Changing lifestyles have had an impact on the health of the general populace in recent decades. The current research assesses the importance of numerous elements linked to nutritious diets, food quality, dietary habits, modernization, and environmental factors impacting human health. The surveys were undertaken in several states of India to understand people's dietary habits with regard to education, economic status, social standing, and so on, in order to analyze their food preferences and health issues related with it. A survey and case studies were conducted to evaluate the quality of the most commonly used food items, such as Milk products, Cold Drinks, Juices & other food items in order to ensure the safety of the products for consumption.

Prof. (Dr.) Simerjit Kaur, Ph.D (Mycology), M.Phil, Gold Medallist, Panjab University, Chandigarh. She is Director-IQAC and Head-Life Sciences at Rayat Bahra University, Mohali, India. She has patents/Research publications/Books credited in her name with over 20 years of experience in Administration, Academics & Research.

9786206 792000

Prof. (Dr.) Simerjit Kaur

Prof. (Dr.) Simerjit Kaur

Modernization, Dietary Habits & Related Health Risks

A Survey on In-Depth Analysis of Food habits & Quality Assurance

LAP LAMBERT Academic Publishing

Prof.(Dr.)SimerjitKaur

Modernization,Dietary Habits&RelatedHealth Risks

ASurveyonIn-DepthAnalysisofFoodhabits& QualityAssurance

LAPLAMBERTAcademicPublishing

Imprint

Coverimage:www.ingimage.comP

ublisher:
LAPLAMBERTAcademicPublishing
isatrademark of
DodoBooksIndianOceanLtd.andOmniScriptumS.R.Lpublishing group

120 HighRoad,EastFinchley,London,N2 9ED,UnitedKingdom
Str.Armeneasca28/1,office1,ChisinauMD-2012,RepublicofMoldova, Europe
Printedat:seelastpage
ISBN:978-620-6-79200-0

TABLEOFCONTENTS

Preface

This book contains the work ofnumerous scholars in the fields of food quality evaluation, food products, balanced diet, altering lifestyle, food management, and so on. Each chapter focusesonspecificgoals,variouscontributingfactors,resultsandevidence-based measures.

Changing lifestyles have had an impact on the health of the general populace in recentdecades. The current research assesses the importance of numerous elements linked to nutritious diets, food quality, dietary habits, modernization, and environmental factors impactinghumanhealth.Thesurveyswereundertakeninseveralstatesof Indiato understandpeople'sdietaryhabitswithregardtoeducation,economicstatus,social standing,and so on,in order to analyze their foodpreferences andhealthissues related with it.

A survey was also done to evaluatethe quality of themostcommonlyused fooditems, such asVerkaMilkproducts,ColdDrinks&Juices,andsoon,in ordertoensurethesafetyof the products for consumption.

Case studies of industries were also conducted in order to better understand the techniques used to ensure the food quality of its products.

An Overview on Food Quality and Quality Assurance

Nidhi Singal[1], Simerjit Kaur[2*], Manoj Bali[3]

[1]Associate Professor & Dean, School of Sciences, Baddi University of Emerging Sciences andTechnology, Baddi, Himachal Pradesh,India. E-Mail: hod.ash@baddiuniv.ac.in

[2*]Corresponding Author: Dean & Professor, Department of Life Sciences, Rayat Bahra University, Mohali, Punjab, India. E-Mail: dr.simer07@gmail.com

[3]Dean & Professor, University School of Sciences, Rayat Bahra University, Mohali, Punjab, India, E-mail drmanojbali@gmail.com

Abstract

Food analysis is necessary to ascertain product quality, carry out regulatory enforcement, verifyconformitywithnationalandinternationalfoodstandards,contractspecifications and satisfy nutrient labeling requirements. Nutritional value, which is a component of food quality, is determined by how well-balanced a meal or diet is in terms of essential elements including carbohydrates, fats, proteins, minerals, and vitamins in relation to the nutrient requirementsof consumers.In order to ensurethe safety, health andwell-beingof people withrelation tofood,newtechniquesandtechnologiesmustfocuson physical,biological and chemical agents or their mixtures. Quality control (QC) is a proactive technique used to identifyandcorrectdefectsinfinishedproducts.Findingandremovingtheoriginsof qualityproblemswillensurethattheclient'sexpectationsareregularlyaddressed. Accreditedproductcertificationisthemosteffectivetechniquetoverifyandconvey productquality.In ordertodeliverhigh-quality productsandservices,qualityassurance (QA)standardsarefrequentlyused.WhileQCfocusesonidentifyingandcorrecting mistakescommittedbefore,duringoraftertheproductdevelopmentprocess,QAattempts todelivergoodsandservicesthataredefect-freeorthatarerightthefirsttimewithlittleto norework.Theauthorshaveattemptedtoassemblein thischaptersomepointsofviewon the state of food quality and assurance today, from farm to fork.

Keywords: Foodquality,Foodsafety,nutritionalvalue,qualitycontrol,qualityassurance.

1. INTRODUCTION

Comparedtoshelterandclothing,foodisahuman'smostfundamentalnecessity.Itmeets the body's needs for development, upkeep, restoration, and reproduction. Foods with vital nutrientsincluding carbohydrates,lipids, proteins,vitaminsandminerals can be foundin bothplant-andanimal-basedsources.Followingconsumption,foodtypicallypasses through a number of metabolic processes that ultimately result in the creation of energy, maintenance of life and/or encouragement of growth.

Inthemodernfoodeconomy,foodqualityisamajorconcern[1].Inrecentyears, consumers' worries about leading healthierlives and protecting the environment havechangedboth their food purchasingintents and theirperceptions offood quality. Because theirpurchasingdecisionsarebasedontheseframes,understandinghowcustomers perceive the quality of food is extremely important [2]. To ensure that consumers consume safefooditemsandprotectedfromtherisksassociatedwithcontaminatedmeals,itis crucial to control food quality [3]. Labelling is unquestionably one of the tools that enables consumerstomakeaninformeddecision[4,5].Numerousstudiesviewlabellingasaway tocommunicateproductqualitiesrelatedtotheenvironmentandhealthinaggregate [6,7,8]. It also lowers the likelihood that purchasers would deal with dishonest vendors andend up with subpar items.

NutritionalAnalysisofFood

Food analysis is required in order to determine product quality, conduct regulatory enforcement, verification of compliance with national and international food standards, contract specifications and nutrient labelling requirements.
Size, consistency, appearance, freshness, hygienic practices, flavor, safety, and maturity are among the crucial food quality factors. The food products are then categorized based on the proportion of requirements met. As a result, buyers may distinguish between products with similarclassificationsbasedon quality andcost.Duetothecategorization code'slegibility on food packaging, it is easily recognized and accessible to consumers. This also applies to food production, animal feed and raw & processed foods [9].

Globalhumanexistencewassignificantlyimpactedbytheearlyshutdownbroughtonby the coronavirus disease 2019 (COVID-19). People had been confined to their homes for a considerableamountoftimeduetothemeasuresimplementedin themajorityofstates, along with the closure of many businesses, including restaurants. There is no doubt that the COVID-19 problem hastened, consumers' demands for safer and more reasonably priced mealsastheybecamemoreconcernedabouttheirhealth[10,11,12]. Researchfindings

havedescribedhowsuchnon-intrusiveandpotentanalyticalapproachescanbeemployed for quick andprecisemeasurements of quality parametersin various circumstances [13].

A variety ofviewpoints on the current development of food quality and quality assurancehavebeen presentedin thischapter.Whilewe donot claimin thistextto cover all elements toguaranteefoodquality,ourgoalistodrawattentiontothefactorsandinformation which, in our opinion, is most crucial.

FoodSafety

Thegrowthofnewwaysoffoodcontrolandsafetyhasbeenrecognizedasnecessaryby the European Food Safety Authority (EFSA) which has recorded the current huge hazard around the globe. Undeniably a crucial element in achieving such aims is the methodology development level. The development of new techniques and tools must concentrate on physical,biologicalandchemicalagentsortheircombinationsinordertoensurethe security,healthandwellbeingofpeoplewithregardtofoods.Becauseofthenumerous laws and guidelines that have been issued by the authorities, quick, accurate and sensitive techniques of detection are recommended for food risk management[14].

Foodqualityandfoodsafetycanoccasionallybeusedinterchangeably.Foodsafetyrefers to all risks, whether they are acute or chronic, that could cause food to be harmful to the consumer'shealth.Itcannotbenegotiated.Alladditional characteristicsthataffecta product's value to the consumer are included in quality.

Foodquality

Sinceitis a dynamic conceptinfluencedby both objective and subjective factors, food qualityisahighlybroadandcomplicatedtermthathaschangedquiteswiftlyoverthepast

few years and is predicted to continue. Food quality can be viewed as the culmination of all efforts made by all parties involved in the food chain to avoid production, storage,distribution,marketing,anddifficultieswithfoodtraceabilityandsafety.Thisisbecause foodqualityinvolvestheaccumulation ofeffortsoveralongperiodoftime[15].The conceptoffoodqualityshouldalwaystakespecificfactorslikeafood'snutritionalvalue intoaccount.Awell-balancedratiooftheVitalnutrientssuchascarbohydrates,fats, proteins, minerals and vitamins in meals or diets related to the nutrient requirements of consumers, is measured as nutritional value as well as a part of food quality. However, the massive rise in the prevalence of chronic diseases worldwide has prompted a change in the way thatnutritionisthoughtof,takingintoaccounttheuniquetraitswhicharedetermined byanindividual'sgenotypeanddailyroutine[16].Morethan85%ofthese"early" fatalities,which affect 15million people aged30-69 eachyear,take placein low- and middle-income nations. The leading cause of death worldwide (17.9 million fatalitiesannually) is cardiovascular disease, which is followed by cancer (9.0 million), respiratory illnesses (3.9 million) and diabetes (1.6 million). Tobacco smoking, along with lack of exercise,excessivealcoholconsumptionandunrestricteddietarychoicesincreasetherisk of dying from one of these illnesses [17].

Advantagesofqualityisenhancedreliability.Byensuringthatproductsorservicesmeet the required quality standards,businesses can increase the reliability oftheir offerings, leading to increased customer trust and loyalty.

QualityControlintheFoodIndustry

Thefoodsectorworkswithproductsthatarequitesensitive.Itisessentialforparticipants in the food sector to uphold quality standards and criteria and this is one of the fundamental justifications for doing so. The reputation of the brand could be damaged by even a minor instance where product quality has been compromised. Therefore, it's possible that the company'searningswill plummet.Asaresult,brandssellingfoodgoodsmustadopt adequate quality control procedures seriously.

Quality control (QC) is a reactive process that seeks to find and fix flaws in final goods. To ensure that theneeds ofthe client are consistently met,it can be accomplishedby locating andeliminatingthesourcesofqualityissues.Usually,theaccountabilityforitfallswithin the quality management inspection component.

Themajority offood assurance schemes functionas product certification programmes and use routine independent inspections to ensure that participants are adhering to the program's requirements.Thescopeofensuredfoodprogrammesincludesbothprimaryfood production and the procedures that apply tothe whole of the foodchain up to retail sales.

2. Objectives

To protect consumers from tainted,unsafe, wrongly marked or polluted food.To support economic growth by preserving consumer faith in the food system.
Toestablishastrongregulatoryframeworkforbothdomesticandinternationalfoodtrade.

ImportanceofQualityControl

A few reasonswhy brandsdealingin fooditemsmustnotignore quality control havebeen identified:

ReducedProductionCost

Companies in the food sector can drastically cut their production costs by using effective inspectionandcontrolmeasuresin theoperationsandprocesses.Productionexpensesare also driven up by wastages and subpar goods. The production cost is greatly reduced when waste and themanufacture of subpar goods are controlled throughquality control.

SuperiorGoodwill

Quality control helps the company's reputation by creating goods of higher quality andmeetingclientneeds.As aresult, thebrandgains asolid reputation andgains strongword- of-mouth marketing on both offline and online platforms. A reputable company can readily raisecapitalfromthemarket.Acompany'sprospectsofsurvivinginthefiercely competitive market are likewise great when it has improved goodwill.

PriceFacilitation

Companies in the food business can guarantee the production of uniform goods of the same qualitybyimplementingqualitycontrolprocedures.Thisconsiderablyfacilitatestheissue offoodproductpricefixing.Theconcern overcommodities'pricingfluctuatingcontinually is also removed.

ExpandSales

By ensuring the manufacture of high-quality goods, quality control plays a crucial role in luring more consumers to the product and boosting sales. It is highly advantageous in preservingthecurrentdemandforthecompany'sproductsaswellasgeneratingnew demand.Additionally, with theincreasedusage of social media, itismoreimportant than ever forbrands to stay alert.Thebrandimage couldbeimpactedby anyunfavorable feedback from customers.

NewProductionMethods

Quality control makes sure that goods are produced at acceptable rates and to the desired standards.Italsoensuresbetterproduction techniquesanddesignsby providingtechnical and engineering data for the product and manufacturing processes.

Increasedmorale

An efficientquality control system isvery helpfulin raisingstaffmorale.Employeesare moreinclinedandmotivatedtoworktowardsthegoalsofthefirmwhen they begin to believe that they are employed by a company that produces good, high-quality products. Additionally,theseworkersaremorelikelytoadheretotheorganization'scriteriafor quality control in their work.

Qualityattributes

Aspect of appearance- Itis a visual appeal assessedby thesense of sight using criteria like:

a) Size and shape wholesomeness:It is clearly visible to the eye. Deviceslike a screen,scale, micrometer etc. are used for precision and standards, though.

b) Damage,defectsandextraneousmaterial:Defectsresultfromthepresenceof undesirable materials. One type of defect is insect damage or injury caused by bruising, crushing etc.

c) Presenceofforeignmaterial:Evenifit'ssafe,extraneousmaterialshouldn'tbeeaten.

d) Deformed fruit and vegetable shapes caused by the environment or a genetic component and/ or other processed foods caused by a processing error. Color, gloss, transparency, turbidity etc. are all considered tobe spectral.The spectral dispersion of light is responsible forcolorandgloss.Viscosity,gelflowandspreadareallexamplesofconsistency. Viscosity is one of the most important qualities of foods including ketchups, juices, creams, jamsandothers.Viscosity measurementsreveal theuniformity ofthefinishedproductas well as the quality control measures used on the raw materials and throughout processing to get the intended outcome.

Kinestheticaspect

It is evaluated by the sense of touch, specifically through the mouth and hands such as softness, chewiness, stickiness etc. The way that food's structural elements are arranged in micro ormacro structures as well as the way that these structures are manifested on the outsideareknownaskinestheticcharacteristicsortexture.Itcontainsaspectsoffoodthat thetongue,palate,orteethmayfeel.Thevarietyoftextureiswideandaqualityflaw occurs when the texture differs from what is intended.

Forinstance-Firm apples, softmangoes and plums,juicy sweet corn and crisp potato chipsare all expected for good quality.

Flavorcomponent

It is evaluated using the senses of smell and taste. It encompasses the senses of taste such as sweet,sour,salty&bitteraswellasthesensationofoff-flavorlikeenzymatic, physiological,chemical,contaminatedandovercooked.Consumersusetheirsensesof smell and taste to assess flavor qualities.

Foodcanbepreservedwithdesiredflavorby-

a) Avoidinglossofflavorduringheattreatment,handling,transitandstorage.
b) Preventingthegrowthofunfavorableflavor.Forexample- Metallictasteandoxidative rancidity of canned goods.
c) Creating and retaining flavor as in the roasting of coffee beans, bread baking, wine agingetc.
d) ReintroducingnaturalflavorsthatarelostduringprocessingbyfortifyingfoodFOR AUTHOR USE ONLY.

Systems for Product Certification and Food Quality Assurance on Marketing Aspects

The best way to validate and communicate product quality is through accredited product certification. The use of quality assurance (QA) standards is regarded as a tried-and-true methodofprovidinghigh-qualitygoodsandservices[18].Strictersafetyrequirementsand a much higher number of quality assurance programs have been introduced on both an internationalandEuropeanUnion(EU)levelasaresultofthegrowingendeavorto guaranteehigherfoodsafetyandquality[19].Beyondthebenefitthatthesequality assurance programs provide to consumers, "quality" has come to be recognized as a critical componentofmarketing,givingcompaniesafantasticopportunitytostandoutinthe market and add value to their goods [20]. Production standards are established by theassurance scheme and vary amongst the schemes, often addressing food safety andtraceability,animalwelfareandenvironmentalprotection.Membersofacertainscheme mayusethescheme'smarkontheirgoodsormakeaspecificclaimtoinformconsumers that the product hasbeen producedin accordance with these requirements [21].

The proprietor of the scheme is the owner of the "Q Mark" for food products. After being judged tobein compliance with all of the scheme standardsby the certification body (CB), the producer whointends tousethismarkon his product has toacquire formal clearance from the scheme owner for the use of the mark. As reliable certification becomes more and moreimportanttointernationaltrade,organizationslikeTheInternationalAccreditation

Forum (IAF) and International Laboratory Accreditation Cooperation (ILAC) continuously seek to maintain a high standard. Without the additional legitimacy of recognized certifications, this cannot be accomplished. The standards for several widely used product certificationprogramsinthefoodindustryhaveincreaseddramatically[21].Nowadays, there are more conventional-plus food products on themarket that convey a certain quality that also applies to comparable organic items. Therefore, these items can be thought of as goods that fall between conventional and organic goods. Given this similarity in certain characteristics, conventional plus goods can face competition from organic ones depending upontheinterestofthecustomers[22].Thegoalistocreateparticularcertification schemes and certification methods for foodstuffs in line with EN ISO/IEC 17065:2012 in contrasttoexistingcertification schemesinotherproductionsectors,whichoftenjust validatethattheproductconformstotherequirements.Theplanmustbeableto demonstrate how, if at all, the plan's requirements go above the required minimum by law.The National Accreditation Board for Certification Bodies (NBCB) grants accreditation to CertificationBodiesbasedonassessmentoftheircompetenceinaccordancewiththe Board'scriteriaandinaccordancewithInternationalStandardsandGuidelines.The approval of the certifying organizations by the scheme owner is conditional upon NBCB accreditation.Theseprogramsaredesignedtoenablethevalidationandcommunicationof a specific product's qualitative features thatin some way constitute a competitive advantageon themarket.They are optional product certification programs.In other words,ifyou believeyourproducthasafeaturethatsetsitapartfromsimilaritemsonthemarketand you want people to know that it has been independently verified.Then these certification procedures whichinclude developing requirements,validating, certifying, communicatingandmonitoringmustbe adopted.The certification markis attached to the product and directly communicates the quality to the customer. With expansion comes the necessity to upholdstandardsforqualityandotherfactors,regardlessofchangesinconsumerdemand orforanyothercause.Allofthisrequirescooperationbetweenmachinesandhumans, whichis known as artificialintelligence,becauseneithera personnora computer can doit on their own.

Artificialintelligenceisprimarilyusedinthefoodsectorsinceitcanactbothlikearobot and like a person at the same time. By considering all the variables, including raw material quality, environmental temperature, fermentation, and bacterial development in the product while acquiring the final goods, artificial intelligence may help produce the finest results. However,manyindustriesandprocessesarestillnotfullyutilizingAI'sbenefits.Once fullyembraced,itwillsurelyhelpusachievethegoaloffullyautomatedmanufacturing that can be run with a single click [23].

HowdoesQualityAssuranceoutperformQualityControlineffectiveness?

Quality

According to the simplest definition, quality is the culmination of a product's attributes thatarecrucialindeterminghowmuchaclientwillacceptit.Qualityshouldbefocusedon thepresentandfutureneedsoftheclient,accordingtoSirEdwardsDeming.Asaresult,it is possibleto define quality as thelevel of goodness that consumers orcustomers'mark.

2.5.2QualityControl

Implementingqualitycontrolisonemethodforraisingthestandardofthefinalproduct.It is a set of operational methods and procedures used to meet quality standards. It includes correctiontoolswithareactivefocus.Theinstrumentsforqualitycontrolassistin identifying flaws in the goods or services and in taking the appropriate corrective action to offer high-quality goods or services.

QualityAssurance

Quality assurance is crucial for a higher-performing system. In order to give consumers enough trust that a product or service will meet quality standards, quality assurance is a planned and systematic activity that is conducted. It is a mechanism put into place by an organization that guarantees external parties that the data generated is of recognized and verified quality and satisfies end user needs. Documentation of the process, the procedures,the capabilities and their monitoring are crucial to this assurance.

Image source: https://www.creaform3d.com/blog/pun5th75ef_wp/wp-content/uploads/imagerie-QC-vs-QA-vs-QS.jpg

WhichcomesfirstQualityAssuranceorQualityControl?

Assuring the quality of any good or service is more effective than other methods. Product-focused activities include quality control and process-focused activities include quality assurance. Quality product production cannot be achieved without ensuring process quality. The term "quality assurance" refers to a comprehensive strategy that can be carried out by a manager,aclient,orevenathird-partyreviewer.Itdescribesthemethodutilizedto producedeliverables.QC,ontheotherhand,isexclusivelyconcernedwiththedelivery itself and requires technical expertise to perform. While QA aims to provide items andservicesthat aredefect-free, orthat areright the first time withlittle tono rework, QC focuses on discovering and fixing errors made during or after the product developmentprocess to manage the system's total quality, however, quality control and quality assuranceare equally crucial, and both must be put into practice to meet the institution's quality objectives.

3. References

[1] Grunert K.G. Food quality and safety: Consumer perception anddemand. Eur. Rev.Agric. Econ. 2005; 32:369–391.

[2] Van Rijswijk W., Frewer L.J. Consumer perceptions of food quality and safety and their relationtotraceability.Br.FoodJ.2008;110:1034–1046.doi:10.1108/00070700810906642.

[3] SajdakowskaM.,GębskiJ.,GutkowskaK.,Żakowska-BiemansS.Importanceof HealthAspectsinPolishConsumerChoicesofDairyProducts.Nutrients.2018;10:1007. doi: 10.3390/nu10081007. [PMC free article] [PubMed]

[4] PetrescuD.C.,OrolanI.G.,ProorocuM.,MihăiescuT.,PauletteL.,VârbanD.Organic products:Consumptionhabitsandperceptions.Adv.Environ.Sci.2013;5:1–9.

[5] Petrescu-Mag R.,Petrescu D.,Sima N.F.,Sima R.Informed productchoicein the organicfoodsector:Fromguaranteeingthelegalrightstofacingsustainabilitychallenges. J.Environ.Prot.Ecol.2016;17:1111–1121.

[6] CerriJ.,TestaF.,RizziF.ThemoreIcare,thelessIwilllistentoyou:How information,environmental concern andethical production influenceconsumers' attitudes andthepurchasingofsustainableproducts.J.Clean.Prod.2018;175:343–353.doi:10.1016/j.jclepro.2017.12.054.

[7] FestilaA.,ChrysochouP.Implicitcommunicationoffoodproducthealthfulness throughpackagedesign:Acontentanalysis.J.Consum.Behav.2018;17:461–476. doi:10.1002/cb.1732.

[8] Osburg V.-S., Yoganathan V., Brueckner S., Toporowski W. How detailed product informationstrengthenseco-friendly consumption.Manag.Decis.2019doi: 10.1108/MD- 10-2017-1012. In press.

[9] Al-Nemri,B.T.,FoodQualityCertificationCode.PatentNumberUS2020/0242977 A1. United States Patent Application Publication, Published 2020.

[10] Lamarche B., Brassard D., Lapointe A., Laramée C., Kearney M., CôtéM., Bélanger-Gravel A., DesrochesS., Lemieux S., PlanteC.Changes in diet quality and food security amongadultsduringtheCOVID-19–relatedearlylockdown:ResultsfromNutriQuébec Am. J. Clin. Nutr., 2021;113: 984

[11] Murphy B.,BensonT.,McCloatA.,Mooney E.,ElliottC.,Dean M.,LavelleF. Changesinconsumers'foodpracticesduringtheCOVID-19lockdown,implicationsfor diet quality and the food system: Across-continental comparison. Nutrients, 2021;13:20

[12] Jiménez-Rincón S., Dou N., Murray-Kolb L.E., Hudy K., Mitchell D.C., Li R., Na M. Daily food insecurity is associated with diet quality, but not energy intake, in winter and during COVID-19, among low-income adults Nutr. J., 2022; 21:19

[13] Su W.H., Sun D.W. Fourier transform infrared and Raman and hyperspectral imaging techniquesforqualitydeterminationsofpowderyfoods:AReviewCompr.Rev.FoodSci. FoodSaf.,2018;17:104

[14] Olmos E.,Venegas M. Sustainable primary production. LibrosblancosDesafíosCientíficos 2030 del CSIC, vol. 6, Consejo Superior de InvestigacionesCientíficas, Madrid 2021

[15] Chen T.,ZhangJ.,LuoJ.Differential gameevolution offoodquality safetybasedon market supply and demand Food Sci. Nutr.,2021; 9:2414

[16]https://www.ars.usda.gov/is/np/NutritiveValueofFoods/NutritiveValueofFoods.pdf. GoogleScholar

[17] https://www.who.int/es/news-room/fact-sheets/detail/noncommunicable-diseases. GoogleScholar

[18] ManningL.,BainesR.N.,ChaddS.A.Qualityassurancemodelsinthefoodsupply chain Brit. Food. J. 2006;108:91-104

[19] BotonakiA.,PolymerosK.,TsakiridouE.,MattasK.Theroleoffoodquality certification on consumers' food choices Brit.Food. J. 2006; 108:77-90

[20] JervellA.M.,BorgenS.O.Newmarketingchannelsforfoodqualityproductsin Norway ActaAgric. Scand. Sect. C Food Economics2004; 1:108-18

[21] Kirk-Wilson R.Review ofUptake ofFSA FoodAssurance SchemeGuidanceby UK Scheme Operators 2008 (Available at: http://collections.europarchive.org/tna/20101209122142/;http://www.food.gov.uk/multimedia/pdfs/foodassureguidance.pdf)

[22] Stolz H., Stolze M., Hamm U., Janssen M., Rutoc E. Consumer Attitudes Towards OrganicVersusConventionalFoodwithSpecificQuality AttributesNJASWagen.J.Life Sc. 2011;58: 67– 72

[23] SharmaS.,BisoyeeP.,JatharJ.FoodQualityAssuranceusingArtificialIntelligence: A Review Paper Int. Res. J Eng Technol. Aug 2021; 08(08):1841-1847 e-ISSN: 2395-0056 www.irjet.net p-ISSN: 2395-0072

Microalgae as Nutraceuticals-A Potential alternatives to Health Supplements

Manoj Bali[1*], Simerjit Kaur[2], Nidhi Singal[3]

[*1]Corresponding Author: Dean & Professor, University School of Sciences, Rayat Bahra University, Mohali, Punjab, India, E-mail drmanojbali@gmail.com

[2]Dean & Professor, Department of Life Sciences, Rayat Bahra University, Mohali, Punjab, India. E-Mail: dr.simer07@gmail.com

[3]Associate Professor & Dean, School of Sciences, Baddi University of Emerging Sciences andTechnology, Baddi, Himachal Pradesh,India. E-Mail: hod.ash@baddiuniv.ac.in

Abstract

Microalgae have higher pigment concentrations than many plant and floral species. In comparison to traditional sourceslikemeat,poultry, and dairy products, proteins derived from microalgae have full Essential AminoAcids (EAA) profiles and a higher proteincontent. The nutraceutical products are recognized for their health benefits both in terms of prevention and treatment of diseases. The rapidly growing population and ever-increasing burdenoflifestylediseaseshasnecessitatedthesearchforaffordablenutraceuticalswhich are easily accessible. Microalgae present a potential solution to easy accessibility,affordability and excessive demand.Through thischapter, wewill give abrief overviewof thenutraceuticals,differentnutraceuticalcompoundsavailablethroughmicroalgaeand their beneficial effects.

Keywords: Nutraceutical,Phytochemicals,Microalgae,Spirulina,Chlorella.

Introduction

Hippocrates(460–370BC)correctlysaid,"Letfoodbeyourmedicineandmedicinebe your food." The combination of the words "nutrition" and "pharmaceutics" referred to as Nutraceutics is the term used for the products which can be a potentially therapeutic due to their nutritional effects. The term was coined Dr. Stephen De Felice, Chairman of the Foundation for Innovation in Medicine in 1989. The term defined differently in different countries;however,itisgenerallyusedfortheproductsisolatedfromfoodsthatare generallymarketedasproductsofphysiologicalimportanceand/orprotectiveagents againstchronicdiseases.Thenutraceuticalsarereferreddifferentlyindifferentcountries and industries, the other terminologies are "designer foods," "functional foods," "dietary supplements," "medical foods," "pharmafoods" and "phytochemicals" [1].

The belief in nutraceuticals is rising, firstly because the regular consumption of a greatnumber of synthetic drugs used in chronic conditionsis known to cause serious side effects and secondlybecause people aroundthe word don't haveaccess to perfectly balanced foodsin terms of fiber, carbohydrate, protein, and the right amounts of vitamins and minerals to maintaingoodhealth.Thenutritionalimbalancehasbeenassociatedwithmanydiseases likecardiovascular(CVDs),cancer,diabetes,obesityandmanysuchdiseases. Nutraceuticals can provide an easy and affordable solution to these conditions in terms of preventivedietaswellastreatment.Nutraceuticalshavereceivedconsiderableattention and interest from patients and medical fraternity because of their presumed safety, effective results and affordability [2].

General classification of nutraceuticals is done on the basis of natural food source i.e. it is obtained from plants, animals, minerals, or microbial sources, chemical nature they are phenols, amino-acids, carbohydrates, fatty acids, minerals etc. and pharmacological actionlike they are effective against Alzheimer's, cancer, diabetes etc. Nutraceuticals can also be categorized as traditional nutraceuticals, which includes natural food like lycopene in tomatoes,resveratrol in grapes andanother categoryisnontraditionalnutraceuticals which are further subdivided into fortified food and recombinant food. Fortified food are artificial foodspreparedbyaddingbioactivecomponentsbyofphysicalmixinglikeorangejuice with calcium or through artificial breeding of plants or animals.Examples of recombinant food are bread, alcohol, fermented starch, yogurt, cheese, vinegar etc. [3].

Therearenumerouspathologicalconditionswherenutraceuticalshavegiveneffective results. However, when we talk about plant of animal-based nutraceuticals, we confront an enormouslimitation.Theglobal populationisgrowingexponentially andispredictedto reach 9.5 billion by 2050. To meet the global food demand of food and nutrition we will require a twofold increase. This will thus put pressure on agriculture and animal rearing and willrequireescalationofagriculturalarea.Thispressureinturnwillaffecttheproduction of nutraceutics derived from flora and fauna.

1. Introduction

Microalgaeormicrophytesareunicellularmicroscopicalgaeinvisibletothenakedeye. Theirnatural habitatincludesfreshwaterandmarinesystems.Microalgaecan survive throughawiderangeofpH,salinity,temperature,lightintensitiesconditionsinreservoirs or deserts. They adapt to available resources and can grow alone or in symbiosis with other organisms. Microalgae are capable of photosynthesis, consume $CO_2$and are credited with productionofapproximately50%oftheatmosphericoxygen.Thesurvivabilityof microalgaeishighunderextremeconditions.Microalgaeusesunlightinvery efficientway ascomparedtothehigherplants.Thebiodiversityofmicroalgaeisexuberantwith estimated 2 lakh to 8 lakh species in many different genera. Microalgae research is gaining importance and weightage as they are being looked upon as future of food security and nutraceuticals.Asmicroalgaecanbeculturedinnon-arablelandandbrakishwaters,hence

their nurturing does not affect the volume of agricultural land. Microalgae are in use since ancient civilizations such as the Aztecs in Mexico used cultures of A*rthrospira* (S*pirulina) maxima*, a C*yanophyceae*, formaking"Tecuitlatl"a typeof cake.Chadnativesused the samemicroalgaeforpreparationoffoodstuffs. InChina*Nostocflagelliforme* hasbeen used for food for more than 2000 years. Microbiologist Beijerinck was pioneer of scientific studies on microalgae, he succeeded in growing pure cultures of *Chlorella vulgaris*(1890). Microalgaehaverecentlyattractedconsiderablescientificandindustrialattention worldwide,dueto theirextensive application potential in diversefieldslike renewable energy, biopharmaceutical, and nutraceutical industries. The fast renewability makes microalgaesustainableandeconomicalsourcesofbiofuels,bioactivemedicinalproducts andfoodingredients.Furthertheextractionofnutrientsfrommicroalgaeisalsoeasy and cost effective.[4, 5]

2. Nutraceuticalsfromalgae

PhenolicandVolatilecompounds

Phenoliccompoundsareprotectivecompoundsormetabolitesproducedinresponseto stress.Phenolicphytochemicalsdemonstratehighbiologicalactivity;theyareprovedto have to have activities such as antioxidant, anti-inflammatory, and antimicrobial.

The microalgae species are known to have total phenolic content similar or higher thanpopular sources such as kale, shallols, cashew, apple and strawberries. Heptadecane and tetradecaneavailableinS*ipirulina*areknown forgoodantibacterial capacity,itisalso known to have antimicrobial activity by virtue of compounds like β-cycb, α and β-ionone. Preclinical and epidemiological studies have revealed that phenolics retard carcinogenic progress, onset of diabetes and prevents cardiovascular and neurodegenerative diseases[6,7,8].

Phytosterols

Phytosterols arebelieved to be related to many healthbenefits. The activity of phytosterols,on human organs is related to their ability to replace cholesterol in membranes, thus attenuating high cholesterol diet effect. Promising quantity of sterols were found inmicroalgae strains, *Dunaliella tertiolecta and D. salina*.Sterols because of their bioactivity have ability to reduce LDL cholesterol. Sterols also show antibacterial, antiviral andantifungal properties.Phytosterolspreventassembly ofcholesterol esterintochylomicrons by preventing esterification of cholesterol. Sterols exhibit anticarcinogenic activity. Studies have proved their protective affects against colon, prostate and breast cancer. Nervous disorders such as Alzheimer's disease, autoimmune encephalomyelitis, amyotrophic lateral sclerosis are also known to be ameliorated by sterols. With a little manipulations of growth mediummicroalgaecanproduceawiderangeofsterolcompounds,brassicasterol, sitosterol,andstigmasterol.Sterolproduceyieldedbymicroalgaeisevenbetterthen

rapeseedplants.Theproduceisestimatedintherangeof678–6035kgha^{-1}y^{-1}of phytosterol [9,10,11].

Pigments

Pigments derived from microalgae are categorized into chlorophylls a, b, and c, phycobili pigments, and carotenoids. From the bunch of algal pigments Carotenoids are believed to providephotoprotectiontothecellsthroughantioxidativeactivity.Therecentresearch shows that the health effects of pigments are however much wider, for example lutein, zeaxanthin,andβ-carotene,cryptoxanthinandα-carotene,fucoxanthinfrombrownalgae and diatoms show anti-cancer activities. Antioxidant, anti-inflammatory, and anticancer properties have also been demonstrated by Phycobilin pigments.

One of the popular microalgae *Spirulina* yields good quantity of c-phycocyanin, which is already inducted as food and is commercially produced in different parts of the world. *Spirulina*constitute30%ofthetotalbiomassproductionofmicroalgaeworldwide. Dunaliella salina and *Haematococcus pluvialis* are rich sources of powerful antioxidant and anti-inflammatory agent effective in controlling protein degradation, macular degeneration, rheumatoidarthritis,cardiovasculardiseases,neurodegenerativediseasessuchas Parkinson's, and cancers. Though there is a long list of pigment producing microaglae and theirhealthbenefitsthecommercialization ofthese(exceptforthosementionedabove)is still questionable. *Spirulina* is recommended for diet of astronauts because of excellent and compact food [12,13, 14, 15].

Polyunsaturatedfattyacids

Aarachidonicacid(AA),linolenicacid,eicosapentaenoicacid(EPA),docosapentaenoic acid(DPA),anddocosahexaenoicacid(DHA)areessentialforhuman animalnutrition. Thesearepolyunsaturatedasthey havemorethan onedoublebondin theirstructureand have carbon chain of 18 or more carbons. PUFA are well known for their preventive or ameliorating activity against asthma, arrhythmias, atherosclerosis, rheumatoid arthritis,manic-depressive illness, chronic obstructive pulmonary diseases, of cystic fibrosis, prevent relapsesin patients with Crohn's disease. PUFA are also helpfulin improvingbone health and brain functions in children. Microalgae are rich source of PUFAs. *Phaeodactylum tricornutum, Monodus subterraneus, Porphyridium cruentum, Chaetoceros calcitrans* and *Nannochloropsis spp* are prominent producers of PUFAs. The prominent Microalgae producing DHA are *Crypthecodinium cohnii, Isochrysis galbana,* and *Pavlova salina.* Linolenic, and oleic acids are produced in good amount by *Dunaliella salina. Spirulina platensis*providesγ-linolenicacid,lauric,palmitoleic,andoleicacidsandDHAinvery good yield [16,17,18].

VitaminsandMinerals

In many ways, vitamins and minerals are originators of dietary supplement category. The nutritional market is expanding leaps and bounds where multivitamins and minerals remainthe most widely accepted and used supplements as enormous health benefits are usually attached to consumption of vitamins and minerals. Microalgae are excellent sources of vitaminssuchasvitaminA,B1,B2,B6,B12,CandEandmineralssuchaspotassium, iron, magnesium, calcium and iodine. *Chlorella* is an excellent source of minerals, dietary fibers,andvitaminsincludingvitaminB12withgoodbioaviabilitiy.55.2µg/gdryweight of α-tocopherol and 51.3µg/g dry weight γ-tocopherol were extracted from *Porphyridium cruentum.*

Minerals may exist in elemental form like zinc, calcium, magnesium, sodium, iron, sulfur, copper etc. or they may existin combined form with other compounds. Minerals areimportant nutraceuticals required for the optimum health and physiological functions.Minerals can only be taken from external sources as minerals, being elements, cannot be synthesized biochemically by living organisms.Microalgae have the ability to accumulate trace elements, but very few studies have been conducted on the mineral content of microalgae.Appreciablequantitiesofzinc,phosphorus,sodium,iron,potassium, manganese, magnesium, and calcium have been extracted from *D. tertiolecta, Isochrisis galbana, Tetraselmis suecica, C. vulgaris, Sochrisis galbana, S. platensis, and Chlorella stigmatophora* [19, 20, 21, 22, 23].

ProteinsandAminoacids

Foodproteinsarewidelyusedinformulatedfoodsastheyaresafetoconsumeandhave high nutritional value. The effectiveness of nutraceutical products in preventing diseases depends on preserving the bioavailability of the active ingredients this presents challenge in oral administration of nutraceuticals. Lot of research has been dedicated to study functional proteins.The gel forming property of proteinsand polymer-based particulate systemshas been exploited for GRAS (generally recognized as safe) biocompatible carriers for oral administration of sensitivenutraceuticalsin awidevariety of foods.Severalmicroalgal strains such *as Chlorella, Spirulina, Scenedesmus, Dunaliella, Micractinium, Oscillatoria, Chlamydomonas,* and *Euglena* contain proteins of high quality. *Cyanobacteria* such as *S. platensis* and *Porphyridium spp*. contain phycobiliproteins, a group of proteins involved in photosynthesis. The essential amino acids, such as lysine, leucine, isoleucine, and valine contribute to the high quality of microalgal proteins. Many species of microalgae possess protein up to 70% dry weight and are nutritionally similar to proteins like egg and soybean. Generally inactive bioactive peptides on hydrolysis exert hormone like activity on physiological processes. Properties attached to bioactive peptides are cholesterolamelioration,immunityimprovement,antimicrobial,anticancer,antioxidant,atherosclerosis and hypertension controlling effects. Proteins purified from *C. vulgaris, Chlorella,S.platensis,Naviculaincerta,Pavlovalutheri,P.lutheri,Chlamydomonassp.*

and*N.incerta*havetestedpositiveforcombatingdifferentdiseasesincluding carcinogenesis and hepatotoxicity [17,19,20, 21,24,25].

3 Conclusion

It would be appropriate to say that microalgae are amazing organism which can grow in diverse conditions. Many compounds of highnutraceuticals are available from microalgaestill remain vastly unexplored. There is need for research in processes of isolation, identification, and growth optimization of new and locally available microalgal strains. Microalgae have been included in many nutritional studies worldwide, and more nutritional benefitsarelikelytobediscoveredwithincreasedhumanuse.Microalgaeifexploredto full potential may be able to overcome challenges of food and nutritional security,and wemayseerevolutionarychangesintheenergy,pharmaceutical,cosmetics,andfood industries in the coming years.

4 References

1. Nasri H, Baradaran A, Shirzad H, Rafieian-Kopaei M. New concepts in nutraceuticals as alternative for pharmaceuticals. Int J Prev Med. 2014;5(12):1487-99.

2. KianiAK, Dhuli K, DonatoK,Aquilanti B, Velluti V, MateraG,Iaconelli A,Connelly ST, Bellinato F, Gisondi P, Bertelli M. Main nutritional deficiencies. J Prev Med Hyg. 2022;63(2 Suppl 3):E93-E101.

3. Chauhan B, Kumar G, Kalam N, Ansari SH. Current concepts and prospects of herbal nutraceutical: A review. J Adv Pharm Technol Res. 2013;4(1):4-8.

4. Kaur M, Bhatia S, Gupta U, Deckaer E, Tak Y, Bali M, Gupta VK, Dar RA, Bala S. Microalgal bioactive metabolites as promising implements in nutraceuticals and pharmaceuticals:inspiringtherapyforhealthbenefits.PhytochemistryReviews.2023:1-31.

5. Dolganyuk V, Belova D, Babich O, Prosekov A, Ivanova S, Katserov D, Patyukov N, Sukhikh S. Microalgae: A Promising Source of Valuable Bioproducts. Biomolecules. 2020;10(8):1153.

6. Ozdemir G, Ulku Karabay N, Dalay M C, Pazarbasi B. Antibacterial activity of volatile component and various extracts of Spirulina platensis. Phytotherapy Research. 2004; 18(9):754–757.

7. Hajimahmoodi M, Faramarzi MA, Mohammadi N, Soltani N, Oveisi MR, Nafissi-VarchehN,Evaluation ofantioxidantpropertiesandtotal phenoliccontentsofsomestrains of microalgae. Journal of Applied Phycology.2010; 22(1):43–50.

8. Lin, J. Y. and Tang, C. Y. Determination of total phenolic and flavonoid contents in selected fruits and vegetables, as well as their stimulatory effects on mouse splenocyte proliferation. Food Chemistry. 2007;101(1):140–147.

9. Cabral CE, Klein MRST. Phytosterols in the Treatment of Hypercholesterolemia and Prevention of Cardiovascular Diseases.Arq Bras Cardiol. 2017;109(5):475-482.

10. Salehi B, Quispe C, Sharifi-Rad J, Cruz-Martins N, Nigam M, Mishra AP, KonovalovDA,OrobinskayaV,Abu-ReidahIM,ZamW,SharopovF,VenneriT,CapassoR,Kukula-

Koch W, Wawruszak A and Koch W. Phytosterols: From Preclinical Evidence to Potential Clinical Applications. *Front. Pharmacol*. 2021:11.
11. Francavilla M, Colaianna M, Zotti MG, Morgese M, Trotta P, Tucci P, Schiavone S, Cuomo V, Trabace L. Extraction, characterization and invivo neuromodulatory activity of phytosterols from microalga Dunaliella tertiolecta. Current Medicinal Chemistry.2012;19(18):3058–3067.
12. Silva SC, Ferreira ICFR, Dias MM, Barreiro MF. Microalgae-Derived Pigments: A 10-Year Bibliometric Review and Industry and Market Trend Analysis. Molecules. 2020;25(15):3406.
13. Sun H,WangY, HeY, Liu B,Mou H,Chen F, YangS. Microalgae-DerivedPigments for the Food Industry. Mar. Drugs.2023;21:82.
14. SalehiB,QuispeC,Sharifi-RadJ,Cruz-MartinsN,NigamM,MishraAP, Konovalov DA, Orobinskaya V, Abu-Reidah IM,Zam W, Sharopov F, Venneri T, CapassoR, Kukula-Koch W, Wawruszak A and Koch W (2021) Phytosterols: From Preclinical Evidence to Potential Clinical Applications. Front. Pharmacol. 11:599959. doi: 10.3389/fphar.2020.59995
15. Matufi F, Choopani A (2020) Spirulina, food of past, present and future health.Biotechnol Biopharm. 3(4):1–20.
16. Hardman D, Fakaa S. Polyunsaturated Fatty Acids as Dietary Supplements.Int J ClinNutr Diet. 2016:113.
17. Stengel DB, Cannon S, Popper ZA. Algal chemodiversity and bioactivity: Sources of natural variability and implications for commercial application. Biotechnology Advances. 2011;29:483–501.
18. Sathasivam R, Radhakrishnan R, Hashem A, Abd_Allah EF. Microalgae metabolites: A richsourceforfoodandmedicine.SaudiJournalofBiologicalSciences.2019;26(4):709- 722.
19.(a) Becker EW. Micro-algae as a source of protein. Biotechnology Advances.2007; 25:207–210.(b)BeckerEW.Microalgaeforhumanandanimalnutrition.Handb Microalgal Cult John Wiley & Sons.2013:461-503.
20. ShimJY,ShinHS,HanJG,ParkHS,LimBL,ChungKW,OmAS.Protectiveeffects of Chlorella vulgaris on liver toxicity in cadmium-administered rats. Journal of Medicinal Food. 2008; 11:479–485.
21. Tokuşoglu Ö, Üunal MK. Biomass nutrient profiles of three microalgae: Spirulina platensis, Chlorella vulgaris, and Isochrisis galbana. Journal of Food Science.2003;68:1144–1148.
22. Durmaz Y, Monteiro M, Bandarra N,Gokpinar S, Isik O.The effect of low temperature on fatty acid composition and tocopherols of the red microalga, Porphyridium cruentum. Journal of Applied Phycology.2007;19:223–227.
23. FabregasJ,HerreroC.Marinemicroalgaeasapotentialsourceofmineralsinfish diets. Aquaculture. 1986;51:237–243.

24. Amorim ML, Soares J, Coimbra JS, Leite MD, Albino LF, Martins MA. Microalgae proteins: production, separation, isolation, quantification, and application in food and feed.Crit Rev Food Sci Nutr. 2020;61:1–27.
25. Kang KH, Qian ZJ, Ryu B, Kim D, Kim SK. Protective effects of protein hydrolysatefrom marine microalgae Navicula incerta on ethanol-induced toxicity in HepG2/CYP2E1cells. Food Chemistry.2012;132(2):677–685.

1. Influence of Distinct Inserts on the Thermal Augmentation of Nanofluid-Based Heat Exchanger: A Comprehensive Review on Solar-Assisted Technology

In: Nanotechnology Applications ... ISBN: 978-1-68507-451-7
Editors: T. Srinivas et al.

Chapter 4

INFLUENCE OF DISTINCT INSERTS ON THE THERMAL AUGMENTATION OF NANOFLUID-BASED HEAT EXCHANGER: A COMPREHENSIVE REVIEW ON SOLAR-ASSISTED TECHNOLOGY

Sashank Thapa[1,*], Raj Kumar[1], Khushmeet Kumar[2], Robin Thakur[1] and Ritika Rana[1]
[1]School of Mechanical, Civil and Electrical Engineering, Shoolini University, Solan, India
[2]Mechanical Engineering Department, Baddi University, Solan, India

ABSTRACT

Nanofluids are the mixture of metal, metal oxide, and non-metal particles added mainly on the nanoscale at a very low concentration to liquid to increase the thermal enhancement of the system. The present work is the review of nanofluids used in the heat exchanger pipe along

* Corresponding Author's E-mail: mech12400@gmail.com.

2. Characterization and slurry erosion performance of plasma sprayed Ni-Al2O3 coatings on Turbine Steel.

Characterization and Slurry Erosion Performance of Plasma Sprayed Ni–Al_2O_3 and Ni–TiO_2–Al_2O_3 Coatings on Turbine Steel

Vishal Kumar Rana, Vibhu Sharma, and Sushma Singh

Abstract In the Himalayan region, hydro turbine parts are prone to significant erosion, particularly during the rainy season. In the present work, the performance of plasma spray Ni–Al_2O_3, and Ni–Al_2O_3–TiO_2 composite coatings were studied, in order to protect the CA6NM hydro turbine steel from slurry erosion. The microstructural characterization of the as-sprayed coatings was studied using the SEM, EDS, and XRD techniques, whereas, for mechanical characterization, various tests were performed for evaluating the micro-hardness, porosity, fracture toughness, surface roughness, and coating density in the as-sprayed coatings. The test was conducted by using the slurry jet erosion test rig. Impact of different parameters which influence the erosion process namely Inflight velocity, Concentration of slurry particles, and average size of erodent's was also evaluated. The as-sprayed Ni–TiO_2–Al_2O_3 coating outperformed the Ni–TiO_2–Al_2O_3 coating and uncoated steel specimens in terms of slurry erosion resistance for all the experimental conditions.

Keywords Plasma spray · Ni–Al_2O_3 · Ni–TiO_2–Al_2O_3 · Slurry erosion · SEM · EDS and XRD

1 Introduction

The deteriorate of the turbine steel used specifically for the hydro turbine steel due to the slurry erosion is the challenging task for its mitigation. The slurry erosion is commonly seen in the turbine blades, propellers, fluid transfer pipelines, spheres, and other part of the machineries. It is the crucial problem in the exiting power generation systems in order to the meet the power demand and supply. Slurry erosion is undesirable in hydro power systems that is primarily connected with the erosion of exposed parts of the turbine to particles laden fluids [1]. The turbine industry faces huge

V. K. Rana (✉) · V. Sharma · S. Singh
Baddi University of Emerging Sciences and Technology, Baddi, India
e-mail: ranavishal413@gmail.com

V. Sharma
e-mail: vibhu.sharma@baddiuniv.ac.in

K. Geetha et al. (eds.), *Recent Trends in Materials*, Springer Proceedings in Materials 18, https://doi.org/10.1007/978-981-19-5395-8_18

DR. ARUN KANT PAINOLI

SELF BRANDING FOR SELF GROWTH

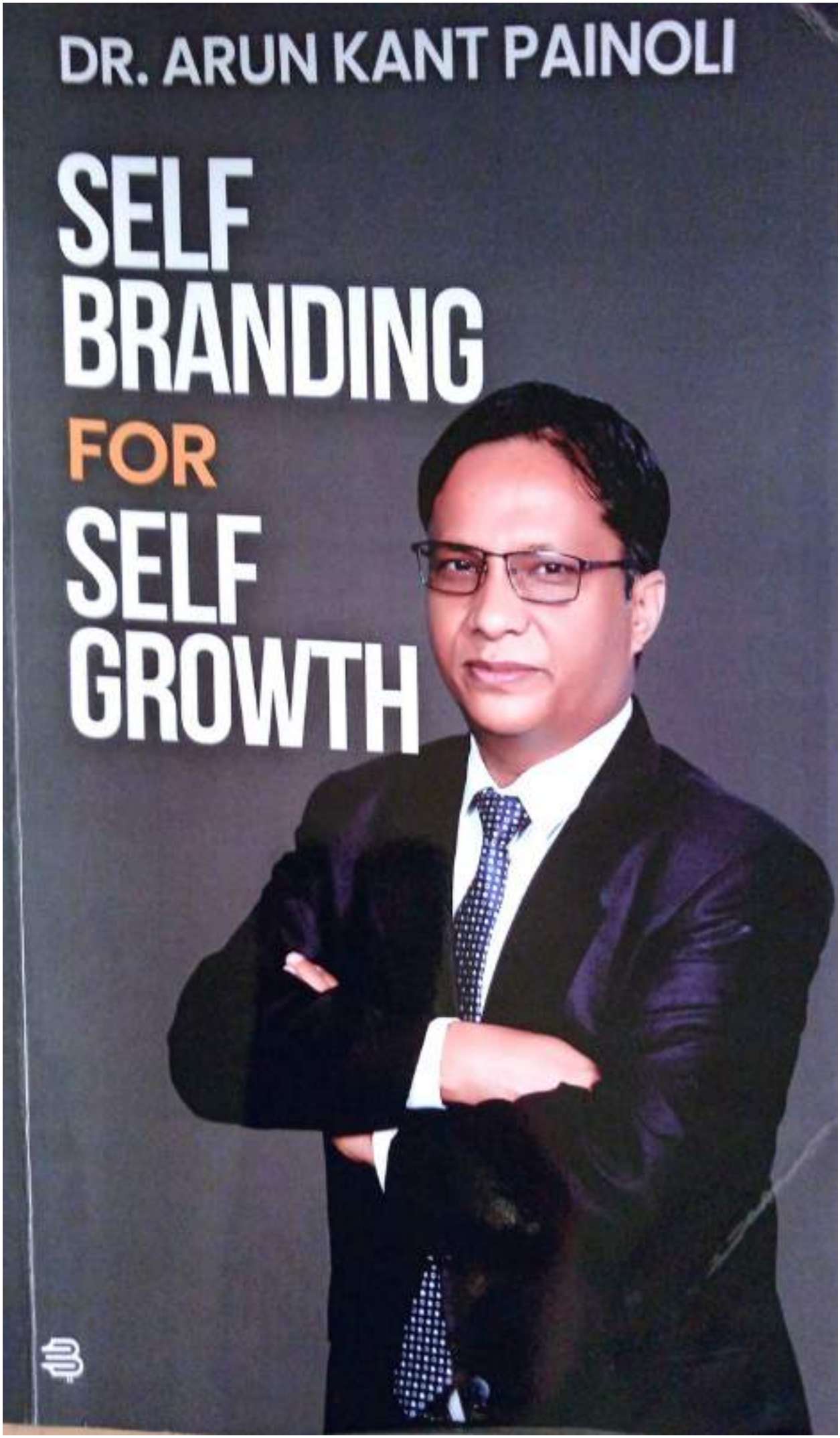

ART OF SELF MANAGEMENT

Dr. Arun Kant Painoli

About the Book

This book is written for the purpose of easy and better understanding of the course curriculum according to the need of Diploma in Pharmacy (D Pharm) students. The syllabus is in compliance with the revised syllabus ER 1998 provided by Pharmacy Council of India. The content of book is framed with precision and specific details about the subject matter and having Board Question Papers from 1996 to 2017. All the questions and the model answers of those questions have been written in a manner that will enable students to get 100% success in MSBTE examinations. Moreover, the content of the book will help not only students but teachers of Diploma Pharmacy. Further, the book content will help to those students who are aspiring for competitive examinations at National (government jobs such as pharmacist, drug inspector and post specific UPSC examination) and International (registered pharmacist or Pharmaceutical Technician in foreign countries) level.

Main features of the book are:

1. Brief outline of each unit's subject matter
2. Short and Long Question Papers of Board examination with their model answers
3. Emphasis on the questions which have been asked repeatedly in Board Examination
4. Lucid and simple Language
5. Crisp and easy to remember answers
6. 100 percent success in all the examinations

About the Authors

Dr. Arti R. Thakkar is alumni of Pharmacy Department, The M. S. University of Baroda, India. She was a visiting scholar at King's College of London, UK (during Ph. D.) and post-doctoral fellow at UNC Eshelman School of Pharmacy, University of North Carolina at Chapel Hill, USA.

Dr. Thakkar has more than 14 years of National & International (India, UK, USA) experience. She has worked in Unison Pharmaceuticals **Ltd as a** QC Chemist. She has worked as a faculty in Parul University, Baroda, ISF College of Pharmacy, Moga, Bodda University and DPSRU. At present she is an Associate Professor, Amity University, Noida. In the past she has developed CDSCO approved/compliant/validated drug testing laboratory ISF AL, Moga.

Dr. **Thakkar** has 37 publications, 66 Presentations, 1 Indian Patent and 1 International Book Chapter, 3 Books, 5 Research Projects (AICTE, ISMAS, DST, NIH and J&J) and 8 awards to her credit. She has guided 33 M. Pharmacy Students and guiding 2 Ph. D Students.

Ms. Prerna Thakur is an Assistant Professor has School of Pharmacy and Emerging Sciences, Baddi University since last 3 years. She has done her B. Pharmacy and M. Pharmacy (Pharmaceutics) from the same college. Before joining in academia Ms. Thakur has worked in Quality Assurance & Quality Control Departments, Fresenius Kabi Oncology Ltd. Baddi.

Ms. Thakur has presented 2 research presentations conferences and one research article to her credit. She is currently teaching D. Pharmacy and B. Pharmacy students.

Paging Publishers
D-1, Acharya Niketan,
Mayur Vihar, Phase - 1, Delhi - 110091
E-mail: info@pagingpublishers.com
Website: www.pagingpublishers.com

Arti • Prerna

Health education and community pharmacy

Health Education and Community Pharmacy

for D. Pharm

10 years, Question & Answer Paper

Dr. Arti R. Thakkar
Ms. Prerna Thakur

About the Book

This book is written for the purpose of easy and better understanding of the course curriculum according to the need of Diploma in Pharmacy (D Pharm) students. The syllabus is in compliance with the revised syllabus ER 1991 provided by Pharmacy Council of India. The content of book is framed with precision and specific details about the subject matter and having Board Question Papers from 1996 to 2017. All the questions and the model answers of those questions have been written in a manner that will enable students to get 100% success in MSBTE examinations. Moreover, the content of the book will help not only students but teachers of Diploma Pharmacy. Further, the book content will help to those students who are aspiring for competitive examinations at National (government jobs such as pharmacist, drug inspector and post specific UPSC examination) and International (registered pharmacist or Pharmaceutical Technician in foreign countries) level.

Main features of the book are:

1. Brief outline of each unit's subject matter
2. Short and Long Question Papers of Board examination with their model answers
3. Emphasis on the questions which have been asked repeatedly in Board Examination
4. Lucid and simple Language
5. Crisp and easy to remember answers
6. 100 percent success in all the examinations

About the Authors

Dr. Arti R. Thakkar is chairperson of Pharmacy Department, The M. S. University of Baroda, India. She was a visiting scholar at King's College of London, UK during Ph. D. and post-doctoral fellow at UNC Eshelman School of Pharmacy, University of North Carolina at Chapel Hill, USA.

Dr. Thakkar has more than 14 years of National & International (India, UK, USA) experience. She has worked Dyssam Pharmaceuticals Ltd as a QC Chemist. She has worked as a faculty in Parul University, Baroda, ISF College of Pharmacy, Moga, Baddi University and DPSRU. At present she is an Associate Professor, Amity University, Noida. In the past she has developed CDSCO approved commercial medical testing laboratory ISFAL, Moga.

Dr. Thakkar has 37 publications, 66 Presentations, 1 Indian Patent and 1 International Book Chapter, 3 Books, 5 Research Projects (AICTE, INMAS, DST, NBI and J&J) and 8 awards to her credit. She has guided 33 M. Pharmacy Students and guiding 2 Ph. D. Students

Ms. Sheetal Sharma is an Assistant Professor has School of Pharmacy and Emerging Sciences, Baddi University since last 3 years. She has done her B. Pharmacy and M. Pharmacy (Pharmaceutics) from the same college. Before joining in academia Ms. Sharma has worked in Quality Assurance Departments, Fresenius Kabi Oncology Ltd., Baddi.

Ms. Sharma has presented 2 research presentations in conferences and one research article to her credit. She is currently teaching D. Pharmacy and B. Pharmacy students.

Paging Publishers
D-1, Acharya Niketan,
Mayur Vihar, Phase - 1, Delhi - 110091
E-mail: info@pagingpublishers.com
Website: www.pagingpublishers.com

Pharmaceutical Chemistry-I

10 years, Question & Answer Paper *for D. Pharm*

Dr. Arti R. Thakkar
Ms. Sheetal Sharma

Arti • Sheetal

Pharmaceutical Chemistry-I

biomedicines

MDPI

Review

Brain-Derived Neurotropic Factor in Neurodegenerative Disorders

Abdallah Mohammad Ibrahim [1], Lalita Chauhan [2], Aditi Bhardwaj [3], Anjali Sharma [4], Faizana Fayaz [4], Bhumika Kumar [5], Mohamed Alhashmi [6], Noora AlHajri [7,*], Md Sabir Alam [8] and Faheem Hyder Pottoo [9,*]

1 Department of Fundamentals of Nursing, College of Nursing, Imam Abdul Rahman Bin Faisal University, Dammam 31441, Saudi Arabia; amsudqi@iau.edu.sa
2 School of Pharmacy & Emerging Sciences, Baddi University of Emerging Sciences & Technology, Baddi 173205, India; lalitachauhan004@gmail.com
3 Department of Pharmaceutical Sciences, Manav Bharti University, Vill. Laddo, Sultanpur (Kumarhatti), Solan 173229, India; aadipharma53@gmail.com
4 Department of Pharmaceutical Chemistry, Delhi Institute of Pharmaceutical Sciences and Research, Sector-3, MB Road, Pushp Vihar, New Delhi 110017, India; anjalish092@gmail.com (A.S.); faizanazargar@gmail.com (F.F.)
5 Department of Pharmaceutics, Delhi Institute of Pharmaceutical Sciences and Research, Sector-3, MB Road, Pushp Vihar, New Delhi 110017, India; bhumika201993@gmail.com
6 College of Medicine and Health Sciences, Khalifa University, Abu Dhabi P.O. Box 127788, United Arab Emirates; 100053507@ku.ac.ae
7 Department of Medicine, Sheikh Shakhbout Medical City (SSMC), Abu Dhabi P.O. Box 127788, United Arab Emirates
8 SGT College of Pharmacy, SGT University, Gurgaon 122505, India; mdsabiralam86@gmail.com
9 Department of Pharmacology, College of Clinical Pharmacy, Imam Abdul Rahman Bin Faisal University, P.O. Box 1982, Dammam 31441, Saudi Arabia
* Correspondence: nalhajri007@gmail.com (N.A.); fhpottoo@iau.edu.sa (F.H.P.)

check for updates

Citation: Ibrahim, A.M.; Chauhan, L.; Bhardwaj, A.; Sharma, A.; Fayaz, F.; Kumar, B.; Alhashmi, M.; AlHajri, N.; Alam, M.S.; Pottoo, F.H. Brain-Derived Neurotropic Factor in Neurodegenerative Disorders. *Biomedicines* **2022**, *10*, 1143. https://doi.org/10.3390/biomedicines10051143

Academic Editor: Marco Segatto

Received: 13 February 2022
Accepted: 30 April 2022
Published: 16 May 2022

Publisher's Note: MDPI stays neutral with regard to jurisdictional claims in published maps and institutional affiliations.

Abstract: Globally, neurodegenerative diseases cause a significant degree of disability and distress. Brain-derived neurotrophic factor (BDNF), primarily found in the brain, has a substantial role in the development and maintenance of various nerve roles and is associated with the family of neurotrophins, including neuronal growth factor (NGF), neurotrophin-3 (NT-3) and neurotrophin-4/5 (NT-4/5). BDNF has affinity with tropomyosin receptor kinase B (TrKB), which is found in the brain in large amounts and is expressed in several cells. Several studies have shown that decrease in BDNF causes an imbalance in neuronal functioning and survival. Moreover, BDNF has several important roles, such as improving synaptic plasticity and contributing to long-lasting memory formation. BDNF has been linked to the pathology of the most common neurodegenerative disorders, such as Alzheimer's and Parkinson's disease. This review aims to describe recent efforts to understand the connection between the level of BDNF and neurodegenerative diseases. Several studies have shown that a high level of BDNF is associated with a lower risk for developing a neurodegenerative disease.

Keywords: brain-derived neurotrophic factor; tropomyosin receptor kinase B; neurodegenerative disorders; Alzheimer's disease; Parkinson's disease

1. Introduction

In the central nervous system, brain-derived neurotrophic factor (BDNF) is a significant neurotrophic factor with a major role in neuronal cell differentiation, maturation [1], and survival [2]. BDNF also has a neuroprotective effect in several pathological conditions, including cerebral ischemia, glutamatergic stimulation, decreased blood glucose, and neurotoxicity [3]. It promotes and regulates neurogenesis [4] in several regions in the central nervous system, such as the cerebral cortex, olfactory system, mesencephalon, basal forebrain, hippocampus, hypothalamus, spinal cord, and the brainstem [1]. Low levels of BDNF protein have been shown to have a role in the development of neurodegenerative

disorders, such as Parkinson's disease (PD) [5], multiple sclerosis (MS) [6], and Huntington's disease [7]. Additionally, BDNF plays a major role in energy homeostasis along with a neuroprotective effect, and has been shown to be able to restrain calorie intake and decrease body weight via peripheral or intracerebroventricular (ICV) administration [8].

BNDF can also be found in the peripheral tissues as it can cross the blood-brain barrier; this peripheral circulating BDNF is not derived from the brain, but can be synthesized in several tissues including the liver, lung, muscles, spleen, and the vascular smooth muscles. Most of the peripheral BDNF is stored inside the platelets while the remaining amount circulates in the plasma. It has been suggested that the level of peripheral BDNF is correlated and regulated by the level of CNS BDNF [9].

According to modern estimates, neurological diseases are major contributors to disability and morbidity, and the percentage of disease occurrence is predicted to be higher in the future [10,11]. The absence of adequate therapy means that such diseases create considerable problems worldwide. The lack of adequate therapy is partially due to insufficient awareness or knowledge about the causes of most neurological disorders. Many diseases related to the central nervous system are closely connected to various environmental stimuli, such as stress [12]. Challenging events create severe risks for people with such diseases, particularly those who are more susceptible to the effects of the disease. A high level of stress sometimes has beneficial effects, such as increased attention and memory. However, stress can have harmful effects on the brain when disquieting actions become part of the daily life of an individual [13]. Various studies have shown that strain is related to metabolic problems, increased risk of heart disease, damage to endocrine functions, fluctuations in mood, and impairment of mental abilities. Stress also leads to greater risk of development of manic and neurologic disorders [13]. Persistent strain causes activation of microglia and increases the secretion of cytokines and pro-inflammatory mediators, leading to the migration of various immune cells into brain tissue, thus creating a suitable environment for the development of numerous brain diseases. In response to sustained stress, brain cells secrete several anti-inflammatory mediators, growth factors, and neurotrophic factors that can help neuronal survival [14]. BDNF has been suggested to be an important factor in various pathological conditions and is a candidate biomarker in therapies of various neuronal diseases [15]. In blood, BDNF levels significantly change in response to current treatments; therefore, it is difficult to completely understand the processes that support alteration in BDNF levels in the diseased state [15], and that reduce BDNF in the CNS and blood [16]. In summary, BDNF has a significant role in the pathology of many neurological diseases, with inflammation of neurons serving as a primary trigger for the development of brain pathologies [16,17].

2. BDNF Expression

BDNF is the fourth member of the neurotrophin family that consists of four structurally related factors which also include neuronal growth factors (NGF), neurotrophin 3 (NT-3) and neurotrophin 4 (NT-4). The gene that encodes BDNF includes 3′ region exons that contain the code of the pro-BDNF proteins, and, in the 5′ region, a promoter region that terminates in the 5′-exon which influences gene expression [16,17]. The gene consists of five exons with the coding region found entirely on exon V; the other four exons have the promotor region on their 5′ flanking region, and, at the 3′ end, contain a splice donor. Exon V has a splice acceptor on the 5′ region and on the 3′ end it has two polyadenylation sites. Therefore, each one of the four exons can have alternative splicing with exon V with the adenylation sites able to produce eight different transcripts of the BDNF [18]. Several experiments have shown that the 5′ region in the four exons has different responses according to various neuronal activities, as both hippocampal and cortical activities can regulate the transcripts that contain exon III [19]. It is thought that the structure of the BDNF gene is related to the stage of development, the type of tissue and the function of the BDNF protein in cellular localization. Despite the similarity of the BDNF gene across different species, there are certain structural differences that are dependent on the specific

function of BDNF in that organism [20]. The gene expression of BDNF is regulated at a high level by a wide range of external and internal factors, such as the level of stress, degree of exercise and activity, brain injury, and food [21]. The level of BDNF expression was found to be very low during fetal development but to increase significantly after birth followed by another decline in expression in adulthood. BDNF is expressed throughout the entire brain with the highest levels found in hippocampal and cerebellar regions [22,23].

BDNF gene translation produces a proneurotrophin (pro-BDNF) [24]. Subsequently, the pro-BDNF protein is cleaved by endoproteases in the cytoplasm to produce the mature BDNF or by plasmin or matrix metalloproteinases (MMP) which occur in the extracellular matrix [25]. Then, the mature and pro-BDNF are secreted and are bound to the p75 neurotrophin receptor (p75NTR) triggering an apoptosis cascade [26]. On the opposite side, cleaved mature BDNF binds to the tyrosine kinase B (TrkB) receptor which is of higher affinity. Binding to the receptor triggers various signaling cascades that include the Ras-mitogen-activated protein kinase (MAPK), the phosphatidylinositol-3-kinase (PI3K), and the phospholipase Cγ (PLC-γ) pathway [27]. These pathways increase the influx of Ca^{2+} which leads to activation of transcription factors by phosphorylation and increased BDNF gene expression (Figure 1) [27].

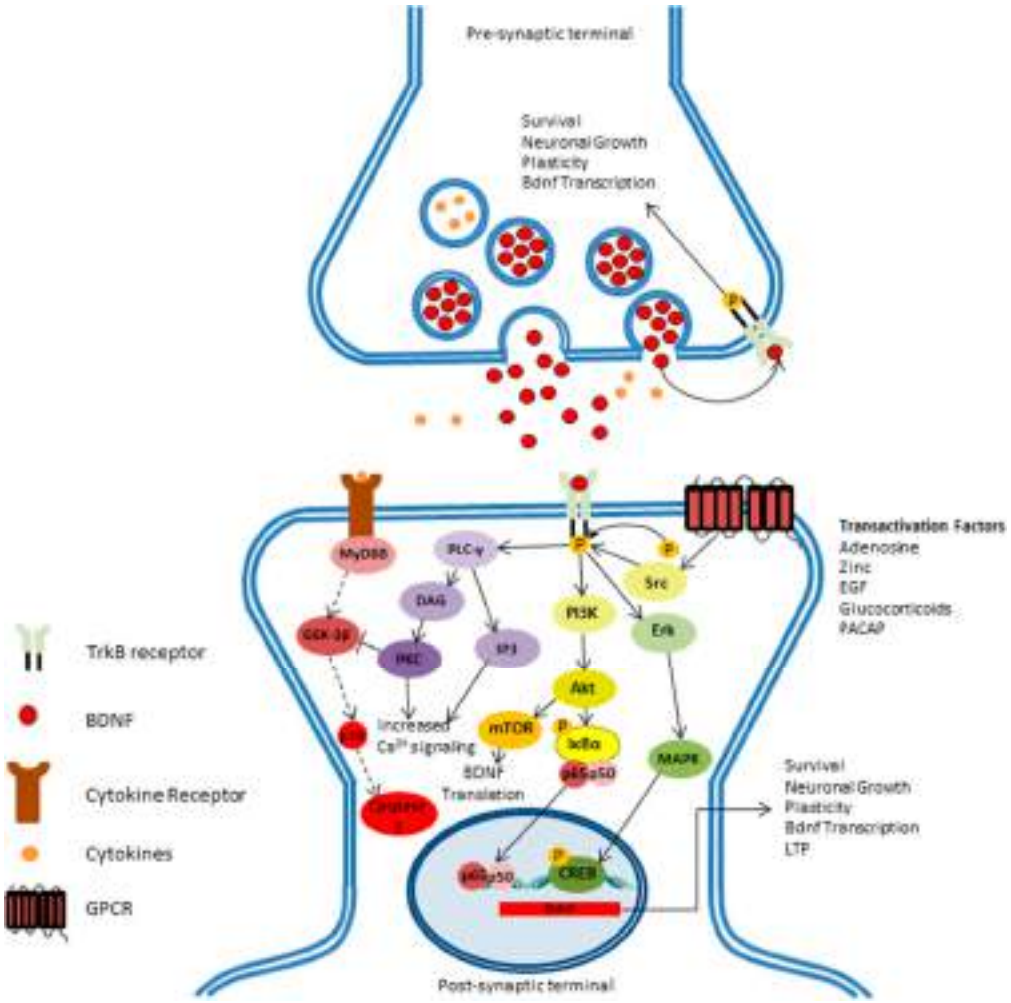

Figure 1. The figure shows the pathways by which BDNF signals can promote the survival of neuronal cells. The binding of BDNF to TrkB receptor switches on 3 different signaling pathways: the first pathway is the activation of the (PLC-γ) pathway which increases the level of Ca^{2+} that will

terminate the apoptosis that is caused by inflammatory mediators (dashed lines), achieved by inhibiting the glycogen synthase kinase 3-beta (GSK-3β). The second pathway is activation of mTOR-dependent translation through the (PI3K) pathway, resulting in the transcription of BDNF mRNA. Additionally, the induction of Akt and Erk downstream enhances gene regulation through the NF-κB and CREB transcription factors. The third pathway is regulated by several factors such as zinc, epidermal growth factor, glucocorticoids, and the so called neurotrophic pathway, which is considered to be independent for BDNF as it can transactivate the TrkB and has a role in its signaling. This figure is adapted after modification from open access [10].

Although pro-BDNF can activate the apoptosis pathway, it is not known if it is secreted by neuronal cells under normal circumstances because the concentration of the pro-BDNF is less than that of mature BDNF [10]. This has been demonstrated in animal research which showed that the mature BDNF concentration was ten times more than the concentration of pro-BDNF [28]. This raises the issue of whether pro-BDNF is an effective factor for signaling. BDNF function is widespread in multiple regions within the brain [21]. The function of BDNF includes participation in neuronal plasticity, the survival of neuronal cells, the synthesis of new synapses, the branching of dendritic cells, and the adjustment of neurotransmitter activity between excitation and inhibition [29]. The activity of BDNF is seen during all developmental stages and within different age groups [30].

These observations suggest that BDNF and pro-BDNF have opposite biological activity; thus, post-transitional control and how pro-BDNF is processed can have an important influence on the biological activity of BDNF [31]. A significant change in the BDNF function could be achieved by the process of adding a pro-domain to the gene of BDNF. This pro-domain has a role in the folding of the BDNF protein [32]. Genetic polymorphism in the pro-domain that arises from a valine to methionine substitution in the 66 codons (Val66Met) results in a change in memory function and affects the BDNF secretion process [33]. This suggests that the pro-domain region is the area which contains most of the function in the gene for BDNF [31]. In transgenic mice where the mutation Val66Met was induced, altered anxiety behavior was expressed [34] as well as alteration in NMDR-dependent neuronal plasticity in the hippocampus region [35]. Experiments performed on hippocampal slices from transgenic mice showed that if mice were injected with BDNF pro-peptide it inhibited LTD in the hippocampus [36]. BDNF's role in transmission at synapses requires further investigation—many pieces of research suggest that it has a significant role in enhancing the efficacy of synaptic transmission in the hippocampus and the cortex [37,38]. Supporting evidence has included the administration of K252a, which is a TrK receptor inhibitor, or TrKB-IgG, which resulted in the prevention of the induction of long-term potentiation in these areas [39].

3. Pathological Mechanism of Action

BDNF and NT-4/5 can bind to the TrkB receptor, in contrast to NGF, which can bind to several receptors, such as Trk A, C subtypes, and NT-3 [40]. TrkB occurs in two similar forms: a full-length type, abbreviated to Gp145 TrkB, with a molecular weight of 145 kDa, and a truncated form, abbreviated as Gp95 TrkB, with a molecular weight of 95 kDa. The truncated form differs from the full length form in that it lacks the tyrosine kinase domain and shows lower affinity to the nerve growth factor receptor (LNGFR); it is denoted p75 NTR [41]. LNGFR is involved in processes that are pro- and anti-trophic, such as neuron growth and death. BDNF and gp145TrkB have broad expression in brain cells; BDNF receptors are also found in the spinal cord, specifically the gray matter neurons [42].

3.1. Activation of TrkB

The signaling of neurotrophin has a significant role in maintaining the survival and proliferation of cells, the reduction of neural precursors, and axon and dendrite growth via TrkB receptors [43]. The NTRK2 gene encodes for neurotrophic tyrosine kinase in human beings [43,44]. TrkB has extracellular domains with multiple glycosylation sites and a transmembrane area with an intracellular domain that has Trk activity. Once activated, G

proteins, such as Ras and MAP kinase, regulate the PI3-kinase and phospholipase-C-γ (PLC-γ) pathways [45]. Signal activation is faster than deactivation; activation needs two minutes, while the deactivation requires around thirty minutes in the spinal cord. Trk signals are regulated by various mediators [40,43]. Nonetheless, other small G protein messengers have a significant role in BDNF signaling, such as Ras, Rap-1, and Cdc-42-Ra [2].

3.2. Secondary Messengers Activation

The Trk receptor family (which includes TrkA-C) and LNGFR regulate the function of the different types of neurotrophins. The pre-synaptic p75 NTR plays a role in regulating the binding to the Trk receptor, ERK activation by Ras, neurite protuberance and activation of terminal kinase (JNK), which causes apoptosis in different neuronal cells [2]. BDNF signaling activates various secondary messengers in the spinal cord, including via ERK signaling, the proto-oncogene c-fos, and neurons that produce nitric oxide [2,46].

3.3. Signaling Cascade in BDNF

Tyrosine residue activation by BDNF leads to the stimulation of pathways that affect neural plasticity, neurogenesis, cell survival, and resistance to stress, which shows the pro-survival function of Trk receptors. BDNF signaling results in the activation of several transcription factors, such as CREB and the CREB-binding protein (CBP), which modulate gene expression that encodes several proteins which participate in different neuronal functions, such as the plasticity of neurons, neuron response to stress, and survival of neurons [43,47,48].

3.4. Ras/MAPK/ERK Pathway

Activation of the TrkB receptor by BDNF leads to dimerization of the receptor and phosphorylation of tyrosine residues; this creates a site for the src-homology domain which contains the Shc adaptor protein and phospholipase C(PLC). The Shc binds to both the receptor and the protein Grb2 through the nucleotide releasing factor SOS. This leads to activation of RAS [49].

Ras activation stimulates the Ras/MAPK-ERK pathway, PI3-K pathway, and PLC pathway. MAPK/ERK is essential for the formation and survival of neurons by activating several genes responsible for the survival of the neurons and inhibition of apoptosis [50]. Research concerning immature neuronal cells showed that activation of the RAS protein via BDNF protected the neurons from MK801-induced apoptosis [51]. In diseases such as schizophrenia, very low levels of ERK signaling proteins in the prefrontal cortex have been observed [52].

3.5. IRS-1/PI3K/AKT Pathway

Other pathways that participate in the actions of BDNF are insulin receptor activation, substrate-1 (IRS-1/2), PI-3K, and protein kinase B (Akt). Ras stops apoptosis by PI3K that activates pkB via deposition of the protein involved in the apoptosis pathway away from their targets [50]. Thus, the Ras-PI3K-Akt pathway is crucial for the survival of neuronal cells, and any deactivation of this pathway will reduce neuronal survival [53]. BDNF can protect hippocampus neurons from the effects of glutamate and norepinephrine via this pathway. In the hippocampus, BDNF autocrine loops result in low stimulation of NMDA receptors which means low glutamate effects and excitotoxicity [54]. Evidence from postmortem studies indicated the relationship between alteration in the Akt and Erk signaling pathways and schizophrenia; there was a low level of AKT1 mRNA proteins in the cortex and the hippocampus [55], and there were some genetic variants of the AKT1 gene0020 that have been linked to schizophrenia [56].

3.6. PLC/DAG/IP3 Pathway

The binding of BDNF to the Trk receptor initiates phosphorylation of the PLC-γ protein that leads to membrane lipids being broken down into inositol 1,4,5 triphosphate (IP3) and

diacylglycerol (DAG) [57], with the former inducing calcium influx and later activating protein kinase C which is needed for neurite outgrowth [58,59].

4. Functions of BDNF

BDNF has generally been recognized in humans as a protein compressed from the BDNF gene. BDNF was initially isolated from the pig [58]. BDNF is the foremost neurotrophic factor that has been discovered [60]. It acts via the protein tyrosine kinase receptor (TrkB) [61] and is generally associated with aspects of nerve growth [49].

BDNF plays a crucial part in the process of neuro-regeneration [62,63] by preventing neuronal death particularly in the peripheral nervous system [64]. It helps to promote the growth of immature neurons and increases the efficiency of adult neurons [65]. Inside the brain, the role of BDNF is essential for the mediation of synaptic function and the morphology of the neurons rather than being a survival factor [66,67]. Furthermore, BDNF plays a significant part in memory function as it has a role in the formation of memory [29], synaptic plasticity [68], synapse formation [69], synaptic efficacy and neuronal connectivity [70]. In the striatum, the loss of BDNF signalling results in spinal atrophy, which is caused by a defect in the GABAergic spiny neuron in the striatum [71]; striatum GABAergic neurons do not produce BDNF, but they obtain it from the presynaptic neurons of the cortico-striatal projections [30]. Disruption in the axonal BDNF transport to the striatum from reduced cortical supply results in the degeneration of striatal neurons, a pathological feature of Huntington's disease [72]. BDNF in the periphery exists in the plasma, platelets, and the serum [73]. The formation of BDNF is generally performed by vascular endothelial cells and secondary blood mononuclear cells [74]. Observations of polymeric markers has demonstrated an association of bipolar disorder with BDNF in large samples, particularly the Neves-Pereira samples [75,76].

Animal studies have shown that neurotrophins are found in high concentrations in the hippocampus and the hypothalamus, suggesting a significant role of BDNF in learning and memory [21,77]. The decline observed during aging involves multiple factors that influence several systems. In the case of learning and memory processes which are severely reduced with aging, it has been found that these cognitive effects result from impaired neuronal plasticity, which is altered in normal aging but particularly so in Alzheimer's disease. Neurotrophins and their receptors, notably BDNF, are expressed in brain areas exhibiting a high degree of plasticity (i.e., the hippocampus, cerebral cortex) and are considered as molecular mediators of functional and morphological synaptic plasticity. The modification of BDNF and/or the expression of its receptors (TrkB.FL, TrkB.T1 and TrkB.T2) have been described during normal aging and in Alzheimer's disease. Interestingly, recent findings have shown that some physiological or pathologic age-associated changes in the central nervous system could be offset by administration of exogenous BDNF and/or by stimulating its receptor expression. These molecules may thus represent a physiological reserve which could determine physiological or pathological aging. These data suggest that boosting the expression or activity of these endogenous protective systems may be a promising therapeutic alternative to enhance healthy aging [21,78,79]. With aging, reduction in neuronal plasticity in the hippocampus and the hypothalamus leads to impairment in learning and memory function [80]. BDNF participates in synaptic plasticity and can protect the neuron from several brain insults [81]. A systematic review and meta-analysis conducted in 2019 found that patients with Alzheimer's disease have lower levels of BDNF, especially during the late stages of the disease [82]. Furthermore, BDNF plays an important role in learning and memory formation; El Hayek et al. found that during exercise in male mice, lactate metabolite enhanced hippocampal-dependent learning via the BDNF pathway [83].

Administration of a single dose of BDNF into the hippocampus resulted in improvement in memory and emotional behaviour in rats [84], while chronic administration of BDNF was shown to have positive potentiation effect in neurotransmission in the hippocampus region [85]. Moreover, a strong connection between the level of BDNF mRNA in

the hippocampus and the memory function has been reported in rats [86]. In the hypothalamus, BDNF can participate in a neurohormonal role via the induction of synthesis, and the release of these hormones [87,88], while the expression of BDNF varies in response to different physiological stimuli [89].

4.1. BDNF and Aging

Aging is a process that consists of multiple declines in endocrine, cognitive, and immunological functions. Several factors play a major role in determining the aging process and the outcome, such as genetic, epigenetic, and environmental factors [90]. In most cases, there is a decline in cognitive capabilities linked to altered hippocampal and cortical functions [91]. Moreover, memory is affected significantly by the aging process, though the degree of memory impairment varies between individuals and the types of memory involved [92]. Generally, effective cognitive function is associated with optimal neural plasticity that is markedly decreased with aging [93]. Change in learning function is not usually associated with neuron loss [94]. The cognitive and learning function changes have been correlated to decreased BDNF expression and signaling [94]. There is impairment in BDNF-induced LTP due to changes in receptor function, which has been attributed to age-related effects.

The administration of Ampakine can induce expression of BDNF, which can revert changes in the neuronal plasticity function, as observed by some researchers [95]. Ampakine modulates AMPA receptors that can restore LTP to the basal dendrites, which is shown to improve memory function in rats [96]. Certain environmental influences can reverse the decline in hippocampal plasticity and reduced neurogenesis in the dentate gyrus, which are also linked to a high level of BDNF in the brain [97]. Numerous studies that have been performed on humans and animals have confirmed that in the aging brain there is a significant decline in BDNF and TrkB receptor expression [98–100], while spatial learning tasks have been shown to reverse or normalize receptor levels, as seen in aged Wistar rats [101]. BDNF system activation has been shown to enhance a healthy aging process, and the administration of exogenous BDNF may be able to regenerate neurons in certain neurodegenerative diseases [21].

4.2. The Role of BDNF and Alzheimer's Disease

There is growing evidence of a relationship between a decreased level of BDNF expression and AD [102,103]. The pathological characterization of AD is associated with the accumulation of β-amyloid peptides (Aβ) in the brain with an increased level of hyperphosphorylated cleaved tau microtubules [104]. The impaired metabolism of the β-amyloid peptides results in neuritic plaque (NP) formation, where the hyperphosphorylated tau causes neurofibrillary tangle (NFT) formation. These events result in neuronal degeneration causing dementia [105]. Several studies have provided evidence that BDNF/TrkB signaling has an essential function in amyloid processing [105,106]. This suggests that BNDF has an important role in LTP and dendritic development, which are crucial elements in memory function, by supporting synaptic integrity through the modulation of the glutamate receptors, AMPA, and NMDA [107]. In neuronal cell culture, BDNF can reduce Aβ amyloid production [95], while in the absence of BDNF, it is elevated [108]. Studies on animal models have shown an increased level of truncated TrkB receptors in the cortex of mice with AD, which has further worsening effects on spatial memory; moreover, overexpressed truncated TrkB receptors disrupted BDNF/TrkB signaling in AD [109]. NFT and NP accumulation within the hippocampus has been shown to be associated with dysregulation of BDNF and TrkB [110]. The BDNF Val66Met polymorphism has been found to be associated with profound memory decline, particularly in the preclinical phase of the disease [111]. According to the above observations, BDNF has protective effects against AD [112]. Thus, studies on AD models suggest the delivery of the BDNF gene as a possible therapeutic option for individuals with AD [113]. Additionally, Wang et al. identified the link between exercise and BDNF levels as a therapeutic method for patients with AD; it was shown

that exercise induces the expression of BDNF, especially within the hippocampus, which facilitates memory and cognitive function [114]. Table 1 summarizes some research that has addressed the relation between BDNF and AD.

Table 1. Levels and effects of BDNF in Alzheimer's disease.

Study Objective	Sample Origin	BDNF Status	Assay Used	Conclusion	Ref.
To determine the stage in which BDNF reduced	Postmortem cortex	Declined	Western plot	The early stages were associated with decreased BDNF.	[103]
A meta-analysis to examine serum BDNF in patients with AD and mild cognitive impairment (MCI) compared to healthy controls	Peripheral serum of BDNF	Declined	NA	A systematic review and meta-analysis, comprising 15 studies, suggested that a significant decline in peripheral BDNF can only be detected in the late stages of Alzheimer's disease.	[82]
To explain the selective vulnerability of certain neurons to AD	Postmortem cortex	Decreased	Western plot	Reduced BDNF may have a role in the selectivity in neuronal degeneration in AD	[115]
To confirm the relation between decreased BDNF and AD development	Postmortem cortex	Low BDNF mRNA	RT-PCR	A decrease in brain-derived neurotrophic factor synthesis could significantly affect hippocampal, cortical, and basal forebrain cholinergic neurons and may account for their selective vulnerability in Alzheimer's disease.	[116]
Investigate plasma proteomic markers in early-onset versus late-onset AD	Plasma BDNF	Elevated	Ultra-sensitive immuno-based assay	BDNF levels were elevated in both early-onset and late-onset AD	[117]
Examination of BDNF serum level in elderly people	Serum samples	No significant change	ELISA	There was no association between gender, depression, and dementia on serum level of BDNF.	[118]
To assess BDNF serum and CSF concentrations in 30 patients at different stages of AD	Serum, CSF	Early stages increased BDNF serum, decreased level in late stage	ELISA	BDNF can be a good determinant in the assessment of the progression of AD.	[119]

4.3. The Role of BDNF in Parkinson's Disease

PD is a neurodegenerative disease with motor and non-motor manifestation. The main pathology is the degeneration of dopaminergic neurons in the substantia nigra (SN) [120]. Studies have suggested that high expression of BDNF in the SN can maintain the survival and differentiation of the dopaminergic neurons [121]. Studies on PD animal models showed that infusion of BDNF can recover the destruction of dopaminergic neurons and D3 receptors [121,122]. The knockout mice did not experience BDNF reduction in the dopaminergic neurons and the D3 receptor [121]. BDNF had a protective effect on hippocampus neurons from oxidative damage that resulted from injury or inflammation that resulted from the induction of heme oxygenase; the protective mechanism was modulated via RAS-MAPK and the P13K-AKT signals, which induced Nrf2 nuclear translocation [123]. Endoplasmic reticulum (ER) stress can induce apoptosis of dopaminergic neurons causing PD [124]. ER stress caused apoptosis by glycogen synthase kinase 3β (GSK3) activation, cyclin D1 suppression, and AKT inactivation. TrkB overexpression stopped these mechanisms via activation of the AKT signal pathway, causing overexpression of cyclin D1 and enhancing the phosphorylation of GSK3, with the net effect of preventing apoptosis of neuronal cells [125]. Furthermore, α-Synuclein (α-syn) mutations were associated with reduced TrkB and BDNF [126,127]. Some studies have found that BDNF/Trkb axonal signaling transport was significantly reduced in axons with an α-syn aggregate [128]. α-syn can interact with the TrkB receptor, specifically the kinase domain; this interaction induces its ubiquitination, reducing TrkB expression [129], as shown in Figure 2. The presence of

BDNF can inhibit this interaction, thus blocking the destruction of it [130]. One recent study has linked the BDNF genotype and response to long-term pharmacological therapy in Parkinson's disease patients, suggesting a role of BDNF in prediction and counseling in the treatment of Parkinson's disease [131]. Further studies should be implemented to assess the possible therapeutic effect of BDNF in PD (Table 2).

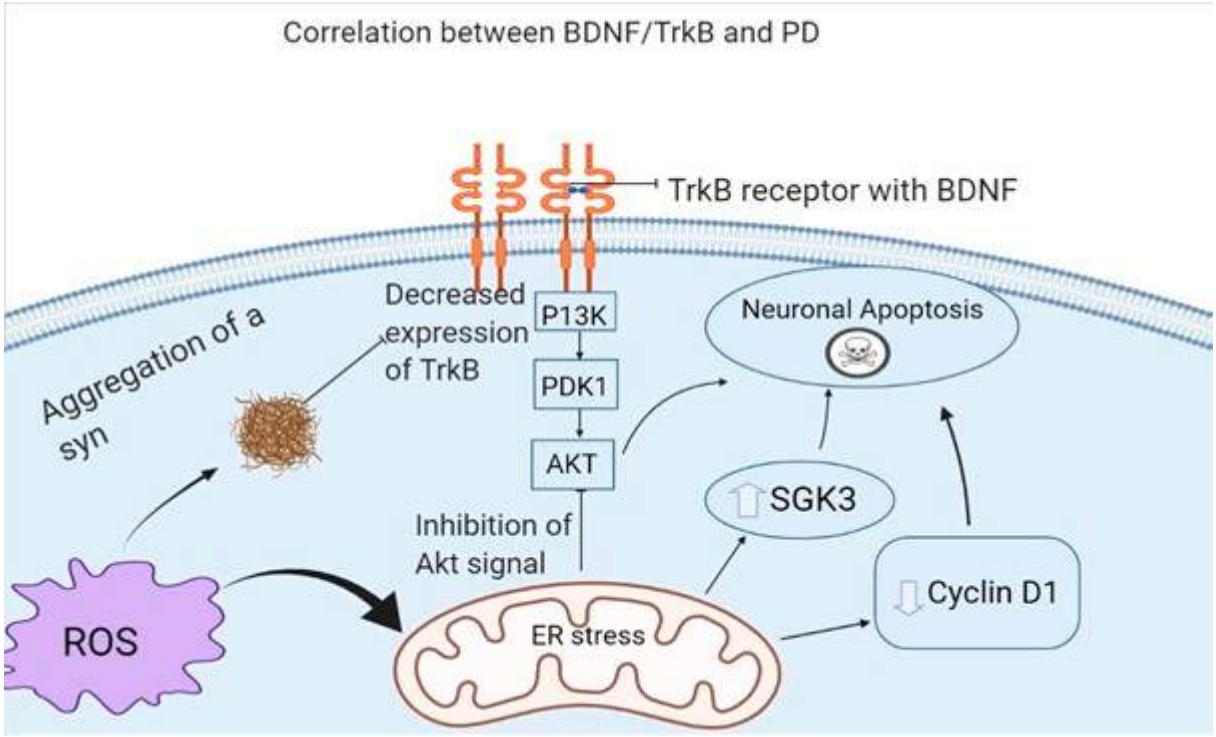

Figure 2. This figure is adapted after modification from open access [132]. The figure shows that ER stress will induce neuronal apoptosis by suppression of cyclin D1, activation of GSK3, and inhibition of Akt signaling from the BDNF/TrkB. A syn aggregation can decrease the expression of the TrkB receptor which will further result in loss of neurons.

Table 2. Levels and effects of BDNF in Parkinson's disease.

Study Objective	Sample Origin	BDNF Status	Assay Used	Conclusion	Ref.
Investigating the effects of BDNF as a neuroprotective factor and as an adjunct therapy in PD	NA	Decreased	NA	In animal PD models, physical activity increased the levels of BDNF and TrkB, which acted as a neuroprotective factor and resulted in symptomatic improvement	[133]
Evaluate salivary cortisol and plasma BDNF levels in PD patients compared to healthy controls	Plasma BDNF	No significant difference in BDNF, but higher cortisol in PD	ELISA	PD patients were in the early stage of the disease, so BDNF is not a suitable biomarker for early cases of PD	[134]
Assess the association between neurotrophic changes and the clinical staging and motor severity of PD	Peripheral BDNF	Decreased	ELISA	A larger decrease in BDNF (and other immune markers) were associated with a higher severity of PD	[135]
Evaluate the levels of serum BDNF in recently diagnosed and untreated PD patients	Serum BDNF	Decreased	Sandwich ELISA	Serum BDNF levels were lower in recently diagnosed and untreated PD patients compared to healthy controls	[136]

Table 2. *Cont.*

Study Objective	Sample Origin	BDNF Status	Assay Used	Conclusion	Ref.
To compare BDNF levels in PD, essential tremor (ET), and healthy controls	Peripheral blood lymphocytes	Decreased in PD	Western blot	BDNF levels were decreased in PD patients, but no significant difference in ET patients	[137]
Investigate the neuroprotective role of BDNF in PD mice	NA	NA	NA	Elevating BDNF levels reduced mitochondrial impairment via increasing electron transport chain (ETC) activity and alleviating dopaminergic loss in PD mice	[138]

4.4. Potential Biological Impact of BDNF Markers

According to a study undertaken by Weinstein et al. relating to the connection between the level of BDNF in the serum and the risk for developing dementia, a ten-year follow up of the effects of BDNF in a particular community showed that, out of 2131 participants, 140 participants had a positive risk of dementia and 117 of them were at positive risk of Alzheimer's disease [125]. Another study found that control participants with higher serum BDNF levels were at minimum risk of developing dementia and AD. Interestingly, this vital relationship of serum BDNF with threat of incidental dementia and AD was restricted to women, participants aged >80 years, and those with a college degree [125]. Further studies suggested that older women were at the highest risk of AD, as they have low serum BDNF, which plays a role in AD growth. Serum BDNF might also operate like a new interpreter in healthy adults [125].

Enzyme-linked immunosorbent assay kits are also known as BDNF antibody [139] of pro-BDNF, which was recognized by Weinstein et al. After use of these kits, there was ease in detecting BDNF forms in humans; it was reported that after using the kits much higher levels of pro-BDNF and mature BDNF were observed in the serum [139].

In a cohort study, given the higher levels of both forms in human serum plus a presumed divergent purpose, it is necessary to measure the individual serum level of both forms (pro-BDNF and mature BDNF) in a technical way [140]. In addition, precautionary drugs, mainly 7,8-dihydroxyflavone (active TrkB), are being used for dementia. These therapeutic drugs enhance recorded low serum BDNF in healthy individuals, and for people who later are likely to developing dementia or AD [140]. The main factors affecting the circulation of BDNF levels in the body are caloric constraints and other physical activities. BDNF acts as an intermediate among the observed links between the threat of dementia and lifestyle [141]. Tracking of original and young applicants was maintained from the year 1992 and the year 1998 for almost ten years in the Framingham study. The study applied Cox models to relate the threat of dementia and AD with levels of BDNF adjusting for probable or potential confounders [125].

BDNF is one of the main modulators of AD risk. Ecological features associated with variation in BDNF brain levels, such as physical activities, might generate neuronal vulnerability and affect risk of AD [114]. Trials (excluding trials on humans) involving the release of BDNF to the brain is a dynamic and new area in translational research for AD. A further study revealed that risk of AD is connected with BDNF blood levels [125]. This study encouraged FHS researchers to explore in more detail the detailed association between BDNF in serum with the threat of dementia and AD [125].

The conclusion reported by Weinstein et al., 2014, in JAMA Neurology was that there was an association between risk of dementia, serum BDNF, and AD in non-demented people who were followed up for up to 10 years [125]. Higher BDNF levels were most frequently related to lesser risk of the disease. Analysis by subgroup suggested the association was restricted mainly to college-going people, women, and in the age group of people over 80 years. Increasing serum BDNF levels led to fewer consequences when account was made for homocysteine levels and other substantial activities affecting AD risk.

The suggestions provided by these perplexing associations are not satisfying and are not easily understood; a more detailed explanation regarding these crucial findings should be less complicated and easier to understand. Certainly, ten years after diagnosis for dementia, levels of serum BDNF were found that were initially observed at the treatment stages of Alzheimer's disease. The symptoms are expressed in terms of slight transformations in primitive functions and biased concerns. Thus, the FHS data showed that BDNF levels act as remedial indicators, highlighting the connection of sequential neurobiology rather than risk modulation of AD with BDNF. Increasingly, work has been conducted to study the BDNF genes and the active process of BDNF delivery to the brain; moreover, detailed studies regarding physical exercise and its involvement in BDNF have been pursued. The risks of reducing homocysteine or inflammation (Lyketsoset al., 2007) were shown to be modulated by the number of therapeutic trials by introducing a blood indicator (collected from the periphery) of AD risk; although the results computed were unsatisfactory. Work on the measurement of BDNF should be sustained as there is strong evidence of its significance.

The study results regarding BDNF levels are quite interesting, but the explanation for these is complex due to various concerns. The main question studied was the connection of serum BDNF with brain levels. Levels of BDNF are affected by additional factors that are considered to influence AD risk, such as physical activity [142] and caloric restriction. Serum BDNF is a relative meandering pointer of these ecological issues rather than a direct modulator of risk. The data collected indicates that the role of BDNF is not clearcut in the mechanism of AD but shows that serum BDNF is strongly associated, being more reactive in the case of dementia. Consideration of peripheral BDNF as a working indicator for the measurement of the effects of remedial interventions is quite premature, and additional studies are necessary to determine the therapeutic and diagnostic importance of the data [143].

One recent meta-analysis study has reported a correlation of BDNF levels with acute stroke; it was concluded that the level of serum BDNF is significantly lower in stroke patients compared to controls. At the same time, there was no correlation between BDNF level and the degree of the infarct or the outcome for the patient [144].

5. Recent Advancements and Challenges

The main challenge in the use of BDNF as a therapeutic intervention in neurological disorders is its ability to reach the CNS in the desired concentration to elicit a therapeutic response [145].

BDNF is a polar protein that is moderate in size; according to these characteristics, it will not cross the blood-brain barrier when administered peripherally. Therefore, it needs to be administered directly into the brain [1].

The administration of BDNF in the ventricles of the brain or intrathecally into the CSF does not result in sufficient penetration to the brain parenchyma [146]. However, the concentration of BDNF is improved when the BDNF is conjugated to polyethylene glycol ('pegylation') as shown in rats, even though this may not produce a sufficient concentration to be suitable for treatment in humans [147].

Moreover, BDNF administration is associated with side-effects with long-term use that cannot be tolerated, including weight loss, dysesthesia, and Schwan cell migration into the subpial space; these side effects result from the penetration of BDNF to the superficial layers [148]. Ideally, BDNF should be administered in a system where it could achieve enough therapeutic concentration in degenerated neurons with limited distribution to other neurons to decrease the side-effects. In addition, the concentration should be maintained for a sufficient time [145]. There are several methods that could be used to enable BDNF as a therapy. These include the following:

BDNF protein infusion which involves the direct intraparenchymal administration of BDNF [149,150]. Several clinical trials performed on Parkinson's disease involved use of implanted devices to infuse BDNF, with high flow rates needed to achieve the

desired concentration in the putamen. The method was associated with tissue damage, as evidenced by MRI. At the same time, the lower rates were not sufficient to elicit a therapeutic response [150,151]. Another observation was that the flowback of the protein in the needle resulted in distribution of the BDNF into the CSF, which caused neuronal death, as shown in animal studies. Therefore, this method needs further improvement to be suitable, such as using an infusion system that can stop the reflux of the protein and a catheter that can distribute the BDNF uniformly into the desired brain regions [152].

The gene delivery method is thought to be a safe and effective way to deliver BDNF into the desired tissue and to decrease the spread to other tissues [153]. This method has been tested in the treatment of Alzheimer's disease, using adenovirus as a viral vector to deliver BDNF gene into the nucleus basalis [153]. It has also been tested in the treatment of Parkinson's disease [154].

Other methods include the use of compounds that can stimulate the synthesis and secretion of BDNF [155]. Moreover, a different approach has been proposed via the enhancement of Trkb receptor activation by agonists such as 7,8-dihydroxyflavone [156], a compound that mimics BDNF such as LMA22A-4 [157], transactivation of Trkb, and, finally, use of facilitators of receptor effects, such as adenosine A2A receptor agonists [158], bearing in mind that the effectiveness of these methods could be altered by the receptor endocytosis effect [159].

6. Conclusions

BDNF is one of the neurotrophic factors that modulate its function through the TrkB receptor. It plays an important role in the central nervous system by the formation and maintenance of a healthy neuronal environment most prominently reflected in cognitive and memory function. Decreased activity of BDNF has been associated with the aging process and with neurodegenerative disorders. The role of BDNF in treatment and as a biomarker for diseases should be investigated thoroughly in future research.

Funding: This research received no external funding.

Conflicts of Interest: The authors declare no conflict of interest, financial or otherwise.

References

1. Acheson, A.; Conover, J.C.; Fandl, J.P.; DeChiara, T.M.; Russell, M.; Thadani, A.; Squinto, S.P.; Yancopoulos, G.D.; Lindsay, R.M. A BDNF autocrine loop in adult sensory neurons prevents cell death. *Nature* **1995**, *374*, 450–453. [CrossRef] [PubMed]
2. Huang, E.J.; Reichardt, L.F. Trk receptors: Roles in neuronal signal transduction. *Annu. Rev. Biochem.* **2003**, *72*, 609–642. [CrossRef] [PubMed]
3. Maisonpierre, P.C.; Le Beau, M.M.; Espinosa, R., III; Ip, N.Y.; Belluscio, L.; Suzanne, M.; Squinto, S.; Furth, M.E.; Yancopoulos, G.D. Human and rat brain-derived neurotrophic factor and neurotrophin-3: Gene structures, distributions, and chromosomal localizations. *Genomics* **1991**, *10*, 558–568. [CrossRef]
4. Zigova, T.; Pencea, V.; Wiegand, S.J.; Luskin, M.B. Intraventricular Administration of BDNF Increases the Number of Newly Generated Neurons in the Adult Olfactory Bulb. *Mol. Cell. Neurosci.* **1998**, *11*, 234–245. [CrossRef]
5. Scalzo, P.; Kümmer, A.; Bretas, T.L.; Cardoso, F.; Teixeira, A.L. Serum levels of brain-derived neurotrophic factor correlate with motor impairment in Parkinson's disease. *J. Neurol.* **2010**, *257*, 540–545. [CrossRef]
6. Sohrabji, F.; Lewis, D.K. Estrogen–BDNF interactions: Implications for neurodegenerative diseases. *Front. Neuroendocrinol.* **2006**, *27*, 404–414. [CrossRef]
7. Mughal, M.R.; Baharani, A.; Chigurupati, S.; Son, T.G.; Chen, E.; Yang, P.; Okun, E.; Arumugam, T.; Chan, S.L.; Mattson, M.P. Electroconvulsive shock ameliorates disease processes and extends survival in huntingtin mutant mice. *Hum. Mol. Genet.* **2011**, *20*, 659–669. [CrossRef]
8. Monteleone, P.; Serritella, C.; Martiadis, V.; Maj, M. Decreased levels of serum brain-derived neurotrophic factor in both depressed and euthymic patients with unipolar depression and in euthymic patients with bipolar I and II disorders. *Bipolar Disord.* **2008**, *10*, 95–100. [CrossRef]
9. Gravesteijn, E. Effects of nutritional interventions on BDNF concentrations in humans: A systematic review. *Nutr. Neurosci.* **2021**, *56*, 3295–3312. [CrossRef]
10. Lima Giacobbo, B.; Doorduin, J.; Klein, H.C.; Dierckx, R.A.J.O.; Bromberg, E.; de Vries, E.F.J. Brain-Derived Neurotrophic Factor in Brain Disorders: Focus on Neuroinflammation. *Mol. Neurobiol.* **2019**, *56*, 3295–3312. [CrossRef]

11. Whiteford, H.A.; Degenhardt, L.; Rehm, J.; Baxter, A.J.; Ferrari, A.J.; Erskine, H.E.; Charlson, F.J.; Norman, R.E.; Flaxman, A.D.; Johns, N.; et al. Global burden of disease attributable to mental and substance use disorders: Findings from the Global Burden of Disease Study 2010. *Lancet* **2013**, *382*, 1575–1586. [CrossRef]
12. Lupien, S.J.; McEwen, B.S.; Gunnar, M.R.; Heim, C. Effects of stress throughout the lifespan on the brain, behaviour and cognition. *Nat. Rev. Neurosci.* **2009**, *10*, 434–445. [CrossRef] [PubMed]
13. McEachan, R.; Taylor, N.; Harrison, R.; Lawton, R.; Gardner, P.; Conner, M. Meta-Analysis of the Reasoned Action Approach (RAA) to Understanding Health Behaviors. *Ann. Behav. Med.* **2016**, *50*, 592–612. [CrossRef] [PubMed]
14. Perry, V.H.; Teeling, J. Microglia and macrophages of the central nervous system: The contribution of microglia priming and systemic inflammation to chronic neurodegeneration. *Semin. Immunopathol.* **2013**, *35*, 601–612. [CrossRef] [PubMed]
15. Hyman, C.; Hofer, M.; Barde, Y.A.; Juhasz, M.; Yancopoulos, G.D.; Squinto, S.P.; Lindsay, R.M. BDNF is a neurotrophic factor for dopaminergic neurons of the substantia nigra. *Nature* **1991**, *350*, 230–232. [CrossRef] [PubMed]
16. Pruunsild, P.; Kazantseva, A.; Aid, T.; Palm, K.; Timmusk, T. Dissecting the human BDNF locus: Bidirectional transcription, complex splicing, and multiple promoters. *Genomics* **2007**, *90*, 397–406. [CrossRef]
17. Aid, T.; Kazantseva, A.; Piirsoo, M.; Palm, K.; Timmusk, T. Mouse and rat BDNF gene structure and expression revisited. *J. Neurosci. Res.* **2007**, *85*, 525–535. [CrossRef]
18. Timmusk, T.; Palm, K.; Metsis, M.; Reintam, T.; Paalme, V.; Saarma, M.; Persson, H. Multiple promoters direct tissue-specific expression of the rat BDNF gene. *Neuron* **1993**, *10*, 475–489. [CrossRef]
19. Lauterborn, J.C.; Rivera, S.; Stinis, C.T.; Hayes, V.Y.; Isackson, P.J.; Gall, C.M. Differential Effects of Protein Synthesis Inhibition on the Activity-Dependent Expression of BDNF Transcripts: Evidence for Immediate-Early Gene Responses from Specific Promoters. *J. Neurosci.* **1996**, *16*, 7428–7436. [CrossRef]
20. Keifer, J. Comparative Genomics of the BDNF Gene, Non-Canonical Modes of Transcriptional Regulation, and Neurological Disease. *Mol. Neurobiol.* **2021**, *58*, 2851–2861. [CrossRef]
21. Tapia-Arancibia, L.; Aliaga, E.; Silhol, M.; Arancibia, S. New insights into brain BDNF function in normal aging and Alzheimer disease. *Brain Res. Rev.* **2008**, *59*, 201–220. [CrossRef] [PubMed]
22. Camuso, S. Pleiotropic effects of BDNF on the cerebellum and hippocampus: Implications for neurodevelopmental disorders. *Neurobiol. Dis.* **2022**, *163*, 105606. [CrossRef] [PubMed]
23. Miranda, M. Brain-Derived Neurotrophic Factor: A Key Molecule for Memory in the Healthy and the Pathological Brain. *Front. Cell. Neurosci.* **2019**, *13*, 363. [CrossRef] [PubMed]
24. Cattaneo, A.; Cattane, N.; Begni, V.; Pariante, C.M.; Riva, M.A. The human BDNF gene: Peripheral gene expression and protein levels as biomarkers for psychiatric disorders. *Transl. Psychiatry* **2016**, *6*, e958. [CrossRef]
25. Kraemer, B.R.; Yoon, S.O.; Carter, B.D. The Biological Functions and Signaling Mechanisms of the p75 Neurotrophin Receptor. In *Neurotrophic Factors*; Lewin, G.R., Carter, B.D., Eds.; Handbook of Experimental Pharmacology; Springer: Berlin/Heidelberg, Germany, 2014; pp. 121–164. [CrossRef]
26. Barkat, M.A. Nanopaclitaxel therapy: An evidence based review on the battle for next-generation formulation challenges. *Nanomedicine* **2019**, *14*, 1323–1341.
27. Minichiello, L. TrkB signalling pathways in LTP and learning. *Nat. Rev. Neurosci.* **2009**, *10*, 850–860. [CrossRef]
28. Matsumoto, T.; Rauskolb, S.; Polack, M.; Klose, J.; Kolbeck, R.; Korte, M.; Barde, Y.A. Biosynthesis and processing of endogenous BDNF: CNS neurons store and secrete BDNF, not pro-BDNF. *Nat. Neurosci.* **2008**, *11*, 131–133. [CrossRef]
29. Bekinschtein, P.; Cammarota, M.; Igaz, L.M.; Bevilaqua, L.R.; Izquierdo, I.; Medina, J.H. Persistence of long-term memory storage requires a late protein synthesis-and BDNF-dependent phase in the hippocampus. *Neuron* **2007**, *53*, 261–277. [CrossRef]
30. Park, H.; Poo, M. Neurotrophin regulation of neural circuit development and function. *Nat. Rev. Neurosci.* **2013**, *14*, 7–23. [CrossRef]
31. Castrén, E.; Kojima, M. Brain-derived neurotrophic factor in mood disorders and antidepressant treatments. *Neurobiol. Dis.* **2017**, *97*, 119–126. [CrossRef]
32. Kolbeck, R.; Jungbluth, S.; Barde, Y.A. Characterisation of Neurotrophin Dimers and Monomers. *Eur. J. Biochem.* **1994**, *225*, 995–1003. [CrossRef] [PubMed]
33. Egan, M.F.; Kojima, M.; Callicott, J.H.; Goldberg, T.E.; Kolachana, B.S.; Bertolino, A.; Zaitsev, E.; Gold, B.; Goldman, D.; Dean, M.; et al. The BDNF val66met Polymorphism Affects Activity-Dependent Secretion of BDNF and Human Memory and Hippocampal Function. *Cell* **2003**, *112*, 257–269. [CrossRef]
34. Chen, Z.Y.; Jing, D.; Bath, K.G.; Ieraci, A.; Khan, T.; Siao, C.J.; Herrera, D.G.; Toth, M.; Yang, C.; McEwen, B.S.; et al. Genetic Variant BDNF (Val66Met) Polymorphism Alters Anxiety-Related Behavior. *Science* **2006**, *314*, 140–143. [CrossRef] [PubMed]
35. Ninan, I.; Bath, K.G.; Dagar, K.; Perez-Castro, R.; Plummer, M.R.; Lee, F.S.; Chao, M.V. The BDNF Val66Met Polymorphism Impairs NMDA Receptor-Dependent Synaptic Plasticity in the Hippocampus. *J. Neurosci.* **2010**, *30*, 8866–8870. [CrossRef]
36. Mizui, T.; Ishikawa, Y.; Kumanogoh, H.; Lume, M.; Matsumoto, T.; Hara, T.; Yamawaki, S.; Takahashi, M.; Shiosaka, S.; Itami, C.; et al. BDNF pro-peptide actions facilitate hippocampal LTD and are altered by the common BDNF polymorphism Val66Met. *Proc. Natl. Acad. Sci. USA* **2015**, *112*, E3067–E3074. [CrossRef]
37. Akaneya, Y.; Tsumoto, T.; Kinoshita, S.; Hatanaka, H. Brain-Derived Neurotrophic Factor Enhances Long-Term Potentiation in Rat Visual Cortex. *J. Neurosci.* **1997**, *17*, 6707–6716. [CrossRef]

38. Kang, H.; Schuman, E.M. Long-lasting neurotrophin-induced enhancement of synaptic transmission in the adult hippocampus. *Science* **1995**, *267*, 1658–1662. [CrossRef]
39. Kang, H.; Welcher, A.A.; Shelton, D.; Schuman, E.M. Neurotrophins and Time: Different Roles for TrkB Signaling in Hippocampal Long-Term Potentiation. *Neuron* **1997**, *19*, 653–664. [CrossRef]
40. Patapoutian, A.; Reichardt, L.F. Trk receptors: Mediators of neurotrophin action. *Curr. Opin. Neurobiol.* **2001**, *11*, 272–280. [CrossRef]
41. Roback, J.D.; Marsh, H.N.; Downen, M.; Palfrey, H.C.; Wainer, B.H. BDNF-activated Sianal Transduction in Rat Cortical Glial Cells. *Eur. J. Neurosci.* **1995**, *7*, 849–862. [CrossRef]
42. Fang, H.; Chartier, J.; Sodja, C.; Desbois, A.; Ribecco-Lutkiewicz, M.; Walker, P.R.; Sikorska, M. Transcriptional activation of the human brain-derived neurotrophic factor gene promoter III by dopamine signaling in NT2/N neurons. *J. Biol. Chem.* **2003**, *278*, 26401–26409. [CrossRef] [PubMed]
43. Kaplan, D.R.; Miller, F.D. Neurotrophin signal transduction in the nervous system. *Curr. Opin. Neurobiol.* **2000**, *10*, 381–391. [CrossRef]
44. Podyma, B. Metabolic homeostasis via BDNF and its receptors. *Trends Endocrinol. Metab.* **2021**, *32*, 488–499. [CrossRef] [PubMed]
45. Roux, P.P.; Barker, P.A. Neurotrophin signaling through the p75 neurotrophin receptor. *Prog. Neurobiol.* **2002**, *67*, 203–233. [CrossRef]
46. Barnabé-Heider, F.; Miller, F.D. Endogenously produced neurotrophins regulate survival and differentiation of cortical progenitors via distinct signaling pathways. *J. Neurosci.* **2003**, *23*, 5149–5160. [CrossRef] [PubMed]
47. Mattson, M.P.; Maudsley, S.; Martin, B. BDNF and 5-HT: A dynamic duo in age-related neuronal plasticity and neurodegenerative disorders. *Trends Neurosci.* **2004**, *27*, 589–594. [CrossRef]
48. Rhee, S.G.; Bae, Y.S. Regulation of Phosphoinositide-specific Phospholipase C Isozymes. *J. Biol. Chem.* **1997**, *272*, 15045–15048. [CrossRef]
49. Pezet, S.; Malcangio, M.; McMahon, S.B. BDNF: A neuromodulator in nociceptive pathways? *Brain Res. Rev.* **2002**, *40*, 240–249. [CrossRef]
50. Brunet, A.; Bonni, A.; Zigmond, M.J.; Lin, M.Z.; Juo, P.; Hu, L.S.; Anderson, M.J.; Arden, K.C.; Blenis, J.; Greenberg, M.E. Akt promotes cell survival by phosphorylating and inhibiting a Forkhead transcription factor. *Cell* **1999**, *96*, 857–868. [CrossRef]
51. Hansen, H.H.; Briem, T.; Dzietko, M.; Sifringer, M.; Voss, A.; Rzeski, W.; Zdzisinska, B.; Thor, F.; Heumann, R.; Stepulak, A.; et al. Mechanisms leading to disseminated apoptosis following NMDA receptor blockade in the developing rat brain. *Neurobiol. Dis.* **2004**, *16*, 440–453. [CrossRef]
52. Yuan, M. Recognition of the SARS-CoV-2 receptor binding domain by neutralizing antibodies. *Biochem. Biophys. Res. Commun.* **2021**, *538*, 192–203. [CrossRef] [PubMed]
53. Vaillant, A.R.; Mazzoni, I.; Tudan, C.; Boudreau, M.; Kaplan, D.R.; Miller, F.D. Depolarization and Neurotrophins Converge on the Phosphatidylinositol 3-Kinase–Akt Pathway to Synergistically Regulate Neuronal Survival. *J. Cell Biol.* **1999**, *146*, 955–966. [CrossRef] [PubMed]
54. Almeida, R.D.; Manadas, B.J.; Melo, C.V.; Gomes, J.R.; Mendes, C.S.; Grãos, M.M.; Carvalho, R.F.; Carvalho, A.P.; Duarte, C.B. Neuroprotection by BDNF against glutamate-induced apoptotic cell death is mediated by ERK and PI3-kinase pathways. *Cell Death Differ.* **2005**, *12*, 1329–1343. [CrossRef] [PubMed]
55. Zhao, M.Z. Promotion on NLRC5 upregulating MHC-I expression by IFN-γ in MHC-I–deficient breast cancer cells. *Immunol. Res.* **2019**, *67*, 497–504. [CrossRef]
56. Emamian, E.S.; Hall, D.; Birnbaum, M.J.; Karayiorgou, M.; Gogos, J.A. Convergent evidence for impaired AKT1-GSK3β signaling in schizophrenia. *Nat. Genet.* **2004**, *36*, 131–137. [CrossRef]
57. Corbit, K.C.; Foster, D.A.; Rosner, M.R. Protein kinase Cδ mediates neurogenic but not mitogenic activation of mitogen-activated protein kinase in neuronal cells. *Mol. Cell. Biol.* **1999**, *19*, 4209–4218. [CrossRef]
58. Barde, Y.A.; Edgar, D.; Thoenen, H. Purification of a new neurotrophic factor from mammalian brain. *EMBO J.* **1982**, *1*, 549–553. [CrossRef]
59. Dimitropoulou, A.; Bixby, J.L. Regulation of retinal neurite growth by alterations in MAPK/ERK kinase (MEK) activity. *Brain Res.* **2000**, *858*, 205–214. [CrossRef]
60. Cohen, S.; Levi-Montalcini, R.; Hamburger, V. A Nerve Growth-Stimulating Factor Isolated from Sarcomas 87 and 180. In *The Saga of the Nerve Growth Factor: Preliminary Studies, Discovery, Further Development*; World Scientific: Singapore, 1997; pp. 156–160.
61. Soppet, D.; Escandon, E.; Maragos, J.; Middlemas, D.S.; Raid, S.W.; Blair, J.; Burton, L.E.; Stanton, B.R.; Kaplan, D.R.; Hunter, T.; et al. The neurotrophic factors brain-derived neurotrophic factor and neurotrophin-3 are ligands for the trkB tyrosine kinase receptor. *Cell* **1991**, *65*, 895–903. [CrossRef]
62. Ebadi, M.; Bashir, R.M.; Heidrick, M.L.; Hamada, F.M.; El Refaey, E.; Hamed, A.; Helal, G.; Baxi, M.D.; Cerutis, D.R.; Lassi, N.K. Neurotrophins and their receptors in nerve injury and repair. *Neurochem. Int.* **1997**, *30*, 347–374. [CrossRef]
63. Eggert, S. Brothers in arms: proBDNF/BDNF and sAPPα/Aβ-signaling and their common interplay with ADAM10, TrkB, p75NTR, sortilin, and sorLA in the progression of Alzheimer's disease. *Biol. Chem.* **2022**, *403*, 43–71. [CrossRef] [PubMed]
64. Sendtner, M.; Holtmann, B.; Kolbeck, R.; Thoenen, H.; Barde, Y.A. Brain-derived neurotrophic factor prevents the death of motoneurons in newborn rats after nerve section. *Nature* **1992**, *360*, 757–759. [CrossRef] [PubMed]

65. Lindsay, J.; Laurin, D.; Verreault, R.; Hébert, R.; Helliwell, B.; Hill, G.B.; McDowell, I. Risk Factors for Alzheimer's Disease: A Prospective Analysis from the Canadian Study of Health and Aging. *Am. J. Epidemiol.* **2002**, *156*, 445–453. [CrossRef] [PubMed]
66. Nikoletopoulou, V.; Lickert, H.; Frade, J.M.; Rencurel, C.; Giallonardo, P.; Zhang, L.; Bibel, M.; Barde, Y.A. Neurotrophin receptors TrkA and TrkC cause neuronal death whereas TrkB does not. *Nature* **2010**, *467*, 59–63. [CrossRef] [PubMed]
67. Pintilie, S.R. Neuroprotective effects of physical exercise: Implications in health and disease. *Rev. Med. Rom.* **2021**, *68*, 383–389. [CrossRef]
68. Pang, P.T.; Teng, H.K.; Zaitsev, E.; Woo, N.T.; Sakata, K.; Zhen, S.; Teng, K.K.; Yung, W.H.; Hempstead, B.L.; Lu, B. Cleavage of proBDNF by tPA/Plasmin Is Essential for Long-Term Hippocampal Plasticity. *Science* **2004**, *306*, 487–491. [CrossRef]
69. Bamji, S.X.; Rico, B.; Kimes, N.; Reichardt, L.F. BDNF mobilizes synaptic vesicles and enhances synapse formation by disrupting cadherin–β-catenin interactions. *J. Cell Biol.* **2006**, *174*, 289–299. [CrossRef]
70. Lu, B.; Chow, A. Neurotrophins and hippocampal synaptic transmission and plasticity. *J. Neurosci. Res.* **1999**, *58*, 76–87. [CrossRef]
71. Li, Y.; Yui, D.; Luikart, B.W.; McKay, R.M.; Li, Y.; Rubenstein, J.L.; Parada, L.F. Conditional ablation of brain-derived neurotrophic factor-TrkB signaling impairs striatal neuron development. *Proc. Natl. Acad. Sci. USA* **2012**, *109*, 15491–15496. [CrossRef]
72. Gauthier, L.R.; Charrin, B.C.; Borrell-Pagès, M.; Dompierre, J.P.; Rangone, H.; Cordelières, F.P.; De Mey, J.; MacDonald, M.E.; Leßmann, V.; Humbert, S.; et al. Huntingtin Controls Neurotrophic Support and Survival of Neurons by Enhancing BDNF Vesicular Transport along Microtubules. *Cell* **2004**, *118*, 127–138. [CrossRef]
73. Yamamoto, H.; Gurney, M.E. Human platelets contain brain-derived neurotrophic factor. *J. Neurosci.* **1990**, *10*, 3469–3478. [CrossRef] [PubMed]
74. Sarchielli, P.; Greco, L.; Stipa, A.; Floridi, A.; Gallai, V. Brain-derived neurotrophic factor in patients with multiple sclerosis. *J. Neuroimmunol.* **2002**, *132*, 180–188. [CrossRef]
75. Neves-Pereira, M.; Cheung, J.K.; Pasdar, A.; Zhang, F.; Breen, G.; Yates, P.; Sinclair, M.; Crombie, C.; Walker, N.; St Clair, D.M. BDNF gene is a risk factor for schizophrenia in a Scottish population. *Mol. Psychiatry* **2005**, *10*, 208–212. [CrossRef] [PubMed]
76. Neves-Pereira, M.; Mundo, E.; Muglia, P.; King, N.; Macciardi, F.; Kennedy, J.L. The Brain-Derived Neurotrophic Factor Gene Confers Susceptibility to Bipolar Disorder: Evidence from a Family-Based Association Study. *Am. J. Hum. Genet.* **2002**, *71*, 651–655. [CrossRef]
77. Tacke, C.D.A.J. Role of a Novel TrkB Agonist Antibody in Positively Modulating the Architecture and Synaptic Plasticity of Hippocampal Neurons in Health and Disease. 2021. Available online: https://publikationsserver.tu-braunschweig.de/receive/dbbs_mods_00069356 (accessed on 1 January 2020).
78. Katoh-Semba, R.; Takeuchi, I.K.; Semba, R.; Kato, K. Distribution of Brain-Derived Neurotrophic Factor in Rats and Its Changes with Development in the Brain. *J. Neurochem.* **1997**, *69*, 34–42. [CrossRef]
79. Araki, T. The effects of microglia- and astrocyte-derived factors on neurogenesis in health and disease. *Eur. J. Neurosci.* **2021**, *54*, 5880–5901. [CrossRef]
80. Eide, F.F.; Vining, E.R.; Eide, B.L.; Zang, K.; Wang, X.Y.; Reichardt, L.F. Naturally Occurring Truncated trkB Receptors Have Dominant Inhibitory Effects on Brain-Derived Neurotrophic Factor Signaling. *J. Neurosci.* **1996**, *16*, 3123–3129. [CrossRef]
81. Schinder, A.F.; Poo, M. The neurotrophin hypothesis for synaptic plasticity. *Trends Neurosci.* **2000**, *23*, 639–645. [CrossRef]
82. Ng, T.K.S.; Ho, C.S.H.; Tam, W.W.S.; Kua, E.H.; Ho, R.C.M. Decreased Serum Brain-Derived Neurotrophic Factor (BDNF) Levels in Patients with Alzheimer's Disease (AD): A Systematic Review and Meta-Analysis. *Int. J. Mol. Sci.* **2019**, *20*, 257. [CrossRef]
83. Hayek, L.E.; Khalifeh, M.; Zibara, V.; Assaad, R.A.; Emmanuel, N.; Karnib, N.; El-Ghandour, R.; Nasrallah, P.; Bilen, M.; Ibrahim, P.; et al. Lactate Mediates the Effects of Exercise on Learning and Memory through SIRT1-Dependent Activation of Hippocampal Brain-Derived Neurotrophic Factor (BDNF). *J. Neurosci.* **2019**, *39*, 2369–2382.
84. Cirulli, F.; Berry, A.; Chiarotti, F.; Alleva, E. Intrahippocampal administration of BDNF in adult rats affects short-term behavioral plasticity in the Morris water maze and performance in the elevated plus-maze. *Hippocampus* **2004**, *14*, 802–807. [CrossRef] [PubMed]
85. Bolton, M.M.; Pittman, A.J.; Lo, D.C. Brain-Derived Neurotrophic Factor Differentially Regulates Excitatory and Inhibitory Synaptic Transmission in Hippocampal Cultures. *J. Neurosci.* **2000**, *20*, 3221–3232. [CrossRef] [PubMed]
86. Schaaf, M.J.M.; Workel, J.O.; Lesscher, H.M.; Vreugdenhil, E.; Oitzl, M.S.; Ron de Kloet, E. Correlation between hippocampal BDNF mRNA expression and memory performance in senescent rats. *Brain Res.* **2001**, *915*, 227–233. [CrossRef]
87. Guerra-Crespo, M.; Ubieta, R.; Joseph-Bravo, P.; Charli, J.L.; Pérez-Martínez, L. BDNF increases the early expression of TRH mRNA in fetal TrkB+ hypothalamic neurons in primary culture. *Eur. J. Neurosci.* **2001**, *14*, 483–494. [CrossRef]
88. Marmigère, F.; Choby, C.; Rage, F.; Richard, S.; Tapia-Arancibia, L. Rapid Stimulatory Effects of Brain-Derived Neurotrophic Factor and Neurotrophin-3 on Somatostatin Release and Intracellular Calcium Rise in Primary Hypothalamic Cell Cultures. *Neuroendocrinology* **2001**, *74*, 43–54. [CrossRef]
89. Givalois, L.; Arancibia, S.; Alonso, G.; Tapia-Arancibia, L. Expression of Brain-Derived Neurotrophic Factor and Its Receptors in the Median Eminence Cells with Sensitivity to Stress. *Endocrinology* **2004**, *145*, 4737–4747. [CrossRef]
90. Crook, T.; Bartus, R.T.; Ferris, S.H.; Whitehouse, P.; Cohen, G.D.; Gershon, S. Age-associated memory impairment: Proposed diagnostic criteria and measures of clinical change—Report of a national institute of mental health work group. *Dev. Neuropsychol.* **1986**, *2*, 261–276. [CrossRef]
91. Hebb, D.O. *The Organization of Behavior: A Neuropsychological Theory*; Psychology Press: London, UK, 2005; 379p.

92. Thoenen, H. Neurotrophins and activity-dependent plasticity. In *Progress in Brain Research*; Neural Plasticity and Regeneration; Elsevier: Amsterdam, The Netherlands, 2000; Volume 128, pp. 183–191. Available online: http://www.sciencedirect.com/science/article/pii/S0079612300280163 (accessed on 12 January 2021).
93. Burke, S.N.; Barnes, C.A. Neural plasticity in the ageing brain. *Nat. Rev. Neurosci.* **2006**, *7*, 30–40. [CrossRef]
94. Barnes, C.A. Normal aging: Regionally specific changes in hippocampal synaptic transmission. *Trends Neurosci.* **1994**, *17*, 13–18. [CrossRef]
95. Gooney, M.; Messaoudi, E.; Maher, F.O.; Bramham, C.R.; Lynch, M.A. BDNF-induced LTP in dentate gyrus is impaired with age: Analysis of changes in cell signaling events. *Neurobiol. Aging* **2004**, *25*, 1323–1331. [CrossRef]
96. Rex, C.S.; Lauterborn, J.C.; Lin, C.Y.; Kramár, E.A.; Rogers, G.A.; Gall, C.M.; Lynch, G. Restoration of Long-Term Potentiation in Middle-Aged Hippocampus After Induction of Brain-Derived Neurotrophic Factor. *J. Neurophysiol.* **2006**, *96*, 677–685. [CrossRef] [PubMed]
97. Granger, R.; Deadwyler, S.; Davis, M.; Moskovitz, B.; Kessler, M.; Rogers, G.; Lynch, G. Facilitation of glutamate receptors reverses an age-associated memory impairment in rats. *Synapse* **1996**, *22*, 332–337. [CrossRef]
98. Hattiangady, B.; Rao, M.S.; Shetty, G.A.; Shetty, A.K. Brain-derived neurotrophic factor, phosphorylated cyclic AMP response element binding protein and neuropeptide Y decline as early as middle age in the dentate gyrus and CA1 and CA3 subfields of the hippocampus. *Exp. Neurol.* **2005**, *195*, 353–371. [CrossRef] [PubMed]
99. Lommatzsch, M.; Zingler, D.; Schuhbaeck, K.; Schloetcke, K.; Zingler, C.; Schuff-Werner, P.; Virchow, J.C. The impact of age, weight and gender on BDNF levels in human platelets and plasma. *Neurobiol. Aging* **2005**, *26*, 115–123. [CrossRef] [PubMed]
100. Mora, F.; Segovia, G.; del Arco, A. Aging, plasticity and environmental enrichment: Structural changes and neurotransmitter dynamics in several areas of the brain. *Brain Res. Rev.* **2007**, *55*, 78–88. [CrossRef] [PubMed]
101. Silhol, M.; Arancibia, S.; Maurice, T.; Tapia-Arancibia, L. Spatial memory training modifies the expression of brain-derived neurotrophic factor tyrosine kinase receptors in young and aged rats. *Neuroscience* **2007**, *146*, 962–973. [CrossRef] [PubMed]
102. Ferrer, I.; Marín, C.; Rey, M.J.; Ribalta, T.; Goutan, E.; Blanco, R.; Tolosa, E.; Martí, E. BDNF and Full-length and Truncated TrkB Expression in Alzheimer Disease. Implications in Therapeutic Strategies. *J. Neuropathol. Exp. Neurol.* **1999**, *58*, 729–739. [CrossRef]
103. Peng, S.; Garzon, D.J.; Marchese, M.; Klein, W.; Ginsberg, S.D.; Francis, B.M.; Mount, H.T.; Mufson, E.J.; Salehi, A.; Fahnestock, M. Decreased Brain-Derived Neurotrophic Factor Depends on Amyloid Aggregation State in Transgenic Mouse Models of Alzheimer's Disease. *J. Neurosci.* **2009**, *29*, 9321–9329. [CrossRef]
104. Selkoe, D.J. Amyloid β-Protein and the Genetics of Alzheimer's Disease. *J. Biol. Chem.* **1996**, *271*, 18295–18298. [CrossRef]
105. Wang, Z.H.; Xiang, J.; Liu, X.; Yu, S.P.; Manfredsson, F.P.; Sandoval, I.M.; Wu, S.; Wang, J.Z.; Ye, K. Deficiency in BDNF/TrkB Neurotrophic Activity Stimulates δ-Secretase by Upregulating C/EBPβ in Alzheimer's Disease. *Cell Rep.* **2019**, *28*, 655–669.e5. [CrossRef]
106. Rohe, M.; Synowitz, M.; Glass, R.; Paul, S.M.; Nykjaer, A.; Willnow, T.E. Brain-Derived Neurotrophic Factor Reduces Amyloidogenic Processing through Control of SORLA Gene Expression. *J. Neurosci.* **2009**, *29*, 15472–15478. [CrossRef] [PubMed]
107. Banerjee, M. Emphasizing roles of BDNF promoters and inducers in Alzheimer's disease for improving impaired cognition and memory. *J. Basic Clin. Physiol. Pharmacol.* **2022**. [CrossRef]
108. Matrone, C.; Ciotti, M.T.; Mercanti, D.; Marolda, R.; Calissano, P. NGF and BDNF signaling control amyloidogenic route and Aβ production in hippocampal neurons. *Proc. Natl. Acad. Sci. USA* **2008**, *105*, 13139–13144. [CrossRef] [PubMed]
109. Numakawa, T.; Odaka, H. Brain-Derived Neurotrophic Factor Signaling in the Pathophysiology of Alzheimer's Disease: Beneficial Effects of Flavonoids for Neuroprotection. *Int. J. Mol. Sci.* **2021**, *22*, 5719. [CrossRef] [PubMed]
110. Ginsberg, S.D.; Malek-Ahmadi, M.H.; Alldred, M.J.; Chen, Y.; Chen, K.; Chao, M.V.; Counts, S.E.; Mufson, E.J. Brain-derived neurotrophic factor (BDNF) and TrkB hippocampal gene expression are putative predictors of neuritic plaque and neurofibrillary tangle pathology. *Neurobiol. Dis.* **2019**, *132*, 104540. [CrossRef]
111. Lim, Y.Y. BDNF VAL66MET polymorphism and memory decline across the spectrum of Alzheimer's disease. *Genes Brain Behav.* **2021**, *20*, e12724. [CrossRef]
112. Kitiyanant, N.; Kitiyanant, Y.; Svendsen, C.N.; Thangnipon, W. BDNF-, IGF-1- and GDNF-Secreting Human Neural Progenitor Cells Rescue Amyloid β-Induced Toxicity in Cultured Rat Septal Neurons. *Neurochem. Res.* **2012**, *37*, 143–152. [CrossRef]
113. Arancibia, S.; Silhol, M.; Moulière, F.; Meffre, J.; Höllinger, I.; Maurice, T.; Tapia-Arancibia, L. Protective effect of BDNF against beta-amyloid induced neurotoxicity in vitro and in vivo in rats. *Neurobiol. Dis.* **2008**, *31*, 316–326. [CrossRef]
114. Wang, R.; Holsinger, R.M.D. Exercise-induced brain-derived neurotrophic factor expression: Therapeutic implications for Alzheimer's dementia. *Ageing Res. Rev.* **2018**, *48*, 109–121. [CrossRef]
115. Michalski, B.; Fahnestock, M. Pro-brain-derived neurotrophic factor is decreased in parietal cortex in Alzheimer's disease. *Mol. Brain Res.* **2003**, *111*, 148–154. [CrossRef]
116. Holsinger, R.M.D.; Schnarr, J.; Henry, P.; Castelo, V.T.; Fahnestock, M. Quantitation of BDNF mRNA in human parietal cortex by competitive reverse transcription-polymerase chain reaction: Decreased levels in Alzheimer's disease. *Mol. Brain Res.* **2000**, *76*, 347–354. [CrossRef]
117. Elahi, F.M.; Casaletto, K.B.; La Joie, R.; Walters, S.M.; Harvey, D.; Wolf, A.; Edwards, L.; Rivera-Contreras, W.; Karydas, A.; Cobigo, Y.; et al. Plasma Biomarkers of Astrocytic and Neuronal Dysfunction in Early- and Late-Onset Alzheimer's Disease. Alzheimers Dement. 24 December 2019. Available online: https://www.sciencedirect.com/science/article/pii/S1552526019353737 (accessed on 28 March 2022).

118. Ziegenhorn, A.A.; Schulte-Herbrüggen, O.; Danker-Hopfe, H.; Malbranc, M.; Hartung, H.D.; Anders, D.; Lang, U.E.; Steinhagen-Thiessen, E.; Schaub, R.T.; Hellweg, R. Serum neurotrophins—A study on the time course and influencing factors in a large old age sample. *Neurobiol. Aging* **2007**, *28*, 1436–1445. [CrossRef] [PubMed]
119. Laske, C.; Stransky, E.; Leyhe, T.; Eschweiler, G.W.; Wittorf, A.; Richartz, E.; Bartels, M.; Buchkremer, G.; Schott, K. Stage-dependent BDNF serum concentrations in Alzheimer's disease. *J. Neural Transm.* **2006**, *113*, 1217–1224. [CrossRef] [PubMed]
120. Elkouzi, A.; Vedam-Mai, V.; Eisinger, R.S.; Okun, M.S. Emerging therapies in Parkinson disease—Repurposed drugs and new approaches. *Nat. Rev. Neurol.* **2019**, *15*, 204–223. [CrossRef] [PubMed]
121. Parain, K.; Murer, M.G.; Yan, Q.; Faucheux, B.; Agid, Y.; Hirsch, E.; Raisman-Vozari, R. Reduced expression of brain-derived neurotrophic factor protein in Parkinson's disease substantia nigra. *Neuroreport* **1999**, *10*, 557–561. [CrossRef] [PubMed]
122. Huang, Y. Serum concentration and clinical significance of brain-derived neurotrophic factor in patients with Parkinson's disease or essential tremor. *J. Int. Med. Res.* **2018**, *46*, 1477–1485. [CrossRef]
123. Bruna, B.; Lobos, P.; Herrera-Molina, R.; Hidalgo, C.; Paula-Lima, A.; Adasme, T. The signaling pathways underlying BDNF-induced Nrf2 hippocampal nuclear translocation involve, R.O.S.; RyR-Mediated Ca^{2+} signals, ERK and PI3K. *Biochem. Biophys. Res. Commun.* **2018**, *505*, 201–207. [CrossRef]
124. Ryu, E.J.; Harding, H.P.; Angelastro, J.M.; Vitolo, O.V.; Ron, D.; Greene, L.A. Endoplasmic Reticulum Stress and the Unfolded Protein Response in Cellular Models of Parkinson's Disease. *J. Neurosci.* **2002**, *22*, 10690–10698. [CrossRef]
125. Weinstein, G.; Beiser, A.S.; Choi, S.H.; Preis, S.R.; Chen, T.C.; Vorgas, D.; Au, R.; Pikula, A.; Wolf, P.A.; DeStefano, A.L.; et al. Serum Brain-Derived Neurotrophic Factor and the Risk for Dementia: The Framingham Heart Study. *JAMA Neurol.* **2014**, *71*, 55–61. [CrossRef]
126. Lotharius, J.; Brundin, P. Pathogenesis of parkinson's disease: Dopamine, vesicles and α-synuclein. *Nat. Rev. Neurosci.* **2002**, *3*, 932–942. [CrossRef]
127. Miller, K.M. Synucleinopathy-associated pathogenesis in Parkinson's disease and the potential for brain-derived neurotrophic factor. *NPJ Park. Dis.* **2021**, *7*, 1–9. [CrossRef] [PubMed]
128. Kohno, R.; Sawada, H.; Kawamoto, Y.; Uemura, K.; Shibasaki, H.; Shimohama, S. BDNF is induced by wild-type α-synuclein but not by the two mutants, A30P or A53T, in glioma cell line. *Biochem. Biophys. Res. Commun.* **2004**, *318*, 113–118. [CrossRef]
129. Volpicelli-Daley, L.A.; Gamble, K.L.; Schultheiss, C.E.; Riddle, D.M.; West, A.B.; Lee, V.M.Y. Formation of α-synuclein Lewy neurite–like aggregates in axons impedes the transport of distinct endosomes. *Mol. Biol. Cell* **2014**, *25*, 4010–4023. [CrossRef] [PubMed]
130. Kang, S.S.; Zhang, Z.; Liu, X.; Manfredsson, F.P.; Benskey, M.J.; Cao, X.; Xu, J.; Sun, Y.E.; Ye, K. TrkB neurotrophic activities are blocked by α-synuclein, triggering dopaminergic cell death in Parkinson's disease. *Proc. Natl. Acad. Sci. USA* **2017**, *114*, 10773–10778. [CrossRef]
131. Sortwell, C.E. *BDNF* rs6265 Genotype Influences Outcomes of Pharmacotherapy and Subthalamic Nucleus Deep Brain Stimulation in Parkinson's Disease. *Neuromodul. Malden Mass.* **2021**. [CrossRef] [PubMed]
132. Jin, W. Regulation of BDNF-TrkB Signaling and Potential Therapeutic Strategies for Parkinson's Disease. *J. Clin. Med.* **2020**, *9*, 257. [CrossRef] [PubMed]
133. Palasz, E.; Wysocka, A.; Gasiorowska, A.; Chalimoniuk, M.; Niewiadomski, W.; Niewiadomska, G. BDNF as a Promising Therapeutic Agent in Parkinson's Disease. *Int. J. Mol. Sci.* **2020**, *21*, 1170. [CrossRef]
134. Costa, C.M.; de Oliveira, G.L.; Fonseca, A.C.S.; de Lana, R.C.; Polese, J.C.; Pernambuco, A.P. Levels of cortisol and neurotrophic factor brain-derived in Parkinson's disease. *Neurosci. Lett.* **2019**, *708*, 134359. [CrossRef]
135. Roy, A.; Mondal, B.; Banerjee, R.; Choudhury, S.; Chatterjee, K.; Dey, S.; Kumar, H. Do peripheral immune and neurotrophic markers correlate with motor severity of Parkinson's disease? *J. Neuroimmunol.* **2021**, *354*, 577545. [CrossRef]
136. Hernández-Vara, J.; Sáez-Francàs, N.; Lorenzo-Bosquet, C.; Corominas-Roso, M.; Cuberas-Borròs, G.; Lucas-Del Pozo, S.; Carter, S.; Armengol-Bellapart, M.; Castell-Conesa, J. BDNF levels and nigrostriatal degeneration in "drug naïve" Parkinson's disease patients. An "in vivo" study using I-123-FP-CIT SPECT. *Parkinsonism Relat. Disord.* **2020**, *78*, 31–35. [CrossRef]
137. Huang, Y.; Huang, C.; Yun, W. Peripheral BDNF/TrkB protein expression is decreased in Parkinson's disease but not in Essential tremor. *J. Clin. Neurosci.* **2019**, *63*, 176–181. [CrossRef] [PubMed]
138. Chang, E.; Wang, J. Brain-derived neurotrophic factor attenuates cognitive impairment and motor deficits in a mouse model of Parkinson's disease. *Brain Behav.* **2021**, *11*, e2251. [CrossRef]
139. Yoshida, T.; Ishikawa, M.; Iyo, M.; Hashimoto, K. Serum Levels of Mature Brain-Derived Neurotrophic Factor (BDNF) and Its Precursor proBDNF in Healthy Subjects. *Open Clin. Chem. J.* **2012**, *5*. Available online: https://benthamopen.com/ABSTRACT/TOCCHEMJ-5-7 (accessed on 7 January 2021). [CrossRef]
140. Hashimoto, K. Sigma-1 receptor chaperone and brain-derived neurotrophic factor: Emerging links between cardiovascular disease and depression. *Prog. Neurobiol.* **2013**, *100*, 15–29. [CrossRef] [PubMed]
141. Erickson, K.I.; Miller, D.L.; Roecklein, K.A. The Aging Hippocampus: Interactions between Exercise, Depression, and BDNF. *Neuroscientist* **2012**, *18*, 82–97. [CrossRef] [PubMed]
142. Oliff, H.S.; Berchtold, N.C.; Isackson, P.; Cotman, C.W. Exercise-induced regulation of brain-derived neurotrophic factor (BDNF) transcripts in the rat hippocampus. *Mol. Brain Res.* **1998**, *61*, 147–153. [CrossRef]
143. Mori, Y. Serum BDNF as a Potential Biomarker of Alzheimer's Disease: Verification Through Assessment of Serum, Cerebrospinal Fluid, and Medial Temporal Lobe Atrophy. *Front. Neurol.* **2021**, *12*, 511. [CrossRef]

144. Karantali, E. Serum BDNF Levels in Acute Stroke: A Systematic Review and Meta-Analysis. *Medicina* **2021**, *57*, 297. [CrossRef]
145. Nagahara, A.H.; Tuszynski, M.H. Potential therapeutic uses of BDNF in neurological and psychiatric disorders. *Nat. Rev. Drug Discov.* **2011**, *10*, 209–219. [CrossRef]
146. Kells, A.P.; Henry, R.A.; Connor, B. AAV–BDNF mediated attenuation of quinolinic acid-induced neuropathology and motor function impairment. *Gene Ther.* **2008**, *15*, 966–977. [CrossRef]
147. Ankeny, D.P.; McTigue, D.M.; Guan, Z.; Yan, Q.; Kinstler, O.; Stokes, B.T.; Jakeman, L.B. Pegylated Brain-Derived Neurotrophic Factor Shows Improved Distribution into the Spinal Cord and Stimulates Locomotor Activity and Morphological Changes after Injury. *Exp. Neurol.* **2001**, *170*, 85–100. [CrossRef] [PubMed]
148. Winkler, J.; Ramirez, G.A.; Kuhn, H.G.; Peterson, D.A.; Day-Lollini, P.A.; Stewart, G.R.; Tuszynski, M.H.; Gage, F.H.; Thal, L.J. Reversible schwann cell hyperplasia and sprouting of sensory and sympathetic neurites after intraventricular administration of nerve growth factor. *Ann. Neurol.* **1997**, *41*, 82–93. [CrossRef] [PubMed]
149. Mucke, L.; Masliah, E.; Yu, G.Q.; Mallory, M.; Rockenstein, E.M.; Tatsuno, G.; Hu, K.; Kholodenko, D.; Johnson-Wood, K.; McConlogue, L. High-Level Neuronal Expression of Aβ1–42 in Wild-Type Human Amyloid Protein Precursor Transgenic Mice: Synaptotoxicity without Plaque Formation. *J. Neurosci.* **2000**, *20*, 4050–4058. [CrossRef] [PubMed]
150. Nutt, J.G.; Burchiel, K.J.; Comella, C.L.; Jankovic, J.; Lang, A.E.; Laws, E.R.; Lozano, A.M.; Penn, R.D.; Simpson, R.K.; Stacy, M.; et al. Randomized, double-blind trial of glial cell line-derived neurotrophic factor (GDNF) in PD. *Neurology* **2003**, *60*, 69–73. [CrossRef] [PubMed]
151. Lang, A.E.; Gill, S.; Patel, N.K.; Lozano, A.; Nutt, J.G.; Penn, R.; Brooks, D.J.; Hotton, G.; Moro, E.; Heywood, P.; et al. Randomized controlled trial of intraputamenal glial cell line–derived neurotrophic factor infusion in Parkinson disease. *Ann. Neurol.* **2006**, *59*, 459–466. [CrossRef]
152. Hovland, D.N.; Boyd, R.B.; Butt, M.T.; Engelhardt, J.A.; Moxness, M.S.; Ma, M.H.; Emery, M.G.; Ernst, N.B.; Reed, R.P.; Zeller, J.R.; et al. Reprint: Six-Month Continuous Intraputamenal Infusion Toxicity Study of Recombinant Methionyl Human Glial Cell Line-Derived Neurotrophic Factor (r-metHuGDNF) in Rhesus Monkeys. *Toxicol. Pathol.* **2007**, *35*, 1013–1029. [CrossRef]
153. Gasmi, M.; Herzog, C.D.; Brandon, E.P.; Cunningham, J.J.; Ramirez, G.A.; Ketchum, E.T.; Bartus, R.T. Striatal Delivery of Neurturin by CERE-120, an AAV2 Vector for the Treatment of Dopaminergic Neuron Degeneration in Parkinson's Disease. *Mol. Ther.* **2007**, *15*, 62–68. [CrossRef]
154. Herzog, C.D.; Brown, L.; Gammon, D.; Kruegel, B.; Lin, R.; Wilson, A.; Bolton, A.; Printz, M.; Gasmi, M.; Bishop, K.M.; et al. Expression, bioactivity, and safety 1 year after adeno-associated viral vector type 2–mediated delivery of neurturin to the monkey nigrostriatal system support cere-120 for parkinson's disease. *Neurosurgery* **2009**, *64*, 602–613. [CrossRef]
155. Fukuchi, M.; Okuno, Y.; Nakayama, H.; Nakano, A.; Mori, H.; Mitazaki, S.; Nakano, Y.; Toume, K.; Jo, M.; Takasaki, I.; et al. Screening inducers of neuronal BDNF gene transcription using primary cortical cell cultures from BDNF-luciferase transgenic mice. *Sci. Rep.* **2019**, *9*, 11833. [CrossRef]
156. Jang, S.W.; Liu, X.; Yepes, M.; Shepherd, K.R.; Miller, G.W.; Liu, Y.; Wilson, W.D.; Xiao, G.; Blanchi, B.; Sun, Y.E.; et al. A selective TrkB agonist with potent neurotrophic activities by 7,8-dihydroxyflavone. *Proc. Natl. Acad. Sci. USA* **2010**, *107*, 2687–2692. [CrossRef]
157. Simmons, D.A.; Belichenko, N.P.; Yang, T.; Condon, C.; Monbureau, M.; Shamloo, M.; Jing, D.; Massa, S.M.; Longo, F.M. A Small Molecule TrkB Ligand Reduces Motor Impairment and Neuropathology in R6/2 and BACHD Mouse Models of Huntington's Disease. *J. Neurosci.* **2013**, *33*, 18712–18727. [CrossRef] [PubMed]
158. Diógenes, M.J.; Costenla, A.R.; Lopes, L.V.; Jerónimo-Santos, A.; Sousa, V.C.; Fontinha, B.M.; Ribeiro, J.A.; Sebastiao, A.M. Enhancement of LTP in Aged Rats is Dependent on Endogenous BDNF. *Neuropsychopharmacology* **2011**, *36*, 1823–1836. [CrossRef] [PubMed]
159. Grimes, M.L.; Zhou, J.; Beattie, E.C.; Yuen, E.C.; Hall, D.E.; Valletta, J.S.; Topp, K.S.; LaVail, J.H.; Bunnett, N.W.; Mobley, W.C. Endocytosis of Activated TrkA: Evidence that Nerve Growth Factor Induces Formation of Signaling Endosomes. *J. Neurosci.* **1996**, *16*, 7950–7964. [CrossRef] [PubMed]

11

ELEPHANT FOOT YAM

Deepak Sharma, Shivani Sharma, Radhika Negi, Dimple Tanwar and Sristi

Botanical Name: *Amorphophallus campanulatus*

Family: Araceae

Chromosome Number: 2n = 28

Introduction

Elephant foot yam, which is also referred as Suran and Zamikand is a potential tuber crop. Even though the crop has an underground stem and lasts for 8–9 months, it is treated as an annual crop. It is widely cultivated for its edible tubers, which are prized secondary crop throughout tropical Asia and a significant source of carbohydrates in India and Indonesia. Because of its eye-catching compound foliage and strikingly distinctive flowering and fruiting structures, it is frequently grown as an ornamental. It has become a commercial crop in India, and the area being cultivated there is growing quickly. Due to its great yield, ease of growing, and tolerance of shade, this lucrative stem tuber crop is gaining favour. Its tolerance to shade, ease of cultivation, high production, low incidence of insect-pests and diseases, consistent demand, and reasonably acceptable pricing, it is a lucrative and profitable stem tuber crop that is gaining popularity. This crop is traditionally grown in the Indian states of Andhra Pradesh, Gujarat, Maharashtra, and Kerala. It can be produced in Orissa under rain-fed conditions with protective irrigation, where the climate is very suited to its production. In Orissa, its wild variants can also be found. Due to their significant calcium oxalate content, wild plants tubers are extremely acidic and can irritate the mouth and throat. Typically, aridity is eliminated by boiling for an extended period of time. However, other

24

SPINACH

Deepak Sharma, Radhika Negi, Dimple Tanwar and Sristi

Scientific Name: *Spinacia oleracea* L.

Family: Chenopodiaceae

Chromosome Number: 2n = 12

Introduction

Spinach is known as "Vilayati palak", a major potherb or leafy vegetable, whose leaves and tender shoots are consumed fresh or processed and grown in USA and Europe. The shape of leaf is somewhat different from that of palak. The edible part is a compact rosette of leaves. It is liked by the common people as a cooked vegetable. The crop is more common in the hilly areas than other parts of India.

The word 'spinach' has been derived from a Spanish word Hispania, however, the Latin meaning of spinach is spiny fruit and oleracea means herbaceous garden herb. *Spinacia tetrandra* and *Spinacia turkistanica*, which have been described in Northwest India and Nepal, are the two diploid relatives of *Spinacia oleracea*. Although it is the most important potherb, its cultivation is restricted to smaller areas in the hills and parts of north as well as South India. It is also a well- suited vegetable in the United States of America, Canada and Europe. France, Germany, Italy, the United States and the Netherlands are the leading countries where it is grown on economic scale for shipment to distant markets and for canning as well as freezing purposes.

Chapter - 4

Global Warming and Effect on Insect Pests

Vijaya and Diksha Abrol

Abstract

Climate change and global warming are much more important to agriculture worldwide and are among the most discussed topics in today's era. Climatic parameters like increased temperature, rising CO_2 levels in the atmosphere, and changing precipitation patterns have significant impact on agricultural production and on insect pests of agricultural importance. Increased temperature can directly or indirectly influence the reproductive rate and survival rate of agricultural crop-pests. Elevated CO_2 can have its impact on the nutritional attributes of the crop plants which ultimately affect the insect pest feeding. Changes in the rainfall pattern can also directly influence the insect-pest population on the host crop plants. Introduction of an invasive insect pest species to a newer environment can also be benefitted due to the alterations in climatic factors. Ineffectiveness of bio-control agents may also be the impact of changed climatic factors like temperature or relative humidity. As a result, there is a great risk of economic production losses and a challenge to global food security in the long term. Climate change significantly affects pest population dynamics, adaptive management strategies are needed to deal with the changing status of insect-pests, therefore, several priorities have to be identified for conducting future research on the effects of climate change on insect pests of agricultural crop plants and for formulating their management strategies.

Keywords: Climate change, insect-pests, temperature, CO_2, management strategies.

Introduction

Global warming and climate change are frequently utilized terms but have unmistakable association. Global warming is the gradual increase in Earth's surface temperature since the pre-industrial era as a result of human activity, mostly the burning of fossil fuels, which contributes to rising levels of greenhouse gases that trap heat. Climate change, on the other hand, refers

Chapter - 14

Crop Protection Strategies: Integrated Pest Management

Authors

Diksha Abrol

Assistant Professor, Baddi University of Emerging Science and Technology, Baddi, Himachal Pradesh, India

Vijaya

Assistant Professor, Baddi University of Emerging Science and Technology, Baddi, Himachal Pradesh, India

Isha Sharma

Research Associate, Dr. Yashwant Singh Parmar University of Horticulture and Forestry, Nauni, Solan, Himachal Pradesh, India

Chapter - 5

Scope for Organic Farming in Himalayan Region

Vinaykumar Rachappanavar, Jeetendra Kumar Sharma, Himanshu Pandey and Kasi Indrakumar

Abstract

Organic farming organization is an integrated approach, where all aspects of farming systems are interlinked with each other and work for each other. A healthy biologically active soil is the source of crop nutrition, on-farm biodiversity controls pests, crop rotation and multiple cropping maintains the system's health and on-farm resource management with integration of cattle ensure productivity and sustainability. Organic management stresses on optimization of resource use and productivity, rather than maximization of productivity and over exploitation of resources on the cost of resources meant for future generations. According to the National Commission on farmers, "Organic farming should be the major tool for the second green revolution in the foot hills area. This region has high potential for organic cultivation as it is already under semi organic cultivation. Non availability of chemical fertilizers and pesticides, organic is not new for and is being followed from ancient terms.

Introduction

There were 57.8 mha of organic agricultural land in 2016, including in conversion areas. The regions with the largest areas of organic agricultural land are Oceania (27.3mha) and Europe (13.5mha). The countries with the most organic agriculture land are Australia (27.4 mha), Argentina (3 mha), and China (2.3 mha). Currently, 1.2 percent of the world agricultural land is organic. Organic farmland increased by 7.5 mha or 15 percent in 2016. This is mainly because 5 m additional hectares were reported from Australia (FiBL-IFOAM, 2012).

Western modern forming has spoiled agriculture in the country. An overuse of chemicals has made land acidic which means it needs even more water to produce which is costly (Narendra singh). India, although comes at

Genotyping of Seeds While Preserving Their Viability

Vinaykumar Rachappanavar, Arushi Padiyal, Jitender Kumar Sharma
Book Editor(s):Humira Sonah, Vinod Goyal, S.M. Shivaraj, Rupesh K. Deshmukh
First published: 01 April 2022

https://doi.org/10.1002/9781119745686.ch6

Summary

Rapid advancement in sequencing technologies facilitated the selection of crop genotypes with desired traits. Functional genomics in agriculture is to link the phenotype with genotype and predict the phenotype of progeny based on their genetic composition. For genetic mapping, and marker-assisted selection, rapid and quality DNA isolation is mandatory to accelerate the whole process. DNA extraction directly from seed without germination can save time and efforts. It is quite difficult to extract DNA from seed for genotyping because of the occurrence of complex molecules such as polysaccharides, proteins, lipids, secondary metabolites such as alkaloids, polyphenols, and tannins, which limits the use of seed as a DNA source. To solve this problem, several modified and crop-specific nondestructive seed DNA extraction protocols are standardized. The seed DNA-based genotyping-by-sequencing could become easy, fast, and less laborious. This can help to identify species and cultivars, varietal mixture, seed-borne diseases, and genetic modifications at seed level.

Chapter 8

Analytical Pipelines for the GBS Analysis

Vinaykumar Rachappanavar, Arushi Padiyal, Jitender Kumar Sharma, Narender Negi
Book Editor(s):Humira Sonah, Vinod Goyal, S.M. Shivaraj, Rupesh K. Deshmukh
First published: 01 April 2022

https://doi.org/10.1002/9781119745686.ch8

Summary

Technological advances in sequencing led to the development of next-generation sequencing (NGS) platforms. Over the period different sequencing platforms are developed based on different chemistry. These platforms have been widely used in the discovery and mapping of single-nucleotide polymorphism (SNPs) in crops. The combination of NGS and reduced representation methods of genotyping has made it possible to simultaneously perform SNPs discovery and genotyping in a single step even in different crop species genotyping-by-sequencing (GBS) is one such method that is comparatively simple, high-throughput, low-cost, attractive complexity reduction method for genotyping in both model and nonmodel species. It has been used in genomic selection (GS), gene mapping, and genome-wide associated studies (GWAS) in various crop species. The NGS generates a huge amount of sequence data. The accurate and efficient computational processing or variant calling in such data is the bottleneck in genomics. To overcome these problems several bioinformatics pipelines have been developed. At present, several GBS bioinformatics pipelines are available to process raw GBS sequence data to identify SNPs. In general, these bioinformatics pipelines are categorized into *de novo* and reference-based GBS data analysis. This chapter discusses the NGS platforms available for sequencing, NGS data analysis, GBS methodology, and the pipelines developed for the GBS data analysis.

POLYMER-DRUG CONJUGATES

Linker Chemistry, Protocols and Applications

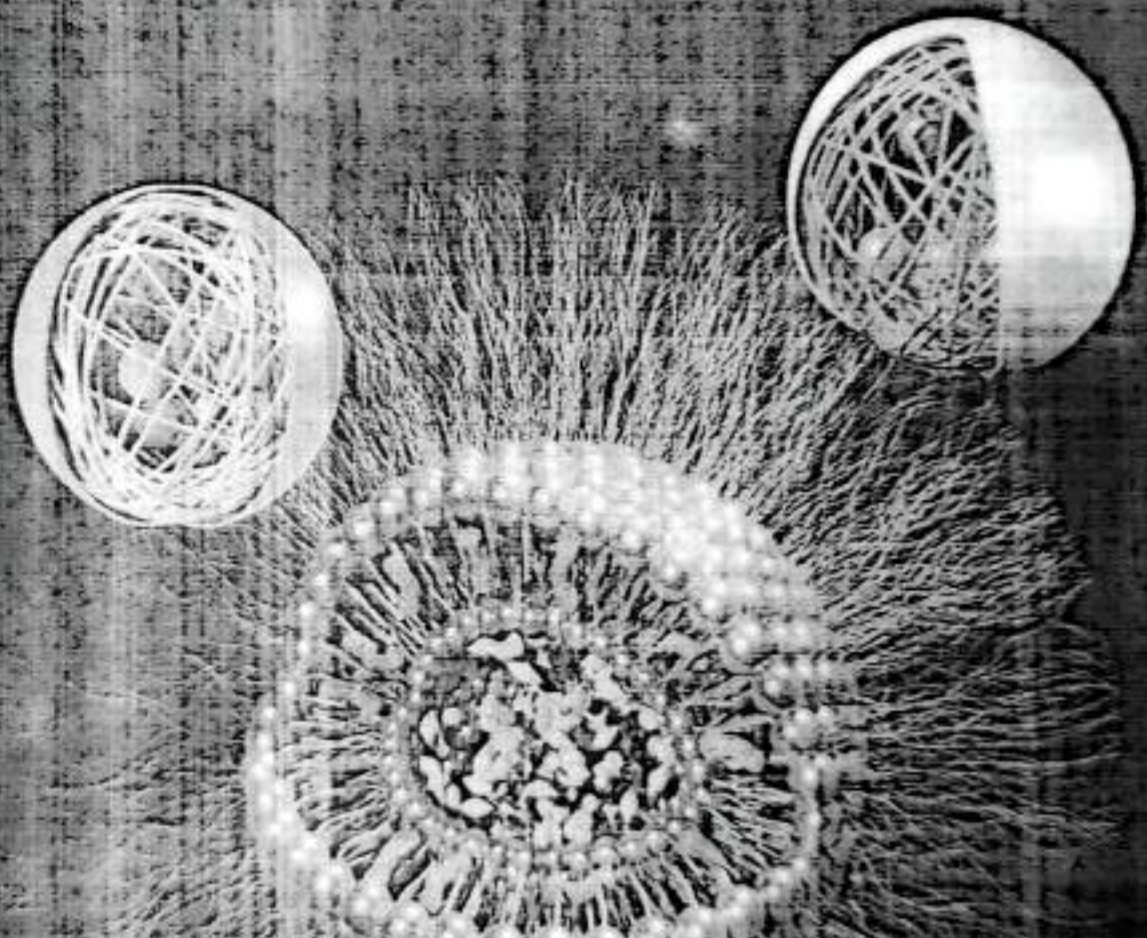

Edited by
Jitender Madan
Ashish Baldi
Monika Chaudhary
Neetu Chopra

AP

Chapter 9

Drug targeting to cancer cells through stimuli-responsive imine bonds: fascinating aspects of site specificity

Ravinesh Mishra, Pallavi Bassi, Roobal and Shivani
School of Pharmacy and Emerging Sciences, Baddi University of Emerging Sciences & Technology, Baddi, Himachal Pradesh, India

1. Introduction

Cancer is a condition when few of the body cells grow out of control and spread to the other body regions. In the millions of cells that make up the human body, cancer can develop anywhere in the body. Roughly 10 million deaths, or nearly one in six deaths, are caused by cancer in 2020, making it the top cause of death globally. Breast, lung, colon, rectum, and prostate cancers are the most prevalent types of cancer [1]. Human cells often divide (via a process known as cell division) to create new cells as the body requires them. New cells replace old ones when they die as a result of aging or damage. Occasionally, this systematic process fails, causing damage or aberrant cells to proliferate when they should not. Tumor, which is tissue mass, could develop from these cells. Tumors can be cancerous or not cancerous (benign). Cancerous tumor can move to the distant parts of the body to produce new tumor, invade neighboring tissues (a process called metastasis). The main reason why cancer patients die is because of widespread metastasis. As cancer progresses, tumor becomes extremely heterogenous, resulting in mixed population of cells with a variety of molecular characteristics and therapeutic responses. The main cause of the development of resistant phenotypes encouraged by a selection pressure after treatment administration is this heterogeneity, which can be observed both at geographical and temporal levels [2].

Chemotherapy continues to be the primary approach for treating cancer despite the major advancements in cancer treatment over the past few decades.

Polymer-Drug Conjugates. https://doi.org/10.1016/B978-0-323-91563-9.00004-7

Polymer-Drug Conjugates

Linker Chemistry, Protocols and Applications

Edited by

Jitender Madan
National Institute of Pharmaceutical Education and Research, Hyderabad, Telangana, India

Ashish Baldi
Pharma Innovation Lab, Department of Pharmaceutical Sciences and Technology, Maharaja Ranjit Singh Punjab Technical University, Bathinda, Punjab, India

Monika Chaudhary
GVM College of Pharmacy, Sonepat, Haryana, India

Neetu Chopra
Safety and Pharmacovigilance Specialist, Syneos Health, Gurgaon, Haryana, India

ACADEMIC PRESS

Academic Press is an imprint of Elsevier
125 London Wall, London EC2Y 5AS, United Kingdom
525 B Street, Suite 1650, San Diego, CA 92101, United States
50 Hampshire Street, 5th Floor, Cambridge, MA 02139, United States
The Boulevard, Langford Lane, Kidlington, Oxford OX5 1GB, United Kingdom

Notices

Knowledge and best practice in this field are constantly changing. As new research and experience broaden our understanding, changes in research methods, professional practices, or medical treatment may become necessary.

Practitioners and researchers must always rely on their own experience and knowledge in evaluating and using any information, methods, compounds, or experiments described herein. In using such information or methods they should be mindful of their own safety and the safety of others, including parties for whom they have a professional responsibility.

To the fullest extent of the law, neither the Publisher nor the authors, contributors, or editors, assume any liability for any injury and/or damage to persons or property as a matter of products liability, negligence or otherwise, or from any use or operation of any methods, products, instructions, or ideas contained in the material herein.

ISBN: 978-0-323-91663-93

Publisher: Stacy Masucci
Acquisitions Editor: Andre G. Wolff
Editorial Project Manager: Sam Young
Production Project Manager: Sajana Devasi P K
Cover Designer: Vicky Pearson Esser

Typeset by TNQ Technologies

biomedicines

MDPI

Brain-Derived Neurotropic Factor in Neurodegenerative Disorders

Abdallah Mohammad Ibrahim [1], Lalita Chauhan [2], Aditi Bhardwaj [3], Anjali Sharma [4], Faizana Fayaz [4], Bhumika Kumar [5], Mohamed Alhashmi [6], Noora AlHajri [7,*], Md Sabir Alam [8] and Faheem Hyder Pottoo [9,*]

1 Department of Fundamentals of Nursing, College of Nursing, Imam Abdul Rahman Bin Faisal University, Dammam 31441, Saudi Arabia; amsudqi@iau.edu.sa
2 School of Pharmacy & Emerging Sciences, Baddi University of Emerging Sciences & Technology, Baddi 173205, India; lalitachauhan704@gmail.com
3 Department of Pharmaceutical Sciences, Manav Bharti University, Vill. Laddo, Sultanpur (Kumarhatti), Solan 173229, India; aadipharma53@gmail.com
4 Department of Pharmaceutical Chemistry, Delhi Institute of Pharmaceutical Sciences and Research, Sector-3, MB Road, Pushp Vihar, New Delhi 110017, India; anjalish092@gmail.com (A.S.); faizanazargar@gmail.com (F.F.)
5 Department of Pharmaceutics, Delhi Institute of Pharmaceutical Sciences and Research, Sector-3, MB Road, Pushp Vihar, New Delhi 110017, India; bhumika201993@gmail.com
6 College of Medicine and Health Sciences, Khalifa University, Abu Dhabi P.O. Box 127788, United Arab Emirates; 100053507@ku.ac.ae
7 Department of Medicine, Sheikh Shakhbout Medical City (SSMC), Abu Dhabi P.O. Box 127788, United Arab Emirates
8 SGT College of Pharmacy, SGT University, Gurgaon 122505, India; mdsabiralam866@gmail.com
9 Department of Pharmacology, College of Clinical Pharmacy, Imam Abdul Rahman Bin Faisal University, P.O. Box 1982, Dammam 31441, Saudi Arabia
* Correspondence: nalhajri007@gmail.com (N.A.); fhpottoo@iau.edu.sa (F.H.P.)

check for updates

Citation: Ibrahim, A.M.; Chauhan, L.; Bhardwaj, A.; Sharma, A.; Fayaz, F.; Kumar, B.; Alhashmi, M.; AlHajri, N.; Alam, M.S.; Pottoo, F.H. Brain-Derived Neurotropic Factor in Neurodegenerative Disorders. Biomedicines 2022, 10, 1143. https://doi.org/10.3390/biomedicines10051143

Academic Editor: Marco Segatto

Received: 13 February 2022
Accepted: 30 April 2022
Published: 16 May 2022

Publisher's Note: MDPI stays neutral with regard to jurisdictional claims in published maps and institutional affiliations.

Abstract: Globally, neurodegenerative diseases cause a significant degree of disability and distress. Brain-derived neurotrophic factor (BDNF), primarily found in the brain, has a substantial role in the development and maintenance of various nerve roles and is associated with the family of neurotrophins, including neuronal growth factor (NGF), neurotrophin-3 (NT-3) and neurotrophin-4/5 (NT-4/5). BDNF has affinity with tropomyosin receptor kinase B (TrKB), which is found in the brain in large amounts and is expressed in several cells. Several studies have shown that decrease in BDNF causes an imbalance in neuronal functioning and survival. Moreover, BDNF has several important roles, such as improving synaptic plasticity and contributing to long-lasting memory formation. BDNF has been linked to the pathology of the most common neurodegenerative disorders, such as Alzheimer's and Parkinson's disease. This review aims to describe recent efforts to understand the connection between the level of BDNF and neurodegenerative diseases. Several studies have shown that a high level of BDNF is associated with a lower risk for developing a neurodegenerative disease.

Keywords: brain-derived neurotrophic factor; tropomyosin receptor kinase B; neurodegenerative disorders; Alzheimer's disease; Parkinson's disease

1. Introduction

In the central nervous system, brain-derived neurotrophic factor (BDNF) is a significant neurotrophic factor with a major role in neuronal cell differentiation, maturation [1], and survival [2]. BDNF also has a neuroprotective effect in several pathological conditions, including cerebral ischemia, glutamatergic stimulation, decreased blood glucose, and neurotoxicity [3]. It promotes and regulates neurogenesis [4] in several regions in the central nervous system, such as the cerebral cortex, olfactory system, mesencephalon, basal forebrain, hippocampus, hypothalamus, spinal cord, and the brainstem [1]. Low levels of BDNF protein have been shown to have a role in the development of neurodegenerative

Considerable interest has been focused recently on the application of magnetic separation technology to solve the various environmental problems. Magnetic carbon-nanocomposites have unique magnetic separation and potential adsorption for pollutants. Carbon matrices avoid the agglomeration of iron oxide nanoparticles and magnetic separation is a substitute to filtration or centrifugation as it avoids the loss of materials. Magnetic separation is quick and operative technique.Functionalized magnetic nanocomposites have distinct advantages over conventional materials due to their selective absorptivity, strong magnetic responsiveness, favorable water dispensability and benign biocompatibility. The semiconductor based carbon-nanocomposite have revealed high ability for the catalytic degradation of contaminants from aqueous segment. While, application of photocatalysis using heterogeneous semiconductor seems to be most pleasant mean and found to be inexpensive, non-toxic, broad absorption spectra with higher absorption coefficients and capability for multi-electron transfer.

Ajay Kumar Mishra (MSc, MPhil, PhD, CSci, FRSC) is currently working as 'Full Professor' for University of South Africa and also working as 'Adjunct Professor' at Jiangsu University, China. His research interests include nanomaterials & water research.
Deepak Pathania is Professor Cum Head Cum Dean, Central University of Jammu, Jammu and Kashmir.

978-620-0-45627-4

Green Nanocomposites

Pathania (Ed.), Mishra (Principal Editor)

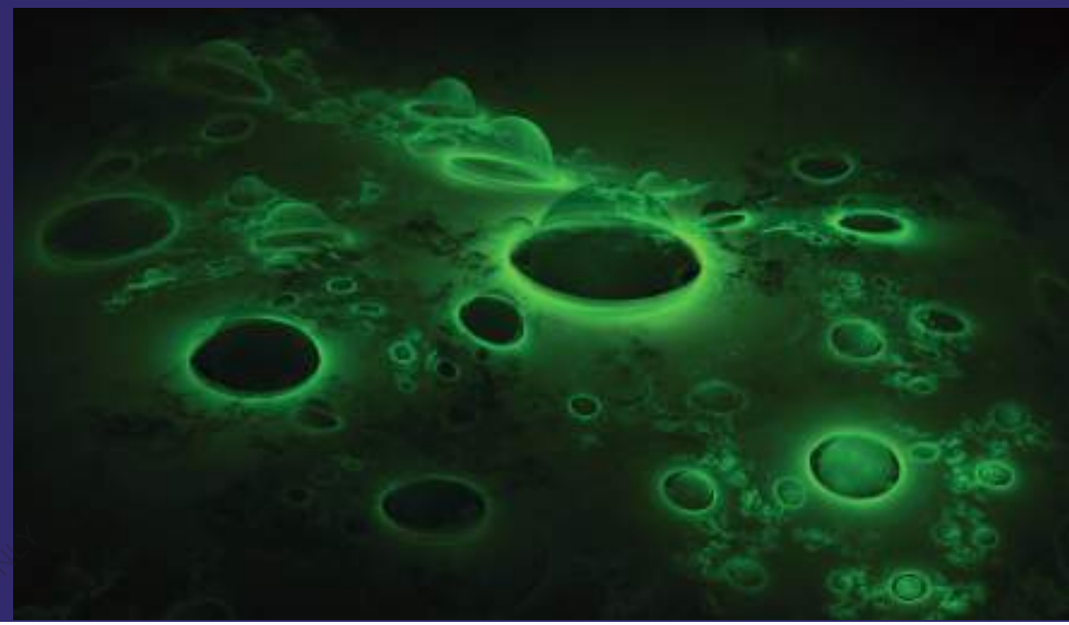

Ajay Kumar Mishra (Principal Editor)
Deepak Pathania (Ed.)

Green Nanocomposites

Advances and Applications in Environmentally Friendly Carbon Nanomaterials

LAP LAMBERT Academic Publishing

Deepak Pathania (Ed.)
Ajay Kumar Mishra (Principal Editor)

Green Nanocomposites

Deepak Pathania (Ed.)
Ajay Kumar Mishra (Principal Editor)

Green Nanocomposites

Advances and Applications in Environmentally Friendly Carbon Nanomaterials

LAP LAMBERT Academic Publishing

Imprint

Cover image: www.ingimage.com

Publisher:
LAP LAMBERT Academic Publishing
is a trademark of
International Book Market Service Ltd., member of OmniScriptum Publishing Group
17 Meldrum Street, Beau Bassin 71504, Mauritius

Printed at: see last page
ISBN: 978-620-0-45627-4

Table of content

Preface

Green nanocomposites are recognized as promising materials for subside environmental problems due to low-cost, potential adsorption and eco-friendliness. Green nanocomposites with the small size of fillers increase the interfacial area as compared to conventional composites. Green nanocomposites usually fabricated by combination of nanomaterials with either natural materials such as biopolymers or derived through green source, are the new trend in the remediation of environmental problems. A composite is a combination of two or more components in which one component acts as a reinforcing agent and other provides compatibility as a matrix. Green nanocomposites have advanced characteristics of excellent adsorption properties and biocompatibility. Green nanocomposites minimized the exposure of metal to the environment what enables special recognition owing to their advanced properties over conventional adsorbents. Various types of functionalized nanomaterials have been developed in the virtue of anchoring specific functional groups on their surface modification.

Current book consists of 10 chapters. Chapter 1 provide details about green nanocomposites and environmental protection- a critical overview and a vision for the future whereas chapter 2 is focused on use of carbon nanomaterials for removing heavy metals from water. Chapters 3 summarizes carbon nanomaterial as the emerging class: current and future perspective whereas Chapters 4 discusses the green synthesis and applications of carbon-based nanocomposites. Chapter 5 details about removal of arsenic and chromium using functional green composites and Chapter 6 summarizes on research and development of green nanocomposites from himalayan medicinal plants. Chapter 7 consists of

biodegradation and dye adsorption studies of gra-cl-poly(aam)-ztip organo-inorganic cation exchanger. Chapter 8 describes the nanoscale understanding and development of materials: a way forward to climate change mitigation and chapter 9 consists of carbon nanotubes: a tool for sustainable environment whereas Chapter 10 describes the details of synthesis methodology of green composite for heavy metal Cr remediation from wastewater.

The current book elucidates on the scientific advancements and recent scientific development in the field of green nanocomposites. Book also covers the research forays, techniques of production, opportunities, challenges and prospects in the field of green nanocomposites.

Book covers the broad aspect of nanocomposites, environmental science and wastewater remediation. Researchers involved in nanomaterials, environmental and water research will be major beneficiaries of the book. Book will be highly beneficial to the researchers who are working for their graduate and postgraduate degrees in this area. The book also provides a platform for all researchers as it covers a huge background for the recent literature and abbreviations.

AK Mishra, Deepak Pathania

Editors

Green Nanocomposites and Environmental Protection- A Vision for the future

Sukanchan Palit[1,2],

[1]Assistant Professor (Senior Scale), Department of Chemical Engineering, University of Petroleum and Energy Studies, Post-Office- Bidholi via Premnagar, Dehradun-248007, India

[2]43, Judges Bagan, Post-Office- Haridevpur, Kolkata-700082, India.

Email-sukanchan68@gmail.com, sukanchan92@gmail.com.

Abstract:

The world of technology and engineering science are today moving at a drastic and rapid pace surpassing one visionary frontier over another. In the similar manner, nanocomposites and nanotechnology are moving towards a path of newer scientific regeneration and vast scientific vision. In this paper the author with immense insight and lucidity delineates the recent scientific endeavor in the field of green nanocomposites and application of nanotechnology in environmental protection. Composite science and material science today stand in the midst of vast scientific ingenuity and deep scientific profundity. Recently, vast attention has been drawn to the use of bio-reinforced composites in automotive, construction, packaging and medical applications due to evergrowing concerns for environmental sustainability. Environmental sustainability and environmental protection is the utmost need of human scientific progress today. Green polymer nanocomposites show excellent scientific properties of combining the advantages of natural fillers and organic polymers. Plant fibre such as jute are found suitable to reinforce polymers. In this paper, the author delves deep into the hidden world of fibre reinforced composites especially jute

reinforced composites. Mankind's immense scientific prowess, man's vast scientific vision and the technological advancements will surely lead a long and visionary way in the true emancipation of nanoscience and nanotechnology. The author also elucidates on the scientific success and the recent scientific endeavor in the field of fibre reinforced composites and the vast world of nanotechnology. This paper also reviews current research forays, techniques of production, opportunities, challenges and prospects in the field of green nanocomposites.

1.0 Introduction:

The world of composite science and environmental engineering science are witnessing immense and drastic challenges as global science and engineering surges forward towards newer visionary directions. In the similar vein, nanotechnology and the vast domain of nanocomposites today stands in the midst of vision and scientific articulation. Technology and engineering science today have few answers to the ever-growing concerns of water purification, drinking water treatment and industrial wastewater treatment. In this chapter, the author deeply delves into the scientific intricacies and the vast scientific ingenuity in the applications of green nanocomposites in environmental remediation. The world of science and engineering should stand perplexed and mesmerized at the ever-growing concerns of loss of ecological biodiversity, environmental disasters and depletion of fossil fuel sources. The author in this paper elucidates the scientific success, the vast scientific imagination and the scientific needs of nanotechnology to human society. Material science, polymer science and composite science are today in the path of newer scientific regeneration and vast technological rejuvenation. The challenges and the vision of environmental protection, groundwater remediation and water purification are immense and groundbreaking today. The status of global environmental

engineering is immensely dismal today. This chapter will open up newer thoughts and newer scientific vision in the field of green nanocomposites in the field of environmental remediation in years to come.

2.0 The vision of the study:

Technology and engineering science are today in the midst of deep scientific divination and immense technological revelation. The vision of this study is to envision and reconstruct the vast world of environmental engineering, chemical process engineering and composite science. Human civilization and human scientific progress are facing immense challenges and vast scientific intricacies. Here is the need of a concerted effort and a targeted research and development initiative in the field of nanotechnology, nanomaterials, composite science and green chemistry. A deep discussion in environmental and energy sustainability is the other pillar of this chapter. Human scientific progress and immense prowess, the marvels of engineering innovations and the needs for green nanotechnology and green chemistry will surely a long and effective way in unraveling the scientific truth of green science and green engineering today. The vision and the challenges of scientific innovations and scientific instinct in the field of nanocomposites and green chemistry are surpassing every boundary. This chapter opens a new window of innovation in the field of environmental remediation and application of nanocomposites in environmental engineering science. Application of nanotechnology today is witnessing newer knowledge dimensions and newer future thoughts. The authors with immense scientific fortitude elucidate and elaborates the success of science, the tremendous scientific vision and ingenuity in the green nanocomposites applications in human society and human scientific progress. Water purification, drinking water treatment and industrial wastewater treatment are today in the threshold of a newer visionary era as global climate change

ushers in grave warnings for the future. This treatise opens up newer research trends and a newer avenue in the nano-science and nano-engineering applications in diverse areas of science and technology.

3.0 The need and the rationale of the study:

The importance of composite science and nanotechnology are immense in today's modern science and present-day human civilization. The need and the rationale behind this study are immense and thought-provoking as science and technology surges forward. The vast and visionary world of nanotechnology today is mesmerizing the scientific fabric of human civilization today. Today global warming and global climate change is urging the scientists and engineers to gear forward towards newer vision and newer scientific innovation. Human civilization and human scientific prowess and profundity today stands in the midst of vision and deep scientific fortitude. The need and the rationale of engineering science and technology are immense, prominent and thought provoking as civilization moves forward. Thus, the imminent need of nanotechnology, composite science, environmental engineering and chemical process engineering. Science and engineering of chemical process technology are huge colossus with a definite vision and sound profundity of its own. Thus, technology and engineering science of environmental remediation are the imminent needs of the human society as environmental disasters and the global climate change devastates the global scientific firmament. The definite vision of this chapter overcomes immense hurdles and scientific intricacies. Environmental engineering science and composite science are the two branches of science and engineering which needs to be re-envisioned and re-envisaged with the passage of scientific history and visionary timeframe. Technology of chemical process engineering and environmental engineering in today's global scenario in the similar vein needs to be

restructured as global vision of engineering and science are reframed. This chapter opens newer thoughts and newer future research trends in the domain of nanotechnology and material science in years to come.

4.0 What do you mean by nanocomposites?

Nanocomposite is a multiphase solid material where one of the phases has one, two or three dimensions of less than 100 nanometers(nm), or structures having veritably nano-scale repeat distances between the different phases that make up the material. The idea behind Nanocomposite is to use building blocks with dimensions in nanometer range to design and create new materials with unprecedented flexibility and improvement in their physical properties. In the broadest sense, this definition can include porous media, colloids, gels and copolymers, but is more usually taken to mean the solid combination of a bulk matrix and nano-dimensional phases differing in properties due to dissimilarities in structure and chemistry. Technological and scientific validation in the field of material science and nanotechnology, the profundity of engineering science and the futuristic vision of material science and technology will veritably open up newer dimensions of research trends in the field of composite science and nano-engineering. Today nanotechnology is veritably connected to human factor engineering and integrated water resource management. This chapter opens up newer vision and newer thoughts in the field of material science, water resource management and the vast world of nanotechnology and human factor engineering.

5.0 What do you mean by green nanocomposites?

Green nanocomposites encompasses bio-reinforced composites in automotive, construction, packaging and medical applications. A greater concern in the field of environmental sustainability is today envisioned and re-envisaged as green nanocomposites enters into a newer era in the field of

composite science and nanotechnology. Green polymer nanocomposites show unique properties of combining the advantages of natural fillers and organic polymers. Plant fibers are found to be suitable to reinforce polymers. Fiber reinforced composites is a branch of green nanocomposites. Plant fibers have relatively high strength and stiffness, low cost of acquisition, low density and produce low carbon dioxide emission. They are also biodegradable and immense tensile strength properties. Success of science and technology, the deep scientific profundity and technological divination are the needs of scientific research efforts in green chemistry and green nanotechnology today. This chapter deeply opens up newer research directions in the field of composite science and fiber science.

6.0 The vision and the scientific doctrine behind nanocomposites applications in environmental protection:

Today globally, the vision behind nanocomposites applications in environmental protection is vast and versatile. In the similar vein the application of nanomaterials and engineered nanomaterials in environmental remediation needs to be re-envisioned and restructured with the passage of scientific history and time. Technology and engineering science has practically no answers to heavy metal and arsenic contamination of drinking water. Here comes the vital importance of nanocomposites, composite applications and the vast world of nanotechnology. The challenges of water purification, drinking water treatment and industrial wastewater treatment are immense and ever-promising. Today science and engineering of environmental remediation are huge colossus with a definite vision and a definite steadfastness of its own. Human civilization's immense scientific prowess, girth and determination, the steadfastness of science and engineering and the vast

vision and intellect of environmental engineering science will veritably uncover the science of environmental sustainability. The scientific doctrine behind nanocomposites applications in environmental protection, ground water remediation and the needs of drinking water treatment are the forerunners towards a larger emancipation in the field of science and technology.

7.0 Environmental sustainability, environmental remediation and the vision for the future:

Sustainable development whether it is environmental, energy, social and economic are the needs of human civilization and human scientific progress. Environmental sustainability and environmental remediation are today two opposite sides of the visionary coin. Water purification, drinking water treatment and industrial wastewater treatment are the imminent needs of human civilization and human scientific progress. Global warming and global climate change are veritably challenging the vast scientific fabric of immense scientific might, vision and scientific perseverance. In this chapter the author pointedly focuses on the scientific necessities of composite science and nanotechnology in mitigating environmental disasters. The vision for the future is absolutely bright and promising. Heavy metal and arsenic groundwater and drinking water contamination are the scientific needs of modern science and present-day human civilization. Mankind's immense scientific prowess, grit and determination of engineering science and the needs of human society will veritably be the forerunners towards a greater realization and a greater emancipation of environmental engineering science. The visionary words of Dr Gro Harlem Brundtland, former Prime Minister of Norway on "sustainability" needs to be re-envisioned and relived as science and technology progresses forward. Today the challenges of technology and engineering science are immense

and thought provoking. The author in this chapter targets the scientific ingenuity and the scientific acuity behind nanotechnology applications in diverse areas of science and engineering. Here the contribution of composite science and material science also assumes immense importance. The futuristic vision of material science, the vast emancipation of nanotechnology and the scientific needs of human society will surely be the forerunners towards a greater scientific understanding and a greater scientific knowledge in the field of environmental engineering science. In the similar vein, chemical process engineering is an ever-growing avenue of science and engineering. In many perspectives today, chemical process engineering and environmental sustainability are two opposite sides of the visionary coin. This chapter, with immense scientific truth and conscience opens up newer windows of innovation in the science of sustainability.

8.0 Technological advances in green nanocomposites and environmental protection:

Technological advances in the domain of green nanocomposites and environmental protection are witnessing drastic and visionary challenges. Green engineering, green chemistry and green nanotechnology are today in the path of newer scientific regeneration. In this treatise, the author elucidates in minute details the vast scientific success, the futuristic vision and the immense scientific ingenuity in the applications of nanocomposites in environmental protection. The challenges, the vision and the targets of environmental engineering science and chemical process engineering are in the avenues of newer beginning and a newer scientific understanding. This treatise will surely give a broad overview of the needs of environmental sustainability and environmental remediation towards the futuristic vision of science and engineering. The challenges, the scientific vision and the targets of nanocomposite applications in environmental engineering science

are immense, inspiring and thought provoking. In this treatise, the author deeply elucidates the scientific success, the scientific provenance and the scientific ingenuity in nanotechnology and composite science applications in environmental remediation. The success of science and engineering in environmental protection are deeply related in this chapter. The needs of science of sustainability in environmental science are the other pillars of this chapter.

Palit et al.(2018)[1] discussed with cogent insight the application of nanocomposites and the wide vision of membrane science. Membrane science and environmental engineering are today scientifically linked with each other by an unsevered umbilical cord.[1] The visionary world of environmental engineering science and chemical process engineering is undergoing drastic and rapid changes. The objective of this research work is to unfold the wide domain of the application of nanocomposites in environmental engineering science and its relevant applications in membrane science and technology. Grave environmental engineering concerns, unmitigated environmental calamities and immense industrial pollution has urged the scientific domain to move towards newer scientific techniques and innovations.[1] The need and the rationale of this study are immense, arduous and far-reaching. Human mankind's immense scientific redeeming and re-envisioning are in the process of newer scientific rejuvenation. Nanocomposites and the vast domain of nanotechnology are the necessities of scientific research pursuit globally today.[1] The authors in this chapter discussed with vast insight fiber-reinforced composites, its engineering applications, medical applications, and a survey of the applications of nanocomposites. The authors also deeply comprehended the recent scientific research pursuit in the field of membrane science and its visionary future. The application of nanotechnology in water pollution control is the utmost need of the hour today. This chapter will surely open

up newer thoughts and newer vision in the field of both environmental engineering and nanotechnology in decades to come.[1]

Ghanghas et al.(2018)[2] discussed with lucidity polymer nanocomposites as nanoadsorbents for environmental remediation. The authors discussed with immense insight advanced processes in nanomaterial science.[2] This chapter also opens up newer discussion in the field of polymer nanocomposites and polymer based nanoadsorbents. A deep discussion on the preparation of polymer-based nanoadsorbents stands as a major pillar of this treatise. Nanoparticles with a size of approximately 1-100 nm have a significant impact in many scientific arenas, including chemistry, electronics, medicine, biology, physics, materials science and vast areas of engineering.[2] The physical and chemical properties of NPs are directly related to their intrinsic compositions, apparent sizes, and extrinsic structures. Technology, engineering and science of nanoparticles are today moving towards definite scientific directions. The authors also discussed in details applications of polymer-based nanoadsorbents.[2] The chapter also discusses magnetic nanocomposites and multi-functional nanocomposites.[2] Environmental remediation and a discussion on applications of nanocomposites in environmental protection is done in minute details. Magnetic polymer nanocomposites are of immense interest today because of the combination of magnetic properties, stability and biocompatibility. There are three types of magnetic nanocomposites: 1)core-shell inorganic nanocomposites, 2)self-assembled nanocomposites and 3)organic-inorganic nanocomposites. [2] This scientific research pursuit will lead a long and visionary way in the true emancipation of composite science and material science today.

Karim et al.(2018)[3] discussed with cogent insight nanocomposite membranes for heavy metal removal from wastewater. The continuous

exposure to heavy metals such as lead, mercury and arsenic has resulted in alarming threats to human health and the human eco-system.[3] The conventionally used chemical precipitation, ion-exchange and electrochemical deposition processes suffer from immense limitations such as energy intensive, excessive toxic sludge production which requires secondary treatment as well as inefficiency to meet environmental regulations and stringent restrictions. Human scientific endeavor's immense prowess, girth and determination and the futuristic vision of the science of environmental protection will be the true forerunners towards proper realization of science and engineering applications today.[3]

9.0 Significant scientific endeavor in the field of green nanocomposites:

Green nanocomposites are veritably the need of science and technology today. Stringent environmental regulations have urged the scientific domain to gear forward towards smart materials and green materials. Green chemistry and green engineering are the scientific needs of human civilization today. The scientific research pursuit in green nanocomposites, green materials and green nanotechnology and its vast scientific rigor are the imminent needs of human civilization today. Provision of basic human needs such as water, food, shelter and education are at deep peril in many nations around the world. Here comes the immediate need a deep deliberation in the field of nanocomposites. The author delves deep into the significant scientific endeavor in the field of green nanocomposites.

Adeosun et al.(2012)[4] deeply discussed with lucid and cogent insight green polymer nanocomposites. In recent years, attention has been drawn to the use of bio-reinforced composites in automotive, construction, packaging and medical applications due to evergrowing concerns for environmental and energy sustainability.[4] Human scientific rigor's

immense prowess, the scientific grit and determination of environmental engineering science and the futuristic vision of nanotechnology will go a long and visionary way in the true realization of composite science and nano-composites today.[4] In modern science today, environmental remediation and nanotechnology are two opposite sides of the visionary coin. Green polymer nanocomposites show promising properties of combining the advantages of natural fillers and organic polymers. The scientific vision and the vast scientific ingenuity in the field of green nanocomposites applications in human society and modern science are immense and immensely thought-provoking.[4] Green chemistry and green nanotechnology are the marvels of science and technology globally today. The authors in this paper discussed with immense insight the importance of green nanotechnology and green nanocomposites to human scientific progress and the advancement of science and engineering.[4] Green engineering is the other side of the visionary coin. The authors discussed with immense zeal and lucidity green polymers, thermoplastic starch based composites, poly-lactic based composites, cellulose based composites, plant oil based composites, polymer-polymer blends based composites, and other biopolymer based composites.[4] The futuristic vision of nanotechnology and composite science, the deep ardor of science and engineering of material science and the veritable needs of human society will surely lead a long and visionary way in the true realization of environmental sustainability and environmental remediation today. Scientific and academic rigor in the field of composite science, material science and polymer technology are today in the path of newer scientific regeneration. The authors in this paper also describes with vast vision and insight nanocomposites processing methods.[4] The prospects and applications associated with nanotechnology and composite applications to human scientific progress are deeply dealt with in this paper. Natural fiber-

reinforced composites using biodegradable polymer as an effective matrix are considered as most promising environmentally friendly material. Here comes the pivotal importance of composite science and nanotechnology. This paper opens up newer thoughts, newer research trends and newer vision in the domain of nanotechnology applications and deeper emancipation of science and engineering today.[4]

Modi et al.(2014)[5] discussed with vast scientific insight and conscience green polymer nanocomposites and their applications. Success of research endeavor in the field of green engineering and environmental protection are highly challenged and veritably stressed.[5] Through this paper, bio-reinforced composites in automotive, construction, packaging, and medical applications are discussed and a window of innovation has ushered in the field of nanotechnology and green nano-composites. The present paper deeply with insight elucidates on green polymer nanocomposites and the application of bio-reinforced composites in automotive, construction, packaging and medical applications due to ever-growing concerns for environmental sustainability.[5] Sustainable development, whether it is energy, environmental, social or economic is the utmost need of the hour. The authors also described on the unique properties of combining the advantages of natural fillers and organic polymers.[5] Plant fibers are found to be extremely suitable to reinforce polymers and the vast domain of fiber-reinforced composites are today in the path of newer scientific regeneration and immense scientific ingenuity. This paper reviews scientific efforts, techniques of production, trends and vast prospects in the field of green polymer nanocomposites. Addition of nanoparticles to base polymers results in improved properties that make them useful in automotive, construction and the vast area of medical science and biomedical engineering. Properties which are immensely promising are mechanical properties (eg- strength, elastic modulus, and

dimensional stability).[5] Nanocomposite materials consisting of polymeric matrix and nano-scale particles which have offered a great opportunity in thermoplastic and rubber industry to make new products and applications with enhanced and unique properties. Human mankind's immense scientific regeneration and ardor, the futuristic vision of nanotechnology and composite science will all lead a long and visionary way in the true realization of environmental sustainability.[5] The world of challenges and the vast and definite vision in the field of nanocomposites will be the future forerunners of greater scientific emancipation in environmental engineering science today. This paper is a veritable eye-opener towards that vision.[5]

Awad et al.(2015)[6] discussed and described with cogent insight and scientific far-sightedness green synthesis, characterization, and anti-bacterial activity of silver/ polystyrene nanocomposite. Technological and scientific validation and ardor are the pillars of scientific pursuit in green nanocomposites, green chemistry and the holistic domain of green nanotechnology.[6] A novel, nontoxic, simple, cost-effective and eco-friendly technique was used to synthesize green silver nanoparticles.[6] The nanomaterials can be synthesized by different techniques including chemical, physical and biological methods. The development of new chemical and physical methods has veritably resulted in environmental contamination since the chemical procedures involved in the synthesis of nanomaterials have resulted in generation of hazardous materials.[6] Today, nanotechnology, nanomaterials and engineered nanomaterials applications are highly challenged as science and technology surges forward.[6] Technological and engineering prowess, the vast scientific ingenuity and the futuristic vision of nanotechnology will all lead a long and visionary way in the true realization of almost every branch of science and technology. Nanotechnology today globally is integrated with every branch of science and engineering.[6] Green nanotechnology is the need of

human scientific progress and that includes safe, clean, eco-friendly and non-toxic methods of nanoparticle synthesis, without the use of high pressure, energy, temperature, and toxic chemicals.[6] The biological methods include synthesis of nanomaterials from the extracts of plant, bacterial, fungal species and so forth. Nanoparticles of silver have been veritably found to exhibit antibacterial activity and the investigation of this phenomenon has gained immense importance due to the increase of bacterial resistance to antibiotics, caused by their overuse.[6] Recently materials have been developed (mainly textiles) containing silver nanoparticles, which exhibit very interesting anti-microbial property. The idea of the present study was the green synthesis of silver nanoparticles by chemical reduction of silver nitrate using orange peel extract as a reducing agent, and the preparation of silver nanoparticles/polystyrene nanocomposite film. The authors in this treatise unfolds the immense scientific necessity and the scientific success in the field of environmental engineering aspects of green nanotechnology.[6]

Tsujimoto et al.(2015)[7] discussed with immense foresight and scientific conscience green nanocomposites from renewable plant oils and polyhedral oligomeric silsesquioxanes. Green nanocomposites based on renewable plant oils and polyhedral oligomeric silsesquioxanes have been developed.[7] Technology and engineering science of nano-science and nanotechnology are witnessing immense challenge, the vast scientific vision and deep scientific profundity.[7] Recently, there has been an immense scientific interest in organic-inorganic nanocomposites as next generation smart materials because of their high potentials to realize novel properties. Polyhedral oligomeric silsesquioxanes consist of inorganic framework made from a proportion of silicon and oxygen.[7] Octahedral derivatives are the most representative ones of this family.[7] The acid-catalyzed curing of epoxidized plant oil and oxirane-containing POSS

produced the transparent nanocomposites, in which the organic and inorganic components components were linked by covalent bonds. The success of science and engineering, the futuristic vision of nano-composites and the scientific needs of human society will be the veritable forerunners towards a newer visionary era in the field of nanotechnology. This paper opens up newer thoughts and newer vision in the field of nanotechnology and nanocomposites with the sole purpose of furtherance of science and engineering.[7]

Uyama et al.(2003)[8] deeply discussed with lucid and cogent insight green nanocomposites from renewable sources which are plant oil-clay hybrid materials. Technological and scientific validation and deep scientific insight are the necessities of innovation in the field of green nanocomposites today. Worldwide potential demands for replacing petroleum-derived raw materials with renewable plant-based ones in production of valuable polymeric materials are quite significant in the present day social and environmental landscape.[8] Therefore using inexpensive renewable resources have greatly attracted the attention of many scientists and researchers around the world. Among them natural oils are expected to be an ideal alternative chemical feedstock since oils, derived from both plant and animal sources are found in immense abundance throughout the world. Triglyceride oils have been extensively used for various applications such as coatings, inks and agrochemicals.[8] These oil based polymeric materials, however, do not show properties of rigidity and strength required for structural applications by themselves. Recently, there has been immense interest in organic-inorganic nanocomposites due to their unexpected hybrid properties derived from the unique combination of their individual properties. [8] This study deals with synthesis of green nanocomposites consisting of the abundant natural resources, plant oils and clay. An epoxidized triglyceride oil was subjected

to intercalation into an organically modified clay, followed by an acid-catalyzed curing of the epoxy- containing triglyceride leading to the production of a new class of biodegradable nanocomposites.[8] This is obtained from inexpensive renewable resources. Technological prowess and ardor, the world of scientific validation and the futuristic vision of nanocomposites will today lead a long and visionary way in the true realization of nanotechnology applications and environmental sustainability emancipation. Thus, this paper explores newer avenues and newer vision in the field of green nanocomposites in years to come.[8]

Pandey et al. (2005) [9] discussed with immense scientific far-sightedness green nanocomposites from renewable resources and the effect of plasticizer on the structure and material properties of clay – filled starch. Nanocomposites of starch were prepared via different addition sequences of plasticizer and clay by the solution method.[9] The extent of dispersion of the filler was evaluated by X-ray diffractometry (WAXD) in the resulting composites.[9] Thermal stability, mechanical properties, and water absorption studies were conducted in minute details to measure the mechanical properties whereas FT-IR spectroscopy was used to study the structure of composites. The sequence of addition of components (starch/plasticizer/ clay) had a significant effect on the nature of composites formed and accordingly properties were altered.[9] In order to develop an environmentally friendly material, efforts are being pursued to solve problems generated by plastic waste, particularly one-time-use materials. Technological validation and deep scientific motivation need to be enshrined and envisioned in the field of green nanocomposites with the passage of time. Most of the research attention should be targeted towards petro-based commodity plastics and biopolymers. The science of biopolymers is in a latent stage and needs to be developed in a rapid and useful manner. Biopolymers have been considered as most promising

materials for this purpose as they may form a cost-effective end-product. The authors in this paper discussed in minute details the preparation of nanocomposites, characterization and measurements, and a deep result and discussion on structure of nanocomposites. The vision and the challenges of applications of green nanocomposites and the futuristic vision of biopolymers are strongly deliberated in details in this paper.[9]

Palit et al.(2017)[10] discussed with immense scientific far-sightedness biopolymers and environmental perspectives. Environmental engineering science is today progressing at a rapid pace surpassing one visionary boundary over another.[10] This chapter opens up new futuristic research trends in the environmental applications of biopolymers. The authors delineate the vast intricacies of the application of biopolymers, its chemistry and the science of environmental sustainability. This chapter discusses the difference between synthetic polymers and biopolymers, recent scientific advances in biopolymers, and the recent scientific advances in the vast domain of biotechnology.[10] The authors also discussed in deep details recent scientific research pursuit in the field of biocomposites and bioplastics. The other areas of this research endeavor are the domain of green chemistry, the scientific success of energy and environmental sustainability and the deep scientific cognizance. A deep scientific introspection in the field of biopolymers, polymer science and environmental remediation are deliberated in deep details in this chapter.[10]

Green nanocomposites are today in the path of newer scientific rejuvenation. Water science and technology needs to be re-envisioned and re-envisaged with the progress and march of scientific history and time. In this entire chapter, the author deeply delves into the scientific rejuvenation, the deep scientific ingenuity and the profundity behind polymer science

and nanotechnology applications in environmental protection. In the similar vein and with a deep scientific conscience, the author relates the scientific and engineering advancements in the field of composite science and materials technology in modern science and present-day human civilization.

10.0 Significant scientific research pursuit in the field of nano-science and nanotechnology:

Nano-science and nanotechnology are changing the vast scientific landscape globally today. Human society and human scientific research pursuit stand in the midst of deep crisis as water shortage, global warming, depletion of fossil fuel resources are changing the face of human civilization. The global water crisis today stands never ending. In this section the author deeply pronounces the needs of engineering science and technology in confronting global environmental issues. Thus, nanotechnology and nanofiltration are the needs of the hour.

Woodrow Wilson International Centre for Scholars Report (2009) [11] discussed with immense scientific conscience next generation nanotechnology. This report discussed in minute details the future of nanotechnology, existing oversight and next-generation nanotechnology, and the future of oversight. Technological vision and motivation of engineering science are the pillars of scientific innovation in nanotechnology and nano-engineering today.[11] Since 1980, the capability of the federal agencies responsible for environmental health, environmental regulations and environmental safety has severely eroded.[11] This paper delineates some of the challenges, focusing on next generation nanotechnologies and also suggests changes that could revitalizes and invigorates these health and safety agencies. Nanotechnology is a revolutionary domain of science and engineering today. Nanotechnology is

today still a new concept in many countries in the developing and the developed world.[11] Oversight of new technologies and its visionary impact in this century will occur in a context characterized by rapid scientific strides, accelerated application of science and frequent product changes. The pillars of nanotechnology are today nanofiltration, water resource management, industrial pollution control and the science of sustainability. [11] This report opens up newer thoughts and newer visionary future trends in the field of nanotechnology applications today. This is an United States of America Federal Government Report and deeply analyses the scientific success, the scientific philosophy and the vast scientific ingenuity in the field of nanotechnology applications in every branch of science and engineering. The other highlights of this paper are the novel characteristics and application of nanomaterials in human society and its environmental and health risks. Scientific sagacity, deep scientific cognizance and the futuristic vision of environmental engineering stands as prerogatives towards the vision of science and engineering in nanomaterials applications today.[11] This report stands as a watershed text in the field of nanotechnology applications and its vast scientific emancipation in the global scientific landscape today.[11]

European Commission Report (2011) [12] discussed and described in minute details successful European Nanotechnology research. Nanotechnology is a frontier science and engineering in Europe and around the world, working at the scale of individual molecules. The authors of this report deeply elucidate the application of nanotechnology in energy and environment, electronics and information and communication technology, industrial applications, textiles, nanomaterials and nanomedicine areas. [12] The environmental and human safety issues are deeply deliberated in minute details in this report. The big issue today is that nanotechnology is not an enabling technology, or merely a method, or a process or a means of

controlling matter at the atomic level. Technology and engineering today has few answers to the scientific intricacies of nanotechnology applications in human society.[12] Here comes a deep scientific understanding and a deep scientific introspection. The main target of this report are the areas of energy and environmental sustainability and a deep scientific redeeming of the needs of nanotechnology applications in sustainable development of human civilization.[12]

Nanotechnology today is in the path of newer scientific regeneration. It is not a latent area yet loots of discoveries needs to be done. Human mankind's immense scientific grit and determination, the vision and the challenges of environmental engineering will surely lead a long and visionary way in true realization of the science of sustainability and nanotechnology.

11.0 Significant scientific research pursuit in the field of fiber-reinforced composites:

Fiber reinforced composites and its applications are changing the face of human scientific progress and the scientific profundity of human civilization today. Mankind's immense scientific prowess and vision, the scientific introspection and articulation in the field of fiber reinforced composites and biopolymers are discussed with immense insight in this section. Engineering science and technology are really challenging the vast scientific landscape of environmental remediation and environmental engineering today. Thus, the need of a strong civil society initiative and a vibrant research and development initiative in the field of bio-composites, fiber-reinforced composites and green nanotechnology. The significant scientific developments are discussed in this section.

Cheung et al.(2009)[13] deeply deliberated in minute details natural fiber-reinforced composites for bioengineering and environmental

engineering applications. Technological and scientific validation, introspection and ardor are the pillars of scientific research pursuit in the field of fiber-reinforced composites today. Conservation of forests, the vision of environmental and energy sustainability and the optimal utilization of agricultural resources are the scientific needs of modern science today. The authors in this treatise deeply discussed natural fibers, plant-based fibers and animal-based fibers with a sole aim towards furtherance of science and engineering.[13] Research on biodegradable polymers and polymeric composites can contribute for green and safe environment. In this paper, a comprehensive review is done on different kinds of natural fiber composites.[13] Their immense potential in future development of different kinds of engineering and domestic products are discussed with vast scientific insight in this paper. Since the past few decades, scientific and engineering interest has dramatically shifted from traditional monolithic materials to fibre-reinforced polymer-based materials due to their unique advantage of high strength to weight ratio, non-corrosive property, and high fracture toughness. These composite materials comprised of high strength fibers such as carbon, glass and aramid, and low strength polymeric matrix and now have dominated the aerospace, leisure, automotive, construction and sporting industries.[13] The vision and the challenge of composite science and engineering and the futuristic vision of fiber-reinforced composites are enumerated in minute details in this paper. The authors discussed in details the environmental concern, the bio-engineering concern, the vast domain of natural fibers and plant fibers, animal based fibers and its vast and varied applications.[13]

Prashanth et al.(2017)[14] discussed and described with lucid and cogent insight fiber-reinforced composites in a review paper. Fiber-reinforced composites are essentially axial particulates embedded in fitting matrices. The primary aim and objective of fiber-reinforced composites is to obtain

materials with high strength in conjunction with higher elastic modulus.[14] Vast technological and engineering vision is needed in today's application of fiber-reinforced plastics globally. In recent years, the advent and scientific needs of composite technology has led to the development of different fiber-reinforced composite systems via varying manufacturing methodologies to obtain advanced material properties. In this paper, a comparative account on various kinds of synthetic fibers and their significance as potential reinforcements with specific emphasis on carbon fibers.[14] Technological vision, deep scientific insight and engineering far-sightedness are the needs of scientific evolution and scientific advancements in carbon fiber technology today. In this paper, the authors stresses on the success of science and engineering of composite science in decades to come. The authors discussed in details important types of fiber-reinforcements such as glass fibers, carbon fibers and Kevlar fibers. This paper also compares a comparative account of glass, carbon and Kevlar fibers. Human civilization's immense scientific prowess, the technological and scientific validation and the world of scientific vision and the challenges will all lead a long and visionary way in the true emancipation and the true realization of nano-composites and composite science today. The reinforcement of fiber upon polymer matrix is found to bring about significant achievements and advancements in mechanical behaviors of polymeric host with added advantages of light weight, high strength to weight ratio, excellent weathering stabilities and enhanced dimensional stabilities in addition to low maintenance cost and excellent material behaviors. Important types of reinforcements are glass fibers, carbon fibers, and Kevlar fibers. A deep technological and engineering insight is the need of the hour as fiber science enters into a newer era of scientific might and vision.

12.0 The world of challenges and the vision in the field of environmental protection and environmental protection:

Human civilization's immense scientific grit, determination and prowess are changing the face of innovations and scientific instinct. The vision and the challenges of environmental protection science are immense and groundbreaking today. Success of environmental engineering tools are few yet groundbreaking. In the similar vein, traditional and non-traditional environmental engineering tools are the needs of human society today. Membrane separation processes and other novel separation processes are also the needs of environmental protection today. In this chapter, the author depicts profoundly the contribution of human factor engineering, systems engineering and integrated water resource management in confronting global water crisis. The challenges, the difficulties and the barriers are immense and needs re-envisioning. [15],[16],[17]

13.0 Arsenic and heavy metal groundwater remediation in South Asia:

Arsenic and heavy metal drinking water contamination in South Asia particularly India and Bangladesh have taken massive proportions. Health effects due to the drinking of polluted water is a challenge to millions of citizens around the globe. Scientific innovations, deep technological discernment and the veritable quest for knowledge are the torchbearers towards a greater understanding and a greater success in the field of environmental engineering and environmental protection. In this chapter the author pointedly focuses on the need of science and engineering in tackling global environmental issues. Novel separation processes, membrane science and advanced oxidation processes are the scientific challenges of today along with environmental remediation. Scientific

endeavor is at a severe risk as science and engineering of environmental protection surpasses vast and versatile frontiers.[18],[19],[20]

14.0 Integrated water resource management, application of nanotechnology and human factors engineering:

Integrated water resource management and human factors engineering are challenging the vast scientific firmament of immense might and vision today. Composite science and material science are changing the face of scientific progress globally. Application of nanotechnology in diverse areas of engineering science are the scientific needs of human civilization and the vast avenue of scientific might, grit and determination. Integrated water resource management and nanotechnology today needs to be merged with the furtherance of science and engineering in mind. In this chapter the author reiterates the vast scientific vision and the scientific ingenuity in the application of nanotechnology and human factors engineering to human scientific advancement. The grit and determination of science and engineering are veritably in the process of newer scientific regeneration. Integrated water resource management and industrial and drinking water treatment are today the scientific needs of human society today. In this chapter the author stresses the importance of nanocomposite applications in environmental remediation. Unit operations in chemical engineering and chemical process engineering are today in the threshold of a newer era of scientific vision and vast scientific might.

15.0 The success of environmental remediation in global scenario:

The domain of environmental remediation today stands in the midst of deep scientific vision and fortitude. Today energy engineering, environmental engineering and sustainability science are linked with each other with scientific might and scientific steadfastness. Renewable energy domain is revolutionizing the scientific and engineering landscape today.

Thus, the scientific need and the importance of nanotechnology and sustainability science and engineering. Groundwater contamination with arsenic and heavy metal has no technological and engineering answers. Globally water shortage and global warming are changing the face of human civilization and the vast scientific landscape. The civil society and a nation's government needs to gear forward toward a greater scientific emancipation and the scientific truth of renewable energy technologies, environmental engineering science and petroleum engineering. Today millions of people around the world lack proper drinking water and absolute lack of sanitation. In the developing and disadvantaged countries around the world, the environmental engineering scenario is worse. Health effects due to arsenic drinking water poisoning are devastating the social and scientific scenario in Bangladesh and the state of West Bengal, India. The global scenario is absolutely grave and thought-provoking. The state of energy engineering science and electrical engineering is in the similar vein immensely dismal as the fate of non-renewable energy scenario is in the process of newer scientific regeneration. Thus, the immediate need of environmental and energy sustainability. Human mankind's immense scientific prowess and girth, the futuristic vision of environmental engineering science and chemical process engineering and the marvels and the profundity of engineering science will lead a long and visionary way in unraveling the scientific truth of sustainability science. Today the world of nanotechnology and environmental engineering has immense challenges and a definite vision of its own. This chapter opens up newer visionary avenues in the field of environmental protection and nanotechnology in years to come.

16.0 Future research trends in application of nanotechnology in environmental protection:

Nanotechnology and its applications are changing the face of human scientific endeavor today. Technology and engineering science today have no answers to the intricate scientific issues of environmental remediation. Water purification, drinking water treatment and the vast domain of industrial wastewater treatment are the fountainhead and the pillars of environmental engineering research pursuit today. Human civilization's immense scientific prowess, scientific grit and determination are the torchbearers towards a newer era in the field of environmental protection today globally. Nano-science and nanotechnology are today integrated with every branch of science and engineering. Future research trends should target the scientific needs, the scientific vision and the vast scientific profundity of novel separation processes, conventional and non-conventional environmental engineering tools, composite science and the vast world of nanotechnology. Human scientific instinct and the deep vision are today in a state of immense disaster and deep hiatus. This chapter will surely unfold the world of challenges in the domain of nanotechnology applications in environmental protection, groundwater remediation and industrial wastewater treatment. The academic and scientific rigor in the field of environmental remediation are vast, versatile and groundbreaking. The authors in this chapter reiterates the scientific success, the immense scientific vitality and vast scientific imagination in the field of environmental protection today.

17.0 Future research and development initiatives in green nanocomposites:

Science and engineering of environmental protection and environmental remediation are today globally huge colossus with an immense vision of its

own. Today there is an imminent need for concerted effort and research and development initiatives in the field nanotechnology, composite science and material science. Technological advancements and vast scientific profundity are the pillars of human innovation and human scientific progress today. Composite science and the field of nanocomposites are challenging the vast scientific firmament of engineering science and nanotechnology today. Green nanocomposites are the scientific ardor and deep scientific vision of engineering and science today. Chemical process engineering, environmental engineering and material science are changing the face of human scientific progress today. Today also introspection of science is the necessity for furtherance of science and engineering. Green nanocomposites and composite science are today challenging the vast scientific might and vision.[21],[22],[23] Future research trends in the field of green nanocomposites should basically follow the following targets:

- A greater scientific emancipation in the field of composite science and material science.
- A wider scientific knowledge in the field of environmental engineering science and environmental remediation.
- Human scientific achievement and a greater scientific understanding in the field of nano-science and nanotechnology.
- Technological and engineering advancements in the field of green engineering and green chemistry.

The challenges, the vision, the pros and cons of environmental protection science are today immense and groundbreaking as science and technology surges forward towards a newer era and newer vision.[21],[22],[23] In this treatise, the author deeply elucidates the scientific success, the scientific redeeming and the deep scientific revelation in the field of environmental remediation and the greater technological emancipation of novel separation

processes, traditional and non-traditional environmental engineering techniques.

18.0 Future flow of thoughts in the field of composite science and environmental engineering:

In today's environmental engineering scenario, science and technology of traditional and non-traditional environmental engineering tools are the deep scientific needs and the scientific vision of human scientific progress. Composite science, material science and polymer science today need to be integrated with all avenues of research endeavor in the field of nanotechnology. Human civilization's immense scientific grit and determination, the marvels of engineering science and the futuristic vision of the science of nanotechnology will go a long and effective way in unraveling the real scientific truth behind composite science and material science. Future flow of thoughts should be targeted towards the larger scientific rigor in the field of novel separation processes, membrane science, advanced oxidation processes and other non-traditional environmental engineering tools. Today water purification, drinking water treatment, industrial wastewater treatment, loss of ecological biodiversity and depletion of fossil fuel resources are challenging the vast scientific fabric of might and vision. Scientific and academic rigor in nanotechnology applications to human society are immense and far-reaching today. This chapter opens up newer avenues and newer visionary perspectives in the field of environmental protection, water treatment and groundwater remediation in particular.

19.0 Conclusion and vast scientific perspectives:

Human civilization's immense scientific prowess today stands in the midst of immense barriers, intricacies and deep vision. Today technology and engineering science has practically no answers to the various issues of

groundwater contamination with heavy metals and arsenic in many developing and developed nations around the world. This treatise profoundly depicts the scientific profundity, the scientific forays and the scientific needs in application of green nanocomposites applications in environmental protection. The perspectives of science and engineering globally are vast and varied. The author in this paper deeply comprehends and elucidates the success of science and engineering in tackling global water issues. Science and technology are today huge colossus with a definite and purposeful vision of its own. Environmental engineering, petroleum engineering, energy engineering and nanotechnology are branches of engineering and science which are highly challenged and needs to be envisioned and re-organized with the passage of scientific history and time. In this chapter, the author reiterates the need of nanotechnology and nano-engineering towards the furtherance of human society and the furtherance of science and technology. Human scientific vision is today in the midst of deep crisis as loss of ecological biodiversity and depletion of fossil fuel resources are devastating the vast scientific firmament. Here comes the challenge of nanotechnology, nanomaterials, engineered nanomaterials and composite science. Human mankind's immense scientific prowess, grit and determination will surely evolve into newer knowledge dimensions as green nanotechnology, green nanocomposites and green chemistry ushers in a newer era of scientific might and profundity. The scientific perspectives of green nano-composites and its applications will also veritably change the future research trends in composite science and usher in a newer era in science and engineering.

20.0 References:

[1] Palit.S., Hussain.C.M.(2018), Frontiers of application of nanocomposites and the wide vision of membrane science- a critical overview and a vision for the future, Chapter 14, Book-Nanocomposites for Pollution Control, Editors- Chaudhery Mustansar Hussain, Ajay Kumar Mishra, Pan Stanford Publishing Pte.Ltd., Singapore, pp-441-476.

[2] Ghanghas.P, Poonia.K., Kumar.D.,(2018), Polymer nanocomposites as nanoadsorbents for environmental remediation,Chapter-6, Book-Nanocomposites for Pollution Control, Editors- Chaudhery Mustansar Hussain, Ajay Kumar Mishra, Pan Stanford Publishing Pte.Ltd., Singapore, pp-173-206.

[3] Karim.Z.A., Sean. G.P.,Ismail.A.F.,(2018),Nanocomposite membranes for heavy metal removal, Chapter-12, Book-Nanocomposites for Pollution Control, Editors- Chaudhery Mustansar Hussain, Ajay Kumar Mishra, Pan Stanford Publishing Pte.Ltd., Singapore, pp-361-402.

[4] Adeosun.S.O., Lawal.G.I., Balogun. S.A.,Akpan.E.I.(2018), Review of green polymer nanocomposites, Journal of minerals & materials characterization & engineering, Vol. 11, No. 4, pp 385-416.

[5] Modi. V.K., Shrives.Y., Sharma. C., Sen. P.K., Bohidar. S.K., (2014), Review on green polymer nanocomposite and their applications, International journal of innovative research in science, engineering and technology, Vol.3, Issue 11, pp17651-17656.

[6] Awad.M.A., Mekhamer. W.K., Merghani.N.M., Hendi.A.A., Ortashi.K.M.O., Al-Abbas.F., Eisa.N.A.(2015), Green synthesis, characterization and antibacterial activity of silver/polystyrene nanocomposite, Journal of Nanomaterials, Volume 2015, pp-1-6.

[7] Tsujimoto.T., Uyama.H., Kobayashi.S., Oikawa. H., Yamahiro.M.,(2015),Green nanocomposites from renewable plant oils and polyhedral oligomeric silsesquioxanes, Metals, 6, pp 1136-1147.

[8] Uyama.H., Kuwabara.M., Tsujimoto.T.,Nakano. M., Usuki.A., Kobayashi. S.,(2003), Green nanocomposites from renewable resources: plant oil-clay hybrid materials, Chemistry of Materials, 15, pp 2492-2494.

[9] Pandey.J.K., Singh.R.P.(2005), Green nanocomposites from renewable resources: effect of plasticizer on the structure and material properties of clay-filled starch, Starch, 57, pp8-15.

[10] Palit.S., Hussain.C.M.,(2017), Biopolymers and environmental perspective, Chapter-2, Book- Biopolymers- structure, performance and applications, Editors- A.K. Mishra, C.M. Hussain, S.B. Mishra, Nova Science Publishers, New York, U.S.A., pp -17-34.

[11] Woodrow Wilson International Centre for Scholars Report , U.S.A., (2009), Oversight of next generation nanotechnology, Author- J.Clarence Davies,.

[12] European Commission Report(2011), Successful European Nanotechnology research: Outstanding science and technology to match the needs of future society, Publications office of the European Union, Luxembourg.

[13] Cheung. H-y, Ho. M-p, Lau.K-t, Cardona.F., Hui.D.,(2009), Natural fiber-reinforced composites for bioengineering and environmental engineering applications, Composites-Part-B, 40, pp655-663.

[14] Prashanth. S., Subbaya. K.M., Nithin.K., Sachhidananda.S.,(2017), Fiber reinforced composites- a review, Journal of Material Science and Engineering, 6:3, pp 1-6.

[15] Andreozzi.R., Caprio.V., Insola.A., Marotta.R.,(1999), Advanced oxidation processes(AOP) for water purification and recovery, Catalysis Today, 53, pp51-59.

[16] Barrow.C.J.(2005), Environmental management and development, (BOOK), Routledge Perspectives on Development, Series Editor- Tony Bines, Taylor and Francis e-library, USA.

[17] Barrow.C.J., (1999), Environmental management for sustainable development, (BOOK), Routledge,USA.

[18] Palit.S.(2017), Application of nanotechnology, nanofiltration and drinking and wastewater treatment- a vision for the future, Chapter-17, Book- Water Purification, Editor- Alexandru Mihai Grumezescu, Academic Press,USA.pp 587-620.

[19] Palit.S.,(2016) Nanofiltration and ultrafiltration- the next generation environmental engineering tool and a vision for the future, International Journal of Chem Tech Research, Vol.9, No.5, 848-856.

[20] Palit.S.,(2016) Filtration: Frontiers of the engineering and science of nanofiltration- a far-reaching review, CRC Concise Encyclopedia of Nanotechnology(Taylor and Francis) ,Editors: Ubaldo Ortiz-Mendez, Kharissova. O.V., Kharisov. B.I.,205-214.

[21] Palit.S.,(2015) Advanced oxidation processes, nanofiltration, and application of bubble column reactor, Nanomaterials for Environmental Protection, Editors: Boris.I. Kharisov,Oxana.V. Kharissova, Rasika Dias.H.V.,(Wiley,USA),207-215.

[22] Palit.S., Hussain.C.M.,(2018), Engineered nanomaterial for industrial use, Chapter-1, Handbook of nanomaterials for industrial applications, Editor- Chaudhery Mustansar Hussain, Elsevier, Netherlands, pp-3-12.

[23] Palit.S.,(2018), Recent advances in the application of engineered materials in the environment industry- a critical overview and a vision for the future, Chapter-47, Handbook of nanomaterials for industrial applications, Editor- Chaudhery Mustansar Hussain, Elsevier, Netherlands, pp-882-893.

21.0 Important websites for reference:

https://pdfs.semanticscholar.org/.../d85db707cb831109b0841dd2db2b7a737903.pdf

https://www.scirp.org/journal/PaperInformation.aspx?PaperID=21051

https://file.scirp.org/pdf/JMMCE20120400004_30264021.pdf

https://pubs.acs.org/doi/abs/10.1021/cm0340227

www.sryahwapublications.com/research-journal-of-nanoscience-and.../pdf/.../5.pdf

https://onlinelibrary.wiley.com/doi/10.1002/9781118911068.ch5

https://www.hindawi.com/journals/jnm/2015/943821/

journals.sagepub.com/doi/full/10.1177/0954008317709891

https://www.ncbi.nlm.nih.gov/pubmed/29410268

https://www.ncbi.nlm.nih.gov/pubmed/29277738

www.insituarsenic.org/

www.insituarsenic.org/innovation.html

www.thestandrewsprize.com/finalist/arsenic-removal-from-water

www.waterrf.org/Pages/Projects.aspx?PID=4299

https://pdfs.semanticscholar.org/e420/20d98afedbea8d91b002cddea2dc6313a432.pdf

https://www.epa.gov/sites/production/files/2015-06/.../arsenic_issue_paper.pdf

https://mpra.ub.uni-muenchen.de/60684/1/MPRA_paper_60684.pdf

https://www.worstpolluted.org/projects_reports/display/76

https://books.google.co.in/books?isbn=1498762433

https://aip.scitation.org/doi/abs/10.1063/1.348741

https://www.sciencedirect.com/topics/earth-and-planetary.../environmental-pollution

https://www.conserve-energy-future.com/causes-and-effects-of-environmental-polluti...

https://www.eartheclipse.com/environment/causes-effects-solutions-to-environmental-...

https://en.wikipedia.org/wiki/Groundwater_remediation

https://www.sciencedirect.com/topics/agricultural-and.../groundwater-remediation

www.iec-nj.com/common-methods-groundwater-remediation/

https://www.energy.gov/em/services/site-facility.../soil-groundwater-remediation

www.understandingnano.com/nanocomposites-applications.html

https://www.nature.com › subjects

www.scielo.br/scielo.php?script=sci_arttext&pid=S1516-14392009000100002

https://www.ttu.ee/public/m/Mehaanikateaduskond/.../Lecture14_Nanocomposites.pdf

https://www.azonano.com/article.aspx?ArticleID=1832

https://www.tandfonline.com/loi/ynan20

www.thwink.org/sustain/glossary/EnvironmentalSustainability.htm

https://study.com/.../environmental-sustainability-definition-and-application.html

www.businessdictionary.com/definition/environmental-sustainability.html

https://www.environmentalscience.org/sustainability

https://en.wikipedia.org/wiki/Sustainability

www.sustainablefriends.com/what-is-environmental-sustainability-why-is-it-important/

https://www.igi-global.com/dictionary/environmental-sustainability/10076

https://www.edx.org/course/environmental-protection-and-sustainability-0

https://www.theguardian.com/global-development/environmental-sustainability

Use of carbon nanomaterials for removing heavy metals from water

Marinela Panayotova[1] and Vladko Panayotov[2]

[1]Dept. of Chemistry, University of Mining and Geology, Sofia, Bulgaria

[2]Bulgarian Academy of Sciences, Sofia, Bulgaria

E.mail: marichim@mgu.bg

Abstract:

Water pollution with heavy metals is of environmental and human health concern. Use of carbon-based nanomaterials is among the advanced and being investigated recently methods for combating water pollution. This chapter presents studies in the last 15 years on application of carbon nanomaterials and composites, as well as graphene, graphene oxide and reduced graphene oxide based materials for the direct elimination of heavy metals from water. Implementation of those materials to immobilize heavy metals (As, Cd, Co, Cr, Cu, Pb, Ni, and Zn - alone or in mixtures) and the factors impacting the heavy metals' removal efficiency are discussed. The relevant kinetic and thermodynamic studies are highlighted. Use of carbon-based nanomaterials and composites for improving the properties of membranes utilized in different membrane processes for the heavy metals' removal is also described.

1 INTRODUCTION

Water is the life. Water is critical for the socio-economic progress, healthy ecosystems and for the human survival itself. The Millennium Ecosystem Assessment noted that the biodiversity loss in freshwater systems is occurring at twice the rate of other natural systems.

Consequently, their ability to provide ecosystem services declines, resulting in negative consequences for human well-being (MEA, (2005)). Nowadays more than 2 billion people lack access to safe drinking water and more than double that number lack access to safe sanitation. At present, an estimated 3.6 billion people live in areas that are potentially water-scarce at least one month per year, and this population could increase to 4.8–5.7 billion by 2050 (WWAP, (2018)). The global demand for water has been increasing at a rate of about 1% per year as a function of population growth, economic development and changing consumption patterns, among other factors, and it will continue to grow significantly over the next two decades (WWAP, (2018)). Water demand for manufacturing is expected to increase by 400 % between 2000 and 2050 globally. By 2050, agriculture will need 60 % more water to produce food globally, and 100 % more - in developing countries (WWAP, (2015)).

About 71 % of the Earth's surface is water-covered but the oceans hold about 96.5 % of all Earth's water. Freshwater is indispensable for sustainable life and development on our planet. However, in all its forms including ice caps, glaciers and permanent snow it represents < 3.454% of the global water (USGS, (2016)). Freshwater is a finite and irreplaceable resource if it is not well managed. Only two ways are available to supply additional fresh water: to purify the wastewater for reuse in industrial facilities or purify sea water. Neither of these frontiers have been conquered cost effectively with existing technology.

On contrary, an estimated 80 % of all industrial and municipal wastewater are released to the environment without any prior treatment, resulting in a growing deterioration of overall water quality with detrimental impacts on human health and ecosystems (WWAP, (2017)).

Heavy metals, are generally defined as metals having densities greater than 5 g/cm^3 and often hazardous metalloids, as arsenic, are also included in this classification. Bearing in mind that there is "no authoritative definition to be found in the relevant literature" (Duffus, (2002)), the term in this chapter will be used for the group of metals and semimetals the most of whose chemical species have been associated with contamination and potential toxicity or ecotoxicity.

Heavy metals are among the most widely spread and important inorganic pollutants found in the wastewaters. Heavy metal ions contamination results mainly from various industrial activities, such as mining, metal processing, electroplating, petroleum refining, textile, tanneries, paint, pigment and pesticides manufacture, battery manufacturing, automobile manufacturing, photographic and printing industries, etc. Agriculture, transportation and domestic activities also "contribute" to the water pollution with heavy metals.

Heavy metals are often considered to be among the most hazardous aqueous contaminants due to their potentially damaging effect on human physiology and other biological systems when the tolerance levels are exceeded, their persistent nature in the environment, and (for some of them) tendency to accumulate in living organisms. Cadmium (Cd), lead (Pb), mercury (Hg), chromium (Cr) and arsenic (As) are widely accepted as bio-accumulating metals. Among the other metals, nickel (Ni) and cobalt (Co) (under consideration) are included in the group of the water priority pollutants (Directive 2013/39/EU, (2013)) together with Cd, Pb and Hg. In addition, copper (Cu) and zinc (Zn) are widely accepted and studied by the scientific community as hazardous (Qiu, (2015)).

Heavy metals can denaturize proteins, block functional groups, combine and replace compounds, modify the normal performance of physiological

functions, hinder transport properties through cell membranes, etc. (Oliveira, (2016)). When heavy metals reach the water bodies, they can affect human health due to their bioaccumulation in ecosystems. Prolonged use of water polluted with heavy metals and their compounds can cause cell intoxication, several types of cancer and mutagenic problems. Table 1 summarizes briefly the health hazard posed by a given metal and the WHO guideline standard for the metal (Hiew et al. (2018)), WHO, (2017)).

Table 1 Health hazards and discharge limits of heavy metals

Metal	Health hazard	WHO guideline, mg/L
As	Gastrointestinal symptoms, death, hepatomegaly, skin lesions, hyperkeratosis, melanosis	0.01
Cd	Renal failure, itai-itai disease, birth defects, anaemia, carcinogenic	0.003
Cr	Genotoxic, alopecia, mutagenic and carcinogenic properties, damage to kidney and liver and at low dosage it causes skin irritation	(Cr_{total}) 0.05
Pb	Kidney failure, gastrointestinal disorder, central nervous system effects, inhibition of some essential elements in human organism, for example, proteins (hemoglobin) and calcium (causing calcium homeostasis and possibly osteoporosis).	0.01
Hg	Kidney disease, death, muscle movement impairment, gum inflammation	0.006
Ni	Anaphylaxis, cancer of lungs, nose and bones, red blood cells loss, nephrotoxic - extreme weakness, dermatitis, headache, dizziness and respiratory distress	0.07
Co	Irritation of skin, throat, eyes; may affect heart, thyroid, liver and kidney, carcinogen	N.a.
Cu	Liver and kidney disease, cancer, stomach irritation, red cells destruction leading to anemia, liver and kidneys problems	2.0
Zn	Dizziness, at long exposure - digestive problems at stomach level or pancreas, it can disturb protein metabolism and cause arteriosclerosis	3.0

The elimination of heavy metals from water (waste and aimed for potable use) is one of the most important environmental problems for research, engineering and technology development. Generally physical (filtration, distillation, membrane processes - membrane distillation, ultrafiltration (UF), nanofiltration (NF), reverse osmosis (RO)), chemical (precipitation, chemical oxidation/reduction), physico-chemical (coagulation and flocculation, flotation, adsorption, ion exchange, electrochemical technologies) and biological methods (microbial water sludge treatment, biosorption, wetlands) have been applied to remedy the problem of heavy metals.

Chemical methods, as well as coagulation and flocculation, require addition of chemicals to transform a soluble compound into an insoluble form (precipitate, flocs most often bonging the heavy metal). The addition of chemicals, as lime, may increase the production of sludge with hazardous properties, requiring further handling. Some metal hydroxides are amphoteric (for example lead, zinc hydroxides) and when we have a mixture of metals, there is no optimal pH to work with and the needed efficiency of the process can not be achieved. The method is practically ineffective for trace metals removing. In ion exchange heavy metal cations are exchanged for H^+ or Na^+. Ion exchange resins are synthetic polymers having active ion group such as $-SO_3H$ (in strong) or -COOH (in weak) acidic resins. Use of ion exchange resins often requires pre-treatment, the resins are not cheap and the issues of resins' regeneration and usage for removing pollutants in very low concentrations are still not entirely solved. The electrochemical technologies such as the electrochemical oxidation/reduction, electroflotation and electrocoagulation have been used for industrial wastewater treatment but the economic constrains are expected with the raising electricity price. Membrane processes, able to remove heavy metals, such as enhanced NF and RO are still expensive due

to needed costs for installations (including membranes), energy, inlet water pretreatment and concentrate treatment.

For the present, adsorption is considered an effective and economic method for heavy metals removal from water, because of its simple design, easy setup and scalability, high capacity, effective removal of pollutants, ease of regeneration and low cost. Different materials have been used to adsorb heavy metals, such as synthetic adsorbents, bio-based sorbents, zeolites, clays, activated alumina, activated carbon, etc. The main selection parameters of adsorbents are their high adsorption capacity, fast kinetics, and low cost.

Low concentrations and small dimensions of some water pollutants are additional obstacles hindering the mitigation of the problem of water pollution by heavy metals. In recent years, nanostructured materials have gained special attention as adsorbents in water purification because these materials possess unique properties compared to the bulk materials. On a mass basis, they have much larger surface areas compared to macro particles. Their chemical affinity towards target compounds can be enhanced with various reacting groups. The higher surface area, surface reactivity and faster kinetics, compared with granular forms, enable the nanoparticles to remediate more material at a higher rate and with a lower generation of hazardous by-products. Nanoparticles can be transported effectively by the groundwater flow. They can also remain suspended for sufficient time in order to launch an in situ treatment sphere. Nanoparticles can be anchored onto a solid matrix, such as a conventional water treatment material like activated carbon, for enhanced strength-to-weight properties of nanocomposites for water treatment.

Adsorptive membrane filtration has emerged as a powerful technique for the removal of heavy metals from effluents due to several advantages over

existing treatment processes, such as greater removal efficiency, lower operating pressure.

Carbon-based materials possess good chemical stability, structural diversity, low density, and suitability for large scale production. In this line, the use of carbon-based nanomaterials (CBNMs) is among the advanced and being investigated in recent years methods for combating water pollution. CBNMs may exist in different forms, such as nanoporous carbon, carbon nanofibres, single-walled carbon nanotubes (SWCNTs), multi-walled carbon nanotubes (MWCNTs), graphene (Gr), graphene oxide (GO), reduced graphene oxide (rGO). All these materials have been studied alone (unmodified or modified) or in different nanocomposites for their ability to remove heavy metals from water.

This chapter presents recent studies on application of CBNMs and composites for the adsorption of heavy metals from water or for improving membranes for heavy metals removal.

In order to facilitate the reader, before describing the findings on preparation and use of different CBNMs, the adsorption phenomenon is presented briefly, as well as the relevant and most used in the today's studies kinetic and thermodynamic models.

2 ADSORPTION - BASICS

Adsorption is a phenomenon where ions or molecules from a gas, liquid or dissolved solid are accumulated through physical or chemical interaction at the interface of two phases (solid-liquid or solid-gas) on the surface of the phase with higher density and well developed surface. The phase with higher density is called adsorbent. The species attached at the interface is called adsorbate. The adsorbed ions or molecules are those that are resistant to washing with the same solvent medium in the case of adsorption from solutions. Physical interaction between the adsorbent and adsorbate is

termed physisorption while chemical interaction is called chemisorption. Generally, physisorption is characterized by weak attraction forces (van der Waals, hydrogen, electrostatic, dipole–dipole and $\pi-\pi$ bonds) between the adsorbate and adsorbent. When the phenomenon is governed by strong interaction between the adsorbate and adsorbent surface through electron exchange, it is chemisorption. Physisorption is a reversible process while chemisorption is practically an irreversible process. Some of the reported adsorption mechanisms in the studies on use of CBNMs as adsorbents for heavy metals removal from water include ionic exchange, complexation, chelation, electrostatic interaction, hydrogen bonding, precipitation, hydrophobic interaction and neutralization.

The efficiency of adsorption depends on the chemical nature of the adsorbate and adsorbent, the specific surface area, surface chemistry (including when applied, the amount of functionalizing reagent) and pore size and structure of the adsorbent. The efficiency of the system is influenced by operating parameters such as mass of adsorbent, concentration of adsorbate, presence of competing ions, solution pH, process temperature, and contact time. The adsorption operation can be batch, semi-batch and continuous. In addition to already mentioned process parameters, in batch and semi-batch process stirring velocity impacts the mass transfer rates, while in column process flow rate of the liquid through the column and the adsorbent bed height influence the efficiency. Practically, the impact of some or all of the described parameters is being studied by the scientists who present the use of carbon nanomaterials-based adsorbents for heavy metals removal from water.

At studying the process, the quantity of adsorbed metal q_t (mg/g) is calculated according to equation (1):

$$q_t = [(C_o - C_t) \times V / m] \qquad (1)$$

where C_o is the initial concentration and C_t is the residual concentration at time t of the metal ion (mg/L), m is the mass of the adsorbent (g) and V is the volume of the solution, containing the metal ions (L).

When equilibrium is reached the relation gives the amount $q_{e,}$ (mg/g) of metal adsorbed per unit mass of the adsorbent at equilibrium (often called adsorption capacity):

$q_e = [(C_o-C_e) \times V / m]$ (1')

and C_e is the residual concentration of the metal ion at equilibrium (mg/L).

The removal efficiency at time t and at the equilibrium is calculated by equations (2) and (2'):

Removal efficiency at time t, % = $[(C_o-C_t) \times 100 / C_o]$ (2)

Removal efficiency at equilibrium, % = $[(C_o-C_e) \times 100 / C_o]$ (2').

In experiments for the adsorbent regeneration, the desorption efficiency is calculated by equation (3):

Desorption efficiency, % = $C_d / C_a \times 100$ (3)

where C_a (mg/L) and C_d (mg/L) are correspondingly the concentration of adsorbed metal ions and the metal ions in solution after the desorption process.

The adsorbent feasibility depends on its ability to be regenerated and to maintain its activity after the regeneration. This is evaluated by using equation (4):

Maintained capacity, % = $q_{e,2} / q_{e,1} \times 100$ (4)

where $q_{e,1}$ and $q_{e,2}$ (mg/g) represent the adsorption capacities before and after the regeneration, respectively.

The kinetics of the adsorption has been evaluated mathematically using different models. In this chapter will be mentioned briefly only those models that have been tested by different authors for their ability to describe the adsorption of heavy metals from water on CBNMs.

The pseudo first order kinetic equation of Lagergren (5):

$dq_t / dt = k_1 \times (q_e - q_t)$ (5)

and after converting to a linear form (5'):

$\log (q_e - q_t) = \log q_e - (k_1 / 2.303) \times t$

where t, q_e and q_t are as described above and k_1 is the rate constant (1/min). The values of k_1, q_e and R^2 for the pseudo-first order model are calculated from a linear plot between $\log (q_e - q_t)$ and t.

The pseudo second order (PSO) kinetic equation - (6):

$dq_t / dt = k_2 \times (q_e - q_t)^2$ (6)

and after converting to a linear form (6'):

$t / q_t = 1 / (k_2 \times q_e^2) + t / q_e$ (6')

where k_2 is the rate constant of PSO adsorption reaction [g/(mg x min)] and t, q_e and q_t are as described above. The values of k_2, q_e and R^2 for the PSO model are calculated from a linear plot between t/q_t and t.

Pseudo first and PSO kinetics are macroscopic models usually applied for explaining the adsorption rate mechanism. The pseudo-first-order kinetic model assumes that physical factors mainly influence the adsorption process. When the adsorption kinetics is best described by the PSO model this indicates that the chemisorption is the rate-limiting step of the adsorption (Pei et al. (2018)).

The intraparticle diffusion model (7) is applied to explain the sorption process when the intraparticle diffusion is the only rate-controlling stage

$q_t = k_i \times t^{1/2} + C$ (7)

where q_t (mg/g) is the adsorption capacity at time t (min), k_i is the intraparticle diffusion rate constant [mg/(g x $min^{1/2}$)] and the intercept C (mg/g) is a constant that approximates the thickness of the boundary layer; a higher C value indicates a higher boundary layer effect and vice versa. If the plot of q_t versus $t^{1/2}$ gives a straight-line passing through the origin, this means that the intraparticle diffusion is the sole rate-controlling mechanism. The non-zero intercept corresponds to a film diffusion mechanism where metal ions are transferred from the bulk solution to the adsorbents' boundary layer (Mortazavian et al. (2018)).

The Boyd model (8) determines whether the actual slowest step in the adsorption process is film diffusion or pore diffusion (Ali, (2018)):

$\ln (1-F) = - k_{fd} \times t$ (8)

where $F = q_t/q_e$, q_t and q_e are the adsorbate uptake at time t and at equilibrium, respectively and k_{fd} [mg/(g x min] is the rate constant.

This model can be approximated as layer (Mortazavian et al. (2018)):

For $F > 0.85$; $B_t = -0.4977 - \ln (1-F)$ (8')

For $F < 0.85$: $B_t = \left(\sqrt{\pi} - \sqrt{\pi - \frac{\pi^2 F}{3}}\right)^2$ (8'')

where B_t is the time constant and it is a mathematical function of F. By plotting B_t versus t (min), it could be stated that intraparticle diffusion is the only rate-controlling mechanism if the graph is linear and passes through the origin. If the graph is nonlinear or it is linear but does not pass through the origin, it can be concluded that the adsorption rate is controlled by a chemical reaction and/or film diffusion.

Less commonly used is the equation of Elovich (9) (Sadegh et al. (2018)):

$dq_t / dt = \alpha \times \exp(-\beta \times q_t)$ (9)

where q_t (mg/g) is the adsorbed amount at time t (min), α initial adsorption rate (mg/(g x min)), β - Elovich constant (g/mg), counting for desorption. In the simplified form the equation can be written as:

$q_t = k_E + \beta \times \ln t$ (9')

where $k_E = \beta \times \ln(\alpha \times \beta)$.

After a certain amount of the pollutant(s) is adsorbed on the adsorbent surface, equilibrium is reached which is described through isotherms, that is, the amount of adsorbed ion on the adsorbent as a function of its final pressure (if gas) or final ion concentration in the solution (if liquid) at constant temperature. The quantity adsorbed is nearly always normalized by the mass of the adsorbent to allow comparison of different materials. To date different isotherm models have been developed. Here briefly will be mentioned only those that have been tested by different authors for their ability to describe the adsorption of heavy metals from water on CBNMs.

Freundlich model (10) is an empirical model that describes non monolayer (and in the most cases multilayer) adsorption process occurring at heterogeneous surfaces, with interaction between adsorbed molecules:

$q_e = K_F \times C_e^{1/n}$ (10)

where q_e, (mg/g) the amount of metal adsorbed per unit mass of the adsorbent at equilibrium, K_F - Freundlich constant [$mg^{(1-1/n)} \times L^{1/n} / g$] or given as [$(mg/g) / (L/mg)^{1/n}$], indicator of sorption capacity, 1/n (dimensionless) – constant for the given conditions, indicator for the adsorption energetics, C_e - aqueous concentration of adsorbate at equilibrium (mg/L). The adsorption is unfavorable process at $1/n > 1$ and favorable if $0 < 1/n < 1$, and in the latter case greater 1/n value is generally interpreted as greater affinity between the adsorbent and adsorbate.

Freundlich constants are obtained from the linear form (10') of the Freundlich equation as slope and intercept:

$\log q_e = \log K_F + 1/n \times \log C_e$ (10') .

The Langmuir isotherm (11) assumes mono-layer coverage on the adsorbent with uniform surface with a finite number of equivalent adsorption sites that are saturable. Maximum capacity of adsorption is achieved when all the sites are saturated with adsorbates. It is assumed that there is not interaction between adsorbed molecules and that adsorption at one site does not affect adsorption at an adjacent site.

$q_e = K_L \times q_{max} \times C_e / (1 + K_L \times C_e)$ (11)

where q_e is the loading of adsorbate on the adsorbent (mg/g) at the equilibrium concentration of the metal C_e (mg/L), q_{max} (mg/g) is the maximum adsorption capacity, and K_L is the Langmuir equilibrium constant (L/mg) related to the energy of adsorption.

The isotherm is most often applied in its linear form:

$C_e / q_e = 1 / (K_L \times q_{max}) + C_e / q_{max}$ (11')

The slope and intercept of plot of C_e/q_e versus C_e are used to calculate q_{max} and K_L.

In addition, a fundamental parameter of the Langmuir model can be represented by a dimensionless constant, R_L, which is determined by the equation (12) :

$R_L = 1 / (1 + K_L \times C_o)$ (12)

where K_L is the Langmuir constant (L/mg) and C_o is the initial concentration (mg/L) of adsorbate in solution. The adsorption is: (i) favorable when $0 < R_L < 1$; (ii) unfavorable if $R_L > 1$; (iii) linear at $R_L=1$; and (iv) irreversible at $R_L=0$.

Except of the Freundlich and Langmuir isotherms that are the most often fitted to the experimental data, other isotherms are tested by the scientific community for their ability to describe the adsorption of heavy metals from water on CBNMs, such as Temkin, Dubinin–Radushkevich, Redlich-Peterson isotherms and more rare - extended Langmuir model, Langmuir-Freundlich (Sips) and Koble-Corrigan isotherms.

Temkin model (13) describes adsorbate-adsorbate interaction on the adsorbent surface. The model assumes that heat of adsorption (function of temperature) of all molecules in the layer would decrease linearly rather than logarithmic with coverage:

$$q_e = (R \times T / b_T) \times \ln (K_T \times C_e) \qquad (13)$$

where, q_e - adsorbed amount (mg/g), C_e (mg/L) = concentration at equilibrium, R - gas constant [8.314 x 10^{-3} kJ/(K x mol)] and T is the absolute temperature (K). K_T - the equilibrium binding constant (L/g)

and B_T - heat of adsorption (J/mol) are the Temkin model constants.

The isotherm is applied in its linear form:

$$q_e = (R \times T / B_T) \times \ln K_T + (R \times T / B_T) \times \ln C_e \qquad (13')$$

A graph between q_e and ln C_e allows the determination of the model constants K_T and B_T from the intercept and the slope.

Dubinin-Radushkevich (D-R) isotherm is generally applied to express the adsorption mechanism with a Gaussian energy distribution onto a heterogeneous surface. The model is usually applied to distinguish the physical and chemical adsorption of metal ions. D-R model is given by the equation (14):

$$q_e = q_{max} \times \exp (-k_{DR} \times \varepsilon^2) \qquad (14)$$

where where, q_{max} - the maximum adsorption capacity (mg/g) and k_{DR} (mol^2/kJ^2) is related to the mean free energy of adsorption and is used to determine the feasibility of adsorption by physical or chemical phenomenon and ε is the Polanyi potential expressed by:

$$\varepsilon = R \times T \times \ln (1 + 1 / C_e) \qquad (15) .$$

The mean free energy (kJ/mol) of adsorption is equal to $1/(2k_{DR})^{1/2}$. The isotherm is applied in its linear form (14'):

$$\ln q_e = \ln q_{max} - k_{DR} \times \varepsilon^2 \qquad (14') .$$

A graph of $\ln q_e$ vs ε^2 is used to determine ε and q_e.

The Redlich-Peterson isotherm model (16) accounts for a mixed mechanism of adsorption that does not follow ideal monolayer adsorption:

$$q_e = k_R \times C_e / (1 + B \times C_e^{\beta}) \qquad (16)$$

where k_R (L/g) and B (L/mg) are the Redlich–Peterson constants, and β (dimensionless) has values in the range of 0-1, C_e is equilibrium liquid-phase concentration of the adsorbate (mg/L), and q_e is equilibrium adsorbate loading on the adsorbent (mg/g). At high liquid-phase concentrations of the adsorbate the isotherm reduces to the Freundlich equation (16'):

$$q_e = (k_R / B) C_e^{1-\beta} \qquad (16')$$

where $k_R / B = K_F$, and $(1-\beta) = 1/n$ of the Freundlich isotherm model.

When $\beta = 1$, the equation reduces to Langmuir equation, where $B = K_L$ (Langmuir adsorption constant, L/mg) and $k_R = K_L \times q_{max}$ (Ayawei et al. (2017)).

The linear form of the Redlich-Peterson isotherm can be expressed as follows (16"):

$\ln (C_e / q_e) = \beta \times \ln C_e - \ln k_R$ (16'').

A plot of $\ln (C_e / q_e)$ versus $\ln C_e$ enables the determination of Redlich-Peterson constants.

Langmuir-Freundlich (Sips) isotherm is a combination of the Langmuir and Freundlich isotherms and it is expressed by the following general equation (17):

$$q_e = K_S \times C_e^{\beta} / (1 + a_S \times C_e^{\beta}) \qquad (17)$$

where K_S is Sips isotherm model constant (L/g), $K_S = N_t \times a_s$, where N_t - the total number of binding sites per gram of adsorbent (analogous to Langmuir q_{max} parameter), a_S (L/mg) the affinity constant for the adsorption and β the index of heterogeneity, which can vary from 0 to 1 (less than 1 for heterogeneous surface) (Vilardi et al. (2018)). The linearized form is given as follows (Ayawei et al. (2017)):

$$\beta \times \ln C_e = - \ln (K_S / q_e) + \ln a_S \qquad (17').$$

The model describes a monolayer solute adsorption on heterogeneous surfaces that shows an asymmetrical quasi-Gaussian distribution of adsorption energies. At low adsorbate concentration this model reduces to the Freundlich model, but at high concentration of adsorbate, it approaches the Langmuir model (monolayer adsorption). The parameters of the Sips isotherm model are pH, temperature, and concentration dependent and isotherm constants differ when found by linearization and nonlinear regression (Ayawei et al. (2017)).

The Koble-Carrigan (K-C) isotherm is usually used to describe heterogeneous adsorption (Vilardi et al. (2018)). The general equation is reported as follows:

$$q_e = A_K \times C_e^{p} / (1 + B \times C_e^{p}) \qquad (18)$$

where A_K is Koble-Carrigan's isotherm constant, related to the thermodynamic equilibrium constant, B is related to the total number of active sites and "p" is the third K-C constant. The linear form of this model is represented by the following equation (Ayawei et al. (2017)):

$$1 / q_e = [1 / (A_K \times C_e^p) + B / A_K \qquad (18')$$

The model is only valid when the constant "p" is greater than or equal to 1. When "p" is < 1, it signifies that the model is incapable of describing the experimental data despite high correlation coefficient or low error value (Ayawei et al. (2017)).

The extended Langmuir model, modified by Jain and Snoeyink, is employed for binary systems modeling. This model is based on the hypothesis that only part of the adsorption process occurs with competition among the two species, and can be expressed by the following equations (Vilardi et al. (2018)):

$$q_1 = (q_{m,1} - q_{m,2}) \times b_1 \times C_1 / (1 + b_1 \times C_1) + q_{m,2} \times b_1 \times C_1 / (1 + b_1 \times C_1 + b_2 \times C_2) \qquad (19a)$$

$$q_2 = q_{m,2} \times b_2 \times C_2 / (1 + b_1 \times C_1 + b_2 \times C_2) \qquad (19b)$$

where q_1 and q_2 are the amounts of solutes 1 and 2 adsorbed per unit weight of adsorbent at equilibrium concentrations, C_1 and C_2, respectively, $q_{m,1}$ (mg/g) and $q_{m,2}$ (mg/g) are the maximum sorption capacities of solutes 1 and 2, respectively, and b_1, b_2 (L/mg) are the two Langmuir constants, they are a function of the energy of adsorption of solutes 1 and 2, respectively.

Considering that $q_{m,1}$ is the total active sites, $q_{m,2}$ is related to the active sites where a competition between the two species occurs and having in mind that in this model $q_{m,1} > q_{m,2}$, the sites number where there is no

competition for molecules of solute 1 is given by the difference ($q_{m,1}$ - $q_{m,2}$). Usually the model is validated by non-linear regression method.

The non-linear regression method can be applied also to the other described isotherms and according to some authors it overcomes the inherent bias resulting from data linearization and avoids the errors affecting the R^2 values when the linear analysis is performed (Vilardi et al. (2018)).

To evaluate whether the adsorption process is spontaneous, exothermic or endothermic the thermodynamic parameters, such as the free energy change (ΔG^o), entropy change (ΔS^o), and enthalpy change (ΔH^o) are calculated by using the following equations:

$$\Delta G^o = - R \times T \times \ln K_d \quad (20)$$

$$K_d = q_e / C_e \quad (21)$$

$$\Delta G^o = \Delta H^o - T \times \Delta S^o \quad (22)$$

$$\ln K_d = \Delta S^o / R - \Delta H^o / (R \times T) \quad (23)$$

where R is the gas constant = 8.314 J/(mol x K), while K_d and T are the distribution coefficient (thermodynamic equilibrium constant) and temperature (K), respectively; q_e (mg/L) and C_e (mg/L) are the equilibrium concentration of the heavy metal ion immobilized on the adsorbent and in solution, respectively.

The value of ΔG^o, ΔH^o and ΔS^o are calculated from the plot $\ln K_d = f (1/T)$. The value of ΔH^o and ΔS^o can be obtained from the slope and intercept and then ΔG^o is calculated. The negative value of ΔG^o is indicative for a spontaneity of the adsorption process. The values of $\Delta S^o > 0$ indicate the increase in randomness at the solid-solution interface during the adsorption that enhances the affinity of the adsorbent towards

adsorbate; $\Delta H < 0$ values indicates that the adsorption process is exothermic. The ΔH^o values are used to distinguish whether the adsorption process can be classified as physisorption or chemisorption. Generally, physisorption processes are dominant when $\Delta H^o < 20$ kJ/mol, chemisorption processes are dominant at ΔH^o in the range 80-400 kJ/mol, and when ΔH^o in the range of 20-80 kJ/mol, the process is mixed (physisorption–chemisorption).

Most of the experiments with CBNMs that studied their ability to remove heavy metals from water are carried out under batch conditions. However, recently some authors are being work on column studies (Mortazavian et al. (2018), Hayati et al. (2018)). In these studies mainly Bohart and Adams, Thomas and the Yoon–Nelson models are applied to describe the adsorption process.

The Adams–Bohart model is based on the surface reaction theory. It assumes that equilibrium is not instantaneous; therefore, the rate of the adsorption is proportional to the adsorption capacity which still remains on the sorbent. Bohart-Adams model (24) determines the basic equation explaining the correlation between C_t/C_o and time t in a fixed bed system:

$$\ln (C_t / C_o) = k_{AB} \times C_o \times t - k_{AB} \times N_o \times Z / F \qquad (24)$$

where C_o and C_t (mg/L) are the influent and effluent metal ions concentration, k_{AB} [L/(mg x min)] is the Bohart-Adams rate constant, F (cm/min) is the linear flow rate computed via dividing the flow velocity to the bed section area, Z (cm) is the bed height of the adsorbent column and N_o (mg/L) is the equilibrium concentration. A linear plot of $\ln (C_t / C_o)$ versus t determines the k_{AB} and N_o values. The Bohart-Adams kinetic model supplies an easy and general approach to investigate fixed bed

adsorption but its validation is limited to the applied conditions and assumptions.

Thomas dynamic model is appropriate for the sorption process when the outside and inside diffusion rates are not the rate limiting steps. The basic assumptions of the Thomas model are: (a) negligible axial and radial dispersion in the fixed bed column, (b) the adsorption is described by a PSO reaction rate principle which reduces to a Langmuir isotherm at equilibrium, (c) constant column void fraction, (d) constant physical properties of the solid-phase and the fluid phase, (e) isothermal and isobaric process conditions, (f) the intra particle diffusion and external resistance during the mass transfer processes are considered to be negligible (Hayati et al. (2018)). The equation of the Thomas dynamic model can be represented as:

$$\ln [(C_o/C_t) - 1] = k_{Th} \times q_e \times W / Q - k_{Th} \times C_o \times t \quad (25)$$

where k_{Th} [mL/(min x mg)] is the Thomas rate constant; q_e (mg/g) is the equilibrium metal ion removal per g of the adsorbent; C_o (mg/L) is the influent metal ions concentration; C_t (mg/L) is the effluent metal ions concentration at time t; W (g), Q (mL/min) and t (min) are the mass of the adsorbent, the flow velocity and flow time, respectively. The intercept and slope of the linear plot of ln $[(C_o/C_t) - 1]$ vs. time (t) is used to determine k_{Th} and q_e.

The Yoon–Nelson model assums that the decrease in the probability of removal of metal ion is proportional to the probability of its adsorption and breakthrough on the adsorbent. The linear form of Yoon–Nelson model is expressed as (Hayati et al. (2018)):

$$\ln [C_t / (C_o - C_t)] = k_{YN} \times t - \tau \times k_{YN} \quad (26)$$

where k_{YN} (1/min) is the Yoon–Nelson constant, τ (min) is the time needed for metal ions in the effluent to reach half of that in the feeding solution. The parameters k_{YN} and τ are calculated from the intercept and slope of the linear plot of ln $[C_t/(C_o-C_t)]$ vs contact time (t).

3 USE OF NANOCARBON, NANOPOROUS CARBON, CARBON NANOFIBRES, NANOCOMPOSITES CONTAINING ACTIVATED CARBON OR BIOCHAR

Different studies have been carried out in this direction. Two carbon nanomaterials were synthesized using turpentine oil in a chemical vapour deposition (CVD) setup by varying the process parameters. Nanocarbon (NC) with varying grain sizes indicative of soot was produced by using cobalt catalyst in N_2 atmosphere. Nanoporous carbon (NPC) with distinctive uniformly porous surface morphology was produced by using silica catalyst in H_2 atmosphere (Ruparelia et al. (2008)). Sorption studies with Cd(II), Pb(II), Ni(II) and Zn(II) were carried out for 12 hours. The sorption capacity is reported over the equilibrium concentration range 10–4000 μeq/g and pH 6.5 for all the metals. NPC revealed greater sorption compared to NC for all studied metal ions. Reported sorption capacities were 1428 μeq/g for Cd(II) and Ni(II) and 2000 meq/g for Pb(II) and Zn(II). It has been found that the adsorption was due to ion exchange and was described by the Langmuir isotherm. The superior performance of NPC as a sorbent is assigned to its unique nanoporous structure.

Xiao and Thomas (2005) produced two series of oxygen and nitrogen functionalized nanoporous activated carbon. A low nitrogen content (≅1 wt %) carbon series (GN) were derived from coconut shell activated carbon and a high nitrogen content (≅18 wt %) carbon series (PANCN) were derived from polyacrylonitrile. In both series, the oxygen contents were varied over the range 2-22 wt %, which was achieved by samples heating at

different temperatures. Materials were utilized to immobilize several heavy metals from water solutions. The process was carried out at 25 ^{o}C for 48 hours. The adsorption followed the Langmuir isotherm. The maximum capacities were determined for the GN with the highest oxygen content, namely 1.37, 0.63, 0.57 and 0.34 mmol/g, correspondingly for Hg(II), Cu(II), Pb(II), and Cd(II). The amount of adsorbed individual metal ions from mixtures decreases compared to an adsorption of a single ion system. The adsorption of aqueous metal ion species on acidic oxygen functional group sites mainly involves an ion exchange mechanism with proton displacement, while the adsorption on nitrogen group sites involves a coordination mechanism. It has been found that the adsorbent's selectivity with respect to metal ions was influenced by the electrostatic effects, multiple speciation of the ions in solution, the accessibility of these species to the porous structure, and the stability constants for interaction with the surface species.

Simultaneous removal of heavy metals such as Pb(II), Cd(II) and Cr(III) ions from water by titania/ activated carbon/ carbonized epoxy (TiO_2/AC/CE) nanocomposite has been demonstrated (Benjwal and Kar (2015)). AC significantly enhances the surface area of the nanocomposite. Around 97% of the Pb(II) ions are removed from aqueous solution at initial concentration 200 mg/L, pH 6.5 and 25 ^{o}C for 10 hours by the TiO_2/AC/CE nanocomposite, while around 80 % removal was achieved by AC/CE nanocomposite. Moreover, the TiO_2/AC/CE composite successfully adsorbed 90% of Cd(II) and Cr(III) impurities.

Magnetic iron oxide nanoparticles loaded sawdust carbon (Fe_3O_4/SC) and EDTA modified Fe_3O_4/SC (EDTA@Fe_3O_4/SC) nanocomposites (ncs) have been synthesized and their application for Cd(II) removal from aqueous medium in batch mode was studied (Kataria and Garg (2018)).

Langmuir isotherm describes the process and the Langmuir maximum adsorption capacity of EDTA@Fe_3O_4/SC ncs is found to be 63.3, 22.4 and 25 mg/g that is greater than maximum adsorption capacity of Fe_3O_4/SC ncs that is 51, 18.9 and 15 mg/g at the adsorbent doses of 0.4, 1.2 and 2.0 g/L, respectively. Cd(II) adsorption kinetic obeyed PSO reaction model. Free energy, enthalpy, and entropy changes showed that the Cd(II) adsorption process is spontaneous and endothermic in nature. The chemisorption of Cd(II) onto EDTA@Fe_3O_4/SC ncs is the proposed mechanism of Cd(II) immobilization. The removal of different metal ions from spiked groundwater sample was studied at natural pH by adding 2.0 g/L adsorbent dose. The removal efficiency of EDTA@Fe_3O_4/SC ncs for different metals was higher than that of Fe_3O_4/SC ncs. By using EDTA@Fe_3O_4/SC ncs, the removal of Cd(II), Zn(II), Cu(II), Pb(II) and Ni(II) was more than 80% and the removal order was Zn(II) > Cd(II) > Cu(II) > Pb(II) >Ni(II) > Co(II) > As(III) >U(VI) > Se(IV). The removal of Cd(II) was about 98% in multimetal spiked ground water sample. The regeneration was achieved with EDTA. The reusability efficiency of EDTA@Fe_3O_4/SC ncs attained up to 83% after 3 reuse cycles and 75% after five cycles.

Multi-functional nitrogen-doped carbon-MoS_2 (NC-MoS_2) nanohybrid composite was synthesized by solvothermal method and applied as heavy metal ions adsorbent (Pei et al. (2018)). The NC-MoS_2 possesses an adsorption capacity of 439.09 mg/g for Pb(II), which is attributed to the integrated physicochemical adsorption resulting from the oxygen-containing functional groups on the surface of nanohybrid composites. The adsorption process of Pb(II) on the surface of NC-MoS_2 can be well fitted with PSO kinetics and a Langmuir isotherm model indicating a monolayer chemisorption. Complex formation and ion-exchange process between the functional sites and target ions control Pb(II) adsorption. The prepared NC-

MoS_2 exhibits good chemical stability and can be reused 7 times with Pb(II) adsorption efficiency over 80%.

A hydroxyapatite-biochar nanocomposite (HAP-BC) was fabricated and adsorption of Pb(II), Cu(II), and Zn(II) by HAP-BC was studied in single and ternary metal systems (Wang et al.(2018)). The results demonstrated that pH influences the adsorption of heavy metals and the adsorption capacity for mixed Pb-Cu-Zn metal ions was the highest at pH 6 within the tested pH range (from 4 to 10). The PSO kinetic model showed the best fit for all three heavy metal ions on HAP-BC. In both single and ternary metal ion systems, the adsorption isotherm of Pb(II) by HAP-BC followed Langmuir model, indicating that Pb(II) likely formed monolayer coverage on HAP-BC. The adsorption of the two other ions followed the Freundlich model in both single and ternary systems implying that Cu(II) and Zn(II) were adsorbed in multilayers. The adsorption of Pb(II) by HAP-BC was related to chemical precipitation, while that of Cu(II) and Zn(II) was related to electrostatic interactions. The calculated maximum adsorption capacities of HAP-BC were 961.54, 854.70, and 980.39 mg/g for Pb(II), Cu(II), and Zn(II), respectively.

A magnetic ceramsite (MC) coated by nano carbon spheres (MCCS) was fabricated, then it was stabilized and functionalized by polyethylenimine (PEI) to obtain a nanocomposite (MCCSP) (Zhou et al. (2018)). The nano carbon spheres (NCS) possessed many amino and oxygen-containing groups (-OH, -COOH) and were distributed homogeneously on the surface of MC. MCCSP demonstrated a high adsorption capacity for Cr(VI) which could be then reduced to low toxic Cr(III)), and the obtained Cr(III) could be chelated on the surface of MCCSP by protonated amine groups. Cr(VI) in initial concentrations of 10 and 20 mg/L can be completely removed by MCCSP within 12 h. At a certain Cr(VI) initial concentration, the removal

capacity increased with the temperature. At initial Cr(VI) concentration of 100 mg/L the highest removal (over 98 %) is achieved at initial solution pH of 1-2 and the removal decreased with pH increasing (around 35 % at pH 11). The loaded MCCSP could be collected from water and soil by a magnetic separation system. The removal capacity for Cr(VI) did not decrease after 4 reuses, and decreased slightly for the fifth reuse.

Iron oxide/activated carbon (Fe_3O_4/AC) nanocomposite was fabricated by co-precipitation method for the removal of Cr(VI), Cu(II) and Cd(II) ions from aqueous solution in batch mode. The activated carbon nanoparticles were prepared from sunflower head waste (Jain et al (2018)). The conditions for the highest removal efficiency of synthesized nanocomposite were pH 2.0 for Cr(VI), and 6.0 for Cu(II) and Cd(II), temperature 25 ±1 °C, initial metal ion concentration 50 mg/L, contact time 45 min for Cr(VI), 90 min for Cu(II) and Cd(II). The experimentally obtained adsorption capacity of Fe_3O_4/AC was 4.4 mg/g for Cr(VI), 2.7 mg/g Cu(II) and 2.9 mg/g Cd(II). The PSO model fitted well to the experimental data indicating chemisorption mechanism. The equilibrium data were well described by Langmuir isotherm, thereby indicating monolayer adsorption. The calculated maximum Langmuir adsorption capacity was 8.06 mg/g for Cr(VI), 3.2 mg/g for Cu(II) and 2.15 mg/g for Cd(II). The obtained negative value of $\Delta G°$ signified that the adsorption process was feasible and spontaneous in nature. With the increase in temperature, the value of $\Delta G°$ decreased indicating that the temperature increase was favorable for the adsorption process. This finding is in agreement with the results obtained from the Langmuir separation factor ($0< R_L < 1$). The positive value of $\Delta H°$ signified an endothermic process. The positive values of $\Delta S°$ indicated that the adsorbent surface had the affinity for Cr(VI), Cu(II) and Cd(II) ions. Desorption studies with 0.1M HCl showed a desorption efficiency of 80% and 83% for Cu(II) and Cd(II)

in first cycle, which decreased gradually till about 50 % in the fourth cycle. In case of Cr(VI), substantially lower desorption efficiency of 23.2% was determined which may be due to the reason that Cr(VI) might be chemically bonded with the Fe_3O_4/AC.

A low-cost adsorbent of graphitic carbon nitride (g-C_3N_4) nanosheets was developed through one-step calcination of guanidine hydrochloride and tested for its ability to adsorb Cd(II), Pb(II), and Cr(VI) (Xiao et al. (2018)). The adsorption on g-C_3N_4 nanosheets occurred rapidly in the first 20 min. After that, the adsorption capacity increased slightly and reached the equilibrium in about 60 min. Kinetic data obtained could be fitted relatively well both by the PSO model and the Elovich model. Data obtained from equilibration studies could be fitted relatively well by Redlich-Peterson isotherm pointing at a hybrid adsorption mechanism, which admits both multilayer and monolayer adsorption. In summary, kinetic and thermodynamic studies have suggested that the adsorption was an endothermic chemisorption process, occurring on the energetically heterogeneous surface based on a hybrid mechanism of multilayer and monolayer adsorption. The tri-s-triazine units and surface N-containing groups of g-C_3N_4 nanosheets are proposed to be responsible for the adsorption process. Study on pH influence demonstrated that electrostatic interaction played an important role. The maximum adsorption capacity of Cd(II), Pb(II), and Cr(VI) on g-C_3N_4 nanosheets is 123.205, 136.571, and 684.451 mg/g, respectively. According to the authors, the observed superior adsorption capacity for Cr(VI) results from a strong complexation between the surface amino groups and the Cr(VI) anions. The adsorbent can be reused for 10 successive cycles with preserving over 80% of its adsorption ability for Cd(II) and Pb(II).

A carbonaceous nanofiber/Ni-Al layered double hydroxide (CNF/LDH) nanocomposites have been synthesized and tested for their ability to remove heavy metals from aqueous solutions (Yu et al. (2018)). The nanocomposites exhibited excellent hydrophilicity and high structural stability in aqueous solutions, guaranteeing the high availability of active sites in these environments. The porous and open nanostructures of CNF/LDH hindered agglomeration of the individual components. The adsorbed amounts of heavy metal ions rapidly increased within the initial 30 min and then reached an equilibrium state after 2 h, yielding a sorption efficiency of approximately 80% for Cu(II) at pH 6.0 and Cr(VI) at pH 4.0. The process is described by PSO kinetic equation. The uptake capacities of 219.6 mg/g (for Cu(II)) and 341.2 mg/g (for Cr(VI)) have been found. The sorption process was best fitted by the Freundlich isotherm model, indicating the presence of heterogeneous binding sites. The dominant interaction mechanisms consisted of surface complexation and electrostatic interaction, as verified by a combination of X-ray photoelectron spectroscopy and Fourier-transform infrared spectroscopy analyses and density functional theory calculations. Regeneration experiments (with 1M Na_2CO_3) showed that the removal decreased from 219.6 to 205.8 mg/g for Cu(II) and from 341.2 to 323.1 mg/g for Cr(VI) after 5 cycles thus suggesting reusability of the material.

Fe_3O_4@C nanocomposite has been prepared using $Fe(NO_3)_3$ and cyclodextrin as raw materials at 200 °C 12 h and tested as adsorbent for Cr (VI) (Ren et al. (2018)). The maximum adsorption capacity, calculated by Langmuir model was 33.35 mg/g. The good adsorption capacity is explained by (a) the large specific surface area and mesoporous structure of the prepared material that can improve the efficiency of adsorption and (b) surface modification by β-cyclodextrin which improves the stability of magnetic particles. The large amounts of oxygen-containing and carboxyl

surface functional groups of carbon ensure chelating of toxic metals, leading to high heavy metals' removal efficiency. The prepared Fe_3O_4@C samples demonstrated facile magnetic separability and good recyclability.

4. USE OF CARBON NANOTUBES

Carbon nanotubes (CNTs) are composed of graphite (sp^2-hybridization of the carbon atom) sheets rolled up into a tube-like structure. They may or may not be capped at their ends. CNTs can be classified as single walled CNTs (SWCNTs), made up of a single layer of carbon atoms, and multi walled CNTs (MWCNTs). MWCNTs are composed of multiple layers and their diameter can reach up to 100 nm while SWCNTs diameters range from 0.4 to 3 nm (Thines et al. (2017)).

Presently, there are four methods to produce CNTs: electric arc discharge, laser ablation, chemical vapor deposition and by thermal plasma. These techniques are relatively expensive due to their high temperature reactions.

CNTs are highly porous and hollow structures, non-corrosive, with low mass density, high mechanical strength, large specific surface area, and tunable surface chemistry. Due to those properties and the possibility for strong interactions between CNTs and pollutants, the applicability of CNTs for removal of hazardous pollutants from aqueous streams by adsorption has been studied extensively.

The hydrophobicity and fibrous structure of CNTs make them prone to aggregation in bundles. There are four possible adsorption sites present in CNT bundles: a) “internal sites” – the hollow interior of individual nanotubes (accessible only if the caps are removed and the open ends are unblocked); b) “interstitial channels” – the interstitial channels between individual nanotubes in the bundles; c) “grooves” – the grooves present on the periphery of a nanotube bundle and the exterior surface of the

outermost nanotubes, where two adjacent parallel tubes meet, and d) "outside surface" – the curved surface of individual nanotubes on the outside of the nanotube bundles. The adsorption reaches equilibrium faster on external sites than on internal sites under same process conditions. The binding energy of the interior sites is the highest, followed by the one of the groove sites on the outside of CNT bundles, and the one of the exterior sites on the convex outer surface is the lowest. The interstitial sites appear to be inaccessible to the adsorbate ions. The fraction of opened and unblocked nanotubes can considerably influence the overall adsorption capacity, since the opened CNTs provide more adsorption sites than closed ones (Gadhave and Waghmare (2014)). Inorganic species adsorb at peripheral groove sites, and the rate might be faster in close-ended CNTs (Das, (2017)).

Generally, the pristine CNTs possess low metal adsorption capacity and thus functionalization of the surfaces of CNTs is needed. Functionalization of CNTs can mediate specific pollutant adsorption, increase CNTs colloidal stability and chemical reactivity. Three different methods have been used for CNTs functionalization, namely: (a) physical non-covalent wrapping, for example by a surfactant application, (b) covalent wet chemical agent treatments, and (c) endohedral filling of CNT hollow cavity (Das, (2017)). Chemical reactions are more selective and straight forward than other processes and simultaneously with functionalization they can remove undesired impurities in the CNTs that are remained from the CNTs synthesis. CNTs are treated with acid or alkaline solutions to remove the impurities. The performance of CNTs can be increased by their functionalization with O, N, and P containing groups which improves dispensability and specific surface area of the CNTs. The functionalization alters the surface of CNTs by attaching an additional functional group on the surface of the CNTs, such as –COOH, –OH, –C=O at the opened end or

at the sidewalls of CNTs. The surface modification by oxidants, such as $KMnO_4$, HNO_3 and organic molecules changes the adsorption ability of CNTs. Generally, oxidized CNTs have high adsorption capacity for metal ions with fast kinetics (Kapinder and Verma (2017)). For example, increasing the surface oxygen content from 3.2 to 5.9 % increased the Pb(II) sorption on oxidized MWCNTs from 74.56 to 106.54 mg /g (Yu et al. (2013)).

The value of pH is an important parameter for aqueous heavy metal removal by use of CNTs, since the pH of the solution affects the ionic forms of heavy metals and functionalized nanomaterials. Generally, heavy metals usually exist in the expected forms under given pH conditions, and functionalized carbon-based nanomaterials are synthesized according to these expected forms.

Major interaction forces between CNTs functionalities and water pollutants are covalent bonding (chemical interaction), hydrogen bonding, van der Waals bonding, electrostatic interactions, ion exchange, hydrophobic interactions, π-π interation (Gadhave and Waghmare (2014)); Das, (2017)). It is considered that chemisorptions processes rather than physisorption processes play the most important role in the heavy metals adsorption by the CNTs (Gadhave and Waghmare (2014)). A brief summary on the adsorption of heavy metal ions by CNTs is presented in Table 2.

CNT-nanocomposites (CNT-NCs) refer to materials that contain two or more ingredients prepared to form a composite mixture with CNTs as the primary host. The combination with other materials improves CNTs dispensability and stability, as well as further handling of CNTs loaded with heavy metals. The combination of features of the different materials enhances the applicability and improves the properties of the obtained

nanocomposites. A brief summary on the adsorption of heavy metal ions by CNTs-NCs is presented in Table 3.

Data presented in Tables 2 and 3 show that many studies have been carried out to test the ability of raw, oxidized and modified CNTs and of CNTs-based composites to remove different heavy metal ions from water (actually mainly from model solutions). For a given pollutant results obtained differ (often considerably) depending on the adsorbent and its modification (in the case of CNTs) or on the adsorbent composition (in the case of CNTs-NCs), as well as on the experimental conditions. Generally, with the research advance in the time higher maximum adsorbed amounts are achieved for a given species under similar conditions. The good news is that potent adsorbents have been found and are still searched for both in the low range and high range of pollutants' concentrations. However, there is still a lot of work to be done to enhance CNTs adsorption properties in future and to avoid aggregation of CNTs in aqueous solution. The surface modification helps to overcome these problems but conventional chemical modification methods use large amounts of chemicals, which causes environmental pollution.

With respect to CNTs based composites - there is still room left to enhance their adsorption properties, selectivity and regenerability. Special attention has to be paid to possible changes in the composite components and their interactions with different (than the studied) chemical species that may present in water (especially in natural water).

5 USE OF GRAPHENE, GRAPHENE OXIDE, REDUCED GRAPHENE OXIDE AND THEIR NANOCOMPOSITES

The material, nowadays referred to as graphene (Gr), is defined by IUPAC in 1995 (McNaught and Wilkinson (1997)): "Graphene is a single carbon layer of the graphite structure, describing its nature by analogy to a

polycyclic aromatic hydrocarbon of quasi innite size. The term graphene should be used only when the reactions, structural relations or other properties of individual layers are discussed." The Gr lattice is 2-dimensional. It is based on the graphite hexagonal honeycomb structure of quasi infnite size. Within the Gr lattice the carbon atoms are sp^2 hybridized. Hence, each carbon is connected via σ bonds to its three neighbors. The σ bonds are responsible for the robustness of the lattice. The unafected p_z orbitals, which are perpendicular to the formed plane, bind covalently with neighboring carbon atoms and form a π bond. Graphene can be produced by top-down and bottom-up strategies. In the top-down strategy powdered raw graphite is attacked to separate its layers and thus to generate graphene sheets. Mechanical exfoliation, chemical exfoliation of graphite and reduction of graphite oxide or graphene oxide, CNTs cutting, etc. are categorized in the top-down strategy. Bottom-up strategy includes the utilization of carbonaceous gas to generate graphene. Methods using bottom-up strategy include pyrolysis, hydrothermal self-assembly, epitaxy (mainly chemical vapor deposition - CVD, but also grow of graphene films on various crystalline surfaces). Generally, large quantities of Gr at low-cost can be produced by the top-down approaches; however, it is difficult to obtain high quality Gr sheets because of introduction of defects during exfoliation. By bottom-up approaches defect-free material can be produced; however, the manufacturing cost is high. The combination of exfoliation–re-intercalation–expansion of graphite can produce high-quality single-layer Gr sheets stably suspended in organic solvents. Large amounts of Gr sheets in organic solvents can be prepared by Langmuir–Blodgett assembly in a layer-by-layer manner (Li et al.(2008)). The microwave assisted method employs a recipe similar to Hummer's method (see below), but excludes $KMnO_4$ and exploits aromatic oxidation by nitronium ions combined with microwave heating instead of traditional heating. Rapid and

simultaneous oxidation of multiple non-neighboring carbon atoms across the entire Gr sheet is ensured, thereby producing only a minimum concentration of oxygen moieties sufficient to enable the separation of Gr sheets (Chiu et al., (2012)).

To prevent the restacking of individual graphene sheets into macro-scale aggregates during adsorption process, three-dimensional (3D) graphene structures are being developed recently. Graphene-based foams, sponges, aerogels and hydrogels are some of the reported 3D graphene structures. The synthesis methods of the 3D configurations can be generally classified into two categories, namely direct synthesis from carbon sources and solution-based synthesis. For each of the synthesis classes, two different approaches are usually applied - template-assisted and template-free methods. The direct synthesis approach offers better control of pore size, pore density and pore size distribution development in the 3D structures. However, this approach is associated with relatively high manufacturing cost. The solution-based synthesis method provides advantages, such as elemental functionalization, potential scalability, higher production yield and lower production cost albeit the random distribution of pores' structure (Hiew et al. (2018)).

Graphene oxide (GO) can be considered as a Gr derivative. It can be produced via the chemical oxidation of graphite to graphite oxide followed by subsequent exfoliation to GO. Graphite oxide can be synthesized by using concentrated sulfuric acid (a) in combination with fuming nitric acid and $KClO_3$ (Brodie/Staudenmaier method), (b) in combination with concentrated nitric acid and $KClO_3$ (Hofmann method) or (c) in the absence of nitric acid but in the presence of $NaNO_3$ and $KMnO_4$ (Hummer method) (Poh et al. (2012)). Hummers' method and its modifications are generally used to fabricate GO based materials at low cost (Weng et al. (2017)). The

graphite oxide can be easily dispersed in aqueous solutions which allows exfoliation by sonication, mechanical stirring, use of microwaves, etc. Due to its solution processability, stability, and ease of synthesis, GO is an attractive precursor for large scale production of Gr. The carbon in graphite oxide / GO is mainly sp^3 hybridized due to rich oxygen functionalities. The GO can be described as a single monomolecular layer of graphite (two-dimensional sheet of covalently bonded carbon atoms) covered by various oxygen containing functionalities such as epoxy, carbonyl, carboxyl and hydroxyl groups on the basal planes and edges. Carbon atoms connected with these groups are in sp^3 hybridization. GO has a much larger interlayer distance than that of natural graphite. This facilitates the synthesis of intercalation compounds (Liu et al. (2016)). The polarised bonds containing functional groups at GO surface and edges are proven to attract metal species easily. GO is also a good oxidizing agent for transition metals (Petnikota et al. (2015)).

The GO can be reduced by the use of different chemical reducing agents or thermal treatment to produce reduced graphene oxide (rGO). The reduction restores the sp^2 hybridization. Reduced graphene oxide resembles Gr but contains residual oxygen and other heteroatoms as well as structural defects (Luedtke, (2019)). Another possibility to produce rGO is to expand graphite oxide into single-layer or few-layered Gr by heat-treatment which yields a simultaneous removal of the oxygen-containing groups (Hantel, (2013)). Graphene can be obtained as a final stage of the GO entire reduction - electrochemical, light induced, laser induced reduction or carried out by thermal treatment under either inert gas atmosphere or Ar/H_2 mixture.

The two-dimensional structure, large surface area and presence of π-bonds render Gr in a good adsorbent but mainly for organic pollutants.

Graphene can be functionalized in order to enhance its loading capacity and specificity for inorganic contaminants, such as heavy metal ions. The approaches adopted for the modification of Gr can be divided into two general categories: covalent functionalization and non-covalent functionalization. Surface functionalization is associated with rehybridization of one or more sp^2 carbon atoms of the carbon network to the sp^3 configuration. Carboxylic (-COOH) and hydroxyl (-OH) groups, can be covalently created on the Gr surface using strong acids and/or oxidants (Wang et al. (2013)).

Graphene oxide has two-dimensional structure that ensures maximum adsorption sites for heavy metals and large surface area. GO possesses hydrophilic oxygen-containing functional groups that increase its adsorption capacity of heavy metals. The functional groups also provide reactive sites for a variety of surface modification reactions aimed at developing functionalized GO and Gr based materials with improved adsorption capacity. Heavy metals adsorption onto GO and its configurations is mainly due to surface complexation, ion exchange and electrostatic interactions. Data modeling suggests that the adsorption generally involves monolayer immobilization of the heavy metals on the adsorbents that is controlled by chemisorption, as proven from the best-fit of the most data to Langmuir isotherm and to PSO kinetic models.

Reduced graphene oxide is more defective and less conductive than Gr but it is relatively easy to be modified by other functional groups. The restoration of graphitic network in the basal plane of rGO facilitates its modification by non-covalent physisorption of polymers and small molecules via π–π stacking or van der Waals interactions (Chowdhury and Balasubramanian (2014)).

The good adsorption ability of graphene-based materials – GBMs (Gr, GO and rGO) and their nanocomposites is related, besides already mentioned properties, with their low weight, chemical stability, mechanical strength, and flexibility.

Various factors, such as oxygen-bearing functional groups presence and their type and amount, the thickness of the GBMs, species of heavy metal ions in solution and experimental conditions (such as pollutants' concentration, pH, temperature, adsorbent dose, time, presence of competing species, etc.) influence the adsorption of heavy metal ions on the surface of GBMs.

The potential application of GBMs as nanoadsorbents depends on their homogeneous dispersion in the liquid phase, as well as their ability to be easily collected and separated from treated water. Chemical functionalization of GBMs or their inclusion in different composites contributes to these problems overcoming. Very often the prepared nanocomposites are not merely a sum of the properties of individual components, but represent a material with new functionalities and properties.

Regeneration of exhausted adsorbents and their re-use in the adsorption process assist in the reduction of overall operating cost and elimination of secondary solid waste formation. Several regeneration methods such as electrochemical treatment, temperature change, pressure swing and use of chemical eluting agents have been applied to regenerate exhausted adsorbents. The majority of the studies has reported that the regeneration of GBMs by using chemical eluting agents (acid, base and organic solvents) was effective.

Some recent studies on the use of GBMs for removal of heavy metals from water are summarized in Tables 4 - 7.

Data presented in Tables 4 -7 show that practically, and understandably due to their inherent properties, pure Gr and pure rGO have not been tested as adsorbents for heavy metal ions, except of the cases of 3D structures (like electrodes, foams). To give it the ability to adsorb metal ions, Gr has been functionalized, decorated or used as a basis for different composites. Due to its easier preparation and structure able to attract metal ions, GO (prepared by different methods) in pure form has been explored as adsorbent for heavy metal ions. Many different nanocomposites, based on Gr, GO and rGO have been prepared and studied as adsorbents for different heavy metals. Usually the adsorption process is relatively fast, which is an advantage when an industrial implementation is considered. As with the CNTs, development in the research and functionalization of the GBMs and preparation of different nanocomposites on the basis of Gr, GO and rGO improved significantly their ability to immobilize heavy metal ions from water. Moreover, good examples are preparation of composites which besides their high adsorption capacity can be easily separated from water and regenerated, such as magnetite-bearing ones.

However, before the possible use of these materials on a large industrial scale, a number of problems have to be solved.

Main part of the studies reported so far in the literature, are based on single solute systems. No many efforts were put in investigating the competitive adsorption. Where the competitive adsorption is studied in the majority of cases all ions are with the same initial concentrations in mg/L, instead of in mol/L or even in equivalent/L, which will be more informative. Such studies are essential for accurate designing of adsorption systems, since the competitive interactions usually cause deterioration in the adsorption capacity with a respect to a given metal ion. Along this line of thinking, the laboratory tests use pure aqueous solutions, only several

attempts have been made to spike real water with the studied heavy metal(s), and according to the literature reviewed very low number of studies (marked with bold in Tables 2-7) applied the developed absorbent(s) for real wastewater. However, industrial effluents contain different types of metal ions and other undesirable substances that most probably would interfere with the process. Studies with real waters will be needed.

The vast majority of studies reported the effects of individual process parameters on the adsorption treatment (while other parameters were kept constant). In a real situation the process parameters usually exercise a combined effect. These limitations can be overcome by optimizing all the process parameters collectively by statistical experimental designs.

The kinetic and equilibrium adsorption data have been empirically correlated with different kinetic and isotherm models that point at the eventual adsorption mechanisms. However, further attempts are needed to interpret the obtained results to go more inside in the mechanisms governing the process. Also, more studies should be pursued to relate the results on the adsorbents' characterization with their performance. All this will ensure more room for the improvement.

In addition, more research is needed to guarantee, simple and convenient separation of loaded GBMs and their composites from water, as well as their regeneration and the reusability.

It is necessary to take into account the fact that the composites include more and more different compounds in order to achieve higher efficiency in retention of the target metal(s), but this may lead to problems with adsorbents' regeneration or even worse - to negative side reactions of some of the components of the adsorbent with other ions or compounds that are present in real water.

Most of the experiments have been carried out in batch mode with very small amounts of the absorbent and polluted solutions. However, in many cases in practice continuous column treatment of water is more convenient and feasible. So, more dynamic adsorption studies are needed. Processes scaling will be another challenge.

In most of the studies Gr, GO and rGO have been synthesized by conventional methods by using toxic chemicals and generating hazardous waste and poisonous gases. Therefore, the development of environmentally benign and costs-effective methods for producing GBMs is a need.

Last but not the least, further studies on the toxicity and ecotoxicity of GBMs are very important requirement.

6. MEMBRANES INCORPORATING CARBON-BASED NANOMATERIALS

Membrane separation technology is widely accepted to desalinate seawater and brackish water and to remove heavy metal ions from polluted and wastewater. Permeability, rejection and selectivity are the most important properties determining the membranes' performance. Pure water flux (water permeability) is expressed by the equation:

$$J_w = Q /(A \times \Delta t) \qquad (27),$$

where J_w is the pure water flux ($kg/(m^2 \times h)$), Q is the amount of permeate collected (kg), Δt is the time interval of permeate collection (h), and A is the membrane area (m^2). Q can be expressed in m^3 or in L, Δt can be expressed in days - with the corresponding changes in the dimension of J_w.

The rejection of solutes (salts, heavy metal ions, etc.) is determined using the equation:

$$R, \% = (1- C_p / C_f) \times 100 \qquad (28)$$

where R is the rejection percentage, C_p and C_f are the concentrations (salt, heavy metal, etc.) in permeate and the feed, respectively.

At steady state, the permeability of component i (P_i) is presented as:

$P_i = K_i \times D_i$, (29)

where K_i is the sorption (or partition) coefficient and D_i is the permeate diffusion coefficient.

The membrane selectivity is used to compare the separating capacity of a membrane for two (or more) species. The membrane selectivity (also known as the permselectivity) for one component (A) over another component (B) is given by the ratio of their permeabilities:

$\alpha_{AB} = P_A / P_B = (K_A / K_B) \times (D_A / D_B)$ (30).

The ratio D_A/D_B can be viewed as the mobility selectivity, reflecting the different sizes of the two solutes. The ratio K_A/K_B is the ratio of the sorption coefficients of the two solutes and can be viewed as the sorption or solubility selectivity.

Membranes with a high permeability, rejection and selectivity are preferred. The higher permeability decreases the membrane area required to treat the water which leads to a decrease in the capital cost of the membrane system. Membrane with a higher rejection and selectivity provides a purer product. The increase in the permeability and selectivity finally will lead to a lower energy consumption.

Except for their permeability, rejection and selectivity membranes are often tested for their water uptake, porosity and mean pore radius. The following expressions are used: (Mahmoudian et al. (2018)):

Water uptake, % = $(W_w - W_d) / W_d \times 100$ (31)

where W_w and W_d are respectively the wet (after 24 h swelling) and dry weight of the samples (g).

$$\varepsilon = (W_w - W_d) / (A \times l \times d_w) \quad (32)$$

where ε - the overall porosity of the samples W_w and W_d - as described above, A is the membrane effective area (cm^2), d_w is the water density (0.998 g/cm^3) and l is the membrane thickness (cm).

$$r_m = [\, 8 \times \eta \times l \times Q \times (2.9 - 1.75 \times \varepsilon) / (\varepsilon \times A \times \Delta P)]^{1/2} \quad (33)$$

where r_m is the mean pore radius (cm), η is the water viscosity (8.9×10^{-4} Pa x s), Q is the volume of the permeated pure water per unit time (m^3/s) and ΔP is the pressure difference between the feed and permeate (Pa), other symbols - as described above.

In addition, contact angle is often measured, since the lower contact angle represents the greater tendency for water to wet the membrane, the higher surface energy and the higher hydrophilicity.

The performance of a membrane is mainly governed by its chemistry and structure. Moreover, it is impacted by the water pH, type and concentration of ions present in the water and the time. The performance of conventional polymer membranes is limited by a trade-off between water permeability and water/salt selectivity. Biofilm fouling is another critical problem in membranes' applications, especially for RO membranes. Recent experiments suggest that by incorporating CBNMs, such as nanoparticles, nanowires, nanofibers (NFs), properly functionalized CNTs and GO, in membranes the described drawbacks can be overcome. Thus obtained membranes can be referred to as new types of hybrid membranes which are made of inorganic materials dispersed in a continuous organic polymer phase and are termed "mixed matrix membranes" (MMM).

The nanocomposite membranes can be roughly classified into three categories: a) conventional nanocomposite membrane, b) thin-film nanocomposite and c) surface coated nanocomposite membrane. The first type is usually synthesized by phase inversion method, where the nanoparticles are loaded onto the pores and substrate of the membrane. For obtaining a thin-film nanocomposite, an ultra-thin film is coated on the substrate as a barrier layer, as widely used in the RO/NF membrane. Nanomaterials are loaded into the thin-film during the phase inversion and interfacial polymerization process. For preparing the third category, functional nanomaterials are coated to membrane surface through self-assembly, in-situ deposition, adsorption or chemical grafting (Zhang et al. (2016)).

A carbonaceous nanowire membrane (CNM) was synthesized by a hydrothermal method. The hydrothermal dehydration and carbonization of mono-saccharide (glucose, 180 ºC, 48 h) can yield one-dimensional carbonaceous nanowires in the presence of tellurium nanowire template. The subsequent solution-evaporation-self-assembly process results in the formation of macro-scale two-dimensional hydrophilic CNM sheet with large specific surface area, developed nanoporosity, and abundant superficial oxygen-containing functional groups. Thus prepared CNM showed high permeability to water molecules and good adsorptive retention of a variety of heavy metals (Zhong et al. (2013)). The CNM was able to eliminate Cd(II) (91-60 % removal efficiency), Cr(VI) (91.5-5 %), Hg(II) (89-57%), Pb(II) (92-63) and Cu(II) (86-59) depending on the water head applied (0.2–1.0 m). Desorption of Cd(II) was carried out by 0.1 M HCl. The CNM loses about 4% capacity after the first static adsorption experiment and about 13% after more than 5 runs.

Mixed matrix activated carbon nanoparticles (ACNPs) embedded polyethersulfone (PES) based nanofiltration membranes (PES-co-ACNPs) were prepared by solution casting technique (Hosseini et al. (2018)). The water contact angle was found to decrease from 54° to 43° by increasing the ACNPs concentration. The increase of the ACNPs concentration up to 0.1 wt.% in the casting solution led to a higher water content in the membrane and higher porosity. The membrane water content and porosity decreased by further increasing the concentration of the additive. The membrane tensile strength was also improved from 2.798 to 3.653 MPa by utilizing nanoparticles up to 0.05 wt% in the casting solution and then showed decreasing trend by a further increase of the nanoparticles content. The membrane with 0.5 wt.% nanoparticles indicated the highest sulfate (95%) and Cu (97%) ions removal. The decrease of the flux ratio due to fouling for a mixed matrix membrane containing 0.5 wt% nanoparticles was about 5% after 60 min of filtration whereas the flux decrease of the unmodified PES membrane was 64%.

Electrospun (CNFs/TiO_2-PAN) hybrid membrane was synthesized using polyacrylonitrile (PAN) polymer, carbon nanofibers (CNF) and TiO_2 nanoparticles at different weight percentage (%) (Kumar et al. (2018)). Hybrid CNFs/TiO_2-PAN membrane showed an enhanced hydrophilic nature when compared to PAN membrane. The water contact angle of CNFs/TiO_2-PAN hybrid membrane decreased from 38° to 18° by addition of different concentration CNFs/TiO_2 (0.5 wt.% to 6 wt. %). The hybrid membrane with 6 wt.% exhibited a higher flux up to 650 LMH with respect to time (180 min). The rejection performance of hybrid CNFs/TiO_2-PAN membrane was evaluated with different metal ions. The maximum rejection values for hybrid membrane were around 87%, 73% and 66%, for Pb(II), Cu(II), and Cd(II), respectively.

Currently, there are two types of CNTs-membranes: (a) vertically aligned (VA) and (b) mixed matrix (MM) CNTs membranes. The VACNTs membranes are synthesized by aligning perpendicular CNTs with supportive filler contents (epoxy, silicon nitride, etc.) between the tubes. The MMCNTs membrane consists of several layers of different composite materials. CNTs-membranes work with low energy consumption because of CNTs' frictionless water transport capability through nanotubes hydrophobic hollow cavity. In addition, due to the CNTs cytotoxicity, the CNTs membranes possess antifouling and self-cleaning abilities (Das, (2017)).

Usually, functionalization of CNTs is a key pre-step for fabrication of CNTs-based composite membranes. CNTs produced by CVD process need purification to remove the residual catalyst, amorphous carbon and other impurities. Due to the presence of van der Waals forces, CNTs tend to form tight bundles which in turn results in the difficulty of CNTs dispersion in most of polymer solvents. To overcome described problems the CNTs are often tailored by introducing active functional groups. Positive ($–NH_3^+$), negative ($–COO^–$, sulfonic acids) and hydrophobic (aromatic) groups can be implanted by using different wet oxidizing agent treatments of CNTs.

Parham et al. (2013) prepared a CNTs-based composite filter for the removal of heavy metal ions from water. Carbon nanotubes were grown in the open pores of a commercial porous ceramic matrix consisting of mainly Al_2O_3 and SiO_2, using a pre-formed nickel catalyst inside the pores and a camphor solution precursor at 780 ^oC. The CNTs filters exhibit hydrophobic behaviour. The CNTs were oxidized to modify their surface behaviour before the filter to be utilised in aquatic systems, where improved wettability is desirable. The oxidation was carried out by acid treatment and by an alternative air oxidation process at 400 ^oC. The initial

adsorption efficiency of an air oxidised 20 mm long CNTs filter for Cu(II) ions (from 12 mg/mL $CuCl_2$) reached 99.99% ± 0.01 at solution flow rates from 2 to 30 mL/h. The ability of filters to adsorb metal ions from their mixture was explored. Functionalized CNTs filters (10 mm long) were immersed in a 30 mL solution of Fe(II), Cu(II), Zn(II) and Mn(II) ions (each at a concentration of 5 mg/L) for 10 h. The air oxidised filter adsorbed most of the Fe(II) and Cu(II) ions, with only a negligible adsorption for Zn(II) and Mn(II). The acid functionalised filter adsorbed 20% of Zn(II) and 20 % of Mn(II) ions under the same conditions.

The polysulfone membranes show high thermal and chemical resistance, but are highly hydrophobic and susceptible to membrane fouling. Functionalized MWCNTs - polysulfone (MWNTs/PSf) composite membranes were synthesized by the phase inversion method using DMF as solvent and water with isopropanol as coagulant (Shah et al. (2013)). Three different functionalities were generated on the nanotube surface i.e., oxidized, amide and azide. The presence of CNTs reduced pore size, thus helping the membranes to be efficient enough for metal ions' removal under continuous filtration operation. The amount of MWNTs in the composite membranes was an important factor influencing the morphology, and permeation properties of the membranes. The rejection of heavy metals was found to increase with increase in amount of MWNTs. Amide functionalized CNTs gave better results as compared to oxidized CNTs and best results were obtained at a pressure of 0.49 MPa and at pH of 2.6. Amide functionalized CNT/PSf composite membranes gave 94.2% removal for Cr(VI) and 78.2% removal for Cd(II), at just 10.2% and 9.9% for the bare PSf membranes, respectively.

Tofighy et al. (2015) fabricated an adsorptive membrane for Ni(II) ions removal from water by implanting CNTs in mullite pore channels of

ceramic membrane substrates via CVD and further oxidation with HNO_3. Rejection of 62.91 % was achieved by the use of CNTs–mullite membranes for Ni(II) solutions with initial concentration of 100 mg/L.

Ar/O_2 plasma treatment technique was employed to functionalize MWCNTs, thus to improve their dispersion capability and adsorption for cationic metal ions in water (Farid et al. (2017)). Further, nanocomposite membranes were fabricated by incorporating functionalized MWCNTs inside a polymeric substrate membranes with hollow-fiber configuration. The adsorptive removal efficiency for Zn(II) from synthetic and real wastewater by the composite membrane with functionalized MWCNTs remained above 90%, regardless of water chemistry conditions. The presence of natural organic matter did not adversely affect Zn(II) removal. The membranes effectively removed Zn(II) from a secondary wastewater effluent in the presence of Na(I), Ca(II), Mg(II), Mn(II) and Fe(II), illustrating the selective adsorption of Zn(II) from wastewater. The adsorption capability of CNTs membranes for Zn(II) was regenerated under acidic condition (0.1 M HCl) showing a reusable potential. The original sorption capacity of the regenerated membrane was maintained after five sorption/desorption cycles.

An alumina-carbon nanotubes (Al_2O_3-CNTs) composite membrane was synthesized through a powder metallurgical method (Shahzad et al. (2018)). Homogeneous dispersion of the CNTs within the alumina matrix was achieved by using gum arabic and sodium dodecyl sulfate as dispersants. The membrane removed 93% of the Cd(II) present in a water solution containing 1 mg/L Cd(II) at pH 6.

GO possesses the following features that benefit its application in membranes: (a) hydrophilic functional groups (e.g., carbonyl, hydroxyl, carboxyl, and epoxy groups), (b) good compatibility with polymer matrix,

(c) a plane structure which allows the GO to be horizontally-aligned and thus to form ultrathin polymer-GO layer (Mahmoudian et al. (2018)). Apart from promoting molecular transport through membranes, graphene-based nanocomposite membranes also possess anti-biofouling properties. These properties are attributed to the presence of oxygen-containing groups, resulting in an increased surface hydrophilicity and enhanced negative zeta potential, which could repel microorganisms through electro-repulsion and impede the surface attachment of the microorganism (Zhang et al. (2016)). That is why graphene-based nanocomposites exhibit huge potential in membrane based water purification, minimizing the transport resistance, maximizing the permeate flux and simultaneously enhancing the ions' rejection.

Cao et al. (2014) blended pristine GO (pGO) and rGO nanosheets with different physical and chemical structures with sodium alginate matrix to fabricate two types of hybrid membranes. Swelling resistance and mechanical stability of the hybrid membranes were both enhanced. The composite membranes, particularly rGO-filled membranes, exhibited improved separation performance and high permeation flux. This was ascribed to the presence of oxygen-containing groups, structural defects, edge-to-edge slits and non-oxides regions of GO nanosheets, which could provide abundant water channels. When the rGO content was 1.6 wt%, optimum separation performance with a separation factor of 1566 and a permeation flux of 1699 g/(m^2 x h) was achieved. The membrane displayed a good long-term operation stability.

A GO impregnated MMM was prepared by non-solvent induced phase inversion method (Mukherjee et al. (2016)). The developed MMM showed high adsorption capacity for Pb(II) (79 mg/g), Cu(II) (75 mg/g), Cd(II) (68 mg/g) and Cr(VI) (154 mg/g) at pH 6.7, 6.5, 6.4 and 3.5, respectively.

Membrane with 0.2 wt.% GO was found to be optimum due to interplay of adsorption, diffusion and convection. The steady state permeate flux was around 30 L/(m^2 x h) for 50 mg/L feed concentration at 414 kPa transmembrane pressure drop and 40 L/h cross flow rate. Rejection of Pb(II), Cu(II), Cd(II) and Cr(VI) was between 90% and 96% for various operating conditions. The long breakthrough time was observed for solutions of individual different heavy metals (12–15 h) as well as for mixed heavy metal solutions (around 8 h) with a small filtration area of 0.008 m^2. The membrane was regenerated in-situ, by acidic solution at pH 5.5.

Cellulose acetate (CA) (Mw = 52,000 Da) membranes containing different amounts of GO were prepared by phase inversion (Mahmoud et al. (2017)). SEM cross sectional images showed even dispersion of GO sheets in the polymeric matrix with no evidence of agglomerations which implies the formation of strong hydrogen bonds between CA and GO sheets. An increase in porosity of CA/GO membranes in comparison with the CA membrane was also noticed. Nitrogen adsorption studies indicated that increasing GO content increased the number of macrovoids at the same final thickness of the nanocomposites. It was found that permeation rates increased with increasing GO due to increased number of hydrophilic sites in the membranes which attracted water molecules and facilitated their movement through the membrane. The membrane with 0.05 wt.% GO showed the highest salt rejection value of 74% and 81% for 2000 mg/L NaCl and 5000 mg/L $MgSO_4$ solutions respectively.

Incorporation of hydrophilic multifunctional compounds into the polymeric membrane's matrix is one of the useful methods for modification of MMMs. Polyethersulfone (PES) mixed matrix membranes with hydrolyzed polymethylmethacrylate (PMMAhyd) grafted on graphene

oxide (GO-PMMAhyd) have been prepared and investigated (Mahmoudian et al. (2018)). The permeability and antifouling properties were improved. The FE-SEM cross-section images have shown that during membrane formation, the membrane surface porosity improves and the hydrophilic GO-PMMAhyd nanoparticles tend to migrate toward the membrane top surfaces which is confirmed by the contact angle measurements showing that the surface hydrophilicity was enhanced after introducing GOPMMAhyd. The rejection percentage for heavy metals follows the order: Cd(II)< Cu(II) <Ni(II) < Zn(II). This is not proportional to the hydrated ionic radius, thus suggesting that size exclusion had a trivial effect on ion rejection and the latter was controlled mainly by electrical repulsion. Like salt rejection results, the highest ion removal was observed for the mixed matrix membrane containing 3 wt.% GO-PMMAhyd.

Bearing in mind the above-described examples, we can say that there is no doubt that CBNMs composite membranes will find their role in the future water purification and desalination, thus addressing critical water issues. Since the research on membranes is still at the premature stage, there are some issues to be solved, for example: (a) Control of fabrication parameters, such as controllable loading of CNTs, and more especially scale-up manufacturing; (b) Membranes' cost; (c) Membranes' degradation at use and the corresponding release of CNTs, Gr, GO, etc. in the treated water and the potential toxicity effects of those materials.

7 TOXICITY AND ECOTOXICITY OF CBNMs

Expected enhanced use of CBNMs in all areas of our life, including for heavy metals removal from water, requires attention to be paid to their possible toxicity and ecotoxicity effects. Toxicity studies focuse on human beings and aim at protecting individuals, while ecotoxicity studies look at various trophic organism levels and intend to protect populations and

ecosystems. Toxicology traditionally assesses adverse effects of a compound once it is absorbed by an organism, while ecotoxicity includes natural uptake mechanisms and the influence of environmental factors on bioavailability and thereby on toxicity (Joner et al. (2008)).

The unique features of nanomaterials, such as very small size, large specific surface area, reactivity, shape, etc. not only make them interesting for technological applications, but also open the possibility for them to enter organisms and travel through tissues, cells and even into cell organelles in ways that larger particles may not.

Studies have shown that the lowest observed effect concentrations (LOEC) mean for freshwater organisms exposed to CNTs are 19.4 ± 32.8 mg/L (mean ± SD) and these values are considerably above the environmental concentrations observed in freshwater systems which are in the order of ng/L (Freixa et al. (2018)). However, many different experiments showed that toxic effects to aquatic organisms are observed at higher concentrations of the CBNMs in short-term experiments. Furthermore, the reported LOEC and the EC_{50} acute toxicity values vary considerably. Reasons for the variations could be the type of aquatic organism, type of CBNMs, exposure time, interactions of the CBNMs with the environment components, and the use of different methods for the CBNMs preparation. For example, the mean EC_{50} values for crustaceans are 14.7 ±13.5 mg/L (n = 27), for algae are 23.7 ± 28.9 mg/L (n = 24), 88.6±101.5 mg/L - for fish (n=6), and 179.4±260.3mg/L - for bacteria (n =16) (mean ± SD) (Freixa et al. (2018)). Having in mind the toxicity ranking scale for acute aquatic toxicity of Pretti et al. (2014) it could be concluded that that CBNMs are slightly toxic for most aquatic organisms (10 mg/L < EC_{50} ≤ 100 mg/L), except for bacteria where they are practically non-toxic (100 mg/L< EC_{50} ≤ 1000 mg/L). Furthermore, the

one-way ANOVA results showed that the type of organisms, the exposure time and the CBNMs preparation methods significantly influence the EC_{50} values, whereas the type of CBNMs did not produce any significant effect. The CBNMs interact (establishing synergistic or antagonistic effects) with other micro-pollutants and the interactions are highly dependent on the chemical properties of each micro-pollutant. CBNMs act either as carriers or as sorbents, thus modifying the original toxicity of the contaminants (Freixa et al. (2018)).

Nowadays, it is still difficult to understand and define the mechanisms of toxicity of carbon nanomaterials in aquatic systems. Broadly speaking, the negative effect of CBNMs to microorganisms is related to: a) the disruption of membrane integrity, b) oxidative stress, c) DNA damage or protein inactivation, d) impurity toxicity leading to conformational changes in microbial enzymes that affect the enzymatic catalytic processes of microbes, which will further disturb the microbial metabolism, e) microorganisms' agglomeration affecting community structure, growth and diversity.

The toxicity of CBNMs to algae can be both directly related to their exposure as well as to some indirect effects, such as shading effects of these nanomaterials on the cells (with consequences in light absorption and photosynthesis) and to the nutrient depletion caused by the adsorption of nutrients on CBNMs.

CBNMs were found toxic for the zebra fish embryos by in vivo tests (Cheng et al. (2007)), Felix et al. (2016)). Souza et al. (2017) found that GO exposure induced significant toxic effects in the physiology of adult zebrafish. Short-term exposure resulted in apoptosis and necrosis as well as oxidative stress responses, probably due to the strong GO interaction with and accumulation on cell membranes. There was no evidence of

genotoxicity, which indicates that at the concentrations evaluated, GO did not cause DNA damage in blood cells. Chronic exposure resulted in significant alteration of gills and liver, demonstrating the organ-specific effects of GO. These results show that although no lethality was observed among zebrafish following acute exposure to GO, sub-lethal effects could be significant and harmful to fish species in a long-term.

The current knowledge on CBNMs ecotoxicity is mainly based on short-term tests, using relatively high concentrations of CBNMs applied to single-species studies. Performing long-term experiments are needed where environmentally relevant concentrations of CBNMs are used in order to understand long-term ecotoxic effects, and the possible recovery and adaptation capacity in key organisms. The inclusion of organisms from different trophic levels, in order to understand the complex mechanisms and interactions (possible bioaccumulation and biomagnification) in the aquatic food webs is desirable. Studying the interaction between CBNMs and other micropollutants co-occurring in the environment is necessary.

CBNMs, when used to remove heavy metals from water, can contact with humans during the technological process of their application (mainly through inhalation and skin contact) and when are presenting as a residue in already treated water (by a skin contact or oral administration). CNTs can be bio-persistent and have the potential to exist as fibre-like structures. All biopersistent CNTs, or aggregates of CNTs, of pathogenic fibre dimensions, could be considered as presenting a potential fibrogenic and mesothelioma hazard unless demonstrated otherwise by appropriate tests (CSIRO, 2012). Proper measures should be taken for their safe handling to prevent their entering in lungs.

As skin, together with lungs, displays the highest exposure to CBNMs, a comprehensive study was carried out on HaCaT keratinocytes, an *in vitro*

model of skin toxicity, on which the effects of four graphene-based materials were evaluated: a few layer graphene (FLG), and three samples of GO with different degree of oxidation (Pelin et al. (2017)). Even though no significant effects were observed after 24 h, after 72 h the less oxidized compound (FLG) was the less cytotoxic, inducing mitochondrial and plasma-membrane damages with EC_{50s} of 62.8 μg/mL (WST-8 assay) and 45.5 μg/mL (propidium iodide uptake), respectively. The largest and most oxidized compound, was the most cytotoxic, inducing mitochondrial and plasma membrane damages with EC_{50} of 5.4 and 2.9 μg/mL, respectively. These results suggest that only high concentrations and long exposures to FLG and GOs could impair mitochondrial activity associated with plasma membrane damage, suggesting low cytotoxic effects at the skin level.

The number of studies on the impact of CBNMs when they are already introduced in a mammal (human) body are increasing in the recent decade. Currently, the literature is insufficient to draw definite conclusions about the potential hazards of CBNMs. Two opposite opinions have emerged: some researchers suggested that these materials are harmless and biocompatible while other studies reported adverse biological responses and cytotoxicity. For example, Zhang et al. (2010) proved that Gr and SWCNTs induced cytotoxic effects in human neural cells were concentration- and shape-dependent. On the contrary, Sasidharan et al. (2012) studied both pristine and functionalized Gr interactions with murine macrophage RAW 264.7 cells and human primary blood components. The study clearly suggested that the observed toxicity effects of pristine Gr towards macrophage cells can be easily averted by surface functionalization and that both the systems show excellent hemocompatibility.

Comprehensive reviews and summaries on the effect of CNMs on mammals (human cells, organs) are already available (Chen et al. (2018), Ou et al. (2016)).

At present, it is widely believed that the oxidative stress is one of most important toxicity mechanisms of CBNMs towards mammals/humans. Others toxicity mechanisms of CBNMs are destruction of cellular structures, mitochondrial damage, DNA damage, cell inflammatory response (inflammatory cell infiltration, pulmonary edema and granuloma formation at high doses via intratracheally instillation), apoptosis, autophagy, fibrosis, necrosis, epigenetics changes (DNA methylation, genomic imprinting, maternal effects, gene silencing, and RNA editing).

Various factors determine the toxicity of CBNMs to mamals, including the lateral size, surface structure, functionalization, charge, impurities, aggregations, etc.

Increasing number of studies on CBNMs toxicity to animals reveals that the problem is becoming more serious. For example, not only CNTs had toxic effect, but they could also contribute to intensification of the toxic effects of heavy metals presenting in the same environment. However, except the already mentioned studies on physicochemical factors influencing the CBNMs toxicity, more universal methodology needs to be established to study especially mammals / human toxicity, including observational criteria, parameters and selection of experimental methods, selection of cell lines for tests, period of exposure, the long-term changes and fate of CBNMs after entering the body or being taken up by cells, etc. (Ou et al. (2016)).

8 CONCLUSION

Examples provided in this chapter show that CBNMs can be useful in solving the worldwide problem of water pollution by heavy metals.

However, before trying to implement them at large scale some important issued have to be discussed and solved. Research is still needed for multi-component systems, where real waters (wastewater or potable water) are applied. Pilot-plant and large scale experiments both batch and in columns and fixed bed systems are necessary. Especially important in the last case is the selection of suitable supporting materials for nanoparticles. In order to be effective adsorbents in batch applications CBNMs are employed as a slurry, consisting of extremely small particles and additional separation process is needed to retain them. Membrane filtration could be one of the possible separation methods but further studies for developing the feasible separation are needed. Regeneration of loaded adsorbents, and especially their reusability without compromise with their effectiveness is still a challenge. Utilization or disposal of loaded and already inactivated adsorbent has to be thought of.

Commercialization of a technology depends on its raw ingredients' costs and quality. Cheaper and with a good quality CBNMs are economically viable for an industrial based water purification technology. The high cost of Gr-based materials and pure CNTs limits their industrial application. The inherent hydrophobicity of CNTs and the nanoparticles' natural tendency to aggregate in fluidized systems and preparation of CBNMs with predetermined properties represent an additional technological challenge needing solution.

Last, but probably the most important - not only removal of targeted metals needs to be studied but also eventual side reactions with CBNMs participation, by-products formation, as well as antagonistic and synergistic effects. Presence of CBNMs could potentially stimulate the oxidation of other metals and the release of toxic ions in aquatic environment. The behavior and fate of the nanomaterials in water and wastewater treatment

process and the impact of nanomaterials on the aquatic environment and human health have to be properly studied and fully understood before the application CBNMs in the real life.

9 REFERENCES

Ali I. (2018). Microwave assisted economic synthesis of multi walled carbon nanotubes for arsenic species removal in water: Batch and column operations. *J. Mol. Liq.*, **271**: 677–685.

Ali MEA. (2018). Synthesis and adsorption properties of chitosan-CDTA-GO nanocomposite for removal of hexavalent chromium from aqueous solutions. *Arab. J. Chem.*, **11**: 1107–1116.

Apostolović T, Tričković J, Šućurović A, Isakovski MK, Maletić S, Rončević S, Dalmacij B. (2018). Adsorption kinetics of divalent metals on amino-functionalized carbon nanomaterials. *Zastita Materijala*, **59**(2): 216-225.

Atieh MA, Bakather OY, Tawabini BS, Bukhari AA, Khaled M, Alharthi M, Fettouhi M, Abuilaiwi FA. (2010). Removal of chromium(III) from water by using modified and nonmodified carbon nanotubes. *J. Nanomater.,* Article ID 232378, 9 pp.

Atieh MA. (2011). Removal of Chromium (VI) from polluted water using carbon nanotubes supported with activated carbon. *Proc. Environ. Sci*., **4**: 281–293.

Awad FS, Abou-Zeid KM, El-Maaty WMA, El-Wakil AM, El-Shall MS. (2017). Efficient Removal of Heavy Metals from Polluted Water with High Selectivity for Mercury(II) by 2-Imino-4-thiobiuret–Partially Reduced Graphene Oxide (IT-PRGO). *ACS Appl. Mater. Inter.*, **9**: 34230- 34242.

Ayawei N., Ebelegi AN, Wankasi D. (2017). Modelling and Interpretation of Adsorption Isotherms. *Hindawi J. Chem.*, Article ID 3039817, 11 pages.

Bandaru NM, Reta N, Dalal H, Ellis AV, Shapter J, Voelcker NH. (2013). Enhanced adsorption of mercury ions on thiol derivatized single wall carbon nanotubes. *J. Hazard. Mater.,* **261**: 534–541.

Benjwal P, Kar KK. (2015). Simultaneous photocatalysis and adsorption based removal of inorganic and organic impurities from water by titania/activated carbon/carbonized epoxy nanocomposite. *J. Environ.Chem. Eng.,* **3**: 2076–2083.

Bhunia P, Kim G, Baik C, Lee H. (2012). A strategically designed porous iron–iron oxide matrix on graphene for heavy metal adsorption. *Chem. Commun.,* **48**: 9888–9890.

Cao KT, Jiang ZY, Zhao J, Zhao CH, Gao CY, Pan FS, Wang BY, Cao XZ, Yang J. (2014). Enhanced water permeation through sodium alginate membranes by incorporating graphene oxides. *J. Membr. Sci.,* **469**: 272–283.

Carpio IEM, Mangadlao JD, Nguyen HN, Advincula RC, Rodrigues DF. (2014). Graphene oxide functionalized with thylenediamine triacetic acid for heavy metal adsorption and anti-microbial applications. *Carbon*, **77**: 289–301.

Chandra V, Kim KS. (2011). Highly selective adsorption of Hg^{2+} by a polypyrrole–reduced graphene oxide composite. *Chem. Commun.,* **47**(13): 3942–3944 .

Chandra V, Park J, Chun Y, Lee JW, Hwang IC, Kim KS. (2010). Water-dispersible magnetite-reduced graphene oxide composites for arsenic removal. *ACS Nano*, **4**(7): 3979–3986.

Chauke VP, Maity A, Chetty A. (2015). High-performance towards removal of toxic hexavalent chromium from aqueous solution using graphene oxide-alpha cyclodextrin-polypyrrole nanocomposites. *J. Mol. Liq.,* **211**: 71-77.

Chen CL, Hu J, Shao DD, Li JX, Wang XK. (2009). Adsorption behavior of multiwall carbon nanotube/iron oxide magnetic composites for Ni(II) and Sr(II). *J. Hazard. Mater.*, **164**: 923–928.

Chen CL, Wang XK. (2006). Adsorption of Ni(II) from aqueous solution using oxidized multiwall carbon nanotubes. *Ind. Eng. Chem. Res*., **45**: 9144–9149.

Chen H, Li J, Shao D, Ren X, Wang X. (2012). Poly(acrylic acid) grafted multiwall carbon nanotubes by plasma techniques for Co(II) removal from aqueous solution. *Chem. Eng. J.,* **210**: 475–481.

Chen JH, Xing HT, Sun X, Su ZB, Huang YH, Weng W, Hu SR, Guo HX, Wu WB, He YS. (2015). Highly effective removal of Cu(II) by triethylenetetramine-magnetic reduced graphene oxide composite. *Appl. Surf. Sci.,* **356**: 355-363.

Chen L, Chen N, Wu H, Li W, Fang Z, Xu Z, Qian X. (2018). Flexible design of carbon nanotubes grown on carbon nanofibers by PECVD for enhanced Cr(VI) adsorption capacity. *Sep. Purif. Technol.*, **207**: 406–415.

Chen M, Zhou S, Zhu Y, Sun Y, Zeng G, Yang C, Xu P, Yan M, Liu Z, Zhang W. (2018). Toxicity of carbon nanomaterials to plants, animals and microbes: Recent progress from 2015-present. *Chemosphere*, **206**: 255-264.

Cheng J, Flahaut E, Cheng SH. (2007). Effect of carbon nanotubes on developing zebrafish (Danio rerio) embryos. *Environ. Toxicol. Chem.,* **26**(4): 708–716.

Chiu PL, Mastrogiovanni DDT, Wei D, Louis C, Jeong M, Yu G, Saad P, Flach CR, Mendelsohn R, Garfunkel E, He H. **(**2012). Microwave- and Nitronium Ion-Enabled Rapid and Direct Production of Highly Conductive Low-Oxygen Graphene. *J. Am. Chem. Soc.*, **134**(13): 5850-5856.

Chowdhury S, Balasubramanian R. (2014). Recent advances in the use of graphene-family nanoadsorbents for removal of toxic pollutants from wastewater. *Adv. Colloid. Interfac.*, **204**: 35–56.

CSIRO (Commonwealth Scientific and Industrial Research Organization). (2012). *Guide, Safe handling and use of carbon nanotubes*, Canberra, Australia.

Cui L, Wang Y, Gao L, Hu L, Yan L, Wei Q, Du B. (2015). EDTA functionalized magnetic graphene oxide for removal of Pb(II), Hg(II) and Cu(II) in water treatment: Adsorption mechanism and separation property. *Chem. Eng. J.*, **281**: 1–10.

Das R. (2017) *Nanohybrid Catalyst based on Carbon Nanotube (A Step-By-Step Guideline from Preparation to Demonstration)*, Springer International Publishing AG, DOI 10.1007/978-3-319-58151-4_2.

De la Luz-Asunción M, Pérez-Ramírez EE, Martínez-Hernández AL, Castano VM, Sánchez-Mendieta V, Velasco-Santos C. (2018). Non-linear modeling of kinetic and equilibrium data for the adsorption of hexavalent chromium by carbon nanomaterials: Dimension and functionalization, *Chin. J. Chem. Eng*., https://doi.org/10.1016/j.cjche.2018.08.024

Di ZC, Ding J, Peng XJ, Li YH, Luan ZK, Liang J. (2006). Chromium adsorption by aligned carbon nanotubes supported ceria nanoparticles, *Chemosphere*, **62**: 861–865.

Di ZC, Li YH, Luan ZK, Liang J. (2004). Adsorption of chromium (VI) ions from water by carbon nanotubes. *Adsorpt. Sci. Technol*., **22**: 467–474.

Directive 2013/39/EU of the European Parliament and of the Council of 12 August 2013 amending Directives 2000/60/EC and 2008/105/EC as regards priority substances in the field of water policy (Text with EEA relevance), *Official J. of the EU*, L 226/1, 24.8.2013**.**

Dong Z, Wang D, Liu X, Pei X, Chen L, Jin J. (2014). Bio-inspired surfacefunctionalization of graphene oxide for the adsorption of organic dyes and heavy metal ions with a superhigh capacity. *J. Mater. Chem.,* **A2:** 5034–5040.

Duffus JH. (2002). Heavy metals - a meaningless term? (IUPAC Technical Report). *Pure Appl. Chem.*, **74(5)**: 793–807.

Fan L, Luo C, Sun M, Li X, Qiu H. (2013). Highly selective adsorption of lead ions by water-dispersible magnetic chitosan/graphene oxide composites. *Colloids Surf*., **B103**: 523–529.

Fang F, Kong L, Huang J, Wu S, Zhang K, Wang X, Sun B, Jin Z, Wang J, Huang XJ, Liu J. (2014). Removal of cobalt ions from aqueous solution by an amination graphene oxide nanocomposite. *J. Hazard. Mater*., **270**: 1-10.

Farid MU, Luan HY, Wang Y, Huang H, An AK, Khan RJ. (2017). Increased adsorption of aqueous zinc species by Ar/O_2 plasma-treated carbon nanotubes immobilized in hollow-fiber ultrafiltration membrane. *Chem. Eng. J.*, **325**: 239–248.

Felix LC, Ede JD, Snell DA, Oliveira TM, Martinez-Rubi Y, Simard B, Luong JHT, Goss GG. (2016). Physicochemical properties of functionalized carbon-based nanomaterials and their toxicity to fishes. *Carbon N. Y.* **104**:78–89.

Freixa A, Acuña V, Sanchís J, Farré M, Barcelób D, Sabater S. (2018). Ecotoxicological effects of carbon based nanomaterials in aquatic organisms. *Sci. Total Environ.,* **619–620**: 328–337.

Fu W, Huang Z. (2018). Magnetic dithiocarbamate functionalized reduced graphene oxide for the removal of Cu(II), Cd(II), Pb(II), and Hg(II) ions from aqueous solution: Synthesis, adsorption, and regeneration. *Chemosphere*, **209**: 449-456.

Gadhave A, Waghmare J. (2014). Removal of heavy metal ions from wastewater by carbon nanotubes (CNTs). *Int. J. Chem. Sci. Applications*, **5(2)**: 56-67.

Ge H, Ma Z. (2015). Microwave preparation of triethylenetetramine modified graphene oxide/chitosan composite for adsorption of Cr(VI). *Carbohydr. Polym*., **131**: 280-287.

Ge Y, Li Z, Xiao D, Xiong P, Ye N. (2014). Sulfonated multi-walled carbon nanotubes for the removal of copper(II) from aqueous solutions. *J. Ind. Eng. Chem*., **20**: 1765–1771.

Guo X, Du B, Wei Q, Yang J, Hu L, Yan L, Xu W. (2014). Synthesis of amino-functionalized magnetic graphenes composite material and its application to remove Cr(VI), Pb(II), Hg(II), Cd(II) and Ni(II) from contaminated water. *J. Hazard. Mater*., **278**: 211–220.

Gupta A, Vidyarthi SR, Sankararamakrishnan N. (2014). Enhanced sorption of mercury from compact fluorescent bulbs and contaminated water streams using functionalized multiwalled carbon nanotubes, *J. Hazard. Mater.*. **274**: 132–144.

Hadavifar M., Bahramifar N, Younesi H, Rastakhiz M, Li Q, Yu J, Eftekhari E. (2016). Removal of mercury(II) and cadmium(II) ions from synthetic wastewater by a newly synthesized amino and thiolated multi-walled carbon nanotubes. *J. Taiwan Inst. Chem. Eng.,* **67**: 397–405.

Hadavifar M., Bahramifar N., Younesi H., Li Q. (2014). Adsorption of mercury ions from synthetic and real wastewater aqueous solution by functionalized multi-walled carbon nanotube with both amino and thiolated groups. *Chem. Eng. J.*, **237**: 217–228.

Hantel MM. (2013). *Graphite oxide and graphene oxide based electrode materials for electrochemical double layer capacitors*, Dr. Sci. Dissertation, ETH, Zurich.

Hao L, Song H, Zhang L, Wan X, Tang Y, Lv Y. (2012). SiO_2/graphene compos- ite for highly selective adsorption of Pb(II) ion. *J. Colloid. Interf. Sci*., **369**(1): 381–387 .

Hayati B, Maleki A, Najafi F, Daraei H, Gharibi F, McKay G. (2016). Synthesis and characterization of PAMAM/CNT nanocomposite as a super-capacity adsorbent for heavy metal (Ni^{2+}, Zn^{2+}, As^{3+}, Co^{2+}) removal from wastewater. *J. Mol. Liq.*, **224**: 1032–1040.

Hayati B, Maleki A, Najafi F, Gharibi F, McKay G, Gupta VK, Puttaiah SH, Marzban N. (2018). Heavy metal adsorption using PAMAM/CNT nanocomposite from

aqueous solution in batch and continuous fixed bed systems. *Chem. Eng. J.*, **346**: 258–270.

He C, Yang Z, Ding J, Chen Y, Tong X, Li Y. (2017). Effective removal of Cr(VI) from aqueous solution by 3-aminopropyltriethoxysilane-functionalized graphene oxide. *Colloids Surf. A: Physicochem. Eng. Asp*., **520**: 448–458.

Henriques B, Gonc AG, Emami N, Pereira E, Vila M, Marques PAAP. (2016). Optimized graphene oxide foam with enhanced performance and high selectivity for mercury removal from water. *J. Hazard. Mater.,* **301**: 453–461.

Hiew BYZ, Lee LY, Lee XJ, Gopakumar ST, Gan S, Lim SS, Pan GT, Yang TCK, Chiu WS, Khiew PS. (2018). Review on synthesis of 3D graphene-based configurations and their adsorption performance for hazardous water pollutants, *Process Saf. Environ.,* **116**: 262–286.

Hoan NTV, Thu NTA, Duc HV, Cuong ND, Khieu DQ, Vo V. (2016). Fe_3O_4/reduced graphene oxide nanocomposite: synthesis and its application for toxic metal ion removal. *J. Chem*., Article ID 2418172, 10 pages.

Hosseini SM, Amini SH, Khodabakhshi AR, Bagheripour E, Van der Bruggen B. (2018). Activated carbon nanoparticles entrapped mixed matrix polyethersulfone based nanofiltration membrane for sulfate and copper removal from water. *J. Taiwan Inst. Chem. Eng.,* **82**: 169–178.

Hosseinzadeh H, Ramin S. (2018). Effective removal of copper from aqueous solutions by modified magnetic chitosan/graphene oxide nanocomposites, *Int. J. Biol. Macromol.*, **113**: 859–868.

Hu J, Chen C, Zhu X, Wang X. (2009). Removal of chromium from aqueous solution by using oxidized multiwalled carbon nanotubes. *J. Hazard. Mater.,* **162**(2-3): 1542–1550.

Hu J, Wang SW, Shao DD, Dong YH, Li JX, Wang XK. (2009). Adsorption and Reduction of Chromium(VI) from Aqueous Solution by Multiwalled Carbon Nanotubes. *Open Environ. Pollut & Toxicol J.,* **1**: 66-73.

Hu Xj, Liu Yg, Wang H, Chen Aw, Zeng Gm, Liu Sm, Guo Ym, Hu X, Li Tt, Wang Yq, Zhou L, Liu Sh. (2013). Removal of Cu(II) ions from aqueous solution using sulfonated magnetic graphene oxide composite. *Sep. Purif. Technol.,* **108**: 189-195.

Hu Z, Qin S, Huang Z, Zhu Y, Xi L, Li Z. (2017). Stepwise synthesis of graphene oxide-wrapped magnetic composite and its application for the removal of Pb(II). *Arab. J. Sci. Eng.,* **42**: 4239-4247.

Huang Z-n, Wang X-l, Yang D-s. (2015). Adsorption of Cr(VI) in wastewater using magnetic multi-wall carbon nanotubes. *Water Sci. Eng.,* **8**(3): 226-232.

Ihsanullah FAAK, Abusharkh B, Khaled M, Atieh MA, Nasser MS, Laoui T, Agarwal S, Tyagi I. Gupta VK. (2015). Adsorptive removal of cadmium(II) ions from liquid phase using acid modified carbon-based adsorbents. *J. Mol. Liq.,* **204**: 255–263.

Jabeen H, Chandra V, Jung S, Lee JW, Kim KS, Kim SB. (2011). Enhanced Cr(VI) removal using iron nanoparticle decorated graphene. *Nanoscale*, **3**: 3583-3585.

Jassal, V., Shanker, U., Gahlot, S. Green synthesis of some iron oxide nanoparticles and their interaction with 2-amino, 3-amino and 4-aminopyridines. Mater. Today Proc. 2016a, 3, 1874–1882.

Jassal, V., Shanker, U., Gahlot, S., Kaith, B. S., Kamaluddin, Md. A. I., Samuel, P. (2015a) Sapindus mukorossi mediated green synthesis of some manganese oxide nanoparticles interaction with aromatic amines. Applied Physics A., 122, 271–282.

Jassal, V., Shanker, U., Kaith, B. S. (2016b) Aegle marmelos mediated green synthesis of different nano-structured metal hexacyanoferrates: Activity against photodegradation of harmful organic dyes. Scientifica., 1–13.

Jassal, V., Shanker, U., Kaith, B. S., Shankar, S. (2015b), Green synthesis of potassium zinc hexacyanoferrate nanocubes and their potential application in photocatalytic degradation of organic dyes. RSC Adv., 5, 26141–26149.

Jassal, V., Shanker, U., Shankar, S. Synthesis, characterization and applications of nano- structured metal hexacyanoferrates. J. Environ. Anal. Chem. 2015c, 2, 1000128–1000141.

Jain M, Yadav M, Kohout T, Lahtinen M, Garg VK, Sillanpää M. (2018). Development of iron oxide/activated carbon nanoparticle composite for the removal of Cr(VI), Cu(II) and Cd(II) ions from aqueous solution. *Water.Resour.Ind.*, **20**: 54–74.

Joner EJ, Hartnik T. Eds. (2007). *Norwegian Pollution Control Authority (2008) Environmental fate and ecotoxicity of engineered nanoparticles. Report no. TA 2304/2007.* Amundsen. Bioforsk, Ås. 64 pp.

Jung C, Heo J, Han J, Her N, Lee SJ, Oh J, Ryu J, Yoon Y. (2013). Hexavalent chromium removal by various adsorbents: Powered activated carbon, chitosan and single/multi-walled carbon nanotubes. *Sep. Purif. Technol.*, **106**: 63-71.

Kabbashi NA, Atieh MA, Mamun AA, Mirghami MES, Alam MDZ, Yahya N. (2009). Kinetic adsorption of application of carbon nanotubes for Pb(II) removal from aqueous solution. *J. Environ. Sci.,* **21**: 539–544.

Kabiri S, Tran DNH, Azari S, Losic D. (2015). Graphene-diatom silica aerogels for efficient removal of mercury ions from water. *ACS Appl. Mater. Inter.*, **7**:11815–11823.

Kabiri S, Tran DNH, Cole MA, Losic D. (2016). Functionalized thre-dimensional (3D) graphene composite for high efficiency removal of mercury. *Environ Sci: Water Res. Technol*., **2**: 390-402.

Kandah MI, Meunier J. (2007). Removal of nickel ions from water by multi-walled carbon nanotubes. *J. Hazard. Mater.,* **146**: 283–288.

Kapinder DM, Verma AK. (2017). Exploiting the Potential of Nanotechnological Applications in Rural Areas to Effectively Eliminate Pollutants from Water Bodies. *J. Pharm. Res.*, **11**(8): 943-950.

Kataria N, Garg VK. (2018). Green synthesis of Fe_3O_4 nanoparticles loaded sawdust carbon for cadmium (II) removal from water: Regeneration and mechanism. *Chemosphere*, **208**: 818-828.

Khazaei M, Nasseri S, Ganjali MR, Khoobi M, Nabizadeh R, Gholibegloo E, Nazmara S. (2018). Selective removal of mercury(II) from water using a 2,2-dithiodisalicylic acid-functionalized graphene oxide nanocomposite: Kinetic, thermodynamic, and reusability studies. *J. Mol. Liq.*, **265**: 189–198.

Kosa SA, Al-Zhrani G, Salam MA. (2012). Removal of heavy metals from aqueous solutions by multi-walled carbon nanotubes modified with 8-hydroxyquinoline. *Chem. Eng. J.*, **181–182**: 159– 168.

Kumar ASK, Jiang SJ, Tseng WL. (2015). Effective adsorption of chromium(VI)/Cr (III) from aqueous solution using ionic liquid functionalized multiwalled carbon nanotubes as a super sorbent. *J. Mater. Chem.,* **A3**: 7044–7057.

Kumar PS, Venkatesh K, Gui EL, Sundaramurthy J, Singh G, Arthanareeswaran G. (2018). Electrospun carbon nanofibers/TiO_2-PAN hybrid membranes for effective removal of metal ions and cationic dye. *Environ. Nanotechnol., Monitor. & Manage.,* **10**: 366–376.

Kumar R, Ansari MO, Alshahrie A, Darwesh R, Parveen N, Yadav SK, Barakat MA, Cho MH. (2019). Adsorption modeling and mechanistic insight of hazardous chromium on para toluene sulfonic acid immobilized-polyaniline@CNTs nanocomposites. *J. Saudi Chem Soc.*, **23**(2): 188-197, https://doi.org/10.1016/j.jscs.2018.06.005

Kumar S, Nair RR, Pillai PB, Gupta SN, Iyengar MAR, Sood AK. (2014). Graphene oxide–$MnFe_2O_4$ magnetic Nanohybrids for efficient removal of lead and arsenic from water. *ACS Appl. Mater. Inter.*, **6**(20): 17426–17436.

Lee YC, Yang JWJ. (2012). Self-assembled flower-like TiO_2 on exfoliated graphite oxide for heavy metal removal. *J. Ind. Eng. Chem.*, **18**: 1178-1185.

Li JX, Chen SY, Sheng GD, Hu J, Tan XL, Wang XK. (2011). Effect of surfactants on Pb(II) adsorption from aqueous solutions using oxidized multiwall carbon nanotubes. *Chem. Eng. J.,* **166**: 551–558.

Li L, Fan LL, Sun M, Qiu H, Li X, Duan H, Luo CN. (2013). Adsorbent for chromium removal based on graphene oxide functionalized with magnetic cyclodextrin–chitosan. *Colloids Surf. B: Biointerfaces*, **107**: 76–83.

Li L, Luo C, Li X, Duan H, Wang X. (2014). Preparation of magnetic ionic liquid/chitosan/graphene oxide composite and application for water treatment. *Int. J. Biol. Macromol*., **66**: 172-178.

Li W, Gao S, Wu L, Qiu S, Guo Y, Geng X, Chen M, Liao S, Zhu C, Gong Y, Long M, Xu J, Wei X, Sun M, Liu L. (2013). High-Density Three-Dimension Graphene Macroscopic Objects for High-Capacity Removal of Heavy Metal Ions. *Sci. Rep.-UK*, **3**: 2125 | DOI: 10.1038/srep02125.

Li X, Ai L, Jiang J. (2016). Nanoscale zerovalent iron decorated on graphenenanosheets for Cr(VI) removal from aqueous solution: surface corrosion retardinduced the enhanced performance. *Chem. Eng. J.*, **288**: 789–797.

Li X, Zhang G, Bai X, Sun X, Wang X, Wang E, Dai H. (2008). Highly conducting graphene sheets and Langmuir–Blodgett films. *Nat. Nanotechnol.*, **3**: 538–542.

Li X, Zhou H, Wu W, Wei S, Xu Y, Kuang Y. (2015). Studies of heavy metal ion adsorption on Chitosan/Sulfydryl-functionalized graphene oxide composites, *J. Colloid Interf. Sci.,* **448**: 389-397.

Li YH, Di Z, Ding J, Wu D, Luan Z, Zhu Y. (2005). Adsorption thermodynamics, kinetic and desorption studies of Pb^{2+} on carbon nanotubes. *Water Res.,* **39**: 605–609.

Li YH, Ding J, Luan Z, Di Z, Zhu Y, Xu C, Wu D, Wei B. (2003). Competitive adsorption of Pb, Cu and Cd ions from aqueous solutions by multiwalled carbon nanotubes. *Carbon*, **41**: 2787–2792.

Li YH, Liu FQ, Xia B, Du QJ, Zhang P, Wang DC, Wang ZH, Xia YZ. (2010). Removal of copper from aqueous solution by carbon nanotube/calcium alginate composites. *J. Hazard. Mater.,* **177**: 876–880.

Li YH, Luan Z, Xiao X, Zhou X, Xu C, Wu D, Wei B. (2003). Removal of Cu^{2+} ions from aqueous solutions by carbon nanotubes. *Adsorpt. Sci. Technol.,* **21**: 475–485.

Li YH, Wang S, Luan Z, Ding J, Xu C, Wu D. (2003). Adsorption of cadmium(II) from aqueous solution by surface oxidized carbon nanotubes. *Carbon*, **41**: 1057–1062.

Li YH, Wang S, Wei J, Zhang X, Xu C, Luan Z, Wu D, Wei B. (2002). Lead adsorption on carbon nanotubes. *Chem. Phys. Lett.*, **357**: 263–266.

Liang J, Liu J, Yuan X, Dong H, Zeng G, Wu H, Wang H, Liu J, Hua S, Zhang S, Yu Z, He X, He Y. (2015). Facile synthesis of alumina-decorated multi-walled carbon nanotubes for simultaneous adsorption of cadmium ion and trichloroethylene. *Chem. Eng. J.*, **273**: 101–110.

Lingamdinne LP, Kim IS, Ha JH, Chang YY, Koduru JR, Yang JK. (2017). Enhanced Adsorption Removal of Pb(II) and Cr(III) by Using Nickel Ferrite-Reduced Graphene Oxide Nanocomposite. *Metals*, **7**: 225, doi:10.3390/met7060225, 5 pp.

Lingamdinne LP, Koduru JR, Roh H, Choi YL, Chang YY, Yang JK. (2016). Adsorption removal of Co(II) from waste-water using graphene oxide. *Hydrometallurgy*, **165**: 90–96.

Liu J, Ge X, Ye X, Wang G, Zhang H, Zhou H, Zhang Y, Zhao H. (2016). 3D graphene/d-MnO_2 aerogels for highly efficient and reversible removal of heavy metal ions. *J. Mater. Chem*., **A4**: 1970–1979.

Liu W, Jiang J, Wang H, Deng C, Wang F, Peng G. (2016). Influence of graphene oxide on electrochemical performance of Si anode material for lithium-ion batteries. *J. Energy Chem.,* **25**: 817–824.

Liu X, Huang Y, Duan S, Wang Y, Li J, Chen Y, Hayat T, Wang X. (2016). Graphene oxides with different oxidation degrees for Co(II) ion pollution management. *Chem. Eng. J*., **302**: 763-772.

Liu Y, Xu L, Liu J, Liu X, Chen C, Li G, Meng Y. (2016). Graphene oxides cross-linked with hyperbranched polyethylenimines: Preparation, characterization and their potential as recyclable and highly efficient adsorption materials for lead(II) ions. *Chem. Eng. J.,* **285**: 698-708.

Liu Z, Chen L, Zhang Z, Li Y, Dong Y, Sun Y. (2013). Synthesis of multi-walled carbon nanotube–hydroxyapatite composites and its application in the sorption of Co(II) from aqueous solutions. *J. Mol. Liq*., **179**: 46–53.

Lu C, Chiu H. (2006). Adsorption of zinc(II) from water with purified carbon nanotubes. *Chem. Eng. Sci.,* **61**: 1138–1145.

Lu C, Liu C, Rao GP. (2008). Comparisons of sorbent cost for the removal of Ni^{2+} from aqueous solution by carbon nanotubes and granular activated carbon, *J. Hazard. Mater.* **151**: 239–246.

Lu CY, Liu CT, Su FS. (2009). Sorption kinetics, thermodynamics and competition of Ni^{2+} from aqueous solutions onto surface oxidized carbon nanotubes. *Desalination*, **249**: 18–23.

Luedtke, A. (2019). Applications of graphene oxide and reduced graphene oxide, (accessed on 15 January 2019) http://www.sigmaaldrich.com/technical-documents/articles/technology-spotlights/graphene-oxide.html

Luo C, Wei R, Guo D, Zhang S, Yan S. (2013). Adsorption behavior of MnO_2 functionalized multi-walled carbon nanoubes for the removal of cadmium from aqueous solutions. *Chem. Eng. J.*, **225**: 406-415.

Ma L, Zhang YW, Hu QH, Yan D, Yu ZZ, Zhai M. (2012). Chemical reduction and removal of Cr(VI) from acidic aqueous solution by ethylenediamine-reduced graphene oxide. *J. Mater. Chem.,* **22**: 5914–5916.

Ma MD, Wu H, Deng ZY, Zhao X. (2018). Arsenic removal from water by nanometer iron oxide coated single-wall carbon nanotubes. *J. Mol. Liq.*, **259**: 369–375.

Madadrang CJ, Kim HY, Gao GH, Wang N, Zhu J, Feng H, Gorrings M, Kasner ML, Hou S. (2012). Adsorption behavior of EDTA-graphene oxide for Pb (II) removal. *ACS Appl. Mater. Inter*., **4**: 1186–1193.

Mahmoud M, Ramadan AR, Esawi AMK. (2017). A Study on the Modification of Cellulose Acetate Membranes with Graphene Oxide Nanofillers for Water Treatment. *Proceedings of the Nanotech France 2017 International Conference Paris*, France, DOI: https://doi.org/10.26799/cp-nanotechfrance2017.10, 1-6.

Mahmoudian M, Kochameshki MG, Hosseinzadeh M. (2018). Modification of graphene oxide by ATRP: A pH-responsive additive in membrane for separation of salts, dyes and heavy metals. *J. Environ. Chem. Eng.,* **6**: 3122–3134.

McNaught AD, Wilkinson A. (1997). *IUPAC. Compendium of Chemical Terminology, 2nd ed. (the "Gold Book"),* Blackwell Scientific Publications: Oxford, XML on-line corrected version: https://doi.org/10.1351/goldbook.G02683 (accessed on 15 January, 2019).

MEA - Millennium Ecosystem Assessment. (2005). *Concepts of Ecosystem Value and Valuation Approaches*, Island Press, Washington DC.

Mi X, Huang G, Xie W, Wang W, Liu Y, Gao J. (2012). Preparation of graphene oxide aerogel and its adsorption for Cu^{2+} ions. *Carbon*, **50**(13): 4856–4864.

Mishra AK, Ramaprabhu S. (2011). Functionalized graphene sheets for arsenic removal and desalination of sea water. *Desalination*, **282**: 39–45.

Moghaddam HK, Pakizeh M. (2015). Experimental study on mercury ions removal from aqueous solution by MnO_2/CNTs nanocomposite adsorbent. *J. Indus. Eng. Chem*., **21**: 221–229.

Moradi O. (2011). The removal of ions by functionalized carbon nanotube: equilibrium, isotherms and thermodynamic studies. *Chem. Biochem. Eng. Quart*., **25**: 229–240.

Mortazavian S, An H, Chun D, Moon J. (2018). Activated carbon impregnated by zero-valent iron nanoparticles (AC/nZVI) optimized for simultaneous adsorption and reduction of aqueous hexavalent chromium: Material characterizations and kinetic studies. *Chem. Eng. J.*, **353**: 781–795.

Moustafa YM, Morsi RE, Fathy M. (2014). Mercury Removing Capacity of Multiwall Carbon Nanotubes as Detected by Cold Vapor Atomic Absorption Spectroscopy: Kinetic and Equilibrium Studies. *Int. J. Chem., Molec., Nucl., Mater. Metallurg Eng.,* **8**(7): 724-730.

Mubarak NM, Alicia RF, Abdullah EC, Sahu JN, Haslija ABA, Tan J. (2013). Statistical optimization and kinetic studies on removal of Zn^{2+} using functionalized carbon nanotubes and magnetic biochar. *J. Environ. Chem. Eng.,* **1**: 486–495.

Mubarak NM, Sahu JN, Abdullah EC, Jayakumar NS, Ganesan P. (2015). Microwave assisted multiwall carbon nanotubes enhancing Cd(II) adsorption capacity in aqueous media. *J. Ind. Eng. Chem.*, **24**: 24-33.

Mubarak NM, Sahu JN, Abdullah EC, Jayakumar NS. (2016). Rapid adsorption of toxic Pb(II) ions from aqueous solution using multiwall carbon nanotubes synthesized by microwave chemical vapor deposition technique. *J. Environ. Sci.*, **45**: 143-155.

Mubarak NM, Sahu JN, Abdullahd EC, Jayakumar NS, Ganesan P. (2015). Novel microwave-assisted multiwall carbon nanotubes enhancing Cu (II) adsorption capacity in water. *J. Taiwan Inst. Chem. Eng.,* **53**: 140–152.

Mukherjee R, Bhunia P, De S. (2016). Impact of graphene oxide on removal of heavy metals using mixed matrix membrane, *Chem. Eng. J.*, **292**: 284–297.

Musico YLF, Santos CM, Lourdes M, Dalida P, Rodrigues DF. (2013). Improved removal of lead(II) from water using a polymer-based graphene oxide nanocomposite. *J. Mater. Chem.*, **A1**: 3789–3796.

Najafi F., Moradi O, Rajabi M, Asif M, Tyagi I, Agarwal S, Gupta VK. (2015). Thermodynamics of the adsorption of nickel ions from aqueous phase using graphene oxide and glycine functionalized graphene oxide. *J. Mol. Liq.*, **208:** 106–113.

Ntim S., Mitra S. (2012). Adsorption of arsenic on multiwall carbon nanotube– zirconia nanohybrid for potential drinking water purification. *J. Colloid Interf. Sci.*. **375**: 154–159.

Ntim SA, Mitra S. (2011). Removal of trace arsenic to meet drinking water standards using iron oxide coated multiwall carbon nanotubes. *J. Chem. Eng. Data*. **56**: 2077–2083.

Oliveira ARL. (2016). *Heavy Metal Ions Removal from Aqueous Solutions by Multiwalled Carbon Nanotubes*, Dept. of Chem. Eng., Faculty of Science and Technology, University of Coimbra, Portugal.

Ou L, Song B, Liang H, Liu J, Feng X, Deng B, Sun T, Shao L. (2016). Toxicity of graphene-family nanoparticles: a general review of the origins and mechanisms. *Part. Fibre Toxicol.*, **13**:57, 24 pp.

Pan M, Wu G, Liu C, Lin X, Huang X. (2018). Enhanced Adsorption of Zn(II) onto Graphene Oxides Investigated Using Batch and Modeling Techniques. *Nanomaterials*, **8**(10): E806, 13 pp, doi:10.3390/nano8100806

Parham H, Bates S, Xia Y, Zhu Y. (2013) A highly efficient and versatile carbon nanotube/ceramic composite filter. *Carbon*. **54**: 215–223.

Pei H, Wang J, Yang Q, Yang W, Hu N, Suo Y, Zhang D, Li Z, Wang J. (2018). Interfacial growth of nitrogen-doped carbon with multi-functional groups on the MoS_2 skeleton for efficient Pb(II) removal. *Sci. Total Environ.,* **631–632**: 912–920.

Pelin M, Fusco L, León V, Martín C, Criado A, Sosa S, Vázquez E, Tubaro A, Prato M. (2017). Differential cytotoxic effects of graphene and graphene oxide on skin keratinocytes, *Sci. Rep.-UK,* **7**: 40572 | DOI: 10.1038/srep40572, 12 pp.

Peng W, Li H, Liu Y, Song S. (2016). Comparison of Pb(II) adsorption onto graphene oxide prepared from natural graphites: Diagramming the Pb(II) adsorption sites. *Appl. Surf. Sci.,* **364**: 620–627.

Peng X, Luan Z, Ding J, Zechao D, Li Y, Tian B. (2005). Ceria nanoparticles supported on carbon nanotubes for the removal CeO_2-CNTs) of arsenate from water. *Mater. Lett.*, **59**: 399–403.

Petnikota S, Marka SK, Banerjee A, Reddy MV, Srikanth VVSS, Chowdari BVR. (2015). Graphenothermal reduction synthesis of 'exfoliated graphene oxide/iron (II)

oxide' composite for anode application in lithium ion batteries. *J. Power Sources*, **293**: 253-263.

Pillay K, Cukrowska EM, Coville NJ. (2013). Improved uptake of mercury by sulphur-containing carbon nanotubes. *Microchem. J*., **108**: 124–130.

Poh HL, Šaněk F, Ambrosi A, Zhao G, Sofer Z, Pumera M. (2012). Graphenes prepared by Staudenmaier, Hofmann and Hummers methods with consequent thermal exfoliation exhibit very different electrochemical properties. *Nanoscale*, **4**(11), 3515-22.

Pourbeyram S. (2016). Effective removal of heavy metals from aqueous solutions by graphene oxide–zirconium phosphate (GO–Zr-P) nanocomposite. *Ind. Eng. Chem. Res.,* **55**: 5608–5617.

Pretti C, Oliva M, Di Pietro R, Monni G, Cevasco G, Chiellini F, Pomelli C, Chiappe C. (2014). Ecotoxicity of pristine graphene to marine organisms. *Ecotoxicol. Environ. Saf.,* **101**: 138–145.

Qiu Y.W. (2015). Bioaccumulation of heavy metals both in wild and mariculture food chains in Daya Bay, South China. *Estuar. Coast. Shelf S.*, **163, Part B**: 7-14.

Ren L, Lin H, Meng F, Zhang F. (2018). One-step solvothermal synthesis of Fe_3O_4@Carbon composites and their application in removing of Cr (VI) and Congo red. *Ceram. Int.,* https://doi.org/10.1016/j.ceramint.2018.11.132

Ren XM, Shao DD, Zhao GX, Sheng GD, Hu J, Yang ST, Wang XK. (2011). Plasma induced multiwalled carbon nanotube grafted with 2-vinylpyridine for preconcentration of Pb(II) from aqueous solutions. *Plasma Process Polym*. **8**: 589–598.

Ruparelia J.P., Duttagupta S.P., Chatterjee A.K., Mukherji S. (2008). Potential of carbon nanomaterials for removal of heavy metals from water. *Desalination*, **232**(1):145-156.

Sadegh H, Ali GAM, Makhlouf ASH, Chong KF, Alharbi NS, Agarwal S, Gupta VK. (2018). MWCNTs-Fe_3O_4 nanocomposite for Hg(II) high adsorption efficiency. *J. Mol. Liq.*, **258**: 345–353.

Sahraei R, Sekhavat-Pour Z., Ghaemy M. (2017). Novel magnetic bio-sorbent hydro-gel beads based on modified gum tragacanth/graphene oxide: removal of heavymetals and dyes from water. *J. Clean. Prod.*, **142**(4): 2973–2984.

Salam MA, Makki MSI, Abdelaal MYA. (2011). Preparation and characterization of multi-walled carbon nanotubes/chitosan nanocomposite and its application for the removal of heavy metals from aqueous solution. *J. Alloys Comp*., **509**: 2582–2587.

Salam MA. (2013). Removal of heavy metal ions from aqueous solutions with multi-walled carbon nanotubes: Kinetic and thermodynamic studies. *Int. J. Environ. Sci. Technol.,* **10**: 677–688.

Samuel MS, Shah SS, Subramaniyan V, Qureshi T, Bhattacharya J, Singh NDP. (2018). Preparation of graphene oxide/chitosan/ferrite nanocomposite for Chromium(VI) removal from aqueous solution. *Int. J. Biol. Macromol.,* **119**: 540–547.

Sankararamakrishnan N, Jaiswal M, Verma N. (2014). Composite nanofloral clusters of carbon nanotubes and activated alumina: An efficient sorbent for heavy metal removal. *Chem. Eng. J.*, **235**: 1-9.

Sasidharan A, Panchakarla LS, Sadanandan AR, Ashokan A, Chandran P, Girish CM, Menon D, Nair SV, Rao CNR, Koyakutty M. (2012). Hemocompatibility and Macrophage Response of Pristine and Functionalized Graphene. *Small*, **8**(8): 1251-1263.

Shah P, Murthy CN. (2013). Studies on the porosity control of MWCNT/polysulfone composite membrane and its effect on metal removal. *J. Membr. Sci.,* **437**: 90–98.

Shahzad HK, Hussein MA, Patel F, Al-Aqeeli N, Atieh MA, Laoui T. (2018). Synthesis and characterization of alumina-CNT membrane for cadmium removal from aqueous solution. *Ceram. Int.*, **44**: 17189–17198.

Shawky HA, Aassar AHME, Zeid DEA. (2012). Chitosan/carbon nanotube composite beads: preparation, characterization, and cost evaluation for mercury removal from wastewater of some industrial cities in Egypt. *J. Appl. Polym. Sci*., **125**: E93–E101.

Sheikh AHE, Degs YSA, Asad RMA, Sweileh JA. (2011). Effect of oxidation and geometrical dimensions of carbon nanotubes on Hg(II) sorption and preconcentration from real waters. *Desalination*, **270**: 214–220.

Sheng G, Li J, Shao D, Hu J, Chen C, Chen Y, Wang X. (2010). Adsorption of copper(II) on multiwalled carbon nanotubes in the absence and presence of humic or fulvic acids. *J. Hazard. Mater.,* **178**: 333–340.

Sitko R, Turek E, Zawisza B, Malicka E, Talik E, Heimann J, Gagor A, Feist B, Wrzalik R, (2013). Adsorption of divalent metal ions from aqueous solutions using graphene oxide. **Dalton Trans.**, **42**: 5682-5689.

Sitko, R., Musielak, M., Zawisza, B., Coik, E., Gagor, A. (2016). Graphene oxide/cellulose membranes in adsorption of divalent metal ions. *RSC Adv.* **6**: 96595–96605.

Souza JP, Baretta JF, Santos F, Paino IMM, Zucolotto V. (2017). Toxicological effects of graphene oxide on adult zebrafish (Danio rerio). *Aquat. Toxicol.*, **186**:11–18.

Sreeprasad TS, Maliyekkal SM, Lisha KP, Pradeep T. (2011). Reduced graphene oxide–metal/metal oxide composites: facile synthesis and application in water purification. *J. Hazard Mater.,* **186**(1): 921–31.

Stafiej A, Pyrzynska K. (2007). Adsorption of heavy metal ions with carbon nanotubes. *Sep. Purif. Technol.*, **58**: 49–52.

Su H, Ye Z, Hmidi N. (2017). High-performance iron oxide–graphene oxide nanocomposite adsorbents for arsenic removal. *Colloids Surf. A: Physicochem. Eng. Asp.*, **522**: 161–172.

Sui N, Wang L, Wu X, Li X, Sui J, Xiao H, Liu M, Wan J, William WY. (2015). Polyethylenimine modified magnetic graphene oxide nanocomposites for Cu^{2+} removal. *RSC Adv*., **5**: 746-752.

Tan P, Sun J, Hu Y, Fang Z, Bi Q, Chen Y, Cheng J. (2015). Adsorption of Cu^{2+}, Cd^{2+} and Ni^{2+} from aqueous single metal solutions on graphene oxide membranes. *J. Hazard. Mater.,* **297**: 251-260.

Tang WW, Zeng GM, Gong JL, Liu Y, Wang XY, Liu YY, Liu ZF, Chen L, Zhang XR, Tu DZ. (2012). Simultaneous adsorption of atrazine and Cu(II) from wastewater by magnetic multi-walled carbon nanotube. *Chem. Eng. J*., **211**: 470–478.

Tawabini BS, Khaldi SFA, Khaled MM, Atieh MA. (2011). Removal of arsenic from water by iron oxide nanoparticles impregnated on carbon nanotubes. *J. Environ. Sci. Health A Toxic Hazard. Subst. Environ. Eng*., **46**: 215–223.

Thines RK, Mubarak NM, Nizamuddin S, Sahu JN, Abdullah EC, Ganesan P. (2017). Application potential of carbon nanomaterials in water and wastewater treatment: A review. *J. Taiwan Ins. Chem. Eng.,* **72**: 116–133.

Tian Y, Gao B, Morales VL, Wu L, Wang Y, Munoz-Carpena R, Cao C, Huang Q, Yang L. (2012). Methods of using carbon nanotubes as filter media to remove aqueous heavy metals. *Chem. Eng. J.*, **210**: 557-563.

Tofighy MA, Mohammadi T. (2011). Adsorption of divalent heavy metal ions from water using carbon nanotube sheets. *J. Hazard. Mater.,* **185**: 140–147.

Tofighy MA, Mohammadi T. (2015). Nickel ions removal from water by two different morphologies of induced CNTs in mullite pore channels as adsorptive membrane. *Ceram. Int*., **41**: 5464–5472.

USGS Water Science School, *https://water.usgs.gov/edu/earthhowmuch.html* (accessed on 17 January 2019).

Varma S, Sarode D, Wakale S, Bhanvase BA, Deosarkar MP. (2013). Removal of Nickel from Waste Water Using Graphene Nanocomposite. *Int. J. Chem. Phys. Sci. IJCPS,* **2**: 132-139.

Velickovic Z, Vukovic GD, Marinkovic AD, Moldovan MS, Grujic AAP, Uskokovic PS, Ristic MD. (2012). Adsorption of arsenate on iron(III) oxide coated ethylenediamine functionalized multiwall carbon nanotubes. *Chem. Eng. J*., **181**: 174–181.

Vilardi G, Mpouras T, Dermatas D, Verdone N, Polydera A, Palma LD. (2018). Nanomaterials application for heavy metals recovery from polluted water: The combination of nano zero-valent iron and carbon nanotubes. Competitive adsorption non-linear modeling. *Chemosphere*, **201**: 716-729.

Vilela D, Parmar J, Zeng Y, Zhao Y, Sanchez S. (2016). Graphene-based microbots for toxic heavy metal removal and recovery from water. *Nano Lett.,* **16**: 2860–2866.

Vu HC, Dwivedi AD, Le TT, Seo SH, Kim EJ, Chang YS. (2017). Magnetite graphene oxide encapsulated in alginate beads for enhanced adsorption of Cr(VI)and As(V) from aqueous solutions: role of crosslinking metal cations in pH control. *Chem. Eng. J.*, **307**: 220–229.

Vukovic GD, Marinkovic AD, Colic M, Ristic MD, Aleksic R, Grujic AAP, Uskokovic PS. (2010). Removal of cadmium from aqueous solutions by oxidized and ethylenediamine-functionalized multi-walled carbon nanotubes. *Chem. Eng. J.,* **157**: 238–248.

Vuković GD, Marinković AD, Škapin SD, Ristić MP, Aleksić R, Perić-Grujić AA, Uskoković PS. (2011). Removal of lead from water by amino modified multi-walled carbon nanotubes. *Chem. Eng. J.*, **173**: 855– 865.

Wang H, Yuan X, Wu Y, Huang H, Peng X, Zeng G, Zhong H, Liang J, Ren MM. (2013). Graphene-based materials: Fabrication, characterization and application for the decontamination of wastewater and wastegas and hydrogen storage/generation. *Adv. Colloid. Interfac.*, **195–196**: 19–40.

Wang H, Yuan X, Wu Y, Huang H, Zeng G, Liu Y, Wang X, Lin N, Qi Y. (2013). Adsorption characteristics and behaviors of graphene oxide for Zn(II) removal from aqueous solution. *Appl. Surf. Sci.,* **279**: 432–440.

Wang H, Zhou A, Peng F, Yu H, Yang J. (2007). Mechanism study on adsorption of acidified multiwalled carbon nanotubes to Pb (II). *J. Colloid Interf. Sci.*, **316**: 277–283.

Wang HJ, Zhou AL, Peng F, Yu H, Chen LF. (2007). Adsorption characteristic of acidified carbon nanotubes for heavy metal Pb(II) in aqueous solution. *Mater. Sci. Eng.,* **A 466**: 201–206.

Wang Q, Li J, Chen C, Ren X, Hu J, Wang X. (2011). Removal of cobalt from aqueous solution by magnetic multiwalled carbon nanotube/iron oxide composites. *Chem. Eng. J*., **174**: 126–133.

Wang SG, Gong WX, Liu XW, Yao YW, Gao BY, Yue QY. (2007). Removal of lead (II) from aqueous solution by adsorption onto manganese oxide-coated carbon nanotubes. *Sep. Purif. Technol.*, **58**: 17–23.

Wang W, Cai K, Wu X, Shao X, Yang X. (2017). A novel poly(m-phenylenediamine)/reduced graphene oxide/nickel ferrite magnetic adsorbentwith excellent removal ability of dyes and Cr(VI). *J. Alloys Compd*., **722**: 532–543.

Wang Y, Liang S, Chen B, Guo F, Yu S, Tang Y. (2013). Synergistic Removal of Pb(II), Cd(II) and Humic Acid by Fe_3O_4@Mesoporous Silica-Graphene Oxide Composites. PLoS One, **8**: 65634, 19 pp.

Wang YY, Liu YX, Lu HH, Yang RQ, Yang SM. (2018). Competitive adsorption of Pb(II), Cu(II), and Zn(II) ions onto hydroxyapatite-biochar nanocomposite in aqueous solutions. *J. Solid State Chem.*, **261**: 53–61.

Weng SC, Brahma S, Chang CC, Huang JL. (2017). Synthesis of MnO_x/reduced graphene oxide nanocomposite as an anode electrode for lithium-ion batteries. *Ceram. Int*., **43***:* 4873–4879.

WHO - World Health Organization. (2017). *Guidelines for drinking water quality:fourth edition incorporating the first addendum*. WHO, Geneva.

Wu CH. (2007). Studies of the equilibrium and thermodynamics of the adsorption of Cu^{2+} onto as-produced and modified carbon nanotubes. *J. Colloid Interf. Sci.,* **311**: 338–346.

Wu S, Zhang K, Wang X, Jia Y, Sun B, Luo T, Meng F, Jin Z, Lin D, Shen W, Kong L, Liu J. (2015). Enhanced adsorption of cadmium ions by 3D sulfonatedreduced graphene oxide. *Chem. Eng. J.,* **262**: 1292–1302.

WWAP - United Nations World Water Assessment Programme. (2015). *The United Nations World Water Development Report 2015: Water for a Sustainable World,* UNESCO, Paris.

WWAP - United Nations World Water Assessment Programme. (2017). *The United Nations World Water Development Report 2017. Wastewater: The Untapped Resource,* UNESCO, Paris.

WWAP - United Nations World Water Assessment Programme. (2018). *The United Nations World Water Development Report 2018: Nature-Based Solutions for Water*, UNESCO, Paris.

Xiao B, Thomas K. (2004). Competitive adsorption of aqueous metal ions on an oxidized nanoporous activated carbon. *Langmuir*, **20**(11): 4566–78.

Xiao B, Thomas K. (2005). Adsorption of aqueous metal ions on oxygen and nitrogen functionalized nanoporous activated carbons. *Langmuir*, **21**(9): 3892–902.

Xiao G, Wang Y, Xu S, Li P, Yang C, Jin Y, Sun Q, Su H. (2018). Superior Adsorption Performance of Graphitic Carbon Nitride Nanosheets for Both Cationic and Anionic Heavy Metals from Wastewater. *Chinese J. Chem. Eng., Cjche,* doi:10.1016/j.cjche.2018.09.028

Xing HT, Chen JH, Sun X, Huang YH, Su ZB, Hu SR, Weng W, Li SX, Guo HX, Wu WB, He YS, Li FM, Huang Y. (2015). NH_2-rich polymer/ graphene oxide use as a novel adsorbent for removal of Cu(II) from aqueous solution. *Chem. Eng. J.,* **263**: 280–289.

Xu YJ, Rosa A, Liu X, Su DS. (2011). Characterization and use of functionalized carbon nanotubes for the adsorption of heavy metal anions. *New Carbon Mater.,* **26**: 57–62.

Xu Z, Zhang Y, Qian X, Shi J, Chen L, Li B, Niu J, Liu L. (2014). One step synthesis of polyacrylamide functionalized graphene and its application in Pb(II) removal. *Appl. Surf. Sci.,* **316**: 308 -314.

Yang ST, Li JX, Shao DD, Hu J, Wang XK. (2009). Adsorption of Ni(II) on oxidized multi-walled carbon nanotubes: effect of contact time, pH, foreign ions and PAA. *J. Hazard. Mater.,* **166**: 109–116.

Ye Y, Yin D, Wang B, Zhang Q. (2015). Synthesis of three-dimensional Fe_3O_4/Graphene aerogels for the removal of arsenic ions from water. *J. Nano-mater*., Article ID 864864, 6 pages.

Yoon Y, Park WK, Hwang TM, Yoon DH, Yang WS, Kang JW. (2016). Comparative evaluation of magnetite–graphene oxide and magnetite-reduced grapheneoxide composite for As(III) and As(V) removal. *J. Hazard. Mater*., **304**: 196–204.

Yu F, Wu Y, Ma J, Zhang C. (2013). Adsorption of lead on multi-walled carbon nanotubes with different outer diameters and oxygen contents: Kinetics, isotherms and thermodynamics. *J. Environ. Sci.,* **25**(1): 195–203.

Yu P, Wang HQ, Bao RY, Liu Z, Yang W, Xie BH, Yang MB. **(**2017). Self-Assembled Sponge-like Chitosan/Reduced Graphene Oxide/Montmorillonite Composite Hydrogels without Cross-Linking of Chitosan for Effective Cr(VI) Sorption. *ACS Sustain. Chem. Eng.,* **5**: 1557−1566.

Yu S, Liu Y, Ai Y, Wang X, Zhang R, Chen Z, Chen Z, Zhao G, Wang X. (2018). Rational design of carbonaceous nanofiber/Ni-Al layered double hydroxide nanocomposites for high-efficiency removal of heavy metals from aqueous solutions. *Environ. Pollut.*, **242**: 1-11.

Yuan X, Wang Y, Wang J, Zhou C, Tang Q, Rao X. (2013). Calcined graphene/MgAl-layered double hydroxides for enhanced Cr(VI) removal. *Chem. Eng. J.,* **221**: 204-213.

Zandi-Atashbar N, Ensafi AA, Ahoor AH. (2018). Magnetic Fe_2CuO_4/rGO nanocomposite as an efficient recyclable catalyst to convert discard tire into diesel fuel and as an effective mercury adsorbent from wastewater, *J. Clean.Prod.*, **172**: 68-80.

Zhang C, Sui J, Li J, Tang Y, Cai W. (2012). Efficient removal of heavy metal ions by thiol-functionalized superparamagnetic carbon nanotubes. *Chem. Eng. J.,* **210**: 45–52.

Zhang F, Wang B, He S, Man R. (2014). Preparation of Graphene-Oxide/Polyamidoamine Dendrimers and Their Adsorption Properties toward Some Heavy Metal Ions. *J. Chem. Eng. Data*, **59**: 1719-1726.

Zhang K, Li H, Xu X, Yu H. (2018). Synthesis of reduced graphene oxide/NiO nanocomposites for the removal of Cr(VI) from aqueous water by adsorption. *Micropor. Mesopor. Mater*., **255**: 7-14.

Zhang Y, Peng W, Xia L, Song S. J. (2017). Adsorption of Cd(II) at the Interface of water and graphene oxide prepared from flaky graphite and amorphous graphite. *Environ. Chem. Eng*., **5**: 4157-4164.

Zhang Y, Wu B, Xu H, Liu H, Wang M, He Y, Pan B. (2016). Nanomaterials-enabled water and wastewater treatment. *NanoImpact,* **3–4**: 22–39.

Zhang Y, Yan L, Xu W, Guo X, Cui L, Gao L, Wei Q, Du B. (2014). Adsorption of Pb(II) and Hg(II) from aqueous solution using magnetic CoFe2O4-reduced graphene oxide. *J. Mol. Liq.*, **191**: 177–182.

Zhang Y, Ali SF, Dervishi E, Li Z, Casciano D, Biris AS. (2010). Cytotoxicity Effects of Graphene and Single-Wall Carbon Nanotubes in Neural Phaeochromocytoma-Derived PC12 Cells. *ACS Nano*, **4**(6), 3181–3186.

Zhang YJ, Chi HJ, Zhang WH, Sun YY, Liang Q, Gu Y, Jing RY. (2014). Highly efficient adsorption of copper ions by a PVP-reduced graphene oxide based on a new adsorptions mechanism. *Nano-Micro Lett.,* **6**(1): 80–87.

Zhao D, Gao X, Wu C, Xie R, Feng S, Chen C. (2016). Facile preparation of amino functionalized graphene oxide decorated with Fe_3O_4 nanoparticles for the adsorption of Cr(VI). *Appl. Surface Sci.,* **384**: 1–9.

Zhao G, Li J, Ren X, Chen C, Wang X. (2011). Few-layered graphene oxide nanosheets as superior sorbents for heavy metal ion pollution management. *Environ Sci Technol*., **45**(24): 10454–10462.

Zhao G, Ren X, Gao X, Tan X, Li J, Chen C, Huang Y, Wang X. (2011). Removal of Pb(II) ions from aqueous solutions on few-layered graphene oxide nanosheets. Dalton Trans., **40**: 10945-10952.

Zhong YJ, You SJ, Wang XH, Zhou X, Gan Y, Ren NQ. (2013). Synthesis of carbonaceous nanowire membrane for removing heavy metal ions and high water flux. *Chem. Eng. J.*, **226**: 217–226.

Zhou C, Zhu H, Wang Q, Wang J, Cheng J, Guo Y, Zhou X, Bai R. (2017). Adsorption of mercury (II) with an Fe_3O_4 magnetic polypyrrole-graphene oxid enanocomposite, *RSC Adv*., **7**: 18466–18479.

Zhou L, Zhang G, Wang M, Wang D, Cai D, Wu Z. (2018). Efficient removal of hexavalent chromium from water and soil using magnetic ceramsite coated by functionalized nano carbon spheres. *Chem. Eng. J.*, **334**: 400–409.

Zhu H, Xu X, Zhong X. (2016). Adsorption of Co(II) on Graphene Oxides from Aqueous Solution. *Pol. J. Environ. Stud.*, **25**(6): 2675-2682.

Table 2. Brief summary on the adsorption of heavy metal ions by CNTs

Pollutant	Adsorbent characteristics	Adsorption conditions	Max adsorption capacity - experimental (calc)*, mg/g	Kinetic/ isotherm equation	Adsorbent regeneration	Remarks**	Reference
As(V) As(III)	MWCNTs	m / v = 2.0, pH 6.0, C_o = 5-50.0 µg/L, 20 °C, 60 min	At 40 µg/L: As(V) removal 92.0 %, As(III) removal 91.0%; As(V) (625 µg/g), As(III) (620 µg/g)	PSO/ Temkin, Dubinin-Radushkevich, Langmuir, Freundlich	1.0 MHCl CNTs lost 1.0–2.5% capability after 1st use and 3.0–5.5% after 5 runs	Liquid film diffusion mechanism; The column data followed Bohart-Adams and Thomas models; In column operations - 13.5 and 14.0 µg/g arsenite and arsenate removal - by physical and ion exchange adsorption	Ali, (2018)
Cd(II)	CNTs - raw and oxidized	m / v = 0.5, pH5.5, C_o = 1.18 - 9.50, C_e = 4, 25 °C, time - n.a.	1.1, 2.6, 5.1 and 11.0 for the raw CNTs, H_2O_2, HNO_3 and $KMnO_4$ oxidized CNTs	N.a. / N.a.	N.a.	For $KMnO_4$ oxidized CNTs almost 100% at the CNT dosage of 0.8 g/L	Li et al. (2003)
Cd(II)	CNTs- raw and oxidized Ethylenediamine-functionalized MWCNTs	m / v = 0.1, pH 8, C_o = 0.1- 5, 25-45 °C, 100 min	Raw CNTs - 1.3 at C_o=5 mg/L, 25 °C (1.28 - at 25 °C, 3.19 - at 45 °C) Ox CNTs - 22.3 at C_o=5 mg/L, 25 °C (22.39 - at 25 °C, 24.15 - at 45 °C) e-MWCNTs - 20.8 at C_o=5 mg/L, 25 °C (21.67 - at 25 °C, 25.70 - at 45 °C)	PSO / Langmuir	Water acidified to pH < 2with HCl	Mechanism - hemisorption and physisorption	Vukovic et. al. (2010)
Cd(II)	MnO_2/oxidized MWCNTs	m / v = 0.5, pH 5, C_o=5-30, 22-52 °C, >150 min	at 22 °C 35.97 (38.0) at 52 °C - (41.6)	PSO / Langmuir	N.a.	Mechanism - physical and chemical adsorption influenced by external mass transfer, and intraparticle diffusion	Luo et al. (2013)
Cd(II)	MWCNTs	m / v = 1, pH 5, C_o =10-80, room temp.,120 min	82.9 (88.62)	PSO/ Langmuir & Freundlich	pH< 2	Practically, equilibrium is reached in 60 min	Mubarak et al. (2015)

Cd(II)	CNTs -acid modified	m / v = 0.075, pH 7, C_o = 1-10, ambient temp., 2 h	2.02 (4.35)	PSO / Langmuir	N.a.	Mechanism - electrostatic interactions	Ihsanullah et al. (2015)
Co(II)	Raw MWCNTs PAA grafted/ MWCNTs	m /v = 1.0, pH = 6.8, 30-70 °C, 24 h	Raw MWCNT (2.00 - at 30 °C and C_e =18.85) MWCNT-*g*-PAA (8.78 - at 30 °C and C_e = 15.90; 9.78 - at 70 °C and C_e =12.96)	PSO/ Langmuir	N.a.	The sorption of Co(II) is endothermic and spontaneous and highly dependent on the pH; Mechanism - surface complexation	Chen et al. (2012)
Cr(VI)	Raw CNTs	m/v = 1, pH=7.5, C_e = 33.28, 24 h	20.56 (26.88)	N.a. / Langmuir	N.a.	Mechanism - ion exchange; The rate of Cr(VI) adsorption - rapid over the first 20 min	Di et al. (2004)
Cr(VI)	Oxidized MWCNTs	m/v = 1.0, C_o = 1-5, 20 °C,	2.85 at pH 2.88 and C_o = 3 mg/L (2.84 at pH 2.88) (4.26 – at pH 2.05)	PSO/ Langmuir	N.a.	Redox reaction of adsorbed Cr(VI) to Cr(III) and subsequent sorption of Cr(III) on MWCNTs	Hu et al. (2009)
Cr(VI)	Raw MWCNTs	m/v =1.0, pH 2.88, C_e = 2.6, 20 °C, 165 h.	2.5 (2.679)	N.a./ Langmuir	N.a.	The adsorption of Cr(VI) decreased with increasing pH and increased with the rise in temperature and MWCNT dosage.	Hu et al. (2009)
Cr(III)	Raw and modified MWCNTs	m/v = 0.06, pH 7, 2 h	At C_o = 1 mg/L Raw - 0.3718 Modified - 0.5	PSO/ Freundlich	N.a.	The time to achieve equilibrium concentration of Cr (III) is less by using modifies CNTs compared with raw CNTs	Atieh et al. (2010)
Cr(VI)	CNTs-AC	m/v = 0.040, pH=2.0, C_o = 0.2-0.5, 20 °C, 60 min	9.0 at C_e = 0.14 (8.551)	N.a. / Langmuir	N.a.	The particle size play vital role in the Cr(VI) adsorption	Atieh, (2011)
Cr(VI)	SWCNTs MWCXNTs	m/v = 0.1, pH 4, C_o= 0.250-50.0, 20 °C, 12 h	SWCNTs - (20.3) MWCNTs - (2.48)	PSO/ Langmuir	N.a.	Mechanism: both physisorption and chemi sorption; Presence of other anions resulted in negative effects on Cr(VI) adsorption	Jung et al. (2013)
Cr(VI)	CNTs raw and OH- fun ctionalzed	m/v = 6.67, pH 7.8, C_o= 1-2.5 mmol/L, 5 days	Raw (1.856) Modified (28.884)	Na/ Langmuir	N.a.	Mechanism - ion exchange with acidic surface OH^- groups	Jun et. al. (2011)
Cr(VI)	Magnetic MWCNTs	m/v = 0.8, pH 3, C_o = 0.78 - 25, 20- 70 °C, 24 h	11.4 (12.531) - at 20 °C 14.8 (16.234) - at 70 °C	PSO/ Langmuir	N.a.	Adsorption capacity increased with the initial Cr(VI) concentration, but decreased with the increase of adsorbent dose and increase in pH.	Huang et al. (2015)

Cr(VI)	MWCNTs Ionic liquid-functionalized oxi-MWCNTs	Batch: m/v= 7.5,pH=2.5-4.0, C_o = 20-500, 40 min Column studies: flow rate of 6 mL/min, pH 2.8, volume = 2000 mL, C_o= 10 mg/L, 1.5 g adsorbent	MWCNT (13.2) IMWCNTs (85.83)	PSO/ Langmuir	The order of elution: NaOH (98.0%) > KOH (79.4 %) > Na_2SO_3 (65.0%) >NH_4OH(61.0%)	Electrostatic, cation–π interaction, anion– π interaction; The adsorption efficiency of Cr(VI) was not influenced by Cu(II), Cd(II), Co(II), Zn(II), Ni(II), or Pb(II), while Fe(II) and Mn(II) did interfere by reducing Cr(VI) to Cr(III); Adsorbent efficiency after 3 cycles - 99.5%.	Kumar et al. (2015)
Cr(VI)	CNTs grown on carbon nanofibers	m/v= 2.5, pH=3.0, C_o = 20-200, 120 min	250.85 at C_o = 60 mg/L, (227)	N.a. / Langmuir	NaOH solution	High right within the first 20 min.; K_L indicates favorable Cr(VI) adsorption process Above 95% and 84% of the initial adsorption capacity after 3 times and 5 times recycle	Chen et al. (2018)
Cu(II)	CNTs raw & oxidized (with HNO_3)	m/v= 0.5, pH 5.4 (raw), 5.2 (oxidized), C_o = 6-30 mg/L, 20 °C, 2 h	Raw - 14.4 (16.55) Oxidized- 27.6 (28.49)	N.a. / Langmuir	N.a.	Mechanism: oxidized - electrostatic interaction; The Cu(II) ion adsorption capacity increased with increasing CNTs dosage.	Li et al. (2003)
Cu(II)	CNTs raw & modified	m/v= 0.5, pH=6, C_o = 2-115, 27°C, 24 h	As produced - 6.8 (8.25) NaOCl-modified - 46.5 (47.39); HNO_3 modified - 11.8 (13.87)	N.a. / Langmuir	N.a.	Mechanism - electrostatic interactions	Wu et al. (2007)
Cu(II)	MWCNTs	m/v = 1, pH 6, C_o =1-20, 20 °C, 48 h	MWCNTs - 3.7 (3.309 ± 0.167) In presence of HA - 8.50 (7.776 ± 0.538) In presence of FA - 9.1 (8.246 ± 0.336)	Na/ Freundlich	N.a.	The adsorption of Cu(II) on MWCNTs increases with pH increasing from 3.0 to 7.5, and then maintains high level at pH >7.5; A positive effect of humic /fulvic acid on Cu(II) adsorption at pH<7.5, a negative - at pH>7.5.	Sheng et al. (2010)
Cu(II)	MWCNTs GO	GO m/v = 0.1, MWCNTs m/V=0.6, pH =5, C_e =22.24, 30°C, 24h	MWCNTs n.a. (2.034) GO 69.91 (74.99)	N.a. / Langmuir	N.a.	Mechanisms - electrostatic interactions, surface complexation, surface precipitation	Ren et al. (2013)
Cu(II)	MWCNTs - purified &	m/v = 0.5, pH=5, C_o = 10-100 mg/L, 25 °C, 6 h	Purified 37.5 (36.82) Sulfonated 59.6 (43.16)	N.a. / D-R model	N.a.	Purified - physical adsorptiuon; Sulfonated - electrostatic interactions	Ge et al. (2014)

	sulfonated						
Cu(II)	MWCNTs	m/v = 0.4, pH 5.5, C_o = 10-80, ambient temp.,2 h	91 (99)	PSO/ Freundlich	N.a.	More than 90% of maximum equilibrium uptake capacity was reached after 35 min	Mubarak et al. (2015)
Hg(II)	Amino & thiol functionalized MWCNTs	Batch: m/v = 0.4, pH 6, C_o = 5-100, 25°C, 60 min Continuous mode - flow rate 2 mL/min, C_o= 40 mg/L, 7 mm CBH, 25 °C	In batch mode - 82.47(84.66); In continuous mode 105.65	PSO/ Langmuir - in batch, Yan and Thomas - in column tests	Loss in the adsorption capacity of 7.2% for Hg(II) after five cycles	Based on thermodynamic data - exothermic, spontaneous and physisorption in nature; 88.7% removal from **real** chloralkali wastewater	Hadavifar et al. (2014)
Hg(II)	Ox-MWCNTs	m/v = 0.5, pH 7, C_o = 1-10 mg/L, 25°C, time- n.a.	3.70 (3.83)	N.a. / Langmuir	1 M HNO_3	Mechanism: electrostatic interactions	Sheikh et al. (2011)
Hg(II)	Sulfur containing MWCNTs	m/v = 5, pH 12.15, C_o= 100 μg/L, 4 h	99 μg/g (72.8 μg/g)	N.a. / Freundlich	With 0.5% thiourea, adsorbent capacity retained after 6 cycles	Mechanism - chemisorption via Hg-S bond formation; The maximum uptake - at sulphur contents of 3.97%; Presence of competing ions - Pb(II), Cd(II), Cu(II) and Cl^- does not affect the adsorption	Pillay et al. (2013)
Hg(II)	SWCNTs - raw & thiol-derivatized	m / v = 0.25, pH 5, C_o = 10-80, 25 °C, 60 min	Raw SWCNTs- n.a.(40.16) SWCNTs-SH - 74.2 (at C_o=40 mg/L) (131.58)	First-order / Langmuir	2M HCl	Mechanism - chemisorption; Adsorption efficiency of recovered adsorbent- 91% after 5 cycles	Bandaru et al. (2013)
Hg(II)	MWCNTs	m/v = 2.5, pH 6, C_o=0.01 -150, room temp., 20min	82 (71.43)	PSO/ Freundlich	N.a.	Very fast process - equilibrium in 20 min	Moustafa et al. (2014)
Hg(II)	MWCNTs - raw, oxidized, iodide, sulfur incorporated	m / v = 1, pH 6, C_o = 10–120, room temp., 2 h	MWCNTs - 5.0 (5.479) MWCNTs-Ox - 25.0 (27.32) CNTs-I - 124 (123.45) CNTs-S - 157 (151.51)	PSO/ Langmuir	0.5% thiourea in 0.05 N HCl desorbes 85 %	Chemisorption and external diffusion controlled processes; Successful application to **real** polluted water; CNTs-I and CNTs-S - efficient sorbent for Hg (0) vapor	Gupta et al. (2014)
Pb(II)	CNTs oxidized with HNO_3	m / v = 0.5, pH=5.0, C_o = 2- 14, room temp., 6 h	15.6 (17.5)	Na/ both Langmuir & Freundlich	N.a.	The removal of Pb(II) is highly dependent on the solution pH, which affects the surface charge of the adsorbent	Li et al. (2002)

Pb(II)	Acidified MWCNTs	m / v = 0.5, pH 5, C_o = 10-80, 25 °C, 6 h	36.8	PSO / Freundlich	HCl & HNO_3 pH<2	The adsorption is spontaneous endothermic process, very fast in the initial 10 min	Li et al. (2005)
Pb(II)	Acidified MWCNTs	m / v = 0.5, pH 5, C_o = 10-60, 25°C, 6 h	51(49.71)-1h acidification; 85 -at C_o= 50 mg/L with 6 h -acidified MWCNTs	N.a. / Langmuir	HNO_3 - pH< 2	Equilibrium time - 20 min; Pb(II) salt or complex deposited on the surface of CNTs	Wang et al. (2007)
Pb(II)	CNTs	m / v = 40 mg/L, C_e= 0.67, pH 5, 25°C, 80 min	102.04	PSO/ Langmuir	N.a.	The rate controlling step - chemisorption	Kabbashi et al. (2009)
Pb(II)	Ox MWNTs OMWCNTs + TX-100 OMWCNTs + BKC OMWCNTs + SDBS	m / v = 0.75, pH4, 25°C, 2 days; surfactants C_o=0.83 mmol/L: sodium dodecylbenzene sulfonate (SDBS), octyl-phenol-ethoxylate (TX-100), and benzalkonium chloride (BKC),	OMWCNTs - 2.49 at C_e = 19.48 (4.37); OMWCNTs+ TX-100 6.84 at C_e = 16.99 (8.58); OMWCNTs+ BKC 1.66 at C_e = 19.89 (3.27); OMWCNTs+ SDBS 32.32 at C_e = 11.81 (66.95)	N.a. / Langmuir	N.a.	The adsorption process in the Pb –surfactant– OMWCNT ternary system - attributed to electrostatic, hydrophobic and π–π interactions	Li et al. (2011)
Pb(II)	MWCNTs MWCNT-*g*-VP	m / v = 0.4, pH 6.0, 25 °C, 24 h	MWCNTs - 8.5 at C_e = 16.5 (15.9) (MWCNT-*g*-VP) - 31 at C_e = 9.5 (37)	N.a. / Langmuir	N.a.	The strong pH dependent Pb(II) sorption on MWCNTs grafted with 2-vinylpyridine suggests that the sorption of Pb(II) is domina ted by inner-sphere surface complexation	Ren et al. (2011)
Pb(II)	MWCNTs	m / v = 0.4, pH 5, C_o = 10 - 80, 40 min	98.7 at C_o = 80 (104.2)	PSO/Langmuir Freundlich	Acifified water pH<2.5	Mechanism - ion exchange	Mubarak et al. (2016)
Ni(II)	Oxidized MWCNTs	m /v = 0.75, pH 6.55, C_o = 6- 20, 18 °C, 24 h	8.75 (8.77; 9.80 - at 60 °C)	PSO/ Langmuir	With 0.01 M KNO_3 + HNO_3 to pH <2.0	Ni(II) adsorption - strongly dependent on pH and oxidized MWCNT concentration; Ion exchange is the predominant mechanis	Chen et al. (2006)
Ni(II)	MWCNTs-raw & HNO_3 oxidized	m /v = 0.4, pH 6, C_o = 10-200, room temp, 3 h	As produced 12.8 (18.083) Oxidized: 38 (49.261)	N.a./ Both Langmuir & Freundlich	N.a.	Equilibrium time - 20 min	Kandah and Meunier (2007)
Ni(II)	SWCNTs MWCNTs NaOCl	m / v = 0.5, pH 7.0, C_o = 10–80, 25 °C, 12 h	NaClO-SWCNTs 45 (47.85) (28.41)♣ NaClO- MWCNTs 34.	PSO/ Langmuir	90 % desorption with 0.1 M HNO_3, 5 h	Mechanism - electrostatic interactions; The adsorbent performance was maintained after 10 sorption/desorption cycles;	Lu et al (2008)

	oxidized		5(38.46) (18.59)♣ ♣ Zn(II) presence-40 mg/L			Strong competition exerted by Zn(II) on the sorption of Ni(II)	
Ni(II)	MWCNTs Polyacrylic acid (PAA)-MWCNTs	m/v = 0.8, pH 5.4, C_o = 1.17 - 18.78, 20 °C, 24	MWCNTs 2.82 (3.67) PAA-MWCNTs - 3.17 (3.87)	PSO/ Langmuir	N.a.	Adsorption of Ni(II) on oxMWCNTs increa sed from 0 to 99% at pH 2–9; Mechanism - surface complexation and ion exchange; A positive effect of PAA on Ni(II) adsorption at pH < 8, a negative - at pH > 8.	Yang et al. (2009)
Zn(II)	SWCNTs-NaOCl and MWCNTs-NaOCl	m/v = 0.5, pH 7, C = 10-80, 25 °C, 60 min	SWCNTs - 28.22 at C_o=10 mg/L, 39.52 at C_o=60 mg/L (43.66) MWCNTs - 22.58 at C_o=10 mg/L, 30.65 at C_o=60 mg/L (32.68)	N.a. / Langmuir	N.a.	The adsorption of Zn(II) increases with the increase of pH in the pH range of 1–8; Mechanism - ion exchange.	Lu and Chiu (2006)
Zn(II)	Functionaliz ed CNTs	m/v = 0.9, pH 10, C_e = 28.9, 120 min	2.42 (1.05)	PSO/ Langmuir	N.a.	Mechanism - electrostatic interactions 99% Zn(II) removal at C_o = 1.1 mg/L	Mubarak et al. (2013)
Pb(II) Cu(II) Cd(II)	HNO_3 treated MWCNTs	Single ion experiments: m/v = 0.5, pH 5.0,C_o = 10 - 60 for Pb, 5- 30 for Cu and 2 -15 for Cd, room temp., 4h competitive adsorption: m/v= 1, pH 5.0, C_o=5-30 for the 3 ions, room, 4 h	Single ion experiments: Pb - 88 at C_e = 17 (97.08) Cu - 29 at C_e = 17 (28.49) Cd - 9.2 at C_e = 10 (10.86) Competitive adsorption: Pb-27.6 at C_e = 2.4 (34.01) Cu-17.6 at C_e=12.4 (17.04) Cd -7.1 at C_e = 2.9 (3.3)	N.a. / Langmuir	N.a.	Ion exchange is the main mechanism	Li et al. (2003)
Cu(II) Co(II) Pb (II)	CNTs	m/v = 5, pH 9, C_o = 1–20, room temp., 4 h	At C_o = 20: Cu(II) - 3.49, Pb(II) - 2.96, Co(II) - 2.60	N.a. / Freundlich	N.a.	At pH 9 and Zn(II) and Mn(II) presence - the affinity order: Cu(II) > Pb(II) > Co(II) > Zn(II) > Mn(II)	Stafiej and Pyrzynska (2007)
Pb(II) Ag(I) Cu(II) Co(II)	Acidified MWCNTs	m/v = 0.5, pH 5.0, C_o = 5-100 for Pb, = 5-40 for Cu and = 5-50 for Ag, 25 °C, 48 h	Pb (II) - 91; Ag (I) - 40; Cu (II) - 23; Co (II) -15	N.a. / N.a.	N.a.	Main mechanism- electrostatic interaction	Wang t al. (2007)

Pb(II) Cd(II)	MWCNTs-raw, oxidied&modified ethylenediamine, diethylenetriamine, triethylenetetramine (r-MWCNT, o-MWCNT, e-MWCNT, d-MWCNT and t-MWCNT)	m/v = 0.1, pH 6 for Pb(II), pH 7-9 for Cd(II), C_o = 5-100 for Pb(II); for competitive studies C_o= 5 both for Pb (II) and Cd(II), 25-45 °C, 90 min	Pb(II) r-MWCNT (2.94- at 25°C), (5.21- at 45 °C) o-MWCNT (37.36 at 25 °C), (40.79 at 45 °C) e-MWCNT (40.12 at 25 °C), (44.19 at 45 °C) d-MWCNT (54.27 aat 25 °C), (58.26 at 45 °C) Cd(II) - d-MWCNT (31.45 at 45 °C) Competitive adsorption d-MWCNT Pb(II) - 24.2, Cd(II) - 15.2 e-MWCNT Pb(II) - 17.1, Cd(II) - 12.3	PSO/ Langmuir	Acidified water with pH 1.5 - 94 % desorption of Pb(II); Regenerated MWCNT can be reused over 5 times with minimal loss of adsorption capacity	Adsorption of Pb(II) and Cd(II) on MWCNTs strongly depends on pH; Adsorption of Pb(II) on the studied MWCNT is complex and spontaneous process, suggesting that mechanism includes both physisorption and chemisorption;	Vuković et al. (2011)
Cu(II) Zn(II) Pb(II) Cd(II) Co(II)	CNT sheets oxidized with HNO_3	m/v = 2, pH=7, C_o = 100 - 1200, 25 °C, 48 h	at C_o = 1200 Pb(II) 101.05 (117.65) Cd(II) 75.84 (92.59) Co(II) 69.63 (85.74) Zn(II) 58.00 (74.63) Cu(II) 50.37 (64.94)	At C_o=100 - PSO, at C_o= 1200 intrapar ticle diffusion / both Langmuir & Freundlich	N.a.	Preference of adsorption: Pb(II) > Cd(II) > Co(II) > Zn(II) > Cu(II).	Tofighy and Mohammadi (2011)
Pb(II) Cu(II) Cd(II)	SWCNTs SWCNTs-COOH	m/v = 0.050, pH 5, C_o = 10-50, 25 °C, 180 min	SWCNTs Pb(II) (33.55), Cu(II) (24.29), Cd(II) (24.07), SWCNTs-COOH Pb(II) (96.02), Cu(II) (77.00), Cd(II) (55.89)	Langmuir	Desorption of: Pb-diluted HNO_3; Cd(II) and Cu(II) - with HCl	Adsorption on SWCNTs-COOH - chemisorption; on SWCNTs surface - physisorption process.	Moradi (2011)
Cu(II) Pb(II)	MWCNTs-raw &	m/v = 12.5, pH 7.0, C_o = 1, 25 °C, 120 min	r MWCNTs, Cu(II) - 0.080, Pb(II)- 0.064, Cd(II)	N.a. / N.a.	Desorption acidified water	Cu(II) removal >99 % at high concentrations of interfering cations - **real Red Sea water**	Kosa et al. (2012)

Cd(II) Zn(II)	8-HQ-MWCNTs		-0.011, Zn(II) - 0.63; 8-HQ-MWCNTs: Cu(II) - 0.080, Pb(II)- 0.076, Cd(II) - 0.032, Zn(II) - 0.075		pH <2	Removal at the third cycle - 99.5%, 95.8%, 80.1% and 21.9% for Cu(II), Pb(II), Cd(II) and Zn(II), respectively	
Pb(II) Cu(II)	Undispersed MWCNTS Dispersed MWCNTs	Batch.: m/v = 0.5, pH 5.6, C_o= 1- 60, room temp, 12 h Fixed bed: 10 mg CNTs incorporated into 16.8 g of sand for each CNT's-sand packed column, 1 mL/min, 2 h	Batch- single metals: Undispersed CNTs: Pb(II) (74.5), Cu(II) (51.3) Dispersed CNTs: Pb(II) (92.3), Cu(II) (67.8) Batch - both metals: Undispersed CNTs: Pb(II) (49.3), Cu(II) (33.0) Dispersed CNTs: Pb(II) (65.0), Cu(II) (43.6)	N.a./Batch - Langmuir	N.a.	Removal - fixed bed column, mg/g: Single metals, mg/g: - Layered CNTs: Pb 25.9, Cu 12.6; - Mixed CNTs: Pb 44.3, Cu 21.1; - Deposited CNTs: Pb 80.1, Cu 42.6 Both metals, mg/g: - Layered CNTs: Pb 25.3, Cu 15.3; - Mixed CNTs Pb 29.9, Cu 18.0; - Deposited CNTs Pb 40.9, Cu 21.2.	Tian et al. (2012)
Hg(II) Cd(II)	Amino and thiol functionalized MWCNTs	Batch system: m/v = 0.2, pH = 6, C_o = 20-80, room temp., 60 min Continuous mode - flow 1 mL/min, C_o = 20, 14 mm bed height column, pH = 6, room temp.	In batch mode -single system: Hg(II) -160.9 at C_e = 54 (204.64), Cd(II) - 45.0 at C_e = 64 (61.10); binary system: Hg(II) (35.89), Cd(II)(14.09) In continuous system: Hg(II) 39.75; Cd(II) 9.72	PSO/ Yan and Thomas models - in fixed bed column tests	N.a.	The bigger Thomas rate constant (120.77 mL/min/mg for Cd(II) compared to 9.44 mL/min/mg for Hg(II)) indicated that the intensity of adsorption of Cd(II) was higher compared to Hg(II).	Hadavifar et al. (2016)
Pb(II) Cu(II) Cd(II)	Amino-functionalized MWCNTs	m/v - adjustable, C_o = 0.1-1.0, 48 h, 20 °C	Cu - 2.51 at pH 3 Pb 9.90 - at pH 4.5 Cd - 3.13 - at pH 6.0	PSO/ N.a.	N.a.	Adsorption occurs in two steps: external diffusion and intraparticle diffusion. Intra-particle diffusion, although slower than the external diffusion, is not the only limiting step, the adsorption rate also depends on the interactions of the metal ions with the binding sites on the adsorbent.	Apostolović et al. (2018)

In Tables 2-7:

*All calculated values for the maximum adsorption capacity are based on Langmuir adsorption isotherm; ** Stressed on by the corresponding authors; m / v - adsorbent dose, g/L; C_o - initial concentration (range), mg/L, unless otherwise specified; C_e - equilibrium concentration, mg/L, unless otherwise specified; PSO - pseudo second order; N.a. - not available

Remarks:

When adsorption ability and adsorbent capacity are discussed, it is very important to point the studied concentration range of the corresponding pollutant(s) since the initial concentrations are decisive for determining the experimentally measured and calculated maximum adsorption capacity. When data on the initial concentration range are missing then the equilibrium concentration represents an useful parameter showing the experimental pollutants' concentration range and consequently the range of the applicability of the chosen system adsorbent-adsorbate as well of the isotherm equations.

Table 3. Brief summary on the adsorption of heavy metal ions by CNTs - composites

Pollutant	Adsorbent characteristics	Adsorption conditions	Max adsorption capacity - exp. (calc)*, mg/g	Kinetic/ isotherm equation	Adsorbent regeneration	Remarks**	Reference
As(V)	CeO_2-CNTs	m / v = 0.5, room temp., pH 3.1, 24 h	68 at C_e= 120	N.a. / Freunlich	0.1 M NaOH-	At natural pH an increase from 0 to 10 mg/L of Ca^{2+} and Mg^{2+} results in an increase from 10 to 81.9 and 78.8 mg/g in the amount of As(V) adsorbed, resp.	Peng et al. (2005)
As(III)	Fe-MWCNTs	m / v = 0.2, pH 8, 120 min	1.8 at C_o=1; (4.0)	PSO / Langmuir	N.a.	Mechanism: electrostatic interactions	Tawabini et al. (2011)
As(III), As(V)	Iron oxide coated MWCNTs	m / v = 1, pH 4, 1 h and 12 h for As(V) and As(III) respectively	As(III):175 μg/g at C_e = 13 μg/g (1723 μg/g) As (V) : 180 μg/g at C_e=10 μg/g (189 μg/g)	PSO / Langmuir & Freundlich	N.a.	Mechanism: electrostatic interactions; The adsorption of As(V) on Fe-MWCNT was faster than that of As(III)	Ntim and Mitra (2011)
As(III), As(V)	MWCNT-zirconia nanohybrid	m / v = 1, pH 6, 6 h	As (III): 98.6 μg/g - at C_o=100 μg/L (2000 μg/g) As (V): 100.5 μg/g at C_o=100 μg/L (5000 μg/g)	PSO / Langmuir & Freundlich	N.a.	Mechanism: chemisorption/ physisorption; removal efficiency of As(V) - not affected by the presence of competing anions; As(III) removal - reduced by the presence of sulfate and nitrate ions.	Ntim and Mitra (2012)
As(V)	e-MWCNT/Fe^{2+} and e-MWCNT/Fe^{3+}	m / v = 0.1, pH 4, C_o= 0.05- 4, 45 °C, 100 min	on e-MWCNT/Fe^{2+} - 23.2 at C_e=1.7 (23.47) on e-MWCNT/Fe^{3+} - 12.73 at C_e=2.70 (13.74)	PSO/ Freundlich	N.a.	Ethylenediamine functionalized MWCNT (e-MWCNT) loaded with iron(III) oxide in the goethite form; Mechanism: formation of inner-sphere surface complexes; As(V) adsorption is dependent on iron(III)-oxide content, pH and temperature	Velickovic et al. (2012)

As(V)	SWCNT - iron oxide nanoparticle	m / v = 0.4, C_o=50, 25 °C	At pH 8: 42.30 At pH 4: 49.65	PSO/ Freundlich	N.a.	Mechanism: chemical adsorption, non-ideal adsorption on heterogeneous surfaces	Ma et al. (2018)
Cd(II)	Alumina decorated MWCNTs	m / v = 1, pH 7, C_o = 0.1 - 64, 4 h	19.8 (27.21)	PSO / Langmuir	N.a.	Mechanism: electrostatic and hydrogen bond interactions and protonation or hydroxylation of Al_2O_3; The presence of Ca(II) reduced adsorption of Cd(II), of HA - facilitated the adsor ption of Cd(II); For **groundwater** (1.028 mg/L Cd) - 94 % removal	Liang et al. (2015)
Co(II)	MWCNTS/iron oxide composite	m/ v = 0.5, pH 6.4, C_e = 24.8, 20 - 60 °C, 24 h	5.60 (8.83) at 20 °C; 8.54 (10.60) - at 60 °C	PSO/ Langmuir	Magnetic separation	Mechanism - ion exchange, surface complexation; Humic substances affected Co(II) sorption; The capacity decreases slightly after six rounds	Wang et al. (2011)
Co(II)	MWCNTs-hydroxyapatite (MWCNT–HAP) composite	m /v=0.6, pH 6, 20-60 °C, 5 h	At 20 °C and C_e = 14.14 - 10.02 (16.14) At 60 °C and C_e = 11.78 - 12.37 (20.91)	PSO/ Langmuir	0.01M NaCl	Mechanism: surface complexation; K^+, Mg^{2+} and Ca^{2+} ions restrained Co(II) sorption at low pH; ClO_4^-, NO_3^- and Br^- made no obvious effect on, F^- dramatically enhanced Co(II) sorption. The presence of FA and HA enhanced Co(II) sorption at low pH values, but suppressed Co(II) it at high pH values; Sorption capacity decreases slightly after 5 rounds	Liu et al. (2013)
Cr(VI)	CeO_2-CNTs	m/v =1, pH 7,25°C, pH=3.0-7.4, 24 h	30.2 at C_e= 35.3 (31.55)	N.a. / Langmuir	N.a.	Mechanism: ion exchange	Di et al. (2006)
Cr(VI)	Para toluene sulfonic acid-immobilized polyaniline - CNTs	m / v = 1, pH 2, C_o=25-200, 30 °C	147.0 (166.7)	PSO / Langmuir	0.1 M NaOH, 30°C	Higher adsorption in acidic medium due to the electrostatic interaction between the negatively charged chromium ions and positively charged adsorbent surface	Kumar et al. (2018))

Cu(II)	CNTs CNTs/calcium alginate composites (CNTs/CA)	m / v = 0.5, pH 5, C_o= 5-40, 2 h	CNTs–19 at C_e= 5 (26.41) CNTs/CA- 67.9 at C_e= 5 (84.88)	N.a. / Langmuir	N.a.	Mechanism: surface complexation/ion exchange	Li et al. (2010)
Cu(II)	MWCNTs/Fe_3O_4	m / v = 0.2, pH 6, C_o = 10-100, 24 h	27.5 at C_e=93.5 (38.91)	PSO/ Langmuir	20% ethanol pH 3.0	Mechanism: electrostatic interaction; Magnetic separation and effective reuse; after 4 cycles - 88% ads. capacity compared with the initial cycle	Tang et al. (2012)
Hg(II)	MWCNTs-COOH-CS & MWCNTs-CS & SWCNTs-CS beads	m / v = 0.4, pH = 4, C_e=1000, 25°C, 2 h	MWCNTs-COOH-CS - 183.2 (181.8); MWCNTs-CS167.5(169.4);SWCNTs -CS 172.7 (172.4)	N.a./ Langmuir	0.1 M HNO_3	Mechanism: electrostatic interaction; The CNTs - chitosan (CS) beds could be recycled and used several times for the removal of Hg(II).	Shawky et al. (2012)
Hg(II)	MnO_2-coated carbon nanotubes	m / v = 1, pH 7, C_o = 1-50, 25 °C, 24 h	49.5 (58.82)	PSO/ Freundlich	N.a.	Physico-chemical mechanism; Hg (10 mg/L) removal efficiency, % in presence of other metal (20 mg/L): Ni^{2+} (88.1), Co^{2+} (91.7), Cd^{2+} (81.0), Pb^{2+} (90.4), Cu^{2+} (77.5)	Moghaddam and Pakizeh (2015)
Hg(II)	MWCNTs-Fe_3O_4 composite	m / v = 0.4, pH 2, C_o = 10-50, 25 °C, 2 h	266 (238.78)	PSO/ Langmuir	N.a.	Chemisorption - the rate-determining step; Capacity depends on the adsorbent dosage, contact time, pH and initial metal ion concentration	Sadegh et al. (2018)
Pb(II)	MnO_2/CNTs	m / v = 0.5, pH 5, C_o=10-60,25°C, 2 h	83.0 (78.74)	PSO/ Langmuir	N.a.	MnO_2/CNTs with MnO_2 loading of 30 wt.% show the best performance	Wang et al. (2007)
Ni(II)	MWCNTs/ magnetic iron oxide	m/v = 0.75, C_e = 14 25°C, pH6.4, 2days	7.65 (9.18)	Langmuir	Magnetic separation	Mechanism - ion exchange; Ni(II) desorption with 0.01M $NaClO_4$ + HNO_3 to pH < 2.0	Chen et al. (2009)
Cu(II) Cd(II)	MWCNTs chitosan (CS)	C_o= 1 mg/L for every ion pH 7, 25 °C	Removal: Cu(II) - 100% Cd(II) - 99% Zn(II) - 98%	N.a./ N.a.	N.a.	MWCNTs/CS nanocomposite (200 mg) - packed in a glass column, 25 mL of the metal ion flowed at rate	Salam et al. (2011)

Zn(II) Ni(II)			Ni(II) - 90%			= 5 mL/min; Mechanism- electrostatic interaction	
Pb(II) Hg(II)	MPTS - MWCNTs/Fe_3O_4	m / v = 1, pH 6.5, C_o=5-90, 25°C, 24h	Pb(II): 42.12 at C_o= 50 mg/L (65.40);Hg(II)63.65 at C_o= 50 mg/L (65.52)	PSO/ Langmuir	Magnetic separation	The 3-mercaptopropyltriethoxysilane CNTs/Fe_3O_4 nanocomposites exhibit superparamagnetic property; Mechanism - Lewis acid–base interactions	Zhang et al. (2012)
Cd(II) Cu(II) Pb(II) Zn(II)	MWCNTs	m / v = 1.25, pH 7, C_o= 0.5 for each metal ion	Cd(II) - 0.065 at 5 °C, 0.139 at 60 °C; Cu(II) - 0.396 at 5°C, 0.399 at 60 °C; Pb(II) - 0.334 at 5 °C, 0.397 at 60 °C Zn(II) - 0.298 at 5 °C, 0.384 at 60 °C	PSO/ N.a.	N.a.	The adsorption is spontaneous entropy-driven process; adsorption capacity order: Cu(II)>Pb(II)>Zn(II)>Cd(II) at all studied conditions	Salam, (2013)
Cd(II), Cr(VI)	Fe- and Ni- doped CNT and activated alumina nanoclusters	m / v = 2.5, for Cd(II) pH=7.5, for Cr(VI) pH=2, C_o= 100-2000,25°C, 4 h	Cd(II) 220 (229.9) Cr(VI) 250 (264.5)	PSO/ Langmuir & Freundlich	N.a.	The adsorption is favorable process for the both metals ($0<R_L<1$); Mechanism: chemisrption + external + intraparticle diffusion	Sankararama krishnan et al. (2014)
Ni(II) Zn(II) As(III) Co(II)	Coated poly-amidoamine dendrimer /CNTs (PAMAM/CNTs)	m / v = 0.03, pH = 7, C_o= 50-200, 25 °C, 4 h	Ni(II) 3170 (3900) Zn(II) 2900 (3650) As(III) 2800 (3500) Co(II) 3000 (3800)	PSO/ Langmuir		Contact times - 15 min to achieve maximum pollu tant removal; The PAMAM dendrimers have low toxicity and are cost effective; optimum pH=8	Hayati et al. (2016)
Cr(VI) Co(II) Se (VI)	CNTs- nano Zero-Valent Iron	m / v = 3, pH 7, single ions C_o=1-10; competitive	Cr(VI) 2.71 (3.29) Co(II) 2.52 (3.81) Se (VI) 2.35 (3.71)	N.a./ single - Sips model; competitive	Capacity decreased < 50%	In the case of competitive adsorption, Cr(VI) exhibited the highest affinity.	Vilardi et al. (2018)

		adsorption C_o= 1, 24 h		- modified Langmuir	after 3 cycles		
As(III) Co(II) Zn(II)	PAMAM/CNTs nanocomposite	Batch adsorption: m / v = 0.03, pH=7, C_o= 50-200, 25 °C Fixed-bed: bed height = 12.0 cm, C_o= 100, flow rate 3 mL/min, 25 °C	Batch: As(III) 2800 (3676); Co(II) 3000 (4065); Zn(II) 2900 (4016) At breakthrough, capacities (calculated with the Thomas model): As(III) 432; Co(II) 494; Zn(II) 470.	Batch: PSO / Langmuir; For fixed bed ads: Thomas and Yoon-Nelson equations	N.a.	The fixed bed adsorption: a decrease in initial concentration and flow rate and an increase in bed height caused an increase in the breakthrough time. The removal capacity at breakthrough was enhanced with a decrease in flow rate, initial ion concentration and increase in bed height.	Hayati et al. (2018)

Table 4. Brief summary on the adsorption of heavy metal ions by 3D porous graphene and its composites

Pollutant	Adsorbent characteristics	Adsorption conditions	Max adsorption capacity - exp. (calc)*, mg/g	Kinetic/ isotherm equation	Adsorbent regeneration	Remarks**	Reference
As(V)	3D Fe_3O_4/Gr aerogels	m/v=0.2, pH 7, C_o= 0.5-30, 25 °C, 12 h	32 at C_e = 23 (40.05)	PSO / Langmuir	Separation with external magnete	The loaded adsorbent can be easily separated from water	Ye et al. (2015)
Cu(II)	Graphene oxide (GO) aerogels	m/v = 0.6, pH 6.3, C_o = 20 -100, 10 - 40 °C, 30 min.	At 10 °C:16.80 (17.73) At 25 °C: 9.05 (19.65) At 40 °C: 29.85 (29.59)	PSO / Langmuir	N.a.	A fast adsorption rate of Cu(II) - due to the interconnected pore structure of GO aerogels; The adsorbed amount increased with the increase in pH, which indicates an ion-exchange mechanism.	Mi et al. (2012)
Cu(II) Ni(II) Pb(II) Cd(II)	Three-dimension Gr macroscopic electrodes	Electrolytic deposition process under i = 0.05 A for 20 min	Cu(II) 3820 Ni(II) 1683 Pb(II) 882 Cd(II) 434	N.a./ N.a.	Desorption by electrodes reversal at 0.1 A for 1 min	The fabricated electrodes possess conductivity of 12 S/cm and surface area of 560 m^2/g	Li et al. (2013)
Hg(II)	Graphene-diatom silica self-assembled aerogel	m / v = 0.04, pH 6.5, C_o = 50-400, 21 °C, 90 min	>300 (>500) 528 at C_o= 400	PSO/ Langmuir	N.a.	Mechanism - physical trapping, electrostatic interaction, chemical bonding by functional group; No major interfer ence for the removal efficiency **for tap and river water** spiked with Hg(II) to provide 100 mg/L Hg (II)	Kabiri et al. (2015)

Pb(II) Cd(II) Cu(II)	3D graphene/δ-MnO_2 aerogels	m / v = 0.065, pH 2, C_o = 1-200, 25 °C, 200 min	Pb(II) (643.62) Cd(II) (250.31) Cu(II) (228.46)	N.a. / Langmuir	Regeneration - HCl followed by KOH	Mechanism - chemical reaction, electrostatic interaction, ion exchange, interlayer trapping; Adsorbtion on the surface of graphene/δ-MnO_2 and intercalation into the interlayer gaps of MnO_2; The regenerated adsorbents can be used for > 8 cycles without performance degradation; Easily separation.	Liu et al. (2016)
Hg(II)	GO foam (3DGON)	m / v = 0.001-0.020, C_o=50 μg/L, pH 5, 21 °C, 48 h	17 at C_e=35 μg/L (35.02)	PSO, Elovich / Langmuir	N.a.	Mechanism - chemical interaction, ionic exchange; 3DGON (10 mg/L) removes up to 96% of Hg(II) in 24 h - a residual concentration in solution close to the guideline value for drinking water (1 μg/L); Affinity order: Hg(II) > Pb(II) > Cd(II) - with removal 91%, 10% and 5%, respectively	Henriques et al. (2016)
Hg(II)	Gr nanosheets+ αFeOOH + porous silica	m / v = 0.04, pH = 6.5, C_o = 10-500, 25 °C, 90 min	881± 32 at C_o = 300 mg/L (1000)	PSO/ Langmuir	N.a.	Efficient (~100%) removal of low (4 mg/L) and high (120 mg/L) concentration of Hg samples in **real** water	Kabiri et al. (2016)

Table 5. Brief summary on the adsorption of heavy metal ions by functionalized graphene and Gr-based composites

Pollutant	Adsorbent characteristics	Adsorption conditions	Max adsorption capacity - exp. (calc)*, mg/g	Kinetic/ isotherm equation	Adsorbent regeneration	Remarks**	Reference
As (V) As (III)	Functionalized Gr sheets based super capacitor water filter (f-HEG)	50 mg of f-HEG loading at each electrode, pH 7, C_o= 50-300, 1 V DC voltage applied	As (V) 195 (142) As (III) 162 (139)	intra-particle diffusion / Freundlich	N.a.	f- HEG provides good contact between electrodes and water, result - high removal from aqueous solution and sea water; Good cyclic repeatability of electrodes at high concentration of As ions in solution and sea water	Mishra and Ramaprabhu (2011)
Cr(VI)	Iron nanoparticle decorated graphene	m / v = 0.2, pH 4.5, C_o= 25 – 125, 25 °C, 4 h	137 (162.59)	PSO / Langmuir	N.a.	-	Jabeen et al. (2011)
Cr(VI)	Nanozerovalent iron decorated Gr	m / v = 1, natural pH, C_o=15-35, room temp, 180 min	22.0 (21.72)	pseudo first / Langmuir	0.01M HCl	Gr coupling facilitates the electron transfer in the NZVI and retards the surface passivation of the NZVI; The Cr(VI) removal efficiency is closely correlated to the graphene amounts in the NZVI/GNS.	Li et al. (2016)
Pb (II)	SiO_2 / graphene	m / v = 0.3, pH 6, C_o=10-50, 25 °C, 60 min	129 (113.6)	PSO / Langmuir	N.a.	A 95% of total Pb(II) - removed in 10 min; Electrostatic interaction between Pb(II) cations and negative surface charge and/or C π electrons of the composite - the main adsorption interactions. 84.23% of Pb(II) is immobilizet at pH 4.8 from mixed solution containing Cu(II), Pb(II), Ni(II), Co(II),	Hao et al. (2012)

						Cd(II), and Cr(III) each one at C_o= 20 mg/L	
Pb(II)	PAM-g-Gr Raw GO	m / v = 0.1, pH 6, C_o = 5–100, 22 °C, 24 h	PAM-g-Gr 440.4 (at 90 min, C_o=45) (819.67); Raw GO (604.00)	PSO / Langmuir	N.a.	The adsorption processes on polyacrylamide grafted graphene reaches equilibrium in 30 min; One-step synthesis	Xu et al. (2014)
Ni(II)	Grnanosheets /δ-MnO_2	m / v = 0.2, C_o= 14 g/L, 3h	770.8	PSO/ N.a.	N.a.	GNS/δ-MnO_2 composite is prepared by a microwave-assisted method	Varma et al. (2013)
Cr(VI) Pb(II) Hg(II) Cd(II) Ni(II)	Gr sheet with ferro-ferric oxide (Fe_3O_4-GS)	m / v = 0.2, pH 6–7 for Pb(II), Cd(II), Hg(II) and Ni(II); pH 1–3.0 for Cr(VI), C_o - n.a. for isotherm, 20 °C, 3 h; For kinetic studies C_o = 3 for Cr(VI), Pb(II), Hg(II), Cd(II) and 5 for Ni(II)	Cr(VI)7.29(39.92) Pb(II)27.95 (157.9) Hg(II)23.03(167.8) Cd(II)27.83(163.6) Ni(II)22.07(158.5)	PSO / Freundlich	Magnetic separation, desorption Cr(VI) - 0.2 MNaOH Pb(II) – 0.01 M HCl	Magnetic separation within one minute; The metals sorption - mainly via chelation or ion exchange; The adsorption - endothermic and spontaneous in nature; At the end of the fifth cycle, the Fe_3O_4-GS retained > 70% and 80% of its original Cr(VI) and Pb(II) adsorption capacity.	Guo et al. (2014)

Table 6. Brief summary on the adsorption of heavy metal ions by GO and GO-based composites

Pollutant	Adsorbent characteristics	Adsorption conditions	Max adsorption capacity - experimental (calc)*, mg/g	Kinetic/ isotherm equation	Adsorbent regeneration	Remarks**	Reference
As(III) As(V)	Magnetite-GO, Magnetite-rGO composite	m / v = 0.1, pH 7, C_o =0.15 - 1.0 mg/L, 25 °C, 24 h	M-GO: As(III) 85 (42.9) As(V) 38 (18.8); M-rGO:As(III) 57 (29.8) As(V) 12 (8.42)	PSO / Freundlich	N.a.	As(III) was more favorably adsorbed than As(V) onto both M-GO and M-rGO; The higher As(III) adsorption capacity - in the pH range of 6-9, the higher As(V) - at pH 4.	Yoon et al. (2016)
As(III) As(V)	Iron oxide/GO nanocomposite	m / v = 0.8, pH 7 for As(III) and pH 3 for As(V), C_o = 0.0001-1200 mg/L, 23°C, 24 h	For composite with 80 % FeO_x: As(III) - 135 (147) As(V) - 115.5 (113)	PSO / Langmuir	N.a.	Mechanism - surface complexation- As(III), electro static reactions - As(V); As(III) & As(V) in treated solutions <0.02 µg/L from 118(As(III)) or 108(As(V)); High As(III) adsorption despite the excessive presence of SO_4^{2-}, CO_3^{2-}, and PO_4^{3-}.	Su et al. (2017)
Cd(II)	GO	m / v = 30, pH 4, C_o = 10-1100, 25 °C, 120 min	GO-AG - 2079.72 (1792.60) GO-FG - 1551.06 (1531.70)	PSO / Langmuir &Freundlich	N.a.	From the SEM-EDS images, Cd(II) were uniformly adsorbed on graphene oxides – both on GO generated by using amorphous graphite (GO-AG) & GO prepared by using flaky graphite (GO-FG)	Zhang et al. (2017)
Co(II)	GO-NH_2	m / v = 0.3, pH 6, C_e = 55, 25 °C, 2 h	106 (116.35)	PSO / Langmuir	Desorption ratio of 97.17% at pH = 0.81 (HNO_3 solution)	Membrane filtration experiments (membranes thick ness 0.2–1.2 mm, flow rate 0.5–5 mL/min, C_o = 1–90) - removal depended on all experiment parameters; The highest percentage removal of Co(II) exceeds 98%.	**Fang et al. (2014)**
Co(II)	GO	m / v = 1, pH 5.5, C_o = 2-25, 25 °C, 60 min	19.23 (21.28)	PSO / Freundlic	GO precipitated upon loading	The adsorption – due to physical and chemical interactions between Co(II) and oxygen-containing	Lingamdinne et al.

				h	with metal ions	surface functional groups, –C–O and –C═O, and the π–π bonds electrons (–C═C–, –C═O) of GO	(2016)
Co(II)	GO	m/v = 0.1, pH = 6.8, 60 min	At 30 °C: 54.2 at C_e= 49.5 (66.67); At 60 °C 65.9 at C_e =48.3 (79.36)	PSO / Langmuir	N.a.	The presence of humic acid reduces Co(II) adsorption at pH<8, but no obvious effect when pH>8	**Zhu et al. (2016)**
Co(II)	Ozonized GO	m/V = 0.1, pH 6.8, 30 °C, 6 h	GO oxidized for 6 hours: 320 at C_e= 35 (371.90)	PSO / Langmuir	N.a.	Increased degree of oxidation improves the adsorption capacity; Co(II) can complex with the oxygen-containing functional groups on GO surface	**Liu et al. (2016)**
Cr(VI)	Gr–MgAl-LDH nano composite	m/v = 1, pH 2, C_o = 50 –250, 20 °C, 24 h	172.55 at C_o = 250 mg/L (183.82)	PSO / Freundlich	Elution - 0.1 M NaOH + 0.1 M Na_2CO_3	Mechanism - surface adsorption on Gr and memory effect of calcined LDH; Calcination at 500 °C regene rates eluted Gr-MgAl-layered double hydroxides (Gr–MgAl-LDH); After 6 cycles - 87.6% removal of Cr(VI) compared to the original nanocomposite	Yuan et al. (2013)
Cr(VI)	Cyclodextrin–chitosan/GO	m/v = 1, pH 3, C_o = 5 - 50 mg/L, 30 °C, 5 h	52.5 (67.66)	PSO / Langmuir	Magnetic separation, then with 0.1 M NaOH- 5h	Efficiency in solutions with low pH; The decrease in the adsorbed amount of Cr(VI) < 5% after 5 cycles.	Li et al. (2013)
Cr(VI)	MC-GO-IL composites	m/v = 1, pH 3.0, C_o = 60 -200, 30 °C, 40 min	(145.35)	PSO / Langmuir	Magnetic separation	Biodegradable biosorbent - magnetic chitosan and GO-ionic liquid; The MCGO-IL could be repeatedly used without obvious structure and performance degradation	**Li et al. (2014)**
Cr(VI)	T-GOCS composite	m/v = 0.4, pH 2, C_o = 16 - 206, 30 °C, 2 h	216.9 (219.5)	PSO / Langmuir	1 M NaOH	Cr(VI) adsorption on triethylenetetramine modified GO chitosan (TGOCS) - a chemical process partly by electrostatic attraction; After 5 cycles, the uptake of Cr(VI) on TGOCS maintained > 80% of initial uptake	Ge and Ma (2015)
Cr(VI)	GO-αCD-PP nanocomposite	m/v = 0.5, pH 2.0, C_o = 100-700, 25-45 °C, 24 h	600 (606.06) - at 25 °C	PSO / Langmuir	Cr(VI) desorption-0.5M NaOH	No significant effect on the Cr(VI) ad sorption by coex isting ions; The GO- functionalized with α cyclodex trin and modified with polypyrrole nanocomposite can	**Chauke et al. (2015)**

			670 (666.67) - at 45 °C			be re-used up to 3 cycles after regeneration with 2 M HCl.	
Cr(VI)	Amino – GO - Fe_3O_4 nanoparticle	m/v = 0.2, pH 2, 25-45 °C, 12 h	At 25 °C: 123.4 at C_e = 32 (124.5) At 45 °C: 150 at C_e = 26 (151.6)	PSO / Langmuir	Magnetic separation - 40 s, followed by 0.1 M NaOH	Electrostatic interaction, chemical reduction by π electrons transfer; The removal process by the amino functionalised GO decorated with Fe_3O_4 nanoparticles - pH dependent, endothermic and spontaneous; Both the Cr(VI) adsorption and subsequent reduction of the adsorbed Cr(VI) to Cr(III) contributed to the removal.	Zhao et al. (2016)
Cr(VI)	3-aminopropyl triethoxysilane functionalized GO	m/v = 0.4, pH 2, C_o = 50-200, 10-55 °C, 24 h	At 10 °C: 180 at C_e = 128 (186.6) At 55 °C: 206 at C_e = 117 (215.2)	PSO / Langmuir	N.a.	Cr(VI) removal - due to the Cr(VI) adsorption on surface functional groups (protonated amine groups and Si-OH groups) and the reduction of Cr(VI) to Cr(III); Cl^-, NO_3^- and PO_4^{3-} (in 100-200 mg/L) had no significant influence on the Cr(VI) adsorption; The presence of SO_4^{2-} sharply reduced the Cr(VI) removal.	He et al. (2017)
Cr(VI)	CS-CHDTTAA-GO	m/v = 2, pH 3.5, C_o = 1-750, room temp., 60 min	166.98 (169.49)	PSO / Langmuir	0.1% H_2SO_4 followed by DI water	The chitosan-1,2-cyclohexylene dinitrilotetraacetic acid – GO nanocomposite adsorbent can be regenerated > 3 times	**Ali, (2018)**
Cr(VI)	GO/chitosan/ ferrite nano composite-GCF	m/v = 0.125, pH 2.0, C_o = 10 - 125, 27 °C, 600 min	263 (270.27)	PSO / Langmuir	Washing the loaded GCF - 0.1 N NaOH, then d. water	An increase in the concentration of co-existing NO_3^- and SO_4^{2-} decreased the GCF uptake capacity for Cr(VI); Increased concentrations of Fe^{3+} and Mg^{2+} lead to increased uptake capacity for Cr(VI) .	Samuel et al. (2018)
Cr(VI)	Raw SWCNTs Ox-SWCNTs Raw MWCNTs Ox-MWCNTs	m/v = 1, pH =2, C_o = 10 - 60, 25 °C, 60 min	RawSWCNTs-(33.396) Ox-SWCNTs- (33.556) RawMWCNTs-(20.940) Ox-MWCNTs-(22.268)	PSO / Langmuir	N.a.	Mechanism: electrostatic interactions and hydrogen bonding; The surface area, oxygenated functional groups, pore size and dimension of the CBNMs perform an important role on the adsorption process of Cr(VI).	De la Luz-Asunción et al. (2018)

	GO r-GO		GO-(40.933); r-GO - (17.141)				
Cu(II)	Magnetic GO composite (SMGO)	m/v = 0.18, pH 5, C_o = 20-80, 10-50 °C, 6 h	45.5 (50.678) at 10 °C 54.5 (56.857) at 30 °C 62.0 (62.73) at 50 °C	PSO / Langmuir	Magnetic separation	The adsorption - endothermic and spontaneous; Film diffusion and intraparticle diffusion were simultaneous ly occurring during the adsorption process.	Hu et al. (2013)
Cu(II)	TEA-magnetite rGO composite	m/v = 0.25, pH 6, C_e =160 20 °C, 24 h	210.97 (209.1)	PSO / Langmuir	Magnetic separation,then with 0.1 M HCl	Excellent adsorption selectivity toward Cu(II); The total adsorption capacity of the composite after 5 cycles remains 75% of its original value.	Chen et al. (2015)
Cu(II)	Poly-allylamide hydrochloride/ GO composite	m/v = 0.1, pH 6, C_o = 10-210, 20 °C, 24 h	348 (349)	PSO / Langmuir	0.1 M HCl	Surface complexation, metal coordination, electrostatic interaction; Competitive adsorption- Cu(II) is adsorbed much preferable to Cd(II) and Ni(II) ions; The total capacity of composite - 87.6 % after 5 cycles of use	Xing et al. (2015)
Cu(II)	GO/Fe_3O_4/ Polyethylenimi ne (PEI) nano composites	m/v = 1, pH 5.0, 25 °C, 10 h	150 at C_e = 350 (157.5)	PSO / Langmuir	Soaking in 0.1 M HCl for 5 h, then magnetic separation	Mechanism - formation of amino group–metal complex es on the surface of adsorbent; Coexisting ions do not affect Cu(II) adsorption of GO/Fe_3O_4/PEI; After 5 cycles, the removal efficiency remained 84 %.	**Sui et al. (2015)**
Cu(II)	Magnetic chitosan/GO nanocomposite (MCGON)	m/v = 0.2 pH 7, 25 °C, g/L, 140 min	126 at C_e = 300 (217.4)	PSO / Langmuir	Magnetic sepa ration followed by 1M HNO_3	Adsorbent - composed of GO modified by ethylenedia mine, Fe_3O_4 nanoparticles and chitosan-g-poly(acrylic acid-co-2-acrylamido-2-methylpropane sulfonic acid) copolymer;No significant loss of capacity after 5 cycles	Hosseinza deh and Ramin (2018)
Hg(II)	Magnetic poly pyrrole-GO nanocomposite	m/v = 0.05, pH 7, C_o = 20 – 100, 27 - 47 °C, 720 min	At 27 °C: 365 (400) At 47 °C: 735 (769.2)	PSO / Langmuir	Magnetic separation	The overall adsorption process involved chemisorption and intra-particle diffusion; High removal efficiency (> 99%) for Hg(II) from **real electroplating effluent**.	Zhou et al. (2017)

Hg(II)	2,2-Dithiodisalicylic acid-functionalized magnetic GO	m/v = 0.1, pH 5.5, C_o = 1 -10, 5-50 ºC, 60 min	At 5 ºC and C_e = 4 (141.1) At 50 ºC and C_e= 1.6 (283.5)	PSO/ Sips	With 0.01 N EDTA - recovery of > 84% of the adsorbed Hg(II)	The equilibrium - in 10 min; Selective removal of Hg(II) in the presence of Cd(II), Co(II), Zn(II), and Ni(II) - each 20 mg/L - even after several regeneration cycles; Excellent adsorptive properties for Hg(II) from **natural ion matrices** - drinking water samples.	Khazaei et al. (2018)
Pb(II)	Few-layered graphene oxide (FGO)	m/v = 0.1, pH 6, 20-60 ºC, 24 h	At 20 ºC: 800 - at C_e = 78 (842); At 40 ºC: 1140 at C_e = 75 (1150); At 60 ºC: 1800 at C_e = 90 (1850)	N.a. / Langmuir	N.a.	Spontaneous and endothermic process; The process is dominated by strong surface complexation; The adsorption of Pb(II) on FGO increases with the pH increasing from 1 to 8, and then at pH > 8 decreases with increasing pH.	Zhao et al. (2011)
Pb(II)	GO EDTA-GO EDTA-rGO	m/v = 0.125, pH 6.8, C_o = 5 - 300, 25 ± 2 °C, 24 h.	GO - 328± 39 (367) EDTA-GO 479 ± 46 (525) EDTA-rGO n.a. (228)	N.a. / Freundlich	Washing with HCl pH <5.0	Removal of Pb(II) with EDTA-GO: ion-exchange reaction between Pb(II) and –COOH or –OH groups and surface complexation of Pb(II) with EDTA. Equilibrium reached in 10 to 30 min; 90% desorption from EDTA-GO surface at pH <2.0.	Madadrang et al. (2012)
Pb(II)	Magnetic chitosan / GO	m/v = 0.8, 30 ºC, pH 5, 60 min	78.56 (76.94)	PSO / Langmuir	HCl, pH 1	Desorption capacity- 90.3 %; Pb(II) ions sorption was strongly dependent on pH.	Fan et al. (2013)
Pb(II)	GO Poly(N-vinylcarbazole) blended with GO (PVK–GO)	m/v = 0.1, pH 7, C_o = 5-300, 25 ºC, 4 h	GO: 658.83 (692.66) PVK–GO: 887.98 (982.86) at 10 : 90 wt % ratio of PVK : GO	N.a. / Langmuir	N.a.	The polymer forms a π–π stacking interaction with GO through the carbazole group that stabilizes the dispersion of the nanocomposite and facilitates the exposure of the functional groups to the heavy metals; The adsorbent with the most GO % has the best Pb(II) adsorption capacity; Higher capacity at higher pH	Musico et al. (2013)

Pb(II)	Mobile GO-based microbots	C_o =1, average velo cities of the microbots around 500 µm/s	> 0.95 mg/L	N.a. / N.a.	With HCl (pH 1)	Pb(II) is decreased from 1000 ppb to below 50 ppb for 60 min; Adsorption of Pb (II) - due to the formation of electron donor–acceptor complexes; GO microbots can be reused after chemical detachment of Pb(II)	Vilela et al. (2016)
Pb(II)	GO cross-linked with hyperbranched polyethylenimines (GO-HPEI)	Model water: m/v = 0.1, pH 5.0-6.0, C_o = 5 - 300, 25 °C, 8 h; **Real** wastewater: 46.5 mg/L Pb(II), m/v = 0.035	GO-HPEI1.8K - 407±31, (438.60) GO-HPEI10K - 368±25 (393.43) GO-HPEI750 - 315 ± 21 (336.33)	PSO / Langmuir	0.1 M HNO_3 Only a slight decrease after 8 cycles	GO-HPEI1.8K contains HPEI with M_n = 1800 GO-HPEI10K -HPEI - with M_n= $1x10^4$ HPEI750K - HPEI - with M_n =7.5 x 10^5 g/mol; Adsorbent – insoluble in water - easy separation from the wastewater	**Liu et al. (2016)**
Pb(II)	GOs prepared from flaky, lump and amorphous graphite	m/v = 0.060, pH 5.0, C_o = 10.37 - 259.25, 30 °C, 180 min For kinetic studies: C_o = 103.7, 5–180 min	GO-FG: 746.2♦(768.4) GO-LG: 738.5♦ (765.7) GO-AG:766.8♦(789.9) ♦ experimental from kinetic studies	PSO / Langmuir	N.a.	Complexation reaction between Pb(II) and hydroxyl or carboxyl groups	**Peng et al. (2016)**
Pb(II)	GO-wrapped magnetic composite	m/v - n.a., C_o = 50-400, room temp., pH 6, 12 h	225.6	N.a./ N.a.	Magnetic separation then - with 0.01M HCl	Mechanism - chelation, electrostatic interaction, covalent bonding; 80% of adsorption capacity is maintained after 5 cycles	Hu et al. (2017)
Ni(II)	GO - glycine functionalized	m/v = 1, pH 6, C_o = 10 - 25, 25 °C, 50 min,	22 (38.61)	N.a./ Freundlich	N.a.	The optimized experimental parameters: 50 min, dose 1 g/L, pH 6 and Ni(II) - 15 mg/L	Najafi et al. (2015)
Zn(II)	GO	m/v=0.07, pH 7.0, C_o =10–100,20-45◦C, 12h	at 20 °C (246) At 45 °C (225)	PSO / Langmuir	With 0.01M HCl	Ion exchange mainly, the electrostatic interaction could also contribute; Exothermic and spontaneous process	Wang et al. (2013)

Zn(II)	GO	m/v = 0.12, pH 7, C_o = 10-25 mg/L, 20 °C, 6 h	166.84 (208.33)	PSO / Freundlich	0.1 M HCl	The interaction mechanism - mainly inner-sphere complexation; GO could maintain 92.23% of its initial capability after 6 cycles	Pan et al. (2018)
Cd(II) Co(II)	GO nanosheets	m/v = 0.1, pH 6, C_o = 20-30, 30 - 60 °C, 24 h	At 30 °C: Cd(II) 93 at C_e = 47 (106.3); Co(II) 54.5 at C_e = 51 (68.2) At 60 °C: Cd(II) 135 at C_e = 41.5 (167.5); Co(II) 66 at C_e = 49 (79.8)	N.a. / Langmuir	N.a.	Cd(II) and Co(II) sorption - strongly dependent on pH and weakly dependent on ionic strength; The presence of humic acid reduced Cd(II) and Co(II) sorption on GO nanosheets for pH < 8; The sorption of Cd(II) and Co(II) on GO nanosheets is endothermic and spontaneous process.	Zhao et al. (2011)
Zn(II) Cd(II) Pb(II)	Pristine GO GO–TiO_2 hybrids treated at 100°C-6 h GO–TiO_2 hybrids treated at 100 °C -12 h	m/v = 0.025, pH 5.6, C_o = 50 for each metal ion, 12 h	Pristine GO Zn(II) 30.1±2.5; Cd(II) 14.9±.5; Pb(II) 35.6±1.3 GO –TiO_2 - 6 h Zn(II) 44.8±3.4; Cd(II) 65.1±4.4;Pb(II) 45.0±3.8 GO –TiO_2 - 12 h Zn(II) 88.9±3.3; Cd(II) 72.8±1.6;Pb(II) 65.6±2.7	N.a. / N.a.	N.a.	Longer treatment times resulted in an increase in the surface area of GO-TiO_2 hybrid and thus its removal capacity of heavy metal increased	Lee et al. (2012)
Cd(II) Pb(II)	PEI-magnetic mesoporous silica - GO	m/v = 0.1, pH 7, 25 °C, 24 h	Pb(II) 318 at C_e = 86 (333.0); Cd(II) 118 at C_e = 100 (167.0)	PSO / Langmuir	N.a.	Presence of humic acid enhances adsorption of heavy metals by the composites - polyethylenimine-modified magnetic mesoporous silica and GO	**Wang et al. (2013)**
Cu(II) Zn(II)	GO	m/v = 0.1, pH = 5, 25 °C, 2 h	Cu(II) 296 at C_e = 142 (294); Zn(II) 340 at C_e = 95 (345); Cd(II) 475 at	PSO / Langmuir	N.a.	Strong surface complexation of metal ions with the oxygen-containing groups on the surface of GO; pH optimum ranges: 3–7 for Cu(II), 5–8 for Zn(II), 4–8 for	Sitko et al. (2013)

Cd(II) Pb(II)			C_e = 75 (530); Pb(II) 1125 at C_e = 148 (1119)			Cd(II), 3–7 for Pb(II); Adsorption of Cd(II) and Zn(II) on GO decreased sharply if Cu(II) and Pb(II) present; The affinity order: Pb(II)>Cu(II)>>Cd(II)>Zn(II).	
Pb(II) Cu(II)	GO silanized with N-(trimeth oxysilylpropyl) EDTA	m/v = 0.025, pH 3 for Pb and pH 5 for Cu, C_o = 1-100, 25 °C, 90 min	Pb(II) 380 at C_e = 95 (454.6) Cu(II) 90 at C_e = 95 (108.7)	N.a./ Langmuir	N.a.	The composite has improved anti-microbial properties compared to GO alone; No cytotoxicity was observed towards human corneal epithelial cell lines hTCEp after 24 h exposure to the composite.	Carpio et al. (2014)
Pb(II) Cu(II) Cd(II) Hg(II)	Poly-dopamine (PD) + GO (PF/GO) composite	C_o = 50 for all ions pH 4.0–5.4 for Pb(II) pH 5.2–6.8 for Cu(II) pH 5.2–6.8 for Cd(II) pH 3.5–4.0 for Hg(II)	Pb(II) 53.6 Cu(II) 24.4 Cd(II) 33.3 Hg(II) 15.2	N.a. / Langmuir	N.a.	Synergistic effect of individual components in designing new functional composites	Dong et al. (2014)
Pb(II) As(III) As(V)	Pristine GO GO–$MnFe_2O_4$ nanohybrids (GONH)	m/v = 0.2, pH 5 for Pb(II), pH 4 for As(V), pH 6.5 for As(III), C_o = 1 - 400, 25 °C, 20 h	Pristine GO Pb(II) (305);As(V) (113) As(III) (77) GONH Pb(II) (673);As(V) (207) As(III) (146)	PSO / Langmuir	Desorption of arsenic ions - with 1 M NaOH, Pb(II) desorption with 0.2 M HCl	Easy magnetic separation and reusability; HCO_3^- and HPO_4^{2-} decrease the adsorption capacity of GONH; No considerable change in adsorption and desorption efficiencies, even after 5 cycles	Kumar et al. (2014)
Pb(II) Cd(II) Cu(II)	GO/Polyamido amine dendri mers - PAMAMs/GO	pH 5 for Cd(II), pH 4.5 for Pb(II), C_o=1- 6 mmol/L for each ion, 25 °C, 4 h	Cd(II) (253.81) Pb(II) (568.18) Cu(II) (68.68)	PSO / Langmuir	N.a.	The adsorption process practically achieves equilibri um in 60 min; The adsorption efficiency is strongly dependent on pH, temperature and adsorbent dosage.	**Zhang et al. (2014)**
Cu(II)	Chitosan/Sulfy	m/v = 1, pH 5, C_o =	Single metal ion system	PSO /	HNO_3 (0.01 M)	The equilibrium - in 30 min; The adsorption efficiency	**Li et al.**

Pb(II) Cd(II)	dryl-functionalized GO CS/SH/GO	10-500, 20 °C, 90 min	Cd(II)- (177.0); Pb(II)-(447.0); Cu(II) - (425.0) Competitive asdorption: Cd(II) - 80 > Cu(II) - 50 > Pb(II) - 35.	Freundlich		- strongly dependent on pH, temperature and adsorbent dosage; The recycled materials could be obtained at about 85% recovery level on desorbing metal ions after 3 cycles.	**(2015)**
Cu(II) Cd(II) Ni(II)	Highly ordered layered GO membranes	m/v = 0.2, pH 5.7, C_o = 5-100, 30 °C, 50 min	Cu(II) (72.6) Cd(II) (83.8) Ni(II) (62.3)	PSO / Langmuir	1 M HCl	Ion exchange mechanism; The GO membranes can be regenerated > 6 times with a slight loss in the capacity	Tan et al. (2015)
Pb(II) Hg(II) Cu(II)	EDTA functionalized magnetic GO (EDTA-mGO)	m/v = 2 for Pb(II), = 4.8 for Hg(II), = 4 for Cu(II), pH = 4.2 for Pb(II), 4.1 for Hg(II), 5.1 for Cu(II), 45 °C, 40 min for Pb (II), 50 min for Hg(II), 90 min for Cu(II)	Pb(II) (508.4) Hg(II) (268.4) Cu(II) (301.2)	PSO / Freundlich and Temkin	Magnetic separation of loaded material - 25 s followed by 0.1 M HCl	Endothermic and spontaneous adsorption process; After 5 recycles - 86.4% removal efficiency for Pb(II), 85.9% - for Hg(II) and 87.6% - for Cu(II).	Cui et al. (2015)
Pb(II) Cd(II) Cu(II) Zn(II)	GO/zirconium phosphate nanocomposite	m/v = 1.5, pH 6, C_o = 5 - 400, room temp., 400 min	Pb(II) - 363.4 Cd(II) - 232.4 Cu(II) - 328.6 Zn (II) - 251.6	PSO / Freundlih		Mechanism - chemisorption, mainly through surface complexation; A removal efficiency of 99% - in 20 min, at 50 mg/L heavy metals.	Pourbeyram, (2016)
Co(II) Ni(II) Cu(II) Zn(II) Cd(II)	GO/cellulose membrane	m/v = 0.080, pH 4.5, C_o = 0.5–20 for Cu(II), 1–12 for Zn(II), 1–14 for Co(II), 0.5–17 for Ni(II), 1–20 for Cd(II), 4–40 for Pb(II), 25 °C,	Co(II) - 15 (15.5) Ni(II) - 14 (14.3) Cu(II) - 26 (26.6) Zn(II) - 15.8 (16.7)	PSO / Langmuir	The membrane can be used >10 cycles	Ions immobilization is controlled by the chemical adsorption involving the strong surface complexation of metal ions; The competitive adsorption order: Pb > Cu > Cd > Zn ≥ Ni ≥ Co	Sitko et al. (2016)

Pb(II)		180 min	Cd(II) - 26 (26.8) Pb(II) - 101 (107.9)				
As(V) Cr(VI)	Magnetite GO encapsulated in alginate beads	m/v = 5, pH 5 for Cr(VI) and pH 7 for As(V), C_o = 10 - 200, 20 °C, 24 h	As (V) 6.7 at C_e = 142 (6.86) Cr (VI) 9.5 at C_e = 110 (14.90)	PSO / Langmuir	With an external magnet	Mechanism - electrostatic interaction, chemical interaction; The mGO/beads could be reused for at least 5 cycles without the leaching of core mineral contents	Vu et al. (2017)
Pb(II) Cu(II)	PVA modified gum tragacanth / GO hydrogel	m/v = 1, pH 6, C_o = 20 - 100, 25 °C, 6 h	Pb (II) 81.78 (88.49) Cu (II) 69.67 (76.92)	PSO / Langmuir	HNO_3 solution	Mechanism - electrostatic interaction, chelation, ionic exchange; Column application of magnetic beads are also highly feasible; The adsorption decreased with 2.75% for Pb(II), 6.5% for Cu(II), after 3 cycles.	Sahraei et al. (2017)

Table 7. Brief summary on the adsorption of heavy metal ions by rGO and rGO-based composites

Pollutant	Adsorbent characteristics	Adsorption conditions	Max adsorption capacity - experimental (calc)*, mg/g	Kinetic/ isotherm equation	Adsorbent regeneration	Remarks**	Reference
As(III) As(V)	Magnetite rGO (M-rGO)	m / v = 0.2, pH 7, C_o = 3-7, 20 °C, 2 h	As(III) 8.5 (13.10) As(V) 4.3 (5.83)	PSO/ Langmuir & Freundlich	Magnetic separation	The temperature of the maximum adsorption is 30 °C; Mechanism- surface complexation; >99.9% arsenic removal; M-rGO composites - superparamagnetic	Chandra et al. (2010)
As(III) As(V)	Magnetite-GO Magnetite-rGO	m / v = 0.1, pH 7, C_o =0.15-1.0, 25 °C, 24 h	M-rGO: As(III) 57 (29.8); As(V) 12 (8.42) M-GO: As(III) 85 (42.9) As(V) 38 (18.8)	PSO/ Freundlich	N.a.	The adsorption mechanism of As(III) - surface complexation; The electrostatic interaction between the positively charged surface of adsorbents and anionic As(V) species - a major factor for the removal	Yoon et al. (2016)
Cd(II)	3D sulfonated rGO aerogel (3DSrGO)	m / v = 0.1, pH 6, C_o= 2-50, 25-65 °C, 24 h	93 at C_o=10 mg/L At 25 °C and C_e=50 mg/L – 169; At 65 °C and C_e=50 mg/L - 209 (234.8)	PSO/ Langmuir	HNO_3 solution at pH = 0.3	Cation exchange of H by Cd and formation of Cd complex are the important mechanisms for Cd removal; > 93% of Cd(II) - removed in 20 min; HNO_3 solution (pH 0.3) desorbs 97.23% Cd(II) from the loaded 3DSrGO.	Wu et al. (2015)
Cr(VI)	ED-rGO sheets	m/v=1, pH 2, C_o=100, room temp, 24 h	89	N.a./ N.a.	N.a.	Cr(VI) can be reduced to low toxic Cr(III) species at low pH; Reduction - with the aid of π electrons on the carbocyclic six-membered ring of ED-rGO.	Ma et al. (2012)

Cr(VI)	Poly(phenylenediamine)/ rGO/nickel ferrite magnetic adsorbent PmPD/rGO/NFO	m / v = 0.1, pH 3, C_o =50-250 mg/L, room temp, 90 min	325 at C_o=100 mg/L (502.5)	PSO/ Langmuir	Magnetic separation	A rapid adsorption in the first 10 min; The immobilization of Cr(VI) involves: (1) Direct adsorption- by the electrostatic interaction between the negatively charged Cr(VI) species and the protonated quinoid imine groups as well as the surface positive charge on PmPD/rGO/NFO, (2) Indirect adsorption: Cr(VI) is reduced to Cr(III), and positively charged Cr(III) - removed by electrostatic interaction with negatively charged groups of rGO.	Wang et al. (2017)
Cr(VI)	Chitosan (CS)/rGO (rGO)/montmorillonite composite	m / v = 1, pH 2, C_o= 0-240, 15 °C, 3 h,	84.0 (87.03)	PSO/ Langmuir	1 M NaOH	The composite hydrogel can restore to the original shape and dimension after compressive deformation and show good stability in acidic conditions	**Yu et al. (2017)**
Cr(VI)	RGO/NiO	m / v = 0.333, pH 4, C_e=110, 25 °C,	187 (198)	PSO/ Langmuir	0.1 M HCl	pH 3–5 favored for Cr (VI) adsorption; The optimal GO amount- 20 wt%; 83% efficiency after 5 cycles	Zhang et al. (2018)
Cu(II)	Polyvinylpyrrolidone-rGO	m / v = 2.5, pH 3.5, C_o =3.5-17.5 g/L, 10 min	1689 at C_o = 7 g/L,	Na/ N.a.	N.a.	Physisorption of Cu ions on Gr modified by PVP. Density functional theory (DFT) is applied.	Zhang et al. (2014)
Hg(II)	Polypyrrole – reduced graphene oxide (PPy-rGO)	m / v = 0.2, pH 3, C_o = 50-250, 20 °C, 3 h	580 at C_o=130 mg/L; (980)	PSO/ Langmuir	HCl, pH 3,2; 1	The capacity of the PPy-RGO - due to enhanced adsorption sites for Hg(II) in the presence of Gr sheets. The desorption capacities for 50 mL HCl at pH3,2, & 1 are 45,63 & 92.3% respectively.	Chandra et al. (2011)
Hg2+	rGO –MnO_2 and	m / v = 0.025, C_o = 1,	Both for RGO –MnO_2	pseudo-	N.a.	The immobilized RGO composites was prepared	Sreeprasa

	rGO-Ag	30 °C	and RGO-Ag - distribution coefficient (K_d) > 10 L/g for Hg(II) uptake	first-order		without the use of any external acid; The size of the nanoparticles formed can be tuned by controlling the precursor concentration added.	d et al. (2011)
Hg2+	Magnetic spinel Fe_2CuO_4/rGO nanocomposite	m / v = 0.8, pH 7.0, 24 °C, 60 min	(1250) at C_e=500 mg/L	PSO/ Langmuir	N.a.	The composite was used as a a catalyst to pyrolyze discard tires and after its deactivation - as adsorbent The adsorption is referred to the impact of sulfur compounds, deposited on it during the tire pyrolysis	Zandi-Atashbar et al. (2018)
As(III) Cr (VI) Hg(II) Pb(II) Cd(II)	rGO–Fe_3O_4; rGO–Fe(0)–Fe_3O_4; rGO–Fe(0) composites	m / v = 0.05, pH 7, C_o = 2-6, 25 °C, 60 min	For As(III) rGO–Fe_3O_4 - 21 rGO–Fe(0) - 37 r GO–Fe(0)–Fe_3O_4 - 44; For other metals: rGO–Fe(0)–Fe_3O_4: Cr (VI) - 33; Hg(II)-23; Pb(II) - 22; Cd(II) - 3	Na/ Langmuir	na	rGO–Fe(0)–Fe_3O_4 composite was applied to **natural water samples** with C_o for As(III) = 0.98 - 4.82 ppb with > 90% adsorption efficiency	Bhunia et al. (2012)
Pb(II) Hg(II)	$CoFe_2O_4$-rGO	m/v 0.16 for Pb(II) & 0.14 for Hg(II); pH = 5.3 for Pb(II) & 4.6 for Hg(II), C_o - n.a., 25 °C,120 min	Pb(II) 123.3 at C_o= 20 mg/L (299.4); Hg(II) - 27.91 at C_o= 5 mg/L (157.9)	PSO/ Langmuir	Magnetic separation in 2 min.	The adsorption processes is chemisorption	Zhang et al. (2014)

As(V) Ni(II) Pb(II)	Fe_3O_4-rGO nanocomposite	m / v = 0.4, pH 5.5–6 for As(V) and Pb(II), pH 4.7–5.2 for Ni(II), C_o= 2-100 for As(V), C_o = 11.69-51.12 for Ni(II), C_o = 13.10 - 75.80 for Pb(II), 25 °C, 4 h	As(V) - 43.0 (54.48) Ni(II)- 52.5 (76.34) Pb(II) - 44.5 (65.79)	PSO/ Langmuir	Magnetic separaion	Mechanism: Electrostatic interaction, protonation and ionization; Fe_3O_4/rGO exhibits superparamagnetic properties at room temperature	Hoan et al. (2016)
Pb(II) Cr(III)	rGO -inverse spinel nickel ferrite nanocomposite (rGONF)	m / v = 0.4, pH 5.0 (for PbII), pH 4.0 (for CrVI), C_o = 2.0 -25.0, 25 °C, 30 min	Pb(II) – 80 (121.95) Cr(III) – 80 (126.58)	Na/ Langmuir	1 M HNO_3	Monolayer adsorption on a homogeneous surface of rGONF, the adsorption occurs through an inner-sphere surface complex; The rGONF can be re-used up to 4cycles with more than 99% adsorption of both metal ions.	Lingamdinne et al. (2017)
Hg(II) Cu(II) Pb(II) Cr(VI) As(V)	2-Imino-4-thiobiuret–Partially reduced GO (IT-PrGO)	m / v = 1, pH = 5 Hg(II), 5.5 Pb(II) and Cu(II), 3 Cr(VI), 2.5 As(V); C_o = 25-1100 Hg(II), 10-500 Pb(II), 10-300 Cr(VI), 10-250 Cu(II), 5-150 As(V); 25 °C, 4 h	Hg(II) 624 (at C_o=900 mg/L) (657.9) Cr(VI) 63.0 (66.3) As(V) 19.0 (20.8) Cu(II) 37.0 (37.9) Pb(II) 101.5 (102.2) At C_o (Hg) = 50 mg/L -	PSO/ Langmuir	Different solutions – see next column	IT-PrGO shows exceptional selectivity for Hg(II) In a mixture of 6 metal ions containing 10 ppm of each ion, the IT-PRGO shows a removal of 3% Zn(II), 4% Ni(II), 9% Cd(II), 21% Cu(II), 63% Pb(II), and 100% Hg(II); Chemisorption mechanism via the amidinothiourea groups grafted on the RGO; Desorption of the metal ions Hg(II), Cu(II), Pb(II), Cr(VI), and As(V) reaching 96%, 100%, 100%, 96%, and 100%, respectively; Desorption: Hg(II) - by 6%	**Awad et al. (2017)**

			100 % removal in 90 min			thiourea + 2 M HNO_3; Pb(II) and Cu(II) - by 1.5 M HNO_3; As(V) and Cr(VI) - by 1 M NaOH solution.	
Cu(II) Cd(II) Pb(II) Hg(II)	Dithiocarbamate (DTC) functionalized magnetic rGO (rGO-DTC/Fe_3O_4).	m / v = 0.4, pH 6, C_o=100 mg/L for each of the metal ions, 25 °C, 1 h	Cu(II) - 96 (113.64) Cd(II) - 114 (116.28) Pb(II) - 134 (147.06) Hg(II) – 76 (181.82)	PSO/ Langmuir	Elution - 0.1 M HCl followed	The adsorption processes - mainly controlled by ion exchange between sodium ions of rGO-PDTC/Fe_3O_4 composite and heavy metal ions. Fast kinetics and easy adsorbent regeneration; The adsorption capacities for Cu(II), Cd(II), Pb(II), and Hg(II) ions in the second cycle decreased approximately 5.48%, 5.29%, 8.15% and 7.26%, respectively. In the next 3 cycles, the adsorption capacities become stable.	Fu and Huang (2018)

Carbon Nanomaterial as Emerging Class: Current and Future Perspectives

Ajay Kumar[a*], Arush Sharma[b*], ManitaThakur[c]

[a*]Department of Chemistry, IEC University, Solan, Himachal Pradesh, India

[b*] School of Sciences, Baddi University of Emerging Sciences and Technology (BUEST), BaddiSolan, Himachal Pradesh, India

[c]Department of Chemistry, Maharishi Markandeshwar University (MMU), Solan (H.P), India

E.mail: arush766@gmail.com

Abstract

Today's cutting-edge technology is moving forward for those materials, which are eco-friendly as well as cost effective. Natural or agronomic materials, which are present in bulk quantities offers low-cost and discarded without any expensive regeneration. Thus, abundance and availability of lignocellulosic materials obtained from various agronomic products make them excellent precursors for the preparation of carbon. These carbon nanomaterials act as emerging class of materials, which are being used over the globe in vast areas due to their unique properties such as high mechanical strength, flexible structural moieties, boosted surface area, legitimate thermal and electronic properties etc. These reliable properties account the carbon nanomaterials in the various field of research, whether it is relevant to the green energy production or environmental detoxification. The presence of various contaminants in the environment has recently gained major concern regarding their potential threat to human health and aquatic ecosystem. The recent investigations have shown that

various carbon nanocomposites perform diverse function including photo catalysts, adsorbents, sensors and antimicrobial agents etc. Hence, making them a neoteric benchmark against all major water contaminants. The articles presents a comprehensive summary on the role of carbon based nanomaterials/quantum dots for the detoxification of noxious pollutants from water system and proposed some strategies for designing the highly efficient multifunctional carbon nanocomposites for deteriorating the environmental crisis.

1. Introduction

The present technology has immense focuses on the development of cost effective and ecofriendly materials for the wide area application. Carbon based nanomaterials are the class of those materials on which various scientific communities doing research for multidirectional utilization. Carbon nanotubes, fullerenes, graphene, reduced graphene oxide, activated carbon etc. are such carbon based materials which attract the present scenarios of research. These materials has various application in all the fields of global research such as adsorption, photocatalysis, biomedical application, catalysis, green fuel synthesis etc. Despite carbon based nano materials regarded as the most suitable materials for environmental remediation applications, a diverse combination of such materials has been accomplished beyond their limitations in terms of ease of availability of raw materials, stability and ecofriendly. Recent trends in the designing, fabrication and utilization of carbon nanomaterial has been highlighted in this review which summarizes the recent work in the respective fields.

2. Carbon nanotubes

Carbon nanotubes (CNTs) have been explored in scientific research area more than fifteen years due to their exclusive properties which encode their potential applications. In 1952, Radushkevich and Lukyanovich firstly

reported nanomaterial's having "worm-like" carbon formations [1]. Meanwhile in late 1990s, the production of carbon nanotubes (CNTs) increases globally nearly 60% per year. In last few years, the production and manufacturing of materials that lies in nanometre scale immensely raised. These novel materials has been made up of organic and inorganic materials. Carbon nanotubes (CNTs) are one of them with superior properties. Carbon nanotubes (CNTs) are allotropes of carbon and also known as buckytubes. CNTs have cylindrical nanostructure carbon molecules with exceptional properties which make them potentially valuable in nanotechnology, electronics, optics, and in different areas of materials science and technology. CNTs has been designed from identical graphite sheet comprised of many structures, differing in length, thickness, helicity and number of layers. The electrical properties differ depending on these variations and may be act as either metals or semiconductors. On the other hand, carbon can build closed and open cages with atomic arrangement like honeycomb and in 1985, C60 molecule was discovered by Kroto et al [2].

2.1 Structure and Bonding

Carbon nanotubes belongs to fullerene family of carbon allotropes and termed as tubular fullerenes consist of cylindrical graphene sheets. They have cylindrical molecules with hexagonal arrangement of sp^2-hybridized carbon atoms with C-C bond distance of 1.4 Å. These are hollow cylinders obtained by rolling multiple layers of graphene sheet to obtain different allotropes of carbon like fullerenes, CNTs and graphite. These cylindrical structures have two forms (SWNTs) and multi walled carbon nanotubes (MWNTs). Although, nanotubes can merge together at high pressure producing strong, unlimited length wires with high-pressure nanotube and conversion of some sp^2 bonds to sp^3 bonds [3, 4].

2.3 Types of carbon nanotubes

CNTs has been classified into four major categories including single-walled CNTs, double-walled CNTs, multi-walled CNTs and types on the basis of chirality. But out of these, two single and multiple walled carbon nanotubes has been explored widely as discussed in detail below.

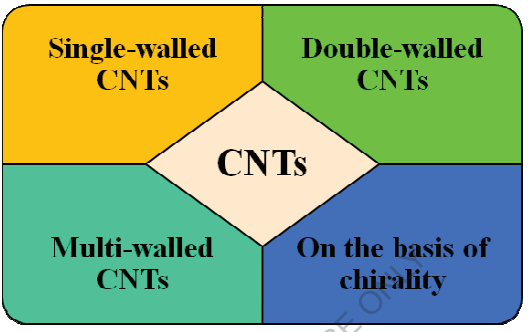

Figure 1: Classification of CNT's

2.3.1 Single-walled CNTs

Single-Walled Nanotubes (SWNTs) are an important range of carbon nanotubes and made up of single graphene sheet rolled at both ends in a hemispherical arrangement of carbon networks with a diameter of 1–2 nm. SWNT's structure can be formed by wrapping one atom thick layer of graphite. The inclusion of pentagonal and heptagonal C-C structures results closure of the cylinder during the growth process. The graphene sheet has been wrapped and represented by indices (n, m) which are known as chiral vector. In this, n and m correspond number of unit vectors along two different directions in the crystal lattice of grapheme [5-8]. The values at m = 0, nanotubes become zigzag which are named for the pattern of hexagons.If n = m, nanotubes are termed as armchair which denotes one of

the two confirmers of cyclohexene. They are also termed as chiral in which the value of m lies in the middle of zig-zag and armchair structures. The length of SWNT's can fluctuate depending on the synthesis techniques. The band gap of SWNT's may alter from 0 to 2 eV and their electrical conductivity illustrates metallic or semiconducting behavior [9]. SWNTs with nanometer diameters can act as excellent conductors and explored in the development of the first intermolecular field-effect transistors (FET) [10].

2.3.2 Multi-walled CNTs (MWNTs)

Multi-walled nanotubes made up of multiple concentric cylinders of graphitic shellswith 2 to 50 nm diameters depending on the number of graphene tubes. MWNTs have inter-layer distance of 0.34 nm approximately. There are two different models like Russian Doll model and Parchment model has been employed to designate the structures of MWNTs. In Russian Doll model, graphite sheets has been organized in concentric cylinders [11-13]. While, in the Parchment model, single sheet of graphite is rolled in around itself and perceived as a scroll of parchment or a rolled newspaper. However, the interlayer distance (3.4 Å) in MWNTs is similar to the distance between graphene layers in graphite approximately. Although, the Russian Doll structure has been observed mostly and its individual shells can be labelled as Single-walled CNTs which can be either metallic or semiconducting. Single-walled CNTs have a better diameter however MWNTs have structural defects causing less stable nanostructure [14-16]. Table 1 shows the difference between single-walled and multiple-walled carbon nanotubes as mentioned below:

Table 1: Difference between single-walled and multiple-walled carbon nanotubes

S. No.	Single-walled CNTs (SWNTs)	Multi-walled CNTs (MWNTs)
1.	These consists single layer of graphene.	These are made up of multiple layers of graphene.
2.	In SWNTs synthesis catalyst is required.	MWNTs can be produced without using catalyst.
3.	Purity is poor in this type. However high purity up to 80% has been found in arc discharge synthesis method	Purity is high.
4.	Not fully dispersed, and form bundled structures.	Homogeneously dispersed with no apparent bundled formation.
5.	Characterization, evaluation of SWNTs is easy and duringfunctionalization chance of defect is high.	MWNTs has very complex structure and chance of defect is less when synthesized using arc-discharged method.
6.	These can be easily twisted, more flexible and less accumulated in human body.	These cannot be easily twisted and more accumulation in body.

2.4 Methods for the synthesis of carbon nanotubes

Carbon nanotubes are synthesized by using three main techniques including arc discharge, laser ablation and chemical vapour deposition as shown in Figure 2. Although researchers has been finding more economic ways to synthesize these structures.

Figure 2: Different techniques used for the synthesis of CNT's

2.4.1 Arc Discharge

The arc discharge method is the most common and easiest way to produce carbon nanotubes and initially used for producing C-60 fullerenes. In this method, nanotubes has been created by arc-vaporization of two carbon rods placed end to end (separated by approximately 1mm) inan enclosure which is filled with inert gas at low pressure. Although, it is also possible to create nanotubes with arc method in liquid nitrogen. In this, a direct current of 50 to 100 Angstrom has been driven which creates a high temperature discharge between the two electrodes. This discharge vaporizes from one of the carbon rods and forms a small rod shaped deposit on another rod. Nanotubes has been produced in high yield if there is uniformity of the plasma arc and the temperature of the deposit which is formed on the carbon electrode. The growth mechanism have been increasing and measurements shown that different diameter distributions are observed due to the mixture of helium and argon. These mixtures have different diffusions coefficients, thermal conductivities which affect the speed of carbon and catalyst molecules diffuse and cool [17-19].

2.4.2 Laser ablation

In this, oven is filled with helium or argon gas to maintain pressure at 500 Torr and very hot vapour plume forms then expands and cools rapidly.

As the cooling occurs, small carbon molecules and atoms condense quickly to form larger clusters like fullerenes. The catalysts used also begin to condense slowly at first and attached with carbon clusters to prevent their closing into cage structures. Tubular molecules grow into single-wall carbon nanotubes until the catalyst particles become too large or conditions have cooled appropriately. The particles has been coated with a carbon layer that they cannot absorb more and the nanotube stops growing. The SWNTs has formed in this case are bundled together by Vander Waals forces. Laser ablation is almost similar to arc discharge including the optimum background gas and catalyst mix is similar. This was due to very similar reaction conditions and same mechanism in the reactions probably occur [20, 21].

2.4.3 Chemical vapor deposition

In this method, synthesis is attained by putting a carbon source in the gas phase and using an energy source such as a plasma to transfer energy to a gaseous carbon molecule. A mixture of hydrocarbon gas, acetylene, methane or ethylene and nitrogen has been introduced into the reaction chamber. Then, carbon diffuses towards the substrate which is heated and coated with a catalyst such as Ni, Fe or Co where it will bind. Thermal annealing results in cluster formation on the substrate, from which the nanotubes will grow. Nanotubes has been formed during the reaction on the substrate by decomposition of the hydrocarbon at temperatures (ranges 700°C–900°C) and atmospheric pressure. The nanotubes are obtained at lower temperature, lower quality and the catalyst can be deposited over the substrate which allows CNTs to adopt well-organized structures [22-24].

2.5 Applications of CNT's

2.5.1 Biomedical applications

In genetic engineering, CNTs has been used to manipulate genomes and atoms in the development of bio imaging genomes, proteomics and tissue engineering. Their tubular nature proved them as a vector in gene therapy. The unwound DNA winds around single walled nanotubes by connecting its specific nucleosides and causes change in its electrostatic properties.

Miniature sized nanotubes and nanohorns get attached with other proteins and amino acids avoiding rejection for implants [25]. They can also be used as implants in the form of artificial joints without host rejection reaction. Due to their high tensile strength, carbon nano tubes filled with calcium and grouped in the structure of bone can act as bone substitute. Protein/enzyme filled nanotubes have been employed as implantable biosensors because of their fluorescence ability in the presence of specific biomolecules [26]. Nanosize robots and motors with nanotubes can be used in studying cells and biological systems. Gelatin CNT mixture (hydro-gel) has been used aspotential carrier system for biomedicals. Anticancer drug Polyphosphazene platinum given with nanotubes had enhanced permeability, distribution and retention in the brain due to controlled lipophilicity ofnanotubes [27].

2.5.2 Catalyst and Preservative

Nanohornshave large surface area and hence, the catalyst at molecular level can be incorporated into nanotubes in large amount. At the same time can be released in required rate at particular time. Hence, reduction in the frequency and amount of catalyst addition can be achieved by using CNTs. Carbon nanotubes and nanohorns are antioxidant in nature. Therefore, they has been used to preserve drugs formulations prone to oxidation. Their antioxidant property is used in antiaging cosmetics and sunscreen [28, 29].

2.5.3 Lithium ions batteries

Lithium is widely used for the manufacturing of efficient batteries due to its lowest electronegativity therefore electrons has been easily donated from Lithium. But it is also high reactive which limits its applicability as the metal loses its efficiency. This problem can be solved by intercalating Li ions within CNTs. This enables Lithium ions to migrate from a graphitic anode to the cathode separated by using polyolefin. The charge and discharge phenomena in these batteries are controlled by the Li^+ intercalation and de-intercalation rates. Therefore, to enhance their storage capacity and lifetimes, many electronics companies have begun to use CNT's as the electrodes in Li^+ batteries [30-32].

2.5.4 Sensors

Sensors are widely used in different fields and the efficiency of biosensors and molecular sensors can be enhanced by attaching CNTs onto them. Wong et al demonstrated that it is possible to sense functional chemical groups attached onto the ends of CNTs. Thus, it is possible to construct different types of sensors containing nanotube composite pellets. CNT's are very sensitive to gases and can be used to monitor leaks in chemical plants. In addition to gas sensing, CNTs and its composites has been also used as sensitive environmental pressure sensors. CNTs are very sensitive to liquid immersion or polymer-embedding processes because nanotubes slightly deform in the presence of different liquid media [33-34].

2.5.5 Supercapacitors and actuators

CNTs are excellent materials for use in electrochemical devices due to their large surface area as well as their high electrical conductivity. It is possible to achieve very high specific capacitances in devices containing 38 wt% of H_2SO_4 as the electrolyte using sheet electrodes of pyrolytically grown MWNTs. CNT super capacitors has been used in devices that

require high power capabilities and higher storage capacities. CNT-embedded super capacitors can be used to provide fast acceleration and store braking energy electrically for hybrid electric vehicles. CNT-modified actuators has been prepared by several researchers. Actuators are important devices but their efficiency decreases with increase in temperature. These work at relatively low voltages and at high temperatures. Maximum stress observed in SWNT actuators was 26 MPa [35-37].

3. Graphene

Graphene is the sheet of2-D network of carbon atom arranged in a honeycomb motif which attracted extensive research owing to its high mechanical, thermal, optical, and electrical properties. The last decade has engaged with graphene in multidisciplinary research in the fields of bio-sensing, nano-electronicspolymer composites, capacitors, catalysisetc [38,39]. Its unique properties such as high thermal conductivity about ~5000 W m^{-1} $K^{-1}$with a charge carrier mobility of 200000 cm^2 V^{-1} s^{-1} and high specific surface area 2600 m^2/g makes it a suitable carbon material to mitigate the various research related hitches[40].

3.1 Synthesis strategies

In the early 1975, B. Lang et al demonstrated the thermal decomposition of carbon on Pt substrate but due to failure of product benefits identification, the process was not studied over a long period of time[41]. Later Novoselov et al in 2004 successfully prepared graphene by exfoliation methods[42]. Further various researcher has discovered and developed various methods for the efficient synthesis of graphene. Some of these are summarized below.

Graphite is the basic raw material used for the graphene synthesis via the two main synthesis strategies top-down and bottom-up method[43].Figure 3 depict the methodology adopted for graphene synthesis.

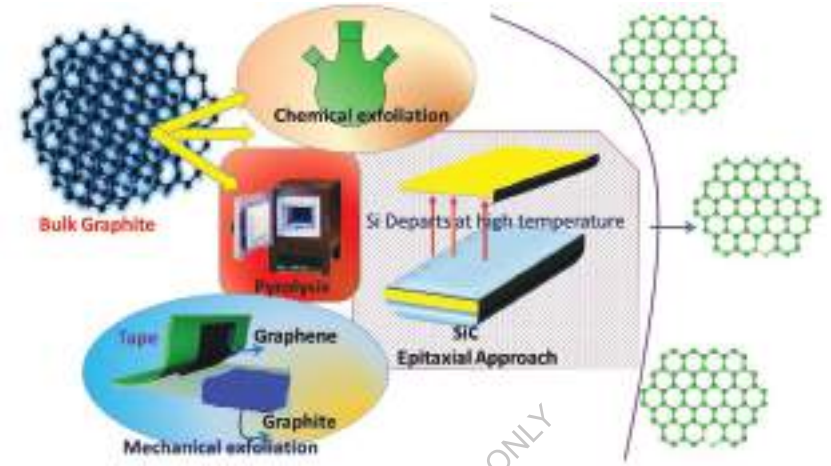

Figure3: Different methods for graphene synthesis from graphite

3.1.1 Chemical exfoliation

Most commonly the Hummer's method is adopted for chemical exfoliation for the indirect synthesis of Graphene through oxidative-reduction of graphite [44]. Initially a strong oxidizing agent $H_2SO_4/KMnO_4$ is used to oxides graphite powder into its oxidized product graphite oxide. Which further reduced into reduced graphene oxide and graphene. The common reducing agents such as hydrazine [45], sodium borohydride [46], ascorbic acid [47], hydro-iodic acid [48] etc. has been used as reducing agent.

3.1.2 Mechanical exfoliation

Mainly the graphite is the scaffold of graphene layer which involve the staking of graphene layers by Van-der Wall and chemical forces. The bond energy between two layers of graphene in graphite is $2eV/nm^2$ [49]

however for mechanical exfoliation of a single layer a force of ~ 300nN/μm^2 is required[50]. The mechanical exfoliation is basically peeling off the thin layer of graphene from the solid graphite substrate. The common peeling agent such as scotch tape, ultra-sonication, electric field has been used for mechanical exfoliation [51-53].

3.1.3 Pyrolytic treatment

Pyrolysis involve the high temperature treatment of graphite oxide (GO) at 1500-2000°C which leads to the formation of thin layer graphene sheets. The elevated temperature degrade the oxygen containing functional moieties of oxidized GO into CO or CO_2 which expend the pressure on the stacked layer ultimately resulted in the formation of graphene sheets[54].

3.1.4 Epitaxial Approach

As the name suggests *epi* means above and *taxis* mean ordered, this approach involve the formation of graphene from a carbon substrate such as SiC under ultra-high vacuum condition[55]. But the productivity is greatly influenced by the operating parameters such as pressure and heating rate.

3.2 Wide mode of application

3.2.1. Utilization for environmental remediation

The key feature of graphene i.e 2-D scaffold of honeycomb motif which contain conjugated π –electron which give it high conductivity for charge carrier as discussed earlier. This property has been efficiently explored for the various photocatalytic operation[56]. The phenomenon of adsorption also has been studied by sole graphene and chemically modified graphene according to the targeted species.

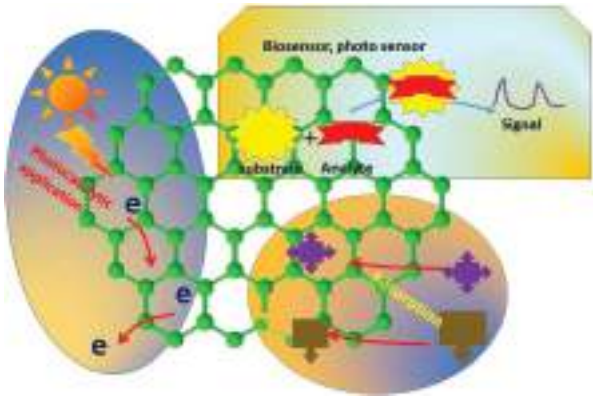

Figure 4: Various mode of applications

Thus various graphene and its derivative based nano-composites has been continuously analysed for the various application in the field of photocatalysis and adsorption. Various composites for adsorption has been prepared in composition with graphene and listed in **Table 2.**

Table 2: Various graphene based composite for adsorption based application

Sr. no	Composite	Pollutants	Ref
1	polyamide-graphene	Antimony(III)	57.
2	Bi2WO6/graphene	MB	58.
3	GO	Anionic azo-dyes	59.
4	GO	Cationic dyes	60.
5	RGO	Malachite green dye	61.
6	RGO/TiO_2	2,4-DCP	62.
7	A-rGO/cobalt oxide	Rhodamine B	63.
8	RGO/CF/PANI	Uranium	64.
9	salicylaldoxime/polydopamine graphene oxide	Uranium	65.
10	CNT/rGO	Phosphate and aluminum	66.
11	GO-NiFe LDH	Congo red, methyl orange and Cr(VI)]	67.
12	GO–Ag	Malachite green and ethyl violet	68.
13	graphene nanoplatelets	Aspirin, acetaminophen and caffeine	69.
14	chitin/graphene oxide	Black and neutral Red	70.
15	magnetite/reduced graphene oxide	1-naphthol	71.

Photocatalysis in another process which is cost effective and easy to operate. Productivity of this process is depending on the efficacy of employed photocatalysts for the targeted operation which is directly influenced by the amount of charge recombination rate of respective photocatalysts. Furthermore, the charge recombination rate depends on the life of photo-generated electrons and hole. And the life is depending upon the availability of charge movement in the photocatalysts. Abundance of conjugation in graphene and its derivative provides sites for the charge transferred and increased life-time of photoinduced electron and hole. In this view various photocatalysts has been developed with graphene for various photocatalytic operation and listed in Table3.

Table 3: Various graphene based composite for photocatalysis based application

Sr. no		**Composite**	**Pollutants**	**Ref**
1		Ag–AgBr/TiO_2/RGO	Photocatalytic degradation of penicillin G	72.
2		Ag-Cu2O/rGO	photodegradation of phenol	73.
3		TiO2 –rGO	Degradation and mineralization of perfluoro-octanoic acid	74.
4		Ag-AgBr-RGO	Degradation of rhodamine B and p-nitrophenol	75.
5		Ag3PO4@MS2(M = Mo, W)/rGO	4-nitrophenol degradation	76.
6		rGO/ZnS-MoS_2	Degradation of nitrophenol	77.
7		rGO@ZnCo2O4	Photocatalytic NO oxidization	78.
8		BiOI/rGO	Methylene blue, levofloxacin	79.
9		$CuCo_2S_4$/RGO	Photodegradation of malachite green	80.

10		Pb-$BiFeO_3$/rGO	Degradation of perfluorooctanoic acid	81.
11		rGO/CuInS2	Photocatalytic removal of nitrophenol	82.
12		SnS_2/RGO	Degradation of remazol brilliant red and remazol brilliant blue	83.
13		$BiFeO_3$/RGO	Degradation of Methylene blue	84.
14		AuCu-P25-rGO	Photodegradation 2-nitrophenol	85.
15		CdWO4-RGO	Degradation of methylene blue	86.

3.2.2 Utilization for clean energy productionvia hydrogen evolution reaction

Splitting of water into hydrogen via hydrogen evolution reaction (HER) is regarded as clean and sustainable strategy. Various research communities has acknowledge it as a future energy carrier[87]. HER needs a catalysts to overcome various kinetic barrier for an efficient productivity. Some commonly used catalysts for HER are Pt, Ag, Pd etc. The use of such metal based catalysts for HER limits their epidemic use. Thus we have to see the alternates which are not only coast effective but also mitigate the physical and chemical properties those are essential requirements for a catalyst in HER. Graphene possesses a high surface are, high electrical conductivity and stability in very harsh condition. Thus various graphene based composites has been studied for HER and listed in Table 4.

Table 4: Various graphene based composite for adsorption based application

Sr. no	**Composite**	**Electrochemical activity potential for HER**	**Ref**
1	Mo_2N–Mo_2C/HGr	11 mV (0.5 m H2SO4) and 18 mV (1 m KOH)	88.

2	N-doped graphene nanosheets	−135 mV at 10 mA cm^{-2} in 0.5 m H2SO4	89.
3	3D-Graphene	18 mV in 0.5 m H2SO4	90.
4	Co/NCNT/NG	123 mV at 10 mA cm^{-2} in 0.5 M H_2SO_4	91.
5	Ni-rGO	Tafel slope (b = 77 mV $dec^{-1}$and (j_0 = 3.408 mA cm^{-2})	92.
6	NiS2/rGO)	10 mA cm^{-2} Vs − 200 mV, Tafel slope of 52 mV dec^{-1})	93.
7	CoP/GA	121 mV at 10 mA cm^{-2}, a Tafel slope of 50 mV dec^{-1}	94.
8	MoS2/GR	----------	95.
9	S-doped graphene	178 mV at 10 mA cm^{-2}	96.
10	MoS2/N-RGO-180	−5 mV, a small Tafel slope of 41.3 mV dec^{-1}, current density of 7.4×10^{-4} A cm^{-2},	97.
11	CoPnanoparticles/N-doped graphene	10 mA cm^{-2} at a cell voltage of 1.58 V	98.
12	MoO2Mo2C/G	----------	99.
13	CoP2/RGO	1.56 V at 10 mA cm^{-2}	100.
14	CoNi@N-C/rGO	Tafel slope of ∼133.7 mV).	101.
15	MoFeNiS/rGO	−140 mV at 10 mA cm^{-2}, Tafel slope of 48.68 mV dec^{-1}	102.

3.2.3 Biomedical application

Graphene based nanocomposite also has been utilized for various biomedical application such as bio sensing, bio-imaging, drug delivery, antibacterial properties etc. Some unique features such as cell growing potential and biocompatibility makes it a sustainable material for biological application[103]. However very limited work has been carried in the biomedical application, some of them has been enumerated in Table 5.

Table 5: Various graphene based composite for biomedical application

Sr. no	Composite	Utilized for biomedical application	Ref
1	ZnO-RGO	Antibacterial activity against E. coli	
2	Fe3O4/GO	Targeting drug carriers	
3	NGO	Live cell imaging and loading doxorubicin, a widely used cancer drug	
4	GO–CS	Delivering both anticancer drugs and genes.	
5	GONPs	Potentiate Anticancer Effect of Cisplatin	
6	GO-PVP and GO-β-CD	Release and delivery of poorly water soluble anticancer drug	
7	Graphene	Biosensor for early detection of Zika virus infection	
8	GO	Biosensor for detecting micro-RNA	
9	MoS2/GO	Targeting and enhanced drug loading/tumor-killing efficacy	
10	GQDs	Fluorescence imaging and tumor-targeted drug delivery	
11	GO-AgNPs	Preventing Viral Entry and Activation of	

		the Antiviral Innate Immune Response	
12	GQD	As HIV Inhibitors	
13	GO	Fluorometric detection of influenza viral RNA	
14	GO	Fluorescence sensing of protein-DNA interactions	
15	GO	Dengue E Protein Detection	

4. Fullerenes

Fullerenes is the allotropic form of carbon described by the general chemical formula C20 + 2Hwhere H is the number of hexagonal faces. Buckminsterfullerene or C_{60}, is often described as a soccer ball. It has the geometry of a truncated icosahedron with 12 pentagonal faces and 20 hexagonal faces. Fullerene C_{60} consists of 60 carbons arranged in symmetrical structures with nano dimensions in a closed-shell configuration which constitute 60 π-electrons with 30 bonding molecular orbitals. Fullerene have in between chemical behavior of aromatic and straight chain alkenes which makes it a suitable template for various reaction [119]. Moreover fullerenes has much potential to explore it for wide area of research.

4.1 Synthesis

4.1.1 Arc Discharge Method

This method is operated at high temperature in an electrical furnaces [120]. A tube made up of quartz, electrodes of carbon, a water cooling jacket and a high voltage pulsed power input is required. For thermal annealing process of carbon clusters, a buffer gas is allowed to pass through the quartz tube. The bulk carbon cluster substrate is then allow to

heat in quartz tube between 25 and 1000°C. The flow rate of the buffer gas is maintained at 300 cm^3/s. Pressure of the buffer gas is maintained at 500 Torr. The input power supply provides pulsated high voltage of 1.1 kV, 22 A and 50–300 sec duration. By this method, electrode at negative terminal is consumed. Then the carbon after condensation is annealed to form fullerenes. The fullerene and other carbon particles are then collected on the water cooled trap.

4.1.2 Chemical Synthesis

However the chemical synthesis of fullerene is very complicated, but various chemist has approached different methodologies such as mobilization between two identical hemisphere hydrocarbons. Furthermore, the hitch which has to face in the fullerene synthesis is the introduction of curvature in the carbon scaffold. The fragment corannulene which contained curvature is first synthesized by Barth and Lawton [121]. But due to low productivity the method is not become so much successful. Further Scott and co-workers has proposed a three step synthesis of corannulene molecule [122]. The first step is a Knoevenagel–Diels–Alder reaction between acenaphthoquinone, heptane-2,4,6-trione, and norbornadiene to give 7,10-diacetylfluoranthene. Followed by conversion step of acetyl groups to 1-clorovinyl side chains. Finally FVP generates terminal alkynes in situ by thermal elimination of HCl from the a-chlorovinyl chains, leading to the formation of corannulene. By the time various research work has been done for the chemical synthesis and various efficient methodologies has been developed for the fullerene synthesis [123-125].

4.2 Mode of utilization

Various fullerene based composites has been explored for the environmental application in the field of photocatalysis, sorption, drug

delivery, clean energy production, electrical energy storage devices etc. wide mode of utilization has been presented in table 6.

Table 6: Wide mode of utilization of fullerenes based nano-composite

Sr. no	Composite	Utilized for biomedical application	Ref
1	TiO_2/FNP	Degradation of the herbicide mesotrione	**126.**
2	C_{60}/Ag_3PO_4	Degradation of Methyl Orange	**127.**
3	$BiVO_4/Fe_{3O}4/C_{60}$	Degradation of methylene blue	**128.**
4	Fullerene-WO_3	Photocatalytic activity for the generation of hydrogen energy	**129.**
5	$Ag_3PO_4/Fe_3O_4/C6_0$	Photocatalytic, catalytic and antibacterial activities	**130.**
6	F-TiO_2(B)/fullerene	Sono-photo degradation of crystal violet dye	**131.**
7	C_{60}-Fe_2O_3	Degradation of methylene blue (MB), rhodamine B (RhB), methyl orange (MO), and phenol	**132.**
8	C_{60}/g-C_3N_4	Oxidation of Sulfides into Sulfoxides	**133.**
9	C_{60}/CNTs/g-C_3N_4	Oxidation of organic pollutant Rh B	**134.**
10	C_{60}/BiOCl	Degradation of phenol and Rh B	**135.**
11	fullerene C_{60}	Sorption of TCC	**136.**
12	C_{60} Fullerene	Naphthalene Adsorption and Desorption	**137.**
13	C_{60} Fullerene	Adsorption of Atrazine	**138.**
14	C_{60} Fullerene nanoparticle	Uptake of Trichloroethylene in Phytoremediation Systems	**139.**

15	N-C_{60}	Catalyst for Hydrogen Fuel Cells	**140.**
16	C_{60} Fullerene	$LiBH_4$ hydrogen uptake and release	**141.**
17	ullerene-like cages	Heterojunctions for organic photovoltaics	**142.**
18	Fullerene Multiadducts	Reduced Efficiencies of Organic Solar Cells	**143.**
19	Fullerene C_{60}	Multifunctional system for drug and gene delivery	**144.**
20	C_{60}–PEI–DOX	pH-responsive drug delivery system	**145.**
21	Fullerene (C_{60}) Derivatives	Nonviral Gene-Delivery Vectors	**146.**
22	Fullerene C_{60}	Glycosidase Inhibition	**147.**
23	Fullerene C_{60}	Doxorubicin Efficiency against Leukemic Cells In Vitro	**148.**
24	Fullerene C_{60}	Cancer Targeted Therapy	**149.**
24	Hydrated C_{60} fullerene	Antioxidant properties	**150.**
26	Pt/C_{60}/TiO_2/Sb_2Se_3	Photo-Electrochemical Water Splitting	**151.**
27	Cationic fullerene derivatives	Anti-HIV properties	**152.**
28	Fullerene C_{60}	Human immunodeficiency virus-reverse transcriptase inhibition	**153.**
29	Boron-Doped Fullerene	Lithium-Ion Battery Application	**154.**
30	Sn-C60	Silicon monoxide oxidation	**155.**

5. Exploration of carbon nanomaterial for future perspective

Carbon nanomaterial as Graphene, RGO, GO, carbon nanotube, fullerene etc. possesses high poetical for wide area research not only for environmental, clean energy production but also for multipurpose biological application. The novel research on these material has proved that they are demanding material to mitigate the essential requirement in various field. However, there are many challenges associated with synthesis and application which has to deal to overcome the efficacy of these nanomaterials. To boost the efficiency we have to discover various strategies to fulfill the need of objective, which demand the rooted investigation including structural analysis, identifying the alternation strategies for morphological changes in the respective areas.

6. Conclusion

The present chapter summarizes potential of various carbon nanomaterials such as nanotubes, graphene, RGO and fullerenes. The different strategies of synthesis which has been approached by different researchers were discussed. The study shows that carbon nano material composites possesses high potential for wide area application including photocatalysis, adsorption, drug delivery, water pollution remediation, evolution of hydrogen, anti-cancerous activity, antibacterial properties etc. However pure metal based composite shows good efficiency for these application. But carbon nanomaterials contribute remarkable which is millstone in the respective field regarding coast effective and ease of availability of raw materials.

References

1. L. V. Radushkevich and V. M. Lukyanovich, Zh. Fiz. Khim., 1952, 26, 88–95.
2. H. W. Kroto, J. R. Heath, S. C. O'Brien, R. F. Curl & R. E. Smalley, C60: Buckminsterfullerene, Nature 318, 162 - 163 14 November 1985.
3. Wilder JW, Venema LC, Rinzler AG, Smalley RE, Dekker C. Electronic structure of atomically resolved carbon nanotubes. Nature. 1998 Jan;391(6662):59.
4. Arnold MS, Green AA, Hulvat JF, Stupp SI, Hersam MC. Sorting carbon nanotubes by electronic structure using density differentiation. Nature nanotechnology. 2006 Oct;1(1):60.
5. Dillon A, Jones KM, Bekkedahl TA, Kiang CH, Bethune DS, Heben MJ. Storage of hydrogen in single-walled carbon nanotubes. Nature. 1997 Mar;386(6623):377.
6. O'connell MJ, Bachilo SM, Huffman CB, Moore VC, Strano MS, Haroz EH, Rialon KL, Boul PJ, Noon WH, Kittrell C, Ma J. Band gap fluorescence from individual single-walled carbon nanotubes. Science. 2002 Jul 26;297(5581):593-6.
7. Chen J, Hamon MA, Hu H, Chen Y, Rao AM, Eklund PC, Haddon RC. Solution properties of single-walled carbon nanotubes. Science. 1998 Oct 2;282(5386):95-8.
8. Odom TW, Huang JL, Kim P, Lieber CM. Atomic structure and electronic properties of single-walled carbon nanotubes. Nature. 1998 Jan;391(6662):62.
9. Chen RJ, Zhang Y, Wang D, Dai H. Noncovalent sidewall functionalization of single-walled carbon nanotubes for protein immobilization. Journal of the American Chemical Society. 2001 Apr 25;123(16):3838-9.
10. Nikolaev P, Bronikowski MJ, Bradley RK, Rohmund F, Colbert DT, Smith KA, Smalley RE. Gas-phase catalytic growth of single-walled carbon nanotubes from carbon monoxide. Chemical physics letters. 1999 Nov 5;313(1-2):91-7.
11. Bottini M, Bruckner S, Nika K, Bottini N, Bellucci S, Magrini A, Bergamaschi A, Mustelin T. Multi-walled carbon nanotubes induce T lymphocyte apoptosis. Toxicology letters. 2006 Jan 5;160(2):121-6.
12. Yu MF, Lourie O, Dyer MJ, Moloni K, Kelly TF, Ruoff RS. Strength and breaking mechanism of multiwalled carbon nanotubes under tensile load. Science. 2000 Jan 28;287(5453):637-40.

13. Monteiro-Riviere NA, Nemanich RJ, Inman AO, Wang YY, Riviere JE. Multi-walled carbon nanotube interactions with human epidermal keratinocytes. Toxicology letters. 2005 Mar 15;155(3):377-84.

14. Dillon A, Jones KM, Bekkedahl TA, Kiang CH, Bethune DS, Heben MJ. Storage of hydrogen in single-walled carbon nanotubes. Nature. 1997 Mar;386(6623):377.

15. Li GY, Wang PM, Zhao X. Mechanical behavior and microstructure of cement composites incorporating surface-treated multi-walled carbon nanotubes. Carbon. 2005 May 1;43(6):1239-45.

16. De Jonge N, Lamy Y, Schoots K, Oosterkamp TH. High brightness electron beam from a multi-walled carbon nanotube. Nature. 2002 Nov;420(6914):393.

17. Hutchison JL, Kiselev NA, Krinichnaya EP, Krestinin AV, Loutfy RO, Morawsky AP, Muradyan VE, Obraztsova ED, Sloan J, Terekhov SV, Zakharov DN. Double-walled carbon nanotubes fabricated by a hydrogen arc discharge method. Carbon. 2001 Apr 1;39(5):761-70.

18. Shi Z, Lian Y, Zhou X, Gu Z, Zhang Y, Iijima S, Zhou L, Yue KT, Zhang S. Mass-production of single-wall carbon nanotubes by arc discharge method. Carbon. 1999 Jan 1;37(9):1449-53.

19. Zhao X, Ohkohchi M, Wang M, Iijima S, Ichihashi T, Ando Y. Preparation of high-grade carbon nanotubes by hydrogen arc discharge. Carbon. 1997 Jan 1;35(6):775-81.

20. Journet C, Maser WK, Bernier P, Loiseau A, de La Chapelle ML, Lefrant DS, Deniard P, Lee R, Fischer JE. Large-scale production of single-walled carbon nanotubes by the electric-arc technique. Nature. 1997 Aug;388(6644):756.

21. Scott CD, Arepalli S, Nikolaev P, Smalley RE. Growth mechanisms for single-wall carbon nanotubes in a laser-ablation process. Applied Physics A. 2001 May 1;72(5):573-80.

22. Singh C, Shaffer MS, Windle AH. Production of controlled architectures of aligned carbon nanotubes by an injection chemical vapour deposition method. Carbon. 2003 Feb 1;41(2):359-68.

23. Meyyappan M. A review of plasma enhanced chemical vapour deposition of carbon nanotubes. Journal of Physics D: Applied Physics. 2009 Oct 6;42(21):213001.

24. Milne WI, Teo KB, Chhowalla M, Amaratunga GA, Lee SB, Hasko DG, Ahmed H, Groening O, Legagneux P, Gangloff L, Schnell JP. Electrical and field emission investigation of individual carbon nanotubes from plasma enhanced chemical vapour deposition. Diamond and Related Materials. 2003 Mar 1;12(3-7):422-8.

25. Bianco A, Kostarelos K, Partidos CD, Prato M. Biomedical applications of functionalised carbon nanotubes. Chemical Communications. 2005(5):571-7.

26. Khabashesku VN, Margrave JL, Barrera EV. Functionalized carbon nanotubes and nanodiamonds for engineering and biomedical applications. Diamond and Related Materials. 2005 Mar 1;14(3-7):859-66.

27. Yang W, Thordarson P, Gooding JJ, Ringer SP, Braet F. Carbon nanotubes for biological and biomedical applications. Nanotechnology. 2007 Sep 12;18(41):412001.

28. Futaba DN, Hata K, Namai T, Yamada T, Mizuno K, Hayamizu Y, Yumura M, Iijima S. 84% catalyst activity of water-assisted growth of single walled carbon nanotube forest characterization by a statistical and macroscopic approach. The Journal of Physical Chemistry B. 2006 Apr 20;110(15):8035-8.

29. Nessim GD, Hart AJ, Kim JS, Acquaviva D, Oh J, Morgan CD, Seita M, Leib JS, Thompson CV. Tuning of vertically-aligned carbon nanotube diameter and areal density through catalyst pre-treatment. Nano Letters. 2008 Oct 7;8(11):3587-93.

30. Yoo E, Kim J, Hosono E, Zhou HS, Kudo T, Honma I. Large reversible Li storage of graphene nanosheet families for use in rechargeable lithium ion batteries. Nano letters. 2008 Jul 24;8(8):2277-82.

31. Frackowiak E, Beguin F. Electrochemical storage of energy in carbon nanotubes and nanostructured carbons. Carbon. 2002 Aug 1;40(10):1775-87.

32. Landi BJ, Ganter MJ, Cress CD, DiLeo RA, Raffaelle RP. Carbon nanotubes for lithium ion batteries. Energy & Environmental Science. 2009;2(6):638-54.

33. Sotiropoulou S, Chaniotakis NA. Carbon nanotube array-based biosensor. Analytical and Bioanalytical Chemistry. 2003 Jan 1;375(1):103-5.

34. Modi A, Koratkar N, Lass E, Wei B, Ajayan PM. Miniaturized gas ionization sensors using carbon nanotubes. Nature. 2003 Jul;424(6945):171.

35. Torop J, Palmre V, Arulepp M, Sugino T, Asaka K, Aabloo A. Flexible supercapacitor-like actuator with carbide-derived carbon electrodes. Carbon. 2011 Aug 1;49(9):3113-9.

36. Shin SR, Lee CK, So IS, Jeon JH, Kang TM, Kee CW, Kim SI, Spinks GM, Wallace GG, Kim SJ. DNA-wrapped single-walled carbon nanotube hybrid fibers for supercapacitors and artificial muscles. Advanced Materials. 2008 Feb 4;20(3):466-70.

37. Torop J, Sugino T, Asaka K, Jänes A, Lust E, Aabloo A. Nanoporous carbide-derived carbon based actuators modified with gold foil: prospect for fast response and low voltage applications. Sensors and Actuators B: Chemical. 2012 Jan 3;161(1):629-34.

38. Geim AK. AK Geim and KS Novoselov, Nat. Mater. 6, 183 (2007). Nat. Mater.. 2007;6:183.

39. Geim AK. Graphene: status and prospects. science. 2009 Jun 19;324(5934):1530-4.

40. Carbon H. A Review of Graphene Allen, Matthew J.; Tung, Vincent C.; Kaner, Richard B. Chemical Reviews (Washington, DC, United States). 2010;110(1):132-45.

41. Lang B. A LEED study of the deposition of carbon on platinum crystal surfaces. Surface Science. 1975 Dec 1;53(1):317-29.

42. Novoselov KS, Jiang D, Schedin F, Booth TJ, Khotkevich VV, Morozov SV, Geim AK. Two-dimensional atomic crystals. Proceedings of the National Academy of Sciences. 2005 Jul 26;102(30):10451-3.

43. Edwards RS, Coleman KS. Graphene synthesis: relationship to applications. Nanoscale. 2013;5(1):38-51.

44. Bhuyan MS, Uddin MN, Islam MM, Bipasha FA, Hossain SS. Synthesis of graphene. International Nano Letters. 2016 Jun 1;6(2):65-83.

45. Zhang Y, Small JP, Pontius WV, Kim P. Fabrication and electric-field-dependent transport measurements of mesoscopic graphite devices. Applied Physics Letters. 2005 Feb 14;86(7):073104.

46. William S, Hummers JR, Offeman RE. Preparation of graphitic oxide. J. Am. Chem. Soc. 1958;80(6):1339-.

47. Gudkov MV, Gorenberg AY, Shchegolikhin AN, Shashkin DP, Mel'nikov VP. Explosive reduction of graphite oxide by hydrazine vapor at room temperature. InDoklady Physical Chemistry 2018 Jan 1 (Vol. 478, No. 1, pp. 11-14). Pleiades Publishing.

48. Jose PP, Kala MS, Kalarikkal N, Thomas S. Reduced graphene oxide produced by chemical and hydrothermal methods. Materials Today: Proceedings. 2018 Jan 1;5(8):16306-12.

49. Fernández-Merino M, Guardia L, Paredes JI, Villar-Rodil S, Solís-Fernández P, Martínez-Alonso A, Tascón JM. Vitamin C is an ideal substitute for hydrazine in the reduction of graphene oxide suspensions. The Journal of Physical Chemistry C. 2010 Mar 4;114(14):6426-32.

50. Fernández-Merino M, Guardia L, Paredes JI, Villar-Rodil S, Solís-Fernández P, Martínez-Alonso A, Tascón JM. Vitamin C is an ideal substitute for hydrazine in the reduction of graphene oxide suspensions. The Journal of Physical Chemistry C. 2010 Mar 4;114(14):6426-32.

51. Moon IK, Lee J, Ruoff RS, Lee H. Reduced graphene oxide by chemical graphitization. Nature communications. 2010 Sep 21;1:73.

52. Hahn DG. Viscoelastic polymer-assisted mechanical exfoliation of large area highly oriented pyrolytic graphite(Doctoral dissertation, Georgia Institute of Technology).

53. Skaltsas T, Ke X, Bittencourt C, Tagmatarchis N. Ultrasonication induces oxygenated species and defects onto exfoliated graphene. The Journal of Physical Chemistry C. 2013 Oct 17;117(44):23272-8.

54. McAllister MJ, Li JL, Adamson DH, Schniepp HC, Abdala AA, Liu J, Herrera-Alonso M, Milius DL, Car R, Prud'homme RK, Aksay IA. Single sheet functionalized graphene by oxidation and thermal expansion of graphite. Chemistry of materials. 2007 Sep 4;19(18):4396-404.

55. Berger C, Conrad EH, de Heer WA. Silicon carbide and epitaxial graphene on silicon carbide. InPhysics of Solid Surfaces 2018 (pp. 683-688). Springer, Berlin, Heidelberg.

56. Li Q, Li X, Wageh S, Al-Ghamdi AA, Yu J. CdS/graphene nanocomposite photocatalysts. Advanced Energy Materials. 2015 Jul;5(14):1500010.

57. Saleh TA, Sarı A, Tuzen M. Effective adsorption of antimony (III) from aqueous solutions by polyamide-graphene composite as a novel adsorbent. Chemical Engineering Journal. 2017 Jan 1;307:230-8.

58. Yang J, Chen D, Zhu Y, Zhang Y, Zhu Y. 3D-3D porous Bi2WO6/graphene hydrogel composite with excellent synergistic effect of adsorption-enrichment and photocatalytic degradation. Applied Catalysis B: Environmental. 2017 May 15;205:228-37.

59. Konicki W, Aleksandrzak M, Moszyński D, Mijowska E. Adsorption of anionic azo-dyes from aqueous solutions onto graphene oxide: equilibrium, kinetic and thermodynamic studies. Journal of colloid and interface science. 2017 Jun 15;496:188-200.

60. Konicki W, Aleksandrzak M, Mijowska E. Equilibrium, kinetic and thermodynamic studies on adsorption of cationic dyes from aqueous solutions using graphene oxide. Chemical Engineering Research and Design. 2017 Jul 1;123:35-49.

61. Gupta K, Khatri OP. Reduced graphene oxide as an effective adsorbent for removal of malachite green dye: plausible adsorption pathways. Journal of colloid and interface science. 2017 Sep 1;501:11-21.

62. Alwan SH, Alshamsi HA, Jasim LS. Rhodamine B removal on A-rGO/cobalt oxide nanoparticles composite by adsorption from contaminated water. Journal of Molecular Structure. 2018 Jun 5;1161:356-65.

63. Alwan SH, Alshamsi HA, Jasim LS. Rhodamine B removal on A-rGO/cobalt oxide nanoparticles composite by adsorption from contaminated water. Journal of Molecular Structure. 2018 Jun 5;1161:356-65.

64. Dat TQ, Ha NT, Van Thin P, Tung NV, Hung DQ. Synthesis of RGO/CF/PANI Magnetic Composites for Effective Adsorption of Uranium. IEEE Transactions on Magnetics. 2018 Jun;54(6):1-6.

65. Qian Y, Yuan Y, Wang H, Liu H, Zhang J, Shi S, Guo Z, Wang N. Highly efficient uranium adsorption by salicylaldoxime/polydopamine graphene oxide nanocomposites. Journal of Materials Chemistry A. 2018;6(48):24676-85.

66. Wang Y, Yang Q, Huang H. Effective adsorption of trace phosphate and aluminum in realistic water by carbon nanotubes and reduced graphene oxides. Science of The Total Environment. 2019 Jan 25.

67. Zheng Y, Cheng B, You W, Yu J, Ho W. 3D hierarchical graphene oxide-NiFe LDH composite with enhanced adsorption affinity to Congo red, methyl orange and Cr (VI) ions. Journal of Hazardous Materials. 2019 Feb 6.

68. Naeem H, Ajmal M, Qureshi RB, Muntha ST, Farooq M, Siddiq M. Facile synthesis of graphene oxide–silver nanocomposite for decontamination of water from multiple pollutants by adsorption, catalysis and antibacterial activity. Journal of environmental management. 2019 Jan 15;230:199-211.

69. Al-Khateeb LA, Almotiry S, Salam MA. Adsorption of pharmaceutical pollutants onto graphene nanoplatelets. Chemical Engineering Journal. 2014 Jul 15;248:191-9.

70. González JA, Villanueva ME, Piehl LL, Copello GJ. Development of a chitin/graphene oxide hybrid composite for the removal of pollutant dyes: adsorption and desorption study. Chemical engineering journal. 2015 Nov 15;280:41-8.

71. Zhao G, Li J, Wang X. Kinetic and thermodynamic study of 1-naphthol adsorption from aqueous solution to sulfonated graphene nanosheets. Chemical Engineering Journal. 2011 Sep 1;173(1):185-90.

72. Wang P, Tang Y, Dong Z, Chen Z, Lim TT. Ag–AgBr/TiO 2/RGO nanocomposite for visible-light photocatalytic degradation of penicillin G. Journal of Materials Chemistry A. 2013;1(15):4718-27.

73. Wei Q, Wang Y, Qin H, Wu J, Lu Y, Chi H, Yang F, Zhou B, Yu H, Liu J. Construction of rGO wrapping octahedral Ag-Cu2O heterostructure for enhanced visible light photocatalytic activity. Applied Catalysis B: Environmental. 2018 Jul 5;227:132-44.

74. Gomez-Ruiz B, Ribao P, Diban N, Rivero MJ, Ortiz I, Urtiaga A. Photocatalytic degradation and mineralization of perfluorooctanoic acid (PFOA) using a composite TiO2– rGO catalyst. Journal of hazardous materials. 2018 Feb 15;344:950-7.

75. Yang Y, Zhang W, Liu R, Cui J, Deng C. Preparation and photocatalytic properties of visible light driven Ag-AgBr-RGO composite. Separation and Purification Technology. 2018 Jan 8;190:278-87.

76. Zhang W, Li G, Wang W, Qin Y, An T, Xiao X, Choi W. Enhanced photocatalytic mechanism of Ag3PO4 nano-sheets using MS2 (M= Mo, W)/rGO hybrids as co-catalysts for 4-nitrophenol degradation in water. Applied Catalysis B: Environmental. 2018 Sep 15;232:11-8.

77. Hu X, Deng F, Huang W, Zeng G, Luo X, Dionysiou DD. The band structure control of visible-light-driven rGO/ZnS-MoS2 for excellent photocatalytic degradation performance and long-term stability. Chemical Engineering Journal. 2018 Oct 15;350:248-56.

78. Xiao S, Pan D, Liang R, Dai W, Zhang Q, Zhang G, Su C, Li H, Chen W. Bimetal MOF derived mesocrystalZnCo 2 O 4 on rGO with High performance in visible-light photocatalytic NO oxidization. Applied Catalysis B: Environmental. 2018 Nov 15;236:304-13.

79. Niu J, Dai P, Zhang Q, Yao B, Yu X. Microwave-assisted solvothermal synthesis of novel hierarchical BiOI/rGO composites for efficient photocatalytic degardation of organic pollutants. Applied Surface Science. 2018 Feb 1;430:165-75.

80. Vadivel S, Paul B, Habibi-Yangjeh A, Maruthamani D, Kumaravel M, Maiyalagan T. One-pot hydrothermal synthesis of CuCo2S4/RGO nanocomposites for visible-light photocatalytic applications. Journal of Physics and Chemistry of Solids. 2018 Dec 1;123:242-53.

81. Shang E, Li Y, Niu J, Li S, Zhang G, Wang X. Photocatalytic degradation of perfluorooctanoic acid over Pb-BiFeO3/rGO catalyst: Kinetics and mechanism. Chemosphere. 2018 Nov 1;211:34-43.

82. Xie C, Lu X, Deng F, Luo X, Gao J, Dionysiou DD. Unique surface structure of nano-sized CuInS2 anchored on rGO thin film and its superior photocatalytic activity in real wastewater treatment. Chemical Engineering Journal. 2018 Apr 15;338:591-8.

83. Dashairya L, Sharma M, Basu S, Saha P. SnS2/RGO based nanocomposite for efficient photocatalytic degradation of toxic industrial dyes under visible-light irradiation. Journal of Alloys and Compounds. 2019 Feb 5;774:625-36.

84. Si YH, Xia Y, Shang SK, Xiong XB, Zeng XR, Zhou J, Li YY. Enhanced visible light driven photocatalytic behavior of BiFeO3/reduced graphene oxide composites. Nanomaterials. 2018 Jul;8(7):526.

85. Wen H, Long Y, Han W, Wu W, Yang Y, Ma J. Preparation of a novel bimetallic AuCu-P25-rGO ternary nanocomposite with enhanced photocatalytic degradation performance. Applied Catalysis A: General. 2018 Jan 5;549:237-44.

86. Azimirad R, TourchiMoghadam M, Babamoradi M. Effect of hydrothermal reaction temperature on the photocatalytic properties of CdWO4-RGO nanocomposites. Journal of Nanostructures. 2018 Jun 17.

87. Qi J, Zhang W, Cao R. Solar-to-Hydrogen Energy Conversion Based on Water Splitting. Advanced Energy Materials. 2018 Feb;8(5):1701620.

88. Yan H, Xie Y, Jiao Y, Wu A, Tian C, Zhang X, Wang L, Fu H. Holey reduced graphene oxide coupled with an Mo2N–Mo2C heterojunction for efficient hydrogen evolution. Advanced Materials. 2018 Jan;30(2):1704156.

89. Ma J, Wang M, Lei G, Zhang G, Zhang F, Peng W, Fan X, Li Y. Polyaniline Derived N-Doped Carbon-Coated Cobalt Phosphide Nanoparticles Deposited on N-Doped Graphene as an Efficient Electrocatalyst for Hydrogen Evolution Reaction. Small. 2018 Jan;14(2):1702895.

90. Wang H, Li XB, Gao L, Wu HL, Yang J, Cai L, Ma TB, Tung CH, Wu LZ, Yu G. Three-Dimensional Graphene Networks with Abundant Sharp Edge Sites for Efficient Electrocatalytic Hydrogen Evolution. AngewandteChemie. 2018 Jan 2;130(1):198-203.

91. Yang L, Lv Y, Cao D. Co, N-codoped nanotube/graphene 1D/2D heterostructure for efficient oxygen reduction and hydrogen evolution reactions. Journal of Materials Chemistry A. 2018;6(9):3926-32.

92. Wang L, Li Y, Xia M, Li Z, Chen Z, Ma Z, Qin X, Shao G. Ni nanoparticles supported on graphene layers: An excellent 3D electrode for hydrogen evolution reaction in alkaline solution. Journal of Power Sources. 2017 Apr 15;347:220-8.

93. Chen R, Song Y, Wang Z, Gao Y, Sheng Y, Shu Z, Zhang J, Li XA. Porous nickel disulfide/reduced graphene oxide nanohybrids with improved electrocatalytic performance for hydrogen evolution. Catalysis Communications. 2016 Oct 5;85:26-9.

94. Zhang X, Han Y, Huang L, Dong S. 3D graphene aerogels decorated with cobalt phosphide nanoparticles as electrocatalysts for the hydrogen evolution reaction. ChemSusChem. 2016 Nov 9;9(21):3049-53.

95. Biroju RK, Das D, Sharma R, Pal S, Mawlong LP, Bhorkar K, Giri PK, Singh AK, Narayanan TN. Hydrogen evolution reaction activity of graphene–MoS2 van der Waals heterostructures. ACS Energy Letters. 2017 May 11;2(6):1355-61.

96. Tian Y, Wei Z, Wang X, Peng S, Zhang X, Liu WM. Plasma-etched, S-doped graphene for effective hydrogen evolution reaction. International Journal of Hydrogen Energy. 2017 Feb 16;42(7):4184-92.

97. Tang YJ, Wang Y, Wang XL, Li SL, Huang W, Dong LZ, Liu CH, Li YF, Lan YQ. Molybdenum Disulfide/Nitrogen-Doped Reduced Graphene Oxide Nanocomposite with Enlarged Interlayer Spacing for Electrocatalytic Hydrogen Evolution. Advanced Energy Materials. 2016 Jun;6(12):1600116.

98. Yu X, Zhang S, Li C, Zhu C, Chen Y, Gao P, Qi L, Zhang X. Hollow CoPnanopaticle/N-doped graphene hybrids as highly active and stable bifunctional catalysts for full water splitting. Nanoscale. 2016;8(21):10902-7.

99. Li X, Ci S, Jia J, Wen Z. Graphene loading molybdenum carbide/oxide hybrids as advanced electrocatalysts for hydrogen evolution reaction. International Journal of Hydrogen Energy. 2016 Dec 14;41(46):21246-50.

100. Wang J, Yang W, Liu J. CoP 2 nanoparticles on reduced graphene oxide sheets as a super-efficient bifunctional electrocatalyst for full water splitting. Journal of Materials Chemistry A. 2016;4(13):4686-90.

101. Chen L, Yang S, Qian K, Wei W, Sun C, Xie J. In situ growth of N-doped carbon coated CoNi alloy with graphene decoration for enhanced HER performance. Journal of Energy Chemistry. 2019 Feb 1;29:129-35.

102. Askari MB, Salarizadeh P, Rozati SM, Seifi M. Two-dimensional transition metal chalcogenide composite/reduced graphene oxide hybrid materials for hydrogen evolution application. Polyhedron. 2019 Jan 24.

103. Shareena TP, McShan D, Dasmahapatra AK, Tchounwou PB. A review on graphene-based nanomaterials in biomedical applications and risks in environment and health. Nano-micro letters. 2018 Jul 1;10(3):53.

104. Sandhya PK, Jose J, Sreekala MS, Padmanabhan M, Kalarikkal N, Thomas S. Reduced graphene oxide and ZnO decorated graphene for biomedical applications. Ceramics International. 2018 Sep 1;44(13):15092-8.

105. Wang J, Fang J, Fang P, Li X, Wu S, Zhang W, Li S. Preparation of hollow core/shell Fe3O4@ graphene oxide composites as magnetic targeting drug nanocarriers. Journal of Biomaterials science, Polymer edition. 2017 Mar 4;28(4):337-49.

106. Sun X, Liu Z, Welsher K, Robinson JT, Goodwin A, Zaric S, Dai H. Nano-graphene oxide for cellular imaging and drug delivery. Nano research. 2008 Sep 1;1(3):203-12.

107. Bao H, Pan Y, Ping Y, Sahoo NG, Wu T, Li L, Li J, Gan LH. Chitosan-functionalized graphene oxide as a nanocarrier for drug and gene delivery. Small. 2011 Jun 6;7(11):1569-78.

108. Rosli NF, Fojtů M, Fisher AC, Pumera M. Graphene Oxide Nanoplatelets Potentiate Anticancer Effect of Cisplatin in Human Lung Cancer Cells. Langmuir. 2019 Feb 11.

109. Karki N, Tiwari H, Pal M, Chaurasia A, Bal R, Joshi P, Sahoo NG. Functionalized graphene oxides for drug loading, release and delivery of poorly water soluble anticancer drug: A comparative study. Colloids and Surfaces B: Biointerfaces. 2018 Sep 1;169:265-72.

110. Afsahi S, Lerner MB, Goldstein JM, Lee J, Tang X, Bagarozzi Jr DA, Pan D, Locascio L, Walker A, Barron F, Goldsmith BR. Novel graphene-based biosensor for early detection of Zika virus infection. Biosensors and Bioelectronics. 2018 Feb 15;100:85-8.

111. Fan X, Qi Y, Shi Z, Lv Y, Guo Y. A graphene-based biosensor for detecting microRNA with augmented sensitivity through helicase-assisted signal amplification of hybridization chain reaction. Sensors and Actuators B: Chemical. 2018 Feb 1;255:1582-6.

112. Liu Y, Peng J, Wang S, Xu M, Gao M, Xia T, Weng J, Xu A, Liu S. Molybdenum disulfide/graphene oxide nanocomposites show favorable lung targeting and enhanced drug loading/tumor-killing efficacy with improved biocompatibility. NPG Asia Materials. 2018 Jan 5;10(1):e458.

113. Dong J, Wang K, Sun L, Sun B, Yang M, Chen H, Wang Y, Sun J, Dong L. Application of graphene quantum dots for simultaneous fluorescence imaging and tumor-targeted drug delivery. Sensors and Actuators B: Chemical. 2018 Mar 1;256:616-23.

114. Du T, Lu J, Liu L, Dong N, Fang L, Xiao S, Han H. Antiviral Activity of Graphene Oxide–Silver Nanocomposites by Preventing Viral Entry and Activation of the Antiviral Innate Immune Response. ACS Applied Bio Materials. 2018 Oct 30;1(5):1286-93.

115. Iannazzo D, Pistone A, Ferro S, De Luca L, Monforte AM, Romeo R, Buemi MR, Pannecouque C. Graphene Quantum Dots Based Systems As HIV Inhibitors. Bio conjugate chemistry. 2018 Aug 14;29(9):3084-93.

116. Jeong S, Kim DM, An SY, Kim DH, Kim DE. Fluorometric detection of influenza viral RNA using graphene oxide. Analytical biochemistry. 2018 Nov 15;561:66-9.

117. Pallares RM, Sutarlie L, Thanh NT, Su X. Fluorescence sensing of protein-DNA interactions using conjugated polyelectrolytes and graphene oxide. Sensors and Actuators B: Chemical. 2018 Oct 15;271:97-103.

118. Kamil YM, Bakar MH, Yaacob MH, Syahir A, Lim HN, Mahdi MA. Dengue E Protein Detection Using a Graphene Oxide Integrated Tapered Optical Fiber Sensor. IEEE Journal of Selected Topics in Quantum Electronics. 2019 Jan;25(1):1-8.

119. Chai B, Liao X, Song F, Zhou H. Fullerene modified C 3 N 4 composites with enhanced photocatalytic activity under visible light irradiation. Dalton Transactions. 2014;43(3):982-9.

120. Senin RM, Ion I, Oprea O, Vasile B, Stoica R, Ganea R, Ion AC. Sorption of Bisphenol A (BPA) in Aqueous Solutions on Fullerene C60. REVISTA DE CHIMIE. 2018 Jun 1;69(6):1309-14.

121. Yadav J. Fullerene: Properties, Synthesis and Application. Research & Reviews: Journal of Physics. 2018 Jan 2;6(3):1-6.

122. Barth WE, Lawton RG. Dibenzo [ghi, mno] fluoranthene. Journal of the American Chemical Society. 1966 Jan;88(2):380-1.

123. Scott LT, Hashemi MM, Meyer DT, Warren HB. Corannulene. A convenient new synthesis. Journal of the American Chemical Society. 1991 Aug;113(18):7082-4.

124. Seiders TJ, Baldridge KK, Siegel JS. Synthesis and characterization of the first corannulenecyclophane. Journal Of the American Chemical Society. 1996 Mar 20;118(11):2754-5.

125. Sygula A, Rabideau PW. A practical, large scale synthesis of the corannulene system. Journal of the American Chemical Society. 2000 Jul 5;122(26):6323-4.

126. Djordjevic A, Merkulov DŠ, Lazarević M, Borišev I, Medić I, Pavlović V, Miljević B, Abramović B. Enhancement of nano titanium dioxide coatings by fullerene and polyhydroxy fullerene in the photocatalytic degradation of the herbicide mesotrione. Chemosphere. 2018 Apr 1;196:145-52.

127. Song L, Yang J, Chen Q, Zhang S. Enhanced photocatalytic activity of Ag_3PO_4 via Fullerene C60 modification. Applied Organometallic Chemistry. 2018 Sep;32(9):e4472.

128. Sepahvand S, Farhadi S. Preparation and characterization of fullerene (C60)-modified $BiVO_4/Fe_3O_4$ nanocomposite by hydrothermal method and study of its visible light photocatalytic and catalytic activity. Fullerenes, Nanotubes and Carbon Nanostructures. 2018 Jul 3;26(7):417-32.

129. Bilal Tahir M, Nabi G, Rafique M, Khalid NR. Role of fullerene to improve the WO_3 performance for photocatalytic applications and hydrogen evolution. International Journal of Energy Research. 2018 Dec;42(15):4783-9.

130. Sepahvand S, Farhadi S. Fullerene-modified magnetic silver phosphate ($Ag_3PO_4/Fe_3O_4/C_{60}$) nanocomposites: hydrothermal synthesis, characterization and study of photocatalytic, catalytic and antibacterial activities. RSC Advances. 2018;8(18):10124-40.

131. Panahian Y, Arsalani N, Nasiri R. Enhanced photo and sono-photo degradation of crystal violet dye in aqueous solution by 3D flower like F-TiO_2 (B)/fullerene under visible light. Journal of Photochemistry and Photobiology A: Chemistry. 2018 Oct 1;365:45-51.

132. Zou CY, Ji WC, Liu SQ, Shen Z, Zhang Y, Jiang NS. Preparation of a fullerene [60]-iron oxide complex for the photo-fenton degradation of organic contaminants under visible-light irradiation. Chinese Journal of Catalysis. 2018 Jun 30;39(6):1051-9.

133. Chen X, Deng K, Zhou P, Zhang Z. Metal-and Additive-Free Oxidation of Sulfides into Sulfoxides by Fullerene-Modified Carbon Nitride with Visible-Light Illumination. ChemSusChem. 2018 Jul 20;11(14):2444-52.

134. Lin X, Zhao R, Xi Y, Li X, Shi J, Yan N. Metal-free C60/CNTs/g-C3N4 ternary heterostructures: synthesis and enhanced visible-light-driven photocatalytic performance. Royal Society open science. 2018 May 16;5(5):172290.

135. Ma D, Zhong J, Peng R, Li J, Duan R. Effective photoinduced charge separation and photocatalytic activity of hierarchical microsphere-like C60/BiOCl. Applied Surface Science. 2019 Jan 28;465:249-58.

136. Ion I, Ivan GR, Senin RM, Doncea SM, Capra L, Modrogan C, Oprea O, Stinga G, Orbulet O, Ion AC. Adsorption of triclocarban (TCC) onto fullerene C60 in simulated environmental aqueous conditions. Separation Science and Technology. 2019 Feb 21:1-4.

137. Cheng X, Kan AT, Tomson MB. Naphthalene adsorption and desorption from aqueous C60 fullerene. Journal of Chemical & Engineering Data. 2004 May 13;49(3):675-83.

138. Gai K, Shi B, Yan X, Wang D. Effect of dispersion on adsorption of atrazine by aqueous suspensions of fullerenes. Environmental science & technology. 2011 Jun 21;45(14):5959-65.

139. Ma X, Wang C. Fullerene nanoparticles affect the fate and uptake of trichloroethylene in phytoremediation systems. Environmental Engineering Science. 2010 Nov 1;27(11):989-92.

140. Gao F, Zhao GL, Yang S, Spivey JJ. Nitrogen-doped fullerene as a potential catalyst for hydrogen fuel cells. Journal of the American Chemical Society. 2013 Feb 20;135(9):3315-8.

141. Wellons MS, Berseth PA, Zidan R. Novel catalytic effects of fullerene for LiBH4 hydrogen uptake and release. Nanotechnology. 2009 Apr 24;20(20):204022.

142. Roncali J. Linear π-conjugated systems derivatized with C 60-fullerene as molecular heterojunctions for organic photovoltaics. Chemical Society Reviews. 2005;34(6):483-95.

143. Faist MA, Shoaee S, Tuladhar S, Dibb GF, Foster S, Gong W, Kirchartz T, Bradley DD, Durrant JR, Nelson J. Understanding the reduced efficiencies of organic solar cells employing fullerene multiadducts as acceptors. Advanced Energy Materials. 2013 Jun;3(6):744-52.

144. Montellano A, Da Ros T, Bianco A, Prato M. Fullerene C 60 as a multifunctional system for drug and gene delivery. Nanoscale. 2011;3(10):4035-41.

145. Shi J, Liu Y, Wang L, Gao J, Zhang J, Yu X, Ma R, Liu R, Zhang Z. A tumoral acidic pH-responsive drug delivery system based on a novel photosensitizer (fullerene) for in vitro and in vivo chemo-photodynamic therapy. Actabiomaterialia. 2014 Mar 1;10(3):1280-91.

146. Sitharaman B, Zakharian TY, Saraf A, Misra P, Ashcroft J, Pan S, Pham QP, Mikos AG, Wilson LJ, Engler DA. Water-soluble fullerene (C60) derivatives as nonviral gene-delivery vectors. Molecular pharmaceutics. 2008 May 28;5(4):567-78.

147. Compain P, Decroocq C, Iehl J, Holler M, Hazelard D, Barragán TM, Mellet CO, Nierengarten JF. Glycosidase inhibition with fullerene iminosugar balls: a dramatic multivalent effect. AngewandteChemie International Edition. 2010 Aug 2;49(33):5753-6.

148. Grebinyk A, Prylutska S, Grebinyk S, Prylutskyy Y, Ritter U, Matyshevska O, Dandekar T, Frohme M. Complexation with C 60 Fullerene Increases Doxorubicin Efficiency against Leukemic Cells In Vitro. Nanoscale research letters. 2019 Dec 1;14(1):61.

149. Bilobrov V, Sokolova V, Prylutska S, Panchuk R, Litsis O, Osetskyi V, Evstigneev M, Prylutskyy Y, Epple M, Ritter U, Rohr J. A Novel Nanoconjugate of Landomycin A with C 60 Fullerene for Cancer Targeted Therapy: In Vitro Studies. Cellular and Molecular Bioengineering. 2019 Feb 15;12(1):41-51.

150. Gudkov, S.V., Guryev, E.L., Gapeyev, A.B., Sharapov, M.G., Bunkin, N.F., Shkirin, A.V., Zabelina, T.S., Glinushkin, A.P., Sevost'yanov, M.A., Belosludtsev, K.N. and Chernikov, A.V., 2019. Unmodified hydrated C60 fullerene molecules exhibit antioxidant properties, prevent damage to DNA and proteins induced by reactive oxygen species and protect mice against injuries caused by radiation-induced oxidative stress. Nanomedicine: Nanotechnology, Biology and Medicine, 15(1), pp.37-46.

151. Tan J, Yang W, Oh Y, Lee H, Park J, Boppella R, Kim J, Moon J. Fullerene as a Photoelectron Transfer Promoter Enabling Stable TiO2-Protected Sb2Se3 Photocathodes for Photo-Electrochemical Water Splitting. Advanced Energy Materials. 2019.

152. Marchesan S, Da Ros T, Spalluto G, Balzarini J, Prato M. Anti-HIV properties of cationic fullerene derivatives. Bioorganic & medicinal chemistry letters. 2005 Aug 1;15(15):3615-8.

153. Mashino T, Shimotohno K, Ikegami N, Nishikawa D, Okuda K, Takahashi K, Nakamura S, Mochizuki M. Human immunodeficiency virus-reverse transcriptase inhibition and hepatitis C virus RNA-dependent RNA polymerase inhibition activities of fullerene derivatives. Bioorganic & medicinal chemistry letters. 2005 Feb 15;15(4):1107-9.

154. Sood P, Kim KC, Jang SS. Electrochemical Properties of Boron-Doped Fullerene Derivatives for Lithium-Ion Battery Applications. ChemPhysChem. 2018 Mar 19;19(6):753-8.

155. Razavi R, Abrishamifar SM, Kahkha MR, Vojood A, Najafi M. Sn-adopted fullerene nanocage as acceptable catalyst for silicon monoxide oxidation. Bulletin of Materials Science. 2018 Dec 1;41(6):152.

Green Synthesis and Applications of Carbon-Based Nanocomposites

[1]Mita Dutta, [2]Sapna and [1]Dinesh Kumar*

[1]School of Chemical Sciences, Central University of Gujarat, Gandhinagar 382030, India

[2]Department of Chemistry, Banasthali Vidyapith, Banasthali, Tonk 304022, Rajasthan, India

**Corresponding author, email:* dinesh.kumar@cug.ac.in

Abstract

Carbon-based nanocomposites are viewed as model materials for polymeric reinforcement due to their excellent properties at nanoscale. For environmental sustainability, currently a significant consideration has been pinched to the use of green routes to synthesize carbon-based nanocomposites in automotive, construction, packaging, and medical applications. This chapter explores current research efforts, techniques of production, challenges and application prospects of green carbon-based nanocomposites including polymer/carbon nanotubes (CNTs) and metal oxides. Generally, polymerized CNTs have been prepared by the interfacial polymerization in the presence of CNTs using green solvents like water and an ionic liquid, dimethyloldihydroxyethyleneurea was used as a crosslinker to prepare the green material from methyl methacrylate grafted starch softwood flour and functionalized multiwalled carbon nanotube (MWCNT). This chapter also includes special properties of CNTs such as low density, high specific surface area, and thermal and mechanical stability. Nanocomposites also showed antifogging and anti-icing properties. Lightweight conductive polymer composites (CPCs) have been considered as the most promising alternatives to metal–based shields for

electromagnetic interference. The UV–Vis absorption spectrum authenticates the existence of strong quantum confinement in the various well–purified nano-diamond grains have perfect crystalline structure with negligible fractions of nano-diamond carbon nanocomposites. Nanostructures of aligned polyaniline (PANI) exhibited excellent electrochemical properties. PANI/MWCNTs/CMC are suitable nanocomposites material for apply electroactive/conducting ink and membrane which could be used in electrochemical and sensor applications. Palladium (Pd) based nanoparticles (NPs), Pd/graphene nanocomposites are synthesized and examined for hydrogen sorption and storage. This chapter would help to improve understanding the current status of green synthetic methods for carbon–based nanocomposites and their societal applications. The pros and cons of synthetic methods for green nanocomposites are discussed. Lastly, the challenges and perspective of applications of green nanocomposites in diverse fields are discussed.

1. Introduction

Composites materials are made up by two or three different components. A composite product always shows a designed solution that surpasses the performance of the starting materials. While nanocomposites are generally multiphasic solid materials, the particles of nano ranges are added to other standard materials to compose a solid matrix. To get nanocomposites add just 0.5–5% of the NPs by weight. These composites are having drastic changes in properties from respective bulk materials like conductivity, thermal and electrical, mechanical strength, surface modification, toughness etc. Depending upon the size range of NPs, various properties can be evaluated as shown in Table 1.

Table 1: The effect of size of the nanocomposites particle at which significant changes occur, Camargo et al. (2009).

Size (nm)	Property
<5	Catalytic activity
<20	Tune hard magnetic material into soft magnetic material
<50	To change refractive index change
<100	Producing superparamagnetism and other electromagnetic phenomena, modifying hardness and plasticity, and Producing strengthening and toughening

Basically, due to two reasons, nanocomposites materials show such changes in their physical and chemical properties, one due to the bond between bulk materials and NPs, and second due to extremely high surface to volume ratio. The first interference on nanocomposites is reported as early in 1992. After that more than 150000 papers on this topic have been published, nano particle of having 3 nm can have 50% of an atom in its surface, whereas of 30 nm particle can have 15% of an atom on its surface that makes nanocomposites unique from bulk. Also, they have strong tendency to agglomerate to avoid it requires a proper environment.

Some of the NPs are usually transparent due to scattering of the light as they are nano. Three main types of composites are metal matrixes (Fe–Cr/Al_2O_3, Ni/Al_2O_3, Co/Cr, Fe–MgO), ceramic matrixes (Al_2O_3/SiO_2, SiO_2/Ni, SiO_2/TiO_2, TiO_2/SiC, etc.), and polymer matrixes (polymer/CNTs, Polyester/CNTs, Polymer/layer double hydroxides etc.). All these nanocomposites are gaining attention due to their applications in the respective fields. The various types of carbon-based nanocomposites and their applications are given in Table 2.

Table 2. Different types of carbon-based nanocomposites and their applications.

Carbon nanocomposites	**Application**
CNTs/Fe@C	Dye removal activity, Ma et al. (2018)
V_2O_5@carbonbased nanocomposites	Supercapacitor, Majumdar et al. (2019)
Carbon-containing Ni–Sn alloy	Anode material in lithium batteries, Milanova et al. (2015)
Carbon-based nanocomposites of $CuFe_{12}O_{19}$	Photocatalyst of erythrosine as an anionic dye, Mahdiani et al. (2018)
Carbon supported butan–1–sulphanic acid	*Environmentally compatible catalyst for the synthesis of 1,8–dioxo–octahydroxanthanes, Boroujeni et al. (2016)*
Carbon nanotube ionic liquid–epinephrine composite	*gel modified electrode as a sensor for glutathione, Benzhi et al. (2015)*

Raja et al. (2019) synthesized $ZnFe_2O_4/CeO_2$ nanocomposites, which used as a visible light photocatalyst for wastewater treatment. It can be used to remove malachite green an organic water pollutant under visible light irradiation.

2. Carbon Based Nanocomposites

Recent research has been much focused on carbon-based nanocomposites, and various types of nanocomposites have been synthesized till date like CNTs as 1D, 2D, 3D, graphene, graphene oxide, carbon nanosheet, buckminsterfullerene, nanodiamond etc. Different forms of carbon nanotubes shown in Figure 1.

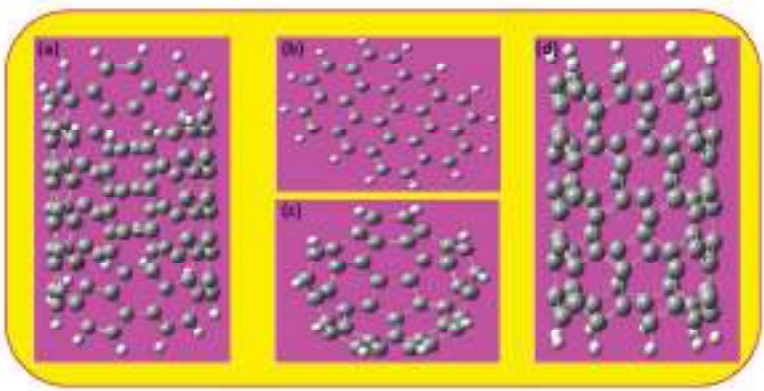

Figure 1. Different form of carbons (a) (5, 5 armchair) carbon nanotube (b) graphite (c) c_{60} fullerene (d) (9, 0 Zigzag) carbon nanotube.

Carbon nanotube was discovered in 1991, after that so many publications basically highest no of research work on this topic is reported. As a composite material, it gains significant attraction due to it's higher thermal and electrical conductivity. Generally, CNTs are of two types of single–walled and multi-walled. It is also a member of the fullerene family its shape is the cylindrical type. There are various synthesized materials have been published as carbon nanotube composites, for examples, MWCNT–TiO_2, CNT/Fe, Co, Ni, CuO–CNT entangled with CNT, CNTs/Zinc sulfide and so forth. Some recent *in vitro* studies have reported increased cytotoxicity of CNTs due to their cellular uptake, agglomeration, and induced oxidative stress.

Allou et al. (2019) reported carbon-based nanocomposites and used as a control vehicle of antibiotics. It has been synthesized by layer double hydroxide (LDH) and surface modified carbon. The surface of its negatively charged. After the deposition of the LDH over activated carbon surface area increase from 0.78 to 1.33 nm. These composite molecules then intercalated with antibiotic molecule norfloxacin (NOR), it shows a gradual release of NOR from AC–LDH–NOR nanocomposites suggest its

prospective application as an effective delivery system for prolonged drug release.

Yang et al. (2017) developed carbon nanotube/nitrogen doped reduced graphene oxide and used as a supercapacitor; it has a higher porosity, super excellent surface area and high potential for improving power and energy density of supercapacitors. Nitrogen-doped reduced graphene oxide nanocomposites, hybrid carbon-based materials are of greatest use as an electrode for energy storage and conversion device. Reduced graphene oxide plays a good role over this. After nitrogen doped surface area of the graphene, oxide nanosheet increases enormously. The specific surface area of nitrogen doped reduced graphene oxide (NrGO) was increased to 633 m^2g^{-1} compared to that of rGO, 450 m^2g^{-1}.

Yun et al. (2018) reported performance of lithium storage by using strongly surface bonded MoO_2/carbon nanocomposites with nitrogen-doped as an anode. Carbon alleviates the volume change of MoO_2 and enhances the electron transfer of the electrode. They produced a core structure of MoO_2, in that carbon shell, doped with nitrogen, as a result, a strong Mo–N bond was obtained. The strongly coupled MoS_2/C nanocomposites show well electrochemical performance.

2.1. Green approach for carbon-based nanocomposites

There are several methods till date which are impregnations the polymeric precursor like chemical vapour deposition (CVD), ball milling, and sol-gel.

Da silva et al. (2019) used an amperometric biosensor for tyramine (Tyr) measurement in food and beverages. A glassy carbon electrode modified by gold nanoparticles (AuNPs) was synthesized using green reducing agent. This biosensor under optimized experimental condition exhibits a linear response to tyramine in the range of 10–123 μM.

Xu et al. (2019) produced water compatible polymer/carbon nanocomposites with beads on a string nanostructure. This is developed by a facile one-step co-assembly of an amphiphilic random copolymer with MWCNTs; it is successfully applied as an effective electrode material for electrochemical sensing. This is actually prepared by green approach, firstly an ambiphilic photo cross–linked co-polymerpoly (AA–co–VMc–co–EHA) (PAVE) synthesized from one step radical generation, then this copolymer was co-assembled with MWCNTs in selective solvent non covalently (Figure 2). The excellence of this sensor is due to large surface area and high electric conductance of “Beads on a string" structured PAVE–CNTs NCs.

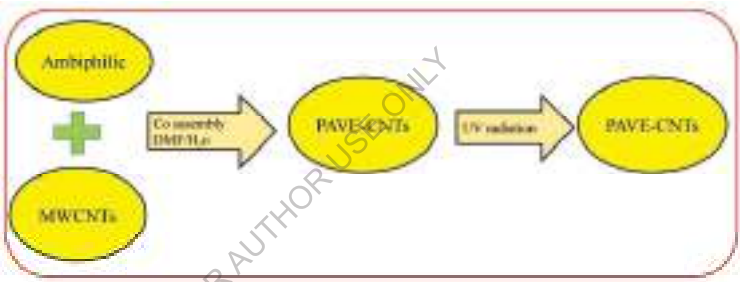

Figure 2. Schematic description of the green preparative process of PAVA–CNTs NCs

Zaho et al. (2019) used a green synthesis process for the synthesis of carbon-based FeS nanocomposites (FeS/C). They used bio waste eggshell membrane as intrinsic source material for C and S, and FeS NPs were fabricated via in situ adsorption–carbonization approach. The FeS NPs are well dispersed in carbon nanowires. It has been used in energy application as an anode material of the electrochemical cell, where it shows the good reversible capacity of 503.5 mAh/g after 100 cycles at 200 mA/g.

Sun et al. (2018) reported a green method to prepare sandwich–like reduced graphene oxide/carbon black/amorphous cobalt borate

nanocomposites (rGO/CB/Co–B). Cobalt ions were mixed with graphene oxide via electrostatic interaction, then some amount carbon black (CB) particle were added and sonicated for few hours, this whole process reduced disperse Co(II)/Go/CB composites. The additions of sodium borohydrate reduced GO and at the same time it simultaneously grew up the amorphous cobalt borate nanosheets. These nanocomposites are used as bifunctional cathode electrocatalyst in zinc air batteries

Atchudan et al. (2018) produced nitrogen-doped carbon dot (N–CDs) and titanium dioxide nanoparticles@ carbon (TiO_2NPs@C) at once applying green affordable hydrothermal method. TiO_2NPs were prepared from titanium isopropoxide, alcohol and water mixture in optimum amount, after vigorous mixing concentrated H_2SO_4 was added to this until the pH reached 3.5, this mixture was then centrifuged, washed with deionised water, dried and calcinated, finally obtained TiO_2NPs. They used peach juice to prepare TiO_2NPs@C. Peach juice, and aqueous ammonia mixed well and transferred into the Teflon lined stainless steel autoclave. The resultant TiO_2NPs@C nanocomposites show good photocatalytic activity towards degradation of organic pollutant, and N–CDs show biocompatibility as for it is used as a fluorescent probe in cell imagining.

Moradi et al. (2018) synthesized photo luminescent nano carbon dots through environmentally friendly biopolymers, gum tragacanth (GT), and chitosan via hydrothermal method. Two types of carbon dot were prepared by pure GT solution and an equal amount of GT and chitosan solution, both were taken in an autoclave for 45 min, after that filtration, washed followed by centrifugation, the supernatant collected and dried. Carbon dots based on biopolymer have been used as ideal non–toxic markers, in biosensing, biological labeling, medical diagnostics, optoelectronic devices, and bioimaging.

Muthuchamy et al. (2018) prepared zinc nanoparticle embedded nitrogen-doped carbon nanosheet based composites (ZnO@NDCS) for enzymatic glucose sensing. The peach extract, Zn powder and ammonia solution were used as a precursor for the synthesis NPs as mentioned above for synthesis of TiO_2NPs. This shows high reproducible sensitivity; the lower range of detection limit is 6.3 μM with $R^2 = 0.998$. This result is encouraging us to obtain an electrode material as an enzymatic sensor by green approach.

Another green route used by Karmakar et al. (2018) for the synthesis of carbon nanocomposites, they used solvothermal treatment of banana (*Musa balbisiana*) bark extract to produce TiO_2@carbon nanocomposites. These so produced nanocomposites demonstrated yellow–green photoluminescent features as well as photocatalytic activity towards degradation off methylene blue under UV–Vis irradiation.

Aravind et al. (2011) developed a solvent-free preparative method to synthesize graphene–MWNT composites. Graphene oxide (GO) is used as starting material, GO was expose to intense solar radiation via a convex lens of 90 mm diameter, after getting a hydrophobic GO further functionalized by refluxing with conc HNO_3, this process is needed so that the produced GO will be much dispersible in a polar medium such as water or ethylene glycol. By the same way MWNT (prepared from catalytic vapor decomposition) are functionalized, thus a 1:1 GO–fMWNT is formed. The exfoliated product, *i.e.* sG–f–MWNT was employed for the synthesis of nanofluids without further chemical treatment.

2.2.Carbon dot conjugated gold nanocomposites

Alarfaj et al. (2018) synthesized a low–cost simple carbon quantum dot/gold nanocomposite, a fluorescence immunosensing solution via a green method. It was synthesized by 15% aqueous solution of AuNPs. The solution was heated by microwave heating, after that CDQs/Au composites

were obtained by simple reduction reaction using CDQs and NH_3 as reducing reagent. It detects CA 19–9(pancreatic tumor maker) from human serum. In the surface of CQDs/Au–nanocomposites, anti–CA 19–9–labeled horseradish peroxidase enzyme (Ab–HRP) was tied up though peptide interaction between carboxylic acid and amine group. A sandwich capping antibody-antigen enzyme formed by trapping another monoclonal antibody coated with microliter wells, this exhibit tunable fluorescence property detection limit 420–530 nm. The fluorescence intensity of nanocomposites immunosensing solutios proportional with CA 19–9 antigen concentration.

Guo et al. (2019) prepared composite by using a green efficient nanocatalyst for removal of organic pollutant. This composite actively degrades peroxymonosulfate (PMS) from 2, 4– dichlorophenol (DCP), acid orange II, reactive brilliant red X–3B, rhodamine B and methylene blue.

Ruiying et al. (2018) used naphthol and talcum composite film modified hydrogen peroxide electrochem sensor. The preparation method includes preparation of aqueous talcum nanosheet colloidal solution and green naphthol solution treated with negative charge glassy carbon electrode sheet in the two kinds of solution to assemble alternately with water to obtain green naphthol talcum multilayer composite film modified electrochemical sensor. The invention has the advantages of water talcum nanosheet as electrochemically active substances through its own redox reaction of hydrogen peroxide to generate electrocatalytic layer–by–layer self–assembly method, so that the active ingredient in the molecular level with controllable nano level in the film, the resulting high orientation film so that the sensor has good response current.

2.3. Special properties of carbon nanotubes (CNTs)

Carbon nanotubes are longfiberlike structure, made up by sp^2 bonded carbon atoms. These are classified as single-walled carbon nanotubes (SWCNTs) and multi-walled carbon nanotube (MWCNTs), SWCNTs are consisted a single graphene layer rolling into seamless tube whereas MWCNTs are consists a bunch of SWCNTs in a close-packed manner. CNTs are of having hexagonal close packing structure, with some sp^3 carbon at the edges as a defect. The uniqueness of CNTs arises as there is strong interaction between the atoms in layers but little interaction between adjacent layers.

Carbon nanotubes are considered as a flexible low cost and high–performance thermoelectric material as these have excellent thermal and mechanical properties. Through special strategies called thermoelectric carbon nanotubes are shows desirable features for both n-type and p-type semiconductor. CNT–polymer hybrids are creating a good record in thermoelectric (TE) performance in organic materials now potentially used for flexible electric devices. Mg–CNTs matrix was fabricated using nanoscale Mg grains through insitu on the surface of carbon nanotubes. Here a nanoscale contacts and diffusion bonding occurred at the CNT–Mg surface. These composites prove special properties of microhardness, ultimate tensile strength and breaking elongation; therefore, composites are very suitable to use as in the field of light weighted structural materials. Carbon nanotubes are gaining much attention in drug delivery system.

Ghasemi–Kooch et al. (2017) explored adsorption property of oleuropein in different types of SWCNTs at both the position inside and outside including the chiral, zigzag and armchair with a different diameter. In their study after an investigation by radial distribution graph and amount of Lennard–Jones energy between oleuropein and carbon nanotube, it has been proved that oleuropein is adsorbed on all the nanotubes. Inner surface

contributes to strong interaction rather than the outer side, strongest interaction occurs at 13 nm, whereas chirality does not play any role in that case. Interaction in inner became weaker with diameter but the outer surface is not. Outer surface interaction shows improvise with solvent modification. This is a reflection of the highly anisotropic property. The extraordinary electrical, thermal, and mechanical properties are the ideal properties along the axial direction inside SWCNTs.

Ram et al. (2018) reported MWCNTs electromagnetic interference (EMI) shielding material as composites with polyvinylidene fluoride (PVDF). Here MWCNTs play the role of reinforcing filler for PVDF matrix. The PVDF matrix shows MWCNT–dependent EMI shielding effectiveness, skin depth, and morphology, mechanical and dynamic mechanical properties

Leont'ev et al. (2017) explored results of multiobjective optimization of lightly weighted autoclave aerated concrete modify with carbon nanotube dispersion. By the dispersion of CNTs, there is an enhancement of strength properties of thermal insulation autoclave aerated concrete. A special type of pours nanofiber tube was prepared to invent a novel electrode material in the technical field. An electrode made by two layers one is carbon nanolayer and another is graphene layer. A nitrogen mixed matrix was produced by an embedded nitrogen atom in the lower surface of the graphene layer, by that way a heterogeneous atomic layer matrix covers both upper and lower surface. The connection of the graphene layer and the nitrogen atomic layer in this structure constrict it as a high–performance anode material

2.4. Single-walled carbon nanotubes specific chirality control growth

In the field of nanotechnology and nanomaterial SWNTs are regarded as star material as it has some extraordinary properties like electrical, thermal, mechanical and optical. It is a challenge to control the growth of CNTs,

there are various methods among them chirality control growth recognizes as a successful method for the diameter, the wall number, the chiral angle, and conductive property. To use a special approach to synthesize CNTs with controllable properties, iron nanoparticle is produced by spin coating micellar solution of iron modified poly (cyclohexyl methacrylate)–block–poly (2–vinyl pyridine) (PCMA–b–P2VP) block copolymer in methanol, after that a uniformly sized iron NPs are formed through thermal decomposition of polymer template on Si substrate. These nanoparticles are showing an excellent catalyst for growing CNTs by plasma enhance thermal chemical vapor decomposition. In addition, the diameter of the nanotubes is controllable by varying grow time.

2.5. CNT/polymer recent advances in electrical and mechanical property

To reach optimum mechanical property nanotube should have maximized insolubility, dispersion and stress transfer. Among the various polymers, polymethylmethacrylate (PMMA) has been extensively used to develop carbon nanotube composites to enhance the electrical and structural applications.

Mathur et al. (2008) reported composites which mainly prepared by solvent casting, melt mixing and in–situ polymerization. The important properties associated with this composite are tensile, elastic modulus, fracture toughness, flexible modulus, flexural strength and so forth.

3. Graphite

Graphite is a crystalline allotrope of carbon. It is very light weighted and extremely soft a layered structure in which six-membered rings of carbons are arranged as a 2D atomic sheet. Graphite nanosheet has unusual mechanical, thermal, and electrical properties to make the researcher more study on this. But preparation of nongraphite sheet is typically difficult as it is not easily dispersible on polymer matrixes, whereas graphite oxide is

much suitable in polymer matrixes that's why research is concentrated toward GO nanosheet. GO is dispersible in aqueous media and exhibits a broader range of physical properties than pure graphite due to structural heterogeneity. There are a various methods and huge applications on GO nanocomposites.

Another important arena is graphite carbon nitride generally formulate as g–C_3N_4, a non-metallic species exhibits well semiconductor properties. It is mainly prepared by polymerization of cyanamide, dicyanamide or melamine and electrodeposition on Si. In nano range, it appears as well crystallized form. Various methods have been published in this field, they will be discussed below in the chapter. Graphite carbon nitride is very popular as nanocomposites materials mainly in photocatalytic reaction. It can also cause CO_2 reduction, water splitting, environment pollution remediation, and production of lithium batteries.

Nithya et al. (2016) reported composites of magnetite and graphite on behalf of supercapacitor as an electrode. The synthesis method single pot co-precipitation is quite suitable and simple method. The thing to be noted here that is low–cost materials being used which are considered an asset to sustainable manufacturing. The CV measurement shows an excellent supercapacitive nature of the composites, the specific conductance of the composites shows a much higher value than pure Fe_2O_3 and that of graphite.

4. Nano-diamond composites

Diamond particle in nanoscale first produced in 1960s, whereas it comes as a breakthrough in the begging of 1990s. Nano-diamonds exhibit very excellence in mechanical and optical properties, it is non–toxic as well. These properties make it a very useful tool in biomedical research. The chemical reactivity of the surface of nano-diamond allowed a variety of wet and gas chemistry techniques to be employed to tailor the properties of

nano-diamond for use as composites. Well purified nano-diamond grains can have an almost perfect crystalline structure with negligible fractions of nano-diamond carbon.

5. Green synthesis, we can synthesize any materials by applying any methods, but we call it green synthesis when the process does not include any toxic materials, or it minimizes toxicity. In chemical synthesis, toxicity arises from using hazard solvents, the evolution of some toxic gases like CO, NO_2, SO_2 etc. and using toxic reagents. Recent studies very much focused on how to reduce these toxic materials by applying green methods. Green chemistry approaches use of plan mediated resources and water as a solvent by a great extent in the synthesis process. These methods can make a synthesis to be green itself. Other than these two, a green synthesis also reveals to use of renewable sources, use of the catalyst in place to use that of high cost or toxic reagent, improve atoms efficiency and minimization of time consumption as well as energy. Till date we have synthesized so many numbers of the nanoparticles by using plant resources, like plant-mediated synthesis of nanoparticles is a green chemistry approach that connects nanotechnology with plants. A few preparations methods of nanoparticles can make a synthesis to be green itself discuss below:

1. Gold ions of dodecahedral and icosahedral shapes of 20–40 nm could be reduced and stabilized by extracts of *Pelargonium graveolens* (rose geranium),

2. *A. indica* juice can reduce silver nitrate to a silver nanoparticle of spherical shape with 5–25 nm size.

3. The In_2O_3 particle of 5–50 nm can be produced by leaf extract of *Aloe barbadensis* (aloe vera).

4. Pain (apigenin glycoside) was extracted from *Lawsonia inermis* (lawsonite thornless, henna) and used for the synthesis of

anisotropic gold and quasi spherical silver nanoparticles with an average size of 21–30 nm

5. Carbon-based nanocomposites are also bought into contact of green synthesis.

Liu et al. (2015) synthesized single and multilayer graphene through exfoliation of graphite sheets collaborated with intercalant ($FeCl_2$) under hydrothermal conditions. Hydrothermal exfoliation nowadays gets attention over the potential application in the exfoliation carbon nanotube, nanoribbon, nanoparticle and also another layer compound like BN (boron nitride), MoS_2 etc. Likewise, hydrothermal process there are other methods included in the green synthesis process, the simple ultrasonic method produces carbon nanohorn–carbon nanotube by Zhu et al. (2019).

By application carbon-based nanocomposites are captured top interest in the research field as well we need to discover these materials through green approach so that society and environment both would feed by such materials. Advances in application still progress with high expectation.

6. Biobased green adsorbent

Mahmoodi et al. (2018) used activated carbon as a nucleation agent for Cr–MOF with different ratios. Here activated carbon (AC) as taken from cucumber peel purchased from local market. To get AC synthesis process includes the following steps as shown in the flow chart given below (Figure 3).

Figure 3. Flow chart of AC synthesis process

Carbon/Cr–MOF are used for removing acid green 25 (AG25) and Reactive Yellow 186 (RY186) dyes from the binary systems.

Shi et al. (2018) prepared g–C_3N_4/carbon nanosphere/Cu by using green template named sodium alginate. Sodium alginate is prepared from Alginic acid which basically distributed in the cell wall brown algae (seaweeds). This is a high–performance polymeric material showing highly desirable fire safety property. Here the Cu particle and g–C_3N_4 were dispersed in carbon nanoparticle, this ternary monohybrid was well distributed in thermoplastic polyurethane (TPU) solution.

In 2018, Al Enizi et al. synthesized nitrogen–doped carbon–based nanocomposites with Sn/SnO_2 nanoparticles to use as fast and high–performance NH_3 gas sensor. The composites have 148.09 m^2g^{-1} surface area. After SEM imagination it shows that both Sn and SnO_2 particles are well dispersed in nitrogen–doped carbon matrix. After characterization with various concentrations of NH_3 gas this sensor response excellent at 65 °C and 300 ppm concentration of NH_3, and recovery time is 55 s and 60 s. So, with all these sensing reports and characterization techniques, these composites could be used as an industrial scale.

7. Oxygen reduction reaction (ORR) catalysis

Tang et al. (2018) reported well–known ORR catalyst, Pt/C is commercially high–cost material, carbon-based nanocomposites have

shown a promising role in this field as an electrocatalyst. Recently, a composite is developed which shows facile electrocatalytic activity towards ORR. One-dimension porous nitrogen doped graphite nanofiber embedded with metal/metal oxide (M/MO) nanoparticle produced by two-step method: electrospinning followed by annealing. Among metal/metal oxide couples, Co_3O_4 shows comparable more catalytic activity with superior stability and methanol tolerance.

8. Applications of Carbon–Based Nanocomposites

Ma et al. (2018) synthesized the novel magnetic CNTs/Fe@C through a one-pot method for the dye removal and achieved high specific surface area 186.3 m^2/g which confirmed through BET. It has been further characterized by various techniques like SEM, XRD, FTIR, XPS, and Raman spectroscopy. Adsorption experiments showed significant differences between single and binary dye systems. It showed maximum adsorption capacities 132.58, 16.53, and 98.81 mg/g for methylene blue, methyl orange and neutral red, respectively. Adsorption equilibrium time with initial adsorption capacities was reported 80, 40, and 10 min, respectively. Both methylene blue and methyl orange exhibited cooperative adsorption whereas methylene blue and neutral red showed competitive adsorption. The electrostatic attraction and π–π stacking interactions and change of surface charge on CNTs/Fe@C make the favorable to the cooperative adsorption. Whereas the competitive adsorption occurred mainly due to the electrostatic repulsion and active site competition between methylene blue and neutral red onto CNTs/Fe@C. The adsorption data and their mechanism have been checked by using several kinetic and isotherms models. The mechanism of interactions between dyes and their corresponding solution, and adsorption mechanisms onto CNTs/Fe@C were described via FTIR, Raman spectra and zeta potential techniques.

Wang et al. (2018) prepared hybrid nanocomposite as anionic polypeptide poly(γ–glutamic acid) (γ–PGA) functionalized magnetic Fe_3O_4–GO–(o–MWCNTs) by using simple one–pot reaction. The involvement of o–MWCNTs solved the biggest problem aggregation of GO and provides the more grafted sites to the GO for the bonding to a large amount of γ–PGA molecule chains. This novel composite showed higher specific surface area and provides many surface adsorption sites. The hybrid nanocomposite also could be separated easily from solution medium. It shows the adsorption behavior towards the heavy metals like Cd(II), Cu(II) and Ni(II) and showed the very good adsorption capacity. Adsorption capacity was checked by varying optimizing parameters including solutions pH, initial concentrations of ions and contact time. They attained good adsorption capacity between the pH range of 2–10. The adsorption capacity well described by the Langmuir model and the pseudo–second-order kinetics model in given optimizing conditions. The highest removal capacity was 625.00, 574.71 384.62 mg/g for Cd(II), Cu(II) and Ni(II), respectively. Additionally, the adsorption mechanism may involve characteristic coordination bonding and electrostatic attraction between γ–PGA–Fe_3O_4–GO–(o–MWCNTs) and metal ions. This composite might be recycled and regenerated up to consequently three adsorption-desorption cycles. All properties like good adsorption capacity and the easy interactions with toxic heavy metals make the composite highly promising as an advanced adsorbent material for the removal of health hazardous metals.

Sahu et al. (2018) demonstrated a hydrothermal technique for the synthesis of novel CeO_2/Fe_2O_3/graphene nanocomposite for the removal arsenic. They were employed the Box–Behnken design to optimize adsorptive removal of As(III) and As(V) from aqueous solutions. The batch study was performed for the adsorption experiments in which three input

variables have been given including adsorbent dosage 0.1 –0.2 g/L, initial concentration 10–50 mg/L, and pH 3–10. The adsorption experiment data showed good fitness with the quadratic polynomial model. They obtained the higher regression (R^2) value for As(III) and As(V) was 0.9957 and 0.9929 respectively. The maximum removal of As(III) achieved at optimum initial concentration, adsorbent dose, and pH, 10.52 mg/L, 0.198 g/L and 7.84, respectively. For the removal of As(V), they were achieved maximum performance at initial concentration 10.78 mg/L, adsorbent dose 0.197 g/L, and pH 3.05. Overall removal percentage of CeO_2/Fe_2O_3/graphene nanocomposite for the As(III) and As(V) was reported to be 98.53% and 97.26% at given optimal conditions. These all results favored CeO_2/Fe_2O_3/graphene nanocomposite seems to be an efficient adsorbent.

Luan et al. (2018) reported the functionalized of CNTs through harsh chemical conditions. Magnetron sputtering technique was utilized to functionalize the CNTs. The deposition of Cu onto pre-synthesized CNTs membranes without given chemical treatment. This synthesis determines that magnetron sputtering seems to be a promising greener technology for the productions of metal–CNTs composite membranes for environmental applications. Among substrate mixed cellulose ester membranes, the polymeric membrane sputtered with Cu, or the polymeric membrane coated with CNTs, Cu/CNTs membrane showed the good adsorption capacity of the arsenite from aqueous solutions under maintaining ionic strength and pH conditions. Other co-existing ions like SO_4^{2-} and PO_4^{3-} compete with the As(III) plays a negative role in the removal of As(III). So, therefore, pretreatment is required for the source water which contains competing anions and inhibits the target metal ion in removal. With the help of HPLC–ICP–MS and XPS results they determined the mechanism of the removal Cu/CNTs membrane of As(III). Basically, two major steps are

involved; firstly oxidation occurred from As(III) to As(V) by aqueous oxygen under the catalysis of sputtered Cu nanoparticles, and second is the adsorption of As(V) onto copper hydroxides on the composite membrane.

Mehta et al. (2018) designed a novel method for the detection of highly toxic ion lead based on kill waste by the waste approach. Fluorescence carbon quantum dots (CQDs) utilized for the detection of Pb(II) present in the wastewater. Further with the Pb–CQDs TiO_2 were impregnated and works for the photodegradation of health hazardous industrial dyes. The CQDs act as nanosensor for detection of Pb(II) ion with good sensitivity (0.070 μM) and effective selectivity. By implication, wet impregnation method fabrication Pb–CQDs–TiO_2 (PCT) nanocomposite occurred with 3.2 to 2.8 eV energy gaps which makes the composite highly active in visible light irradiation. The TiO_2 nanocomposite showed the 100% removal for the reactive brilliant red X–3BS(RB)X dye and 1.8 μmols of CO_2 evolution was observed 1in 60 min.

Ali et al. (2018) prepared the low-cost MWCNTs of 10–40 nm with 9.0 m^2/g surface area. These MWCNTs were used for the elimination of fenuronpesticide from the wastewater. At various optimizing conditions such as the effect of contact time (60 min), adsorbent dosage (2.0 g/L), pH (2.0), initial concentration (100.0 μg/L), and temperature (25 °C) and showed 90% removal of fenuron pesticide. The adsorption experimental data was well explained by Langmuir, Freundlich, Temkin, and Dubinin–Radushkevich models. The supramolecular mechanism of fenuron adsorption onto CNTs was fixed by simulation studies and the binding energy and binding affinity of fenuron with CNTs were −6.5 kcal/mol and $5.85 \times 104\ M^{-1}$, respectively.

Agrawal et al. (2018) synthesized the micron or nano size filters which have needed for the separation of adsorbent from the water after the rejection of adsorbate. There is a serious problem like even after filtration

some amount of adsorbent remains in purified water, which has worsened the quality of water for drinking purpose. So, by using a sacrificial template process MWCNTs loaded carbon foam (CF) was fabricated to eradicate these problems. In the present method for the impregnation of the polyurethane (PU) template MWCNTs and phenolic resin mixture played an important role. After the impregnation, PU foam stabilized and carbonized to get MWCNTs embedded and further utilizes to trap the As(V) from the water. The maximum adsorption capacity achieved 90.5 μg/g at the optimized condition of time, pH, and initial concentration of metal ion, which is excellent in comparison to several other materials utilized for removal of As(V).

Sharma et al. (2018) utilized combustion technique for the development of nanosized tin ferrous oxide ($Sn_{0.95}Fe_{0.05}O_2-\delta$) decorated graphene oxide (GO) based adsorbents. In terms of material morphology, structures, stability, binding, and the specific surface area developed adsorbents were characterized by SEM, XRD, TGA, XPS, and BET. In comparison to bare GO and nano tin ferrous oxide, $Sn_{0.95}Fe_{0.05}O_2-\delta$ decorated GO sheets showed four times higher adsorption capacity. The adsorption kinetics and the thermodynamics well described by the pseudo-second–order and the Langmuir isotherm model equilibrium. $Sn_{0.95}Fe_{0.05}O_2-\delta$ decorated GO NPs attained higher adsorption capacity at equilibrium was 105 mg/g than $Sn_{0.95}Fe_{0.05}O_2-\delta$ and GO was 27, 23 mg/g respectively. The adsorption study also checked in a packed bed column and investigated its feasibility for large–scale operations.

Samuel et al. (2018) demonstrated the removal of chromium (VI) from aqueous solution by the utilization of magnetically modified graphene oxide/chitosan/ferrite nanocomposite (GCF). To check the notable adsorption capacity nanocomposite goes through various parameters like a dose of adsorbent, pH condition, initial metal ion concentration, contact

time in the batch experiment. The higher adsorption value for Cr (VI) was observed at pH 2.0 was 270.27 mg/g. The GCF adsorption experiment data was well defined by Langmuir isotherm and pseudo–second-order kinetic model, with a high regression coefficient. On the basis of all these results, GCF nanocomposite material proved as an efficient adsorbent for rejection of Cr(VI) from wastewater.

Wu et al. (2019) developed three–dimensional α–Fe_2O_3/amino–functionalization carbon nanotube as a α–Fe_2O_3/CNT–N sponge for the removal of organic pollutant Tetrabromobisphenol A (TBBPA) present in the aqueous system. The adsorption capacity was 41.35 ± 6.09 mg/g at 303 K and pH 7.0 ± 0. Maximum adsorption capacity was maintained in the pH range of 3–7. The adsorbed organic pollutant TBBPA on the α–Fe_2O_3/CNT–N sponge could degrade after addition of peroxymonosulfate (PMS) which generate hydroxyl and sulfate radicals. The functional groups such as –$CONH_2$, –C=O and π–π* bonds played a significant role in the activation of PMS. After four to five cycles of adsorption-desorption it still maintained the adsorption efficiency. Therefore, it can be considered good adsorbent for the wastewater treatment due to their higher adsorption capacity, good regeneration tendency and easy separation from water.

Sherlala et al. (2018) demonstrated the adsorption As(III) from aqueous solution. They synthesized the high potential magnetic graphene oxide (MGO). The adsorption experiment performed to check the adoption capacity of the adsorbent. During the batch experiment, various parameters were considered and played an important role in the adsorption. They carried change in the adsorbent dosage amount, pH range, and contact time. The maximum adsorption capacity attained by MGO at optimum conditions of utilized parameters. At initial As(III) concentration was 100 mg/L, pH at 7, adsorbent dosage at 0.3 g/L and contact time around 77 min showed 99.95% of As(III) removal. The adsorbent dosage and pH

parameters were the most significant parameters which affect the adsorption efficiency. As(III) adsorbed over the surface of MGO through the complexation between surface functional groups of the MGO and the oxyanions of As(III). Resultant adsorption mechanism of As(III) on to MGO confirmed by the FTIR analysis. After even four cycles of adsorption-desorption still maintained the significant adsorption capacity of MGO. Hence, the synthesized MGO has great potential to be used for the exclusion of arsenic from aqueous solution.

Hayati et al. (2018) used CNT coated polyamidoamine dendrimer (PAMAM) for the adsorption of As(III), Co(II), and Zn(II) from aqueous system. Based on their results confirmed that the dendrimer functionalized CNTs have been favorably synthesized. The fixed bed adsorption results outcome indicates that a decline flow rate, as well as initial concentration and increment in bed height, enhances the breakthrough time and removal capacity. The maximum adsorption reported at fixed bed breakthrough were 432, 494, 470 mg g^{-1} for As(III), Co(II), Zn(II) at 12.0 cm, 100 mg L^{-1}, 0.5 m/L/min bed height, influent concentration, flow rate, respectively. At last adsorption, results were checked using the Yoon–Nelson, Bohart–Adams and Thomas models. They found that the empirical breakthrough best–fitted curves which produced by the Thomas and Yoon–Nelson equations.

9. Conclusions

Nanocomposites materials are most important discovery in our material science, where carbon-based nanocomposites bring highest attention due to its day by day increasing application in various fields of catalysis, water purification, solar cell, bio sensor, energy storage, bio medical etc. Recent days, scientist take one step more to developed efficient and economical method to apply carbon-based nanocomposites. Advances in application still progress with high expectation. We have discussed some of green

approaches that already been discovered, to benefited more quantifiably from these nanocarbon composites further investigation should be focused on their reproducibility and reusability. Research need to consider mostly on health and energy issue related problems deals by greenery produced carbon nanomaterial.

10.Acknowledgment

We gratefully acknowledge support from the Ministry of Science and Technology and Department of Science and Technology, Government of India under the Scheme of Establishment of Women Technology Park, for providing the necessary financial support to carry out this study vide letter No, F. No SEED/WTP/063/2014.

11.References

Agrawal, P. R., Singh, N., Kumari, S, and Dhakate, S. R. (2018). Multiwall carbon nanotube embedded phenolic resin–based carbon foam for the removal of As(V) from contaminated water, *Mater. Res. Express,* **5**, pp. 1–9.

Ahadian, S., Obregon, R., Ramon-Azcon, J., Salazar, G., Shiku, H., Ramalingam, M. and Matsue, T. (2016). Carbon nanotubes and graphene-based nanomaterials for stem cell differentiation and tissue regeneration, *J. Nanoscience Nanotechnol.*, **16**, pp. 8862–8880

Alarfaj, N., El-Tohamy, M. and Oraby, H. (2018). CA 19-9 pancreatic tumor marker fluorescence immunosensing detection via immobilized carbon quantum dots conjugated gold nanocomposite. *Inter. J. mole. Sci.,* **19,** pp.1162.

Al-Enizi, A. M., Naushad, M., Al-Muhtaseb, A. H., Ruksana, Alshehri, S. M., Alothman, Z. and Ahamad, T. (2018). Synthesis and characterization of highly selective and sensitive Sn/SnO_2/N-doped carbon nanocomposite (Sn/SnO_2@NGC) for sensing toxic NH_3 gas, *Chem. Eng. J.*, ***345***, pp. 58–66.

Ali, I., Alharbi, Omar., ALOthman, Z. A., Al–Mohaimeed, AM. and Alwarthan, A. (2018). Modeling of fenuron pesticide adsorption on CNTs for mechanistic insight and removal in water, *Environ. Res.,* **170**, pp. 389–397.

Allou, N. B., Saikia, J., Bordoloi, P., Yadav, A., Pal, M. and Goswamee, R. L. (2019). Layered double hydroxide and microwave assisted functionalized carbon-based nanocomposites as controlled release vehicle for antibiotics, *J. Drug Deliv. Sci. Technol.,* ***49***, pp. 243–253.

Aravind, S. S. and Ramaprabhu, S. (2013). Graphene–multiwalled carbon nanotube-based nanofluids for improved heat dissipation, *RSC Adv.*, ***3,*** pp. 4199–4206.

Atchudan, R., Edison, T. N., Perumal, S., Vinodh, R. and Lee, Y. R. (2018). In-situ green synthesis of nitrogen-doped carbon dots for bioimaging and TiO_2 nanoparticles@nitrogen-doped carbon composite for photocatalytic degradation of organic pollutants, *J. Alloys Compd.,* ***766***, pp. 12–24.

Ayahi, H., Mohsenzadeh, F., Darabi, H. R. and Aghapoor, K. (2019). Facile and economical fabrication of magnetite/graphite nanocomposites for supercapacitor electrodes with significantly extended potential window, *J. Alloys Compd.,* ***778,*** pp. 633–642.

Boroujeni, P. K., Heidari, Z. and Khalifeh, R. (2016). Carbon Nanotube-Supported Butyl 1-Sulfonic Acid Groups as a Novel and Environmentally Compatible Catalyst for the Synthesis of 1,8-Dioxo-octahydroxanthenes. *Acta. Chimica. Slovenica.,* **63**, pp. 602–608.

Byrne, M. T. and Gun'ko, Y. K. (2010). Recent advances in research on carbon nanotube-polymer composites, *Adv. Mater.,* ***22***, pp. 1672–1688.

Camargo, P. H., Satyanarayana, K. G. and Wypych, F. (2009). Nanocomposites: synthesis, structure, properties and new application opportunities. *Mater. Res.,* ***12***, pp.1–39.

da Silva, W., Ghica, Mariana E., Ajayi, Rachel F., Iwuoha, Emmanuel I. and Brett, Christopher M. A. (2019). Tyrosinase based amperometric biosensor for determination of tyramine in fermented food and beverages with gold nanoparticle doped poly(8-anilino-1-napthalene sulphonic acid), *Food Chem.,* **282**, pp.18–26

Dong, S., Peng, L., Wei, W. and Huang, T. (2018). Three MOF-templated carbon nanocomposites for potential platforms of enzyme immobilization with improved electrochemical performance, *Acs Appl. Mater. Inter.,* **10**, pp. 14665–14672.

Ghasemi-Kooch, M., Dehestani, M., Housaindokht, M. R. and Bozorgmehr, M. R. (2017). Oleuropein interactions with inner and outer surface of different types of

carbon nanotubes: Insights from molecular dynamic simulation, *J Mol Liq.,* ***24***, pp. 367–373.

Guo, F., Wang, K., Lu, J., Chen, J., Dong, X., Xia, D., Aiqing Zhang and Wang, Q. (2019). Activation of peroxymonosulfate by magnetic carbon supported Prussian blue nanocomposite for the degradation of organic contaminants with singlet oxygen and superoxide radicals, *Chemosphere,* ***218****,* pp. 1071–1081.

Hayati, B., Maleki, A., Najafi, F., Gharbia, F., McKay, G., Gupta, V. K., Puttaiah, S. H. and Marzban, N. (2018). Heavy metal adsorption using PAMAM/CNT nanocomposite from aqueous solution in batch and continuous fixed bed systems*, Chem Eng J.,* **346**, pp. 258–270.

Guo, F., Xu, Y., and Wang, C. (2011). Sulfur-impregnated disordered carbon nanotubes cathode for lithium–sulfur batteries, *ACS Nano. Lett.,* **11**, pp. 4288–4294

Karmakar, S., Biswas, S., Kumbhakar, P. and Ganguly, T. (2017). Optical properties of TiO_2@C nanocomposites: Synthesized by green synthesis technique, *Adv. Mater. Lett.,* ***8***, pp. 449–457.

Leont'ev, S., Shamanov, V., kurzanov, A. and Yakovlev, G. (2017). Multiobjective optimization of the lightweight autoclaved aerated Concrete modified with carbon nanotubes dispersions, *Stroitel'nye Materialy,* ***745***, pp. 31–40.

Li, H., Dai, X., Zhao, L., Li, B., Wang, H., Liang, C. and Fan, J. (2019). Microstructure and properties of carbon nanotubes-reinforced magnesium matrix composites fabricated via novel in situ synthesis process, *J. Alloys Compd.,* ***785***, pp. 146–155.

Liu B., Wang M., and Xiao B. (2015). Application of carbon nanotube–ionic liquid–epinephrine composite gel modified electrode as a sensor for glutathione, *J. Electroanal. Chem.,* **757**, pp. 198–202.

Liu, Y., Xie, J., Ong, C. N., Vecitis, C. D. and Zhou, Z. (2015). Electrochemical wastewater treatment with carbon nanotube filters coupled with in situ generated H_2O_2*, Environ. Sci-Wat Res.,* **1**, pp. 769–778.

Lu, J., Ju, J., Bo, X., Wang, H. and Guo, L. (2013). Cobalt(II) Schiff base/large mesoporous carbon composite film modified electrode as electrochemical biosensor for hydrogen peroxide and glucose, *Electroanal.,* **25**, pp. 2531–2538

Luan, H., Zhang, Q., Cheng, G. A. and Huang, H. (2018). As (III) removal from drinking water by carbon nanotube membranes with magnetron–sputtered copper: performance and mechanisms*, ACS Appl. Mater. Interfaces,* **10**, pp. 20467–20477.

Ma, J., Ma, Y. and Yu, F. (2018). A novel one–pot route for Large–scale synthesis of novel magnetic CNTs/Fe@C hybrids and their applications for binary dye removal, *ACS Sustainable Chem. Eng.,* **6**, pp. 8178–8191.

Ma, J., Ma, Y. and Yu, F. (2018). As-prepared carbon nanotubes for water purification: pollutant removal and magnetic separation. *Nanotechnology for Sustainable Water Resources,* pp. 329–370

Ma, Z., Yang, J., Wang, L., Shi, L., Li, P., Chen, G., Miao G. and Mei, C. (2018). Highly-curved carbon nanotubes supported graphene porous layer structure with high gravimetric density as an electrode material for high-performance supercapacitors, *J. Alloys. Compd., **745***, pp. 688–695.

Mahdiani, M., Soofivand, F., Ansari, F. and Salavati-Niasari, M. (2018). Grafting of $CuFe_{12}O_{19}$ nanoparticles on CNT and graphene: Eco-friendly synthesis, characterization and photocatalytic activity, *J. Clean. Prod.*, ***176***, pp. 1185–1197.

Mahmoodi, N. M., Taghizadeh, M. and Taghizadeh, A. (2019). Activated carbon/metal-organic framework composite as a bio-based novel green adsorbent: Preparation and mathematical pollutant removal modelling, *J. Mole. Liq.,* **277,** pp.310–322.

Majumdar, D., Mandal, M. and Bhattacharya, S. K. (2019). V_2O_5 and its Carbon-Based Nanocomposites for Supercapacitor Applications, *ChemElectroChem.*, doi.org/10.1002/celc.201801761.

Mathur, R., Pande, S., Singh, B., and Dhami, T. (2008). Electrical and mechanical properties of multi-walled carbon nanotubes reinforced PMMA and PS composites. *Polymer Composites, **29***, pp. 717–727.

Mehta, A., Mishra, A., Kainth, S. and Basu, S. (2018). Carbon quantum dots/TiO_2 nanocomposite for sensing of toxic metals and photodetoxification of dyes with kill waste by waste concept, *Mater. Design,* **155**, pp. 485–493.

Milanova, V.L., Piskin, V.L., Petrov, T.I., Stankulov, T.E., Denev I.D and Markov I.N. (2015). Ni-Sn alloy carbon-containing nanocomposites as alternative anode materials to the graphite electrodes in Li-ion batteries, *Rev. Adv. Mater. Sci.,* **41,** pp. 52–60.

Moradi, S., Sadrjavadi, K., Farhadian, N., Hosseinzadeh, L. and Shahlaei, M. (2018). Easy synthesis, characterization and cell cytotoxicity of green nano carbon dots using hydrothermal carbonization of Gum Tragacanth and chitosan bio-polymers for bioimaging. *J. Mole. Liquids, **259***, pp. 284–290.

Muthuchamy, N., Atchudan, R., Edison, T. N., Perumal, S. and Lee, Y. R. (2018). High-performance glucose biosensor based on green synthesized zinc oxide nanoparticle embedded nitrogen-doped carbon sheet, *J. Electroanal. Chem.,* ***816***, pp. 195–204.

Muthuchamy, N., Atchudan, R., Edison, T. N., Perumal, S., Vinodh, R., Park, K. H., and Lee, Y. R. (2019). An ultrasensitive photoelectrochemical biosensor for glucose based on bio-derived nitrogen-doped carbon sheets wrapped titanium dioxide nanoparticles. *Biosens. Bioelectron.,* ***126***, pp. 160-169.

Nithya, V. D., and Sabari Arul, N. (2016). Progress and development of Fe_3O_4 electrodes for supercapacitors. **Mater. Chem. A, 4**, pp. 10767–10778.

Ram, R., Khastgir, D. and Rahaman, M. (2018). Physical properties of polyvinylidene fluoride/multi-walled carbon nanotube nanocomposites with special reference to electromagnetic interference shielding effectiveness, *Adv. Polym. Tech., **37,*** pp. 3287–3296. Raja, V., Karthika, A., Lok Kirubahar, S., Suganthi, A., and Rajarajan, M. (2019). Sonochemical synthesis of novel $ZnFe_2O_4/CeO_2$ heterojunction with highly enhanced visible light photocatalytic activity, *Solid State Ionics,* **332,** pp. 55–62.

Ranabhat, K., Pylinina, A. I., Skripkin, K. S., Sofronova, E. A., Revina, A. A., Kasatkin, V. E., Patrikee I. N and Lapshinsky, V. A. (2016). Effect of mono- and bimetallic nanoparticles Fe, Ni, & Fe/Ni based on carbon nanocomposites on electrocatalytic properties of anodes. *IOP Conference Series: Mater. Sci. Eng., **151***, pp. 012–023.

Sahu, U. K., Mahapatra, S. S. and Patel, R. K. (2018). Application of Box–Behnken Design in response surface methodology for adsorptive removal of arsenic from aqueous solution using CeO_2/Fe_2O_3/graphene nanocomposite, *Mater. Chem. Phys.,* **207**, pp. 233–242.

Samuel, M. S., Shah, S. S., Subramaniyan, V., Qureshi, T., Bhattacharya, J. and Singh, N. P. (2018). Preparation of graphene oxide/chitosan/ferrite nanocomposite for Chromium (VI) removal from aqueous solution, *Int. J. Biol. Macromol.,* **119**, pp. 540–547.

Shahrokhian, S. and Saberi, R. (2011). Electrochemical preparation of over-oxidized polypyrrole/multi-walled carbon nanotube composite on glassy carbon electrode

and its application in epinephrine determination, *Electrochimica. Acta.,* **57**, pp. 132–138.

Sharma, M., Ramakrishnan, S., Remanan, S., Madras, G. and Bose, S. (2018). Oxide sheets for efficient nano tin ferrous oxide decorated graphene arsenic (III) removal, *Nano–Structures Nano–Objects,* **13**, pp. 82–92.

Sharma, M., Joshi, M., Nigam, S., Shree, S., Avasthi, D. K., Adelung, R., Srivastava, S. K. and Mishra, Y. K. (2019). ZnO tetrapods and activated carbon-based hybrid composite: Adsorbents for enhanced decontamination of hexavalent chromium from aqueous solution, *Chem. Eng. J,* **358**, pp. 540–551.

Sherlala, A. I. A., Raman, A. A. A. and Bello, M. M. (2018). Synthesis and characterization of magnetic graphene oxide for arsenic removal from aqueous solution, *Environ. Technol.,* https://doi.org/10.1080/09593330.2018.1424259, pp. 1–32.

Shi, Y., Wang, L., Fu, L., Liu, C., Yu, B., Yang, F. and Hu, Y. (2019). Sodium alginate-templated synthesis of g-C3N4/carbon spheres/Cu ternary nanohybrids for fire safety application. *J. Colloid Inter. Sci.,* **539,** pp.1–10.

Sinar, A., NurAzni, M. A., Zainuddin, F., Hazizan, M. A., Siti Shuhadah, M. and Sahrim, H. (2014). Treatment method for dispersion of carbon nanotubes: A Review, *Mater. Sci. Forum, **803**,* pp. 299–304.

Sun, H., Zhang, H., Liu, S., Ning, N., Zhang, L., Tian, M. and Wang, Y. (2018). Interfacial polarization and dielectric properties of aligned carbon nanotubes/polymer composites: The role of molecular polarity, *Compos. Sci. Technol., **154**,* pp. 145–153.

Sun, J., Yang, D., Lowe, S., Zhang, L., Wang, Y., Zhao, S., Liu P., Wang Y., Tang Z., Zaho H. and Yao, X. (2018). Sandwich-like reduced graphene oxide/carbon black/amorphous cobalt borate nanocomposites as bifunctional cathode electrocatalyst in rechargeable zinc-air batteries, *Adv. Energy Mater., **8***, pp. 1–9.

Tan, X. Q., Cheng, X. L., Zhang, L., Wu, B. W., Liu, Q. H., Meng, J., Xu H. Y. and Cao, J M. (2014). Multi-walled carbon nanotubes impair Kv4.2/4.3 channel activities, delay membrane polarization and induce bradyarrhythmias in the rat, *PLoS ONE, **9**,* e101545.

Tang, H. (2018). Electrocatalytic N-Doped Graphitic Nanofiber - Metal/Metal Oxide Nanoparticle Composites, *Small,* **14,** 1703459.

Tang, L., Li, T., Li, C., Ling, L., Zhang, K. and Yao, Y. (2016). Correction: CoPt/CeO_2 catalysts for the growth of narrow diameter semiconducting single-walled carbon nanotubes, *Nanoscale*, ***8***, pp. 5386–5386.

Umeyama, T., Kadota, N., Tezuka, N., Matano, Y. and Imahori, H. (2007). Photoinduced energy transfer in composites of poly[(p-phenylene-1,2-vinylene)-co-(p-phenylene-1,1-vinylidene)] and single-walled carbon nanotubes, *Chem. Phys. Lett.,* ***444***, pp. 263–267.

Wang, L., Hu, D., Kong, X., Liu, J., Li, X., Zhou, K., Zhao, H and Zhou, C. (2018). Anionic polypeptide poly (γ–glutamic acid)–functionalized magnetic Fe_3O_4–GO–(o–MWCNTs) hybrid nanocomposite for high–efficiency removal of Cd(II), Cu(II) and Ni(II) heavy metal ions, *Chem. Eng. J.,* **346,** pp. 38–49.

Wu, Y., Wang, Y., Lin. Z., Wang, Y., Li. Y., Liu, S., Gui, X. and Yang, X. (2019). Three–dimensional α–Fe_2O_3/amino–functionalization carbon nanotube sponge for adsorption and oxidative removal of tetrabromobisphenol A, *Sep. Purification Technol.,* **211**, pp. 359–367.

Xia, Q., Gong, C., Gu, F., Wang, Z., Hu, C., Zhang, L., Qiang L., Ding X., Gao S. and Gao, Y. (2018). Functionalized multi-walled carbon nanotubes for targeting delivery of immunostimulatory CpG oligonucleotides against prostate cancer, J. Biomed. Nanotechnol, 14, pp. 1613–1626.

Xu, S., Wei, Z., Lin, G., Wu, Q., Xu, M., Xuewen, H., Luo J., Zhu Y., and Liu, X. (2019). long conducting and water-compatible polymer/carbon nanotubes nanocomposite with "Beads-on-a-String" structure as a highly effective electrochemical sensing material, ACS Sustainable Chem. Eng., 7, pp. 3556–3566

Yang, C. M., Tsai, M., Huang, C. H., Yen, P., Pan, C. M., Wu, W., Kung-Hwa, Lan-Rong D and Tseng, T. (2017). Carbon nanotube/nitrogen-doped reduced graphene oxide nanocomposites and their application in supercapacitors, *J. Nanosci. Nanotechnol.*, ***17,*** pp. 5366–5373.

Yun Y., Shi Z., Shao J., Qu Q., Gao Y., Chen Z., Chen Y. and Zheng H. (2018). Strongly surface-bonded MoO2@carbon nanocomposites by nitrogen-doping with outstanding capability for fast and stable Li storage, Chem. Nanomat., 4, pp.1248–1253.

Zaho, J., Ali Sayed, J., Wen, X., Lu, H. and Meng, X. (2019). Green synthesis of FeS anchored carbon fibers using eggshell membrane as a bio-template for energy storage application, J. Alloy Compd., 777, pp. 974–981.

Zhang, X., Cui, H., Gui, Y. and Tang, J. (2017). Mechanism and application of carbon nanotube sensors in SF_6 decomposed production detection: A Review, Nanoscale Res. Lett., 12, pp. 1–6.

Zhang, Y., Wang, A. and Zhang, T. (2010). A new 3D mesoporous carbon replicated from commercial silica as a catalyst support for direct conversion of cellulose into ethylene glycol, Chem. Commun., 46, pp. 862–864.

Zhang, Z., Guo, C., Zhang, S., He, L., Wang, M., Peng, D., Tan j. and Fang, S. (2017). Carbon-based nanocomposites with aptamer-templated silver nanoclusters for the highly sensitive and selective detection of platelet-derived growth factor. *Biosens. Bioelectron.*, *89*, pp. 735–742.

Zhu, G., Fiston, M. N., Qian, J. and Kingsford, O. J. (2019). Highly sensitive electrochemical sensing of para-chloronitrobenzene by using carbon nanohorns-nanotubes hybrids modified electrode, *Anal. Methods.*, 11, pp. 1–22.

REMOVAL OF ARSENIC AND CHROMIUM USING FUNCTIONAL GREEN COMPOSITES

Sangeeta Adhikari[1], Sandip Mandal[2], Pu Shengyan[2], Ajay Kumar Mishra[3]

[1]School of Chemical Engineering, Chonnam National University, Gwangju, Republic of Korea.

[2]State Key Laboratory of Geohazard Prevention and Geoenvironment Protection (Chengdu University of Technology), 1#, Dongsanlu, Erxianqiao, Chengdu 610059, Sichuan, PR China

[3]Nanotechnology and Water Sustainability Research Unit, College of Engineering, Science and Technology, University of South Africa, Johannesburg, South Africa.

E.mail: adhikari.sangeeta8@gmail.com

Abstract:

The anthropogenic activities have increased the water related environmental problems creating havoc in both human life and aquatic system. Among the environmental pollutants, heavy metals such as arsenic and chromium are known to have detrimental effect on human health and also is one of the root causes of environmental hazards. A significant development has been made to remediate these heavy metals, but the treatment technology is still in embryonic stage. Most of the treatment technologies uses different classes of materials in combination with remediation methodologies. In concern to the environmental credential and sustainability of the material, functional 'green' composites has emerged as promising materials due to its biodegradable nature. The constituent of these composites are derived from natural occurring resources which makes them fascinating. This chapter will discuss about different classes of green composites that includes, natural fibers as reinforcement, biodegradable polymer as matrix, and functionalization of these derived composites for

effective utilization in removal of arsenic and chromium from aqueous solution. The factors governing the removal efficiency depends on the material attributes such as processing technique and its properties for improving the interfacial characteristics. The challenges and problems concerned towards green composites in the mean to increase the removal efficiency has been addressed in this chapter.

1. Background

Heavy metal pollution has become a matter of global concern due to rapid growth in industrial sectors. The mere presence of the heavy metals in certain forms in both water and surrounding atmosphere is accumulating due to the anthropogenic activities making the human survival in threat [1]. The elements such as arsenic, copper, chromium, lead, mercury, nickel, zinc, and cadmium are considered as potential heavy metals. The specific characteristic of these heavy metals are their density being greater than 5 g/cm^3. Based on the geological factors, these change their chemical compositions which are vital along with their mobility to travel large distances, if present in surface waters and soil [2]. The major sources of these heavy metals include mining, metal-based industries, foundries, metal refineries, coal and petroleum power plants, and nuclear power plants as well, whereas other sources like paper processing plants, textiles, and microelectronics, which also contribute in their exposure and corresponding contamination [3]. The poisoning of heavy metals in humans and other anthropogens could be partially through the food chain process due to metal corrosion, soil erosion or leaching of metal ions in soil and atmospheric deposition [4]. Among all the heavy metals, arsenic and chromium hold potential and serious environmental risks. However, WHO (World Health Organization), US-EPA (United states Environmental Protection Agency) and other national environmental agency of different developing countries constantly monitors the limits of these heavy metals

in different waterbodies with simultaneous understanding of their effects on human health [5, 6]. Today, the technological advancement has made possible remediation of such potential contaminants in the anthroposphere.

2. Hazards of Arsenic

Arsenic, the 53rd abundant element on earth with a density of 5.72 g cm^{-3} is known to be a human carcinogen. Arsenic is considered as a weak acid oxyanion forming complexes for easy removal with hydroxides of metal. It can be found in both organic and inorganic forms in air and water. Although, arsenic is found in four oxidation states namely arsenide (-3), arsenite (+3), arsenate (+5); and metal arsenic (0), but the most predominant species is in the form of pentavalent arsenate (AsO_4^{3-}), existing as arsenic acid or dihydrogen arsenate in strong and weak acidic conditions. Another species commonly found is trivalent arsenite (AsO_3^{3-}) [7, 8]. The mentioned species can be frequently found in water sources as well as in sediments, where As(III) exhibits anaerobic stability and As(V) shows aerobic stability thermodynamically. The toxicity of arsenite is sixty times more than the arsenate because of its high mobility and its prevalence in reducing atmosphere [8]. However, high amount of arsenic in groundwater is not related to the high content present in source rocks, but environmental factors such as closed basins, dry climate and reducing aquifers originating from alluvial and regions certain geothermal influence affects the presence of arsenic in the ground water [9]. The choice of method to remove arsenic depends on several factors such as the species of arsenic, the influence of other chemical species present in the environment, hardness, capacity and complexity level with the technique and finally the cost effectiveness. The safe limit in drinking water as recommended by World Health Organization (WHO) is 10 μg/L [10]. In accordance with the U.S. Environmental Protection Agency (US-EPA), the methodologies that are well recognized for removal of arsenic from water are membrane

filtration, ion-exchange, precipitation/co-precipitation and also permeable reactive barriers (PRBs) [11]. The efficiency of such treatment techniques is via development and use of active materials that are cheap, exhibits high removal efficiency, easy recovery, low cost of operation and less requirement of energy.

3. Hazards of Chromium

Chromium (Cr), a geochemical element is both mutagenic and carcinogenic to human beings and every living organism. In the recent years, the level of chromium has increased significantly affecting the aquatic and ecosystem [12]. The most stable oxidation states of Cr are trivalent Cr(III) and hexavalent Cr(VI) which are mostly released from industries such as metallurgy, textile, tanneries, pigments, electroplating and other anthropogenic sources [13]. Among both the prevalent chromium, Cr(VI) is quite toxic and harmful causing teratogenic effects due to intermediate transition formed by Cr(V/IV) intracellular reduction. However, Cr(III) is helpful in carbohydrate metabolism [14]. According to USEPA, the chromium discharge to surface water has a permissible limit to 0.05 mg/L, whereas WHO allows a limit of about 50 µg/L in drinking water and from 5- 500 µg/L in the waste water systems [15]. The presence of Cr(VI) in the drinking water is from the percolation of waste water to soil which reaches the ground water and finally consumed for drinking purpose exhibiting serious health effects. The nanoparticles of chromium if inhaled can cause serious respiratory problems such as asthma, bronchitis, pulmonary fibrosis larynx inflammation, pneumonia, trachea and lung cancer as well [16]. Cr(VI) is known for less interaction with inorganic materials advocating the high stability of this species, whereas any type of Cr(III) species is removable under alkaline and neutral pH through adsorption. Industrial wastewater contains oxyanions of Cr(VI) such as CrO_4^{2-}, $Cr_2O_7^{2-}$, and $HCrO_4^-$ depending on the parameters of the pre-

processing in industries [17]. Technologies such as reverse osmosis, electro dialysis, ultrafiltration, adsorption and ion-exchange are quite famous in this perspective for chromium removal [18]. In the perspective of available technologies, the waste formation after the treatment process is huge and disposed to the very environment and which has led to development of green nanocomposites which are biodegradable, sustainable and environment friendly.

4. Green Composites

Lately, there have been interest in the functional green composites in the mean to develop sustainable materials that are commonly biodegradable and cost effective [19]. Complimentary reports on green composites have been well documented by Dicker et al. [20] and Shekar et al. [21]. Green composites are composed of natural fibers and biopolymers, where the natural fibers are from vegetable, animal and plant, however, biopolymers are artificial fibers mainly thermosetting or thermoplastic polymers which contain the composition of natural fibers derived chemically [22]. These polymers include cellulose and alginate mimicking the animal fiber; poly(lactic acid), and polysaccharides impersonating the plant fibers. In comparison to the man-made biopolymers, the structure of natural fibers are quite complex [23]. The advantages of green composites are that they exhibit high mechanical properties, and variation in the properties is observed due to difference in the fiber nature, they are renewable, biodegradable, cost effective, and they also exhibit high hydrophilicity which enhances the water absorption. These materials are also non-toxic, biocompatible and bioactive having lower impact on the sustainability of the environment [20]. Despite these advantages, the green composites suffer from non-stability at elevated temperatures ranging between 170^{o}C - 200^{o}C liming its versatility [20, 21].

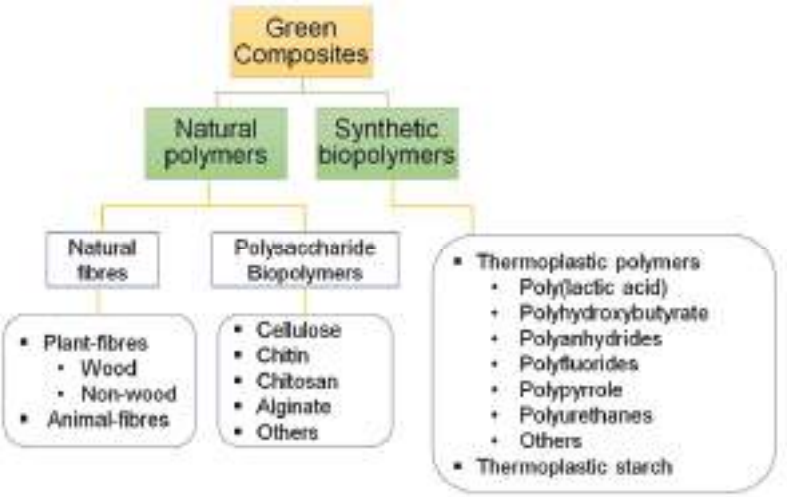

Figure 1. Flowchart classifying the types of green composites and sub-composites.

The durability of the green composites are quite low and is rapidly affected by the presence of moisture with time forming fungus and bacteria degrading the material [22]. In this perspective, the green composites are functionally modified with incorporation of different materials that could enhance the durability of the materials on the basis of practical applicability. Looking through the active applications of the green composites includes tissue engineering and scaffold development in biomedical applications [24], equipment development for sports such as bicycle frames, and snowboards which are non-biodegradable and also they have been applicable in many electronics companies [25-27]. They are also actively applied for automotive applications [28]. Recently, environmental remediation via green composites has become hot topic due to concern over good sustainability after the processing. Apart from the mechanical and characteristic development of the composite, another important criterion is to minimize the environmental hazard through the advantageous compatibility of green composites with the environment. In this perspective, a detail study of the removal of heavy metals specifically,

arsenic and chromium using the green composites via different processing has been presented in the later sections. A flowchart classifying of different green composites is shown in **Figure 1**.

5. Functional green composites for arsenic and chromium removal

5.1. Natural/Reinforced Bio-fibers

5.1.1. Rice Husk

Reinforced bio-fibers are naturally derived from plants, such as bagasse, rice husk, sawdust and others. High cellulose containing rice husk is an active material which can be effectively used for removal of arsenic and chromium from aqueous solutions after chemical modifications. Acid and alkali treatment of rice husk can reduce the content of hemicellulose, lignin, and also increases the porosity of rice husk by decreasing the cellulose crystallinity [29]. A study by Pehlivan et al. [30], presented the modification of rice husk by extracting the lignocellulosic material which was further surface modified by coating iron using the process of hydrolization using ferric nitrate. The modified material was effectively used for removal of arsenic. The positive charge developed due to surface RH-FeOOH group and formation of chelated complexes with rice husk due to presence of carbonyl and carbonyl functional groups were responsible for the 94% adsorption of arsenate species via Coulombic interactions at an optimum pH 4.0. In another study, rice husk has been transformed to biochars and similar biochars were formed from sewage sludge, municipal solid waste and also sandy loam soil for aqueous removal of As(V), Cr(III) and Cr(VI). Although soil is an effective material for removing As(V) but the transformed anions are not stable in them in comparison to the biochars. The biochar from sewage sludge was effective in removal of Cr(VI) due to more Fe_2O_3 content [31].

5.1.2. Sugarcane bagasse/fly ash

Sugarcane bagasse is another plant fiber and a prominent solid waste from sugar industries. This component is rich in cellulose, polyols and lignin making it a composition having high hydroxyl and phenolic groups [32]. The bagasse fly ash has been proved as efficient adsorbent for uptake of chromium and lead by Gupta and Ali et al. [33]. The obtained bagasse fly ash were chemically treated with hydrogen peroxide to get rid of any organic matter adhered and then dried at 100 ^{o}C flowed by grinding and sieving for further use. The mechanism behind the uptake of chromium and lead was particle diffusion and the nature of adsorption reported to be exothermic in nature. The flow column operated at the flow rate of 0.5 ml/min was able to remove about 95% of both the metal ions. The study also indicated high adsorption capacity for chromium than lead, where reasons were not discussed. In another study, bagasse fly ash (BFA) was obtained from a bio fuel producer and sponge iron char (SIC, industrial waste) was obtained from a sponge iron industry. There was no iron detected in the BFA after acidification, thus it was soaked in 2M $FeCl_3$ solution followed by drying at 105^{o}C to be used as final adsorbent (BFA-IC). SIC was granuled by ball milling and sieved to obtain a size of 110 microns. Both the modified materials BFA-IC and SIC measured the respective surface areas to be 168 and 78.63 m^2/g, which were used to test the adsorption capacity of the arsenic in aqueous solution. The Langmuir isotherm determined the monolayer adsorption capacity of As(V) and As(III) to be 25.82 mg/g and 39.53 mg/g; and 28.58 mg/g and 27.85 mg/g for BFA-IC and SIC, respectively [34]. This study proves that some heavy industrial waste such as sponge iron could be a potential material for removal of hazardous environmental heavy metals.

5.1.3. Bamboo fiber

In a mean to develop low cost adsorbents, bamboo-based materials are also studied for heavy metal remediation. Iron-modified bamboo biochar (BC-Fe) was developed by alkali treatment of bamboo charcoal followed by treatment with $FeCl_3$ solution with pH adjusted to 2.5. The SEM micrograph of raw and iron modified bamboo charcoal has been presented in **Figure 2a and 2b,** respectively. The micrographs well shows that the porosity in BC-Fe with surface area of 277.89 m^2/g, which is 4% less due to iron impregnation in comparison to the pristine bamboo charcoal. The maximum arsenic adsorption capacity of BC-Fe were 7.23 and 19.77 mg/g for As(III) and As(V), respectively. There was significant influence of pH on adsorption of both the species of arsenic, where As(V) exhibited decrease in removal upon increase in pH, however, wide pH range from 2-9 exhibited fairly good removal efficiency. The rate of adsorption was controlled by both intra-particle and film diffusion mechanism [35]. Wang et al. [36] chemically modified the bamboo charcoal by iron and cobalt forming binary oxide loaded adsorbent with microwave heating technique for effective removal of Cr(VI) from aqueous solution. The formation of bamboo biochar was via carbonization of four-year old Makino bamboo at 500^{o}C under nitrogen atmosphere at flow rate 500 ml/min with heating rate 10^{o}C/min. Prior to use, biochar was washed by soaking in boiling water to get rid of impurities, if any followed by desiccation. Cr(VI) adsorption over the designed adsorbent decreased with increasing alkalinity and temperature suggesting the reaction dominant by the spontaneous ion-exchange process, which is exothermic and the maximum chromium adsorption capacity derived from Langmuir model is 51.7 mg/. Among the efficient sorption materials, activated carbon has been the most applicable material for adsorption of heavy metals due to the high surface area. Researchers have been trying to find a mean to develop low cost activated

carbon using the plant waste. Activated carbon derived from cheap plant waste like bamboo, date pits, jute fiber, rice husk and palm-shell waste are used as cheap starting materials. Jais et al. [37] used the palm-shell waste to produce activated carbon (PSAC), which was magnetized by hydrothermal wet impregnation (MPSAC) and further lanthanum was wet-impregnated followed by calcination at 500 ^{o}C (MPSAC-La). The preparation methodology has been shown in **Figure 2c** with the mechanism for arsenic removal and its magnetic separation has been presented as well. The La to Fe weight ratio of 0.36 in MPSAC-La showed the highest arsenic removal efficiency in aqueous solution with maximum adsorption capacity of 227.6 mg/g in comparison to other adsorbents. The removal of arsenate is via precipitation at pH lower than 8, whereas at higher pH arsenate complexes with the $La(OH)_3$ on its surface. However, it is worth mentioning that the Nano magnetite stabilizes the lanthanum due to strong bonding and also does not allow dissolution of lanthanum in aqueous medium.

Figure 2. SEM micrographs of (a) raw bamboo charcoal; (b) iron modified bamboo charcoal; and (c) Schematic of preparation of MPSAC-La (La to Fe ratio 0.36) and arsenate removal mechanism with images of magnetic separation.

5.1.4. Coconut coir/husk

Coconut waste has also been explored for treatment of heavy metals. The presence of functional groups such as hydroxyl and carboxyl are beneficial for sorption. Both coconut shell and coir pith are useful in the perspective to be used for heavy metal remediation. The raw coconut coir has been effectively used for the treatment of sulphochromic waste as an active bio-adsorbent. The hexavalent chromium sorption was via oxidation of organic matter and the uptake of chromium as confirmed from the Fourier transform infrared spectra (FTIR). It was also confirmed that more than 73% of the active adsorption sites were phenolic compounds from lignin in the bio-sorbent, determined from the potentiometric titration. The adsorption capacity of the coconut coir was improved by grinding the coir to increase the overall surface area of the material. The chromium sorption capacity was estimated to be 26.8 mg/g which was observed to be better than the other reported values. Consequently, the results indicated that coconut coir are effective in sulphochromic waste water treatment and greater than 60% of chromium in original mass can be reduced to Cr_2O_3 by calcination [38]. Activated carbon derived from coconut husk was impregnated with copper to use as sorbent for arsenite adsorption where the sorbent can be easily regenerated with the 30% hydrogen peroxide solution in 0.5M nitric acid solution [39].

5.1.5. Sawdust

Sawdust from different plants is highly fibrous containing all the three important compounds namely hemicellulose, cellulose and lignin with some polyphenolic groups which is beneficial for binding the toxic metal ions via different mechanism [40]. There are two different types of sawdust such as hardwood and softwood [41]. The pristine sawdust can remove the arsenic species but for anion extraction, the sawdust surface should be

chemically modified with functional groups which are electron deficient. Taking this into account, sawdust was modified with incorporation of lanthanum and zirconium oxide for easy adsorption and extraction of arsenic anions. Prior to the oxide incorporation, the sawdust surface was modified with glutamic acid after lignin removal with alkali treatment. Surface immobilization of ZrO_2 and La_2O_3 were prepared by mixing salts of Zr and La followed by keeping in the ammonia chamber to form respective oxides on the surface of sawdust. The experimental observation revealed that ZrO_2-sawdust had enhanced extraction capacities of arsenite and arsenate as 29 and 12 mg/g, whereas with La_2O_3-modified sawdust showed 22 and 28 mg/g of extraction of anions. They also reported on complete regeneration of La_2O_3-sawdust, whereas, ZrO_2-based exhibited half the adsorption efficiency. The adsorption of arsenic was via electrostatic interaction in La_2O_3-sawdust by surface hydroxyl groups and from ligand exchange, which was the main reason for arsenic binding in ZrO_2 sawdust with enhanced selectivity [42]. Diethylenediamine crosslinked with pine sawdust has also been explored for active aqueous removal of both chromium and arsenic [43]. The mechanistic probability for removal was electrostatic interaction at acidic pH as presented in equations below (Eq. 1 and Eq.2), where the amine groups provided the protonation effect. The presence of co-existing anions was sequentially selective as dichromate>bicarbonate>sulfate>nitrate>chloride>dihydrogen arsenate.

$$-NH_3^+ \cdots R^- + HCrO_4^- \leftrightarrow -NH_3^+ \cdots HCrO_4^- + R^- \quad (1)$$

$$-NH_3^+ \cdots R^- + H_2AsO_4^- \leftrightarrow -NH_3^+ \cdots H_2AsO_4^- + R^- \quad (2)$$

The sorption capacity of the modified sawdust was observed to be 238.6 mg/g and 71.23 mg/g for chromium and arsenic at pH-6 having adsorbent dose of 0.5g at controlled temperature of 50ºC. The pH variation revealed maximum adsorption capacity of Cr(VI) between the values 2-6 and for As(V), pH 5-6 was found to be favorable.

5.1.6. Wheat

Agricultural bio wastes from wheat such as wheat bran and straw from wheat milling industries has been explored widely for the effective usage in treatment of heavy metals [44, 45]. The initial acid treatment of any natural waste helps in increasing the affinity towards further functionalization or adsorption process. Sulfuric acid treatment of wheat bran is helpful in increasing the surface area of the bran by converting macrospores to micro pores for adsorption of heavy metals [46]. The magnetic Fe_3O_4 nanoparticles were embedded into wheat straw using in-situ co-precipitation method for enhanced adsorption of arsenic. Wheat straw has been used as template for embedding the magnetic nanoparticles and also as matrix so that feasible separation of the composite becomes easy by using the magnetic field. High magnetic nanoparticles in the template led to enhanced adsorption capacity by well-fitting the Langmuir model. Arsenate adsorption was depleted with increasing pH, whereas arsenite had the highest adsorption capacity between pH 7-9. The developed adsorbent was easily regenerated using 0.1 mol/L NaOH solution [47]. The well exploitation of wheat bran has been carried out for environmentally hazardous heavy metals. In another study, wheat straw was amine treated to be used as adsorbent for chromium ions. Initially, wheat straw was oxidized using nitric acid for availability of more carboxyl and hydroxyl groups for grafting of tetraethylenepentamine on the surface of wheat straw. The enhancement in the amine groups on the wheat straw surface

showed positive zeta potential below pH 9.8. According to Langmuir fitting, at pH 2.2, the maximum sorption capacity was 454 mg/g. The amino functionalized adsorbent showed enhanced hexavalent chromium selectivity and high adsorption capacity in the presence of co-existing anions. The electrostatic attraction was the main reason for chromium adsorption on the amino functionalized wheat straw, where Cr(VI) adsorbed on the surface was reduced to Cr(III) followed by chelation of the formed Cr(III) cations on the surface again after getting released in the solution [48].

5.1.7. Others

There are few other natural fibers such as maize corncobs, cotton, and spent grain that has been used with potential surface modifications or functionalization to be used as adsorbent. The acid and amine based modifying agents such as phosphoric acid, triethanolamine, diethyelenetriamine and 1, 4-diaminobutane were used for estimated removal of methyl orange and arsenic species. The study plays with the natural surface chemistry of the maize as natural sorbent. Phosphorylation of maize corncobs in the presence of ammonia shows arsenite adsorption capacity of 11 mg/g (total concentration - 550 g As), corresponding to 98% removal efficiency with adsorbent dose of about 50 mg/ml. The maize corncobs modified with phosphoric acid and urea removed about 11 mg/g arsenate from the total concentration of 300 mg/g of As solution [49].

Hexavalent chromium has been treated with chitosan coated cotton fibers, where the role of ester bonds was crucial for the adsorption process. Alkali treated cotton fibers exhibited five times greater reactivity with further modification using citric acid and chitosan solution. NaOH treatment of cotton fiber favors the formation of ester bonds than the amide bonds on the cotton fiber surface. The formed ester bonds increase the

surface exposure of amino groups from chitosan which increases the adsorption capacity of the modified cotton fibers and hence removal is significantly higher. The mechanism behind the efficient removal was electrostatic attraction observed due to negative charge chromium ions in aqueous solution and the surface of the adsorbent containing protonated amino groups [50]. The results have opened ventures of functionalized cotton fiber for heavy metal remediation.

Most of the breweries disposes spent grain (SG, a solid waste) having lignin and cellulose as basic composition. From the past studies, it is quite well understood that adsorbent surface functionalized with carboxyl, hydroxyl, amino, amide and others have led to high removal efficiency and selectivity in the presence of co-existing anions. Some studies have revealed a pre-oxidation step to convert As(III) to As(V) for enhancing the removal efficiency of As(III) [51]. This step may cause generation of unwanted contaminants which could be fatal. A study uses anionic, cationic, and nonionic polyacrylamide polymers (PAM) have been used to functionalize the spent grain for direct removal of arsenite from aqueous solutions. The experimental study revealed a trend of arsenite adsorption on the modified sorbent as anionic PAM-SG> cationic PAM-SG> nonionic PAM-SG. The functional group contributing for the arsenite adsorption were amino group ($-NH_2$), carbonyl group (C=O), C-N bond from amide group ($CONH_2$) and also surface hydroxyl groups (O-H). The tubular structure developed on the surface of anionic PAM modified spent grain increased the surface area favoring the arsenite adsorption [52].

5.2. Biopolymer composites

In general, the polymeric materials derived from biological resources are termed biopolymers. Biopolymers are emerging materials that can be effectively used for treatment of heavy metals [53]. They are extensively

used due to their non-toxicity, eco-friendliness and biodegradable nature. Some of the renowned biopolymers that has been used for treatment and removal of heavy metals are cellulose, chitin, chitosan, and alginate [54-56]. The characteristic of these biopolymers, and their functional modifications has been discussed with their application towards removal of chromium and arsenic.

5.2.1. Cellulose

Cellulose is basically derived from natural wood and cotton. It is a polysaccharide which consist of linear polymer chains having numerous hydroxyl groups. The adsorption of heavy metals via cellulose is possible by chemical modification of the polysaccharide surface starting with carbon 6 due to availability of primary hydroxyl groups with probability of modification in secondary hydroxyl groups at carbon 2 and 3 [54, 57]. Functionalization of cellulose takes place through processes such as oxidation, esterification and halogenation.

Biopolymer cellulose-montmorillonite was designed for chromium detoxification and prior to the polymerization, surfactant as cetyltrimethylammoniumbromide (CTABr) was used to modify sodium montmorillonite (Na-MMT) clay to make it more organophilic and to enhance the molecular interaction between Na-MMT and cellulose. The maximum adsorption capacity with the designed biopolymer composite was estimated to be 22.2 mg/g with a good Langmuir model fit. Chromium uptake in the biopolymer-clay composite is via hydrogen bonding between oxygen atoms in dichromate anion and hydroxyl protons in cellulose [58]. Hybrid magnetic bio-composites were developed using cellulose (Cel), hydrotalcite (CelHT) and hydroxyapatite (CelHAp), which were coated with iron oxide nanoparticles for remediating the hexavalent chromium. Three possible mechanism were put forward for chromium removal, which

is electrostatic interaction, ion exchange mechanism and reduction of Cr(VI). The positive metal ions in the bio-composite electrostatically attracts the $HCrO4^-$ anion. The CO_3^{2-}, in interlayer of Fe_3O_4@CelHT gets exchanged with the $HCrO_4^-$ ions, whereas OH^- ions gets exchanged in Fe_3O_4@CelHAp bio-composite. Also, the matrix of cellulose contains reducing aldehyde groups that can possibly reduce Cr(VI) to Cr(III). The mechanism of the preparation of bio-composite and chromium uptake has been shown in **Figure 3** [59]. Medical cotton has been used as cellulose source to prepare cellulose@iron oxide magnetic nanoparticles via one-step co-precipitation and using an aqueous solution containing NaOH-thiourea-urea, where alkali was used to precipitate the iron oxide nanoparticles. The green pathway synthesized cellulose@ironoxide nanoparticles showed enhanced magnetically induced sensitivity towards external magnetic field. The maximum adsorption capacity of the arsenite and arsenate was estimated to 23.16 and 32.11 mg/g using Langmuir isotherm model [60].

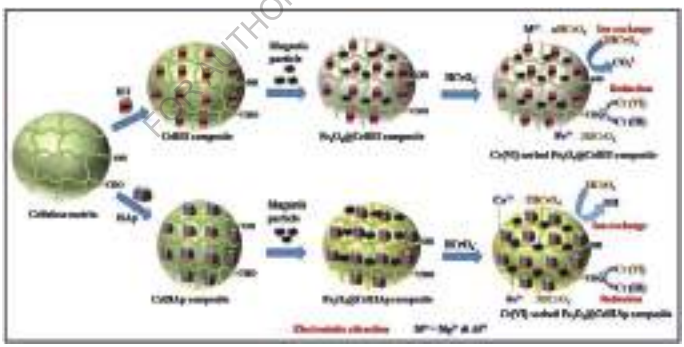

Figure 3. Possible Cr(VI) sorption mechanism pathway onto Fe_3O_4@CelHT and Fe_3O_4@CelHAp bio-composite.

5.2.2. Chitin

Chitin is also a polysaccharide, known for its reinforcement and strength and mostly found in the anthropods. It is the second most abundant

biopolymer. Apart from the monomer units of glucose, it has amine and acetamide functional groups at carbon 2 position, which makes it different from cellulose. It is hydrophobic in nature and shows insolubility in water and common organic solvents [55]. The poor solubility of chitin has led to surface modification using different functional groups to be used as active material. Functionalization of chitin with polypyrrole was carried out via in-situ polymerization method for adsorption of chromate anions. The percentage removal of hexavalent chromium was quite low at alkaline conditions in comparison to acidic pH explaining the sorption mechanism through electrostatic interaction between the protonated -NH groups with the $HCrO_4^-$ or $Cr_2O_7^{2-}$ ions under acidic conditions. In alkaline conditions, competition to occupy the sorption sites among OH^- and Cr(VI) ions increases and also the electrostatic repulsion increases due to negative surface charge of the adsorbent. Langmuir model fitting determines the maximum adsorption capacity to be 35.22 mg/g [61]. Chemical and mechanical treatment of chitin nanofiber was performed after extraction from shrimp shells and cysteine was grafted by mixing cysteine, N-hydroxysuccinimide and 1-ethyl-3-[3-dimethylaminopropyl] carbodiimidehydrochloride. Thiol-modified chitin nanofibers with cysteine availed a greater number of active sites for arsenic sorption, which was quantified for Thiol groups with Ellman's reagent. Arsenic ions exhibited strong affinity towards the functionalized thiol groups at pH-7 for enhanced adsorption showing maximum adsorption capacity of 149 mg/g [62]. A study reported onto production of micron-sized chitin loaded with magnetic nanoparticles for adsorption of hexavalent chromium. The ephippial eggs of Daphnia longispina which is a crustacean was used for extraction of chitin micro cages which was further deproteinized and acid treated for depigmentation from ephippia. For magnetic particle loading, it was mixed with salts of

iron to produce magnetite particles. Chemical ion-exchange led to removal of chromium ions as estimated from the sorption study with higher removal of 1.29 mmol/g in comparison to pristine chitin microcages which exhibited 0.77 mmol/g of capacity. Surface negativity after magnetic particles loading eliminated the chance of adsorption by electrostatic process [63]. The functionalization based on the surface groups in biopolymers are beneficial to targeted sorption of heavy metals.

5.2.3. Chitosan

Chitosan is a linear co-polymer which is derived from chitin. It is polyaminosaccharide derived from alkaline n-deacetylation of chitin which involves deprotonation and deacetylation [64]. Chitosan is a very useful biopolymer for heavy metal removal due to the presence of amino group (-NH_2) and hydroxyl group (-OH) as its backbone [65]. Chitosan is known for its sensitivity towards pH of the solution. Chitosan upon cross-linking with other functional reagents is beneficial for metal binding [66]. Chitosan has been modified using polyhexamethylene biguanide (Ch-PHMB) and simultaneously magnetic chitosan (M-Ch) was also prepared to have a comparative study for removal of hexavalent chromium. Response surface methodology was implemented to understand the behavior of both the adsorbents. Above neutral pH efficient removal of chromium ions was observed where higher removal efficiency found with Ch-PHMB of about 70% in comparison of M-Ch, but the former was more toxic than the later as evaluated from toxicity tests [67]. Nanofiber of chitosan was fabricated by electrospinning process and doped with iron for trace evaluation of arsenate in water. Exceptional adsorption was observed with the designed adsorbent with more than 90% removal under neutral pH conditions with maximum adsorption capacity to be 11.2 mg/g. The adsorbent was easily regenerated, and the removal rate was about 98% after ten consecutive

cycles of adsorption-desorption. As(V) adsorption over adsorbent was via chemisorption which indicates significant interaction between the surface functional group and arsenic ions. Weber and Morris model put forward three possible steps for adsorption which includes controlled pore diffusion, controlled intra-particle pore diffusion in the pore and stereo-hindrance from adsorbed species leading to slow sorption. The dominant contribution towards arsenic adsorption was from -NH, -OH and -CO group in the adsorbent [68].

Chitosan is also used as a stabilizing agent in some studies. Chitosan stabilized bimetallic Fe/Cu (Ch-Fe-Cu) nanoparticles were synthesized to be used for hexavalent chromium removal. Higher removal efficiency was achieved with Ch-Fe/Cu in comparison with the bare nZVI and bimetallic Fe/Cu nanoparticles. The reactivity and stabilization of zerovalent iron was compromised due to surface coated with chitosan and Cu. Higher efficiency was explained with the increased surface area and the galvanic cell. The zerovalent iron has some oxidized iron as well, thus, after reaction, the complete oxidation of trivalent iron takes place due to electron contribution. On the other hand, Cu exists as metal Cu and Cu_2O converting to CuO after the reaction. This process is governed by precipitation and co-precipitation phenomena, where the initiation take place from Cu^{2+} accepting electrons from zerovalent iron forming Fe^{2+} and hydroxides of iron (Fe_xO_y) proceeding to cover all metallic Cu nanoparticles. Fe_xO_y precipitates Cr(VI) during the process and adsorption of chitosan increases the precipitation and co-precipitation of metallic copper which is responsible for effective removal of chromium. Conclusively, the designed Ch-Fe/Cu exhibited dual functionalization from copper being galvanic and chitosan adsorption to enhance the removal of hexavalent chromium with high concentration in aqueous under wide pH

range 3-9 [69]. The schematic of the possible synthesis and mechanism of chromium removal is shown in **Figure 4a**.

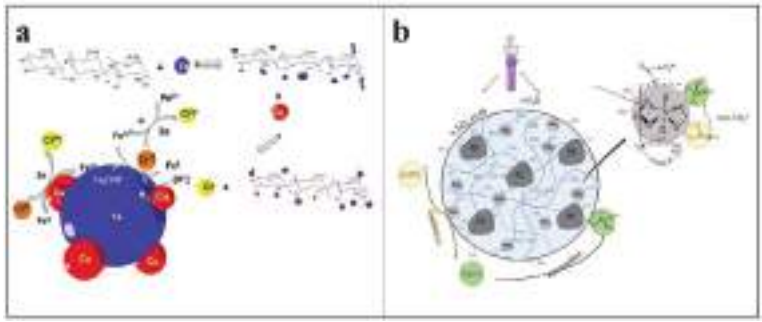

Figure 4. (a) Hypothesizing the possible synthesis process of chitosan-stabilized Fe/Cu and removal mechanism of Cr(VI). (b) Schematic diagram of mechanisms involved in the adsorptive-photoactive removal of As by n.TiO_2.FS.CS.

An eco-friendly bio-photocatalytic composite with nano-TiO_2/feldspar embedded with chitosan developed for abatement of the arsenic in aqueous solution. The chitosan matrix was immobilized with nano-TiO_2 and fine particles of feldspar (**Figure 4b**). Removal of arsenate using the bio-photocatalyst was over a wide pH range with a negligible drop in the removal upon increasing the pH. However, there was no significant influence of pH over arsenite removal using the biocatalyst. Arsenate removal as quite selective in the presence of foreign ions which includes fluoride and sulfate with little competition from phosphate ions at higher concentrations was observed. Linear and non-linear Langmuir modeling estimated the maximum adsorption capacities to be 2000 and 2025 mg/g in respective. High removal efficiency was achieved for both the species of arsenic under UV light irradiation varying from 33% to 73% for arsenate and 23% to 84% for arsenite, respectively. The reaction was experimentally proved to be thermodynamically favorable and spontaneous. The

adsorptive-photoactive sites was provided by -NH_2 and -OH group in chitosan and also metal oxide [70].

5.2.4. Alginate

Alginate, a natural polysaccharide (having sequences of uronic units: 1–4 linked α-l-guluronic and β-d-mannuronic acids) is known for its non-toxicity, renewable, biodegradable and biocompatible nature [71]. It is extracted naturally from brown seaweeds. These biopolymers can be altered to tailor the materials pristine form for excellent sorption properties [72]. Upon cross-linking alginate with divalent and trivalent cations, gel phased adsorbents are prepared which makes the handling much easier than the powder counterparts. Such gel-based formulations occur due to the presence of carboxylic acids in the gel phase that helps in the formation of complexes in aqueous solutions with metal ions [73]. Pentavalent arsenic ions were removed in a fixed bed column using the Fe(III) crosslinked alginate nanoparticles. The removal of arsenic in bed column was dependent of factors like bed depth, concentration of arsenic as influent and also the flow rate of influent played major role. Lowest flow rate exhibited better removal performance and the increase in bed height increases the column bed capacity and the time of exhaustion. The adsorption bed capacity decreases significantly from 0.066 to 0.022 mg/g upon varying the initial arsenic concentration from 0.5 mg/L to 1.5 mg/L. The experimental data were also further fitted with Bed Depth Service Time model which was in agreement with the breakthrough curves [74]. The removal of hexavalent chromium was carried out with nanocomposite of alginate and chitosan cross linked using glutaraldehyde. Prior to nanocomposite formation, ionic gelation method was followed to form alginate nanoparticles using Rajaonarivony's method. Gelification with sodium alginate and calcium chloride was carried out followed by suspension

stabilization through aging and finally centrifuged and free dried to obtain the alginate nanoparticles. The higher adsorption of chromium onto nanocomposite was via multilayer adsorption as confirmed from the well-fitted experimental data to Freundlich isotherm. The developed nanocomposite proved to be a potential bio-sorbent for chromium removal from wastewater [75]. The separation of the sorbent using magnetic nanoparticles is not only fascinating but also the presence of magnetic nanoparticles contributes in the heavy metals remediation processes. However, the instability of magnetic particles limits its application in treatment process. In this perspective, magnetite graphene oxide has been encapsulated inside alginate for high and efficient uptake of Cr(VI) and As(V) from waste water. Alginate helps in stabilization of the magnetite graphene oxide and also hinders the aggregation of the powdered magnetite graphene oxide enhancing the performance towards extraction of heavy metals. The present study was also compared with carbon nanotube and activated carbon and superior adsorption efficiency were observed with the developed magnetic graphene oxide alginate bead upon comparison. There was no leaching observed for the developed magnetic graphene oxide embedded into alginate beads. Fe^{3+}-crosslinked with magnetic graphene oxide on alginate beads aided the release of Fe^{3+} ions favoring the chromium removal. The uptake of Cr(VI) was controlled by the pH changes in the solution. On the contrary, there was no alteration observed in As(V) uptake over a wide range of pH. The release of Fe^{3+} forms hydronium ions in the solution which decreases the pH of the solution favoring chromium adsorption with selectivity. However, Ca^{2+} crosslinked with magnetic graphene oxide on alginate beads reduces the pH below 3 favoring chromate species adsorption under acidic condition. The results suggested that Fe^{3+} binds strongly with the available functional groups of alginate [76]. Detailed mechanism in schematic has been displayed in

Figure 5 . Crosslinking of polyvinyl alcohol (PVA), with sodium alginate has been carried out using boric acid and calcium chloride for formation of alginate beads to be effectively used as adsorbent for removal of hexavalent chromium. The main functionalization of PVA is to provide mechanical strength, biodegradability and high solubility for crosslinking. It was justified that UV light illumination to PVA-alginate beads enhanced the adsorption rates tremendously due to increased surface sites and is affected by the initial dose of PVA and sodium alginate. Superior adsorption activity was observed with optimum 12 g PVA and 2.5 g sodium alginate forming beads with complete removal within 1.5 hours [77]. The study also put forward another strategy of alginate functionalization for enhancing the surface-active sites and can be a very potential candidate for removal of heavy metals from the industrial waste water systems.

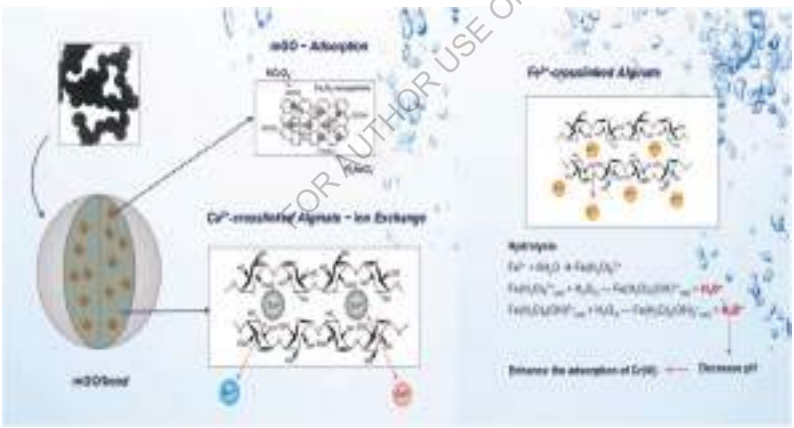

Figure 5. Fabrication and mechanism of Cr sorption with alginate-derived beads and others.

5.3. Synthetic polymer composites

5.3.1. Bio-thermoplastic polymers

Bio-thermoplastic polymers are another group of green composites which includes compounds like poly lactic acid (PLA), polyvinyl alcohol, polyhydroxylbutyrate, polyanhydrides and others [20, 78]. There are two categories of polylactic acid available namely poly(l-lactide) (PLLA) and poly(DL-lactide)(PDLLA) with major difference between them being chiral polyester with semi crystallinity and amorphous, respectively [79]. Electro spun PLLA fibers have been synthesized and architecture of ZnO nanorod arrays has been grown on PLLA as functional materials for adsorption of Cr(VI). The SEM image of electrospun PLLA nanofibers and grown ZnO on PLLA has been presented in **Figure 6a and 6b**, respectively. Both electrostatic and surface interactions were responsible for the adsorption of chromium onto ZnO-PLLA composite with maximum efficiency achieved at pH< 3.5 with desorption efficiency of about 60% [80]. Another study develops a composite of chitosan/PVA/zeolite for removal of chromium, methyl orange and Congo red dye from aqueous solutions. The composite was observed to be stable in both acidic and basic pH conditions, where Congo red adsorption followed flocculation process for removal and methyl orange was adsorbed with flocculation at higher concentrations. The capacity of adsorption of chromium was estimated to be 450 mg/g following the pseudo-second order kinetics [81].

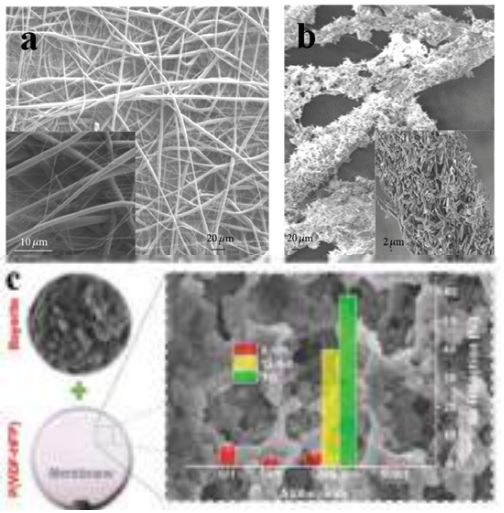

Figure 6. (a) SEM micrographs of electrospun PLLA nanofibers; (b) ZnO grown on PLLA nanofibers. (inset presents high resolution cross-sectional images) ; and (c) Schematic showing membrane composed with bayerite and arsenic rejection with the composite.

Fe^{3+} ion immobilized into PVA matrix has been explored for arsenic removal from water. Electrospun nanofiber mats of PVA/Fe3+ was cross linked with saturated ammonia in a desiccator. The increase in Fe^{3+} immobilization led to rise in glass transition temperature with lower melting peak enthalpy. The maximum adsorption of arsenite and arsenate from spiked aqueous solution were 67 mg/g and 36 mg/g, respectively [82]. A hybrid composite was designed using emulsion-polymerization process without any emulsifier using chitosan, polymethylmethacrylate (PMMA) used for grafting and crosslinked with silica for mechanical strength. The preparation was carried out under nitrogen atmosphere using ammonium persulfate to initiate the chemical reactions. The recovery of Cr (VI) was about 98% with high removal efficiency [83]. Membranes composed of

poly (vinylidene fluoride-hexafluoropropylene) (PVDF-HFP) having aluminum hydroxide as filler and bayerite polymorph were solvent casted to be used as membrane filter for arsenic adsorption and filtration (**Figure 6c**). The porosity degree was estimated between 65-75% with high homogeneity. Dead-end cell filtration tests led to 60% arsenic rejection in 1 hour with standard arsenic solution of 100 μg/L. The positively charged surface from bayerite causes coulombic interaction between the As anions and Al^{3+} in bayerite. The study claims that formation of hydroxides of aluminum is favorable for arsenic adsorption [84].

5.4. Others

Epoxies, polypropylene and polyester are among few other polymers that are processed for effective use of heavy metal remediation. Membranes of polypropylene is known for its ion-exchange properties that can explicitly use for transport of metal ions through the system with high selectivity [85]. In-situ radical polymerization method was used to modify the polymers such as, poly[(ar-vinylbenzyl) trimethylammonium chloride], poly[2 (acryloyloxy) ethyl]trimethylammonium chloride], poly(acrylic acid), poly(2-acrylamidoglycolic acid), poly (glycidylmethacrylate-*N*-methyl-d-glucamine), poly(2-acrylamido-2-methyl-1-propane sulfonic acid), and poly [sodium (styrene sulfonate)] designated as P(ClVBTA), (P(ClAETA), P(AA), P(AGA), P(GMA-NMG), P(AMPS), and P(SSNa), respectively. Furthermore, to make the membranes hydrophilic, the surface was grafted with polyelectrolyte. The modified membranes with P(ClVBTA) was effective in transporting hexavalent chromium ions, whereas P(SSNa) was effective in transport of trivalent chromium ions [86]. Availability of different functional groups from polymers increases the selectivity towards particular chromium ions in the system.

6. Future of functional green nanocomposites

The use of functional green composites will be a boon to the environmental sustainability because of its biodegradable nature and enhancement in the uptake of heavy metals from the environment. These will overtake the market for commercialization because of its self-degrading property after overcoming the basic problems associated with the green composites. The above studies have cleared the picture of functionalization and property enhancement in the green composite by using natural and synthetic biopolymers due to changes in chemical, physical and mechanical properties. Efficient separation after environmental remediation could be addressed by immobilizing magnetic nanoparticles into the green composite. The polymeric structures not only provide surface for functionality but also participate in stabilization and chelation, as support host and also as reducing agents in some cases. In context to the heavy metal adsorption, strong chelation with surface functional groups is of prior significance with high selectivity and sensitivity in the presence of foreign species. It could be speculated that green composites apart from its usage in environmental remediation could be effective in structural applications as well.

References

[1] P.K. Rai, S.S. Lee, M. Zhang, Y.F. Tsang, K.-H. Kim, Heavy metals in food crops: Health risks, fate, mechanisms, and management, Environment International 125 (2019) 365-385.

[2] L. Liu, W. Li, W. Song, M. Guo, Remediation techniques for heavy metal-contaminated soils: Principles and applicability, Science of The Total Environment 633 (2018) 206-219.

[3] P.B. Tchounwou, C.G. Yedjou, A.K. Patlolla, D.J. Sutton, Heavy metal toxicity and the environment, Experientia supplementum (2012) 101 (2012) 133-164.

[4] H.-J. Hapke, Heavy metal transfer in the food chain to humans, in: C. Rodriguez-Barrueco (Ed.) Fertilizers and Environment: Proceedings of the International Symposium “Fertilizers and Environment”, held in Salamanca, Spain, 26–29, September, 1994, Springer Netherlands, Dordrecht, 1996, pp. 431-436.

[5] J.E. Gall, R.S. Boyd, N. Rajakaruna, Transfer of heavy metals through terrestrial food webs: a review, Environmental Monitoring and Assessment 187 (2015) 201.

[6] L. Järup, Hazards of heavy metal contamination, British Medical Bulletin 68 (2003) 167-182.

[7] M.I. Litter, Last advances on TiO_2-photocatalytic removal of chromium, uranium and arsenic, Current Opinion in Green and Sustainable Chemistry 6 (2017) 150-158.

[8] P.V. Nidheesh, T.S.A. Singh, Arsenic removal by electrocoagulation process: Recent trends and removal mechanism, Chemosphere 181 (2017) 418-432.

[9] M.B. Shakoor, N.K. Niazi, I. Bibi, M. Shahid, Z.A. Saqib, M.F. Nawaz, S.M. Shaheen, H. Wang, D.C.W. Tsang, J. Bundschuh, Y.S. Ok, J. Rinklebe, Exploring the arsenic removal potential of various biosorbents from water, Environment International 123 (2019) 567-579.

[10] H. Hernández-Flores, N. Pariona, M. Herrera-Trejo, H.M. Hdz-García, A.I. Mtz-Enriquez, Concrete/maghemite nanocomposites as novel adsorbents for arsenic removal, Journal of Molecular Structure 1171 (2018) 9-16.

[11] M.B. Shakoor, N.K. Niazi, I. Bibi, M.M. Rahman, R. Naidu, Z. Dong, M. Shahid, M. Arshad, Unraveling Health Risk and Speciation of Arsenic from Groundwater in Rural Areas of Punjab, Pakistan, International Journal of Environmental Research and Public Health 12 (2015) 12371.

[12] A.M. Zayed, N. Terry, Chromium in the environment: factors affecting biological remediation, Plant and Soil 249 (2003) 139-156.

[13] R. Saha, R. Nandi, B. Saha, Sources and Toxicity of Hexavalent Chromium, 2011.

[14] A.A. Al-Homaidan, H.S. Al-Qahtani, A.A. Al-Ghanayem, F. Ameen, I.B.M. Ibraheem, Potential use of green algae as a biosorbent for hexavalent chromium removal from aqueous solutions, Saudi Journal of Biological Sciences 25 (2018) 1733-1738.

[15] A. Bakshi, A.K. Panigrahi, A comprehensive review on chromium induced alterations in fresh water fishes, Toxicology Reports 5 (2018) 440-447.

[16] H. Işsever, K. Özdilli, B.A. Özyildirim, B. Hapçioglu, N. ince, H. ince, E. Isik, E. Akçay, Y. Yeğenoğlu, M. Erelel, B. Çalak, N. Ağbaş, Respiratory Problems in Tannery Workers in Istanbul, Indoor and Built Environment 16 (2007) 177-183.

[17] A.F.C. Campos, H.A.L. de Oliveira, F.N. da Silva, F.G. da Silva, P. Coppola, R. Aquino, A. Mezzi, J. Depeyrot, Core-Shell Bimagnetic Nanoadsorbents for Hexavalent Chromium Removal from Aqueous Solutions, Journal of Hazardous Materials 362 (2019) 82-91.

[18] P. Raut, A. Chahande, Y. Moharkar, Various techniques for the removal of Chromium and lead from Waste water:Review, 2015.

[19] S.A. Bhawani, A.H. Bhat, F.B. Ahmad, M.N.M. Ibrahim, 23 - Green polymer nanocomposites and their environmental applications, in: M. Jawaid, M.M. Khan (Eds.) Polymer-based Nanocomposites for Energy and Environmental Applications, Woodhead Publishing2018, pp. 617-633.

[20] M.P.M. Dicker, P.F. Duckworth, A.B. Baker, G. Francois, M.K. Hazzard, P.M. Weaver, Green composites: A review of material attributes and complementary applications, Composites Part A: Applied Science and Manufacturing 56 (2014) 280-289.

[21] H.S.S. Shekar, M. Ramachandra, Green Composites: A Review, Materials Today: Proceedings 5 (2018) 2518-2526.

[22] D.B. Dittenber, H.V.S. GangaRao, Critical review of recent publications on use of natural composites in infrastructure, Composites Part A: Applied Science and Manufacturing 43 (2012) 1419-1429.

[23] K.G. Satyanarayana, G.G.C. Arizaga, F. Wypych, Biodegradable composites based on lignocellulosic fibers—An overview, Progress in Polymer Science 34 (2009) 982-1021.

[24] H. Patel, M. Bonde, G. Srinivasan, Biodegradable Polymer Scaffold for Tissue Engineering, 2011.

[25] S. R. Ramakrishna, J. Mayer, E. Wintermantel, K. Leong, Biomedical applications of polymer-composite materials: A review, 2001.

[26] L. Zhang, The Application of Composite Fiber Materials in Sports Equipment, 2015.

[27] H.L. Wang, Application of Fiber Reinforced Composites in Sports Equipment, Applied Mechanics and Materials 416-417 (2013) 1717-1720.

[28] G. Koronis, A. Silva, M. Fontul, Green composites: A review of adequate materials for automotive applications, 2013.

[29] A. Bazargan, T. Gebreegziabher, D. Hui, G. McKay, The effect of alkali treatment on rice husk moisture content and drying kinetics, 2014.

[30] E. Pehlivan, T.H. Tran, W.K.I. Ouédraogo, C. Schmidt, D. Zachmann, M. Bahadir, Removal of As(V) from aqueous solutions by iron coated rice husk, Fuel Processing Technology 106 (2013) 511-517.

[31] E. Agrafioti, D. Kalderis, E. Diamadopoulos, Arsenic and chromium removal from water using biochars derived from rice husk, organic solid wastes and sewage sludge, Journal of Environmental Management 133 (2014) 309-314.

[32] L. Moghaddam, Z. Zhang, M. Wellard, J. Bartley, I. O'Hara, W. Doherty, Characterisation of lignins isolated from sugarcane bagasse pretreated with acidified ethylene glycol and ionic liquids, 2014.

[33] V.K. Gupta, I. Ali, Removal of lead and chromium from wastewater using bagasse fly ash—a sugar industry waste, Journal of Colloid and Interface Science 271 (2004) 321-328.

[34] L.S. Yadav, B.K. Mishra, A. Kumar, K.K. Paul, Arsenic removal using bagasse fly ash-iron coated and sponge iron char, Journal of Environmental Chemical Engineering 2 (2014) 1467-1473.

[35] X. Liu, H. Ao, X. Xiong, J. Xiao, J. Liu, Arsenic Removal from Water by Iron-Modified Bamboo Charcoal, Water, Air, & Soil Pollution 223 (2012) 1033-1044.

[36] W. Wang, X. Wang, X. Wang, L. Yang, Z. Wu, S. Xia, J. Zhao, Cr(VI) removal from aqueous solution with bamboo charcoal chemically modified by iron and cobalt with the assistance of microwave, Journal of Environmental Sciences 25 (2013) 1726-1735.

[37] F. Mohd Jais, S. Ibrahim, Y. Yoon, M. Jang, Enhanced arsenate removal by lanthanum and nano–magnetite composite incorporated palm shell waste–based activated carbon, 2016.

[38] M. H Gonzalez, G. Labuto, C. B Pelizaro, E. A Menezes, S. Lemos, G. Batista de Sousa, A.R. Nogueira, Coconut coir as biosorbent for Cr(VI) removal from laboratory wastewater, 2008.

[39] G.N. Manju, C. Raji, T.S. Anirudhan, Evaluation of coconut husk carbon for the removal of arsenic from water, Water Research 32 (1998) 3062-3070.

[40] R. Ouafi, Z. Rais, M. Taleb, M. Benabbou, M. Asri, Sawdust in the treatment of heavy metals-contaminated wastewater, 2017, pp. 145-182.

[41] J.R. Dillen, S. Dillén, M.F. Hamza, Pulp and Paper: Wood Sources, Reference Module in Materials Science and Materials Engineering, Elsevier2016.

[42] D. Setyono, S. Valiyaveettil, Chemically Modified Sawdust as Renewable Adsorbent for Arsenic Removal from Water, ACS Sustainable Chemistry & Engineering 2 (2014) 2722-2729.

[43] L. Hao, Q. Liu, X. Li, Z. Du, P. Wang, A potentially low-cost modified sawdust (MSD) effective for rapid Cr(vi) and As(v) removal from water, RSC Advances 4 (2014) 49569-49576.

[44] V. Gupta, A. Nayak, S. Agarwal, Bioadsorbents for remediation of heavy metals: Current status and their future prospects, 2015.

[45] M. Farajzadeh, A. Boveiri Monji, Adsorption characteristics of wheat bran towards heavy metal cations, 2004.

[46] A. Özer, Removal of Pb(II) ions from aqueous solutions by sulphuric acid-treated wheat bran, Journal of Hazardous Materials 141 (2007) 753-761.

[47] Y. Tian, M. Wu, X. Lin, P. Huang, Y. Huang, Synthesis of magnetic wheat straw for arsenic adsorption, Journal of Hazardous Materials 193 (2011) 10-16.

[48] X. Yao, S. Deng, R. Wu, S. Hong, B. Wang, J. Huang, Y. Wang, G. Yu, Highly efficient removal of hexavalent chromium from electroplating wastewater using aminated wheat straw, RSC Advances 6 (2016) 8797-8805.

[49] M.P. Elizalde-González, J. Mattusch, R. Wennrich, Chemically modified maize cobs waste with enhanced adsorption properties upon methyl orange and arsenic, Bioresource Technology 99 (2008) 5134-5139.

[50] S.I. Rojas, D.C. Duarte, S.D. Mosquera, F. Salcedo, J.P. Hinestroza, J. Husserl, Enhanced biosorption of Cr(VI) using cotton fibers coated with chitosan – role of ester bonds, Water Science and Technology 78 (2018) 476-486.

[51] L. Chai, Q. Li, Y. Zhu, Z. Zhang, Q. Wang, Y. Wang, Z. Yang, Synthesis of thiol-functionalized spent grain as a novel adsorbent for divalent metal ions, Bioresource Technology 101 (2010) 6269-6272.

[52] Y. Chen, C. Xiong, Adsorptive removal of As(III) ions from water using spent grain modified by polyacrylamide, Journal of Environmental Sciences 45 (2016) 124-130.

[53] M. Rahim, M.R.H. Mas Haris, Application of biopolymer composites in arsenic removal from aqueous medium: A review, Journal of Radiation Research and Applied Sciences 8 (2015) 255-263.

[54] M. Ahmad, S. Ahmed, B. Lal Swami, S. Ikram, Adsorption of heavy metal ions: Role of chitosan and cellulose for water treatment, 2015.

[55] I. Anastopoulos, A. Bhatnagar, D.N. Bikiaris, G.Z. Kyzas, Chitin Adsorbents for Toxic Metals: A Review, International journal of molecular sciences 18 (2017) 114.

[56] L. Zhang, W. Xia, B. Teng, X. Liu, W. Zhang, Zirconium cross-linked chitosan composite: Preparation, characterization and application in adsorption of Cr(VI), Chemical Engineering Journal 229 (2013) 1-8.

[57] D.W. O'Connell, C. Birkinshaw, T.F. O'Dwyer, Heavy metal adsorbents prepared from the modification of cellulose: A review, Bioresource Technology 99 (2008) 6709-6724.

[58] A.S.K. Kumar, S. Kalidhasan, V. Rajesh, N. Rajesh, Application of Cellulose-Clay Composite Biosorbent toward the Effective Adsorption and Removal of Chromium from Industrial Wastewater, Industrial & Engineering Chemistry Research 51 (2012) 58-69.

[59] S. Periyasamy, V. Gopalakannan, N. Viswanathan, Fabrication of magnetic particles imprinted cellulose based biocomposites for chromium(VI) removal, Carbohydrate Polymers 174 (2017) 352-359.

[60] X. Yu, S. Tong, M. Ge, J. Zuo, C. Cao, W. Song, One-step synthesis of magnetic composites of cellulose@iron oxide nanoparticles for arsenic removal, Journal of Materials Chemistry A 1 (2013) 959-965.

[61] R. Karthik, S. Meenakshi, Synthesis, characterization and Cr(VI) uptake studies of polypyrrole functionalized chitin, Synthetic Metals 198 (2014) 181-187.

[62] R. Yang, Y. Su, K.B. Aubrecht, X. Wang, H. Ma, R.B. Grubbs, B.S. Hsiao, B. Chu, Thiol-functionalized chitin nanofibers for As (III) adsorption, Polymer 60 (2015) 9-17.

[63] G. Arslan, I. Sargin, M. Kaya, Hexavalent chromium removal by magnetic particle-loaded micro-sized chitinous egg shells isolated from ephippia of water flea, International Journal of Biological Macromolecules 129 (2019) 23-30.

[64] W. S. Wan Ngah, L.C. Teong, M.A.K. Megat Hanafiah, Adsorption of Dyes and Heavy Metal Ions by Chitosan Composites: A Review, 2011.

[65] A. Khan, S. Badshah, C. Airoldi, Dithiocarbamated chitosan as a potent biopolymer for toxic cation remediation, 2011.

[66] V.M. Boddu, K. Abburi, J.L. Talbott, E.D. Smith, R. Haasch, Removal of arsenic (III) and arsenic (V) from aqueous medium using chitosan-coated biosorbent, Water Research 42 (2008) 633-642.

[67] H. Aslani, T. Ebrahimi Kosari, S. Naseri, R. Nabizadeh, M. Khazaei, Hexavalent chromium removal from aqueous solution using functionalized chitosan as a novel nano-adsorbent: modeling and optimization, kinetic, isotherm, and thermodynamic studies, and toxicity testing, Environmental Science and Pollution Research 25 (2018) 20154-20168.

[68] L.-L. Min, L.-B. Zhong, Y.-M. Zheng, Q. Liu, Z.-H. Yuan, L.-M. Yang, Functionalized chitosan electrospun nanofiber for effective removal of trace arsenate from water, Scientific reports 6 (2016) 32480-32480.

[69] D. Jiang, D. Huang, C. Lai, P. Xu, G. Zeng, J. Wan, L. Tang, H. Dong, B. Huang, T. Hu, Difunctional chitosan-stabilized Fe/Cu bimetallic nanoparticles for

removal of hexavalent chromium wastewater, Science of The Total Environment 644 (2018) 1181-1189.

[70] M. Yazdani, A. Bhatnagar, R. Vahala, Synthesis, characterization and exploitation of nano-TiO2/feldspar-embedded chitosan beads towards UV-assisted adsorptive abatement of aqueous arsenic (As), Chemical Engineering Journal 316 (2017) 370-382.

[71] A. Pettignano, D.A. Aguilera, N. Tanchoux, L. Bernardi, F. Quignard, Chapter 17 - Alginate: A Versatile Biopolymer for Functional Advanced Materials for Catalysis, in: S. Albonetti, S. Perathoner, E.A. Quadrelli (Eds.) Studies in Surface Science and Catalysis, Elsevier 2019, pp. 357-375.

[72] L. Dehabadi, L. D Wilson, Polysaccharide-based materials and their adsorption properties in aqueous solution, 2014.

[73] C. Menakbi, F. Quignard, T. Mineva, Complexation of Trivalent Metal Cations to Mannuronate Type Alginate Models from a Density Functional Study, The Journal of Physical Chemistry B 120 (2016) 3615-3623.

[74] P. Singh, S.K. Singh, J. Bajpai, A.K. Bajpai, R.B. Shrivastava, Iron crosslinked alginate as novel nanosorbents for removal of arsenic ions and bacteriological contamination from water, Journal of Materials Research and Technology 3 (2014) 195-202.

[75] S. Gokila, T. Gomathi, P.N. Sudha, S. Anil, Removal of the heavy metal ion chromiuim(VI) using Chitosan and Alginate nanocomposites, International Journal of Biological Macromolecules 104 (2017) 1459-1468.

[76] H.C. Vu, A.D. Dwivedi, T.T. Le, S.-H. Seo, E.-J. Kim, Y.-S. Chang, Magnetite graphene oxide encapsulated in alginate beads for enhanced adsorption of Cr(VI) and As(V) from aqueous solutions: Role of crosslinking metal cations in pH control, Chemical Engineering Journal 307 (2017) 220-229.

[77] L. Te Chuan, N. Manap, H. Abdullah, M. Idris, Polyvinyl Alcohol-Alginate Adsorbent Beads for Chromium (VI) Removal, 2018.

[78] M. Jamshidian, E.A. Tehrany, M. Imran, M. Jacquot, S. Desobry, Poly-Lactic Acid: Production, Applications, Nanocomposites, and Release Studies, Comprehensive Reviews in Food Science and Food Safety 9 (2010) 552-571.

[79] G. Narayanan, V.N. Vernekar, E.L. Kuyinu, C.T. Laurencin, Poly (lactic acid)-based biomaterials for orthopaedic regenerative engineering, Advanced drug delivery reviews 107 (2016) 247-276.

[80] T. Burks, F. Akhtar, M. Saleemi, M. Avila, Y. Kiros, ZnO-PLLA Nanofiber Nanocomposite for Continuous Flow Mode Purification of Water from Cr(VI), 2015.

[81] U. Habiba, T.A. Siddique, T.C. Joo, A. Salleh, B.C. Ang, A.M. Afifi, Synthesis of chitosan/polyvinyl alcohol/zeolite composite for removal of methyl orange, Congo red and chromium(VI) by flocculation/adsorption, Carbohydrate polymers 157 (2017) 1568-1576.

[82] N. Mahanta, S. Valiyaveettil, Functionalized poly(vinyl alcohol) based nanofibers for the removal of arsenic from water, RSC Advances 3 (2013) 2776-2783.

[83] T.R. Sethy, P.K. Sahoo, Highly toxic Cr (VI) adsorption by (chitosan-g-PMMA)/silica bionanocomposite prepared via emulsifier-free emulsion polymerisation, International Journal of Biological Macromolecules 122 (2019) 1184-1190.

[84] H. Salazar, J. Nunes-Pereira, D.M. Correia, V.F. Cardoso, R. Gonçalves, P.M. Martins, S. Ferdov, M.D. Martins, G. Botelho, S. Lanceros-Méndez, Poly(vinylidene fluoride-hexafluoropropylene)/bayerite composite membranes for efficient arsenic removal from water, Materials Chemistry and Physics 183 (2016) 430-438.

[85] S. Jiang, B.P. Ladewig, High Ion-Exchange Capacity Semihomogeneous Cation Exchange Membranes Prepared via a Novel Polymerization and Sulfonation Approach in Porous Polypropylene, ACS Applied Materials & Interfaces 9 (2017) 38612-38620.

[86] Y. Tapiero, J. Sánchez, B. L. Rivas, Ion-selective interpenetrating polymer networks supported inside polypropylene microporous membranes for the removal of chromium ions from aqueous media, 2015.

Research and Development of eco- friendly Green nanocomposites for cancer therapy

Indu Hira[1], Prachi Vaid[1], Neeraj Kumar Saini[2], Adesh K. Saini[3*], Reena V. Saini[1*]

[1] Faculty of Applied sciences and Biotechnology, Shoolini University of Biotechnology and Management Sciences, Solan, HP, India

[2] Department of Microbiology and Immunology, Albert Einstein College of Medicine, Bronx, New York 10461, USA

[3] Faculty of Basic Sciences, Shoolini University of Biotechnology and Management Sciences, Solan, HP, India

Email ID: reenavohra10@gmail.com, sainiade@gmail.com

Abstract

The chapter describes the preparation, characterization techniques and various biomedical applications of green synthesized nanocomposites. Himalayan plants are a major contributor to the herbal pharmaceutical industry both of India and other countries. The use of medicinal herbs has increased in biomedical applications as they have negligible side effects than that of modern synthetic drugs. Green synthesis of nanocomposites using plant material is an inexpensive and eco-friendly approach. As single component materials cannot satisfy the basic requirements such as biocompatibility, biodegradability and appropriate mechanical properties for effective therapy. The biomedical use of nanocomposite depends on their properties of interaction between the chosen matrix and the filler. In the present chapter, the use of green nanocomposites to improve drug delivery, targeted drug delivery to cells, co-delivery of drugs for combined treatment and visualization and biodistribution of the therapeutic agents with imaging modalities has been employed successfully for treating cancer.

1.1 Cancer

Cancer is a group of diseases involving abnormal cell growth having the potential to invade other parts of the body. It has become a big threat to human beings globally and also major causes of death in developed countries, together with cardiac and cerebrovascular diseases (Velusamy *et al.,* 2016). Cancer is a major public health problem worldwide and is the second leading cause of death in the United States. Around 1,688,780 new cancer cases and 600,920 cancer deaths occurred in the United States in 2017. In men, the cancer incidence rate is 20% higher and the cancer death rate is 40% higher than in women (Siegel *et al.,* 2017). The world's population is expected to be 7.5 billion by 2020 and it is predicted that about 15.0 million new cancer cases will be diagnosed with the deaths of about 12.0 million cancer patients in India (Ali *et al.,* 2011). It has been predicted by the International Agency for Research on Cancer GLOBOCAN that in India cancer burden will nearly double in the next 20 years. So, from a million new cases in 2012 to more than 1·7 million by 2035 (Ferlay *et al.,* 2015). The cancer treatment is targeted at its proliferation potential and its ability to metastasize, and hence the majority of treatments are targeted at rapidly dividing cells and at molecular targets that represent the bulk of the tumor. The type of treatment depends on the type of cancer and its stage (Reya *et al.,* 2001). The most common types of cancer treatments are surgery, chemotherapy, radiation therapy, and many others. Current therapies may treat cancer, but all these are limited due to their side effects.

1.2 Nanobiotechnology and Cancer treatment

A nanotechnology-based therapeutics is an essential tool for improving efficacy and safety of cancer treatments it has become one of the most promising technologies for treating and diagnosing cancer. Nano-strategies has been shown to improve delivery of weakly water soluble drugs, longer

circulating lifetime of drugs in the body, targeted drugs delivery to cells, co-delivery of drugs for combined treatment and visualization of sites of drug delivery (Chen *et al*., 2015). Nanotechnology alters electrical, magnetic, structural, morphological, chemical, and physical properties of nanomaterials which are comparable in size to naturally occurring biomolecules that makes them applicable for biological applications. Thus nanomaterials have the potential to be used in medicine and especially in the area of cancer. Quantum dots (QD), gold nanoparticles, magnetic nanoparticles, carbon nanotubes, gold nanowires are the `nanostructures that have been developed from the past few years which can be used as biomarkers for cancer detection. Biomarkers in relation to nanotechnology and biosensors have opened up a new era of early cancer diagnosis and precise drug delivery (Choi, *et al*., 2010).

1.3 Green Nanotechnology

Nature has a stake of comrades to help the developing world that is tending to several diseases. Consumption of naturally available plant derived products has been used to prevent as well as treat various diseases for many centuries by mankind. The natural compounds present in the plants, namely phytochemicals has been extensively exploited for its anticancer property. Green nanobiotechnology means synthesizing nanoparticles or nanomaterials using biological routes such as those involving microorganisms, plants, and viruses or their byproducts, such as proteins and lipids, with the help of various biotechnological tools. The principles of green chemistry can be applied to produce safer and more sustainable nanomaterials and more efficient and sustainable nano-manufacturing processes. Plants have shown great potential to accumulate heavy metal and detoxification (Yang *et al*., 2005). It has been shown that the metal nanoformulations produced by plants are more stable in

comparison with those produced by other organisms. Plants (especially plant extracts) can reduce metal ions faster than fungi or bacteria. Furthermore, in order to use an easy and safe green method in scale-up and industrial production of well-dispersed metal nanoparticles, using plant extracts is a better approach (Iravani, 2011).

Nanoparticles/nanocomposite synthesized by chemical and physical approaches are expensive and harmful to the environment. Therefore, there is a need for biodegradable and biocompatible material for the synthesis of nano-formulations with enhanced target specificity and effective drug delivery system (Dziadek *et al*., 2017). Plants have a unique property of heavy metal tolerance that can be exploited for nanoparticles synthesis. Plant-mediated synthesis of nanoparticles is conferred due to the presence of biomolecules such as proteins, amino acids, vitamins, polysaccharides, polyphenols, terpenoids etc. These molecules also stabilize the nanoparticles formed with desired size and shape. Studies have indicated that biomolecules not only play a role in reducing the ions to the nanosize, but also play an important role in the capping of nanoparticles (Collera-Zuniga *et al.,* 2005). Zinc oxide nanocomposite has been synthesised using seaweed *Sargassum muticum* water extract and hyaluronan biopolymer (HA/ZnO nanocomposite). *In vitro* cytotoxicity assay depicted significant toxicity of HA/ZnO nanocomposite towards pancreatic adenocarcinoma (PANC-1), ovarian adenocarcinoma (CaOV-3), colonic adenocarcinoma (COLO205) and acute promyelocytic leukemia (HL-60), but no toxicity was exhibited towards normal human lung fibroblast (MRC-5) cell line (Namvar *et al.,* 2016). Another green nanocomposite has been synthesized by encapsulating chlorophyll (Chl) extracted from vegetables into polymer (pluronic F68, Plu) micelles. It has been shown that Chl encapsulated nanocomposite could be used for cancer imaging after vein injection or oral administration. The Chl encapsulated nanocomposite also exhibited

therapeutic effects as mouse melanoma tumours were eliminated after 15 days of irradiation via intratumorally injected nanocomposites mainly due to photothermal and photodynamic properties of Chl (Chu *et al.,* 2014).

Recently, graphene and graphene-based materials have been used increasingly for various biological applications due to their extraordinary physicochemical properties. Silver doped highly reduced graphene oxide nanocomposites (PGE-HRG-Ag) were synthesized by using *Pulicaria glutinosa* extract (PGE) as a reducing agent. The PGE-HRG-Ag nanocomposite was able to induce apoptotic pathways and were more toxic than the standard drug in A549 cells (lung adenocarcinomas) (Khan *et al.,* 2016). Similarly, gold-reduced graphene oxide (Au- rGO) nanocomposite was developed using the fruit of *Piper pedicellatum* and was found to be cytotoxic towards PC3 (human prostate carcinoma cell line) and RWPE-1(non-malignant human prostate epithelial cells) (Saikia *et al.,* 2016). Further, reduced graphene oxide–silver nanoparticle nanocomposites (rGO–Ag) were synthesized using R-phycoerythrin (RPE) and were shown to mediate cell death in human ovarian cancer cells (A2780 cell line) via apoptosis (Gurunathan *et al.,* 2015). The green graphene oxide–metal nanocomposites synthesised by using a black pepper extract have been shown to detect epidermal growth factor receptor, a biomarker for cancer detection (Ali *et al.,* 2017).

1.4 Different methods for synthesizing green nanocomposite.

Various methods of formulating novel nanocomposites with desired properties and functions have been developed. These methods produce materials in which the unique properties of the nanoparticles were preserved. These methods can be classified into two general approaches; as direct compounding, and in situ synthesis. The direct compounding refers to the mixing of already synthesised nanomaterials and polymers followed

by blending using a different method. Different techniques applied for blending are solvent casting, melt blending, template synthesis, electrospinning and self-assembly. In situ polymer nanocomposite synthesis involves a combination of precursors of nanocomposite (metal ions for nanomaterials or monomers for polymer) leading to the generation of nano-entity. These reactions can be catalyzed with heat, radiation or an agent initiator (Nadagouda., 2012). The biological synthesis of nanoparticles/nanocomposite using plant tissue extracts is a suitable alternative to chemical procedures and physical methods as discussed above. Green Synthesis of nanoformulations using plant extracts is very cost effective and efficient.

Synthesis of nanocomposite using a biological method has been shown in Fig. 1. The method includes the choice of solvent, an ecofriendly reducing agent, and a nontoxic material as a capping agent for stabilization of synthesized nanocomposite (Mohanpuria *et al*., 2008; Ingale and Chaudhari, 2013). The pH of the solution, temperature, the concentration of extracts, the concentration of the raw materials used, size, and method followed for the synthesis process are various factors that affect the synthesis of nanoparticles/nanocomposite. (Baker *et al*., 2013). Target specific NPs might change the stability, solubility, and pharmacokinetic properties of the carried drugs and shelf life, aggregation, leakage, and toxicity of materials that were used to make nanoparticles (Jain *et al*., 2011; Kendall and Holgate, 2012).

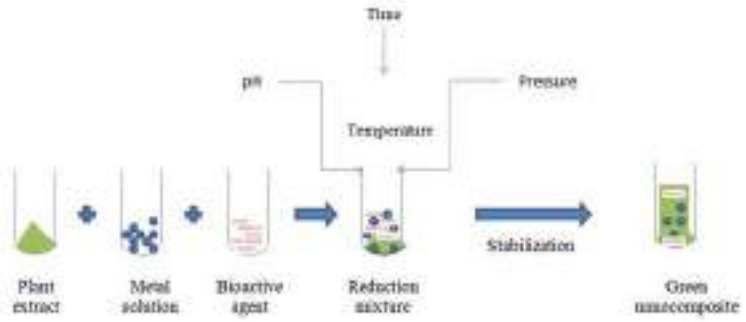

Figure 1: Scheme for biosynthesis of green nanocomposite

1.5 Characterization techniques for green nanocomposite

Many different nanoparticles/nanocomposite characterization techniques are available. The techniques include thermogravimetric analysis (TGA), FT-IR differential scanning calorimetry, transmission electron microscopy (TEM), scanning electron microscopy (SEM), X - ray diffraction (XRD), nuclear magnetic resonance (NMR), IR spectroscopy, Raman spectroscopy, X-ray photoelectron spectroscopy, dielectric relaxation spectroscopy, atomic force microscopy, electron spin resonance, continuous - wave and pulsed ESR spectroscopy, etc. (Bana and Banthia, (2009); Sain and Oksman , 2014).

Nanoparticles/nanocomposites synthesized using biological methods or green technology have diverse natures, with greater stability and appropriate dimensions since they are synthesized using a one-step procedure. Various undesirable processing conditions are thus eliminated by allowing the synthesis to proceed at physiological temperatures, pH, pressure, and, at the same time, a negligible cost (Ingale and Chaudhari, 2013). Thus, specific characterization techniques may be employed to characterize the physiochemical components of the synthesized nanoformulations.

1.6 Applications of the green nanocomposite in cancer therapy and detection

The green synthesis of nanocomposite from plants sources has become an emerging field due to their safer, eco-friendly, simple, fast, energy efficient, low cost and less toxic nature. The applications of green nanocomposite include cellular visualization, targeted drug delivery, anti-cancer activity, photo-thermal therapy for cancer.

1.6.1 Nanotechnological Approaches for Screening of Cancer

The number of research developments in the nanotechnology area has been conducted to utilize nanomaterials to detect cancers at early stages. Nanomaterials have unique physical, optical and electrical properties that have proven to be very useful in sensing. Quantum dots, gold nanoparticles, carbon nanotubes, gold nanowires and proteins, antibody fragments, DNA fragments, and RNA fragments have been served as cancer biomarkers that have been used as targets in cancer detection and monitoring (Lungu et al., 1995; Choi et al., 2010).

The nanocomposites containing biomarkers especially antibodies/ antigens are generally termed as immunosensors. Martirosyan *et al*., 2009 has developed a biodegradable nanocomposite of poly (methyl methacrylate) with single-walled carbon nanotubes (SWCNT) to visualize the precise location of radioactive titanium seeds by using magnetic resonance imaging (MRI). The nanocomposite was used as an encapsulating material containing cobalt based and gadolinium-based contrast agents for monitoring and treatment of prostate cancer. (Martirosyan *et al*., 2009).

Deng *et al*., has developed a novel aptamer-guided nanocomposite consisting of mesoporous metal-organic frameworks (MOFs) based on iron (III) carboxylate materials and up-conversion luminescent

$NaYF_4$:Yb^{3+}/Er^{3+}nanoparticles (UCNPs) core. Anticancer aptamer AS1411 (a 26-mer guanine-rich oligonucleotide), was used for targeting cancer cells and enhancing intracellular uptake, since it has an affinity for nucleolin, a tumor cells specific membrane receptor. The 5' end of AS1411 aptamer was conjugated to fluorescein isothiocyanate for fluorescence labelling. The doxorubicin (DOX) loaded UCNPs@MOF nanocomposite showed specificity towards cancer cells, enhanced cellular internalization and unique up-converting green emission under laser excitation at 980 nm (Deng *et al.,* 2015).

The reduced graphene oxide silver (RGO–Ag) nanocomposite was prepared utilizing the extract of a medicinal mushroom, *Ganoderma lucidum.* The green and one-step synthesis approaches were developed for the formulation of RGO-Ag nanocomposite that can be utilized for the detection of H2O2, an important biomarker for cancer progression (Bai *et al.,* 2016).

A multifunctional nanoparticle with biomolecules conjugated to QDs have been used in cancer detection and targeted drug delivery. (Rosenthal *et al.,* 2011) Cadmium telluride (CdTe) QD-attached nanogels (QD-NGs) were found to be another type of nanoformulation with potential drug delivery and cell imaging abilities. Nanogels were synthesized using lysozyme and carboxymethylcellulose. The cellular uptake indicated that the QDs-NGs can protect QDsfrom decomposition in cytoplasm and retain the native fluorescence intensity. MTT assay demonstrated that the QDs-NGs greatly decreased the cytotoxicity of the QDs. Moreover, the methotrexate (MTX) loaded QDs-NGs distinctly enhanced the availability of drug. The QDs-NGs are potential nanocarriers for the cell imaging and drug delivery (Li *et al.,* 2015).

Additionally, Bwatanglang *et al*., synthesized a green nanocomposite by encapsulating luminescent Mn:ZnS quantum dots (QDs) in chitosan and conjugated to folic acid (FA) for specific targeting of folate receptor (FR) expressing cancer cells. The cell viability and proliferation studies demonstrated that the synthesized composites do not exhibit any toxicity toward the human breast cell lines. The *in vitro* fluorescence imaging studies showed that the composite conjugated with FA demonstrated specific attachment towards human breast cancer lines (MCF-7 and MDA-MB-231) that expressed FRs and are emitting fluorescence from the QDs. Therefore, this nanocomposite can be used as a theranostic agent for simultaneous targeted drug delivery and cellular imaging (Bwatanglang *et al.,* 2016).

Another nano-formulation was fabricated through complexing dimethylmaleic acid (DMMA) and PEG functionalized poly(allyamine) (PEG-(PAH/DMMA)) with cisplatin(IV) prodrug covalently functionalized carbon dots (CDs-Pt(IV)) by electrostatic interaction. This CDs-Pt(IV)@PEG-(PAH/DMMA) carrier was tumor extracellular microenvironment-sensitive prepared for image-guided drug delivery. *In vivo* experiments of these CDs exhibited high tumor inhibition ability and minimal side effects (Feng *et al.,* 2016).

1.6.2 Green nanocarriers for drug delivery system for cancer cells targeting

Nanocarriers, owing to their high surface area to volume ratio, have the ability to alter basic properties and bioactivity of drugs. Improved pharmacokinetics and biodistribution, decreased toxicities, improved solubility and stability, controlled release and site-specific delivery of therapeutic agents are some of the features that nanocarriers can incorporate in drug delivery systems. The common carriers that were

employed ranged from micelles with the polymeric base, dendrimers, liposomes and nanoparticles. The phytochemicals were found to become more soluble when delivered by the nanocarriers and exhibited a remarkable effect on the cancer cells compared to its free form.

1.6.2.1. Polymeric nanocomposite as a drug delivery system

Polymers, both natural and synthetic, due to their versatility and characteristics have been widely used in the development of a drug delivery system. Natural polymers are highly biocompatible and biodegradable and present functional groups (e.g., -OH, $-NH_2$) that can be easily modified (Ulery *et al*., 2011). Synthetic polymers, in turn, have the possibility of being prepared with tailored compositions, and their properties can be easily adjusted, to match a specific application (Nair and Laurencin, 2005). Polymer nanocomposite consist of polymer or copolymer with nanoparticles dispersed in the polymer matrix which is the one way to decrease toxicity and increase safety of the loaded drugs.

The bioabsorbable materials that are commonly used in cancer therapy are polyesters, polyanhydrides, polyphosphoesters, polysaccharides (chitosan, dextran, hyaluronic acid), and proteins (albumin, gelatin). The aliphatic polyester poly(lactic acid) (PLA), the copolymer poly(lactic-co-glycolic acid) (PLGA), and poly(ε-caprolactone) (PCL) are by far the most used bioabsorbable synthetic polymers in the biomedical field (Ratner *et al*., 2004).

A conventional radical polymerization technique was used to prepare nanogel from dextrin and poly(lactide) by using a homo-bifunctional cross-linker. In vitro cytocompatibility studies against human mesenchymal stem cells (hMSCs) proposed that the native nanogel had nontoxic effects on cancer cells, while doxorubicin (DOX)-loaded nanogels demonstrated high toxicity toward MG 63 cancer cells (Human osteosarcoma cell lines) (Das

et al., 2016). A novel reactive oxygen species-cleavable diblock polymer was prepared with hydrophilic PEG shells and a hydrophobic PLGA core. This new nanocompound with high stability, efficient drug delivery, excellent sensitivity, and good compatibility has been used for cancer chemotherapy (Li et al., 2016)

Chen et al synthesized biodegradable tricomponent graft copolymers, chitosan-PCL-PEG (chitosan-poly(ε-caprolactone)-poly(ethylene glycol) (CPP)) using paclitaxel and rutin as model drugs for the evaluation of the controlled released capacity of copolymers (Chen et al., 2011).

Tu et al prepared QC/BSA, QC-REC/BSA and QC-REC/BSA/DOX nanoparticles (Quaternized chitosan –Bovine Serum Albumin – Rectorite) and concluded that the release of doxorubicin was effectively decreased with the addition of REC, decreasing more in basic conditions (stimulated intestinal fluid) than in the acidic conditions (stimulated gastric fluid) (Tu et al., 2015).

The choice of polymers for drug conjugation is very critical. Polymers must be water-soluble with functional groups for covalent attachment of the drugs. The simplest form of polymer-drug conjugates is the attachment of poly(ethylenne glycol) (PEG) to drugs, a process known as pegylation. Various proteins therapeutics have been modified by PEG to improve proteins' solubility and reduce immunogenicity. Polymeric nanocomposites consist of a combination of polymers and nanofillers, which are used to support the polymer and to provide better characteristics. Polymeric nanocomposites are of two types, carbon nanotubes (CNTs) and layered silicates, in which they differ in the nanofillers used (Bhattacharya *et al*., 2008). Drug delivery using polymers as matrix/ encapsulation material involves the embedding of the NPs within organic particles that serve as delivery vectors for the drugs. EPR effect can facilitate the enhanced and

targeted drug delivery inside tumors. Drug circulation time and cancer specificity can be further enhanced by encapsulation of the NPs by polymers with active targeting biomarkers.

It has been shown that Her–Fe3O4@PLGA–PVP (HER-2 ligand conjugated, Poly-Vinyl-Pyrrolidone (PVP) stabilized core-shell iron oxide nanocomposite), nanocomposites facilitated the encapsulation of Tamoxifen. Nanocomposite recognized the target breast cancer cells through binding of Herceptin antibody to HER2, a cell surface receptor expressed by to promote HER2 receptor mediated endocytosis and induced apoptosis in breast cancer cells (Vivek R, 2016).

Green synthesis of CNTs was shown to be green catalyst-assisted to overcome the cytotoxic effect of metals. The synthesis has been shown to be non-toxic in nature as green catalysts used were organic compounds and were free from metal impurities. An eco-friendly and safe graphene nanosheet–CNT–iron oxide (GN–CNT–Fe823O) NP hybrid has been used as a new composite for attaching and carrying antitumor drugs (Fan *et al.,* 2013) Additionaly, a transactivator of transcription (TAT) peptide was conjugated to chitosan followed by addition of multiwalled CNTs (MWCNTs). The TAT–chitosan-conjugated MWCNTs (MWCNTs-TC) showed significant promising properties, such as water solubility, low toxicity, cell-penetrating capability, and accumulation in tumors (Dong *et al.,* 2015).

PEG 2000N modified Fe3O4@carbon quantum dots (CQDs) coated SWNTs were fabricated. These magnetofluorescent SWCNTs-PEG-Fe3O4@CQDs were conjugated with a sgc8c aptamer and doxorubicin for targeted dual modal fluorescence/magnetic resonance imaging, for inducing photodynamic and photothermal ablations, and was found to release DOX following irradiation with pH/NIR laser (Zhang et al., 2018).

It has been shown in our previous work that nanocomposite of pectin-guar gum- zinc oxide prepared by coprecipitation method (Fig. 2) acts as a immunostimulator of human peripheral-blood lymphocyte thus increasing their cytotoxicity towards lung cancer (A549 cell lines) and breast cancer cells (MCF-7 cell lines). It was also concluded that with increase in effector: target ratios from 2.5:1 to 20:1 there was increase in cancer cell death (Hira et al., 2018)

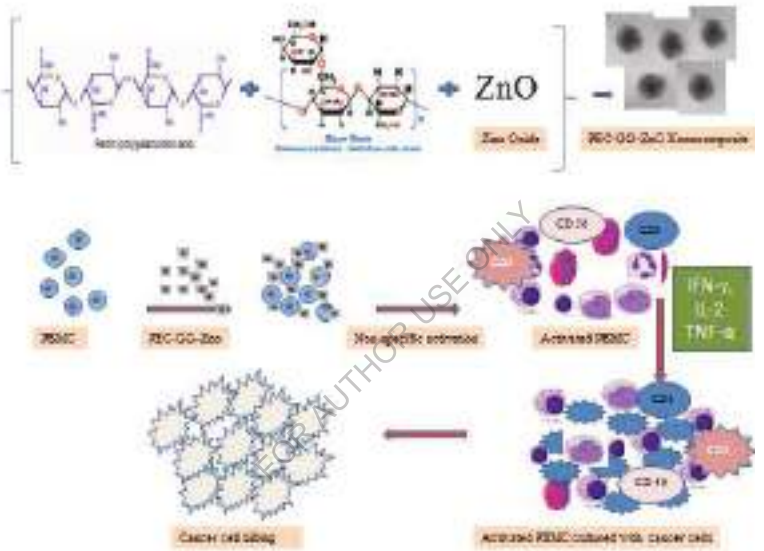

Figure 2: Synthesis and immunomodulatory potential of pectin-guar gum-zinc oxide nanocomposite (Hira *et al.*, 2018)

1.6.2.2. Liposomal nanocarriers as drug delivery for cancer

Liposomes have been widely used as a carrier for delivering both *in vitro* and *in vivo* (Deng *et al*., 2013) Since their bilayer membrane structure is similar to cell membrane composing of lipid and cholesterol molecules, liposomes exhibit a number of unique characteristics such as good biocompatibility and biodegradability. Particularly, the hydrophilic drugs

can be encapsulated into the hydrophilous core and hydrophobic drugs into the lipid bilayer (Allen and Cullis, 2013). Kang *et al*., reported the synthesis of lipid-coated gold nanocomposites using thermosensitive phospholipids onto the surface of anisotropic gold nanoparticles (AuNPs).These lipid-coated nanohybrids were loaded with the drug docetaxel (DTX) by a thin-film formation, hydration, and sonication method. The results showed that DTX-loaded anionic lipid-coated gold nanorod (AL_AuNR_DTX) and cationic lipid-coated gold nanoparticle (CL_AuNP_DTX) possess effective anticancer abilities (Kang and Ko, 2015).

Rengan *et al*., 2015, has reported that the liposome gold nanoparticles (LiposAu NPs) were capable of killing MCF-7 (breast) and HT1080 (fibrosarcoma) cancer cells through photothermal therapy. The pharmacokinetic study of LiposAu NPs performed in a small animal model indicates *in situ* degradation in hepatocytes and further getting cleared through the hepato-biliary and renal route (Rengan, *et al*., 2015)

1.6.2.3. Micelles as the drug delivery system

Polymeric micelles, core–shell-type nanoparticles formed through the self-assembly of block copolymers, are one of the most promising nanocarriers. The release rate and drug incorporation efficiency can be altered by designing the constituent block copolymers because of their critical features such as size, stability. Indocyanine green (ICG) was encapsulated in the core of a polymeric micelle, which self-assembled from ampiphilic PEG-polypeptide hybrid triblock copolymers of poly(ethylene glycol)-b-poly(L-lysine)-b-poly(L-leucine) (PEG-PLL-PLLeu), with PLLeu as the hydrophobic core and PEG as the hydrophilic shell. PEG-PLL-PLLeu-ICG micelles displayed high cellular uptake rate, passive tumor targeting and long circulation time under *in vivo* conditions. Besides

its application in tumor diagnosis and imaging, PEG-PLL-PLLeu-ICG also exhibited utility in tumor photothermal therapy (Wu *et al.,* 2013).

Drug conjugated micellar constructs were fabricated using triblock dendron-linear polymer conjugates where a hydrophilic linear polyethylene glycol (PEG) chain was flanked by well-defined hydrophobic biodegradable polyester dendrons bearing an antiangiogenic drug, combretastatin-A4 (CA4). The hydrophobic-hydrophilic-hydrophobic character of these constructs made them suitable for passive tumor targeting through enhanced permeability and retention (EPR) effect thus acting as controlled drug delivery agents (Sumer *et al.,* 2016).

Conclusions

Nanomedicine plays an essential role in developing alternative and more effective treatment strategies for cancer theranostics. The green synthesis of nanocomposites from plants and microbial sources has become an emerging field due to their safer, eco-friendly, simple, fast, energy efficient, low cost and less toxic nature. Green nanotechnology-driven drug delivery systems, receive great attention in the biomedical research area. Cancer is one of the most common health problems responsible for outnumbered deaths worldwide. The present chapter discussed the use of green chemistry design, and application principles and eco-friendly synthesis techniques of green nanocomposite for the treatment of cancer with low side effects. Green nanoformulations are effective in the diagnosis of tumor at the initial stage by allowing cellular visualization. Furthermore, prospective applications of green nanocomposite include targeted drug delivery, anti-cancer activity, photo-thermal therapy and bio-imaging. The present chapter provides perspective on the use of anti-cancer green bionanomaterials with a focus on their present status and prospects in the theranostics of cancer.

References

1. Velusamy B, Kaliyaperumal S, and Raju A. (2016). Collection and data-mining of bioactive compounds with cancer treatment properties in the plants of *fabaceae* family. *International Journal of Pharmaceutical Sciences and Research*, **7**(5), 2065.
2. Siegel RL, Miller KD, Jemal A. (2017). Cancer Statistics, 2017. *CA Cancer J Clin.*, **67**:7-30.
3. Ali I, Wani WA, and Saleem K. (2011). Cancer Scenario in India with Future Perspectives. *Cancer therapy*, **8**.
4. Ferlay J, Soerjomataram I, Dikshit R, Eser S, Mathers C, Rebelo M, and Bray F. (2015). Cancer incidence and mortality worldwide: sources, methods and major patterns in GLOBOCAN 2012. *International journal of cancer*, **136**(5), E359-E386.
5. Reya T, Morrison SJ, Clarke MF, and Weissman IL. (2001). Stem cells, cancer, and cancer stem cells. *Nature*, **414**(6859), 105.
6. Chen J, Gu W, Yang L, Chen C, Shao R, Xu K, and Xu ZP. (2015). Nanotechnology in the management of cervical cancer. *Reviews in medical virology*, **25**, 72-83.
7. Choi YE, Kwak JW, and Park JW. (2010). Nanotechnology for early cancer detection. *Sensors*, **10**(1), 428-455.
8. Yang X, Feng Y, He Z, and Stoffella PJ. (2005). Molecular mechanisms of heavy metal hyperaccumulation and phytoremediation. *Journal of trace elements in medicine and biology*, **18**(4), 339-353.
9. Iravani S. (2011). Green synthesis of metal nanoparticles using plants. *Green Chemistry*, **13**(10), 2638-2650.
10. Dziadek M, Stodolak-Zych E, and Cholewa-Kowalska K. (2017). Biodegradable ceramic-polymer composites for biomedical applications: a review. *Materials Science and Engineering: C*, **71**, 1175-1191.
11. Collera-Zúñiga O, Jiménez, FG, and Gordillo RM. (2005). Comparative study of carotenoid composition in three Mexican varieties of *Capsicum annuum* L. *Food Chemistry*, **90**(1-2), 109-114.

12. Namvar F, Azizi S, Rahman HS, Mohamad R, Rasedee A, Soltani M, and Rahim RA. (2016). Green synthesis, characterization, and anticancer activity of hyaluronan/zinc oxide nanocomposite. *OncoTargets and therapy*, **9**, 4549.
13. Chu M, Li H, Wu Q, Wo F, and Shi D. (2014). Pluronic-encapsulated natural chlorophyll nanocomposites for in vivo cancer imaging and photothermal/photodynamic therapies. *Biomaterials*, **35**(29), 8357-8373.
14. Khan M, Khan M, Al-Marri AH, Al-Warthan A, Alkhathlan HZ, Siddiqui MRH, and Adil SF. (2016). Apoptosis inducing ability of silver decorated highly reduced graphene oxide nanocomposites in A549 lung cancer. *International journal of nanomedicine*, **11**, 873.
15. Saikia I, Sonowal S, Pal M, Boruah PK, Das MR, and Tamuly C. (2016). Biosynthesis of gold decorated reduced graphene oxide and its biological activities. *Materials Letters*, **178**, 239-242.
16. Gurunathan S, Han JW, Park JH, Kim E, Choi YJ, Kwon DN, and Kim JH. (2015). Reduced graphene oxide–silver nanoparticle nanocomposite: a potential anticancer nanotherapy. *International journal of nanomedicine*, **10**, 6257.
17. Ali MA, Singh C, Srivastava S, Admane P, Agrawal VV, Sumana , and Malhotra BD. (2017). Graphene oxide–metal nanocomposites for cancer biomarker detection. *RSC Advances*, **7**(57), 35982-35991.
18. Nadagouda MN. (2012). Green synthesis of nanocrystals and nanocomposites. In *Modern Aspects of Bulk Crystal and Thin Film Preparation*. InTech.
19. Mohanpuria P, Rana NK, and Yadav SK. (2008). Biosynthesis of nanoparticles: technological concepts and future applications. *Journal of nanoparticle research*, **10**(3), 507-517.
20. Ingale AG, and Chaudhari AN. (2013). Biogenic synthesis of nanoparticles and potential applications: an eco-friendly approach. *J Nanomed Nanotechol*, **4**(165), 1-7.
21. Baker S, Rakshith D, Kavitha KS, Santosh P, Kavitha HU, Rao Y, and Satish S. (2013). Plants: emerging as nanofactories towards facile route in synthesis of nanoparticles. *BioImpacts: BI*, **3**(3), 111.
22. Jain AK, Das M, Swarnakar NK, and Jain S. (2011). Engineered PLGA nanoparticles: an emerging delivery tool in cancer therapeutics. *Critical Reviews™ in Therapeutic Drug Carrier Systems*, **28**(1).

23. Kendall M, and Holgate S. (2012). Health impact and toxicological effects of nanomaterials in the lung. *Respirology*, **17**(5), 743-758.

24. Bana R, and Banthia AK. (2009). Preparation and characterisation of green nanocomposites of biodegradable poly (vinyl-alcohol-co-ethylene) and wood dust. *Pigment & Resin Technology*, **38**(5), 275-279.

25. Sain M, and Oksman K. (2014). Introduction to Biobased Composite Materials: Their Processing, Properties, and Industrial Applications. In *HANDBOOK OF GREEN MATERIALS: 4 Biobased composite materials, their processing properties and industrial applications*, 1-5.

26. Ingale AG, and Chaudhari AN. (2013). Biogenic synthesis of nanoparticles and potential applications: an eco-friendly approach. *J Nanomed Nanotechol*, **4**(165), 1-7.

27. Lungu O, Sun XW, Wright Jr TC, Ferenczy A, Richart RM, and Silverstein S. (1995). A polymerase chain reaction-enzyme-linked immunosorbent assay method for detecting human papillomavirus in cervical carcinomas and high-grade cervical cancer precursors. *Obstetrics & Gynecology*, **85**(3), 337-342.

28. Choi YE, Kwak JW, and Park JW. (2010). Nanotechnology for early cancer detection. *Sensors*, **10**(1), 428-455.

29. Martirosyan KS, Stafford RJ, Elliott AM, and Frank SJ. (2009). PMMA/SWCNTs composites for prostate brachytherapy MRI contrast agent markers. In *NSTI-NanoTech.* **2**, 44-47.

30. Deng K, Hou Z, Li X, Li C, Zhang Y, Deng X, and Lin J. (2015). Aptamer-mediated up-conversion core/MOF shell nanocomposites for targeted drug delivery and cell imaging. *Scientific reports*, **5**, 7851.

31. Bai RG, Muthoosamy K, Shipton FN, Pandikumar A, Rameshkumar P, Huang NM, and Manickam S. (2016). The biogenic synthesis of a reduced graphene oxide–silver (RGO–Ag) nanocomposite and its dual applications as an antibacterial agent and cancer biomarker sensor. *RSC Advances*, **6**(43), 36576-36587.

32. Rosenthal SJ, Chang JC, Kovtun O, McBride JR, and Tomlinson ID. (2011). Biocompatible quantum dots for biological applications. *Chemistry & biology*, **18**(1), 10-24.

33. Li Z, Xu W, Wang Y, Shah BR, Zhang C, Chen Y, and Li B. (2015). Quantum dots loaded nanogels for low cytotoxicity, pH-sensitive fluorescence, cell imaging and drug delivery. *Carbohydrate polymers*, **121**, 477-485.

34. Bwatanglang IB, Mohammad F, Yusof NA, Abdullah J, Hussein MZ, Alitheen NB, and Abu N. (2016). Folic acid targeted Mn: ZnS quantum dots for theranostic applications of cancer cell imaging and therapy. *International journal of nanomedicine*, **11**, 413.

35. Feng T, Ai X, An G, Yang P, and Zhao Y. (2016). Charge-convertible carbon dots for imaging-guided drug delivery with enhanced in vivo cancer therapeutic efficiency. *ACS nano*, **10**(4), 4410-4420.

36. Ulery BD, Nair LS, and Laurencin CT. (2011). Biomedical applications of biodegradable polymers. *Journal of polymer science Part B: polymer physics*, **49**(12), 832-864.

37. Nair LS, and Laurencin CT. (2005). Polymers as biomaterials for tissue engineering and controlled drug delivery. In *Tissue engineering I*. Springer, Berlin, Heidelberg, 47-90.

38. Ratner BD, Hoffman AS, Schoen FJ, and Lemons JE. (2004). *Biomaterials science: an introduction to materials in medicine*. Elsevier.

39. Das D, Patra P, Ghosh P, Rameshbabu AP, Dhara S, and Pal S. (2016). Dextrin and poly (lactide)-based biocompatible and biodegradable nanogel for cancer targeted delivery of doxorubicin hydrochloride. *Polymer Chemistry*, **7**(17), 2965-2975.

40. Li Q, Wen Y, Wen J, Zhang YP, Xu XD, Victorious A, and Xu X. (2016). A new biosafe reactive oxygen species (ROS)-responsive nanoplatform for drug delivery. *RSC Advances*, **6**(45), 38984-38989.

41. Chen C, Cai G, Zhang H, Jiang H, and Wang L. (2011). Chitosan-poly (ε-caprolactone)-poly (ethylene glycol) graft copolymers: Synthesis, self-assembly, and drug release behavior. *Journal of Biomedical Materials Research Part A*, **96**(1), 116-124.

42. Tu H, Lu Y, Wu Y, Tian J, Zhan Y, Zeng Z, and Jiang L. (2015). Fabrication of rectorite-contained nanoparticles for drug delivery with a green and one-step synthesis method. *International journal of pharmaceutics*, **493**(1-2), 426-433.

43. Bhattacharya SN, Gupta RK, and Kamal MR. (2008). Polymeric nanocomposites. *Hanser, Munich*.

44. Namvar F, Azizi S, Rahman HS, Mohamad R, Rasedee A, Soltani M, and Rahim RA. (2016). Green synthesis, characterization, and anticancer activity of hyaluronan/zinc oxide nanocomposite. *OncoTargets and therapy*, **9**, 4549.

45. Vivek R, Thangam R, Kumar SR, Rejeeth C, Sivasubramanian S, Vincent S, and Kannan S. (2016). HER2 Targeted Breast Cancer Therapy with Switchable "Off/On" Multifunctional "Smart" Magnetic Polymer Core–Shell Nanocomposites. *ACS applied materials & interfaces*, **8**(3), 2262-2279.

46. Fan X, Jiao G, Gao L, Jin P, and Li X. (2013). The preparation and drug delivery of a graphene–carbon nanotube–Fe 3 O 4 nanoparticle hybrid. *Journal of Materials Chemistry B*, **1**(20), 2658-2664.

47. Dong X, Liu L, Zhu D, Zhang H, and Leng X. (2015). Transactivator of transcription (TaT) peptide–chitosan functionalized multiwalled carbon nanotubes as a potential drug delivery vehicle for cancer therapy. *International journal of nanomedicine*, **10**, 3829.

48. Zhang M, Wang W, Cui Y, Chu X, Sun B, Zhou N, and Shen J. (2018). Magnetofluorescent Fe3O4/carbon quantum dots coated single-walled carbon nanotubes as dual-modal targeted imaging and chemo/photodynamic/photothermal triple-modal therapeutic agents. *Chemical Engineering Journal*, **338**, 526-538.

49. Hira I, Kumar A, Kumari R, Saini AK, and Saini RV. (2018). Pectin-guar gum-zinc oxide nanocomposite enhances human lymphocytes cytotoxicity towards lung and breast carcinomas. *Materials Science and Engineering: C*, **90**, 494-503.

50. Deng ZJ, Morton SW, Ben-Akiva E, Dreaden EC, Shopsowitz KE, and Hammond PT. (2013). Layer-by-layer nanoparticles for systemic codelivery of an anticancer drug and siRNA for potential triple-negative breast cancer treatment. *ACS nano*, **7**(11), 9571-9584.

51. Allen TM, and Cullis PR. (2013). Liposomal drug delivery systems: from concept to clinical applications. *Advanced drug delivery reviews*, **65**(1), 36-48.

52. Kang JH, and Ko YT. (2015). Lipid-coated gold nanocomposites for enhanced cancer therapy. *International journal of nanomedicine*, **10**(Spec Iss), 33.

53. Rengan AK, Bukhari AB, Pradhan A, Malhotra R, Banerjee R, Srivastava R, and De A. (2015). In vivo analysis of biodegradable liposome gold nanoparticles as efficient agents for photothermal therapy of cancer. *Nano letters*, **15**(2), 842-848.

54. Wu L, Fang S, Shi S, Deng J, Liu B, and Cai L. (2013). Hybrid polypeptide micelles loading indocyanine green for tumor imaging and photothermal effect study. *Biomacromolecules*, **14**(9), 3027-3033.

55. Sumer Bolu B, Manavoglu Gecici E, and Sanyal R. (2016). Combretastatin A-4 conjugated antiangiogenic micellar drug delivery systems using dendron–polymer conjugates. *Molecular pharmaceutics*, **13**(5), 1482-1490.

Biodegradation and dye adsorption studies of GrA-cl-poly (AAm)-ZTIP organo-inorganic cation exchanger

Rachna Sharma[*1], Balbir Singh Kaith[1]and Rajeev Jindal[1]

[1]*Department of Chemistry*

Dr. B. R. Ambedkar National Institute of Technology, Jalandhar 144 011 (Pb.), India

E-mail: sharmarachna3110@gmail.com

Abstract

Hydrogels are three-dimensional high molecular weight materials. These are also known as crosslinked polymeric networks which have the capacity to hold water or biological fluids within its porous structure without getting disintegrated. These are also called as super absorbents because they can absorb water more than 90%. In 1960, first time hydrogel was synthesized the based on 2-hydroxymethylmethacrylate and ethylene dimethacrylate. This copolymer was used in ophthalmology. Such properties are because of presence of functional groups like –OH, –COOH, $–CONH_2$ and $–SO_3H$. Maximum biocompatible materials can be synthesized through hydrogels because they look like natural tissues. They have high absorption capacity, smoothness, elasticity and low interfacial tension with solutions which makes it worthy for that. They are also called as smart materials because they can react with modification in external environments such as physiological pH, ionic strength, temperature and electric currents. These three-dimensional hydrophilic networks have been used extensively in various fields including biomedical, pharmaceutical, agriculture, horticulture and waste-water treatment.

Classification of hydrogels

Hydrogels can be classified on the basis of their source of origin, monomer composition, structure and ionic charges.

Classification based on origin of source

Natural hydrogels

Hydrogels derived from natural backbones are termed as natural hydrogels e.g. *Gum xanthan*, *Guar gum*, *Psyllium,Gum acacia*.

Synthetic hydrogels

Synthetic hydrogels are derived from synthetic monomers or polymers. For example poly(vinylalcohol), poly(acrylicacid), poly(hydroxyethyl methacrylate) and poly(vinylacetate).

Classification based on monomer composition

Homopolymer hydrogels

These hydrogels are referred to polymer network derived from a basic structural unit *i.e*. monomer. Homopolymers can be crosslinked according to the nature of the monomer and polymerization method used. For example poly(2-hydroxypropylmethacrylate), poly(2-hydroxyethyl methacrylate), poly(ethylene glycol), poly(acrylonitrile), poly(acrylamide) and poly(crotonic acid).

Copolymer hydrogels

Hydrogels of these types have two or more different monomeric units and atleast one of the monomers is hydrophilic in nature. These hydrogels exist in different arrangements for example random, block and alternative on the basis of main polymeric chain. Triblock hydrogel of poly(ethylene glycol)-poly(ε-caprolactone)-poly(ethyleneglycol) has been prepared by some researcher and used it for drug delivery system.

Interpenetrating Polymeric Hydrogels (IPN)

These hydrogels comprise of two unrestricted polymeric networks. In this case, one of the polymeric networks swells within the network of other and resulted the development of IPN possessing cross-linked uncross-linked components.

Classification based on structure

Amorphous hydrogels

These types of hydrogels are optically transparent isotropic networks with unsystematically arranged polymeric chains. The amorphous hydrogel network contained non-homogenous arrangements. They undergo transformation between two phases i.e. from rubbery to glassy state without any demarcation at temperature conditions. Because of such properties, these materials are used in biomedical applications requiring optical transmittance.

Semi-crystalline hydrogels

They consist of complex mixtures of amorphous and crystalline phases with compressed areas of arranged polymeric chains. In these materials, semi-crystalline polymers are immersed in an aqueous medium resulting in the swelling of amorphous regions without any effect on the crystalline part.

Classification based on charge

Neutral Hydrogels

Hydrogels consists of neutral monomeric units are known as neutral hydrogels. Crosslinked monomeric units to form three-dimensional networks might be homopolymeric or copolymeric in nature. Some examples of these type of hydrogels are poly(acrylamide) derivatives, poly(N-vinyl caprolactam) and poly(N-vinyl pyrrolidinone).

Ionic Hydrogels

Monomers with negative and positive charge used to prepare these hydrogels. They can be made through changes in neutral polymers by adding additional of polyelectrolytes.

Anionic hydrogels

These are homopolymers or copolymers of negatively charged acidic or anionic monomers. Nonionic hydrogels can be converted into anionic hydrogels through modification like partial hydrolysis with poly(hydroxyl alkyl methacrylates) or by using additional polyanions. The swelling ratio of anionic hydrogels increases with increase in pH. For example poly(crotonic acid) and poly(acrylicacid).

Cationic hydrogels

Cationic hydrogels are the homopolymers or copolymers of positively charged basic or cationic monomers. These hydrogels can also be synthesized by the modifications of the existing neutral hydrogels. Examples of cationic hydrogels are poly(4-vinyl pyridine) and poly(aminoethyl methacrylate).

Ampholytic Hydrogels

Hydrogels with both cationic and anionic monomeric units are called ampholytic hydrogels. Proteins have positive charge below than its isoelectric point and estimated to react with hydrocolloids with negative charge to get polyion complex hydrogels.

Metals with relatively densities and atomic weight are known as heavy metals. These metals are less reactive than lighter metals and have less soluble sulfides and hydroxides. These metals are using in nearly all aspects of life such as in electronic components, electrodes, and wiring, solar panels, diagnostic imaging, electron microscopy, nuclear science,

colour of glass, ceramic glazes, paints, pigments, and plastics, etc. Heavy metals have serious toxic effects also such as cancer, brain damage, skin and other body parts damage. So, many researchers are working to remove heavy metal ions from the environment.

In this chapter synthesis of zirconium-tungstoiodophosphate based multi-component ion exchangers by incorporating into crosslinked graft copolymers and various parameters such as ion-exchange capacity, thermal stability, pH, chemical stability and distribution studies were studied. Ion-exchangers were characterized using FT-IR, SEM and XRD. Further, they have been evaluated for their thermal behaviorusing TGA/DTA/DTG techniques. After that, synthesized sample has been used to remove heavy metal ions.

GrA-cl-poly(AAm)-ZTIP was synthesized under pressure reaction condition and it showed ion exchange capacity 1.9 $meqg^{-1}$. Effect of temperature on ion exchange capacity was studied and it was observed that hybrid cation exchanger found to possessed higher thermal stability and could retain ion-exchange capacity 0.12 $meqg^{-1}$ at 160^{o}C in GrA-cl-poly(AAm)-ZTIP-UP, respectively. pH titration studies were done with NaCl-NaOH and KCl-KOH solutions and it was observed that cation exchangers synthesized under different reaction conditions are strong exchangers. This study was done with different chemical solutions to find out the effect of ion exchange capacity of the cation exchangers and it was observed that the synthesized cation exchangers are quite stable in water, fairly stable with acids of moderate concentration and unstable in basic solutions. Distribution studies clearly showed that the cation exchangers were found to possess high preference in K_d values in the following order Pb^{+2}> Cd^{+2}> Ca^{+2}> Mg^{+2} in DMW and hence considered to be selective for Pb(II).

FTIR spectrum of GrA-cl-poly(AAm)-ZTIP cation exchanger revealed that peak at 3193.27 cm^{-1} was due to the grafting of poly(acrylamide) chains containing –NH functional groups. Peaks at 1655.09 cm^{-1} and at 1316.36 cm^{-1} were due to –C=O stretching and –NH bending of an amide group, respectively. FTIR spectrum of cation exchanger also revealed the presence of PO_4^{3-}, IO_3^-, WO_4^{2-} and ZrO groups by exhibiting a peak at 1070.90 cm^{-1}, 810.72 cm^{-1}, 612.73 cm^{-1} and 494.90 cm^{-1}, respectively. Cation exchanger showed coherence length more than *Gum rosin* and less than reduced *Gum rosin* which indicated semi-crystalline nature of the sample. SEM showed changes in the surface morphology which confirmed the functionalization of crosslinked graft copolymers with inorganic materials (zirconium-tungstoiodophosphate). Thermal studies of cation exchanger showed that it has good thermal stability due to the functionalization of crosslinked graft copolymers with zirconium-tungstoiodophosphate inorganic materials. IDT of synthesized cation exchangers under pressure was at 186.8 ^oC and FDT was also observed at 743.3 ^oC, respectively. TGA data was also confirmed by DTA and DTG results.

Biodegradation of ion-exchangers were studied using soil composting method and soil burial methods. It was observed that *Gum rosin* was not degraded but derivatized *Gum rosin* degraded completely within 7days. Zirconium(iv)tungstoiodophophate ion-exchanger was found to degrade to the extent of 71.34% after 70 days.

In soil burial method, ion-exchangers synthesized under pressure conditions GrA-cl-poly(AAm)-ZTIP-UP showed 65.28% degradation, after 70 days.

Biodegradation through soil burial was found to show lower weight loss in comparison to the composting method. This can be explained on the

basis that soil contains a lesser number of essential micro-organism colonies required for the biodegradation of the samples, in comparison to the active species of microorganism present in the compost.

The % organic carbon was 0.70%, and 0.74% in control soil and GrA-cl-poly(AAm)-ZTIP-UP, respectively. Thus, % organic carbon was observed higher in polymer degraded samples than control soil sample. Phosphorus and potassium components in control soil sample have been observed 16.9 gm^{-2} and 29.1 gm^{-2}, respectively, whereas, in polymer degraded samples it was found to be in the range of 10.3 gm^{-2} and 25.8 gm^{-2}, respectively.

1.1 Introduction

This chapter deals with the synthesis and characterization of GrA-cl-poly(AAm)-ZTIP crosslinked ion-exchanger synthesized by graft copolymerization using zirconium-tungustoiodophosphate as multicomponent ions with acrylamide-*N'N*-methylene bisacrylamide monomer-crosslinker system onto derivatized *Gum rosin* with potassium persulphate as an initiator in-air reaction condition. Various parameters such as ion-exchange capacity, thermal stability, pH, chemical stability and distribution studies were studied.

Ion exchangers play prominent role in water processing and chemical industries. During last 2-3 decades, many researchers focused on the synthesis of different types of ion-exchangers. The term ion-exchange denotes the processes of decontamination of aqueous solutions with solid ion exchangers. Topp and Pepper (1949) studied cation-exchange properties due to the presence of strongly acidic -SO_3H, weakly acidic -COOH or very weak phenolic -OH group. However, in case of anion-exchanger weakly basic amino groups are responsible for anion-exchange. Hu and Peter (1998) synthesized zirconia based polymeric cation exchangers for the HPLC analysis of proteins. Tetravalent metal acid salts

derivatized by organic moieties in the presence of such groups –OH, –COOH, $–SO_3H$ and –NH into organo–inorganic ion exchangers. A polymeric ion-exchanger is an interesting material, because it has good mechanical stability. Alberti *et al.* (1979) synthesized zirconium bis-(carboxymethanephosphonate) and studied its properties. Khan and Alam (2003) synthesized polymeric ion exchanger,polyanilineSn(IV) tungstoarsenate, with high ion-exchange capacity and stability. Poly(methyl methacrylate) Zr(1V)phosphate ion-exchanger was prepared by methyl methacrylate and Zr(IV) phosphate (Siddiqui *et al.,* 2007). Many researchers worked on masking of the unpleasant taste of drugs using ion-exchange resins. Sriwongjanya and Bodmeier (1998) observed drug release behaviour of ion exchange resins. Kankkunen *et al,* (2002) studied effect of pH-adjusted ion exchange fibers on levodopa drug. Bhise *et al,* (2008) used ion-exchange resins as drug carrier and tastemaker. Junyaprasert and Manwiwattanakul (2008) studied the sustained release behaviour of diltiazem-resin microcapsules.

In the present work an attempt has been made to synthesize the multicomponent organic-inorganic ion-exchanger GrA-cl-poly(AAm)-ZTIP ion under pressure reaction condition.

1.2 Materials and method

1.2.1 Ion-exchange materials

Gum rosin (Gr) and potassium persulphate (KPS) were procured from Himedia and Sd-Fine Chemicals Pvt. Ltd., respectively. *N, N'*-methylene-bis-acrylamide (MBA) and acrylamide (AAm) were purchased from MERCK and used as received. Zirconium oxychloride, sodium tungstate, potassium iodate and orthophosphoric acid were purchased from Sd-Fine Chemicals Pvt. Ltd. Deionized water was used for all types of reactions.

1.2.2 Synthesis

A solution of 0.1 molar zirconium oxychloride was mixed with the 0.5 molar solution of sodium tungstate, potassium iodate and 1 molar solution of orthophosphoric acid, in various volume proportions. Preoptimized amounts of potassium persulphate, MBA and AAm were mixed with reduced *Gum rosin* (1g) and taken in a reaction flask. Reaction was accomplished at preoptimized temperature for a definite time. After completion of reaction the resulting ion-exchanger was cooled to room temperature followed by washing with acetone and was dried. The sample was placed into distilled water (DW) and finally dried at 40ºC. The sample was kept for 24 hours in 1M HNO_3 to adapt the hydrogen ion form. Excess of acid from the obtained material was removed by washing with DW and dried at 40 ºC. The resulting organo-inorganic hybrid ion-exchanger GrA-cl-poly(AAm)-ZTIP was crushed to fine powder (Siddiqui and Khan, 2007).

1.3 Physico-chemical properties of ion-exchanger

1.3.1 Ion exchange capacity (IEC)

The column process was used to determine the IEC of cation exchanger synthesized under pressure, in diverse alkali and alkaline earth metal solutions **(Table 1)**. 0.5g ion-exchanger in H^+ manner was positioned in glass column over the glass wool and excess of acid was removed with distilled water from the cation exchanger. 1.0M solution of diverse alkali and alkaline earth metal chlorides were used in ion exchanger process. The effluent was collected and titrated in contradiction of 1.0M NaOH standard solution of using phenolphthalein indicator to determine total H^+ ions released.

Maximum IEC for K^+ ion was observed to be 1.66 $meqg^{-1}$ for GrA-cl-poly(AAm)-ZTIP-UP. The alkali and alkaline metal ions showed the

following sequence $K^+ > Na^+ > Li^+$ and $Ca^{+2} > Mg^{+2}$. The trend in IEC confirmed that it is dependent upon both ionic radii and hydrated form of the ions (Chand *et al.,* 2011).

Table 1: Ion-exchange capacity of GrA-cl-poly(AAm)-ZTIP-UP with respect to various ions

Exchanging Ions	pH	Ionic Radii (Å)	Hydrated Ionic Radii (Å)	IEC ($meqg^{-1}$)
Li^+	7.0	0.68	3.40	0.73
Na^+	7.0	0.97	2.76	0.89
K^+	7.0	1.33	2.32	1.93
Mg^{2+}	7.0	0.78	7.00	0.81
Ca^{2+}	7.0	1.06	6.30	0.95

where, IEC = maximum ion exchange capacity

1.3.2 Effect of temperature on ion-exchange capacity

The consequences of heat on weight and IEC of the cation exchanger was studied using hot-air oven in which temperature up to 200 ^oC was maintained. For studying the thermal stability, six equal parts of 0.5 g each of the cation exchanger were heated at different temperatures (40-160 ^oC) for one hour in hot-air oven. After heating at specific temperature for a fixed time the samples were cooled down to room temperature in desiccator and were weighed to find the weight loss. IEC of sample was also determined in order to find out the effect of temperature on IECs **(Table 2)**. It was detected from the results that hybrid cation exchanger found to possessed higher thermal stability and could retain ion-exchange capacity $0.23meqg^{-1}$ at 160^oC in GrA-cl-poly(AAm)-ZTIP-UP (Kunhikrishnan and Janardanan, 2002).

Table 2: Ion exchange capacity of GrA-cl-poly(AAm)-ZTIP-UP after heating at different temperatures for 1hr

Temperature (°C)	Change in colour	IEC ($meqg^{-1}$)
50	Light orange	1.93
80	Light orange	0.63
100	Light orange	0.53
120	Light orange	0.44
140	Light orange	0.23
160	Light orange	0.12

where, IEC = maximum ion-exchange capacity

1.3.3 pH Titrations

pH titrations were done by using batch performance (Topp and Pepper, 1949; Chand *et al.,* 2011) **(Table 3. 4)**. The cation exchanger (0.5g) was treated separately using 50 ml NaCl-NaOH and KCl-KOH solutions. Samples were prepared by varying NaCl-NaOH and KCl-KOH solution ratios. Samples were shaked for 6 hours using Electric Rotary shaker and were kept undisturbed for 24 hours to maintain the equilibrium. This was followed by the determination of pH of each solution. It was observed that cation exchangers synthesized under different reaction conditions are strong cation exchangers as showed by the pH value of the solutions at the initial stage when no hydroxyl ions were mixed in system. This might be due to placing the sample in H^+ form in NaOH solution, the ion exchange initiates and the solution become acidic. This was further confirmed through pH titration curves that showed the monofunctional behavior (Pan *et al.,* 2007).

Table 3: pH titrations using different NaCl – NaOH solutions through GrA-cl-poly(AAm)-ZTIP-UP

NaCl Solution (ml)	NaOH Solution (ml)	pH Value
50	0	2.101
45	5	2.108
40	10	2.111
35	15	2.121
30	20	2.137
25	25	2.139
20	30	2.156
15	35	2.159
10	40	2.169
5	45	2.178
0	50	2.204

Table 4: pH titration using different KCl – KOH solutions through GrA-cl-poly(AAm)-ZTIP-UP

KCl Solution (ml)	KOH Solution (ml)	pH Value
50	0	2.181
45	5	2.216
40	10	2.229
35	15	2.242
30	20	2.253
25	25	2.256
20	30	2.261

15	35	2.268
10	40	2.278
5	45	2.288
0	50	2.305

1.3.4 Chemical stability

This study was done to find out the consequences of diverse chemical solutions on IEC of the cation exchangers. 0.5g of sample was equilibrated separately with 25 ml of different chemical solutions for 24 hours. After equilibration, filtration and washing of sample was done by purified water. It was followed by drying at 40 ^{o}C. IEC of the material was observed (Reilley *et al.,* 1959; Chand *et al.,* 2011) and it is clear from the **Tables 5** that the synthesized cation exchangers are quite stable in water, acids of moderate concentration and unstable in basic solutions as the weight loss was observed.

Table 5: Chemical stability of GrA-cl-poly(AAm)-ZTIP-UP in different solutions

Solution	**Weight Before Treatment (g)**	**Weight After Treatment (g)**	**IEC ($meqg^{-1}$)**
DMW	0.50	0.50	1.93
1M HCl	0.50	0.41	0.48
2M HCl	0.50	0.35	1.71
1M HNO_3	0.50	0.40	0.50
2M HNO_3	0.50	0.36	1.66
1M H_2SO_4	0.50	0.41	0.73
2M H_2SO_4	0.50	0.38	2.63

1M CH_3COOH	0.50	0.36	0.27
2M CH_3COOH	0.50	0.34	1.17
1M NaOH	0.50	Dissolve Completely	-
2M NaOH	0.50	Dissolve Completely	-
1M KOH	0.50	Dissolve Completely	-
2M KOH	0.50	Dissolve Completely	-

1.3.5 Distribution studies

In case of cation exchangers synthesized under different reaction conditions distribution studies are shown in **Table 6**. 0.5g of each cation exchanger sample was treated with 20 ml of diverse metal ion solutions. These solutions were shaked for 6hrs to maintain the equilibrium using Electric Rotary shaker and afterwards were kept undisturbed for some time at room temperature. This was followed by titration of the solution against EDTA solution (Reilley *et al.*, 1959). Simultaneously metal ion solutions without cation exchanger were also titrated against EDTA solution. The distribution coefficient (K_d) values were calculated for different metal ions with the help of the following equation:

$$K_d = \frac{I - F}{F}\frac{A}{W}$$

where, I = burette reading for the different metal ion solutions before treatment with a cation exchanger.

F = burette reading for the different metal ion solutions after treatment with a cation exchanger.

A = capacity of different metal ion solution taken

W = weight of the sample

Distribution studies clearly revealed that the cation exchangers have high preference of K_d values in the following order $Pb^{+2} > Cd^{+2} > Ca^{+2} > Mg^{+2}$ in DMW and hence considered to be selective for Pb(II) which is a main contaminating agent in water. This could be explain on the basis of the Donnan membrane effect which is known for the performance of charged particles near a semi-permeable membrane which occasionally fail to distribute consistently across the dual sides of the membrane. Thus, the charged groups in cation exchanger improve permeation of the metal ions and significantly uptake the lead (Pan *et al*., 2007).

Table 6: K_d values of metal ions in DMW using GrA-cl-poly(AAm)-ZTIP-UP

Metal Ion	Taken as	Titrated against	Indicator used	Endpoint color change	K_d (mLg^{-1})
Ca (II)	Nitrate	EDTA	Calcon	Red-Blue	38.70
Mg (II)	Nitrate	EDTA	Erio T	Red-Blue	25.00
Cd (II)	Nitrate	EDTA	Erio T	Red-Blue	57.00
Pb (II)	Nitrate	EDTA	Erio T	Violet-Blue	60.00

where, EDTA = ethylenediaminetetraacetic acid; K_d = distribution coefficient

1.3.6 Dye adsorption studies

The adsorption of industrial dyes such as malachite green (MG) and methylene blue (MB) was studied by batch experiments. Solutions with varied concentrations ranging from 10-50 ppm were prepared. A known weight of ion-exchanger sample was placed in 500 mL dye solution and the effects of initial concentration of dye, physiological pH, sample concentration and temperature on adsorption behaviour were studied. The absorbance of dye solution was measured at 618 nm. The amount of dye

adsorbed per unit mass of hydrogel (q_t) was determined using following equation (Shirsath *et al.,* 2013):

$$q_t = \frac{C_0 - C_t}{M} V$$

where, V = volume of the dye solution, M = the mass of dry hydrogel, C_0 and C_t are the initial and at different time concentrations of dye in mgL^{-1}.

% dye removal was evaluated by the equation.

$$\%\ Dye\ Removal = \frac{C_0 - C_{eq}}{C_0} X\ 100$$

where, C_o is the initial concentration and C_{eq} is the equilibrium concentration of dyes solutions in mgL^{-1}.

1.4 Malachite green and methylene blue dyes removal

Synthesized sample GrA-cl-poly(AAm)-ZTIP cation-exchanger was evaluated for its efficiency in the removal of MG from the water. Different parameters like initial concentration of dye, feed concentrations, physiological pH and temperature were optimized in order to get the maximum uptake of dye through the test sample.

1.4.1 Effect of initial concentration of dye

The effect of malachite green and methylene blue dyes were investigated by varying the initial concentration of dye from 10-50 ppm. It was observed that the percentage dye removal **(Figs. 1a-2a)** through GrA-cl-poly(AAm)-ZTIP-UP cation-exchanger decreases from 96%-80.1% and 95%-73%, respectively. The obtained trends can be due to strong electrostatic interaction between functional groups of the GrA-cl-poly(AAm) and dye molecules resulting in high adsorption and removal. Thus, at concentration 10-50 ppm of MG dye, percentage dye removal decreases (Zheng *et al.,* 2014).

1.4.2 Effect of feed concentration

The effect of GrA-cl-poly(AAm)-ZTIP dose on the removal of MG dye was observed by using different amounts of sample. Percentage dye removal was found to increase with increase in feed dose. The higher dye removal 96.4% and 95% was obtained with 500mg dose through GrA-cl-poly(AAm)-ZTIP-UP cation-exchanger **(Figs. 1b-2b)**. It was observed that higher amount of sample dose provides a large number of active adsorbent sites for the removal of dye (Patel and Patel, 2013).

1.4.3 Effect of pH of aqueous medium

The pH of aqueous medium interrupts the external charge of the cation-exchanger alongwith and adsorption of other ions. The adsorptive process also affected by a change of pH through disconnection of functional groups on the active spots of the exchanger. Effect of pH on % removal of MG with GrA-cl-poly(AAm)-ZTIP cation-exchanger is shown in **Figs. 1c-2c**. GrA-cl-poly(AAm)-ZTIP cation-exchanger prepared in-air had maximum adsorption 96% over the pH 7.0. Malachite green becomes protonated at lesser pH and deprotonated at greater pH. Since, dye molecules have great positive charge density at a lesser pH, so, an electrostatic repulsion occurred between the +ve charged exchanger and dye molecule at lower pH. Thus, it is comprehended that adsorption increases with rise in pH. However, at higher pH (more than 7.0) lower adsorption of dye was found because of the presence of an excess of negative ions which forms a screen between surface ions and dye ions. Thus, it may be seen that dye removal is extreme at pH 7.0 (Iqbal *et al.,* 2007).

1.4.4 Effect of temperature

The effect of temperature on % dye removal has been studied ranging from 30 ^{o}C–70 ^{o}C and results are shown in **Figs 1d-2d**. Maximum percentage dye removal 97% and 96% observed at 30 ^{o}C followed by decreasing trend at higher temperature as the adsorption process exists as an exothermic procedure. It could be clarified basis of solubility of dye; adsorbate–adsorbent interactions decreased with increase in solubility and resulted in decreased percentage dye removal at a higher temperature. Desorption process was also observed at higher temperature (Bajpai *et al.,* 2012).

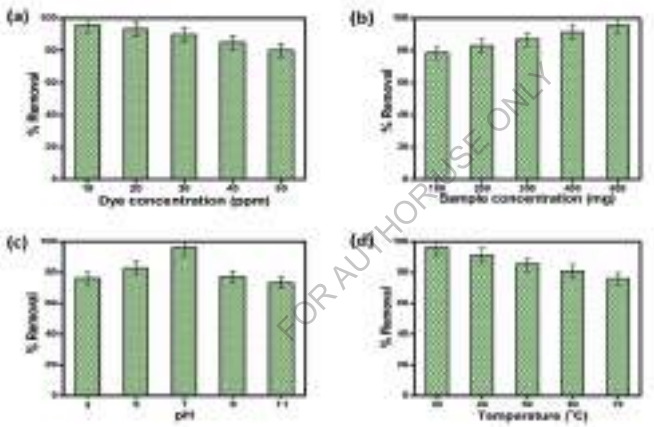

Figs 1.0 a-d: (a) Effect of MG dye concentration, (b) Effect of sample dose, (c) Effect of pH and (d) Effect of temperature on MG dye removal using GrA-cl-poly(AAm)-UP

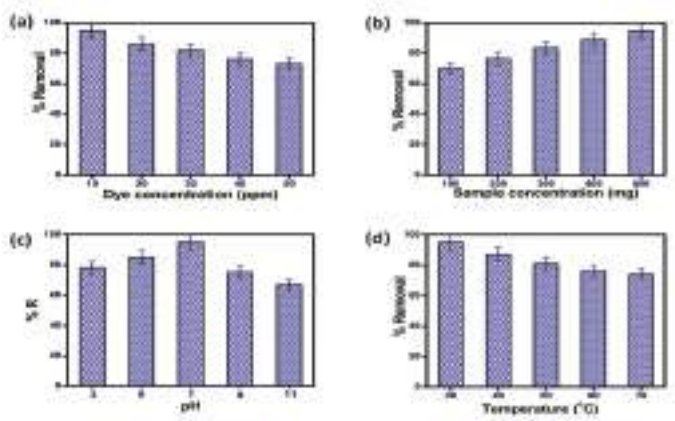

Figs. 2.0 a-d: (a) Effect of MB dye concentration, (b) Effect of sample dose, (c) Effect of pH and (d) Effect of temperature on MB dye removal using GrA-cl-poly(AAm)-UP

1.5 Biodegradation studies of the synthesized hydrogels and ion-exchangers

1.5.1 Composting method

Gum rosin and synthesized crosslinked samples were exposed to biodegrade by composting method (Mittal *et al.,* 2013; Saruchi *et al.,* 2015). The compost was contained in the pots. 10 samples with known weights were taken and hidden in the compost at equidistance. As we know, the compost contained the diversities of actively developing microbial species to degrade the samples. Therefore, aqueous solution from the dump release was used regularly to feed the microbial species in the compost to preserve the population balance. The aqueous level of the pots was sustained in a way that it was just touched to the outside of the compost. Water was added at each alternative day to prevent drying through evaporation. Weights of polymers were taken at regular interval of 7days by rinsing with water and drying at 50 ^{o}C. Percentage degradation

(%D) was calculated as using following equation (Saruchi *et al.,* 2015; Sharma *et al.,* 2016).

$$\%D = \frac{W_i - W_f}{W_i} X\ 100$$

where, W_i is initial weight and W_f is and final weight of samples, respectively.

1.5.2 Soil burial method

Gum rosin and synthesized samples were exposed to biodegrade by soil burial process. The soil for these studies was collected from the garden of NIT Jalandhar and the samples were hidden into soil. The water level was sustained in a way that it was just touched to the outside of the soil. Water was added each day to refill the drying through vaporization. The polymers were placed 3cm spaced out in the soil. Weights of polymers were observed at each 7 days.

1.5.3 Biodegradation study using composting method

Biodegradation of *Gum rosin* based hydrogels and ion-exchangers were studied using soil composting method. No degradation was observed in case of *Gum rosin* because of hydrophobic nature which is mainly due to hydrophenanthrene group but derivatized *Gum rosin* degraded completely due to hydrophilic nature within 7 days **(Table 6)**. Ion-exchanger prepared under pressure condition with zirconium(iv)tungstoiodophophate was found to degrade to the extent of 71.34% after 70 days **(Table 6, Fig. 3a)**.

During soil composting method, calculation of % wt loss is a significant technique to check the biodegradation performance of samples. Moreover, biodegradation of samples under composting medium occurred because of attack of microbes that caused in discontinuity of chemical bonds.

1.5.4 Biodegradation Studies using Soil Burial Method

No degradation was observed in case of *Gum rosin* even after 70 days but instead, derivatized *Gum rosin* was completely degraded after 7 days **(Table 7)**. Ion-exchangers synthesized under pressure reaction condition i.e., GrA-cl-poly(AAm)-ZTIP-UP showed 65.28% degradation after 70 days **(Table 7, Fig. 3b)**.

Biodegradation through soil burial method was observed with lesser weight loss than the composting method. The reason behind this might be presence of less microbe colonies in soil burial in comparison to the microorganism existing in the compost. The ion-exchangers synthesized under pressure reaction conditions degraded underneath soil burial method as a result of destruction of the big molecular chains into low molecular weight parts and breakage of covalent bonds by active bacterial species present in the soil (Mittal *et al*., 2013a).

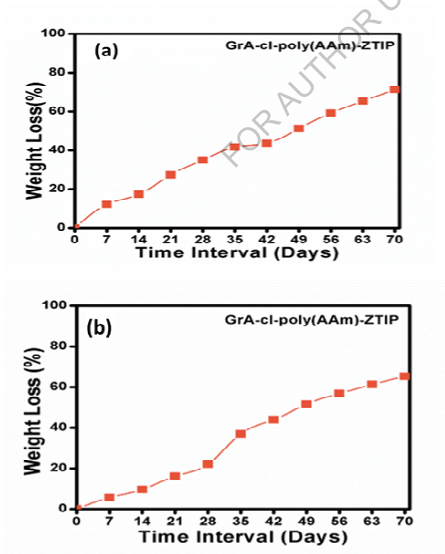

Figs. 3.0a-b: Biodegradation Studies of Samples Synthesized Under Pressure (a) Soil Composting Method (b) Burial Method

Table 6: Biodegradation Studies of Ion-exchanger using Soil Composting Method

Sample Code	% weight loss at different time intervals (Days)									
	7	**14**	**21**	**28**	**35**	**42**	**49**	**56**	**63**	**70**
Gum rosin	0.0	0.0	0.0	0.0	0.0	0.0	0.0	0.0	0.0	0.0
Der. *Gum rosin*	100.00	100.0	100.0	100.0	100.0	100.0	100.0	100.0	100.0	100.0
GrA-cl-poly(AAm)-ZTIP-UP	12.15	17.29	27.42	35.05	41.68	43.68	51.23	59.18	65.42	71.34

Table 7: Biodegradation Studies of Ion-exchanger using Soil Burial Method

Sample Code	% weight loss at different time intervals (Days)									
	7	**14**	**21**	**28**	**35**	**42**	**49**	**56**	**63**	**70**
Gum rosin	0.0	0.0	0.0	0.0	0.0	0.0	0.0	0.0	0.0	0.0
Der. *Gum rosin*	100.00	100.0	100.0	100.0	100.0	100.0	100.0	100.0	100.0	100.0
GrA-cl-poly(AAm)-ZTIP-UP	5.73	9.63	16.15	22.13	37.01	43.98	51.65	56.84	61.28	65.28

1.5.5 Impact of biodegradation of synthesized samples on soil

Soil analysis has been done to study the impact of biodegradation of samples on soil fertility. Sandy loam soil was used for soil burial method. Soil pH, organic C, K and P contents were analyzed.

Control soil and samples of degraded soil were chemically analyzed and it was observed that control soil possessed pH 7.5 (i.e. neutral pH), whereas soil containing degraded ion-exchanger sample showed pH 7.2. It is clear that there was no extreme change in pH of soil samples and it was found under permissible range (6.5-8.7). The % organic carbon was 0.70% and 0.74% in control soil and GrA-cl-poly(AAm)-ZTIP-UP, respectively. Thus, %organic carbon was observed higher in degraded ion-exchanger samples than control soil sample. Phosphorus and potassium components in control soil sample have been observed 16.9 gm^{-2} and 29.1 gm^{-2}, respectively, whereas in degraded ion-exchanger samples it was found to be in the range of 10.3 gm^{-2} and 25.8 gm^{-2}, respectively **(Table 8)**.

Table 8: Analysis of soil samples containing biodegraded chemically synthesized candidate polymers

S. No.	Samples	pH	C (%)	P (g/m^2)	K (g/m^2)
1	Control	7.5	0.70	16.9	29.1
2	GrA-cl-poly(AAm)-ZTIP-UP	7.2	0.74	10.3	25.8

where, C = organic carbon; P = phosphorus; K = potassium.

1.6 Conclusions

GrA-cl-poly(AAm)-UP exhibited good ion-exchange capacity. This was due to more functionalization of organic matrix with inorganic ions as compared to the samples synthesized in-air and under vacuum. The synthesized ion exchangers were found to be more selective towards the removal of Pb^{2+} followed by Cd^{2+}> Ca^{2+} and Mg^{2+} metal ions. The synthesized ion exchangers were further found to remove efficiently the malachite green and methylene blue dyes from aqueous medium.

In case of soil composting method, it has been found that %D was higher in synthesized hydrogels as compared to ion-exchangers. After the period of 70 days, ion-exchangers exhibited 71% degradation, respectively. In ion-exchanger, there is ZTIP interpenetrates in hydrogels matrix, which makes it more complex and difficult for bacteria to degrade the samples. Similar behavior of percentage degradation has been found in case of burial conditions. It has also been observed that degradation of ion-exchangers was higher in case of composting method as compared to soil burial method. Presence of the large number of bacterial colony in compost degraded the samples through the cleavage of both primary and secondary bonding at a faster rate.

References

Alberti, G., Costantino, U., Giovagnotti, M. L. L. 1979. "Synthesis and ion-exchange properties of zirconium bis-(carboxymethanephosphonate), a new organic-inorganic ion exchanger." Journal of Chromatography A, 180, 45–51.

Bajpai, S. K., Chand, N., Mahendra, M. 2012. "The adsorptive removal of cationic dye from aqueous solution using poly (methacrylic acid) hydrogels: part-I. equilibrium studies." Int J Environ Sci, 2, 1609–1624.

Bhise, K., Shaikh, S., Bora, D. 2008. "Taste mask, design and evaluation of an oral

formulation using ion exchange resin as drug carrier." AAPS PharmSciTech, 9, 557–562.

Chand, S., Seema, A., Chahal, C. V. 2011. "Synthesis, characterization and ion exchange properties of a new ion exchange material: bismuth (iii) Iodophosphate." Recent Research in Science and Technology, 3, 1-8.

Hu, Y., Carr, P. W. 1998. "Synthesis and characterization of new zirconia-based polymeric cation-exchange stationary phases for high-performance liquid chromatography of proteins." Analytical Chemistry, 70, 1934–1942.

Iqbal, M. J., Ashiq, M. N. 2007. "Adsorption of dyes from aqueous solutions on activated charcoal." Journal of Hazardous Materials, 139, 57–66.

Junyaprasert, V. B., Manwiwattanakul, G. 2008. "Release profile comparison and stability of diltiazem--resin microcapsules in sustained release suspensions." International Journal of Pharmaceutics, 352, 81–91.

Kankkunen, T., Huupponen, I., Lahtinen, K., Sundell, M., Ekman, K., Kontturi, K., Hirvonen, J. 2002. "Improved stability and release control of levodopa and metaraminol using ion-exchange fibers and transdermal iontophoresis." European Journal of Pharmaceutical Sciences, 16, 273–280.

Khan, A. A., Alam, M. M. 2003. "Synthesis, characterization and analytical applications of a new and novel 'organic--inorganic'composite material as a cation exchanger and Cd (II) ion-selective membrane electrode: polyaniline Sn (IV) tungstoarsenate." Reactive and Functional Polymers, 55, 277–290.

Kunhikrishnan, M. J., Janardanan, C. (2002). "Synthesis and analytical application of lead selective thorium iodate cation exchanger." Indian Journal of Chemical Technology, 9, 420–423.

Mittal, H., Fosso-Kankeu, E., Mishra, S. B., Mishra, A. K. 2013. "Biosorption potential of Gum ghatti-g-poly (acrylic acid) and susceptibility to biodegradation by B. subtilis." International Journal of Biological Macromolecules, 62, 370–378.

Pan, B. C., Zhang, Q. R., Zhang, W. M., Pan, B. J., Du, W., Lv, L., Zhang, Q. J., Xua, Z. W., Zhang, Q. X. 2007. "Highly effective removal of heavy metals by polymer-based zirconium phosphate: a case study of lead ion." Journal of Colloid and Interface Science, 310, 99–105.

Patel, Y. N., Patel, M. P. 2013. “Adsorption of azo dyes from water by new poly (3-acrylamidopropyl)-trimethylammonium chloride-co-N, N-dimethylacrylamide superabsorbent hydrogel—Equilibrium and kinetic studies.” Journal of Environmental Chemical Engineering, 1, 1368–1374.

Reilley, C. N., Schmid, R. W., Sadek, F. S. 1959. “Chelon approach to analysis: I. Survey of theory and application.” J. Chem. Educ, 36, 555.

Saruchi., Kaith, B. S., Jindal, R., Kumar, V., 2015. “Biodegradation of Gum tragacanth acrylic acid based hydrogel and its impact on soil fertility.” Polymer Degradation and Stability, 115, 24–31.

Sharma, K., Kumar, V., Chaudhary, B., Kaith, B. S., Kalia, S., Swart, H. C. 2016. “Application of biodegradable superabsorbent hydrogel composite based on Gum ghatti-co-poly (acrylic acid-aniline) for controlled drug delivery.” Polymer Degradation and Stability, 124, 101–111.

Shirsath, S. R., Patil, A. P., Patil, R., Naik, J. B., Gogate, P. R., Sonawane, S. H. 2013. “Removal of Brilliant Green from wastewater using conventional and ultrasonically prepared poly (acrylic acid) hydrogel loaded with kaolin clay: a comparative study.” Ultrasonics Sonochemistry, 20(3), 914–923.

Siddiqui, W. A., Khan, S. A. 2007. “Synthesis, characterization and ion exchange properties of zirconium (IV) tungstoiodophosphate, a new cation exchanger.” Bulletin of Materials Science, 30, 43–49.

Sriwongjanya, M., Bodmeier, R. 1998. “Effect of ion exchange resins on the drug release from matrix tablets.” European Journal of Pharmaceutics and Biopharmaceutics, 46, 321–327.

Topp, N. E., Pepper, K. W. 1949. “Properties of ion-exchange resins in relation to their structure. Part I. Titration curves.” Journal of the Chemical Society, 3299–3303.

Zheng, Y., Zhu, Y., Wang, A. 2014. “Highly efficient and selective adsorption of malachite green onto granular composite hydrogel.” Chemical Engineering Journal, 257, 66–73.

Eco-Friendly Nanomaterials: A Way Forward to Climate Change Mitigation

Shweta Yadav

Department of Environmental Sciences, Central University of Jammu, Bagla (Rahya Suchani), Samba, Jammu (J&K) – 181143

E.mail: Shweta.evs@cujammu.ac.in

Abstract:

Nanoscale understanding and development of eco-friendly materials with cognizance of other techniques assist in introducing new, innovative and sustainable energy efficient alternatives. Climate change is a long term consequence of human expansion and it may further amplify with increasing green house gases (GHGs) emissions and particulate pollution. The use of eco-friendly nano-composites with low cost and biodegradable nature such as bio-fibers and bio-polymers can replace plastics and thus provide a green and clean solution. Nanotechnology provides a two way approach in providing respite from the problem of climate change. The development and application of green composites reduce the burden on usage of fossil fuels, decrease GHGs emissions and as are biodegradable, need no expensive waste disposal techniques. On the other hand, nanotechnology helps in developing energy efficient innovations to meet the increasing demand for living. From testing of nanomaterial based batteries and fuel cells for electric vehicles to the revolution of photovoltaics for harnessing solar energy, biodegradable nanomaterials have shown an opportunity to address the issue of climate change. The advanced solar cells with nanoparticles are cheaper as well as efficient in producing more solar energy than the traditional ones. Recent research shows that the use of nanoparticles as fuel additives has resulted into

saving of tonnes of carbon dioxide per year. This chapter summarizes the priority areas where testing and usage of biodegradable nanoparticles has shown the climate change mitigation potential.

1. Introduction

The climate system is complex and it is important to understand the climate and its associated short term and long term variations. Global warming is defined as an increase in combined surface air and sea surface temperatures averaged over the globe and over a 30-year period. The Global warming of 1.5 °C or so has resulted into consequences like sea level rise, floods hazards, intense droughts and extreme events, which has further posed a major threat to human health and biodiversity (IPCC special report on Global warming of 1.5 °C). The present warming levels are due to anthropogenic influence and thus the scientific community is searching for solutions to combat the alarming levels of pollution and greenhouse gases.

Nanotechnology has emerged as a promising field and can be used in various sectors to control and contribute towards combating the problem of global warming and alarming levels of pollution. The important areas where nanotechnology can be applied are: a) environmental remediation, b) clean energy alternatives, c) energy storage devices, d) fuel additives, e) green synthesis of noble metals etc. Figure 1 shows the application of nanotechnology in various sectors. The application of nanomaterials has significant direct and indirect implications on the climate system.

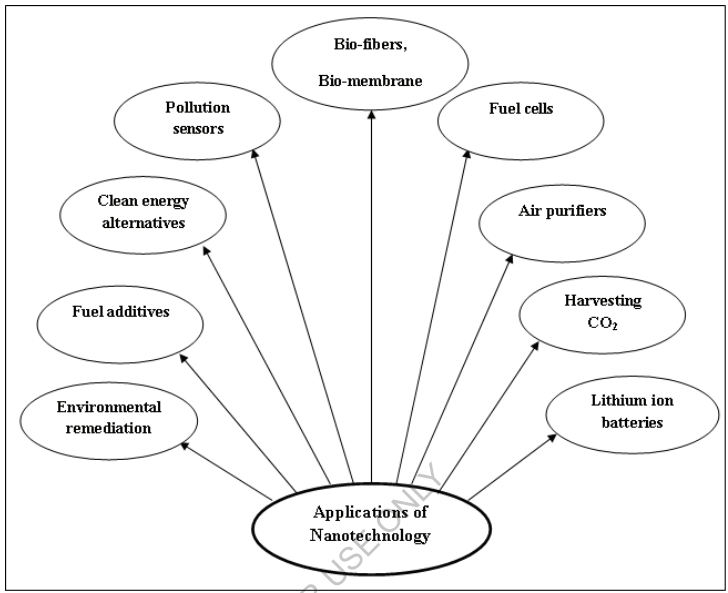

Figure 1: Application of nanotechnology in various sectors.

The environmental friendly approaches to use natural products in nanomaterials result in pollution control at source, while the nanodevices to measure and control the pollutants already present in environment offer promising solutions to the increasing problem of pollution. The nano scale fuel additives can cut down the Green house gas emissions and can directly contribute to reduce the threats posed by global warming. The usage of fuel additives should result in improved engine efficiency, saving of millions of carbon dioxide per annum and also reduction of the harmful emissions in form of particulates and gases. Though, the impacts of fuel additives on human health, biodiversity and overall environment need to be evaluated. There is an ongoing quest to test and produce newly improved and advanced nanomaterials to address the challenge of climate change.

2. Nanomaterials and environmental remediation

Industrialization along with increasing population pressure has led to high levels of environmental pollution in the form of air, water and soil contaminants. These environmental pollutants have adverse health effects and also results in long term implications to our climate. Nanomaterials consisting of organic and inorganic constituents are commonly used in purification of air, water and soil through physical, chemical and biological treatment. Their nano size allows much greater surface area, better adsorbtion properties and efficient interactions/reactions to remove impurities (Yunus et al. 2012). The waste water treatment plants use nanomaterials in beads, powder or slurry form to remove heavy metals and other contaminants. The two methods of water purification include: a) Pump and Treat Method (PTM) and b) Permeable Reactive Barrier (PRB). The nanometrials made up of zero valent Iron (ZVI) are efficiently used in treatment of contaminants like Cu^{2+}, CrO_2^{2-} etc. The antimicrobial nanomaterials fall into two broad categories: Naturally occurring and artificially engineered nanomaterials. They directly and indirectly interact with microbes (Li et al., 2008). Nanotechnology and Nanomaterials have been used to abate the problem of air pollution in several different ways. Nano-catalysts with increased surface area could be used in catalytic convertors to transform harmful exhaust gases/vapours from vehicles and industries into harmless gases. One such catalyst is manganese oxide nano particle based nanofibre catalyst that has been used to treat industrial emissions for volatile organic compounds. Nano particles of Gold have also been proved very effective in catalyzing the conversion of highly toxic CO to CO_2. Chen and Goodman (2006) hypothesized that it is the quantum size effect of gold nanoparticles responsible for this oxidative conversion of CO into CO_2.

2.1 Removal (Reduction) of Air Pollution

Carbon nanotubes (CNTs) have exhaustively been studied for their role in purification of air owing to their unique structural features with abundant pores, large surface-to-volume ratio, and strong adsorption and desorption capabilities for gases. The use of CNTs as efficient gas absorbent is based on the findings that absorption of gas molecules on the surface of CNTs changes the shape of CNTs and trigger redistribution of electrons, leading to a macroscopic change in resistance (Zhang et al. 2010). CNT can trap gases up to a hundred times faster than other methods, allowing integration into large-scale industrial plants and power stations feasible.

Use of nanostructured membranes having pores small enough to separate methane or CO_2 from exhaust could be another approach, which can be used to reduce air pollution at source. Kowalczyk and Holyst (2008) reported that nanostructured membranes composed of single-walled carbon nanotubes (SWCNTs) can efficiently be utilized as nanoscale vessels for selective encapsulation of tetrafluoromethane and, the rate of adsorption is directly related to the pore size of the nanotubes. Unlike conventional membranes that can either only separate or process gaseous substances, this CNT-based technology is capable of doing both separation and processing effectively even for large volumes of gas. Using CNT-based technology, a method has been developed to filter and collect soot particles from diesel fuel emissions and recycle it to synthesize the SWCNT filter through laser vaporization (Uchida et al., 2006). Long and Yang (2001) reported that CNTs could also be used as an adsorbent for the removal of NO. Here also, NOx adsorption relied on the unique structures, electronic properties and surface functional groups of CNTs. When NO and O_2 pass through CNTs, NO is

oxidized to NO_2 and then adsorbed on the surface of nitrate species. This idea was also supported by Mochida et al. (1997).

Pitoniak et al. (2005) studied mercury vapour removal efficacy of Silica-Titania nanocomposites. They tried to amalgamate, high surface area of nanosilica and unique photoctalytic property of titania molecules to make a novel nanocomposite for improved mercury absorption. They have shown that reduced contact angle up to 10° ensures superior mercury removal efficiency by this silica-titania nanocomposite. Sinha and Suzuki (2007) developed a new material comprising of highly porous manganese oxide with gold nanoparticles that is very effective for removing Volatile Organic Compounds (VOCs) from air at room temperature. They also tested the performance of this material three major indoor organic air pollutants: acetaldehyde, toluene and hexane and found that all three pollutants in the air were very effectively removed and degraded by this catalyst compared with the conventional catalyst systems based on photocatalysts, adsorbents such as activated carbon or ozonolysis.

Nanofiber based membrane air filters, with fiber diameters in the range of 10 to 1000 nm, have demonstrated better efficiency in comparison to conventional microfibrous air filters for $PM_{2.5}$ removal. These nanofibrous membrane air filters are endowed with high specific surface area, high porosity, inter-connected porous structure, low resistance to airflow, more active sites, easy functionalization ability, and good mechanical strength (Chang et al., 2018). As $PM_{2.5}$ particles are mostly polar in chemical nature as comprised of different ionic species, nanofibrous membranes with high polarity have been made to aim at high adhesion interactions between $PM_{2.5}$ and the nanofibers. It has also been observed that the $PM_{2.5}$ capture continues with the attachment of incoming particles onto a pre-

existing particle along the fibers and finally merge together leading to stable sphere-shaped aggregates around the nanofibers (Liu et al., 2015).

2.2 Sensors for Air Pollutants

Fast, precise and sensitive sensors able to detect pollutants at low level of concentrations are highly desirable in the present era of rapid urbanization to monitor criteria pollutants ensuring healthy ambient atmosphere. Nanocontact sensors have been developed with potential to detect some metal ions without preconcentration. With the development of such sensors, it has been possible to detect some heavy metals including radioactive elements onsite in very economical manner. Because of their miniature size construction and their automatic operations, these nanocontact sensors can easily be used onsite. In addition, as these sensors are made with conventional microelectronics manufacturing equipment using simple electrochemical techniques, their use in large monitoring networks becomes very cost effective (Masciangioli and Zhang, 2011).

Detection of gaseous pollutants such as NO_2 and NH_3 using single walled carbon nanotubes (SWCNTs) based sensors have shown a faster response and higher sensitivity than the conventional probes those are currently used. In these sensors, pollutant gas molecules are directly bonded to the surface of SWCNTs leading to corresponding change in electrical resistance of the sensor. These SWCNTs based sensors have been proved advantageous as they achieve high sensitivity at room temperature (Smart et al., 2006).

2.3 Carbon dioxide Capture

In this era of industrialization, we are forced to depend in fossil fuels. In such scenario, to reduce ever-increasing effects of the global warming, it is a pressing need to develop cost effective and energy efficient technologies for carbon dioxide

(CO_2) capture (Ashley et al., 2012). Yaghi et al. (1995) have also developed new materials for inexpensively capture of CO_2 efficiently and selectively. This development was based on the organic ligand molecules that can get associated with multiple metal ions forming an extended porous network. So, materials based on metal organic frameworks (MOFs) were used to make tiny "cages" capable of capturing CO_2. These MOFs were found to be 2–3 times more efficient than conventional sorbents in absorbing CO_2. The captured CO_2 can be released from the MOF by pull of a vacuum and can then be pumped deep into the Earth where it becomes stable in the form of carbonate minerals. For the purpose of CO_2 capture, MOF 210, with highest surface area and highest selectivity, an amine functionalized mmen-CuBTri MOF have been used most routinely. Recently, new materials have been developed based on MOFs having potential for gas separation and CO_2 capture (Eddaoudi et al., 2002; Wang et al., 2008; Furukawa et al., 2010). These MOFs are built of self-assembly of metal ions and organic linkers and have large surface areas, adjustable pore sizes, and controllable surface properties, imparting them unique characteristics, including high selectivity for CO_2 (Wu et al., 2010). Significant amount of CO_2 can be absorbed even at low pressure by high-density of open metal sites present in these MOFs (Yazaydın et al., 2009). Now, it is the ability of the investigator to design these MOFs as adsorbents that can be fine-tuned in pore size, shape, and chemical functionality. Researchers have also been attempting to increase the adsorption capacity of MOFs along with increasing CO_2 selectivity. In order to accomplish this, they have to use a nitrogen-functionalized organic linker while retaining a porous MOF that interacts with CO_2 (Ortiz et al., 2011). Overall, studies focusing on the carbon capture by MOFs based nano-materials suggest the significant advantage of MOFs over the more traditional zeolites in both adsorption selectivity and capacity (Rajamani, 2012).

Microporous organic polymers (MOPs), in which the processability of polymers are combined with the high surface area of porous materials, are also of great interest for carbon capture. Specifically, polymers of intrinsic microporosity (PIMs) have been studied as they display good solubility, high gas permeability and selectivity, and slow physical aging. In order to improve CO_2 separation in MOPs, tetrazole groups, which have a high CO_2 affinity, have also been combined with PIMs (Du et al., 2011). Recently Supported Ionic Liquid Membranes (SILMs) technique has attracted the interest of scientific community for their usage in CO_2 capture. SILMs comprises of organic cation balancing with an inorganic anion embedded in porous membrane support such as polyvinylidene fluoride, nylon and Nafion membrane etc. In these membranes, ionic liquids are liquids at room temperature with various advantages such as non-flammability, high thermal stability, low volatility (Rogers and Seddon, 2003; Noble and Gin 2011).

3. Clean energy options for sustainable future

The development of clean energy solutions is the need of hour to combat climate change and associated implications. To follow and sustain on the path of development which is environment friendly, economically viable and socially acceptable, there is an urgent need to search for technological advancement in this field. Renewable sources of energy present a practical, environment friendly and cost effective solution to the increasing energy demand. The use of nanomaterials in various types of renewable energy sources viz. solar, wind, tidal, biomass, hydrogen, geothermal has improved the renewable energy sources to the next level. The solar collectors and devices depend upon the amount of solar energy reaching the earth's surface, which generally varies at different times of the day and in different seasons in a year. The efficiency of these devices has been improved by intervention of nanomaterials. The use of nanomaterials facilitates the larger

exposure of conducting surface and also result in enhanced release of electrons per photon received from sun. Three types of solar cells with nanomaterial based improvements include: a) Dye-sensitized solar cell (DSSC), b) Organic-polymer-based PV solar cell (OPV) and c) Hot carrier solar cells. The details are described elsewhere (Hussein 2015). The use of advanced nanomaterials in solar devices increase the efficiency in various ways: Efficient absorption of sunlight falling on the panel, improved performance of the receiver, selective absorption of solar energy by nanofluids, easy passage of nano scale size particles through pumps, improved thermal conductivity of nanofuids, decreased pollution levels, diverted angle of exciton diffusion by unique nano-wire based solar collector etc. (Taylor et al., 2011; Otanicar and golden, 2009, Yuhas and Yang, 2009).

The hydrogen energy capture by fuel cells has resulted into a new revolution for providing alternative energy source. The fuel cell works on the principle of conversion of chemical energy of selected fuels like hydrogen into the electrical energy in presence of an oxidizing agent. The larger surface to volume ratio allows the use of nanomaterials as catalysts and electrodes in fuel cells. In harnessing hydrogen energy, one of the biggest challenges remains is the efficient storage of hydrogen. The eco-friendly carbon nanotubes, nanofilters and nanoblades are increasingly used for efficient storage of hydrogen. The use of carbon nanotubes in fuel cells results in improvement of mechanical strength of electrolyte membranes, efficient adsorption of hydrogen and thus overall performance of the fuel cell, (Zuttel et. al, 2002, Zhang and Silva, 2011). Hydrogen energy in internal combustion engines is considered a cleaner fuel as it does not result in emission of harmful gases. The new and improved designs of diesel engines also include the usage of nanomaterials for efficient combustion processes. The alumina coated

aluminium nanoparticles have shown a promising alternative for highly efficient designs of diesel engines (Kao et al., 2005).

Another form of renewable source of energy is the biomass energy. The easy availability of biomass (Organic material coming from plants and animals) and the cost effective approach of harnessing biomass energy with almost no harmful environmental effects has made it a very attractive source of energy in today's scenario. The biomass stores the sun's energy through a very natural process of photosynthesis. The important types of biomass include: animal waste and sewage, woods, agricultural waste, crop residue, plant refuse, garbage etc. When biomass is burnt, the chemical energy stored in biomass is released as heat. Apart from this, biomass can be used to produce biofuels and biogas. The efficient conversion of biomass energy into other forms is done by a process called nanobiocatalysis. The intervention of nanotechnology in biocatalysis has made the process quite cost effective and less time consuming. The nano scale enzyme immobilization with the advancement in coatings of enzyme aggregates have resulted in reduced enzyme loadings and increased stability. Nanomaterials based upon nickel and cobalt have resulted into very efficient biofuel production. When used separately or in combination, these nanomaterials have resulted into increased biofuel yields and selective reduction of certain functional groups. The nanosize TiO_2 based photocatalysts are used as very good substitutes in many applications. The conventional methods often result in low yields and time consuming processes. Another good example is the biofuel production from spent tea. It has been noticed that the biofuel production from spent tea can be efficiently done at a much faster rate in the presence of nanoparticles of cobalt as green catalysts. The use of nanoparticles as catalysts in biofuel production from algal biomass has been optimized in recent times and the best added advantage of this relatively faster

process is organism survival at the end of the process (Malik and Sangwan, 2012 and references therein).

The green synthesis of Titanium dioxide nanoparticles for usage in Lithium ion batteries can improve the electrochemical efficiency and overall performance of Lithium ion batteries. Kashale et al., 2016 discussed the biosynthesis of Titanium dioxide nanoparticles using waste water from soaked Bengal gram beans. Their experiments show that on soaking, the autolysis of cell wall results in release of pectin from Bengal gram beans, which gets bound to Titanium, on addition of $TiCl_4$ and at the end nano scale TiO_2 particles are formed after calcinations (Kashale et al. 2016).

4. Cellulose based nanomaterials and their role in combating Global warming

Cellulose is a most abundant naturally occurring polymer with unique morphological structure. It is a polysaccharide with highly porous network consisting of microfibrils, which permits the passage of ions, and other molecules through cell wall. The unique properties of cellulose allow ion diffusion applications and thus have resulted in its increased usage in energy storing devices, green synthesis of nanoparticles of noble metals etc. Figure 2 shows the products, advantages and applications of various nanomaterials derived from cellulose. The use of cellulosic nanomaterials has an added advantage of holding the carbon dioxide captured during the process of photosynthesis. However ultimately, the cellulosic products will return the carbon dioxide to the atmosphere through the process of burning or decaying but atleast for some time the process will remain on hold and will lead to transitory carbon sequestration mechanism. This small contribution from the usage and application of cellulosic nanomaterials will contribute to reduce the increasing burden of global warming and its associated

effects. The embedded network of fibers with semicrystalline structure of cellulose allows the usage of cellulose in production of cellulosic nanofibers and colloidal nanocrystals. The cellulosic nanofibers retain some of the amorphous part of cellulose and are manufactured through mechanical treatment like grinding or paper beating etc. The dried form of these nanofibers is used as nanopapers. The cellulose derived nanopapers possess a much improved intrinsic strength and is used further in many applications like thermoelectric products, transparent paper. The unique optical properties of cellulosic nanofibers has been used to form transparent papers termed as 'glassine'. The process of formation of colloidal nanocrystals includes hydrolysis of cellulose in presence of strong acids. These cellulose derived nanocrystals are known to have interesting properties like stabilization oil-water emulsions. However, the biggest challenge in this area is the sustenance of aqueous dispersions and self assembly of cellulosic nanocrystals. In the process of hydrolysis, several acids are used for this purpose but recent investigations show that phosphoric acid works best in maintaining the aqueous dispersions of cellulosic nanocrystals. The cellulosic nanocrystals and their composite products are used in inks, paints and several other industrial applications (Eichhorn et al. 2018).

Figure 2: Products from cellulosic nanomaterial and its advantages and applications in various fields

Supercapacitors are important devices for energy storage. The paper made up of cellulose fibre can be used in multiple ways in these energy storing devices. The application of cellulose fibers as a) substrate with higher surface area, b) interior electrolyte reservoir and c) electrode when coated with additional carbon nanotubes coating provides a greener alternative to increase the performance of supercapacitors. Paper made up of cellulose in combination with carbon nanotubes is used in hybrid electrodes for improved capacitor performance (Gui et al. 2013). Apart from energy storing devices, the cellulose fibers have also been used in synthesis of nanoparticles of noble metals like silver, gold, platinum and palladium. The nanoparticles can further be used for many applications in nanotechnology. The two main characteristics of cellulose fibers include: 1) Highly

nanoporous structure and 2) High oxygen density. These two unique properties make them ideal nanoreactors, where the insitu synthesis of nanoparticles of important noble metals is possible (He et al., 2003). Though there is a considerable advancement in understanding the structure of cellulose for making its best use in several applications, still there are some limitations which need more research and developmental interventions.

References:

Ashley M, Magiera C, Ramidi P, Blackburn G, Scott TG, Gupta R, Wilson K, Ghosh A, Biswas A (2012) Nanomaterials and processes for carbon capture and conversion into useful by-products for a sustainable energy future. Greenhouse Gas Sci Technol. 2:419–444.

Chang J, Zhang L and Wang P (2018) Intelligent environmental nanomaterials. Environ. Sci.: Nano 5: 811.

Chen M, Goodman DW (2006) Catalytically active gold: from nanoparticles to ultrathin films. Acc Chem Res 39:739–746

Du N, Park HB, Robertson GP, Dal-Cin MM, Visser T, Scoles L and Guiver MD (2011), Polymer nanosieve membranes for CO2 capture applications. Nature Materials 10(5):372–375.

Eddaoudi M, Kim J, Rosi N, Vodak D, Wachter J, O'Keeffe M and Yaghi OM (2002), Systematic design of pore size and function-ality in isoreticular MOFs and their application in methane storage. Science 295(5554):469–472.

Eichhorn SJ, Rahatekar SS, Vignolini S, Windle AH (2018) New horizons for cellulose nanotechnology Subject Areas : 1–5

Furukawa H, Ko N, Go YB, Aratani N, Choi SB, Choi E et al. (2010), Ultrahigh porosity in metal-organic frameworks. Science 329(5990):424–428.

Gui Z, Zhu H, Gillette E, et al (2013) Natural Cellulose Fiber as Substrate for Supercapacitor. 6037–6046. doi: 10.1021/nn401818t

He J, Kunitake T, and Nakao, A (2003) Facile In Situ Synthesis of Noble Metal Nanoparticles in Porous Cellulose Fibers. Chem. Mater. 15 (23), pp 4401–4406, DOI: 10.1021/cm034720r.

Hussein AK (2015) Applications of nanotechnology in renewable energies — A comprehensive overview and understanding. 42:460–476

Kashale AA, Gattu KP, Ghule K, et al (2016) SC. Compos Part B. doi: 10.1016/j.compositesb.2016.06.015

Kao M, Lin B, Tsung T (2005) The study of high-temperature reaction responding to diesel engine performance and exhaust emission by mixing aluminium nanofluid in diesel fuel. In: 18th internal combustion engine symposium. Jeju, Korea.

Kowalczyk P, Holyst R (2008) Efficient adsorption of super greenhouse gas (tetrafluoromethane) in carbon nanotubes. Environ Sci Technol 42:2931–2936

Liu C, Hsu PC, Lee HW, Ye M, Zheng G, Liu N, Li W and Cui Y (2015) Transparent air filter for high-efficiency PM2.5 capture. Nat. Commun. 6: 6205.

Long RQ and Yang RT (2001) Carbon nanotubes as a superior sorbent for nitrogen oxides. Ind. Eng. Chem. Res. 40:4288–4291.

Malik, P. and Sangwan A (2012) Nanotechnology: A tool for Improving Efficiency of. 1:37–49

Masciangioli T and Zhang WX (2011) Environmental technologies at the nanoscale. Environ. Sci. Technol. 37: 102A–108A.

Mochida I, Kawabuchi Y, Kawano S, Matsumura Y, and Yoshikawa M (1997) High catalytic activity of pitch-based acti-vated carbon fibers of moderate surface area for oxidation of NO to NO2 at room temperature: Fuel 76:543–548.

Ortiz G, Brandès S, Rousselin Y and Guilard R (2011), Selective CO2 adsorption by a triazacyclononane bridged microporous metal-organic framework. Chem Eur J 17(24):6689–6695.

Otanicar T, Golden J (2009) Comparative environmental and economic analysis of conventional and nanofluid solar hot water technologies. Environ Sci Technol;43:6082–7.

Pitoniak E, Wu C, Mazyck DW, Powers KW, Sigmund W (2005) Adsorption enhancement mechanisms of silica-titania nanocomposites for elemental mercury vapor removal. Environ Sci Technol 39:1269–1274

Rajamani K (2012), Adsorptive separation of CO2/CH4/CO gas mixtures at high pressures. Microporous and Mesoporous Materials 156:217–223.

Rogers RD and Seddon K (2003), Ionic Liquids - Solvents of the future? Science 302:792–793.

Noble RD and Gin DL (2011), Perspective on ionic liquids and ionic liquid membranes. J Membrane Sci 369:1–4.

Sinha AK and Suzuki K (2007) Novel mesoporous chromium oxide for VOCs elimination., Appl. Catal. B: Environ. 70: 417–422.

Smart SK, Cassady AI, Lu GQ and Martin DJ (2006) The biocompatibility of carbon nanotubes, Carbon 44:1034–1047.

Taylor R, Phelan P, Otanicar T, Walker C, Nguyen M, Trimble S, et al. (2011) Applicability of nanofluids in highflux solar collectors. J Renewable Sustainable Energy; 3:1–15.

Uchida T, Ohashi O, Kawamato H, Yoshimura H, Kobayashi K, Tanimura M, Fujikawa N, Nishimoto T, Awata K, Tachibana M, Kojima K (2006) Synthesis of single-wall carbon nanotubes from diesel soot. Jpn J Appl Phys 45:8027–8029.

Wang B, Cote AP, Furukawa H, O'Keeffe M and Yaghi OM (2008), Colossal cages in zeolitic imidazolate frameworks as selective carbon dioxide reservoirs. Nature 453(7192):207–211.

Wu D, Xu Q, Liu D and Zhong C (2010), Exceptional CO2 capture capability and molecular-level segregation in a Li-modified metal organic framework. J Phys Chem C 114(39):16611–16617.

Yaghi OM, Li G, Li H (1995) Selective binding and removal of guests in a microporous metal–organic framework. Nature 378:703–706.

Yazaydın AO, Snurr RQ and Park TH (2009), Screening of metal-organic frameworks for carbon dioxide capture from flue gas using a combined experimental and modeling approach. J Am Chem Soc 131(51):18198–18199.

Yuhas B, Yang P (2009) Nanowire-based all-oxide solar cells. J Am Chem Soc;131:3756–61.

Yunus IS, Kurniawan A, Adityawarman D, et al (2012) Nanotechnologies in water and air pollution treatment. 2515:. doi: 10.1080/21622515.2012.733966.

Zhang XX, Liu WT, Tang J, Xiao P (2010) Study on PD detection in SF6 using multi-wall carbon nanotube films sensor. IEEE Trans Dielectr Electr Insul 17:838–844.

Zhang W, Silva S (2011) Application of carbon nanotubes in polymer electrolyte based fuel cells. Rev Adv Mater Sci;29:1–14.

Zuttel A, Sudan P, Mauron P, Kiyobayashi T, Emmenegger C, Schlapbach L (2002) Hydrogen storage in carbon nanostructures. Int J Hydrogen Energy;27:203–12.

CARBON NANOTUBE BASED GREEN NANOCOMPOSITES FOR SUSTAINABLE ENVIRONMENT

Samjeet Singh Thakur[1], Alpana[2], Manish Kumar[3], Pankaj Thakur[4], Sunil Kumar[5]*

[1] Department of Chemistry, RGM Govt. College JoginderNagar (Mandi), H. P. India

[2]Department of Physics, MCM DAV College Kangra, H. P. India

[3]Department of Chemistry, Sri Sai University, Palampur, H.P. India

[4]Department of Chemistry, Shoolini University, Solan, H.P. India

*[5] Department of Chemistry, Govt. Degree College, Khundian (Kangra), H. P. India

E-mail: samjeet23chem@gmail.com ; sunil678kumar@rediffmail.com

Abstract

Our surrounding air, water and soil are being contaminated by industrial by-products due to increasing human activities and the population burden on our planet. We need to overcome those problems with the best use of green material. Sustainable and eco-friendly biopolymers are mostly derived from the renewable resources like polysaccharides and proteins, which have received a great deal of research attention as probable substitutes to the conventional petrochemical-based materials. Carbon Nanotubes (CNTs) are one-dimensional and one of allotropic form of carbon. Variety of CNTs ranging from single walled to multi walled and crosslinking through functionalized biopolymers are promising candidates as green nanocomposites in various applications, such as waste water treatment, enzyme mobilization, pharmaceutics, biotechnological and bioengineering applications. CNT's and biopolymers based green nanocomposites are efficient, cost-effective, environmentally benign CNT dispersion and alignment technologies. Its versatility scale-up CNT dispersion and alignment methods for nanomanipulation,

nanopatterning, and nanocomposite fabrication without any limitations on synthetic polymer/biopolymer system selection. This chapter will include various advances in CNTs and CNT-biopolymer based findings in biomedical applications, energy storage applications, waste water treatments, catalysis, molecular electronics, as conductive adhesives, as thermal materials and water filtration *etc*. for environmental remediation and concerns.

1.1. Introduction

Carbon is the most versatile element in the Periodic Table. In many ways it is a unique element, it is crucial for life on earth as we know it since the human body is to a large extent made up out of carbon (Iijima, (1991)). Technically, the whole huge field of organic chemistry deals entirely with carbon and its compounds, whereas; in the field of physics it is one of the most intensively studied materials. There exists an international journal named "*Carbon*" specifically devoted to carbon. ***Carbon is as beautiful as diamond and fullerenes but, as ugly as charcoal***. Pure carbon compounds are known as allotropes in the language of chemistry and they come in many different incarnations with different effective dimensionalities. These are molecules and structures entirely made up of carbon atoms, some of which have generated much excitement over the last three decades. Diamond and graphite are three dimensional allotropes of carbon, which are crystalline solids. Diamonds is the hardest substance on this planet, because carbon atom exhibits sp^3 hybridization and all the four *C*-atoms are oriented at the corners of tetrahedron which makes 3-dimensional rigid network with high stiffness, poor electrical conductivity but, high thermal conductivity. Graphites have layer over layer structure in which its *C*-atom are sp^2 hybridized and each *C*-atom is connected evenly to three other carbons with 120° bond angle each in a trigonal plane (*xy*) as a result, a weak π bond is present in the perpendicular *z*-axis

in a hexagonal (honeycomb) lattice. This makes its slippery nature and used as lubricant and it is electrical conductor, but less stiff than diamond. Carbon also forms low-dimensional allotropes (which may be two-dimensional, one-dimensional or zero-dimensional) collectively known as carbon nanomaterials. Examples of such nanomaterials are 0D fullerenes, 1D carbon nanotubes (CNTs) and 2D graphenes (Thakur *et al*. (2016)). *Korto* and his coworkers discovered a new form of zero-dimensional carbon allotropic nano-material, Buckminster fullerene in 1985 which are known to show superconductivity! Their discoveries have marked the development of nanoscale carbon allotropes followed by one dimensional carbon nanotubes and more recently graphenes in two-dimension (Hwang *et al.* (2010).). In the list of carbon nanomaterials, graphene is known as 2D single layer of graphite. Chen *et al.* (2011) reported that sp^2 bonds in graphene are stronger than sp^3 bonds in diamond and it makes graphene the strongest material.

One-dimensional carbon nanotubes (CNTs) are obtained when a graphene layer is rolled along the longitudinal axis. A zero-dimensional (0D) fullerene is obtained when the same graphene sheet is wrapped in a ball structure (Bianco *et al.* (2005)). Thus, quasi-one-dimensional carbon nanotubes (CNTs) were first reported by Ijima in 1991 when he discovered multi-walled carbon nanotubes (MWCNTs) in carbon soot made by an arc-discharge method (Iijima, (1991)). CNTs have tubular shape and made out of graphite with a typical diameter of a few nanometers (from which the name stems) and their lengths can be as large as a few *mm*. Carbon nanotubes are interesting in many ways and can be both, metallic or semiconducting depending on the diameter and how the tube is rolled up. The finite size of graphene layers has dangling bonds, which corresponds to higher energy states (Thakur *et al*. (2017)). Carbon nanotubes formation eliminates

dangling bonds and increases strain energy as a consequence the total energy of the molecules decreases (Guldi & Costa (2013).).

Paul McEuen, an American Physicist quoted that, "*Carbon nanotubes are amazing because they're really good electrical conductors, yet they are only a few atoms in diameter. You can make transistors out of them in the same way you can with silicon. At Berkeley, we made the narrowest device anybody had ever made. It was basically a single molecule.*"

History and development of Carbon Nanotubes breakdown:

1952: *Radushkevich and Lukyanovich publish a paper in the Soviet Journal of Physical Chemistry showing hollow graphitic carbon fibers that are 50 nanometers in diameter*

1979: *John Abrahamson presented evidence of carbon nanotubes at the 14th Biennial Conference of carbon at Pennsylvania State University*

1981: *A group of Soviet scientists published the results of chemical and structural characterization of carbon nanoparticles produced by a thermocatalytical disproportionation of carbon monoxide*

1991: *Nanotubes discovered in the soot of ac discharge at NEC, by a Japanese researcher, Sumio Ijima*

CNTs can be made by chemical or physical routes and broadly classified into two types: single-wall carbon nanotubes (SWCNTs) and multi-walled carbon nanotubes (MWCNTs) (Rao *et al*. (2018)) as shown in Figure 1. Topologically, a single-wall CNT (SWCNT) can be constructed by rolling up a single layer of graphite or graphene along a certain direction into a tiny cylinder with a possible diameter from sub nanometer to a few nanometers (Dillon *et al*. (2008)).

Fascinatingly, the rolling-up direction and diameter or the chirality of an SWCNT determine its fundamental properties. To obtain chirality-pure SWCNTs has been a dream for a long time, because the electrical and optical properties of SWCNTs are dominated by their chirality (Seo, *et al.* (2004)). Some SWCNTs have small energy band gaps, showing semiconducting characteristics, whereas others do not have the band gap and they are metallic ones. Structurally MWCNTs consist of multiple layers of graphite superimposed and rolled in on them to form a tubular shape (Han & Ostrikov (2012)). MWCNTs are polymers of pure carbon and can be reacted and manipulated using the rich chemistry of carbon (Hemraj-Benny & Wong (2006); Tan *et al.* (2011)).

McEuen *et al.*, (2002) and Avouris *et al.*, (2003) have also reviewed experimental demonstrations of transistors made out of carbon nanotubes. The CNTs have amazing properties and are specifically interesting for the industry. The combination of these impressive properties enables a whole new variety of useful and beneficial applications.

(a) *CNTs have interesting electronic properties*

(b) *CNTs are as conductive as copper, meaning thereby these have Electrical conductivity.*

(c) *CNTs are up to hundred times stronger than steel. All in all, these have high strength.*

(d) *CNTs are six times lighter than steel. These have high elastic stiffness.*

(e) *CNTs are known to show high thermal conductivity. These have same thermal*

conductivity as that of diamond and *more than five times that of copper.*

Table1: A comparison between SWCNTs and MWCNTs

S. No.	Single Wall Carbon Nano Tubes (SWCNTs)	Multi-Walled Carbon Nano Tubes (MWCNTs)
1	*Nanotubes of carbon which have only one cylinder wall or consist up of just one layer of carbon are called single-walled carbon nanotube (SWCNT)*	*It can form multiple concentric cylinders made of pure carbon atoms. Each concentric nanotube is kept away from the other by the inter-atomic force. These are known as multi-walled carbon-nanotubes (MWCNT).*
2	*Average diameter of SWCNT is 0.5 to 1.5 nm* and a *length of (1-3) μm*	*Thin MWCNT of carbon purity (90%) confirms an average diameter of 20 nm with a high-aspect-ratio (>150)*
3	*Composed entirely of sp^2 bonds and Band Gap is* 0-1*e*V	*Composed entirely of sp^2 bonds and Band Gap is greater than* 1*e*V and the interlayer distance is 3.4 Å
4	*Well characterized structure and properties*	*MWCNTs have many structural defects*

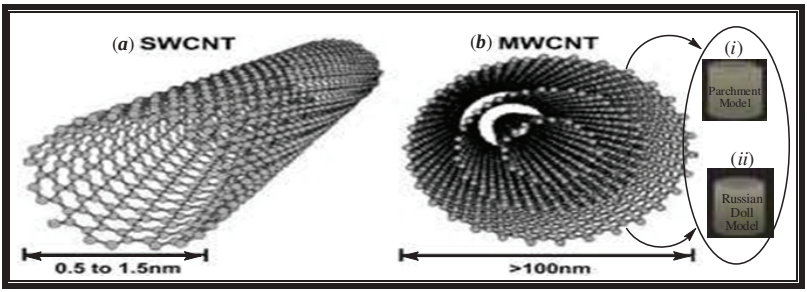

Figure 1: (***a***) SWCNTs (***b***) MWCNTs (Parchment Model & Russian Doll Model)

Precisely controlling CNT synthesis parameters and carefully selecting the catalysts used are confirmed to be the key factors that affect the chirality distribution of the grown CNTs (Pierce *et al.* (2017)). A large number of post-treatment processes have been reported to sort CNTs in terms of their semiconducting or metallic properties, their thickness and lengths, etc. (Yang *et al.* (2008)).

Carbon nanotubes (CNTs) are distinguished for being excellent conductors of electricity and temperature, which finds them numerous applications all over the industrial spectrum:

(a) Versatile Applications: The excellent heat and electrical conducting properties of these nanotubes make them excellent for numerous applications in material science and technology, apart from nano-technology, optics and electronics and therefore, are capable when it comes to conducting electricity, due to the loose electron in each atom forming the nano-cylinder (Avouris (2002)).

(b) Additive: Carbon-nanotubes (CNTs) are not always used singularly, but are also used as additives to other structural materials to make them stronger and safer (Vijayan *et al.* (2012)).

(c) Strength Factor – It is formed through sp^2-hybrid chemical bonding between the carbon atoms, which makes it stronger than most of the saturated hydrocarbons and even diamond. The carbon atoms for a strong bond with their loose electron, forming an efficient hexagonal shape of carbon molecules. Aforementioned makes the nanotubes of carbon stronger than conventional steel at least 100 times (Mora *et al.* (2008)).

(d) Shapes and Sizes: Apart from being single-walled and multi-walled, carbon-nanotubes (CNTs) are also available as *carbon peapod*, *nanobud*,

nanocones and *nanofibers*. These are extremely thin, only about 1 *nm* to 3 *nm* in diameter, making them around 10,000 times thinner than a human hair (Hu *et al.* (2010)).

(e) Prospective of Use: Carbon nanotubes are estimated to find widespread application including, mainly, in nano-technology engineering. Apart from this, it is also set to be used in building blocks of *three dimensional macroscopic* carbon devices, manufacturing electrically-conductive fiber for wearable electronic devices (Avouris (2002)).

(f) Significantly Safe: It has been deemed safe for use by ***Europe's Registration, Evaluation, Authorization and Restriction of Chemicals*** (REACH) regulations (Kim *et al.* (2014)).

(g) Effective heat conductor: The nanotubes are also able to adequately conduct heat, thus making them ideal for application in even high-temperature environments (Tan *et al.* (2011)).

1.2. Threats to Environment

Different synthetic strategies for the production of *carbon nanotubes* are used (Yang *et al.* (2005). At first sight all the CNTs material looks similar, however, on comparison by doing close examination; the materials vary considerably in terms of their crystalline structure, morphology and the content of the residues. The use of carbon nanotubes has increased substantially in last few decades, and is expected to continue to increase strongly in the future, because the properties of carbon nanotubes are versatile but, the exposure situations that exist during production, processing and the handling of products containing carbon nanotubes are known as the toxicology of carbon nanotubes (Bhaskar *et al.* (2013). Therefore, increased production, handling and machining have increased the risk of exposure

in different work environments. Nowadays, the production of carbon nanotubes takes place mainly in non-Nordic countries, but in the Nordic countries, carbon nanotubes are used in research and development work only. Carbon nanotubes are used mainly as a reinforcement material in various types of polymers and other material where this all exposure takes place (Schnorr & Swager (2010)). These are active materials of printed electronics (conductive ink), anti-fouling coatings, high-durability epoxy-paints, L*i*-ion batteries, antistatic thermoplastic, conductive textile, thin heating mats, high performance sporting goods and microscopy probes *etc.* (Zhang *et al.* (2014); Ballesteros *et al.* (2007)).

The risk assessment for carbon nanotubes is made more difficult by a lack of knowledge at several levels: *Carbon nanotubes can be found in a large number of variants that are likely to have different levels of toxicity*; *the toxicological data is inadequate but literature indicates that there is a risk of inflammatory reaction and pulmonary fibrosis when inhaled at relatively low doses; there is also the risk of producing a DNA-damaging effect*; *exposure levels for the commercial handling of carbon nanotubes are incompletely characterized even today* (Alshehri *et al.* (2016); Shen *et al.* (2009)).

The production method and properties that triggers the nanotubes toxicity are used to interpret the observed bio-chemical effects (Ju & Papadimitrakopoulos (2008)). Toxicological studies of CNTs should include a detailed description of the physical and chemical properties that may be relevant to the biological response (Baoukina *et al.* (2013)). Another important issue in respect of threat to environment and toxicological impact is whether the physical characteristics of the carbon nanotubes in the exposure study are the same as those what expected in an actual exposure situation. Examples of this are if the carbon nanotubes are inhaled as single tubes, or as bundles of tubes, or rolled into larger agglomerates. For

example, agglomerates or aggregates often have a larger aerodynamic diameter than individual tubes and will therefore, to a greater extent, deposit in the upper respiratory airways, where other mechanisms remove or degrade the tubes compared with those in the alveoli. To suspend the carbon nanotubes to an airborne state in a controlled and reproducible way is a problem in toxicological inhalation studies. Other models of lung deposition were also reported, such as in tracheal instillation or aspiration (Silva *et al.* (2014)); Wang *et al.* (2010)). The aggregation condition has not only an effect on where in the lung the carbon nanotubes are deposited but also on the biological response (Mercer *et al*., (2008); Shvedova *et al*., (2005). Two methods used in the suspension of carbon nanotubes into the air is to spray droplets of a solution of carbon nanotubes and to dry out the fluid so that only the tubes remain (Lee *et al*., 2011) or directly by suspending a powder (Maynard *et al*., 2004). The proposed international occupational exposure limits are at very low levels. Airborne exposure arises from the manufacture, handling, and use of carbon nanotubes and in the machining of products containing carbon nanotubes. Established technical protective measures such as encapsulation and process ventilation should be applied in conjunction with personal protective equipment such as respiratory protective equipment, protective gloves and protective clothing. Toxicological studies strongly indicate that exposure to certain CNTs may be associated with long-term adverse health effects in test-animals to the human beings. The primary routes of CNTs hazardous exposures are dermal contact, oral uptake and inhalation. Systemic effects partly depend on the ability of the CNTs in the translocation of the other organs of the body. Therefore, the toxicological overview is presented according to current knowledge on CNT fate and translocation, pulmonary, oral and dermal toxicology is very little in the literature. In the mechanistic study of CNT Toxicity it is reported that CNT

exposed cells undergo oxidative stress due to induction of oxidants and toxic enzymes as a result the higher level of oxidative stress leads to inflammation and cytotoxicity (Witzmann *et al.* (2006); Xiao *et al.* (2003)).

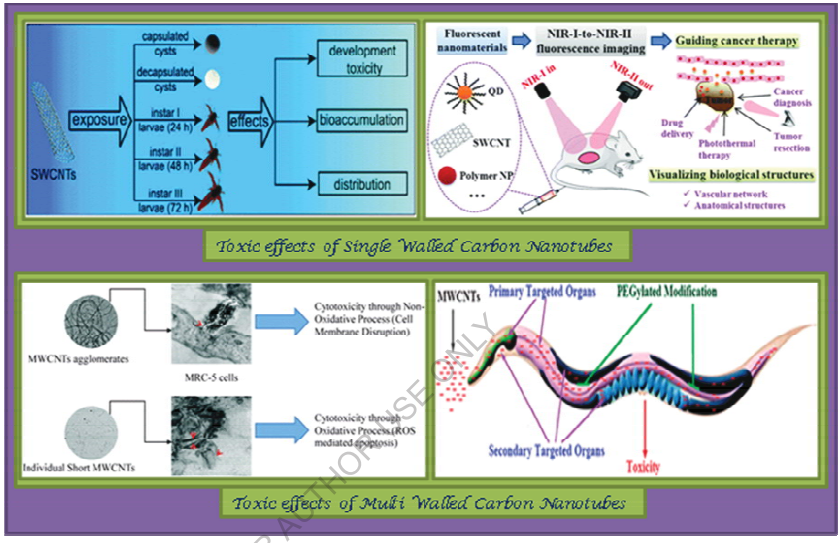

Figure 2: Toxic Effects of SWCNT & MWCNT

CNTs mainly led to the formation of *free radical formation, reactive oxygen species (ROS), increased inflammatory responses, granuloma formation, apoptosis* etc. are the main causes related to oxidative stress. The excess free radicals oxidize lipids, protein, and DNA and therefore, oxidative stress may up-regulate redox sensitive transcription factors, activator protein-1 and kinases that cause inflammatory responses. The slow clearance caused due to agglomeration as well as accumulation of these CNTs nanoparticles which actually produces free radicals, into the organs of Reticulo Endothelial System (RES) as a consequence organs like spleen, kidneys and lungs are made available as a soft targets for this

oxidative stress (Wang *et al.* (2011)). Reactive oxygen species are chemically active oxygen containing molecules that are formed as side products of the normal metabolism of oxygen. However, their concentration may increase due to environmental stress such as exposure to radiation, foreign particles *etc*. Therefore, it may lead to harmful effects in cells like apoptosis, DNA damage, amino acid oxidation and inactivity of enzymes (Valko *et al.* (2007)). It is also reported in the literature that SWCNTs damage DNA, cause changes in the cell cycle and generated apoptotic signals by generating ROS. Most cells grown in the medium containing CNTs changes the G1 phase of their cell cycle (Azad *et al.* (2013)). Wang *et al*. (2011) have determined that apoptosis of PC12 cells was induced by 4 to 5 fold higher concentrations of ROS in cells exposed to SWCNTs (200 µg/ ml). MWCNTs have been shown to induce ROS in Human Umbilical Vein Endothelial Cells (HUVEC) at 20 µg/ml concentration (Coleman *et al.* (2006); Guo *et al.* (2011)). The physical characteristic and parameters like *fiber shape*, *length* and *the aggregation status* can also influence the immunological responses and their local deposition in tissues (Vittorio *et al.* (2009)). The shape and length of CNTs determines the internalization of CNT by macrophages and hence the immune response. Shorter the CNTs, less toxic they are. It is reported that when shorter CNTs injected subcutaneously in rat, then after 4 weeks they were found in the cytosol of the macrophages, whereas longer CNTs were found to be free floating and causing inflammation (Poland *et al.* (2008)). Thereupon, it is confirmed that the toxicity of MWCNTs was length dependent and comparable with that of asbestos toxicity. A Polish group compared inflammatory responses produced by exposing mice to MWCNTs (Poland *et al.* (2008)). MWCNTs exposure enhances the release of polymorphonuclear leukocytes and protein exudation, indicating an increased inflammatory response. It was attributed that the increased inflammatory

response of long MWCNTs alongwith asbestos to "*frustrated phagocytosis*" in which the macropghages are not able to surround the long needle shaped CNTs. By contrast, in another study done on a mouse macrophage RAW 264.7 cell line, CNTs induced ROS related necrosis, apoptosis and chrosomal damage, but do not induce an inflammatory response (Di Giorgio *et al.* (2011)). CNTs as well as asbestos both were found to cause granulomas in mice exposed for 7 days (Poland *et al.* (2008)). Granuloma is a small nodule or a tiny collection of immune cells formed when the immune system attempts to wall off foreign substances, but is not able to eliminate them. Intratracheal instillation of SWCNTs (diameter 0.7-1.5 *nm*) in the lungs of rats leads to blockage of the large airways as a result of the formation of granulomas, with 15 % mortality within one day (Warheit *et al.* (2004)). SWCNTs caused the maximum apoptosis of five carbon-based nanomaterials when tested for SWCNTs and MWCNTs toxicity on human fibroblast cells (Cui *et al.* (2005)). It was hypothesized that dispersed and hydrophobic materials with small surface area displayed increased toxicity and therefore, it is proposed that the mechanism of toxicity of CNTs was due to extracellular matrix protein signaling which actually results in changes to the cell skeleton and the subsequent dislodgment of organelles, resulting in membrane deformation and finally apoptosis. Cui *et al.* (2005) have reported that CNTs caused apoptosis in several cell types including T- lymphocytes and HEK293 cells. Genes associated with apoptosis (p16, bax, hrk, bak1, p53, p57FGFR2, TGF beta receptor1 (TGFbetaR1) and TNFAIP2) were up-regulated by CNTs. Other studies also indicated the upregulation of genes responsible for apoptosis (Montes-Fonseca *et al.* (2012)). The unfunctionalized (UP-CNTs), purified (P-CNT), and FITC functionalized (FITC-CNTs) all caused decreased cell viability and increased apoptosis (Di Giorgio *et al.* (2011)).

Carbon nanotubes toxicity also arises from the catalyst remainder left after their production and their synthesis involve the use of various metal catalysts like iron (F*e*), Nickel (N*i*), Cobalt (C*o*), Arsenic (A*s*), Molybdenum (M*o*) *etc*. which are also toxic themselves (Pulskamp *et al.* (2007)). These elements are necessarily removed during the purification step; they tend to catalyze oxidative processes by free radical generation. Otherwise, the reductive oxygen species (ROS) generated cause oxidative damage to cells as well as membranes. These catalysts too interfere with the immune system at the cellular level. Since CNTs are surrounded by the macrophages, nicotinamide adenine dinucleotide phosphate–oxidase (NADPH-oxidase) produces superoxides (O_2^-) at the interiors of the cells. Iron based catalysts react with the superoxides formed and form hydroxyl ions which eventually results in oxidative stress and damage at the molecular level (Firme III & Bandaru (2010)). It is also reported in the literature that MWCNTs subjected to oxidation with nitric acid were more toxic to T-lymphocytes than their impure counterparts (Bottini *et al.* (2006)). It is also given in the literature that CNTs with added carbonyl (CO), carboxylic (COOH), and hydroxyl (-OH) groups are more toxic than their pristine counterparts (Magrez *et al.* (2006)). At low concentrations (5 µg-10 µg), the toxic effects of CNTs are almost negligible but, observed higher at higher concentrations level (50 µg-500 µg). To avoid toxicity, CNTs with highest purity have to be used as it minimizes the lethal effects of residual catalysts or surface oxidation (Vittorio *et al.* (2009)).

1.3. Potential of CNTs in environment remediation

In the area of environmental remediation, nanomaterials (nanoparticles, tubes, wires, fibres *etc.*) offer the potential for the efficient removal of pollutants and biological contaminants. CNTs function as adsorbents and catalysts and their composites with polymers/biopolymers are used for the detection and removal of

gases (SO_2, CO, NO_x, *etc.*), contaminated chemicals (arsenic, iron, manganese, nitrate, heavy metals, *etc.*), organic pollutants (aliphatic and aromatic hydrocarbons) and biological substances, such as viruses, bacteria, parasites and antibiotics. These materials show a better performance in environmental remediation than other conventional techniques because of their high surface area (surface-to-volume ratio) and their associated high reactivity.

The contribution of CNTs as their potential respect to sustainable environment and green technologies perspective in water treatment, air pollution control applications, energy storage applications, renewable energy technologies, super capacitors and green nano composites is marvelous. Because of their special physico-chemical properties, MWCNTs and SWCNTs are expected to play a major role in numerous applications.

Saifuddin *et al*. 2012 has reported the remarkable properties and qualities of CNTs as structural materials. Their potential applications include textiles, body armour, concrete, polyethylene, sports equipment, bridges, flywheels and fire protection. In textiles, CNTs can produce waterproof and tear-resistant fabrics. As body armor, CNT fibers are being used as combat jackets, which are used to monitor the condition of the wearer and to provide protection from bullets. In concretes CNTs are used to increase the tensile strength and halt crack propagation. CNT fibers can be used as polyethylene. The CNT based polyethylene can increase the elastic modulus of the polymers by 30 %. CNT plays major role in sports equipments such as golf balls & golf clubs, stronger and lighter tennis rackets, bicycle parts, and baseball bats. CNTs may be able to replace steel in suspension and bridges. In flywheels, the high strength/weight ratios of CNTs enable very high rotational speeds.

Thin layers of buckypaper can potentially protect the object from fire. The dense, compact layer of CNT or carbon fibers in the form of buckypaper can efficiently reflect the heat. CNTs can be fabricated in electromagnetic applications such as in electrical conductors, semiconductors and insulators. Ji *et al*. 2006 reported that the *Buckypaper* thin nanotube sheets are 250 times stronger and 10 times lighter than steel and can be used as heat sink for chipboards, backlight for LCD screens, or Faraday cage to protect electrical devices/aeroplanes. Jornet and Akyildiz 2010 reported that CNTs can be used as alternative to tungsten filaments in incandescent lamps and the strong magnetic field can be generated using multi-walled CNTs coated with magnetite. As solar cells, germanium CNT diode exploits the photovoltaic effect. In some solar cells, nanotubes are used to replace the ITO (indium tin-oxide) to allow the light to pass to the active layers and generate photocurrent as reported in literature by Jeon *et al*. (2015).

As an Electromagnetic antenna CNTs can act as an antenna for radio and other electromagnetic devices due to its durability, light weight and conductive properties reported by Jornet and Akyildiz 2010. Huang *et al*. 2008 reported the skin effect in CNTs is negligible at high frequencies due to additional kinetic inductance which results in lowpower dissipation and high antenna efficiency.

Howarth *et al*. (2016) reported and discussed the application of CNT in the field of electro-acoustic as *Loudspeaker* which can be manufactured from parallel sheets of CNTs. These loudspeaker can generate sound similar to the sound of lightening producing thunder.

CNTs finds remarkable applications in the chemical field also, according to Ong *et al*. (2010) CNTs are one of the best materials for air filters because they possess high adsorption capacity and large specific area. The conductance of CNTs

changes when polluted gas comes in its contact and which helps in detecting and filtering the polluted air. Kusworo *et al*. (2010) also reported that CNT membranes can successfully filter the carbon dioxide from biogas and CNT membranes assisted filtration can reduce distillation costs by three fourth. These membranes are so thin that small particles like water molecules can even pass through them, while larger particles such as the chloride ions in salt were blocked. CNTs have high active site and controlled distribution of pore size on their surface. This increases not only its sorption capabilities, but also its sorption efficiency. According to Ong *et al*. (2010) CNTs have effective sorption capacity over broad pH range (from 7 to 10). Fullam *et al*. (2000) reported that the CNTs finds their applications in nanowire manufacturing using materials such as gold, zinc oxide, gallium arsenide, etc. The gold based CNT nanowires are very selective and sensitive to hydrogen sulphide (H_2S) detection. The zinc oxide (ZnO) based CNT nanowires can be used in applications for light emitting devices and harvesters of vibrational energy. Kuo *et al*. (2007) reported that CNTs based sensors can detect temperature, air pressure, gases (such as CO, NH_3), molecular pressure, strain, *etc*. The working of CNTs based sensor is primarily dependent on the generation of current and voltage. Al-zubaidi *et al*. (2017) reported that electric current is generated by the flow of free charged carrier induced in any material which is characteristically modulated by the adsorption of a target on the CNT surface.

The potential application of CNTs can be found in the mechanical engineering as an oscillator, waterproofs etc. CNTs based Oscillators have achieved higher speeds than other technologies (>50 GHz). Researchers also reported a molecular oscillator with frequencies up to several GHz. The operation of this oscillator is primarily based on the low friction and low wear bearing properties of a multi-walled CNT with a diameter ranging from one to few tens of nanometers (Jiang *et*

al. (2004)). CNTs can be used to prepare super-hydrophobic cotton fabric by dip-coating approach. This approach is exclusively based on the chemical reactions caused by UV-activated nitrene solution. The solution is used to transform the cotton fabric surface from hydrophilic to super-hydrophobic with an apparent water contact angle of 154º. Since CNTs are covalently attached on the surface of the cotton fabric, the super-hydrophobicity possesses high stability and chemical durability.

CNTs are attractive materials in fundamental science and technology as electrical circuits which demonstrated unique electrical properties for building electronic devices, such as CNT field-effect transistors (CNTFETs) and CNT diodes. CNTs can be used to form a *p–n* junction diode by chemical doping and polymer coating (Franklin (2013)). These types of diodes can be used to form a computer chip. CNT diodes can potentially dissipate heat out of the computer chips due to their unique thermal transmission properties.

Avouris (2002) reported that carbon nanotubes (CNTs) have emerged as one of the most potential interconnect material solutions in current nanoscale regime. The higher current density of 1000 MA/sq-cm of an isolated CNT can eliminate the electromigration reliability concerns that plagues the current nanoscale copper interconnects. Therefore, CNT interconnects can potentially offer immense advantages over copper in terms of crosstalk, delay and power dissipation.

Franklin *et al*. (2012) reported that CNTs plays an important role as transistor architectures. CNTs can form conducting channels in transistor configurations whereupon, two different device architectures have been developed for them. In both cases, CNTs connect the source, drain electrodes and show excellence behavior in the area of memory designing, amplifiers, sensors and detectors, etc. In

one device architecture, the source and the drain are connected by a single nanotube whereas in other, random arrays of nanotubes function as a conducting channel. The advantages of CNTFET over S*i*-MOSFET are as reported by Sahoo and Mishra in 2009 that CNTFET demonstrates higher drive current, shows approximately four times higher trans-conductance and its average carrier velocity is almost double as compared to Si-MOSFET.

All in all, this chapter presented the unique properties and applications of carbon nanotubes in terms of structural, electrical, mechanical and thermal base and is primarily dependent on their diameter and chirality. In addition to this, the chapter summarized different production and purification methods for SWNTs and MWNTs

1.4. Variety of CNTs ranging from single walled to multi walled and cross-linking through functionalized biopolymers

Most of the wonderful properties of carbon nanotubes can be best utilized by incorporating the nanotubes into some form of matrix. The exceptional mechanical properties, in particular, have prompted huge interest in the production of composite materials containing nanotubes for structural applications using polymers, ceramics and metals (MacDonald *et al.* (2005)). The materials which form composites with carbon nanotubes are mostly polymers or biopolymers reported elsewhere in the literature. One of the simplest methods for preparing CNTs- polymer composites is mixing the CNTs dispersion with solution of the polymer, and then evaporates the solvent in a controlled way. This method has been used with various polymers such as polyvinyl alcohol, polystyrene, polycarbonate and poly(methyl methacrylate) reported by Spitalsky *et al*. (2010). In order to facilitate solubilization and mixing, the nanotubes are often functionalized before adding to the polymer solution. For example, acid treatment

is used to disperse catalytically produced MWNTs in water, and then nanotubes polymer composite is made by simply mixing one of these dispersions with an aqueous solution of the polymer and casting the mixture as film. The solution mixing approach is limited to polymers that freely dissolve in common solvents. An alternative is to use thermoplastic polymers and apply melt processing techniques (Haggenmueller *et al.* (2000)). One problem associated with this method is that achieving homogeneous dispersions of nanotubes in melts is generally more difficult than with solutions, and high concentrations of tubes are hard to achieve due to the high viscosities of the mixtures. An alternative method for preparing nanotubes polymer composites is to use the monomer rather than the polymer as a starting material, and then carry out *in situ* polymerization (Xia *et al.* (2003)). Ceramics have high stiffness and thermal stabilities but relatively low breaking strengths. Incorporating carbon nanotubes into a ceramic matrix produces a composite with both toughness and high-temperature stability. However, achieving a homogeneous dispersion of tubes in an oxide, with strong bonding between tubes and matrix, presents rather more of a challenge than incorporating tubes into a polymer. CNTs have been used to improve the anti-static properties of fuel-handling components and body panels of automobiles. CNTs-containing sporting equipment (e.g., tennis rackets and high-performance racing bicycles) has been manufactured recently. It has been shown that considerable improvement in the performance of Li-ion batteries can be achieved by the addition of catalytically-produced MWNTs.

Aztatzi-Pluma *et al.* (2016) reported the study of the molecular interactions between functionalized carbon nanotubes and chitosan where molecular dynamics (MD) simulations were performed to calculate the interaction between chitosan at different degrees of deacetylation (DD) and CNTs functionalized with either amine

(−NH_2) or carboxylic (−COOH) groups. Xu *et al*. (2005) reported stable films of biopolymer chitosan and were prepared by a layer-by-layer self-assembly technique for studying the electrochemistry of microperoxaidase-11. Liu *et al*. (2007) reported a novel noncovalent approach is developed for the functionalization of MWNTs using a biopolymer obtained in the cellulose industry with sodium lignosulfonate (SLS). Zykwinska *et al*. (2009) reported layer-by-layer functionalization and non-covalently modification of CNTs with synthetic and natural polyelectrolytes. The adsorbed polyelectrolyte layers were used as anchoring ones to subsequently graft a natural biopolymer. Such post-functionalization creates a way to design new CNTs based biodevices. Gandra *et al*. (2009) reported that Single-walled carbon nanotubes (SWNTs) functionalized with −COOH (along with some sulfonation and nitration) and modified with chitosan were prepared and tested for their singlet oxygen ($^1O_2$) production. *Zamaleeva et al*. (2010) reported the 3D assembly of MWCNTs on the polyelectrolyte-coated living Yeast cells (*Saccharomyces cerevisiae*) using the polyelectrolyte-mediated layer-by-layer approach. Ji *et al* (2009) reported that SWCNTs and MWCNTs are the potential candidates and effective adsorbents for the removal of tetracycline from aqueous solution. To compare the results, a non-polar adsorbate, naphthalene, and two other carbonaceous adsorbents, pulverized activated carbon (AC) and non-porous graphite, were used. It was observed that the remarkably strong adsorption of tetracycline to the CNTs can be attributed to the strong adsorptive interactions due to vander Waals forces π—π electron donor-acceptor interactions, cation- π bonding. Fan *et al*. (2013) reported that hydrothermal synthesis of phosphate-functionalized CNTs containing carbon composites for super-capacitors with highly stable performance phosphate-functionalized carbon nanotubes. (CNT)-containing carbon composites

with hierarchical porous structure have been synthesized by a simple soft-template hydrothermal method followed by heat treatment. The electrochemical performance of the carbon composites as electrode materials for super-capacitors is also investigated and it was observed that CNTs can be uniformly embedded in the carbon matrix, and the phosphate groups are introduced into the carbon composites successfully. Bhattacharya *et al*. (2008) successfully dispersed functionalized SWNTs within hyaluronic acid–water solutions where divinyl sulfone was used as a crosslinker for the Hybrid hyaluronic acid (HA) hydrogels with SWNTs. All in all, it is evident from the literatrure that the functionalization of CNTs(SWCNTs &MWCNTs) led to change in their properties and tune pristine properties like solubility, composite materials, sensitivity & reactivity electron interaction, defects, vibrations. Various functional groups are responsible for the verstality of their nature and properties after functionalization as shown in the figure 3 as reported in the literature.

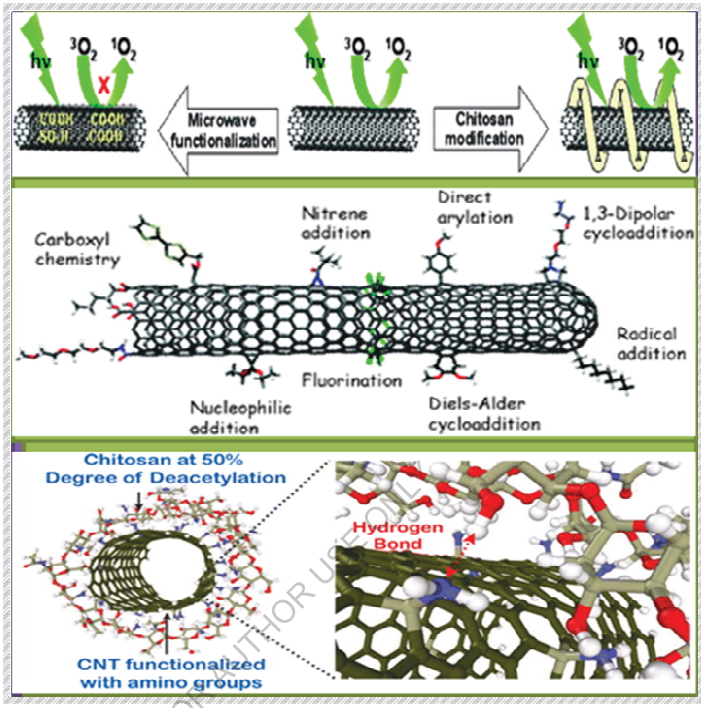

Figure 3: Different method of CNTs functionalization reported in literature

2. Synthetic Strategies of Carbon nanotubes

The report **"***Carbon Nanotubes (CNT) Market by Type (Single, Multi Walled), Method (Chemical Vapor Deposition, Catalytic Chemical Vapor Deposition, High Pressure Carbon Monoxide), Application (Electronics, Chemical, Batteries, Energy, Medical) - Global Forecast to 2023*" The carbon nanotubes market was estimated to be USD 4.55 billion in 2018 and is projected to reach USD 9.84 billion by 2023, at a CAGR of 16.70%. Carbon nanotubes (CNTs) have emerged as one of the most important classes of nanomaterials having enormous potential to spark-off the industrial revolution from the last decade. Multi-walled carbon

nanotubes (MWNTs)-enhanced products, while SWCNT's growth will be steady but not as high as MWCNTs, due to higher prices and limited end-user adaptability such as electrical & electronics market. CNTs market is facing a huge gap between demand and supply due to low volume utilization of CNTs by end users. In order to bridge this gap, manufacturers should be ready to capitalize on that future demand, which is expected to grow rapidly over the next five to ten years. Keeping in view the market analysis CNTs in 3D printing, adhesives, aerospace and aviation, automotive, coatings, composites, electronics (flexible electronics, conductive films and displays; conductive inks; transistors, integrated circuits; memory devices; photonics), energy storage, conversion and exploration (batteries, super-capacitors, photovoltaic cells, fuel cells and hydrogen storage), filtration and separation, life sciences and medical, lubricants, oil and gas, rubber and tires, sensors, smart textiles and apparel etc., the synthesis and production of carbon nanotubes (CNTs) have been attracted huge attention over the past two decades, based on their extraordinary physical and chemical properties that are a result of their intrinsic nano-sized one-dimensional nature. Generally the syntheses and production of both types of CNTs (SWCNTs & MWCNTs) are made with three different techniques, *chemical vapour deposition* (CVD), *arc discharge method* and *laser ablation method*.

2.1. Arc Discharge Method

The **Arc-discharge method** synthesizes nanotubes by using a fairly low voltage power supply to strike an electrical arc between two carbon electrodes (Hou *et al.* (2001)). The carbon anode can be enriched with particles of a transition metal in order to aid synthesis. Nanotubes form in the arc and collect on the anode, along with a host of other carbon byproducts. The nanotubes that are synthesized by this means are typically very ropy and multi-walled.

S. Iijima (1991) was first to report that a DC arc discharge in argon consisting of a set of carbon electrodes was used to prepare CNTs. The temperature of 2000–3000°C was kept at nominal conditions of 100 A of current and 20 V of potential difference for the production of CNTs. This apparatus produced multi walled carbon nanotubes (MWCNTs) in the soot. Later, SWCNTs were grown with the same set-up by arc discharge technique where carbon is released from catalysts doped with catalyst source materials (e.g., Fe, Ni, Co, Ni, Co, Pt, Rh, Pt) (Baddour & Briens (2005); Ishigami *et al.* (2000)). This method is a slightly modified version of the method used for fullerene production. An arc discharge is generated between two graphite electrodes placed face to face in the machine's principal airtight chamber under a partial pressure of inert gas (typically 600 *m*bar of H*e* or A*r*). The resulted electrical discharge brings the temperature up to 6000°C, which is hot enough for the carbon (graphite) to sublime and transform from a solid state to gaseous one without turning into a liquid first. During sublimation, the high energies involved can eject single carbon atoms from the solid forming plasma. These atoms move towards colder zones within the chamber, allowing a nanotubes deposit to accumulate on the cathode. In fact, in the chamber, the gas ionizes to electrons and positively charged ions and produces very hot plasma. The electrons impact the anode with high velocity, and the carbon material is raised to such a high temperature that carbon vapor is produced which follows the ionization of carbon to give carbon ions. Thereafter, the carbon ions and vapor move around to the cathode, which is cooler than the anode electrode due to the decreased temperature and form clusters, by a phase transition to liquid carbon and eventually to solid carbon where it has been found that CNTs are synthesized (Yousef *et al.* (2012)). It has been reported that different kind of substances can be formed in different parts of reactor besides CNT such as large quantities of rubbery soot,

web-like structures between the cathode and the chamber walls, grey hard deposits, and a spongy soft coating like a belt called 'collaret' (Zhang *et al.* (2014)). The type of nanotube produced depends mainly upon the presence of metal catalysts. If small amounts of transition metals such as F*e*, C*o*, N*i* or Y are introduced in the target graphite, then SWCNTs are the dominant product as reported by (Sano *et al.* (2004); Antisari *et al.* (2003)). There are many physical and chemical parameters which affect the arc-discharge process such as the dispersion and concentration of the carbon vapour in the inert gas, the inner temperature of the reactor, addition of promoters, composition of the catalyst, and the presence of hydrogen. The nucleation and the growth of the nanotubes, their inner and outer diameters and the type of nanotubes (SWCNTs, MWCNTs) are the main characteristics which can be influenced by the above-mentioned parameters (Imasaka *et al.* (2006)). Liquid N_2, doubly deionized water and aqueous solutions of N*i*SO_4, C*o*SO_4, F*e*SO_4 and N*a*C*l* have been added to the reaction environment in the arc-discharge method and their precise composition has a huge impact on the characteristics of the products (Zhu *et al.* (2002)). For example, when a liquid nitrogen in the range of 22 – 27 V, a high density of MWCNTs were obtained with distorted morphology, degraded structure and irregular shaped multi-shelled carbon 'onions' (Palkar *et al.* (2007)). Nowadays, this method has been modified to improve the efficiency and properties of CNTs, where the use of an electric field assisted arc-discharge technique resulted in direct synthesis of de-bundled SWCNTs. Antisari *et al.* (2003) has reported, > 50% of SWCTNs were obtained with less than 3 *nm* diameter. Since diameter of individual SWCNT is 1.3 – 2.7 nm, meaning thereby greater than 50% of them were isolated (mostly two bundles of SWCNT).

2.2. Chemical Vapour Deposition (CVD) Method

Chemical vapour deposition (CVD) method is the other means of synthesis for the preparation of CNT. CVD synthesis is achieved by taking a carbon species in the gas phase and using an energy source, such as plasma or a resistively heated coil in order to impart energy to a gaseous carbon molecule. Danafar *et al.* (2009) reviewed catalytic chemical vapour deposition synthesis of carbon nanotubes and found that methane, carbon monoxide, ethylene, propylene and acetylene were the most commonly used sources of gaseous carbon. The energy source is used to "crack" the molecule into a reactive radical species. These reactive species then diffuse down to the substrate, which is heated and coated in a catalyst (usually a first row transition metal such as Ni, Fe, or, Co) where it will bond. The result is that carbon nanotubes will form if the proper parameters are maintained. CVD allows the experimenter to avoid the process of separating nanotubes from the carbonaceous particulate that often accompanies the other two methods of synthesis. Excellent alignment as well as positional control on the nanometer scale can be achieved by the use of CVD method. Control over the diameter, as well as the growth rate of the CNTs can also be maintained. The appropriate metal catalyst can preferentially grow single rather than multi-walled nanotubes. Most CNT appears to be produced by chemical vapour deposition using metal catalysts (e.g., F*e*, N*i*, C*o*) or nanopores in ceramic nanomaterials (e.g, S*i*C, Al_2O_3, T*i*O_2). By this method, later named as catalytic CVD, MWCNTs and SWCNTs both were produced and the decomposition temperature was kept between 650 and 900°C which is less than other methods. More CVD methods are presented in the following.

The hot filament CVD (HFCVD) is an economical technique for the synthesis of CNTs and other carbon nanostructures such as carbon nano-flakes and

carbon nanowalls (Okazaki & Shinohara (2003); Sahoo *et al.* (2014)). In HFCVD, a relatively inexpensive substrate can be used to produce CNT. Bouanis *et al.* (2011) fabricated SWCNTs by the HFCVD method and used R*u*-nanoparticle as a catalyst and methane gas as a carbon source heated by a 2 watt filament. A substrate consist up of clay minerals like kaolinite, sepiolite and nontronite were used to prepare MWCNTs by Pastorková *et al*. (2012). CH_4 was the carbon source and H_2 was the carrier gas fed at a pressure ~ 3 KPa into the reactor, containing the clay mineral as a substrate coated with F*e* to act as a catalyst and heated upto 600°C. They concluded 3D nonaligned CNT and aligned MWCNTs were formed clay mineral substrates. Sanchez-Valencia *et al*. [43] synthesized chiral CNTs using a bottom-up technique using cyclodehydrogenation on a Pt catalyst. $C_{96}H_{54}$ was the precursor that was decomposed at 500°C (approx) under vacuum condition in order to produce (6,6) 'armchair' nanotube seeds. Finally, by epitaxial elongation chiral CNTs grew free of defects. In 2009, Swierczewska *et al*. (2014) first used gadolinium and europium as inner transition metal catalysts to grow SWCNTs by the CVD method, yielding nanotubes with 1.9 nm diameter and a narrow distribution of lengths.

Plasma enhanced CVD (PECVD) is another promising method to fabricate vertically aligned CNT (VACNTs) (Melechko *et al.* (2005)). In this method, a gas containing a carbon source mixed with a carrier gas was injected into a vacuum chamber containing a heated substrate, which was coated with catalyst. The main role of plasma is the dissociation of hydrocarbon molecules in order to produce C atoms and reactive radicals such as $^{\bullet}CH$, $^{\bullet}CH_2$, $^{\bullet 9}CH_3$ and H^+ ions at a lower temperature compared to arc discharge or laser ablation. Saghafi *et al*. (2014) reported VACNTs which were produced from acetylene gas with a silicon substrate and nickel catalyst. The pressure of the vacuum chamber was maintained

10–2 Torr at 65°C and 1.5 – 2 W/cm2DC power to heat the plasma in order to fabricate the VACNTs that had 78 *nm* diameter and 1 – 8 μm length. The variation in plasma power, pressure at which the precursors are injected, temperature of the substrate, and the chamber growth time, catalyst content and catalyst thickness are the most important parameters in the PECVD technique which has been comprehensively investigated by Loffler *et al*. (2011) and Jeong *et al*. (2012).

Radio frequency plasma-enhanced CVD (RF-PECVD) can produce a higher concentration of reactive radicals from the carbon source at a lower temperature in comparison to PECVD. Wang & Moore (2012) synthesized MWCNTs with a N*i* catalyst on S*i*, T*i*N/S*i* and a glass substrate by a RF-PECVD with RF power 600 watt whereas at low temperatures (140°C and 180°C) it is 13.56 MHz and injected CH_4, H_2 and A*r* into the chamber. They evaluated parameters such as substrate temperature and type, plasma intensity, gas flow rate and gas compositions. Dervishi *et al*. (2013) devised an inexpensive method for the preparation of CNTs using a radio frequency generator and an electrical furnace in a H_2/ A*r* atmosphere. They used an iron oxide-graphene substrate without using any hydrocarbon gas at a relatively low temperature between 150 and 500°C. They reported that if they used iron oxide nanoparticles of 5 nm diameter then CNT were formed at 150°C and for 15 nm nanoparticles the temperature needed to be 400°C or higher.

The microwave plasma-enhanced CVD (MPECVD) method is often used for the synthesis of CNTs at low temperature and high yield. Hata *et al*. (2004) also reported that water-assisted CVD (WA-CVD) was presented by adding an amount of water into the CVD reactor so that the catalyst activity, rate of formation and length increases which alter the diameter of CNTs (Wang *et al.* (2012)). WA-CVD is therefore known as d "***super-growth CVD***" due to the improved CNTs synthesis (Yamada *et al.* (2008)). Oxygen and carbon dioxide can also enhance and modify

CVD synthesis method for CNTs. Kim *et al*. (2010) reported that oxygen-assisted MPECVD using a mixture of CH_4/H_2 gases with a F*e*/A*l*$_2$O$_3$/Si substrate at 700°C could give MWCNTs with 4.08 μm length and 5 – 10 *nm* diameter.

It is also reported that, organometallic precursors based CVD combine a carbon source and the catalyst in a single compound using organometallic precursors as ferrocene or nickelocene for CNT synthesis (Rao & Govindaraj (2002). The pyrolysis of these compounds also reported in the literature which depends on the process conditions and carried out using a mixture of methane or acetylene at 1100°C to produce SWCNTs or MWCNTs (Rao & Govindaraj (2002).

A ferrocene and benzene mixture enriched with thiophene as a growth promoter was injected into a hydrogen, where, 0.5–5% by weight of thiophene was added into the stream led to the formation of SWCNTs whereas MWCNT could be formed, If the thiophene was increased to more than 5% (Cheng *et al.* (1998). The use of a ferrocene and xylene mixture can also produce MWCNT as reported in literature by Jasti & Bertozzi (2010).

2.3. Laser Ablation Method

Laser ablation or vaporization method was another among these methods for the preparation of CNTs. A high power laser is restored across a carbon target. In the plasma plume that is generated by the laser, provided that appropriate conditions exist, SWNTs form and are collected downstream from the plasma plume on a "cold finger". Laser ablation may also be used and enables production low-volume high-quality pure SWCNT. The third method of SWCNT synthesis was laser ablation in which laser vaporization of a graphite rod in an oven with C*o* and N*i* as catalysts (Bota *et al.* (2014). In this method, a carbon-metal composition is placed in a heated chamber with a flow of inert gas (A*r*) at a pressure of 500 Torr @ flow

rate of 50 sccm (standard cubic centimeters per minute). When a laser beam is focused on the target and the soot produced was deposited onto a cooled copper collector, then SWCNTs produced are 90% pure with better-graphitize like structure. It can produce a low amount of CNTs but with high purity and vice versa. Arc-discharge method can produce a large amount of CNTs but with significant impurities. Maser *et al*. (2001) reported that in this method, gas flow rate, carrier gas type, catalyst, substrate for nucleation and time are the most important parameters that affect the CNTs structure and growth (Mubarak *et al.* (2014). It is also reported that the composition of the target material is one of the crucial factors in CNT synthesis and in fact using pure graphite targets in laser ablation yields fullerenes and nano-onions rather than nanotubes. Isolated SWCNTs have been reported when monometallic C*o* or N*i* dopants has been used along with graphite as a target material. Otherwise it could have resulted in a high yield of SWCNT bundles w.r.t. bimetallic graphite containing a N*i*/Y catalyst (concentration of N*i* always higher than that of Y, or N*i*/C*o* in equal concentration) (José-Yacamán *et al*. (1993)). In this method, the CNTs best yield and quality depends on the reaction temperature of range 1200°C. It is reported by Maser *et al*. (2001) that the quality of the CNTs diminished and lots of defects appeared at lower temperatures.

Although, laser ablation and arc discharge yield nanotubes with high quality, however these methods suffer from the some shortcomings: obtaining large quantities of graphite is problematic, which limits the CNTs large-scale production, the purification process of the tangled form of nanotubes mixed with unwanted materials is problematic as well as expensive, energy consumption can be very high in these methods. It is also reported that Qin *et al*. (1998) on comparing with other methods, these two methods have a higher reaction

temperature, which imposes another difficulty in designing an industrial process. All the synthesis methods are summarized in the Table 1. As shown below

Method	**Arc discharge method**	**Chemical vapour deposition**	**Laser ablation (Vaporization)**
Who reported first?	Ebbesen and Ajayan of NEC, Japan in 1992	Endo from Shinshu University, Nagano, Japan	Smalley of Rice University USA in 1995
How it works?	connect two graphite rods to a power supply, place them a few *mm* apart from each other and throw the switch. At 100 A, carbon vaporizes and forms a hot plasma.	Place substrate in oven and heated at 600 ^{o}C, slowly add a carbon-bearing gas such as methane. As gas decomposes it frees up carbon atoms, which recombine in the form of CNTs	Blast graphite with intense laser pulses rather than electricity to generate carbon gas from which the CNTs form; optimize the best conditions until hit on one that produces prodigious amounts of SWCNTs
Typical yield	30% to 90%	20% to 100 %	Up to 70%
SWCNTs	Short tubes with diameters of 0.6*nm* to 1.4*nm*	Long tubes with diameters ranging from 0.6*nm* to 4*nm*	Long bundles of tubes (5-20 microns), with individual diameter from 1*nm* to 2*nm*.
MWCNTs	Short tubes with inner diameter of 1 *nm* to 3*nm* whereas outer diameter is 10*nm* (approximately)	Long tubes with diameter ranging from 10*nm* to 240*nm*	Not very much interest in this method, as it is too expensive, but, MWCNT synthesis is possible.
Advan	Can easily produce SWNT, MWCNTs in which	Easiest to scale up to industrial production; long	Primarily SWCNTs with good diameter control and

tages	SWCNTs have few structural defects but, MWCNTs can be produced without catalyst, less expensive, open air synthesis also possible	length, simple process, SWCNTs diameter controllable and are quite pure	few defects. The reaction product is quite pure.
Disad vantages	Tubes tend to be short with random sizes and directions; oftenly needs a lot of purification	CNTs are usually MWCNTs and often riddled with defects	Expensive method, because it requires expensive lasers with high power requirement

3. Applications of Carbon Nanotube Based Green Nanocomposites

Electronic, molecular and structural properties of carbon nanotubes are determined to a large extent by their nearly one dimensional structure because nanotubes are not one, but many materials and consist only of surface atoms. The chemical reactivity of CNTs is enhanced due to the curvature of the CNT surface when compared with a graphene sheet (Park *et al.* (2003)). Carbon nanotubes reactivity is directly related to the π-orbital mismatch caused by an increased curvature. A smaller diameter nanotubes resulted has increased reactivity due to covalent chemical modification of either sidewalls or end caps (Bahr & Tour (2002)). Therefore, a distinction can be made between the sidewall and the end caps of nanotubes and even the solubility of CNTs in different solvents can be controlled. CNTs have been exploited for applications in drug delivery; gene therapy; cancer therapy; vaccine delivery; energy storage; imaging and diagnostics in vacuum fluorescent display (VFD) as white light source, in liquid crystal display (LCD) as backlight, in cathode ray tube (CRT) and field emission display (FED) as emitter, in single electron transistor (SET) as microwave devices & ultra small

diodes high density device composites, in scanning tunneling microscope (STM) and atomic force microscope (AFM) as nano-scale wire, nano-pipettes, nano-capsule and nano-tweezers (Liu *et al.* (2012); Tatami *et al.* (2005)). Carbon nanotubes have potential applications in other fields like energy storage devices, sensors, adsorbents, sports equipments, adhesives as shown in the figure 3. Liu *et al.* (2014) have reported the development of host-guest methodology for separation of single-walled carbon nanotubes (SWCNTs) based diporphyrin nano-tweezers which have unique features due to handedness and diameter with gable-type chiral diporphyrins. They consist up of two porphyrins and rigid spacer in between and are next generations of the host molecules focusing on larger diameter of SWCNTs, named “nano-calipers”

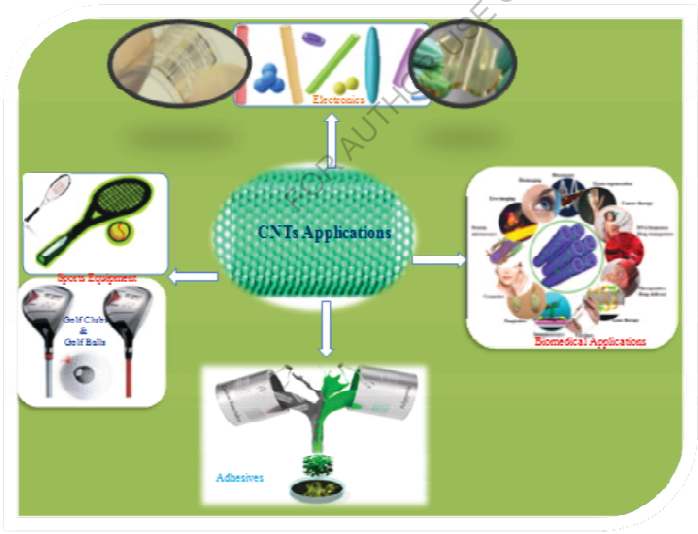

Figure 3: CNTs Applications

3.1. CNTs in Molecular Electronics and Optical Applications

Molecular electronics with CNTs results into field emitting devices as are flat panel displays, tubes in telecom networks, electron guns for electron microscopes, AFM tips and microwave amplifiers (Avouris (2002)). The quantum confinement and band gap in CNTs depends upon structure, however most properties depend on the band gap (Han *et al.* (2007)). Carbon nanotubes can be filled with molecules that have either an electronic or structural property which can be used to represent the quantum bit (Qubit) of information, and which can be associated with other adjacent Qubits (Ranjan *et al.* (2015)). If a solid is subjected to an adequately high electric field, electrons near the *Fermi level* can be extracted from the solid by tunneling through the surface potential barrier. This emission current depends on the strength of the local electric field at the emission surface and its work function indicates the energy necessary to extract an electron from its highest bounded state into the vacuum level. The applied electric field must be kept very high in order to extract an electron. This condition is fulfilled for carbon nanotubes, because their elongated shape ensures very large field amplification (Bonard *et al.* (1999)).

For technological applications, the emissive material should have a low threshold emission field and large stability at high current density. Furthermore, carbon nanotubes possess ideal qualities of being good emitter of nanometer size diameter, structural integrity, high electrical conductivity, a small energy spread and a large chemical stability (Worsley *et al.* (2010)).

CNTs based field effect transistors have excellent operating characteristics that are as good as or better than state-of-the-art silicon devices. CNTs do not have interface states that need passivation, as in the case of the S*i*-S*i*O_2 interface, which makes it easier to integrate the CNTs with high dielectrics (Yang *et al.* (2009)).

Furthermore, the high conductivity and exceptional stability of metallic nanotubes makes them excellent candidates for future use in interconnects (Kreupl *et al.* (2002)). Sahoo and Mishra (2009) reported the advantages of CNTFET over S*i*-MOSFE, where CNTFET demonstrates higher drive current, shows approximately four times higher trans-conductance and the average carrier velocity of CNTFET is almost double. The field-effect transistor is a three-terminal switching device which can be constructed of only one semiconducting SWCNTs. By applying a voltage to a gate electrode, the carbon nanotubes can be switched from a conducting to an insulating state. Such CNTs transistors can be coupled together and working as a logical switch as the basic component of computers (Javey *et al.* (2003)). Two different device architectures have been developed for the transistor configuration. In both cases, CNTs connect the source and drain electrodes and show excellence behavior in the area of memory designing, amplifiers, sensors and detectors, etc (Lin *et al.* (2012); Zaporotskova *et al.* (2016)).

Although CNTs are currently one of the most promising materials for molecular electronics, many challenges remain before they can become a successful technology. Most of these challenges involve the synthesis, separation, and self-assembly of CNTs. Appropriate functionalization of the nanotubes can help achieve the self-assembly of CNT circuits. To a great extent, the future of CNTs electronics is now in the hands of the chemists (Maune *et al.* (2010); Rao *et al.* (2003)).

Theoretical studies have been reported in the literature, where it is revealed that the optical activity of chiral carbon nanotubes disappears if their size becomes larger (Ivchenko & Spivak (2002)). Therefore, it is expected that other physical properties are influenced by these parameters too. Use of the optical activity might result in optical devices in which CNTs play an important role (Rotkin &

Subramoney (2006)). However, a bottleneck in the use of nanotubes for applications is the dependence of the conductivity and emission stability of the nanotubes on the fabrication process and synthesis conditions. Thus, CNTs as field emitting devices are flat panel displays, tubes in telecom networks, electron guns for electron microscopes, AFM tips and microwave amplifiers (Liang *et al.* (2016); Irita *et al.* (2018)).

3.2. CNTs in Energy Storage Applications

3.2.1. CNTs in Hydrogen storage: The first and foremost advantage of hydrogen as energy source is that its combustion product is water and the other is that it can be easily regenerated. Therefore, a suitable hydrogen storage system is necessary and which satisfies a combination of both volume and weight limitations. Because of their cylindrical and hollow geometry, and nano metre-scale diameters, it has been reported that CNTs can store a liquid or a gas in the inner cores through a capillary effect (Lee & Lee (2000)). Since Iijima (1991) reported the synthesis of carbon CNTs, these have been regarded as a good candidate material for hydrogen storage. However, it was 6 years after Dillon *et al.* (1997) reported the first experimental evidence for hydrogen storage in carbon nanotubes. In their first experiment, it was shown that carbon can store considerable amounts of hydrogen at room temperature. Later on, Chen *et al.* (1999) reported that alkali-doped carbon nanotube demonstrate high hydrogen uptake. They investigated lithium- and potassium-doped carbon nanotubes and found hydrogen adsorption of 14% to 20% by weight between 25 to 400 °C (Froudakis (2001)). However, Yang (2000) replicated their experiments and reported that the high uptake is mainly attributed due to the moisture and the weight gained by reactions with the alkali species in the alkali-metal-doped CNTs and hence the contribution from pure hydrogen storage was limited. Kajiura *et al.*

(2003) have reported in his experimental work that the hydrogen storage performance of SWCNTs, MWCNTs, and nanofibers (CNFs), at optimum temperature and up to 8 MPa, cannot surpass 0.43 wt% (obtained for purified SWNTs). Ritschel *et al.* (2002) also studied and reported the hydrogen storage capacity of different carbon nanostructures such as SWCNTs, MWCNTs, and CNFs. According to him, the purified SWCNTs showed a reversible storage capacity of 0.63 % by weight at room temperature and 45 bar, which is higher for SWCNTs as compared to MWCNTs and CNFs. The improvements are still going on to obtain CNT based better hydrogen storage cages (Ghosh *et al.* (2017); Jiang *et al.* (2018)).

3.2.2. CNTs in Lithium intercalation: The basic principle of rechargeable lithium batteries is electrochemical intercalation and deintercalation of lithium in both electrodes. An ideal battery has a high-energy capacity, fast charging time and a long cycle time. The capacity is determined by the lithium saturation concentration of the electrode materials (De las Casas & Li (2012)). For L*i*, this is the highest in nanotubes if all the interstitial sites (inter-shell vander Waals spaces, inter-tube channels and inner cores) are accessible for L*i* intercalation (Gao *et al.* (1999)). SWCNTs have shown to possess both highly reversible and irreversible capacities, because of the large observed voltage hysteresis (Frackowiak & Beguin (2002)). L*i*-intercalation in CNTs is still unsuitable for battery application. This feature can potentially be reduced or eliminated by processing and cutting the nanotubes to short segments (Fang *et al.* (2017)).

3.2.3. CNTs in Electrochemical supercapacitors: Supercapacitors have a high capacitance and potentially applicable in electronic devices. Usually, they are comprised of two electrodes separated by an insulating material which ionically conducts electrochemical devices (Vivekchand *et al.* (2008)). The capacity of

electrochemical supercapacitors depends inversely on the separation between the charge on the electrode and the counter charge in the electrolyte (Conway (2013)). Since, the separation for CNTs in electrodes is about only fewest nanometers, their high surface area results very large capacities which are accessible to the electrolytes. Therefore, a large amount of charge injection transpires if only a small voltage is applied. This charge injection is used for energy storage in CNTs based supercapacitors (Wang *et al.* (2017)).

3.4. CNTs in Thermal and Mechanical Applications

One of the "carbon nanotubes" coveted properties is that they have extreme strength. Walters *et al*. (1999) Yu *et al.* (2000) reported that SWCNTs are said to be around 10 times stronger than steel and 1-2 times stiffer (axial) than diamond and are considered to be one of the stiffest materials. Its excellent mechanical properties come from the strong covalent bonds (sp^2 hybrids) that connect the carbon atoms in the graphene structure. Fundamentally, CNTs are relatively soft and easily deformed. Ruoff *et al.* (1993) has shown that the van der Waals forces from adjacent CNTs are sufficient to deform the tubes which has radial flexibility and can be bent several times up to 90 degrees without being damaged. CNTs have a very large Young's modulus in their axial direction. Therefore, these compounds are potentially suitable for applications in composite materials that need anisotropic properties. Jorio *et al.* (2008) reported that oscillators based on CNTs have achieved higher speeds than other technologies (>50 GHz. The operation of these oscillators is primarily based on the low friction and low wear bearing properties of MWCNTs with a diameter ranging from 1 nm to a few tens of nanometers. CNTs can be used to prepare super-hydrophobic cotton fabric by using dip-coating approach, which is solely based on the chemical reactions caused by UV-activated nitrene solution (Li *et al.* (2010)). The solution is used to

transform the cotton fabric surface from hydrophilic to super-hydrophobic with an apparent water contact angle of 154º. Since, the super-hydrophobicity possesses high stability and chemical durability CNTs gets covalently attached to the fabric surface (Jung *et al.* (2018); Guo *et al.* (2017)).

3.5. CNTs as Nanoprobes and Sensors

Due of the flexible nature, nanotubes can also be used in scanning probe instruments. Since MWCNTs tips are conducting, they can be used in STM and AFM instruments. Advantages are the improved resolution in comparison with conventional Si or metal tips (Zhao *et al.* (2002)). These tips do not suffer from crashes with the surfaces because of their high elasticity. However, CNTs vibration will remain an important issue due to their large length until the shorter nanotubes can be grown controllably. CNTs tips can be modified chemically by attachment of functional groups, therefore, CNTs can be used as molecular probes. A pair of nanotubes can be used as tweezers to move nano-scale structures on their surfaces. Sheets of SWCNTs can be used as electromechanical actuators, mimicking the actuator mechanism present in natural muscles. SWCNTs may also be reported to be used as miniaturized chemical sensors (Salavagione *et al.* (2014)). On exposure to NO_2, NH_3 or O_2 etc. rich environments, the electrical resistance changes. Wu *et al*. (2018) reported that nanoprobes such as single-walled carbon nanotubes (SWCNTs) are capable of label-free detection that benefits from intrinsic and photostable near-infrared fluorescence, whereas Yi *et al*. (2012) reported genetically engineered multifunctional M13 phage which can assemble and functionalized Single-Walled Carbon Nanotubes (SWCNTs) as nanoprobes for Second Near-Infrared Window Fluorescence Imaging of Targeted Tumors. Wei *et al*. (2008) reported Control of Length and Spatial Functionality of

SWCNTs AFM Nanoprobes WCNTs nanofibrils assembled onto conductive atomic force microscopy (AFM) probes with the help of dielectrophoresis (DEP).

3.6. CNTs as Composite Materials

One of the most important applications of CNTs based on their properties which may be used as reinforcements in high strength, low weight, and high performance composites in composite materials (Moniruzzaman & Winey (2006)). However, there have not been many successful experiments that show that CNTs are better fillers than the traditionally used carbon fibers. A main advantage of using nanotubes for structural polymer composites is that CNT reinforcements will increase the toughness of the composites by absorbing energy during their highly flexible elastic behavior (Dyke & Tour (2004)). Other advantages are the low density of the CNTs, an increased electrical conduction and better performance during compressive load. Another possibility is filling of photoactive polymers with CNTs, which is an example of a non-structural application (Liu & Kumar (2014)). PPV (Poly-p-phenylenevinylene) filled with MWCNTs and SWCNTs is a composite, show a large increase in conductivity with only a little loss in photoluminescence and electro-luminescence yields. Another benefit is that the CNT based composite are more robust than the pure polymer. CNTs-polymer based composites could be used in the biochemical field as membranes for molecular separations or for osteointegration (growth of bone cells) (de Menezes *et al.* (2019)). CNTs also exist as templates for hybrid materials, because of the small channels, strong capillary forces which exist among the nanotubes. These forces are strong enough to hold gases and fluids in nanotubes. In this way, it may be possible to fill the cavities of the nanotubes to create nanowires (Ponnamma *et al.* (2014)).

3.7. CNTs in Pharmaceutics, Biomedical **Biotechnological and Bioengineering** Applications

Klumpp *et al*. (2006); Mehra *et al*. (2008); He *et al*. (2013) reported that CNTs are assumed to be biocompatible, non-biodegradable and non-immunogenic in their nature. They are supposed to have highly elastic nature and therefore wide applications in intracellular delivery. CNTs may exhibit minimum cytotoxicity. Beg *et al.* (2013) reviewed that the CNTs can be designed for very specific purposes in the area of biomedicine in especially four main fields: drug delivery, biomedical imaging, biosensors and scaffolds in tissue engineering.

3.7.1. CNTs in Drug delivery: Specific drug delivery is an essential method used in medicine to deliver pharmaceutics to the specific place in the body where it is needed. CNTs based drug delivery shows great promise in cancer therapy since one of the biggest challenges in treating cancer is the severe side effects caused by the chemotherapy (Bianco *et al.* (2005); Liu *et al.* (2011)).

3.7.2. CNTs in Cancer Treatment: CNTs (MWCNTs or SWCNTs) have wide application in the treatment of blood cancer, breast cancer, liver cancer and brain cancer *etc.* Leukemia is a cancer that begins in the bone marrow, which is the soft inner part of some bones, however, moves into the blood (Madani *et al.* (2011)). It can then spread to other parts of the body, such as organs and tissues. Acute lymphoblastic leukemia (ALL) is one of the four main types of leukemia which is slow-growing blood cancer that starts in bone marrow cells called lymphocytes or white blood cells. Once these white blood cells are affected by leukemia, they do not go through their normal process of maturing. An intensified targeted delivery of daunorubicin (Dau) to acute lymphoblastic leukemia was achieved by Taghdisi *et al.* (2011). They developed a tertiary complex of Sgc8c aptamer (targets

leukemia biomarker protein tyrosine kinase-7), daunorubicin, and SWCNT named as Dau-aptamer SWCNTs. Flow cytometric analysis viewed that the tertiary complex was internalized effectively into human T cell leukemia cell (MOLT-4 cells) but not to U266 myeloma cells. Release of Dau-loaded CNTs was pH-dependent. In a slightly acidic solution at pH 5.5, Dau was released from complex in 72 h at 37 ºC, while Dau-aptamer-SWCNTs tertiary complex was pretty stable after the same incubation at pH 7.4. Liu *et al.* (2008)*.,* studied SWCNT delivery of paclitaxel (PTX) into xenograft tumors in mice with higher tumor suppression efficacy than the clinical drug formulation Taxol. The PTX conjugated to PEGylated SWCNTs showed high water solubility and maintains alike toxicity to cancer cells as Taxol *in vitro*. SWCNT-PTX affords much longer blood circulation time of PTX than that of Taxol and PEG ylated PTX, leading to high tumor uptake of the drug through EPR effect. The strong therapeutic efficacy of SWCNT-PTX is shown by its ability to slow down tumor growth even at a lower drug dose. Pan *et al.* (2012) investigated the efficiency of MWCNTs to deliver the gene to the tumor cell for cancer therapy, where they fabricated MWCNTs modified with polyamidoamine dendrimer which were further conjugated with FITC-labelled antisense c-myc oligonucleotides (asODN). Ou *et al.* (2009) synthesized phospholipid-bearing polyethylene glycol (PL-PEG) functionalized SWCNTs conjugated with protein A, which was further coupled with the fluorescein-labeled integrin monoclonal antibody to form SWCNT-integrin monoclonal antibody (SWCNT-PEGmAb).

3.7.3. CNTs in Lymph Node Metastasis

Yang *et al.* (2011) compared the *in vitro* and *in vivo* potential therapeutic effect of gemcitabine (GEM) loaded magnetic MWCNTs (mMWCNTs) with that of gemcitabine loaded magnetic-carbon particles (mACs). Due to the super

paramagnetic behaviour of mMWCNTs-GEM, their magnetic moments tend to align along the applied field leading to net magnetization which greatly affects the interaction of mMWCNTs-GEM with the cellular membrane and thus they were found to be superior than mACs-GEM in successful inhibition of lymph node metastasis after following subcutaneous administration under the impact of magnetic field. Li *et al.* (2011) developed a novel approach of utilizing natural biocompatible polymer chitosan for imaging the tumor cells. Combining the intrinsic properties of CNTs, versatility of chitosan, and folic acid, FITC-CHIT-SWCNT-FA can be used as potential devices for targeting the drug into the tumor cells and also for imaging.

3.7.4. CNTs in Gene therapy

CNTs can deliver a large amount of therapeutic agents, including DNA and RNA, to the target disease sites, Gene therapy and RNA have presented a great potential for antitumor treatment (Bates & Kostarelos (2013)). The wire shaped structure matches with DNA/siRNA diameter and their remarkable flexibility; CNTs can influence the conformational structure and the transient conformational changes of DNA RNA and further enhance the therapeutic effects of DNA/siRNA. The treatment of a human lung carcinoma model *in vivo* using siRNA sequences led to cytotoxicity and cell death using amino-functionalized multiwalled carbon nanotubes (Ren *et al.* (2018).

3.7.5. CNTs in Immune therapy

Chemotherapy faces the issues of accumulative toxicity and drug resistance, anti-tumor immunotherapy usually has few adverse effects, good patient tolerance, and the potential to improve the prognosis significantly (Fadel & Fahmy (2014)). CNTs have also shown the potential to boost the antigenicity of the carried

peptides/proteins. Meng *et al.* (2008) studied that MWCNTs conjugated to tumor lysate protein will enhance the efficacy of an anti-tumor immunotherapy that employs tumor cell vaccine (TCV) in a mouse model bearing the H22 liver cancer. The study showed that MWCNTs conjugated to tumor lysate protein enhanced the specific anti-tumor immune response and the cancer cure rate of a TCV immunotherapy in mice.

3.7.6. CNTs in Biomedical imaging

The unique electrical, mechanical and optical properties properties of CNTs are very useful in applications such as biomedical imaging (Gong *et al.* (2013)). SWCNTs have strong optical absorption from ultraviolet (UV) to near infra-red (NIR) regions and are useful in a range of different imaging techniques. These include photo-acoustic imaging, Raman imaging, fluorescence imaging, and with functionalization of the CNTs also positron emission tomography (PET) imaging and magnetic resonance (MR) imaging. Kam *et al.* (2004) reported the CNTs were functionalized with a specific receptor for internalization into a specific cell type thus imaging these cells with very low auto fluorescence background. In an *in vivo* study the bio-distribution of SWCNTs in live drosophila larvae was monitored by fluorescence imaging. In photo-acoustic imaging deeper tissue penetration can be achieved compared to most other optical imaging techniques (Xie *et al.* (2016)). The technique makes use of certain light absorbing CNTs based molecules that converts laser pulses delivered into the biological tissue to heat. Thereby passing thermo-elastic expansion is induced and giving rise to wideband ultrasonic emission, detected by an ultrasonic microphone. Due to high optical absorption in the NIR range, SWCNTs make a useful contrast agent in this kind of biomedical imaging.

3.7.6. CNTs in Biosensors and Tissue Engineering

Biosensors are used for mentioning biological processes or for recognition of bio-molecules and differ from other sensors by having a sensing element consisting of a biological material such as proteins, polynucleotides or microorganisms. It is reported by Gao *et al*. (2003) that CNT-based biosensors incorporating enzymes have been produced for detection of glucose and other biomolecules.

CNTs are also useful in enhancing tissue matrices and tissue scaffold, which played an important part in tissue engineering, which provides the structural support for the new tissue. It is responsible for defining the space which new tissue occupies, and for aiding the process of tissue development. The scaffolds have high mechanical strength, good biocompatibility (supporting cell adhesion, viability, proliferation and differentiation), and biodegradability and these criteria meet using CNTs in the production of the scaffold and with superior results compared to other materials used in tissue engineering (Edwards *et al*. (2009)). Studies have shown that scaffolds of CNTs seem to be biocompatible both *in vitro* and *in vivo* when mixed with other materials such as in a polymer matrix of chitosan which itself is highly biocompatible.

3.8. CNTs in Catalysis & Enzyme Immobilization Applications

Yan *et al.* (2015) reported that CNTs are used in several catalytic reactions as catalyst or as support for biocatalysts. According to Melchionna *et al.* (2015) Carbon nanotubes have emerged as unique carbon allotropes that bear very interesting prospects in catalysis. In particular liquid phase reactions were studied extensively with MWCNTs. Higher surface area and mesoporous nature resulted in significant decrease in mass transfer limitations compared to activated carbon. N*i*, R*h*, R*u* supported on CNTs were reported to be more active for hydrogenation reactions

compared to when supported on activated carbon. Hydrogenation reactions such as hydrogenation of alkenes and α,β – unsaturated aldehyde have been reported for CNT supported catalysts. Ruthenium nanoparticles supported on MWCNTs showed excellent catalytic activity for hydrogenation of aromatic hydrocarbon. Onoe *et al.* (2007) reported that 5% P*t*/CNT catalyst (by weight) to be significantly more active than 5% P*t*/AC (by weight) for hydrogenation of trans–diphenylethene and trans–β–methylstyrene. Rhodium complex grafted on MWCNTs was reported by Lmus-Yegres *et al.* (2008) that it to be very active for cyclohexene hydrogenation whereas; P*d*/CNT catalyst was found to be active for benzene hydrogenation according to Zhang *et al.* (2004). Lordi *et al.* (2001) has found that Pt supported on SWCNTs were to be active and selective in hydrogenation of prenal (3-methyl-2-butenal) to prenol (3-methyl-2-butenol). Van steen and Prinsloo (2002) investigated that CNTs have been used as catalyst support in Fischer–Tropsch synthesis reactions of methanol, higher alcohols and hydroformylation reactions. Copper promoted F*e*/MWCNT catalysts are active for Fischer-Tropsch synthesis with olefins. Chin *et al.* (2001) exhibited an enhancement in Fischer-Tropsch activity when C*o*-R*e*/Al_2O_3 deposited on MWCNT by dip coating as compared to what observed with a similar system without CNT arrays. MWCNTs also have been used as promoter by Dong *et al.* (2003) for C*u*-Z*n*O-Al_2O_3 based catalysts for methanol synthesis using H_2/CO/CO_2. The complex [HR*h*(CO)(PPh_3)$_3$] has been grafted onto MCWNTs and used for hydroformylation of propene. Higher conversion and higher regioselectivity toward n-butaldehyde have been reported by Zhang *et al.* (1999) for CNT supported catalysts compared to that activated carbon or carbon molecular sieve supported catalysts. The R*u*/C catalysts were studied as an alternative to conventional F*e*-based catalyst for ammonia synthesis at high pressure and temperature. However, it is prone to

deactivation due to metal sintering, metal leaching or methanation of support. The stability of the catalyst is reported to increase on using CNTs as support. R*u*-K/MWCNT catalyst has been found to be significantly more active than R*u* supported on other carbon supports as reported by Chen *et al.* (2005). The catalytic decomposition of ammonia to generate CO free hydrogen for fuel cells has received increasing attention, because it is more economical than using methanol as hydrogen source. Yin *et al.* (2004) reported that The MWCNT supported ruthenium was found to be more active than M*g*O, T*i*O_2 or Al_2O_3 supported R*u*. CNTs were also reported to be used as catalysts supports for anode or cathode catalysis in direct methanol fuel cells or proton exchange membrane fuel cells, where its structure has direct impact on fuel cells performance. The most studied reactions are methanol oxidation (anode catalyst), oxygen reduction (cathode catalyst) and hydrogen oxidation (anode catalyst), where P*t* is most used metal followed by P*t*-R*u* system. The CNT based catalysts are observed to be more active and better resistant to poisoning compared to conventional carbon black support. The advantage of CNT supports for fuel cell applications is due to higher metal dispersion and higher electroactive surface area, higher mesoporous 3D network to facilitates mass transport and excellent conducting properties which improve electron transfer. CNTs have also been used as direct catalyst for some specific reactions such as methanation to produce CO and CO_2 free hydrogen, oxidative dehydrogenation of ethyl benzene to styrene and oxidative dehydrogenation of propane to propene, selective oxidation of H_2S and aniline, esterification and hydroxylations.

CNTs have been used for enzyme immobilization which increases enzyme stability, control of pore size, multiple active sites and reduced mass transfer limitations. Du *et al.* (2015) reported that a two-Enzyme immobilization approach

Using CNTs/Silica as support. Individually pre-immobilized a-amylase and glucoamylase were sequentially co-immobilized on silica microspheres. The permeable sol-gel layer allows the hydrolysis of starch into oligosaccharides by the entrapped CNT-a-amylase, and then the oligosaccharides were subsequently catalyzed into glucose by CNT-glucoamylase. The sequentially co-immobilized enzymes exhibited a higher substrate affinity and comparable specificity and catalytic efficiency in comparison to the mixture of free enzymes. Ke *et al.* (2014) reported an enhanced enzyme activity and enantioselectivity of *Burkholderia cepacia* lipase (BCL) *via* immobilization on modified MWCNTs. CNT–BCL exhibits great advantages and possesses promising potential in industrial application.

3.9. CNTs in Conductive Adhesives Applications

Carbon nanotubes are certainly excellent electrically-conductive and thermally-conductive nano filler for polymers. Yu *et al.* (2010) have reported the use of carbon nanotubes reinforced epoxy as adhesives to join aluminum plates. CNTs reinforced epoxy adhesives were successfully developed by use of mechanical stirring followed by ultrasonication. The carbon nanotubes distributed uniformly in the epoxy matrix with no obvious agglomerations at 1% (by wt) of CNTs. The adhesives were used to bond aluminum plates due to increased bonding strength and durability with the incorporation of CNTs and it is confirmed by *Boeing Wedge* test. Li *et al.* (2019) reported that Gecko-inspired vertically aligned carbon nanotubes (VA-CNTs) exhibit ultra-strong adhesion, dopamine is used to make a modification to this traditional biomimetic material. Li *et al.* (2015) presented a transfer method to fabricate vertically aligned carbon nanotubes (VACNT) array-based dry adhesive materials onto a flexible PET substrate with TPU as the inter-medium. A thermal oxidation process was introduced to obtain free standing VACNTs arrays, resulting in the production of top-transferred and bottom-

transferred structural VACNTs array-based dry adhesive materials. Interfacial bonding strength of the transferred VACNTs array was enhanced dramatically, and an improved adhesive behavior were exhibited. The flexible structure of the transferred VACNTs array showed a better non-fouling state by mimicking the DH motion of the gecko foot. It is a stable structure of VACNTs array-based dry adhesive materials with strong interfacial bonding, high adhesive strength, and ability to keep non-fouling state. It reveals a new direction for the biomimetic design of VACNTs array-based gecko-inspired dry adhesive materials with high reusability and reliable properties. Hu *et al.* (2013) also reviewed progresses in the development of advanced gecko-foot-mimetic dry adhesives based on CNTs. With unique hierarchical fibrillar structures on their feet, gecko lizards can walk on vertical walls or even ceilings. Hu *et al.* (2010) have shown that strong binding along the shear direction and easy lifting in the normal direction can be achieved by friction and adhesion of hierarchical CNT structures for biomimetic dry adhesives multiscale modeling. Sethi *et al.* (2008) reported that design of reversible adhesives requires both stickiness and the ability to remain clean from dust and other contaminants and inspired by gecko feet, CNTs based flexible gecko tapes has the self-cleaning ability. It is also reported by Messina et al. in 2016 that on the addition of a commercially available conductive resin with double-wall carbon nanotubes (DWCNTs) and graphene nano-platelets for hybrid conductive adhesives with enhanced thermal and electrical conductivity is essential for the fabrication of compact microelectronic and optoelectronic power devices. Yu *et al.* (2013) reported a facile synthesis of carbon nanotube-inorganic hybrid materials with improved photoactivity and these modified CNTs act as a scaffold in core–shell composites with a uniform T*i*O_2 coating through esterification and hydrolysis.. Sánchez-Romate *et al*. (2017) reported a novel CNTs-doped adhesive

film, has been developed to detect adhesive deformation and crack propagation along the bonding line by means of the electrical response of the material. Novel graphene/CNTs based composite films with high hydrophobicity, low water adhesion, high conductivity and stable hydrophobic capability under applied potentials are reported by Pu *et al*. (2013); Mionic *et al.* (2012) reported that the UV and temperature processed structures show very good adhesion and reasonably good resistivity with a low concentration of carbon nanotubes. Their reported composite material for inkjet deposition is completely compatible with current MEMS fabrication processes.

3.10. CNTs in Waste Water Treatments

It is indeed a matter of concern about the CNTs potential environmental and human health risks, the expanding use of single-walled carbon nanotubes (SWCNTs) raises environmental concerns. Wastewater treatment systems are potential recipients of SWCNTs containing influent; however some researchers have poorly documented the impacts of SWCNTs on these systems and reported their applications in waste water treatments (Qu *et al.* (2015)). A unique type of carbon nanotubes (CNTs), vertically aligned CNTs (VACNTs) possess the intrinsic, extraordinary nano-scale properties (mechanical, electrical, and thermal) of individual CNTs, but present them in a hierarchical and anisotropic morphology, which holds promise to transform a diverse set of practical environmental application processes from water filtration to energy storage. Shi & Plata (2018), reported vertically aligned CNTs as an example to explore strategies to co-optimize their environmental benefits and costs, which could potentially impact the way all other emerging materials are designed for environmental sustainability purposes. Bisesi Jr *et al.*(2017) suggested that, because of single-walled carbon nanotubes (SWCNTs) adsorptive nature, these can make their way

into aquatic environments and may reduce the toxicity of other waterborne contaminants. Pan & Xing (2008), also reported the adsorption mechanisms of organic chemicals on CNTs. Lin *et al.* (2006) reported a simple and highly effective process for perchlorate removal based on electrically switched ion exchange (ESIX) which was developed by using polypyrrole (PPy) deposited on high surface area carbon nanotubes.

4. Conclusions

It is concluded that, this chapter presented the unique atomic structures, variety of CNTs, properties and applications of CNTs. These are classified as SWCNTs and MWCNTs, are known to display unique combination of strength, tenacity, and stiffness, previously unobserved in any other material. Herein, we summarized different production methods and purification methods are reviewed for the syntheses of SWCNTs and MWCNTs In this chapter, we have also discussed some good applications of functionalized CNTs, elsewhere reported in the literature. CNTs are known to show different applications in different fields such as molecular electronics and optical sensors; as energy storage for hydrogen storage, lithium intercalation, electrochemical supercapacitors, field emission display, microscopy; thermal and mechanical applications due to stiffness and flexibility; as nanoprobes and sensors in biomedicines; as composite materials; pharmaceuticals, biomedical, biotechnological and bioengineering fields; catalysis & enzyme immobilization applications; conductive-adhesives and waste water treatments and so on. All in all we can say that "*CNTs are indeed ……a wonder material*"

Refrences

- Alshehri, R., Ilyas, A. M., Hasan, A., Arnaout, A., Ahmed, F., & Memic, A. (2016). Carbon nanotubes in biomedical applications: factors, mechanisms, and remedies of toxicity: miniperspective. *Journal of medicinal chemistry*, *59*(18), 8149-8167.
- Al-zubaidi, A., Ji, X., & Yu, J. (2017). Thermal charging of supercapacitors: a perspective. *Sustainable Energy & Fuels*, *1*(7), 1457-1474.
- Antisari, M. V., Marazzi, R., & Krsmanovic, R. (2003). Synthesis of multiwall carbon nanotubes by electric arc discharge in liquid environments. *Carbon*, *41*(12), 2393-2401.
- Avouris, P. (2002). Molecular electronics with carbon nanotubes. *Accounts of chemical research*, *35*(12), 1026-1034.
- Avouris, P., Appenzeller, J., Martel, R., & Wind, S. J. (2003). Carbon nanotube electronics. *Proceedings of the IEEE*, *91*(11), 1772-1784.
- Azad, N., Iyer, A. K. V., Wang, L., Liu, Y., Lu, Y., & Rojanasakul, Y. (2013). Reactive oxygen species-mediated p38 MAPK regulates carbon nanotube-induced fibrogenic and angiogenic responses. *Nanotoxicology*, *7*(2), 157-168.
- Aztatzi-Pluma, D., Castrejón-González, E. O., Almendarez-Camarillo, A., Alvarado, J. F., & Duran-Morales, Y. (2016). Study of the molecular interactions between functionalized carbon nanotubes and chitosan. *The Journal of Physical Chemistry C*, *120*(4), 2371-2378.
- Baddour, C. E., & Briens, C. (2005). Carbon nanotube synthesis: a review. *International journal of chemical reactor engineering*, *3*(1).
- Bahr, J. L., & Tour, J. M. (2002). Covalent chemistry of single-wall carbon nanotubes. *Journal of Materials Chemistry*, *12*(7), 1952-1958.
- Ballesteros, B., de la Torre, G., Ehli, C., Aminur Rahman, G. M., Agulló-Rueda, F., Guldi, D. M., & Torres, T. (2007). Single-wall carbon nanotubes bearing covalently linked phthalocyanines− photoinduced electron transfer. *Journal of the American Chemical Society*, *129*(16), 5061-5068.

- Baoukina, S., Monticelli, L., & Tieleman, D. P. (2013). Interaction of pristine and functionalized carbon nanotubes with lipid membranes. *The Journal of Physical Chemistry B*, *117*(40), 12113-12123.
- Bates, K., & Kostarelos, K. (2013). Carbon nanotubes as vectors for gene therapy: past achievements, present challenges and future goals. *Advanced drug delivery reviews*, *65*(15), 2023-2033.
- Beg, S., Rizwan, M., Sheikh, A. M., Hasnain, M. S., Anwer, K., & Kohli, K. (2011). Advancement in carbon nanotubes: basics, biomedical applications and toxicity. *Journal of pharmacy and pharmacology*, *63*(2), 141-163.
- Bhaskar, A., Deepa, M., & Narasinga Rao, T. (2013). MoO2/multiwalled carbon nanotubes (MWCNT) hybrid for use as a Li-ion battery anode. *ACS applied materials & interfaces*, *5*(7), 2555-2566.
- Bhattacharyya, S., Guillot, S., Dabboue, H., Tranchant, J. F., & Salvetat, J. P. (2008). Carbon nanotubes as structural nanofibers for hyaluronic acid hydrogel scaffolds. *Biomacromolecules*, *9*(2), 505-509.
- Bianco, A., Kostarelos, K., & Prato, M. (2005). Applications of carbon nanotubes in drug delivery. *Current opinion in chemical biology*, *9*(6), 674-679.
- Bianco, A., Kostarelos, K., Partidos, C. D., & Prato, M. (2005). Biomedical applications of functionalised carbon nanotubes. *Chemical Communications*, (5), 571-577.
- Bisesi Jr, J.H., Robinson, S.E., Lavelle, C.M., Ngo, T., Castillo, B., Crosby, H., Liu, K., Das, D., Plazas-Tuttle, J., Saleh, N.B. & Ferguson, P. L. (2017). Influence of the gastrointestinal environment on the bioavailability of Ethinyl estradiol Sorbed to single-walled carbon nanotubes. *Environmental science & technology*, *51*(2), 948-957.
- Bonard, J. M., Salvetat, J. P., Stöckli, T., Forro, L., & Chatelain, A. (1999). Field emission from carbon nanotubes: perspectives for applications and clues to the emission mechanism. *Applied Physics A*, *69*(3), 245-254.

- Bota, P. M., Dorobantu, D., Boerasu, I., Bojin, D., & Enachescu, M. (2014). Synthesis of single-wall carbon nanotubes by excimer laser ablation. *Surface Engineering and Applied Electrochemistry*, *50*(4), 294-299.
- Bottini, M., Bruckner, S., Nika, K., Bottini, N., Bellucci, S., Magrini, A., Bergamaschi, A. & Mustelin, T. (2006). Multi-walled carbon nanotubes induce T lymphocyte apoptosis. *Toxicology letters*, *160*(2), 121-126.
- Bouanis, F. Z., Baraton, L., Huc, V., Pribat, D., & Cojocaru, C. S. (2011). High-quality single-walled carbon nanotubes synthesis by hot filament CVD on Ru nanoparticle catalyst. *Thin Solid Films*, *519*(14), 4594-4597.
- Chen, H.B., Lin, J.D., Cai, Y., Wang, X.Y., Yi, J., Wang, J., Wei, G., Lin, Y.Z. & Liao, D. W. (2001). Novel multi-walled nanotubes-supported and alkali-promoted Ru catalysts for ammonia synthesis under atmospheric pressure. *Applied surface science*, *180*(3-4), 328-335.
- Chen, P., Wu, X., Lin, J., & Tan, K. L. (1999). High H2 uptake by alkali-doped carbon nanotubes under ambient pressure and moderate temperatures. *Science*, *285*(5424), 91-93.
- Chen, W., Xiao, P., Chen, H., Zhang, H., Zhang, Q., & Chen, Y. (2018). Polymeric Graphene Bulk Materials with a 3D Cross-Linked Monolithic Graphene Network. *Advanced materials*, 1802403.
- Cheng, H. M., Li, F., Su, G., Pan, H. Y., He, L. L., Sun, X., & Dresselhaus, M. S. (1998). Large-scale and low-cost synthesis of single-walled carbon nanotubes by the catalytic pyrolysis of hydrocarbons. *Applied Physics Letters*, *72*(25), 3282-3284.
- Chin, Y. H., Hu, J., Cao, C., Gao, Y., & Wang, Y. (2005). Preparation of a novel structured catalyst based on aligned carbon nanotube arrays for a microchannel Fischer-Tropsch synthesis reactor. *Catalysis today*, *110*(1-2), 47-52.
- Coleman, J. N., Khan, U., Blau, W. J., & Gun'ko, Y. K. (2006). Small but strong: a review of the mechanical properties of carbon nanotube–polymer composites. *Carbon*, *44*(9), 1624-1652.

- Conway, B. E. (2013). *Electrochemical supercapacitors: scientific fundamentals and technological applications*. Springer Science & Business Media.
- Cui, D., Tian, F., Ozkan, C. S., Wang, M., & Gao, H. (2005). Effect of single wall carbon nanotubes on human HEK293 cells. *Toxicology letters*, *155*(1), 73-85.
- Danafar, F., Fakhru'l-Razi, A., Salleh, M. A. M., & Biak, D. R. A. (2009). Fluidized bed catalytic chemical vapor deposition synthesis of carbon nanotubes—a review. *Chemical Engineering Journal*, *155*(1-2), 37-48.
- De las Casas, C., & Li, W. (2012). A review of application of carbon nanotubes for lithium ion battery anode material. *Journal of Power Sources*, *208*, 74-85.
- de Menezes, B. R. C., Rodrigues, K. F., da Silva Fonseca, B. C., Ribas, R. G., do Amaral Montanheiro, T. L., & Thim, G. P. (2019). Recent advances on the use of carbon nanotubes as smart biomaterials. *Journal of Materials Chemistry B*.
- Dervishi, E., Biris, A. R., Driver, J. A., Watanabe, F., Bourdo, S., & Biris, A. S. (2013). Low-temperature (150° C) carbon nanotube growth on a catalytically active iron oxide–graphene nano-structural system. *Journal of catalysis*, *299*, 307-315.
- Di Giorgio, M. L., Di Bucchianico, S., Ragnelli, A. M., Aimola, P., Santucci, S., & Poma, A. (2011). Effects of single and multi walled carbon nanotubes on macrophages: cyto and genotoxicity and electron microscopy. *Mutation Research/Genetic Toxicology and Environmental Mutagenesis*, *722*(1), 20-31.
- Dillon, A., Jones, K. M., Bekkedahl, T. A., Kiang, C. H., Bethune, D. S., & Heben, M. J. (1997). Storage of hydrogen in single-walled carbon nanotubes. *Nature*, *386*(6623), 377.
- Dillon, E. P., Crouse, C. A., & Barron, A. R. (2008). Synthesis, characterization, and carbon dioxide adsorption of covalently attached polyethyleneimine-functionalized single-wall carbon nanotubes. *Acs Nano*, *2*(1), 156-164.
- Dong, X., Zhang, H. B., Lin, G. D., Yuan, Y. Z., & Tsai, K. R. (2003). Highly active CNT-promoted Cu–ZnO–Al 2 O 3 catalyst for methanol synthesis from H 2/CO/CO 2. *Catalysis letters*, *85*(3-4), 237-246.

- Du, K., Sun, J., Zhou, X., Feng, W., Jiang, X., & Ji, P. (2015). A two-enzyme immobilization approach using carbon nanotubes/silica as support. *Biotechnology progress*, *31*(1), 42-47.
- Dyke, C. A., & Tour, J. M. (2004). Covalent functionalization of single-walled carbon nanotubes for materials applications. *The Journal of Physical Chemistry A*, *108*(51), 11151-11159.
- Edwards, S. L., Werkmeister, J. A., & Ramshaw, J. A. (2009). Carbon nanotubes in scaffolds for tissue engineering. *Expert review of medical devices*, *6*(5), 499-505.
- Fadel, T. R., & Fahmy, T. M. (2014). Immunotherapy applications of carbon nanotubes: from design to safe applications. *Trends in biotechnology*, *32*(4), 198-209.
- Fan, X., Yu, C., Ling, Z., Yang, J., & Qiu, J. (2013). Hydrothermal synthesis of phosphate-functionalized carbon nanotube-containing carbon composites for supercapacitors with highly stable performance. *ACS applied materials & interfaces*, *5*(6), 2104-2110.
- Fang, S., Shen, L., & Zhang, X. (2017). Application of carbon nanotubes in lithium-ion batteries. In *Industrial applications of carbon nanotubes* (pp. 251-276). Elsevier.
- Fernández Sánchez-Romate, X. X., Molinero, J., Jiménez-Suárez, A., Sánchez, M., Güemes, A., & Ureña, A. (2017). Carbon Nanotube-Doped Adhesive Films for Detecting Crack Propagation on Bonded Joints: A Deeper Understanding of Anomalous Behaviors. *ACS applied materials & interfaces*, *9*(49), 43267-43274.
- Firme III, C. P., & Bandaru, P. R. (2010). Toxicity issues in the application of carbon nanotubes to biological systems. *Nanomedicine: Nanotechnology, Biology and Medicine*, *6*(2), 245-256.
- Frackowiak, E., & Beguin, F. (2002). Electrochemical storage of energy in carbon nanotubes and nanostructured carbons. *Carbon*, *40*(10), 1775-1787.
- Franklin, A. D. (2013). Electronics: The road to carbon nanotube transistors. *Nature*, *498*(7455), 443.

- Franklin, A.D., Luisier, M., Han, S.J., Tulevski, G., Breslin, C.M., Gignac, L., Lundstrom, M.S. & Haensch, W. (2012). Sub-10 nm carbon nanotube transistor. *Nano letters*, *12*(2), 758-762.
- Froudakis, G. E. (2001). Why alkali-metal-doped carbon nanotubes possess high hydrogen uptake. *Nano letters*, *1*(10), 531-533.
- Fullam, S., Cottell, D., Rensmo, H., & Fitzmaurice, D. (2000). Carbon nanotube templated self-assembly and thermal processing of gold nanowires. *Advanced materials*, *12*(19), 1430-1432.
- Gandra, N., Chiu, P. L., Li, W., Anderson, Y. R., Mitra, S., He, H., & Gao, R. (2009). Photosensitized singlet oxygen production upon two-photon excitation of single-walled carbon nanotubes and their functionalized analogues. *The Journal of Physical Chemistry C*, *113*(13), 5182-5185.
- Gao, B., Kleinhammes, A., Tang, X. P., Bower, C., Fleming, L., Wu, Y., & Zhou, O. (1999). Electrochemical intercalation of single-walled carbon nanotubes with lithium. *Chemical Physics Letters*, *307*(3-4), 153-157.
- Gao, M., Dai, L., & Wallace, G. G. (2003). Biosensors based on aligned carbon nanotubes coated with inherently conducting polymers. *Electroanalysis: An International Journal Devoted to Fundamental and Practical Aspects of Electroanalysis*, *15*(13), 1089-1094.
- Ghosh, S., & Padmanabhan, V. (2017). Hydrogen storage capacity of bundles of single-walled carbon nanotubes with defects. *International Journal of Energy Research*, *41*(8), 1108-1117.
- Gong, H., Peng, R., & Liu, Z. (2013). Carbon nanotubes for biomedical imaging: the recent advances. *Advanced drug delivery reviews*, *65*(15), 1951-1963.
- Guldi, D. M., & Costa, R. D. (2013). Nanocarbon hybrids: the paradigm of nanoscale self-ordering/self-assembling by means of charge transfer/doping interactions. *The journal of physical chemistry letters*, *4*(9), 1489-1501.

- Guo, X. J., Xue, C. H., Li, M., Li, X., & Ma, J. Z. (2017). Fabrication of robust, superhydrophobic, electrically conductive and UV-blocking fabrics via layer-by-layer assembly of carbon nanotubes. *RSC Advances*, *7*(41), 25560-25565.
- Guo, Y. Y., Zhang, J., Zheng, Y. F., Yang, J., & Zhu, X. Q. (2011). Cytotoxic and genotoxic effects of multi-wall carbon nanotubes on human umbilical vein endothelial cells in vitro. *Mutation Research/Genetic Toxicology and Environmental Mutagenesis*, *721*(2), 184-191.
- Haggenmueller, R., Gommans, H. H., Rinzler, A. G., Fischer, J. E., & Winey, K. I. (2000). Aligned single-wall carbon nanotubes in composites by melt processing methods. *Chemical physics letters*, *330*(3-4), 219-225.
- Han, M. Y., Özyilmaz, B., Zhang, Y., & Kim, P. (2007). Energy band-gap engineering of graphene nanoribbons. *Physical review letters*, *98*(20), 206805.
- Han, Z. J., & Ostrikov, K. (2012). Uniform, dense arrays of vertically aligned, large-diameter single-walled carbon nanotubes. *Journal of the American Chemical Society*, *134*(13), 6018-6024.
- Hata, K., Futaba, D. N., Mizuno, K., Namai, T., Yumura, M., & Iijima, S. (2004). Water-assisted highly efficient synthesis of impurity-free single-walled carbon nanotubes. *Science*, *306*(5700), 1362-1364.
- He, H., Pham-Huy, L. A., Dramou, P., Xiao, D., Zuo, P., & Pham-Huy, C. (2013). Carbon nanotubes: applications in pharmacy and medicine. *BioMed research international*, *2013*.
- Hemraj-Benny, T., & Wong, S. S. (2006). Silylation of single-walled carbon nanotubes. *Chemistry of materials*, *18*(20), 4827-4839.
- Hou, P., Liu, C., Tong, Y., Xu, S., Liu, M., & Cheng, H. (2001). Purification of single-walled carbon nanotubes synthesized by the hydrogen arc-discharge method. *Journal of Materials Research*, *16*(9), 2526-2529.

- Howarth, T.R., Huang, D., Schumacher, C.R., Mayo, N.K., Cox, D.L., Boisvert, J.E., Aliev, A.E. & Baughman, R. H. (2016). Investigation of carbon nanotubes for acoustic transduction applications. *The Journal of the Acoustical Society of America*, *140*(4), 3086-3086.
- Hu, J., Zou, R., Sun, Y., & Chen, Z. (2010). Excellent field emitters: onion-shaped tipped carbon nanotubes. *The Journal of Physical Chemistry C*, *114*(18), 8282-8286.
- Hu, S., Jiang, H., Xia, Z., & Gao, X. (2010). Friction and adhesion of hierarchical carbon nanotube structures for biomimetic dry adhesives: multiscale modeling. *ACS applied materials & interfaces*, *2*(9), 2570-2578.
- Hu, S., Xia, Z., & Dai, L. (2013). Advanced gecko-foot-mimetic dry adhesives based on carbon nanotubes. *Nanoscale*, *5*(2), 475-486.
- Huang, Y., Yin, W. Y., & Liu, Q. H. (2008). Performance prediction of carbon nanotube bundle dipole antennas. *IEEE Transactions on Nanotechnology*, *7*(3), 331-337.
- Hwang, H. J., Jung, S. L., Cho, K. H., Kim, Y. J., & Jang, H. (2010). Tribological performance of brake friction materials containing carbon nanotubes. *Wear*, *268*(3-4), 519-525.
- Iijima, S. (1991). Helical microtubules of graphitic carbon. *nature*, *354*(6348), 56.
- Imasaka, K., Kanatake, Y., Ohshiro, Y., Suehiro, J., & Hara, M. (2006). Production of carbon nanoonions and nanotubes using an intermittent arc discharge in water. *Thin solid films*, *506*, 250-254.
- Irita, M., Yamazaki, S., Nakahara, H., & Saito, Y. (2018, January). Development of a compact FE-SEM and X-ray microscope with a carbon nanotube electron source. In *IOP Conference Series: Materials Science and Engineering* (Vol. 304, No. 1, p. 012006). IOP Publishing.
- Ishigami, M., Cumings, J., Zettl, A., & Chen, S. (2000). A simple method for the continuous production of carbon nanotubes. *Chemical physics letters*, *319*(5-6), 457-459.
- Ivchenko, E. L., & Spivak, B. (2002). Chirality effects in carbon nanotubes. *Physical Review B*, *66*(15), 155404.

- Jasti, R., & Bertozzi, C. R. (2010). Progress and challenges for the bottom-up synthesis of carbon nanotubes with discrete chirality. *Chemical physics letters*, *494*(1-3), 1-7.
- Javey, A., Guo, J., Wang, Q., Lundstrom, M., & Dai, H. (2003). Ballistic carbon nanotube field-effect transistors. *nature*, *424*(6949), 654.
- Jeon, I., Chiba, T., Delacou, C., Guo, Y., Kaskela, A., Reynaud, O., Kauppinen, E.I., Maruyama, S. & Matsuo, Y. (2015). Single-walled carbon nanotube film as electrode in indium-free planar heterojunction perovskite solar cells: investigation of electron-blocking layers and dopants. *Nano letters*, *15*(10), 6665-6671.
- Jeong, K. Y., Jung, H. K., & Lee, H. W. (2012). Effective parameters on diameter of carbon nanotubes by plasma enhanced chemical vapor deposition. *Transactions of Nonferrous Metals Society of China*, *22*, s712-s716.
- Ji, L., Liu, F., Xu, Z., Zheng, S., & Zhu, D. (2009). Zeolite-templated microporous carbon as a superior adsorbent for removal of monoaromatic compounds from aqueous solution. *Environmental science & technology*, *43*(20), 7870-7876.
- Ji, Y., Lin, Y. J., & Wong, J. S. (2006, January). Buckypaper's Fabrication and Application to Passive Vibration Control. In *2006 1st IEEE International Conference on Nano/Micro Engineered and Molecular Systems* (pp. 725-729). IEEE.
- Jiang, H., Yu, M. F., Liu, B., & Huang, Y. (2004). Intrinsic energy loss mechanisms in a cantilevered carbon nanotube beam oscillator. *Physical Review Letters*, *93*(18), 185501.
- Jiang, Y., Song, H., & Xu, R. (2018). Research on the dispersion of carbon nanotubes by ultrasonic oscillation, surfactant and centrifugation respectively and fiscal policies for its industrial development. *Ultrasonics sonochemistry*, *48*, 30-38.
- Jorio, A., Souza Filho, A.G., Brar, V.W., Swan, A.K., Ünlü, M.S., Goldberg, B.B., Righi, A., Hafner, J.H., Lieber, C.M., Saito, R. & Dresselhaus, G. (2002). Polarized resonant Raman study of isolated single-wall carbon nanotubes: Symmetry selection rules, dipolar and multipolar antenna effects. *Physical Review B*, *65*(12), 121402.

- Jornet, J. M., & Akyildiz, I. F. (2010, April). Graphene-based nano-antennas for electromagnetic nanocommunications in the terahertz band. In *Proceedings of the Fourth European Conference on Antennas and Propagation* (pp. 1-5). IEEE.
- José-Yacamán, M., Miki-Yoshida, M., Rendon, L., & Santiesteban, J. G. (1993). Catalytic growth of carbon microtubules with fullerene structure. *Applied physics letters*, *62*(6), 657-659.
- Ju, S. Y., & Papadimitrakopoulos, F. (2008). Synthesis and redox behavior of flavin mononucleotide-functionalized single-walled carbon nanotubes. *Journal of the American Chemical Society*, *130*(2), 655-664.
- Jung, K. K., Jung, Y., Choi, C. J., & Ko, J. S. (2018). Highly Reliable Superhydrophobic Surface with Carbon Nanotubes Immobilized on a PDMS/Adhesive Multilayer. *ACS Omega*, *3*(10), 12956-12966.
- Kajiura, H., Tsutsui, S., Kadono, K., Kakuta, M., Ata, M., & Murakami, Y. (2003). Hydrogen storage capacity of commercially available carbon materials at room temperature. *Applied physics letters*, *82*(7), 1105-1107.
- Kam, N. W. S., Jessop, T. C., Wender, P. A., & Dai, H. (2004). Nanotube molecular transporters: internalization of carbon nanotube-protein conjugates into mammalian cells J Am Chem Soc 126 (22): 6850–6851. *Find this article online*.
- Ke, C., Li, X., Huang, S., Xu, L., & Yan, Y. (2014). Enhancing enzyme activity and enantioselectivity of Burkholderia cepacia lipase via immobilization on modified multi-walled carbon nanotubes. *RSC advances*, *4*(101), 57810-57818.
- Kim, J.E., Kang, S.H., Moon, Y., Chae, J.J., Lee, A.Y., Lee, J.H., Yu, K.N., Jeong, D.H., Choi, M. & Cho, M. H. (2014). Physicochemical determinants of multiwalled carbon nanotubes on cellular toxicity: influence of a synthetic method and post-treatment. *Chemical research in toxicology*, *27*(2), 290-303.
- Kim, Y., Song, W., Lee, S.Y., Shrestha, S., Jeon, C., Choi, W.C., Kim, M. & Park, C. Y. (2010). Growth of millimeter-scale vertically aligned carbon nanotubes by microwave plasma chemical vapor deposition. *Japanese Journal of Applied Physics*, *49*(8R), 085101.

- Klumpp, C., Kostarelos, K., Prato, M., & Bianco, A. (2006). Functionalized carbon nanotubes as emerging nanovectors for the delivery of therapeutics. *Biochimica et Biophysica Acta (BBA)-Biomembranes*, *1758*(3), 404-412.
- Kreupl, F., Graham, A. P., Duesberg, G. S., Steinhögl, W., Liebau, M., Unger, E., & Hönlein, W. (2002). Carbon nanotubes in interconnect applications. *Microelectronic Engineering*, *64*(1-4), 399-408.
- Kuo, C. Y., Chan, C. L., Gau, C., Liu, C. W., Shiau, S. H., & Ting, J. H. (2007). Nano temperature sensor using selective lateral growth of carbon nanotube between electrodes. *IEEE Transactions on Nanotechnology*, *6*(1), 63-69.
- Kusworo, T. D., Ismail, A. F., Widiasa, I. N., & Johari, S. (2010). CO2 removal from biogas using carbon nanotubes mixed matrix membranes. *International Journal of Science and Engineering*, *1*(1), 1-6.
- Lee, K. S., Lee, W. J., Park, N. G., Kim, S. O., & Park, J. H. (2011). Transferred vertically aligned N-doped carbon nanotube arrays: use in dye-sensitized solar cells as counter electrodes. *Chemical communications*, *47*(14), 4264-4266.
- Lee, S. M., & Lee, Y. H. (2000). Hydrogen storage in single-walled carbon nanotubes. *Applied Physics Letters*, *76*(20), 2877-2879.
- Li, G., Wang, H., Zheng, H., & Bai, R. (2010). A facile approach for the fabrication of highly stable superhydrophobic cotton fabric with multi-walled carbon nanotubes– azide polymer composites. *Langmuir*, *26*(10), 7529-7534.
- Li, R., Wu, R. A., Zhao, L., Hu, Z., Guo, S., Pan, X., & Zou, H. (2011). Folate and iron difunctionalized multiwall carbon nanotubes as dual-targeted drug nanocarrier to cancer cells. *Carbon*, *49*(5), 1797-1805.
- li, W.Li, Y., Sheng, M., Cui, S.,Wang, Z., Zhang, X., Yang, C., Yu, Z., Zhang, Y.,Tian, S., Dai, Z. & Xu, Q. Enhanced adhesion of carbon nanotubes by dopamine modification. *Langmuir, Accepted Manuscript, DOI: 10.1021/acs.langmuir.9b00192*

- Liang, X., Xia, J., Dong, G., & Tian, B. (2016). Carbon nanotube thin film transistors for flat panel display application. *Topics in Current Chemistry*, *374*(6), 80.
- Lin, S., Kim, Y. B., & Lombardi, F. (2012). Design of a ternary memory cell using CNTFETs. *IEEE transactions on nanotechnology*, *11*(5), 1019-1025.
- Lin, Y., Cui, X., & Bontha, J. (2006). Electrically controlled anion exchange based on polypyrrole and carbon nanotubes nanocomposite for perchlorate removal. *Environmental science & technology*, *40*(12), 4004-4009.
- Liu, G., Saito, Y., Nishio-Hamane, D., Bauri, A. K., Flahaut, E., Kimura, T., & Komatsu, N. (2014). Structural discrimination of double-walled carbon nanotubes by chiral diporphyrin nanocalipers. *Journal of Materials Chemistry A*, *2*(44), 19067-19074.
- Liu, G., Wang, F., Peng, X., Rahman, A. F. M. M., Bauri, A. K., & Komatsu, N. (2012). Separation of left-and right-handed structures of single-walled carbon nanotubes through molecular recognition. In *Handbook of carbon nano materials*(Vol. 3, pp. 203-232). World Scientific.
- Liu, Y., & Kumar, S. (2014). Polymer/carbon nanotube nano composite fibers–a review. *ACS applied materials & interfaces*, *6*(9), 6069-6087.
- Liu, Y., Gao, L., & Sun, J. (2007). Noncovalent functionalization of carbon nanotubes with sodium lignosulfonate and subsequent quantum dot decoration. *The Journal of Physical Chemistry C*, *111*(3), 1223-1229.
- Liu, Z., Chen, K., Davis, C., Sherlock, S., Cao, Q., Chen, X., & Dai, H. (2008). Drug delivery with carbon nanotubes for in vivo cancer treatment. *Cancer research*, *68*(16), 6652-6660.
- Liu, Z., Robinson, J. T., Tabakman, S. M., Yang, K., & Dai, H. (2011). Carbon materials for drug delivery & cancer therapy. *Materials today*, *14*(7-8), 316-323.
- Löffler, R., Häffner, M., Visanescu, G., Weigand, H., Wang, X., Zhang, D., Fleischer, M., Meixner, A.J., Fortagh, J. Löffler, R., Häffner, M., Visanescu, G., Weigand, H., Wang, X., Zhang, D., Fleischer, M., Meixner, A.J., Fortagh, J. & Kern, D. P. (2011). Optimization of

plasma-enhanced chemical vapor deposition parameters for the growth of individual vertical carbon nanotubes as field emitters. *Carbon*, *49*(13), 4197-4203.

- Lordi, V., Yao, N., & Wei, J. (2001). Method for supporting platinum on single-walled carbon nanotubes for a selective hydrogenation catalyst. *Chemistry of Materials*, *13*(3), 733-737.
- MacDonald, R. A., Laurenzi, B. F., Viswanathan, G., Ajayan, P. M., & Stegemann, J. P. (2005). Collagen–carbon nanotube composite materials as scaffolds in tissue engineering. *Journal of Biomedical Materials Research Part A: An Official Journal of The Society for Biomaterials, The Japanese Society for Biomaterials, and The Australian Society for Biomaterials and the Korean Society for Biomaterials*, *74*(3), 489-496.
- Madani, S. Y., Naderi, N., Dissanayake, O., Tan, A., & Seifalian, A. M. (2011). A new era of cancer treatment: carbon nanotubes as drug delivery tools. *International journal of nanomedicine*, *6*, 2963.
- Magrez, A., Kasas, S., Salicio, V., Pasquier, N., Seo, J.W., Celio, M., Catsicas, S., Schwaller, B. & Forró, L. (2006). Cellular toxicity of carbon-based nanomaterials. *Nano letters*, *6*(6), 1121-1125.
- Maser, W. K., Benito, A. M., Muñoz, E., de Val, G. M., Martínez, M. T., Larrea, Á., & de la Fuente, G. F. (2001). Production of carbon nanotubes by CO2-laser evaporation of various carbonaceous feedstock materials. *Nanotechnology*, *12*(2), 147.
- Maune, H. T., Han, S. P., Barish, R. D., Bockrath, M., Goddard III, W. A., Rothemund, P. W., & Winfree, E. (2010). Self-assembly of carbon nanotubes into two-dimensional geometries using DNA origami templates. *Nature nanotechnology*, *5*(1), 61.
- Maynard, A. D., Baron, P. A., Foley, M., Shvedova, A. A., Kisin, E. R., & Castranova, V. (2004). Exposure to carbon nanotube material: aerosol release during the handling of unrefined single-walled carbon nanotube material. *Journal of Toxicology and Environmental Health, Part A*, *67*(1), 87-107.
- McEuen, P. L., Fuhrer, M. S., & Park, H. (2002). Single-walled carbon nanotube electronics. *IEEE transactions on nanotechnology*, *99*(1), 78-85.

- Mehra, N.K., Jain, A.K., Lodhi, N., Raj, R., Dubey, V., Mishra, D., Nahar, M. & Jain, N. K. (2008). Challenges in the use of carbon nanotubes for biomedical applications. *Critical Reviews™ in Therapeutic Drug Carrier Systems*, *25*(2).
- Melchionna, M., Marchesan, S., Prato, M., & Fornasiero, P. (2015). Carbon nanotubes and catalysis: the many facets of a successful marriage. *Catalysis Science & Technology*, *5*(8), 3859-3875.
- Melechko, A. V., Merkulov, V. I., McKnight, T. E., Guillorn, M. A., Klein, K. L., Lowndes, D. H., & Simpson, M. L. (2005). Vertically aligned carbon nanofibers and related structures: controlled synthesis and directed assembly. *Journal of applied physics*, *97*(4), 3.
- Meng, J., Meng, J., Duan, J., Kong, H., Li, L., Wang, C., Xie, S., Chen, S., Gu, N., Xu, H. & Yang, X. D. (2008). Carbon nanotubes conjugated to tumor lysate protein enhance the efficacy of an antitumor immunotherapy. *small*, *4*(9), 1364-1370.
- Mercer, R.R., Scabilloni, J.F., Wang, L., Kisin, E.R., Murray, A.R., Schwegler-Berry, D., Shvedova, A.A. & Castranova, V. (2008). Alteration of deposition pattern and pulmonary response as a result of improved dispersion of aspirated single walled carbon nanotubes in a mouse model. *American Journal of Physiology-Lung Cellular and Molecular Physiology*.
- Mionić, M., Pataky, K., Gaal, R., Magrez, A., Brugger, J., & Forró, L. (2012). Carbon nanotubes–SU8 composite for flexible conductive inkjet printable applications. *Journal of Materials Chemistry*, *22*(28), 14030-14034.
- Moniruzzaman, M., & Winey, K. I. (2006). Polymer nanocomposites containing carbon nanotubes. *Macromolecules*, *39*(16), 5194-5205.
- Montes-Fonseca, S. L., Orrantia-Borunda, E., Aguilar-Elguezabal, A., Horta, C. G., Talamás-Rohana, P., & Sánchez-Ramírez, B. (2012). Cytotoxicity of functionalized carbon nanotubes in J774A macrophages. *Nanomedicine: Nanotechnology, Biology and Medicine*, *8*(6), 853-859.
- Mora, E., Pigos, J. M., Ding, F., Yakobson, B. I., & Harutyunyan, A. R. (2008). Low-temperature single-wall carbon nanotubes synthesis: feedstock decomposition limited growth. *Journal of the American Chemical Society*, *130*(36), 11840-11841.

- Mubarak, N. M., Abdullah, E. C., Jayakumar, N. S., & Sahu, J. N. (2014). An overview on methods for the production of carbon nanotubes. *Journal of Industrial and Engineering Chemistry*, *20*(4), 1186-1197.
- Okazaki, T., & Shinohara, H. (2003). Synthesis and characterization of single-wall carbon nanotubes by hot-filament assisted chemical vapor deposition. *Chemical physics letters*, *376*(5-6), 606-611.
- Ong, Y. T., Ahmad, A. L., Zein, S. H. S., & Tan, S. H. (2010). A review on carbon nanotubes in an environmental protection and green engineering perspective. *Brazilian Journal of Chemical Engineering*, *27*(2), 227-242.
- Onoe, T., Iwamoto, S., & Inoue, M. (2007). Synthesis and activity of the Pt catalyst supported on CNT. *Catalysis Communications*, *8*(4), 701-706.
- Ou, Z., Wu, B., Xing, D., Zhou, F., Wang, H., & Tang, Y. (2009). Functional single-walled carbon nanotubes based on an integrin αvβ3 monoclonal antibody for highly efficient cancer cell targeting. *Nanotechnology*, *20*(10), 105102.
- Palkar, A., Melin, F., Cardona, C.M., Elliott, B., Naskar, A.K., Edie, D.D., Kumbhar, A. & Echegoyen, L. (2007). Reactivity differences between carbon nano onions (CNOs) prepared by different methods. *Chemistry–An Asian Journal*, *2*(5), 625-633.
- Pan, B., & Xing, B. (2008). Adsorption mechanisms of organic chemicals on carbon nanotubes. *Environmental science & technology*, *42*(24), 9005-9013.
- Pan, Y., Sahoo, N. G., & Li, L. (2012). The application of graphene oxide in drug delivery. *Expert opinion on drug delivery*, *9*(11), 1365-1376.
- Park, S., Srivastava, D., & Cho, K. (2003). Generalized chemical reactivity of curved surfaces: carbon nanotubes. *Nano letters*, *3*(9), 1273-1277.
- Pastorková, K., Jesenák, K., Kadlečíková, M., Breza, J., Kolmačka, M., Čaplovičová, M., Lazišťan, F. & Michalka, M. (2012). The growth of multi-walled carbon nanotubes on natural clay minerals (kaolinite, nontronite and sepiolite). *Applied Surface Science*, *258*(7), 2661-2666.

- Pierce, N., Chen, G., P. Rajukumar, L., Chou, N.H., Koh, A.L., Sinclair, R., Maruyama, S., Terrones, M. & Harutyunyan, A.R. (2017). Intrinsic chirality origination in carbon nanotubes. *ACS nano*, *11*(10), 9941-9949.
- Poland, C.A., Duffin, R., Kinloch, I., Maynard, A., Wallace, W.A., Seaton, A., Stone, V., Brown, S., MacNee, W. & Donaldson, K. (2008). Carbon nanotubes introduced into the abdominal cavity of mice show asbestos-like pathogenicity in a pilot study. *Nature nanotechnology*, *3*(7), 423.
- Ponnamma, D., Sadasivuni, K. K., Grohens, Y., Guo, Q., & Thomas, S. (2014). Carbon nanotube based elastomer composites–an approach towards multifunctional materials. *Journal of Materials Chemistry C*, *2*(40), 8446-8485.
- Pu, J., Wan, S., Lu, Z., Zhang, G. A., Wang, L., Zhang, X., & Xue, Q. (2013). Controlled water adhesion and electrowetting of conducting hydrophobic graphene/carbon nanotubes composite films on engineering materials. *Journal of Materials Chemistry A*, *1*(4), 1254-1260.
- Pulskamp, K., Diabaté, S., & Krug, H. F. (2007). Carbon nanotubes show no sign of acute toxicity but induce intracellular reactive oxygen species in dependence on contaminants. *Toxicology letters*, *168*(1), 58-74.
- Qin, L. C., Zhou, D., Krauss, A. R., & Gruen, D. M. (1998). Growing carbon nanotubes by microwave plasma-enhanced chemical vapor deposition. *Applied Physics Letters*, *72*(26), 3437-3439.
- Qu, Y., Ma, Q., Deng, J., Shen, W., Zhang, X., He, Z., Nostrand, J.D.V., Zhou, J. & Zhou, J. (2015). Responses of microbial communities to single-walled carbon nanotubes in phenol wastewater treatment systems. *Environmental science & technology*, *49*(7), 4627-4635.
- Radushkevich LV, Lukyanovich VM (1952). The structure of carbon forming in thermal decomposition of carbon monoxide on an iron catalyst. *Soviet Journal of Physical Chemistry*, *26*, 88-95.

- Ranjan, V., Puebla-Hellmann, G., Jung, M., Hasler, T., Nunnenkamp, A., Muoth, M., Hierold, C., Wallraff, A. & Schönenberger, C. (2015). Clean carbon nanotubes coupled to superconducting impedance-matching circuits. *Nature communications*, *6*, 7165.
- Rao, C. N. R., & Govindaraj, A. (2002). Carbon nanotubes from organometallic precursors. *Accounts of chemical research*, *35*(12), 998-1007.
- Rao, R., Pint, C.L., Islam, A.E., Weatherup, R.S., Hofmann, S., Meshot, E.R., Wu, F., Zhou, C., Dee, N., Amama, P.B. & Carpena-Nuñez, J. (2018). Carbon Nanotubes and Related Nanomaterials: Critical Advances and Challenges for Synthesis toward Mainstream Commercial Applications. *ACS nano*, *12*(12), 11756-11784.
- Rao, S. G., Huang, L., Setyawan, W., & Hong, S. (2003). Nanotube electronics: Large-scale assembly of carbon nanotubes. *Nature*, *425*(6953), 36.
- Ren, Z., Cai, D., & Jay-Jiguang, Z. H. U. (2018). Nanovectors for penetrating brain tumor tissues to conduct gene therapy. *U.S. Patent Application No. 16/029,809*.
- Ritschel, M., Uhlemann, M., Gutfleisch, O., Leonhardt, A., Graff, A., Täschner, C., & Fink, J. (2002). Hydrogen storage in different carbon nanostructures. *Applied Physics Letters*, *80*(16), 2985-2987.
- Rotkin, S. V., & Subramoney, S. (Eds.). (2006). *Applied physics of carbon nanotubes: fundamentals of theory, optics and transport devices*. Springer Science & Business Media.
- Ruoff, R. S., Tersoff, J., Lorents, D. C., Subramoney, S., & Chan, B. (1993). Radial deformation of carbon nanotubes by van der Waals forces. *Nature*, *364*(6437), 514.
- Saghafi, M., Mahboubi, F., Mohajerzadeh, S., & Holze, R. (2014). Preparation of vertically aligned carbon nanotubes and their electrochemical performance in supercapacitors. *Synthetic Metals*, *195*, 252-259.
- Sahoo, R., & Mishra, R. R. (2009). Simulations of carbon nanotube field effect transistors. *International Journal of Electronic Engineering Research*, *1*(2), 117-125.

- Sahoo, S. C., Mohapatra, D. R., Lee, H. J., Jejurikar, S. M., Kim, I., Lee, S. C., ... & Lee, W. S. (2014). Carbon nanoflake growth from carbon nanotubes by hot filament chemical vapor deposition. *Carbon*, *67*, 704-711.
- Saifuddin, N., Raziah, A. Z., & Junizah, A. R. (2012). Carbon nanotubes: a review on structure and their interaction with proteins. *Journal of Chemistry*, *2013*.
- Salavagione, H. J., Diez-Pascual, A. M., Lázaro, E., Vera, S., & Gomez-Fatou, M. A. (2014). Chemical sensors based on polymer composites with carbon nanotubes and graphene: the role of the polymer. *Journal of Materials Chemistry A*, *2*(35), 14289-14328.
- Sanchez-Valencia, J.R., Dienel, T., Gröning, O., Shorubalko, I., Mueller, A., Jansen, M., Amsharov, K., Ruffieux, P. & Fasel, R. (2014). Controlled synthesis of single-chirality carbon nanotubes. *Nature*, *512*(7512), 61.
- Sano, N., Nakano, J., & Kanki, T. (2004). Synthesis of single-walled carbon nanotubes with nanohorns by arc in liquid nitrogen. *Carbon*, *3*(42), 686-688.
- Schnorr, J. M., & Swager, T. M. (2010). Emerging applications of carbon nanotubes. *Chemistry of Materials*, *23*(3), 646-657.
- Seo, K., Kim, C., Kim, B., Lee, Y. H., & Song, K. (2004). Growth energetics of single-wall carbon nanotubes with carbon monoxide. *The Journal of Physical Chemistry B*, *108*(14), 4308-4313.
- Sethi, S., Ge, L., Ci, L., Ajayan, P. M., & Dhinojwala, A. (2008). Gecko-inspired carbon nanotube-based self-cleaning adhesives. *Nano letters*, *8*(3), 822-825.
- Shen, M., Wang, S.H., Shi, X., Chen, X., Huang, Q., Petersen, E.J., Pinto, R.A., Baker Jr, J.R. & Weber Jr, W. J. (2009). Polyethyleneimine-mediated functionalization of multiwalled carbon nanotubes: synthesis, characterization, and in vitro toxicity assay. *The Journal of Physical Chemistry C*, *113*(8), 3150-3156.
- Shi, W., & Plata, D. L. (2018). Vertically aligned carbon nanotubes: production and applications for environmental sustainability. *Green Chemistry*, *20*(23), 5245-5260.

- Shvedova, A. A., Kisin, E. R., Porter, D., Schulte, P., Kagan, V. E., Fadeel, B., & Castranova, V. (2009). Mechanisms of pulmonary toxicity and medical applications of carbon nanotubes: two faces of Janus?. *Pharmacology & therapeutics*, *121*(2), 192-204.
- Silva, R.M., Doudrick, K., Franzi, L.M., TeeSy, C., Anderson, D.S., Wu, Z., Mitra, S., Vu, V., Dutrow, G., Evans, J.E. & Westerhoff, P. (2014). Instillation versus inhalation of multiwalled carbon nanotubes: exposure-related health effects, clearance, and the role of particle characteristics. *ACS nano*, *8*(9), 8911-8931.
- Spitalsky, Z., Tasis, D., Papagelis, K., & Galiotis, C. (2010). Carbon nanotube–polymer composites: chemistry, processing, mechanical and electrical properties. *Progress in polymer science*, *35*(3), 357-401.
- Taghdisi, S. M., Lavaee, P., Ramezani, M., & Abnous, K. (2011). Reversible targeting and controlled release delivery of daunorubicin to cancer cells by aptamer-wrapped carbon nanotubes. *European Journal of Pharmaceutics and Biopharmaceutics*, *77*(2), 200-206.
- Tan, X. J., Liu, H. J., Wen, Y. W., Lv, H. Y., Pan, L., Shi, J., & Tang, X. F. (2011). Thermoelectric properties of ultrasmall single-wall carbon nanotubes. *The Journal of Physical Chemistry C*, *115*(44), 21996-22001.
- Tatami, J., Katashima, T., Komeya, K., Meguro, T., & Wakihara, T. (2005). Electrically conductive CNT-dispersed silicon nitride ceramics. *Journal of the American Ceramic Society*, *88*(10), 2889-2893.
- Thakur, A., Kumar, S., Pathania, P., Pathak, D., & Rangra, V. S. (2017). SYNTHESIS OF RGO–ZnO COMPOSITES FOR THERMAL, ELECTRICAL AND ANTIBACTERIAL STUDIES. *Surface Review and Letters*, *24*(07), 1750095.
- Thakur, A., Kumar, S., Sharma, M., & Rangra, V. S. (2016). Optical, electrical and antimicrobial studies of chemically synthesized graphite oxide and reduced graphene oxide. *ADVANCED MATERIALS*, *7*(12), 1029-1034.
- Valko, M., Leibfritz, D., Moncol, J., Cronin, M. T., Mazur, M., & Telser, J. (2007). Free radicals and antioxidants in normal physiological functions and human disease. *The international journal of biochemistry & cell biology*, *39*(1), 44-84.

- Van Der Voort, P., Vercaemst, C., Schaubroeck, D., & Verpoort, F. (2008). Ordered mesoporous materials at the beginning of the third millennium: new strategies to create hybrid and non-siliceous variants. *Physical Chemistry Chemical Physics*, *10*(3), 347-360.
- van Steen, E., & Prinsloo, F. F. (2002). Comparison of preparation methods for carbon nanotubes supported iron Fischer–Tropsch catalysts. *Catalysis Today*, *71*(3-4), 327-334.
- Vijayan, B. K., Dimitrijevic, N. M., Finkelstein-Shapiro, D., Wu, J., & Gray, K. A. (2012). Coupling titania nanotubes and carbon nanotubes to create photocatalytic nanocomposites. *Acs Catalysis*, *2*(2), 223-229.
- Vittorio, O., Raffa, V., & Cuschieri, A. (2009). Influence of purity and surface oxidation on cytotoxicity of multiwalled carbon nanotubes with human neuroblastoma cells. *Nanomedicine: Nanotechnology, Biology and Medicine*, *5*(4), 424-431.
- Vivekchand, S. R. C., Rout, C. S., Subrahmanyam, K. S., Govindaraj, A., & Rao, C. N. R. (2008). Graphene-based electrochemical supercapacitors. *Journal of Chemical Sciences*, *120*(1), 9-13.
- Walters, D. A., Ericson, L. M., Casavant, M. J., Liu, J., Colbert, D. T., Smith, K. A., & Smalley, R. E. (1999). Elastic strain of freely suspended single-wall carbon nanotube ropes. *Applied Physics Letters*, *74*(25), 3803-3805.
- Wang, G., Chen, J., Tian, Y., Jin, Y., & Li, Y. (2012). Water assisted synthesis of double-walled carbon nanotubes with a narrow diameter distribution from methane over a Co–Mo/MgO catalyst. *Catalysis today*, *183*(1), 26-33.
- Wang, H., & Moore, J. J. (2012). Low temperature growth mechanisms of vertically aligned carbon nanofibers and nanotubes by radio frequency-plasma enhanced chemical vapor deposition. *Carbon*, *50*(3), 1235-1242.
- Wang, J., Sun, P., Bao, Y., Liu, J., & An, L. (2011). Cytotoxicity of single-walled carbon nanotubes on PC12 cells. *Toxicology in vitro*, *25*(1), 242-250.
- Wang, X., Xia, T., Ntim, S.A., Ji, Z., George, S., Meng, H., Zhang, H., Castranova, V., Mitra, S.& Nel, A. E. (2010). Quantitative techniques for assessing and controlling the

dispersion and biological effects of multiwalled carbon nanotubes in mammalian tissue culture cells. *ACS nano*, *4*(12), 7241-7252.

- Wang, Y., Fugetsu, B., Wang, Z., Gong, W., Sakata, I., Morimoto, S., Hashimoto, Y., Endo, M., Dresselhaus, M. & Terrones, M. (2017). Nitrogen-doped porous carbon monoliths from polyacrylonitrile (PAN) and carbon nanotubes as electrodes for supercapacitors. *Scientific reports*, *7*, 40259.
- Warheit, D. B., Laurence, B. R., Reed, K. L., Roach, D. H., Reynolds, G. A., & Webb, T. R. (2004). Comparative pulmonary toxicity assessment of single-wall carbon nanotubes in rats. *Toxicological sciences*, *77*(1), 117-125.
- Wei, H., Kim, S. N., Zhao, M., Ju, S. Y., Huey, B. D., Marcus, H. L., & Papadimitrakopoulos, F. (2008). Control of length and spatial functionality of single-wall carbon nanotube AFM nanoprobes. *Chemistry of Materials*, *20*(8), 2793-2801.
- Witzmann, F. A., & Monteiro-Riviere, N. A. (2006). Multi-walled carbon nanotube exposure alters protein expression in human keratinocytes. *Nanomedicine: Nanotechnology, Biology and Medicine*, *2*(3), 158-168.
- Worsley, M. A., Pauzauskie, P. J., Olson, T. Y., Biener, J., Satcher Jr, J. H., & Baumann, T. F. (2010). Synthesis of graphene aerogel with high electrical conductivity. *Journal of the American Chemical Society*, *132*(40), 14067-14069.
- Wu, S. J., Schuergers, N., Lin, K. H., Gillen, A. J., Corminboeuf, C., & Boghossian, A. A. (2018). Restriction Enzyme Analysis of Double-Stranded DNA on Pristine Single-Walled Carbon Nanotubes. *ACS applied materials & interfaces*, *10*(43), 37386-37395.
- Xia, H., Wang, Q., & Qiu, G. (2003). Polymer-encapsulated carbon nanotubes prepared through ultrasonically initiated in situ emulsion polymerization. *Chemistry of materials*, *15*(20), 3879-3886.
- Xiao, G. G., Wang, M., Li, N., Loo, J. A., & Nel, A. E. (2003). Use of proteomics to demonstrate a hierarchical oxidative stress response to diesel exhaust particle chemicals in a macrophage cell line. *Journal of Biological Chemistry*, *278*(50), 50781-50790.

- Xie, L., Wang, G., Zhou, H., Zhang, F., Guo, Z., Liu, C., Zhang, X. & Zhu, L. (2016). Functional long circulating single walled carbon nanotubes for fluorescent/photoacoustic imaging-guided enhanced phototherapy. *Biomaterials*, *103*, 219-228.
- Xu, Z., Gao, N., Chen, H., & Dong, S. (2005). Biopolymer and carbon nanotubes interface prepared by self-assembly for studying the electrochemistry of microperoxidase-11. *Langmuir*, *21*(23), 10808-10813.
- Yamada, T., Maigne, A., Yudasaka, M., Mizuno, K., Futaba, D.N., Yumura, M., Iijima, S. & Hata, K. (2008). Revealing the secret of water-assisted carbon nanotube synthesis by microscopic observation of the interaction of water on the catalysts. *Nano letters*, *8*(12), 4288-4292.
- Yan, Y., Miao, J., Yang, Z., Xiao, F. X., Yang, H. B., Liu, B., & Yang, Y. (2015). Carbon nanotube catalysts: recent advances in synthesis, characterization and applications. *Chemical Society Reviews*, *44*(10), 3295-3346.
- Yang, C., Lin, Y., & Nan, C. W. (2009). Modified carbon nanotube composites with high dielectric constant, low dielectric loss and large energy density. *Carbon*, *47*(4), 1096-1101.
- Yang, F., Jin, C., Yang, D., Jiang, Y., Li, J., Di, Y., Hu, J., Wang, C., Ni, Q. & Fu, D. (2011). Magnetic functionalised carbon nanotubes as drug vehicles for cancer lymph node metastasis treatment. *European Journal of Cancer*, *47*(12), 1873-1882.
- Yang, H., Wang, C., & Su, Z. (2008). Growth mechanism of synthetic imogolite nanotubes. *Chemistry of Materials*, *20*(13), 4484-4488.
- Yang, Q., Xu, W., Tomita, A., & Kyotani, T. (2005). The template synthesis of double coaxial carbon nanotubes with nitrogen-doped and boron-doped multiwalls. *Journal of the American Chemical Society*, *127*(25), 8956-8957.
- Yang, R. T. (2000). Hydrogen storage by alkali-doped carbon nanotubes–revisited. *Carbon*, *38*(4), 623-626.
- Yi, H., Ghosh, D., Ham, M. H., Qi, J., Barone, P. W., Strano, M. S., & Belcher, A. M. (2012). M13 phage-functionalized single-walled carbon nanotubes as nanoprobes for second

near-infrared window fluorescence imaging of targeted tumors. *Nano letters*, *12*(3), 1176-1183.

- Yin, S. F., Xu, B. Q., Zhou, X. P., & Au, C. T. (2004). A mini-review on ammonia decomposition catalysts for on-site generation of hydrogen for fuel cell applications. *Applied Catalysis A: General*, *277*(1-2), 1-9.
- Yousef, S., Khattab, A., Osman, T. A., & Zaki, M. (2012, December). Fully automatic system for producing carbon nanotubes (CNTs) by using arc-discharge technique multi electrodes. In *2012 First International Conference on Innovative Engineering Systems* (pp. 86-90). IEEE.
- Yu, M. F., Files, B. S., Arepalli, S., & Ruoff, R. S. (2000). Tensile loading of ropes of single wall carbon nanotubes and their mechanical properties. *Physical review letters*, *84*(24), 5552.
- Yu, S., Tong, M. N., & Critchlow, G. (2010). Use of carbon nanotubes reinforced epoxy as adhesives to join aluminum plates. *Materials & Design*, *31*, S126-S129.
- Yu, Y., Chen, J., Zhou, Z. M., & Zhao, Y. D. (2013). Facile synthesis of carbon nanotube-inorganic hybrid materials with improved photoactivity. *Dalton Transactions*, *42*(43), 15280-15284.
- Zamaleeva, A. I., Sharipova, I. R., Porfireva, A. V., Evtugyn, G. A., & Fakhrullin, R. F. (2009). Polyelectrolyte-mediated assembly of multiwalled carbon nanotubes on living yeast cells. *Langmuir*, *26*(4), 2671-2679.
- Zaporotskova, I. V., Boroznina, N. P., Parkhomenko, Y. N., & Kozhitov, L. V. (2016). Carbon nanotubes: Sensor properties. A review. *Modern Electronic Materials*, *2*(4), 95-105.
- Zhang, H., Bork, M. A., Riedy, K. J., McMillin, D. R., & Choi, J. H. (2014). Understanding photophysical interactions of semiconducting carbon nanotubes with porphyrin chromophores. *The Journal of Physical Chemistry C*, *118*(22), 11612-11619.

- Zhang, Y. L., Hou, P. X., Liu, C., & Cheng, H. M. (2014). De-bundling of single-wall carbon nanotubes induced by an electric field during arc discharge synthesis. *Carbon*, *74*, 370-373.
- Zhang, Y., Zhang, H. B., Lin, G. D., Chen, P., Yuan, Y. Z., & Tsai, K. R. (1999). Preparation, characterization and catalytic hydroformylation properties of carbon nanotubes-supported Rh–phosphine catalyst. *Applied Catalysis A: General*, *187*(2), 213-224.
- Zhao, Q., Gan, Z., & Zhuang, Q. (2002). Electrochemical sensors based on carbon nanotubes. *Electroanalysis: An International Journal Devoted to Fundamental and Practical Aspects of Electroanalysis*, *14*(23), 1609-1613.
- Zhu, H. W., Li, X. S., Jiang, B., Xu, C. L., Zhu, Y. F., Wu, D. H., & Chen, X. H. (2002). Formation of carbon nanotubes in water by the electric-arc technique. *Chemical Physics Letters*, *366*(5-6), 664-669.
- Zykwinska, A., Radji-Taleb, S., & Cuenot, S. (2009). Layer-by-layer functionalization of carbon nanotubes with synthetic and natural polyelectrolytes. *Langmuir*, *26*(4), 2779-2784.

Synthesis methodology of green composite for heavy metal Cr remediation from waste water

Manviri Rani[1] and Uma Shanker*[2]

[1]Malaviya National Institute of Technology JLN Marg, Rajasthan-INDIA

[2]Dr B R Ambedkar National Institute of Technology Jalandhar, Punjab-INDIA

E.mail: manviri.chy@mnit.ac.in : shankeru@nitj.ac.in

Abstract:

Recently, green composites based on nanomaterials are recognized as promising technology for subside environmental problems due to low-cost, potential adsorption cum photocatalysts and eco-friendliness. Natural materials such as chitosan, clay, gels and polymers are mixed with very small amount of nanoparticles (carboneous or metal compounds) to achieve excellent adsorption properties credited to special functional groups arose on the surface. Here, we summarized the updated information on synthesis methodology (hydrothermal, sol-gel, co-precipitation etc) of various green composite and their application in removal of chromium (Cr) a heavy metal (density more than 5g/cm^3) from waste-water. Furthermore, importance of green synthesized nanocomposite is highlighted due to low cost of production and mediated effect of biogenic sources (polyphenols etc). Cr (VI) is carcinogenic, strong mutagenic and tetragenic. For that, conventional techniques like chemical precipitation, ion exchange, membrane filtration, electrochemical methods, solvent extraction, coagulation–flocculation, membrane process, flotation and adsorption have been employed. Among them adsorption was found best in terms of its efficiency and economy as metal bounded adsorbents are compact and strongly bonded. CNTs functionalized with chitosan or

metal, porous carbon-encapsulated iron, amine-graphene oxide along with green composites of metals with natural materials (polypyrrole/ Fe_3O_4, Fe^0-waste rock wool) are used as green adsorbent in the removal of Cr (VI) due to their improved performances. Nanocomposites of nanosilica-immobilized-nanopolyaniline and crosslinked nanopolyaniline, Zeolite–TiO_2 hybrid composites, trialkylamine impregnated macroporous polymeric sorbent, amine-modified polyacrylamide-grafted coconut coir pith and many more have also been reported. Research gaps prevailing and future recommendations have also been provided.

Introduction

During the past few decades, the extensive use of chemicals and unsafe materials around the world has caused several environmental challenges. Water pollution has become menace to living life. Fresh or clean water used by human is very less (0.0008% is available and renew-able) and that's quality is also declining due to increased population growth (4–5 billion people estimated by the year 2025) (Roger, 2006). Hence, management of environment is necessary to get sustainable and better life. Heavy metal ions(density>6 g per cc) precarious water pollutants, even at ultralow concentrations, form potentially carcinogenic and mutagenic compounds within the bio-system (Santhosh et al., 2016). Due to high population density and growth of industrial deeds, heavy metal ions (Cr^{6+}, Cu^{2+}, Cd^{2+}, Pb^{2+} and Zn^{2+}) were reported highly persistent pollutants in wastewater and become lethal if their concentrations exceed certain limits (Goldstein et al., 1971; Renge et al., 2012). Chromium a widely used element in steel production industry as ferrochrome listed as top-priority toxic pollutants by the US-EPA with tolerance limit (0.1 mg/L) in drinking H_2O [Costa, 2003; Barakat et al., 2011; Lv et al. 2012].The hexavalent state Cr^{6+} (common contaminant in soils and water) is easily miscible and movable in water stream and frequently released at levels well above

the regulatory trace limits into the environment [Liu et al. 2010; Zhang et al. 2012; Wei et al. 2013]. In view of strong mutagenic and teratogenic properties Chromium has been categorized as a cancer-causing agent by the International Agency for Research on Cancer [De Flora, 2000]. Furthermore, accidental case also cause environment disaster e.g., Cr(VI) concentration in slag of Nanpan River China reported the concentration 2000 times above the safe level [Fu et al., 2011].

Global chromium production was 31,000 MT in 2017 (Chromium, 2018). According to the US Geological Survey on chromium in 2017, South Africa (15,000 MT) is the largest ferrochrome and chromite ore producer followed by Kazakhstan (5400 MT), India (3200 MT) and Turkey (2800 MT). China is the world's top consumer of chromium, as well as the world's top stainless steel producer. Generally, Chromium mainly exhibit two oxidation states Cr(VI) and Cr(III)in nature [Qu et al., 2013] andCr(VI) typically exists in soluble forms of $HCrO^-_4$, $Cr_2O_7^{2-}$, and CrO^{2-}_4in H_2O below pH 6.5, $HCrO^-_4$ being predominant while change to CrO^{2-}_4 as pH increases, and $Cr_2O^{2-}_7$ is the keyform in solution at low pH.In view of economy and environmental concern, the separation/removal of metals from wastewater by developed cheap, ecofriendly and advance treatment technology are encouraging [Marques et al., 2000; Owlad et al. 2008; Unnithan and Anirudhan, 2001; Zelmanov and Semiat, 2011]. The illustrative depiction of the biological transfer of heavy metal to man has been depicted in

Insert Figure 1 here.

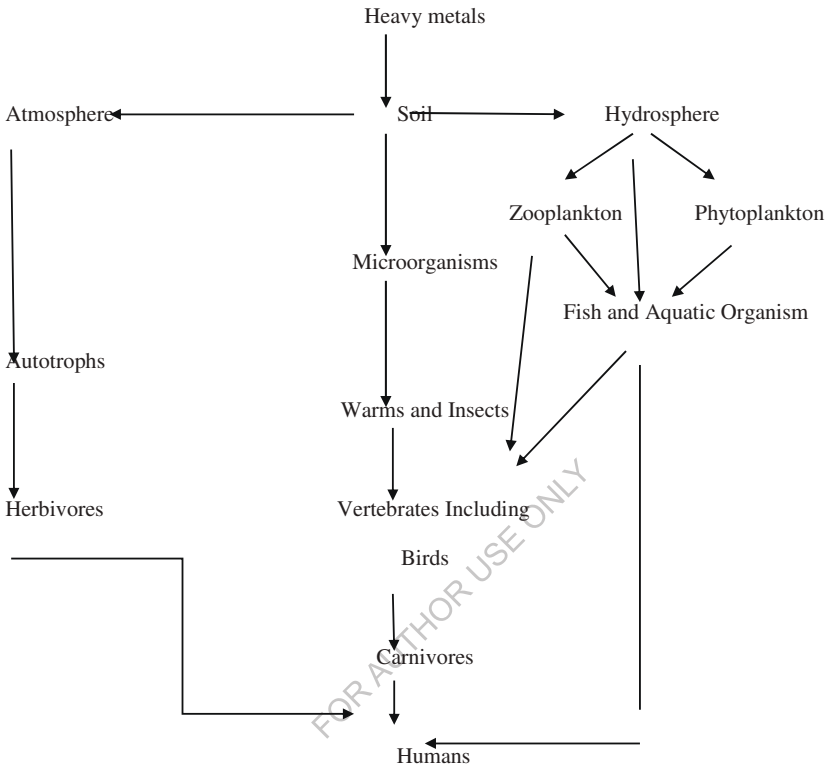

Figure 1: Biological transfer of heavy metals to man

Numerous reviews on heavy metal ions removal revealed the use of ion-exchange resin, chemical-precipitation, and membrane separation-filtration methods have been extensively reported (Fu and Wang, 2011). Such technics suffers various drawbacks like high cost or less effective, therefore, researches around the globe are now in the search of new and effective technologies to combat pollution caused by wastewater. Adsorption with green adsorbent materials (lower cost, satisfactory adsorption properties and environmentally-friendly nature)

was found as high effective process for removal of various pollutants from wastewater in the recent time. Such green adsorbents were obtained from various sources such as agronomic sources, by-products of fruits, vegetables, foods, activated carbons after pyrolysis of agricultural sources etc. Moreover, the removal of such adsorbents found challenging after the adsorption of pollutants. Activated carbon (AC)obtained from agricultural wastes was reported as one of the most comprehensively utilized as adsorbent for pollutants removal through adsorption. High production cost restricted the use of AC in the recent time (Tocchi et al., 2012).

Recently green nanocomposites formed by combination of nanomaterials (carbonadoes and metal based) with either natural materials (polymer, chitosan, clay etc) or they are derived through green source are the new trend in the remediation of environmental problems. A composite is a combination of two or more components in which one component acts as a reinforcing agent and other provides compatibility.

Green nanocomposites have advanced characteristics of excellent adsorption properties and biocompatibility. Moreover, they minimized the exposure of metal to the environment. During the last decades nanomaterials have gained special recognition owing to their advanced properties (high surface area, semiconducting nature) over conventional adsorbents. Various types of functionalized nanomaterials were developed in the virtue of anchoring specific functional groups on their surface modification. A number of reviews on the green adsorbents for wastewater treatment have been reported such as Kyzas and Kostoglou (2014) critical reviewed adsorption capacity; kinetic modeling and critical techno-economical data of green adsorption processes in order to scale-up experiments (from laboratory to industry) with economic analysis and viewpoints of the use of

green adsorbents. Various clays like kaolinite and montmorillonite (natural and modified), agriculture waste, polymer nanocomposites, chemically modified plant waste, were reported for the removal of heavy metals from wastewater (Bhattacharyya and Gupta 2008; Sud et al. (2008); Sonawane et al. 2018; Wan Ngah and Hanafiah 2008; Singh et al. 2014). Several investigators reported by-products from industry like, diatomite (Sheng et al., 2009), lignin (Betancur et al., 2009; Reyes et al., 2009), lignite (Mohan and Chander, 2006), aragonite shells (Kohler et al., 2007), natural zeolites (Apiratikul and Pavasant, 2008a), peat (Liu et al., 2008a), clay (Al-Jlil and Alsewailem, 2009), clino-pyrrhotite (Lu et al., 2006), and kaolinite (Gu and Evans, 2008) etc.Various forms of low-cost, plant material for example black gram husk (Saeed et al., 2005), potato peels (Aman et al., 2008), sugar-beet pectin gels (Mata et al., 2009), sawdust (Kaczala et al., 2009), coffee husks (Oliveira et al., 2008) and citrus peels (Schiewer and Patil, 2008), etc., have been extensively examined as excellent biosorbents for toxic heavy metals. In spite of their easy availability, cheap and eco-friendly nature, uses of these materials are less common because of lesser adsorption capacity and stability. Moreover, these materials are difficult to separate after the adsorption process.

Present chapter deals exclusively with the remediation of heavy metal Cr by various green nanocomposites/adsorbents that functionedvia adsorption and photocatalytic process. Nanomaterials are now in fashion because of their exceptional properties, like high surface area and their high mechanical strength. They have excellent adsorption properties credited to special surface functional groups. A review on removal of Cr (VI)-contaminated water and wastewater was presented by Owlad et al. (2008). Removal of Cr (VI) through adsorption was performed by Fe-functionalized ACobtained from Trapa natans husk (Liu et al. 2010), Iron phosphate (Zhang et al. 2012), iron(III) complex of a carboxylated

polyacrylamide grafted sawdust (Unnithan and Anirudhan, 2001), Iron (Fe^{3+}) oxide/hydroxide nanoparticles-based agglomerates suspension (Zelmanov and Semiat, 2011) and highly active nanoscale zero-valent iron (nZVI)-Fe_3O_4 nanocomposites[Lv et al. 2012]. Updated information on synthesis methodology (hydrothermal, sol-gel, co-precipitation etc) of green composite are summarized. Furthermore, importance of green synthesized nanocomposite is highlighted due to economicalfabrication and intercededoutcome of biogenic sources (polyphenols etc). Research gaps prevailing and future recommendations have also been provided.

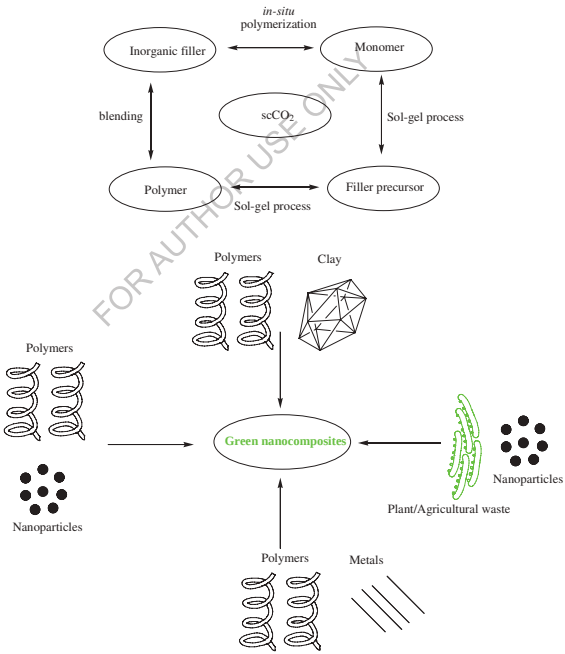

Figure 2. Various types of green nanocomposites

Environmental concern of heavy metals

Literature survey reveals that heavy metals have atomic weights between 63.5 and 200.6 and density greater than 5 g per cubic centimeter [Srivastava and Majumder, 2008; Barakat, 2011; Fu and Wang, 2011]. The fast industrialization during recent years has significantly contributed to heavy metals release into environment. The pollution of water due to discharge of heavy metals from various industrial sources (metal plating facilities, battery manufacturing, fertilizer, mining, paper and pesticides, metallurgical, mining, fossil fuel, tannery) into environment has been instigating disquiet around the globe [Marques et al. 2000]. Heavy metals owing to non bio-degradable nature tend to accumulate in living organisms unlike organic contaminants and this leads to treatment of industrial wastewaters include Pb, Cr, Cd, Hg, As, Ni, Cu and Zn. There are various symptoms of the toxic metals toxicity like high blood pressure, vascular occlusion speech disorders, sleep disabilities, fatigue, aggressive behavior, poor concentration, irritability, mood swings, depression, increased allergic reactions, autoimmune diseases and memory loss [Qu et al. 2013]. Heavy metals like Se, Zn and Mg might dislocate the humanoid cellular enzymes, while cadmium, lead, arsenic and mercury were reported harmful to human body. Although, human body desires few heavy metals (Manganese, iron, chromium, copper and zinc) but large amounts of such metals might be lethal [Qu et al. 2013 Nordberg et al. 2007 Rao et al. 2006]. Table 1 illustrates the permissible concentrations limits for the selected heavy metals, as reported by U.S. Environmental Agency (U.S. EPA, 2015) and World Health Organization (WHO, 2008).

Global discharges of Cr metals (out of 1000 metric tonnes/year) in water, air and soil is 142, 30, and 896 MT/year (Nriagu and Pacyna, 1988).

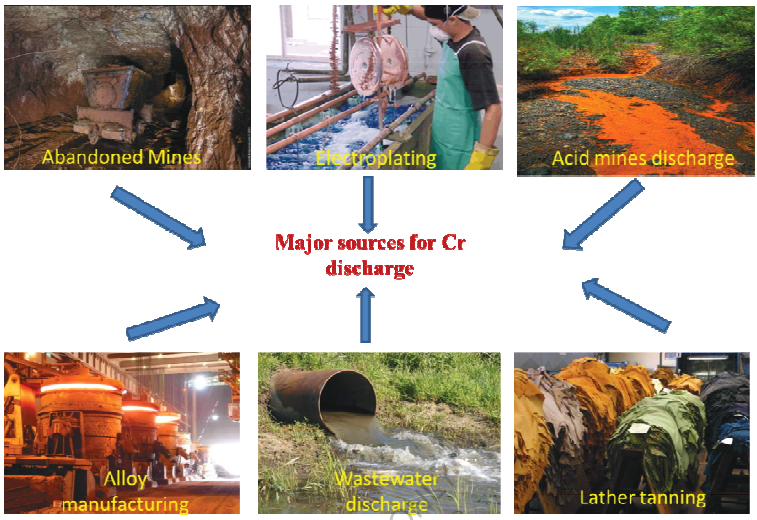

Figure 3. Various sources of chromium discharge

Potential sources of chromium are unauthorized release from various Industries to environment, cooling tower blowdown, Electroplating, Metal plating and coating processes. Chromium has various applications in electroplating, metal furnishing, magnetic tapes, pigments, leather tanning, wood protection, chemical manufacturing, brass, electrical and electronic equipment, catalysis and so on [Kimbrough et al. 1999]. Toxic effect due to excessive chromium includes severe diarrhea, Nausea, Pulmonary congestions liver and kidney damage. Available treatment techniques are Adsorption, Membrane-technologies, Ion-exchange, Floatation, Solvent extraction, Coagulation and Cyanide treatment.

Pollutants from various industries discharge are rich in heavy metal ions (Chromium, Arsenic, Cadmium etc) endure an important environmental issue. Constituents of wastewater have been presented as Table 1(Henze, 1992). Though control methodologies have been used to various industrialized and public sources,

the total amount of such agents discharged to the atmosphere remains staggering (Mohan and pitterman, 2006). The discharge of Cr compounds withgreatvariability of valency states (range: IV to +VI) to H_2O systems may extremelydistressmarine life [Fukai 1967]. In order to meet out the legal limits of 50 µg/L of total chromium concentration for drinking water [Khezami and Capart, 2005] and 100 µg/L for released to surface water (US Environmental Protection Agency standards) [EPA, 1990], chromium should be removed or otherwisereduced into a harmless soluble species [Pandey and Mishra, 2011]. Still, industrialized wastewater usuallycomprises high amount of chromium, from range from 500 to 270,000 µg/L [Patterson 1985], and levels could reach 50–700 µg/L in groundwater [Oze et al. 2007].Highamount of Cr in soil causes reticence on herbevolution, chlorosis in fresh leaves, nutrient inequity, wilting of tops, and root injury [Yadav, 2010]. Notably, Cr in soil inclined to be uptaken by crops and consequently absorbed by humanoid beings, instigating a variety of diseases. Consequently, it was rather significant to decrease the absorption of Cr by crops.

Table 1. Constituents of wastewater (Henze, 1992)

Type	Source	Components	Effects
Microorganisms	Sewage, animals excrement	Pathogenic bacteria, virus, *etc*. e.g. E-Coli, bacillus subtilis, pseudomonas aeruginosa, enterococcus faecalis, *g*iardia lamblia	Water born disease Risk while bathing and eating fish
Organic materials	-	Oxygen depletion in rivers, lakes and fjords	Eutrophication, aquatic death, may contain disease causing microorganisms.

Synthetic organic materials	Industrial waste	Pesticides, fat, oil and grease,dyes, phenols, amines, PAHs, chlorinated compound, tennaries, pharmaceuticals *etc*.	Mutagenicity, pH, Cercogenic, COD, aesthetic inconveniences, bioaccumulation
Nutrients	-	N, P, ammonium, Ca, Na, Mg, K, *etc*.	Eutrophication, oxygen depletion, toxiceffects
Inorganic materials	Soil-erosion, power plants	Acids, bases, heavy metals (Hg, Pb, Cd, Cr, Cu, Ni), Metals/Metalloids, nitartes, phosphates	Corrosion, toxic effect, acidity, hardness, aquatic death, bioaccumulation
Radioactivity	Radiomaterials	Various radioactive elements	Toxic effect, accumulation

Adsorption:

A variety of technologies are presently in use to combat presence in water like biological treatment methods, joint chemicaland biochemical methods (Tocchi et al., 2012), chemical oxidation and photocatalysis (Wang et al., 2014; Hamad et al., 2015a,b). Among all, Adsorption wasdocumented as an effective and cost-effective methodology for heavy metal removal from wastewater. The adsorption procedure offers flexibility in design and operation and in numerous cases will generates high-quality treated effluent. Furthermore, since adsorption is occasionally reversible, adsorbents can be regenerated by appropriate desorption procedure.Indirect method was used for the analysis of heavy metals in wastewaters. For example, AAS and ICP-MS have been preferred for analyzing

the collected aliquot of adsorbate. Commercial used AC is prohibited due to relative expensiveness of AC. Moreover, environmental concern is an issue while using toxic reagents. Therefore, low cost green adsorbents are the need of time for the remediation of heavy metals.

Biosorption of heavy metals from green adsorbents includes bioadsorbents (agricultural wastes, natural substances), and industrial byproducts/wastes. The phenomenon has promising effects of potential removal ofheavy metals even from dilute solution withusage of low-cost bio-sorbents.

The budding source of green adsorbants are biomass of dead (bark, lignin, shrimp, krill, squid and crab shell), algae and microbes (bacteria, fungi and yeast) (Apiratikul and Pavasant, 2008b).

Algae was greatly employed in several research publication for adsorption of metals (Ajjabi and Chouba, 2009; Pavasant et al., 2006 Deng et al., 2007 Ajjabi and Chouba (2009) due to *varied obtainability, low-cost, high adsorption capability along with good excellence (Apiratikul and Pavasant, 2008b)*El-Sikaily et al. (2007) used green alga Ulva lactuca for the biosorption of chromium from wastewater. Bacteria such as Escherichia coli, Bacillus cereus andPseudomonas aeruginosa (Pan et al., 2007; Gabr et al., 2008; Tuzen et al., 2008; Souiri et al., 2009; Quintelas et al., 2009)and fungi like Aspergillus niger,Rhizopus arrhizus, Saccharomyces cerevisiae and Lentinus edodes (Aksu and Balibek, 2007; Bahadir et al., 2007; Chen and Wang, 2008; Cojocaru et al., 2009; Bayramoglu and Arica, 2008 Amini et al., 2009; Tsekova et al., 2010) have also showed efficiency in biosorption of toxic-metals. Moreover,due to small size *Fungi and yeasts can be easily grown into high yields and higher chances of hereditarily and morphologically manipulation.*

Agricultural waste(soybeanhull and jackfruit; sugar beet pulp; fruit and weeds waste; hazelnut shell ;chestnut shell; maize corncob; rice husk; jatropha oil cake and grape seed activated carbon etc) has its own pros (profuse, naturally obtainable and cheap) and cons (environmental concern of load due to unfitting disposal) (Kurniawan et al., 2006;Ho, 2003;Alper˙Is¸ o˘glu., 2005;Wafwoyo et al., 1999), compost, (Pellera et al., 2010; Abdulrasaq and Basiru, 2010; Habib et al., 2007; Odoemelam et al.,2011; Demirbas et al., 2008; Özcimen and Ersoy-Meric¸ boyu, 2009), (Garg et al., 2008; Kumar and Bandyopadhyay, 2006). Lingo-cellulosic fibers (annual global production: 4billion tonnes) with large volume of production from agriculture and forest has been extensively usedas raw or activated for clean-up of waste water (Warren et al., 2005; Ngah and Hanafiah, 2008a). In addition, use of agricultural adsorbents avoids the high research cost of the synthetic adsorbents (Wafwoyo et al., 1999). However, **agricultural waste have limited adsorption capacity for metal e.g.,** 12.42 mg/g and activated carbon produced from agricultural wastes was rendered in view of high manufacture and managements costs (Tocchi et al., 2012). Due to strong binding affinity towards metals, many biopolymers such as, chitosan [Ngah et al. 2011; Aydın and Aksoy, 2009], alginate [Gupta and Babu 2009], and chitin [Baran et al. 2006] were also employed in remediation of toxic metal contaminants. Kaolinite clay has rapid uptake (30 min) with maximum metal (Jiang et al. 2010) while brine sediments and sawdust were used for removal of Zn and Cu (Agoubordea and Navia, 2009). Inspite of *wide-ranging source, cheapness and maximum adsorption capacity, biosorbents are materials of less-choice because of difficulty in separation.*

Hence, in view of those limitations, bioadsorbents were combined or mixed with nanomaterials to obtain green nanocomoposites with extraordinary characteristcs. Nanocomposites have shown their versatility in protection of environment via

photocatalytic mechanisms (separation of electron-hole pairs in UV-Visible). Binary and ternary metal oxides, or heterostructures along with clay, graphene, and graphene oxide and multifunctional cotton fabrics with nanocomposite coating are also in development.

Synthetic methods for green composites nanostructures

For removal of total Cr, nanocomposites are prepared by several methods like Carbothermal, Microwave, Solvothermal, Co-precipitation, Hydrothermal, Sol-gel, Reduction, Impregnation, Micelle and Reverse Micelle, and Miscellaneous (intercalation, precipitation, evaporation etc). The green composites were characterized by Brunauer-Emmett-Teller (BET) analysis for calculation of surface area (N_2 physisorption) porosimetry, X-ray diffractometry (PXRD), to investigate the crystallinity, structure, phase compositionand existence of intercalation in composites; spectroscopic techniques (Fourier transform infrared (FTIR), Raman, X-ray photoelectron spectroscopy (XPS)determine the various functional groups and the different bonds formed upon mixing; microscopic techniques(FE-SEMand high-resolution transmission electron microscope HR-TEM) and band gap calculation by obtaining Diffuse Reflectance Spectra data.Herein we are summarizing some key synthetic methodologies for the generation of green nanocompsites.

1. Carbothermal:

In the carbothermic process reduction of materials, generally metal oxides (MO_2^{-2}), using carbon as the reducing agent at high temperatures. Elemental forms of various elements have been generated via these processes. On the basis of Ellingham diagrams the capability of metals to take part in carbothermic reactions can be expected (Greenwood and Earnshaw, 1997). Carbothermal reactions

generally yieldCO and occasionallyCO_2. The competence of suchtransformations is attributable to the entropy of process: two solids, the metal oxide and carbon, are converted to a new solid (metal) and a gas (CO), the latter having high entropy. Thermal-heating is provided for facilitate the diffusion of the reacting solids.

Carbon-supported nanoiron (C-Fe^0) particles werecarbothermally synthesized by 5 g carbon black (80 m2/g) obtained from Alfa Aesar. It wasadded to 200 mL of aqueous solutions of Fe(II) or Fe(III) salts (50 g of $Fe(NO_3)_3 \cdot 9H_2O$), either by adsorption or by impregnation (Hoch et al. 2008).The solid obtained was then heated to 800 °C to obtain C-Fe0 nanocomposite.XRD pattern reveals that at 600 °C or above oxide was completely converted into elemental iron. The minimum temperature of the carbothermal iron reduction was determined by dividing a sample of carbon black with adsorbed iron (from ferric nitrate solution) into 1 g portions. It was reported that different particles size of synthesized Fe^0 NPs. The deviations in surface area presumablyredirect changes in the remainingquantity and the porosity of the carbon support, meanwhile the specific surface area linked with 50 nm spherical particles of Fe0 should be in the range of ~10 m^2/g.

Zhuang et al. (2014) fabricated a spongy carbon-encapsulated iron (Fe@PC) nanocompositevia reduction of ferric nitrate, starch and sodium chloride. The cost-effective and water-soluble starch was selected as the carbon precursor. NaCl was usedas a solid spacer to inhibit the particles agglomeration. Fe@PC with surface area 378.71 m2/g; pore volume: 0.17 cm3/g) exhibitedhigh, quick removal capability and reductivity for Cr(VI). XRD patternrevealed that iron species existed as Fe3O4 first, and reduced to Fe by carbon under higher temperature.

Kumar et al., 2012, prepared dry prawn shell (P. esculentus) activated carbon after treating 25 g of dried shells with 20 mL of conc. H_2SO_4 at 100 ◦C. Activation

was done in a muffle furnace at 400 ◦C to get activated carbon and care was taken to avoid the formation of ash during the activation process in muffle furnace. **Acharya et al., 2009,**developed activated carbon from Tamarind wood activated with zinc chloride (10g/100mL) with chemical ratio (activating agent/precursor) of 100% . The mixing was performed at 50 ◦C for 1 h followed by vacuum drying at 100 ◦C for 24 h. The resulting samples were heated (5 ◦C/min) to the final carbonization temperature for carbonization times of 40 min. Optimization condition provided by RSM were chemical ratio (296%), activation time (40 min) and carbonization temperature (439 ◦C).

2. Microwave:

The frequency range of microwave heating is between 900 and 2450 MHz. At lower microwave frequencies, conductive currents flowing within the material due to the movement of ionic constituents can transfer energy from the microwave field to the material while at higher frequencies, the energy absorption is mainly due to molecules with a permanent dipole that tend to reorientate under the effect of a microwave electric field. A dielectric material can be processed with energy in the form of high-frequency electromagnetic waves.

For Cr(VI) removal,**Wang et al. (2011)**synthesized *microwave*-assisted Fe-bamboo charcoal adsorbents (Fe–BC) using5 g BC (support) and Fe^{3+} that was obtained by50 mL 20%(w/v) of $Fe_2(SO_4)_3$ and 50 mL of 50% H_2SO_4). Microwave conditions are: 640 W output power; 2.45 GHz frequency for 6 min and 10 mL/min of nitrogen flow. BC is selected as aeconomicauxiliary material for iron oxide coating. Being a decent microwave absorber, temperature of the adsorbent raised quickly and consistently on exposure to radiation. Hence, Fe+3 species maximize their cross-linking with various functional groups on BC surface and

become efficient adsorber for metal removals.Fe-BC has OH and Fe–O group indicated by strong streching band at 3450 cm−1 and 630 cm−1, diagnostic of goethite. [Li et al. 2008; Namduri and Nasrazadani, 2008].Alcoholic, phenolic and carboxylic groups in Fe–BC was confirmed with peak at 1020–1120 cm−1 (Shen et al. 2009; Jung et al. 2001).Coating of iron oxide on BC resulted in decrease of surface area (Fe–BC: 49 m2/g; BC: 64 m2/g), pore volume and pore size. Zhang et al. [2008] and Liu et al. [2010] also observed decreased surface area of activated carbons coated with iron oxide. Moreover, coarse surface of Fe–BC also indicated the presence of iron oxide on BC that was having smooth surface initially.The intensity of the EDS peak at 6.38KeV in composite indicating the redox coating and elevation of oxygen peak with high intensity supported the iron oxide coating.

Gupta et al. 2013 prepared bio-based porous carboni.e., Ficus carica fiber — activated carbon (FC-AC) for adsorption of Cr(VI). The bio-fibre was carbonized and activated with H3PO4 under exposure of microwave radiations.

Kashinath et al. (2018) carried out microwave mediated synthesis of cerium oxide-graphene oxide (CeO2-GO) hybrid nanocomposite in absence of any surfactant or reducing agent. In-situ hexagonal nano cerium oxide particles embedded on the layered surface of GO sheets was used for removal of Cr(VI) ions. Nanocomposites CeO2-GOexhibitedimproved 5-folds of efficieny in UV (ultraviolet) light and showedquickefficacy in the removal of chromium ion superior than the bared GO and CeO_2, thatreticent by capable photosensitive electron injection and suppressing the electron–hole recombination.

3. Solvothermal: In the solvothermal method nonaquesous media is used instead of water as in the hydrothermal method at much higher temperature than that in hydrothermal method, asmany of organic solvents with high boiling points

can be picked. This is a versatile method for the generation of variety of nanoparticles with superior control over size and morphology, crystallanity than hydrothermal methods(Li et al. 2006; Xu et al. 2006; Wang et al. 2005).

Zheng et al., 2012 fabricated tunable sized Fe_3O_4@C core-shell nanoparticles (FCNPs) were by solvothermal reaction [Xuan et al., 2007, Wang et al., 2010] of $FeCl_3$·6H2O, glucose and $CO(NH_2)_2$ in EG solvent. In a typical experiment, 2.5 mmol of $FeCl_3$·$6H_2O$ was dissolved in 30 ml of EG with addition of 25 mmol$CO(NH_2)_2$and 0.5 mmol glucose with stirring for 30 minutes. Followed by transfer to Teflon-lined stainless steel autoclave and heated at 200 ◦C for 12 h.This resulted to solid products whichwere washedand dried. In order to tune the particle size and morphology of the FCNPs, controlled experiments were carried out. The TEM analysis revealed The FCNPs consist of nearly spherical particles with a size range from 70 to 100 nm with particles consist of smaller primary magnetic particles. The HRTEM image revealed that the resolved spacing of about 0.48 nm corresponds to the (111) lattice planes of cubic Fe_3O_4 crystal.

4. Co-precipitation:

Many catalysts withmultiple components(bulk catalysts and support material like Al_2O_3, SiO_2, TiO_2, ZrO_2 etc) can easily be fabricated via co-precipitation method with higher purity and better stoichiometric control. Calcination temperatures are usually lower for co-precipitation than the mixed oxide methods, and the product is more easily milled to finer particle sizes. Generally, the metal hydroxides were precipitated from their precursor salt solution owing to their low solubility. The precipitation of hydroxides can be achieved either by preliminary from an alkaline solution thatcan be acidified or from acidic solution by raising the pH. Typically, ammonia or sodium bicarbonate is employed as the precipitating

agent while extremely soluble inorganic salts like nitrates, carbonates or chlorides are usually used as metal precursors. (Jassal et al.,2015a, b,c; 2016a,b; Shanker et al., 2016a,b; 2017a,b,c).

Agarwal and Singh, (2014) prepared Zinc ferrite–PVA nanocomposite ($ZnFe_2O_4$) by coprecipitation of zinc and iron hydroxides and subsequent calcinations at 500°C.Theproduct was characterized by X-ray powder diffraction (XRD) and scanning electron microscopic (FESEM) techniques. Nanosize ZnFe2O4 (5 wt%) was dispersed in polyvinyl alcohol (PVA) solution and, on evaporation, a film of 1-mm thickness was formed. A PVA film of same dimension was also made. The film was characterized by Fourier Transform Infrared Spectroscopy (FTIR) and electrical conductivity measurement methods.

Nematollahzadeh et al. (2015) synthesized polydopamine (PDA, i.e. catecholamine) coated maghemite nanoparticles (MNP) with strong magnetic attraction for removal of Cr(VI) ions by the adsorbing and bridging effect of PDA. Maghemite (γ-Fe_2O_3) nanoparticles were synthesized by co-precipitation of ferric chloride ($FeCl_3$) (1 M)and ferrous salts $FeCl_2 \cdot 4H_2O$ (2 M), in an alkaline medium [Mirzayi et al. 2014, 2015; Seraj et al. 2014].Liq. NH_3 (2 M) was added dropwise to iron salt solution and obtained MNPs were separated by using magnetic field.An ultra-thin layer of polydopamine (PDA), as a catecholamine, was constructed on the surface of the MNP nanoparticles in an ex-situ process.MNPs (1g)weredistributed in 100 mL dopamine solution and shaken at room temperature for 24 h under ambient oxygen, the modified MNPs were obtained after completion of the self-polymerization of dopamine.

Baig et al., 2015 fabricated polypyrrole– titanium(IV)phosphate (TiP) nanocomposite by in situ oxidative chemical polymerization of pyrrole with $FeCl_3$,

in the presence of TiP particles. TiP was prepared from simple precipitation from aqueous solutions of titanium(IV)sulfate and H3PO4. With vital stirring, H3PO4 was added dropwise into titanium(IV)sulfate solution. The mixture was stirred for 24 h at 25 °C to form an absolute precipitate that was filtered off, dried at 100 °C for 24 h and ground to yield a fine TiP powder.

5. Hydrothermal:

This method is typicallyperformed in autoclaves with or without Teflon liners under precise temperature and/or pressure in aqueous media. The temperature can be raised above the boiling point of water, to reach the pressure of vapor saturation. This method is extensivelyemployed for the generation of small particles in the various industriesand generation of variety of nanoparticles.

Wang et al. (2018) prepared polyvinylpyrrolidone and polyacrylamide intercalated molybdenum disulfide (PVP/MoS2) composites by a simplistic way involving room temperature heating of Na_2MoO_4(0.60 g; 2.91 mM) with CH3CSNH2 (0.40 g; 5.32 mM) in deionized water (50 mL). Followed by addition of 0.10 g of PVP and continuous stirring (30 min), a uniform suspension was obtained. After further treatments (autoclave, centrifugation and washing), the developedmaterial (PVP/MoS2) was vacuum dried (70 °C for 20 h)and used for further studies. For comparative studies, PAM/MoS2 composite was also fabricated on similar lines.

6. Sol-gel:

This method has gained importance in preparation of ceramic materials (Pierre et al. 2002; Lu et al. 2002; Wight and Davis, 2002; Schwarz et al. 1995; Hench and West, 1990).Initially, precursors (inorganic metal salts or metal organic compounds such as metal alkoxides) undergo hydrolysis and polymerization to

give a colloidal suspension (sol) that will convert into a solid gel via complete polymerization and loss of solvent. Aerogel (highly porous material with low-density) is gotten when solvent form wet gel is detached under a supercritical state.Ceramic fibers have been drawn after adjusting viscosity of a sol while ultrafine/uniform ceramic powders can be achieved via precipitation, spray pyrolysis, or emulsion.

Under specified scenario, nanomaterials and nanocomposites of TiO2 was achieved from hydrolysis of a titanium precursor. Doke et al. (2014) prepared Titania ceramic membranes by polymeric sol–gel technique [42]for elimination of Cr(VI) by surfactant boosted microfiltration. In brief, to the titanium tetraisopropoxide (TTIP) solution (0.5 M), ablend of water, nitric acid and 2-propanol was added drop-wise and mixture is stirred, dried at 120°C for 5 h (to get polymeric gel) and calcinated to get TiO2 powder. Later on, aqueous PVA solution (was added with TiO2 powder to get homogenous paste (ratio of PVA/SG-TiO2 = 2% (w/w) and H2O/SG-TiO2 = 1 (w/w); SGstandas for sol–gel). PVA has characteristics of binder with improved dispersion to create homogeneity in the material. The obtained paste is dried and pressed to titania ceramic membrane (diameter: 25 mm; thickness: 2 mm).

7. Reduction

Zhou et al. (2018) prepared the nano Fe^0 functionalized with waste rock wool (RW) for proficientexclusion of Cr (VI). hexavalent chromium.waste RW (50 g) was acid treated to get ARW with micro/nano cracks. To 1 g of ARW, FeSO4·7H2O was added and resulting mixture is stirred. At that time, NaBH4 was added to reduce Fe2+ to Fe0 and stirred for 30 min. Through

magnetic separation, precipitate of ARW/ ZVI composites was collected and dried.

Télleza et al., 2011 studied removal of toxic Cr (VI) in water by iron nanoparticles embedded in orange peel pith. The method used briefly thereparation of biomass followed by biocomposite. Orange peel were dried, milled,sieved andstored under vacuum until use. Fabrication of biocomposite includestirring of mixture of orange peel powder (0.6 g) and iron(II) acetate (15 mL of 1×10^{-2}M)with dropwise addition of sodium borohydride (1×10^{-2}M).

Impregnation method (Incipient wetness**,** capillary or dry)

Impregnation is usual technique for preparation of heterogeneous catalysts from active metal precursor and catalyst support comprising the identical pore-volume like volume of the metal solution. Capillary-action pulls the solution into the pores and addition of excess of solution changed capillary process into a much slower diffusion. After drying and calcination, metal deposited on the catalyst surface was obtained.

Rajesh and co-workers(2011) synthesized trialkylamine impregnated with macroporous polymeric adsorbentfor treatment of Cr(VI) intoxicated industrial wastewater. In brief, Amberlite XAD-1180 (4 g) resin was stirred with 0.05 mol of TOA (octyl) to get homogeneous dispersion of the amine in the polymeric matrix in 2h. the obtained resin has specific surface area (150 to 900 m^2 g^{-1}) and an average pore diameter (4 to 9 nm) with characteristic FT-IR stretching bands (3046 cm^{-1} and 2924 cm-1 for aromatic and aliphatic C—H, 2368 cm-1 for protonated nitrogen, 1605 cm-1 for aromatic C—C, and 1267 cm-1 for C—N). After the Cr(VI)

adsorption, adsorbent showed an additional peaks at 889 cm-1 attributed to stretching of Cr=O in HCrO4 and revealed the protonation of nitrogen to form an ion pair with HCrO4 in the acidic standard.

Unnithan et al. (2004) reported synthesis, and application of amine-modified polyacrylamide-grafted coconut coir as adsorbent for Cr(VI). Here, polyacrylamidewas grafted onto coconut coir pith (CP; 20.0 g)at constant temperature to obtain polyacrylamide-grafted CP (PGCP). PGCP was refluxed with ethylenediamine (en; 25 mL) to change into an anion exchanger. On further treatment with 0.1 M HCl, the functionalized PGCP (PGCP-NH3 +Cl-) was obtained and sieved for studies. CP has characteristic IR peaks at 3407 cm-1forO-H stretching from cellulose structure of the CP. In PGCPNH3 +Cl-, following bands were obtained: broad absorption peaks at 3420 cm-1 for overlapping of C-H, N-H, and CdO stretching vibrations; 1627 cm-1 and 1565 cm-1 are due NH2 group; 1452 and 1020 cm-1 (Not present in the CP) for aliphatic C-N vibration and -CH2NH3 + type nitrogen. Common peak at 2928 and 2925 cm-1 (CP and PGCP-NH3 +Cl-, respectively) indicated the C-H stretching from >CH2. The bands at 1782 and 584 cm-1 are CdO stretching of hemicellulose and α-glucosidic linkage, respectively.IR completely favored the presence of polymeric chain (backbone) and the presence of -NH3 +Cl- functional group in PGCP-NH3 +Cl-. Sorption of Cr(VI) is found best at pH 3.0 and followed a pseudo-second-order kinetic.

Fang Luo et al., 2016, synthesized agarose-Fe nanoparticles hydrogel using green method for Cr (VI) removal. In brief, same volume of Fe2+ solution (0.01 mol/L) and grape leaf aqueous extract (2g/50 mL) was mixed thoroughly, stirred and dried to get Fe NPs which was added to hot agarose solution in order to get final agarose-Fe NPs hydrogel (uniform sized; average diameter of 5.0 mm). The

agarose solution was prepared by adding 0.075 g of agarose into 6 mL of water at its melting point (65–85 ^{0}C). Immobilization of Fe-NPs by agarose to formhydrogel also considered as encapsulation. SEM, XPS, and FTIR showed macroporous center of the agarose-Fe NPs hydrogel and uniformly encapsulated of Fe NPs inside the hollow agarose hydrogel.

Micelle and Reverse Micelle:

Micelles the groups of surfactant particlesdistributed in a liquid colloid are formed when surfactant concentration surpasses the critical micelle concentration (CMC). Amount of lipid decides the self-assemblage of surfactants and lipids molecules, for examples; spherical micelles, elongated pipes and into stacked lamellae of pipes. The form of a micelle is decided by molecular geometry of the surfactant molecules involved and solution conditions (surfactant concentration, temperature, pH, and ionic strength).Contrary to micelles, reverse micelles are obtained in non-aqueous media where hydrophobic groups arepresent towardsoutside the non-aqueous media. CMC is not considered true for reverse micelles in view of less number of assemblage that are not affected by surfactant concentration. TiO_2 nanomaterials were extensively synthesized by micelles and inverse micelles methods (Rachna et al., 2018 a, b; 2019, a,b,c; Rani et al., 2017, a, b; 2018, a,b,c,d,e,f,g,h,I; 2019,a,b,c;).

Miscellaneous:

Chen et al.(2011) prepared magnetic MCM-41 nanosorbents by incorporation of the magnetic iron oxide nanoparticles (10 nm) inside MCM-41 matrix (250 ± 50 nm) via the adding TEOS to the mixture. Briefly, aminopropyls were attached to the pores of the magnetic MCM-41 from 3-aminopropyltrimethoxysilane by reflux. The resulting NH_2–magMCM-41 was converted to Fe^{3+}–magMCM-41 by

overnight adsorption of Fe3+ (50 mM FeCl3 in 2-propanol). Magnetic colloid Fe3O4 nanoparticles was obtained from synthesis solution containing molar composition of 3.2 FeCl3:1.6 FeCl2:CTABr:39 NH4OH:2300 H2O) via sonochemical method. An aliquot of magnetic colloid (20 mL) was added to mixture of 1 CTABr:292 NH4OH:2773 H2O under vigorous mixing.

Lyu et al., 2017 preparedcomposite of nanoscale iron sulfide supported on biochar (CMC-FeS@biochar composite). Initially, Fe^{2+}- CMC complexes was prepared via addition of CMC solution (55 mL of 1%, w/w) to FeSO4.7H2O and then biochar (550 mg, particle size = 0.5–1 mm) was hosted into the mixture. FeS particles deposited on biochar by dropwise addition of Na2S solution (45 mL) under strong magnetic stirring (30 min).Diffraction peaks at 27.0, 31.9, 34.3, 38.0, 46.4, 52.8, 59.2, and 64.1 was for FeS and peak at 22.0 is for existence of biochar in irregular granular CMC-FeS@biochar (<100 nm) [28]. Suppressing the aggregation of FeS by biochar was resulted in increase in sorption sites in composites (CMC-FeS@biochar) due to more surface area, pore size and volume and smaller hydrodynamic diameters (256 ± 3 nm).FTIR data revealed that several functional groups (e.g., -OH, C=C, C=O, O=C-O, C-O, and Si-O)might have contributon in bonding of FeS particles onto the biochar surface. The point of zero charge (Pzc) was 5.7 and 5.0 for biochar and FeS, respectively,but CMC-FeS@biochar was negatively charged from pH 2.3 to 9.0 i.e., Pzc <2.3 for CMC-FeS@biochar.

Boddu et al.(2003) composite chitosan biosorbent (spherical; 100-150 microns; 105.2m2/g; nonporous) by coating the ceramic alumina onchitosan gel. The dried alumina for coating(150 mesh)and chitosan (50 g) were acid treated individually. The acid and chitosan form a viscous mixture (gel) and to this, about 500 g of the acid treated alumina was slowly added. The mixture was allowed to settle and clear

liquid was filtered out. Coating was repeated and the total amount of chitosan on the double coated biosorbent was 21.1 wt % andmicropore area of the biosorbent is only 3.3 m2/g.The XPS spectrum showed the predominance of carbon, oxygen, nitrogen, and aluminum elements based on binding energies at 289 eV (C 1s), 535 eV (O 1s), 402 eV (N 1s), and 78 eV (Al 2p) and hence supported the presence of -CH2OH, -CO, and -NH2 as surface moieties on the composite.

Shaikh et al. (2017) prepared polyhydroxamic acid (PHA) functionalized sorbent by the method [21]. Acrylamide (CH2=CH-CO-NH2) and crosslinker, N, N'–methylene – bis – acrylamide (CH2-CH-CO-NH-CH2-NH-CO-CH-CH2) was dissolved in deionised water with constant stirring to get a clear solution. Ammonium persulfate (initiator) was added and resultant mixture was heated at 60 ^{0}C for about 15 min to initiate the polymerization. The bulk polymer polyacrylamide (PAM) was crushed, and washed with water to remove the excess/un-polymerized reagents. PAM was further treated with hydroxylamine hydrochloride solution for 30 min followed by adjusting the pH of the solution to 12. The mixture was left overnight and neutralized using 3 N HCl. Sorbent thus obtained was washed with water till free from acid, air dried and termed as polyhydroxamic acid (PHA).

Khare et al. (2017) fabricated a nanocomposite of chitosan supported microchannel-embedded metal–carbon–polymer (chitosan/Fe-oxide-CNF/PVA nanocomposite film). A PVA emulsion was set from hydrolysis of PVAc followed by modification with the hydrophobic methyl acrylate and acrylonitrile monomers as reported[Khare et al., 2015]. The Fe-oxide CNFs (Fe-CNFs) were separately prepared involving catalytic chemical vapor deposition and ball milling step [Bikshapathi et al., 2012]. A fixed amount of the PEG-soaked Fe-CNF fillers was mixed into the chitosan solution (4 g in 100 mL) containing 0.1% (v/v)- glutaraldehyde as a cross-linking

agent. To this mixture solution modified PVA emulsion was added and the entire mixture was stirred for 30 min before casting. The cast material was sequentially dried (60 $_{o}$C for 24 h and 150 $_{o}$C for another 12 h).

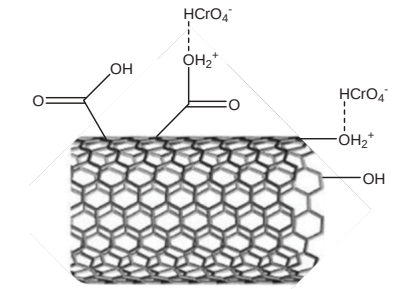

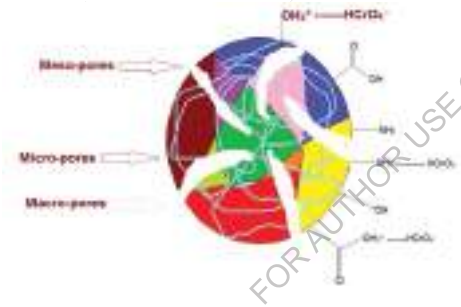

Luo et al. (2013) prepared magnetic nanocomposite of manganese dioxide/iron oxide/acid oxidized multi-walled carbon nanotube **(Fe3O4/o-MWCNTs)**. Initially, raw-MWCNTs were oxidized with a mixture of acid solution (conc. H2SO4 and HNO3 v/v 3:1) at 100 ^{0}C for 4 h to get o-MWCNTs. Deposition–precipitation method was used for deposition of **Fe3O4**on o-MWCNT surfacesusing Fe3+/Fe2+ salt precursors [Cunha et al., 2012]. Concisely, o-MWCNTs (200 mg) were ultrasonicated in deionized water for 30 min and to the suspension $FeCl_{6.}H2O$ (200

mg) and $FeCl_2.4H_2O$ (100 mg) were sequentially added followed by dropwise addition of 6% ammonium hydroxide (30 mL).

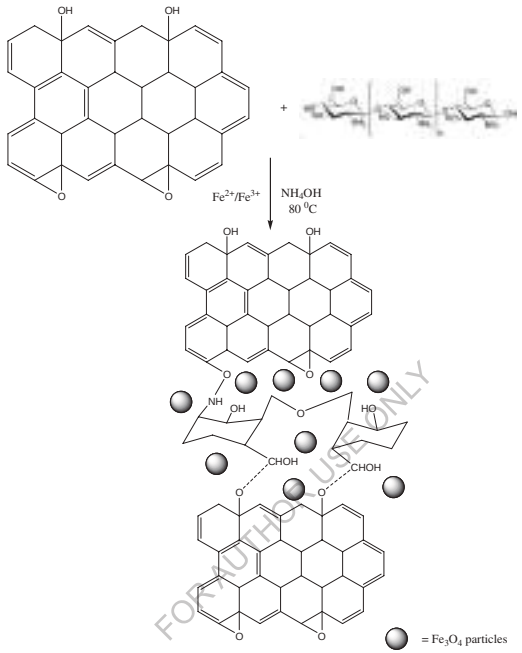

Figure 4. Schematic representation of formation chitosan-graphene oxide nanocomposite

Kumar A.S.K. et al. (2012) prepared celluloseNaMMT composite adsorbent where NaMMT clay was obtained from montmorillonite. Initially, cetyltrimethylammonium bromide (CTABr; 100 mL of 0.001 mol/L) was added to the clay suspension containing sodium ions.The mixture was stirred followed by centrifugation solid material was washed and then dried overnight. Later on, cellulose powder (3 g) was added slowly to organophilic NaMMT, and the

resulting mixture was stirred for 12 h and resulting composite adsorbent was washed, dried for 6 h and used for further studies.

Yang et al. (2018) reported in-situ functionalization of poly(m-phenylenediamine) (PmPD) nanoparticles on bacterial cellulose (BC) by adsorption of mPDs on BC followed by the chemical oxidative polymerization to form PmPD incorporated to BC fibril. Shyaa et al. (2015) synthesized ion exchange resin capable of coordinating with metal ion i.e., polyaniline/ zeolite nanocomposite for the removal of chromium (VI) from aqueous solution. Zeolite was modified with conducting polyaniline by the polymerization of anilinium cation in and outside of zeolite channels and a nanocomposite of polyaniline/zeolite (PANI/zeolite) was obtained by the oxidative polymerization of anilinium cation with the zeolite structure. Characterization indicate that composite (300 and 600 nm) has a high content of PANI.

Khosravi et al. (2018) fabricated ultrasonic assisted green nanocomposite (ZVI-PAC; size 60 nm) by loading GnZVI on powdered activated carbon (PAC) prepared fromPeganum harmala seed. Moreover, plant extract was also used for the synthesis of zero-valent iron nanoparticles (GnZVI). FESEM found that the surface of the produced activated carbon had many pores which indicated the effective role of ultrasonic waves in the process of activation. In addition, the FTIR range confirmed the role of hydroxyl groups generated by organic compounds in the synthesis of nanoparticles. BET test showed that after the loading of Iron nanoparticles the specific surface area of activated carbon reduced from 442 m2/g to 107 m2/g.

Heavy metal treatment methods

Heavy metal could be treated with several techniques associated with their pros and cons. Traditionally used chemical precipitation is simple and cheap but limited to treat high concentration wastewater containing heavy metal ions and thereby generate large amount of sludge. Ion-exchange method is expensive to use at large scale and resins need to be regenerated and hence, further serious secondary pollution. Adsorption involving AC (high cost) and other low cost adsorbents is widely efficient method. Biosorption of heavy metals from aqueous solutions is a relatively new process.Membrane filtration has limitation of high cost, process complexity, membrane fouling and low permeate flux. Coagulation/flocculation could settle good sludges with dewatering characteristics but associated with chemical consumption.Flotation deals several gains over the more conventional methods (Rubio et al., 2002) but involve high cost of initial capital involving maintenance and operation.Electrochemical techniques are rapid and well-controlled but expensive with electricity supply and capital cost. The selection of the most suitable techniques depends on the initial concentration of metal, the component of the wastewater, capital investment and operational cost, plant flexibility and reliability and environmental impact, etc. (Kurniawan et al., 2006).

Removal of Cr

The ground water contamination due to the chromium compounds used in electroplating and tannery industries [Ramos et al. 1994] need efficient treatment and sustainable technologies involving newer adsorbents [Saha et al. 2011]. Environmental Protection Agency (EPA) has set a limit of 0.1 mg L-1 for total chromium [Baral and Engelken, 2002; Xu and Zhao, 2007] in water.

Table 2: WHO and US EPA limitations of selected heavy metal in drinking water.

Contaminant	EPA limitations		WHO provisional guideline value(mg/L)
	Maximum contamination level (MCL) (mg/L)	Maximum contamination limit goal (MCLG) (mg/L)	
Lead	0.015	0	0.01
Chromium	0.1	0.1	0.05
Cadmium	0.005	0.005	0.003
Arsenic	0.010	0	0.01
Mercury	0.002	0.002	0.006
Copper	1.3	1.3	2
Zinc	5	-	3
Nickel	-	-	0.07

Among the low-cost adsorbents, sawdust [Garg et al. 2004], agricultural bio-waste [Park et al. 2008] and activated carbon [Mohan and Pittman Jr, 2006; 48] have showed good adsorption capacity. An electrochemical method involving electrodes of stainless steel nets coated with single walled carbon nanotubes has been used for the removal of chromium from aqueous solutions [Liu et al. 2011].

Novel adsorbents belonging to carbon e.g., graphene and graphene oxide (a graphene derivative) with their unique layer stuructured and several functional groups on its surface have been found fruitful adsorbents for Cr(VI) removal [Rao et al. 2009; Li et al. 2008; Quintana et al. 2013; Zhao et al. 2012; Dreyer et al. 2010; Huang et al. 2011].

Conventional technologies

Several methods such as biological methods, combined chemical and biochemical methods (1; Tocchi et al., 2012), chemical oxidation and photo-catalysis (Wang et al., 2014; 56,57; Hamad et al., 2015a,b),adsorption (Ma et al., 2015), coagulation and membrane treatments, presentlyin trend for the elimination of pollutants from waste water (Staj˘ci´c et al., 2015). Every of these methods have particularbenefits and shortcomings including incomplete metal removal and high cost. In view of above, there isurgentrequirement for the advancedmethodologywhich will be highly inexpensive, selective, more effective and easy to perform.

Adsorption was found as one of the effective technology for cleaning of wastewater with heavy metals [Barakat, 2011]. Activated carbon (AC) and activated carbon fiber (ACF) due to their abundant micropores and huge specific surface areas, they have been extensivelyused for the complete removal of contaminants from the air and water [Chen and Zeng, 2003]. AC and ACF found excellent for the removal of organic pollutants, they can scarcely reduce the concentration of metal ions upto ppb level when used in the removal of metallic pollutants such as Cr(VI) [Zhang et al., 2010 Wang et al., 2011 Pillay et al., 2009]. Various carboneous nanomaterials like Magnetic grapheme (Mg)synthesized using graphene oxide -ferrocene [Gollavelli et al. 2013] adsorb chromium with an

adsorption capacity of 4.86 mg/g. Calcined graphene/MgAl-layered double hydroxides and nanoparticle decorated graphene are reported for Cr(VI) adsorption [Yuan et al. 2013; Jabeen et al. 2011; Ma et al. 2012]. Recently, the interaction of an ionic liquid, Aliquat-336 with graphene oxide for chromium remediation in effluent samples has been reported [Kumar and Rajesh, 2013]. Several adsorbent such as polyaniline nanorods dotted on graphene oxide nanosheets, Amine functionalized Fe3O4 hollow microspheres–graphene oxide composite Poly (amidoamine) modified graphene oxide, polypyrrole/GO composite nanosheets have been extensively studied for the effective adsorption of hexavalent chromium [Zhang et al. 2013; Liu, et al. 2013; Yuan et al. 2013; Li et al. 2012].

Duranoglu et al. (2012) studied kinetics and thermodynamics of Cr(VI) adsorption onto activated carbon derived from acrylonitrile–divinylbenzene copolymer. Tuzen and Soylak, (2007) used multiwalled carbon nanotubes for speciation of chromium in environmental samples.

Kumar et al. (2013) used DBSA doped polyaniline/multi-walled carbon nanotubes composite for high efficiency removal of Cr(VI) from aqueous solution. Riahi et al. (2010) investigated removal of chromium from aqueous solution using polyaniline–poly ethylene glycol composite. Zhang et al. (2013) applied polyaniline nanorods dotted on graphene oxide nanosheets as a novel super adsorbent for Cr(VI). Raji and Anirudhan, (1998) studied kinetics and thermodynamics of Batch Cr(VI) removal by polyacrylamide-grafted sawdust. Deng and Bai, (2004) studied the removal of trivalent and hexavalent chromium with aminated polyacrylonitrile fibers. Senthurchelvan et al. (1996) studied thermodynamic, kinetic, and mechanistic aspects of reduction of hexavalent chromium in aqueous solutions by polypyrrole. Dossing et al. (2011) carried out reduction of hexavalent chromium by ferrous iron: a process of chromium isotope

fractionation and its relevance to natural environments. Lazaridis et al. (2005) studied Cr (VI) sorptive removal from aqueous solutions by nanocrystalline akaganeite. Hu et al. (2009) studied removal of chromium from aqueous solution by using oxidized multiwalled carbon nanotubes.Zhu et al. (2012) carried out one-pot synthesis of magnetic graphene nanocomposites decorated with core@double-shell nanoparticles for fast chromium removal. Li et al. (2013) used N-doped porous carbon with magnetic particles formed in situ for enhanced Cr(VI) removal. Gu et al. (2012) investigated magnetic polyaniline nanocomposites toward toxic hexavalent chromium removal. Wang et al. (2013) prepared polyacrylonitrile/polyaniline core/shell nanofiber mat for removal of hexavalent chromium from aqueous solution. Samani et al. (2010) studied the removal of chromium from aqueous solution using polyaniline–poly ethylene glycol composite.

Table 4. Cr(VI) adsorption by synthetic nanocomposites

Adsorbent /composites	pH/ Det. method	Brief summary	References
cerium oxide-graphene oxide (CeO2-GO) (5 g/L)		85% of Cr removal (100 mL, 30 mg/L) under UV-light.enhanced 5-folds of photocatalytic activities than the pure GO and CeO2;pseudo-second-order adsorption	Kashinath et al. (2018)
Trioctylamine-exfoliated graphene oxide (TOA–EGO)	2.5-3.0	TOA–EGO (99.4)> EGO(73.5) for Cr(VI) removal; Cr(III) removal by TOA–EGO is 92% at pH of 8 to 8.5 Total Cr removal: 96%	ASK Kumar et al. 2013
SiO2-SH/ED3A Thiol-functionalized silica/ethylenediaminetriacetate	1.5–3.0	35 mg/g in less than <15 min	Zaitseva et al 2013
Fe3O4/PANI microspheres	2.0	200 mg/g in 180 min	Han et al 2013

PANI/MWCNTs Nanocomposite (NC)	2.0	56 mg/g in 600 min	Kumar et al. 2013
Polypyrrole /Fe3O4 nanocomposite	2.0	170 mg/g in 30–180 min	Bhaumik et al. 2011
PPY/Fe3O4 microspheres	2.0	209 mg/g in 70 min	Wang et al 2012
Polyacrylonitrile/PPY core/shell nanofiber mat	2.0	62 mg/g in 30-90 min	Wang et al 2013
Polypyrrole (PPY)/γ-Fe2O3 PANI/γ-Fe2O3	2.0	209 mg/g in 15 min 196 mg/g in 35 min	Chávez-Guajardo et al. 2015
PPY-PANI nanofibers	2.0	227 mg/g in 30 min	Bhaumik et al. 2012
PANI/SiO2 composite	4.2	63.41 mg/g	Karthik and Meenakshi, 2014
Magnetically modified MWCNTs	1	14.28 mg/g	Bayazit and Kerkez, 2014
Magnetically modified activated carbon	1	5.07 mg/g	Bayazit and Kerkez, 2014
Aniline formaldehyde condensate coated on silica gel	3	17.0 mg/g	Albino Kumar et al. 2007
PVP coated silica gel	5	3 mg/g	Gang et al. 2000
Imidazole grafted silica	4	113.0 mg/g	Li et al. 2007
Mesoporous aluminosilicate	5.5	112.0 mg/g	Wu et al. 2010
Activated carbo-aluminosilicate	4	92 mg/g	Shawabkeh, 2006
zeoliteNaX	4	6.414 mg/g	Pandey et al. 2010
DMAEMA-g-silica	2.5–5	68.0 mg/g	Qiu et al. 2009
DMAEMA-g-silica	1.5–5.4	51.9 mg/g	Zhao et al.2011
Cyphos IL 104 functionalized silica (SG-2)	0–2	19.31 mg/g	Liu et al. 2010
Cyphos[A336][C272 functionalized silica(SG-5)]	0–2	15.29 mg/g	Liu et al. 2010

Dodecyl-benzene-sulfonic-acid (DBSA) doped PANI/MWNT composite	2 /ICP	55.5	Kumar et al. 2013
PANI/PEG poly ethylene glycol	5 /AAS	68.9	Riahi et al. 2010
PANI/GO	3/ ICP-MS	1149.4	Zhang et al. 2013
TiO2–RGO	6.3/ UV–visible	-	Zhao et al. 2013
Fe 3 O 4 @glycine doped polypyrrole magnetic nanocomposites	2.0	238.0 mg/g in 30–180 min	Ballav et al 2014
polypyrrole– titanium(IV)phosphate nanocomposite 0.2 g		42.7 mg/g; spontaneous and endothermic pseudo-second-order model 88% removal; 19 min, Cr(VI) initial concentration of 200 mg L_1	Baig et al. 2015
Magnetic mesoporous carbon incorporated with polyaniline	2	172.3 mg/g in 120 min	Yang et al. 2014
polyvinylpyrrolidone intercalated molybdenum disulfide composites and polyacrylamide intercalated molybdenum disulfide composites	5	142.24 mg/g on PVP/MoS2 and 84.91 mg/g on PAM/MoS2 spontaneous and endothermic process Cr(VI) ions were fixed on the composite surfaces by electrostatic attraction and then entered into the interlayer and combined with amide groups at the interlamination of the composites	wang et al 2018
MnO2/Fe3O4/ o-MWCNTs acid oxidized		186.9 mg/g150 min;85% pseudo-second-order rate Adsorption: spontaneous and endothermic	Luo et al. 2016
magnetic amino-functionalized composites (Fe 3 O 4 @A/PDA hollow dopamine (DA) and aminosilane	2	284.1 mg/g in 10 min at 25 ^{0}C, pseudo-second-order and Langmuir model; activation energy is 7.17 kJ/mol −1;Adsorption: 70% Cr(VI) removal, spontaneous endothermic	Li et al. 2017

coupling agents (A1, A2, A3 represent APTMS, TSPED and TPDA, respectively)		Hollow Fe3O4@A2/PDA (284.1 mg/g)> PS@Fe3O4@A2/PDA (182.4)>Hollow Fe3O4@/PDA(138.2)>nanoFe3O4(21.3)	
MNP@PDA	3	38.6 mg/g in 240 min	Nematollahzadeh et al. 2015
EDA- Fe 3 O 4	2.0	81.5 mg/g in 120 min	Fang et al 2014
PEI-modified magnetic adsorbent	2	78.1 mg/g in 30 min	Pang et al. 2011

Green adsorbent

Several green nanocomposites of combination of nanomaterials with natural greenfeedstockshave been used for Cr removal via adsorption and reduction mechanism. In view of presence of diverse functional groups in their structure that offers them high capacity and selectivity towards heavy metals, natural organic macromolecules such as biopolymers such as alginate, chitosan, various gums, cyclodextrin, etc. have beenfor the selective removal of chromium from wastewater. Among these, chitosan, a natural polysaccharide produced by the N-deacetylation of chitin was the best example being widely used in many studies [Liu et al, 2013]. This biopolymer ownsdecentadsorption capacity for various heavy metal ions because of its high amino content on the polymer matrix thatoffers selectivity to the adsorption process. To enhance its chemical stability in acidic medium, chitosan is generally cross-linked with another compound (e.g. glutaraldehyde, ethylenediamine, b-cyclodextrin, epichlorohydrin, etc.) into the chain. The amino and hydroxyl groups within the structure of chitosan can interact with heavy metals by ion exchange or complexation reactions along with electrostatic interactions [Wen et al., 2011; Li et al., 2008], However, raw chitosan

has few limitations such as poor chemical stability and mechanical strength and may block the filters or generates secondary pollution [Reddy and Lee, 2013].

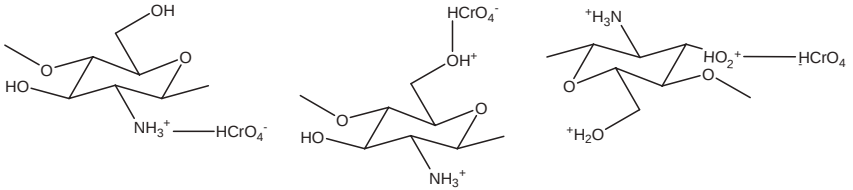

A combination of nanomaterial and biopolymer has fascinated for achieving high efficiency, biocompatibility and inert condition and also avoided direct exposure of metals or their oxides [Huang et al. 2018]. Among making green composites, iron nanomaterials having unique properties of magnetism, stability and high surface-area along with ease of functionalizationis extensively used. Among, metallic iron (cheap and safe moderate reducing reagent) or nano zerovalentiron (nZVI; Fe0) have been widely adopted (Gillham and O'Hannesin 1994; Orth and Gillham 1996; O'Hannesin and Gillham 1998). Working of Fe0 involves the electrochemical/corrosion reactions where iron gets oxidized fromexposure to oxygen and water. Contaminants freely accept the electrons from iron oxidation and reduced according to their stoichiometry.Although nZVI has many advantages, but its efficiency decreases with time because of formation of oxide layers that block its surface active sites. However, coupling of chitosan with the magnetic material (Fe_3O_4) could make its separation easy [Barquist and Larsen, 2010].

The adsorption process faces some challenges namely the separation of the adsorbate from solution. In batch mode, the separation is achieved by gravitational sedimentation or by filtration. However, incomplete sedimentation favors the presence of suspended material particles in the treated solution. The filtration method renders the method more expensive. Thus, magnetic separation presents

the solution to both these problems, where the cost as well as the risk of the presence of the adsorbent media in the treated solution, are both reduced.

Chitosan coated MNPs (proficient of operating in a wide range of pH values without any interferences by sulfate, silicate or phosphate) is potential adsorbents for metallic oxyanions too [Thinh et al., 2013]. Chitosan has tendency to easily protonate at amino groups under lower pH: MNPs@Chitosan-NH2 + H^+ = MNPs@Chitosan-NH^+_3. While removing dichromate by MnFe2O4@-Chitosan, chelation between chitosan and metal ions played a much important role than the electrostatic interactions in the process (Xiao et al., [91].Chromium can be speciated as HCrO4-, $CrO4^{2-,}$ and $Cr2O7^{2-}$based on pH and concentration of the aqueous phase (Luo et al. 2011).Cr (VI) exists primarily as bichromate ion (HCrO4-) in the pH range 3.8-5.5 and dichromate ($Cr2O7^{2-}$) at lower pH values (Suksabye et al. 2007).

During the removal of Cr(IV) by biopolymer based nanocomposite, HCrO4- species is associated as an ion pair with the positively charged nitrogen of biopolymer composite following the hard and soft acids and bases theory [Ho et al., 1975]. On the other hand, there is ligand-exchange reaction between the coordinated nitrate of Fe–crosslinked chitosan complex (Ch–Fe) and HCrO4 – ions (Zimmermann et al. 2010).

At 25 ◦C, Ch–Fe showed maximum adsorption of 325 mg/g of Cr(VI) from water at pH 2. The results indicate that the Langmuir–Freundlich Cr(VI) uptake on the adsorbent decreased on increasing the pH (295 mg/g at pH 2, 295 mg/g and 125 mg/g at pH 4.8 and 8.0, respectively), temperature (295 mg/g at 25 ◦C; 209 mg/g at 65 ◦C).Cr(VI) was analysed spectrophotometrically at 540nm and calculated by difference in their initial and final concentrations [Babu and Gupta, 2008].In

alkaline side, Cr(VI) adsorption is lower because of following reasons 1) high abundance of OH^- io omp t with r(VI) p i for th ad orptio it ; 2)Ch-Fe cannot able to adsorb $CrO4^{2-}$ (significant species at higher pH)(Wu et al., 2007) and 3) At pH > pHzpc, the net surface charge becomes negative that result in repulsive forces between Ch-Fe (pHzpc: 8.9) and Cr(VI) The pHpzc is an important parameter that determined the range of pH sensibility and allows the surface active and adsorption capacities to be predicted [Pintor et al., 2013]. These results are supported by efficient chromium adsorption at lower pH by several adsorbents like waste biomass (42 mg/g at pH 2.0), chitosan beads (58 mg/g at pH of 3.5)[Zubair et al 2008], magnetic beads (108 mg/g at a pH of 2.0) [Bayramoglu and Arica, 2008] and activated carbon(108 mg/g) [Demiral et al. 2008]. Besides chitosan, other organic coatings based on natural or synthetic polymers were found potential adsorbents due to the high content of functional groups on their structure [19,94–101,164–171].

A.S.K. Kumar et al. (2012) used mesoporous cellulose biopolymer – surfactant modified sodium montmorillonite clay composite (adsorption capacity: 22.2 mg/g for treatment of industrial wastewater. The ion pair interaction between positively charged nitrogen biopolymer composite surfacefollowed by the H-bonding interaction with OH-groups of cellulose is more prominentthan the interaction that exists between the quaternary ammonium cation and the hydroxyl groups of the biopolymer. This fact is supported by characteristic peaks of Cr=O and Cr-O at 913 and 765 cm-1, respectively (Singh et al. 2008). Kalidhasan et al. (2011) also observed similar mechanism on effective adsorption of Cr by crystalline cellulose_ionic liquid blend polymeric material. In bioclay, the protonated SiOH2+ also further supported the adsorption of bichromate anion with the positively charged composite adsorbent surface (Hu et al 2006). Langmuir adsorption was

spontaneous (-ΔG) and following second order kinetics. The mesoporous nature of the cellulose-clay composite, nano pore size (1.8 nm; volume: 0.31 cm3/g) and the good surface area (87.09 m2/g) is an indication of effective adsorption of Cr on the polymeric adsorbent (Lin et al 1997). Overall, the percentage adsorption of Cr (VI) as bichromate anion onto the surface of the biocomposite material (0.5-0.6 g; Range: 0.1-1.0 g) was found to be maximium (99.5%) in weakly acidic acondition (pH 3.8-5.5).

Li et al. (2008) foundmaximum biosorption (capacity: 6.73 mg/g) of Cr(VI) at initial concentration 40 mg/l and pH 1.0 and optimum temperature 28 °C in wastewater by bio-functional magnetic beads. The beads were mechanically stable and magnetic separatable and constituted by the powder of Rhizopus cohnii and Fe3O4 particles coated with alginate and polyvinyl alcohol (PVA). The groups of –NH^{+}_{3} , –NH^{+}_{2} and NH– , –, and >NH– played an important role in the Cr(VI) adsorption. Furthermore, The bio-functional magnetic beads were regenerated (by desorption with 0.1 M NaOH solution) and reusable (n=5) with predominant characteristics of adsorption, recovery and magnetism.

Zhou et al. (2018) used nanocomposite of Fe^{0}-functionalized waste acid treated-rock wool (ARWZ) for efficient removal of Cr(VI) (197.69 mg/g) from water and soil through adsorption and reduction due to its higher surface area credited to micro/nano cracks structure (porosity, active groups).Removal efficiency within 1 h followed: ARW/ZVI composites (1:2 w/w)100%>ZVI (73%)>ARW (55%)>waste RW (~3%). Endothermic adsorption was higher with increasing initial Cr(VI) concentration (increasing contact probability between adsorbent and Cr(VI) ions) (Chen et al. 2011) and decreasing pH (197.69 and 68.83 mg/g at pH 2.0 and 11.0, respectively). The positive zeta potential of ARWZ under acidic condition could favor the adsorption of negatively-charged Cr (VI) on ARWZ

through electrostatic attraction and the reduction of Cr (VI) to Cr(III) [Zhang et al. 2011]:

$Cr2\ O7^{-2}+ 14H^{+}+ 6e= 2Cr+3+ 7H2\ O$ ……(1)

López-Téllez et al., 2011 fabricated a biocomposite (iron nanoparticles embedded in orange peel pith) which coupled the reducing capability of iron nanoparticles with the adsorption capacity of cellulose to effectively remove 71%of Cr(VI) from industrial wastewater (10 mg/L) at pH 1 within 60 min. The biocomposite with the nanoparticles exhibited twice the Cr(VI) removal of the unmodified orange peel pith and also possesses over twice the adsorption capacity —5.37 mg/g vs. 1.90 mg/g indicated the potential role of iron. The adsorption seem to have reduction of Cr(VI) to Cr(III)by Fe or Fe(II) followed by adsorption of Cr(III).

Kashinath et al. (2018) found that cerium oxide-graphene oxide (CeO2-GO) hybrid nanocomposite (5 g/L) showed 85% of Cr removal (100 mL, 30 mg/L) under UV-light. Hybrid was multiple times photo-effective than bared ones(GO and CeO2) due to enhanced surface area, charge transferred at the interface. More the absorption of light and transportation of charge, more will be photocatalytic reduction of Cr(VI)owing to synergistic effects of CeO2 and GO (Hu et al., 2015

$CeO_2 + h\upsilon \rightarrow CeO\ (h^{+}+ e-)$

$GO + e- \rightarrow GO\ (e-)$

$Cr_2O_7^{2-} + 14H^{+} + 6e- \rightarrow 2Cr^{3+} + 7H2O$

$2H_2O + 4h+ \rightarrow O_2 + 4H^{+}$

The pseudo-second-order adsorption of $HCrO4^{-}$ and $Cr2O7^{2-}$ on CeO2-GO composite is credited to H-bonding between $HCrO4^{-}$ and composite containing empty 3d orbital of Ce3+. The $HCrO4^{-}$ or $Cr2O7^{2-}$ is the dominant form, and

$CrO4^{-}$ existed in neutral and alkaline medium. The enhanced removal of Cr(VI) at a relatively lower pH is attributed to large amount of H+ ions.

$HCrO4^{-} + 7H^{+} + 3e^{-} \rightarrow Cr^{3+} + 4H2O$ ……..(1)

$Cr2O7^{2-} + 14H^{+} + 6e^{-} \rightarrow 2Cr^{3+} + 7H2O$ …..(2)

$CrO4^{2-} + 4H2O + 3e^{-} \rightarrow Cr(OH)3 + 5OH^{-}$ …(3)

Boddu et al. (2003) used a nonporous biosorbent composite (prepared by coating chitosan , a glucosamine biopolymer, onto nonporous ceramic alumina) for Cr(VI) from synthetic and actual chrome plating wastewater at 25 ◦C. Oxalated dianion was seemed to make a connection between alumina and chitosan (Fig.) byH-bonds with –OH, –CH2OH, or –NH2 groups on the biopolymer. The effect of pH, sulfate, and chloride ion on adsorption was also investigated. The biosorbent (105.2m2/g) have adsorption capacity of 153.85 mg/g chitosan and regenerated using 0.1 M sodium hydroxide solution. Cr(VI) sorption occurred on protonated amine functional groups of the biopolymer as shown in Fig.

M.K.Kim et al. (2015) found synergism effect and complexation interactions in chitosan based multicomponent functional gel (FG) with multiwall carbon nanotube and substituted polyaniline i.e., (MWNT)–poly(acrylic acid) (PAA)–poly(4-amino diphenyl amine) (PADPA) for effective eradication of Cr (VI) from controlled and field samples. Binding -NH2 sites in CS and PADPA while internal H+ ions through PAA increases removal efficiency over a pH range. Moreover,

CS and PAA bestow 3D-hydrogel framework along with controlled swelling/shrinking action of the hydrogel. MWNTs impart stability to the gel during adsorption–desorption cycle and improves re-useability.Gokila et al., 2017 usedchitosan -alginate nanocomposites for removal of Cr (VI) from waste water

under the effects of initial concentration, adsorbent dose, pH (5.0), and agitation time.

Table 5: Cr(VI) adsorption by chitosan based composites

Adsorbent /composites	pH/ Det. method	Brief summary	Mechanism	References
chitosan-Fe^0 nanoparticles		pseudofirst-order reaction kinetics; rate constants favored temperature and iron loading. Lower adsorption at higher Cr(VI) conc and pH.	adsorption of Cr(VI) and reduction to Cr(III)	Geng et al. 2009
Chitosan bead (3 mm)-Fe^O nanocomposite (Tube shape; 58.6 mm; pore size:19.2 to 138.6)	4.5	45 mg/g, 89.4% of 68 mg/L Cr (VI) in 2 h Lower adsorption at higher Cr(VI) conc and pH; electroplating wastewater;	reduction of Cr (VI) to Cr (III)	Liu et al. 2013
Fe–crosslinked chitosan complex (Ch–Fe) 25 mg	2.0–5.0	325 mg/g;adsorption of HCrO4 – (97% of 600 mg/L in 60min at 25 ◦C;): pHzpc of ChFe is 8.9;	ligand-exchange between coordinated nitrate and HCrO4 – ions;	Zimmermann et al. 2010
Crosslinked chitosan–Fe(III) complex (4.17 lm)	4.8	148 mg/g 1.5 h; 380 mg/L	Adsorption-ion exchange	Demarchi, et al 2015
chitosan–magnetite (15–30 nm; spheres) nanocomposite strip		92.33 %, of Cr(VI) removal, better than chitosan strip (29.39 %)	Adsorption and ion exchange	Sureshkumar et al. (2016)
Magnetic chitosan–GO nanocomposite	3		Adsorption - photocatalytic	Debnath et al. 2014
ethylenediamine-modified cross-linked magnetic chitosan resin	2	The maximum adsorption capacities obtained from the Langmuir model are 51.813 mg g−1, 48.780 mg g−1 and 45.872 mg g−1 at 293, 303 and 313 K, respectively; time 6-10	Reduction-Adsorption	Hu et al. 2011

		min		
chitosan/Fe-oxide-CNF/PVA nanocomposite composite;	5.2	80 mg/ g in 1.3 h ; 400 mg/L; CNF= carbon nanofibre PVA=polyvinyl alcohol	Photocatalytic-adsorption	Khare et al. 2016
Magnetic chitosan – iron(III) hydrogel	3.0	135mg/g in 0.3 h; 115 mg/L	Adsorption-ion exchange	Yu et al 2013
composite chitosan biosorbent Chitosan-ceramic alumina (105.2m2/g)	4.0	Adsorption capacity: 153.85[a] mg/g; Cr(VI)= 5000 mg/L chrome plating wastewater at 25 ◦C regeneration: 0.1 M NaOH	Adsorption-reduction	Boddu et al. 2003
hydrolyzed polyacrylamide (HPAM)–chitosan gel	4 AAS	66.1 mg/g; Cr(VI)—82.9% and Cr(III)—67.6%; pseudo-second-order rate kinetics and Langmuir isotherm	Adsorption	Kuang et al. 2012
CS–MWNT–PAA–PADPA/FG chitosan functional gel – MWCNT- substituted polyaniline	2 UV–visible	2000 mg/g; synthetic/ field samples; adsorption; synergism effect; Cr removal mechanism: complexation interactions	Adsorption	Kim et al. (2015)
Chitosan -Alginate nanocomposites	5	removal of Cr (VI) from waste water;second-order kinetics;Freundlich isotherm;multilayer adsorption	Adsorption	Gokila et al., 2017
Chitosan coated with poly 3-methyl thiophene	2	127.6 mg/g Langmuir	Adsorption	Hena, 2010
Chitosan–g-polyaniline composite Cross linked-chitosan–g-polyaniline composite	4.2	165.6 mg/g Freundlich 179.2 mg/g Freundlich	Adsorption-ion exchange	Karthik and Meenakshi, 2014

Si gel- chitosan composite	4	Si-Chitosan (3.5 mg/g) > Si (1.08)	Adsorption	Rajiv Gandhi and Meenakshi. 2012
La(III) encapsulated silica gel chitosan composite	4	240 mg/g	Adsorption	Rajiv Gandhi and Meenakshi. 2012
amino terminated polyamidoamine functionalized chitosan beads			Adsorption-ion exchange	Rajiv Gandhi and Meenakshi. 2013
Hydrolysis product of chitosan (size NA)	3	26 mg/g; 24 mg/L	Adsorption	Ramnani, and Sabharwal, 2006
Xanthated chitosan flakes (0.3 mm)	3	230 mg/g 16.0 h; 10 mg/L	Adsorption	Chauhan, N. Sankararamakrishnan, 2011
Ethylamine-modified chitosan in rice husk-carbon beads (size = NA)	2.0	53mg/g; 300 mg/L	Adsorption	Sugashini, et al. 2012
PNMANI/Ch–HCl composite	4.2	192.4 mg/g Freundlich	Adsorption	Yavuz et al.2011
P2EANI/Ch–HCl composite	4.2	148.7 mg/g Freundlich	Adsorption	Yavuz et al.2011
PNEANI/Ch–HCl composite	4.2	229.8 mg/g Freundlich	Adsorption	Yavuz et al.2011
chitosan-NaMMT (unmodified clay)		9.36	Adsorption	Hyok An and Dultz, 2008
metal ion imprinted chitosan	5.5	51.0 mg/g 1000.0 mg/l	Adsorption	Tan Tianwei et al 2001
metal ion imprinted chitosan cross-linked with epichlorohydrin	5.5	51.0 mg/g 1000.0 mg/l	Adsorption-ion exchange	Tan Tian wei et al 2001
chitosan cross-linked	5.5	56.8 mg/g 1000.0 mg/l	Adsorption	Tan Tianwei et al

with ethylene glycol diglycidyl ether				2001
chitosan cross-linked with epichlorohydrin	5.5	52.3 mg/g 1000.0 mg/l	Adsorption	Tan Tian wei et al 2001
natural and crosslinked chitosan membranes			Adsorption	Baroni et al. 2008
cross-linked chitosan	5.0	50.0 mg/g 1000.0 mg/l	Adsorption	Schmuhl et al 2001
Chitosan (13 g l^{-1}	3	22.09 mg g^{-1} at 30 mg l^{-1} while 102 mg g^{-1} for 100 mg l^{-1}initial Cr(VI); 92.9% Cr(VI) removal	adsorption	Aydın and Aksoy 2009
chitosan	5.0	78.0 mg/g 1000.0 mg/l	Adsorption	Manuel et al. 1995
chitosan	?	27.2 mg/g	Adsorption	Masri et al.1974

[a] Based on the amount of chitosan (21.1 wt %) on the composite biosorbent. This corresponds to maximum capacity of 35.4 mg/g of composite biosorbent

Liu et al. (2013) used enhanced chitosan beads-supported Fe^0-nanoparticles (CS-NZVI) for complete reduction of Cr (VI) to Cr (III) in less than 2 h from electroplating wastewater in permeable reactive barriers. CS-NZVI beads (Tube shape; 58.6 mm; pore size:19.2 to 138.6) enhanced by ethylene glycol diglycidyl ether (EGDE) had a loose and porous surface with a nucleus-shell structure. chitosan (CS) beads were introduced as a support material in permeable reactive barriers (PRBs). The removal rate of Cr (VI) (89.4%), decreased with an increase of pH and initial Cr (VI) concentration. Ozay et al. (2009) fitted bothLangmuir and Freundlich adsorption isotherms for removal of Cr(III) from water with magnetic hydrogels based on 2-acrylamido-2-methyl-1-propansulfonic acid. Sureshkumar et al. (2016) found that chitosan–magnetite (15–30 nm; spheres) nanocomposite strip showed 92.33 %, of Cr removal, better than chitosan strip (29.39 %) from K2Cr2O7 solution containing Cr(VI) ions.

Ostovar et al. (2017) used silver oxide/sawdust nanocomposite (Ag2O/SD NC) (Adsorption capacity: 13.41 mg/g) for removal of Cr (VI) ions from aqueous solutions at different feed solution pH (2, 6, and 10), influent concentration of Cr (VI) (25 mg/L; range: 25-100 mg/L), flow rate (2 mL/min; range: 1-5 mL/min) and bed depth (4-12 cm). Thomas model found best in Adams-Bohart and Bed Depth Service Time (BDST) models used for adsorption kinetics. Nanocomposite can be regenerated using a dilute solution of NaOH (0.01 M).

Shyaa et al. (2015) investigated capacity studies of ion exchange resin capable of coordinating with metal ion i.e., polyaniline/ zeolite nanocomposite for the removal of Cr(VI) from aqueous solution. PANI/zeolite nanocomposite (300-600 nm) has a high content of PANI. The capacity of chromium adsorption on PANI/zeolite increases with initial metal concentration, the metal ion adsorption on surfactant is well represented by the Freundlich isotherm.

Khosravi et al. (2018) used green nanocomposite (ZVI-PAC) prepared by loading of GnZVI on PAC for Cr(VI) removal. Nanocomposite (107 m2/g)with a size of 60 nm has hydroxyl groups and many pores on surface of the activated carbon. Equilibrium adsorption are endothermic and spontaneous and were well-fitted with Langmuir model and Ho pseudo-second order model. Moreover, intraparticle diffusion and film diffusion were the mechanisms involved in the adsorption process.

Unnithan and Anirudhan, (2001) used iron(III) complex of a carboxylated polyacrylamide-grafted sawdust for adsorption (>99.0%) of Cr(VI) (25.0 mg/L in the pH range 2.0–3.0). predominant species being $HCrO_4^-$ was rapidly adsorbed via coordination on unsaturated sites for the iron(III) complex of polymer.Adsorption of Cr(VI) over complex surface was endothermic (144.20 mg/g at 20 °C to 172.74 mg/g at 60 °C) and following second-order kinetic. The L-type adsorption isotherm could be interpreted by the Langmuir and Freundlich equations.

Amine-modified polyacrylamide-grafted coconut coir pith carrying -NH3+Cl- (PGCP-NH3+Cl-) was found more active than Dowex (commercial chloride anion exchanger of quaternary amine) and CP for complete removal of 25.0 mg/L Cr(VI) at 30 °C, pH 3.0, and an adsorbent dosage of 2.0 g/L (Unnithan et al. 2004). Adsorption is favorable at low temperature(exothermic), pH and initial concentration and followed Freundlich model. The removal involve the anion exchange mechanism at pH 3.0 between adsorbent having -NH3 +Cl and dominant Cr (VI) species HCrO4- and $Cr2O7^{2-}$(Bailar et al. 1973)

PGCP-NH3+Cl- + HCrO4- =PGCP-NH3+...HCrO4- + Cl- (3)

2PGCP-NH3+Cl- + Cr2O7 2- =(PGCP-NH3+)2...Cr2O7 2- + 2Cl- (4)

Below pH < 2.5, Cr(VI) polymerized as Cr3O102- and $Cr4O13^{2-}$ whichexchanged Cl ions from the adsorbent surface with difficulty and resulted in a lower adsorption. The explanation of leastadsorption at higher pH is same as discussed earlier involving role of pHzpc (7.6 for PGCP-NH3 +Cl-) and competition from the OH- ions. Adsorption of Cr(VI) was increasing with increase in adsorbent (composites or individual on moss peat and sawdust carbon) dose due to more active sites (Sharma and Forster, 1993; Raji et al. 1997) who studied the adsorption of Cr(VI), respectively. Due to variation in experimental conditions, comparison among adsorbents doesn't make sense but can provide the fruitful scenario.For example, the high adsorption capacity per gram of hydrotalcite hydrotalcite than that of PGCP-NH3+Cl- was attributed to difference in the ion-exchange behavior (Lazaridis et al. 2001; Lazaridis and Asouhidou, 2003)

Hydrotalcite has two kinds of anion retention sites within the interlayer and onto the external surfaces that affect the uptake capacity.

Rajesh et al. (2011) used Macroporous polymeric Trioctylamine impregnated Amberlite XAD-1180showed the efficient removal of Cr(VI) in acidic condition (predominant polymeric species HCrO4- and $Cr2O7^{-2}$) by ion-pair formation (Cabatingan et al. 2001). Exothermic adsorption ($-\Delta H$ due to ion-pair mechanism). For the recovery of Cr (VI) as sodium chromate, desorption efficiency follows the order: sodium nitrite (75 %) < ascorbic acid (88.6 %) < sodiumsulfite (90 %) < sodiumhydroxide (99.5 %), respectively (Kalidhasan and Rajesh, 2009; Kalidhasan et al. 2010).

Table: Cr(VI) adsorption by PANI , polymer and green based composites

Adsorbent /composites	pH/ Det. method	Brief summary	Mechanism	References
polyaniline/ zeolite nanocomposite (300-600 nm)		Cr(VI) water; Freundlich isotherm.		Shyaa et al. (2015)
short chain polyaniline - jute fiber PANI-jute	3	62.9 mg/g; Cr(VI) (50–500 mg/L); 94% within 40–120 min at 20 ◦C; Wastewater Exothermic adsorption: Regeneration:10 min by 2M NaOH.	electrostatic attraction of acid chromate ion with protonated PANI-jute.	Albino Kumar et al. 2008
PANI/humic acid composite	5.0	671 mg g−1; 150 m / i 120 mi ; pseudo-second-order;Freundlich isotherm		Li et al 2011
PANI/sawdust NC	2.0	0.25 mg/g in 20 min		Esfandian et al. 2012
Polyaniline/cellulose fiber	4.8			Liu et al. 2013
Flake-like PANI/montmorillonite NCs	2.0	168 mg/g in 150 min		Chen et al. 2013
sodiumalginate-polyaniline nanofibers	2	73.34 mg g−1;p do-second-order; Langmuir; Removal of 78.63% of Cr(VI) (100 mg/L) in 60 min at 30 ^{0}C	electrostatic interaction between the Cr(VI) ions and SAP nanofibers;	Karthik,and Meenakshi, 2015
polyacrylamide-grafted sawdust	3	28.8 mg/g; Cr(VI) (100 mg l^{-1}) adsorption: 91.0% at 30°C; exothermic; first-order kinetics Freundlich, regenerated using 0.2 M NaOH and 0.5 M NaCl		Raji and Anirudhan, 1998
Cassia marginata seed gum functionalized with PMMA (5 g/L) microwave irradiation	1	16.94 mg/g; 20 mL of 100 ppm Cr(VI) solution at 30 °C. Langmuir and Freundlich; second order kinetics; rate constant =0.10 × 10^{-5} g/(mg min) at 100 mg/L Cr(VI); resuse: 2 M NaOH		Singh et al. 2008
cellulose–clay composite (87.09 m2/g; 1.8 nm; volume: 0.31 cm3/g) 0.5-0.6 g	3.8-5.5	22.2 mg/g; 99.5%; industrial wastewater, spontaneous adsorption, Langmuir isotherm, second order kinetics.		Kumar A.S.K. et al. 2012
amine-modified polyacrylamide-grafted coconut coir pith	3	99.4% (12.43 mg/g) adsorption of 25.0 mg/L Cr (VI) from aqueous solution and wastewater at 30 °C.		Unnithan et al. (2004)

(PGCP-NH3+Cl-) 2.0 g/L				
polyacrylonitrile/pumice (PAn/Pmc) composite	8	adsorption of Cr3+ (100–500 mg/g) from water: PAn/Pmc(87% removal; capacity: 0.268 mmol/g) composite > Pmc(80%; 0.031) in 6h at room temperature Langmuir models	Mechanism-complexation and sorption;	Yavuz et al. 2008
CTAB-silica gelatin composite	7.5	16.6 mg/g		Venditti et al. 2007
Alumina/alginate (AlAlg) composite	2	17.45 mg/g		Gopalakannan et al. 2016
HDTMA modified montmorillonite clay		7.28		Akar et al. 2009
silver oxide/sawdust nanocomposite (Ag2O/SD NC)	2	13.41 mg/g; Cr (VI) (25 mg/L); water; Thomas model for adsorption kinetics. Regenerated: dil NaOH (0.01 M).		Ostovar et al. (2017)

Based on this theme, the same group (ASK Kumar et al. 2013) prepared Trioctylamine (TOA) impregnated exfoliated graphene oxide (EGO) (adsorption capacity: 232.55 mg/g) for the removal of 96% Cr(VI) in wastewater via electrostatic interaction and H-bonding. In acidic medium, the protonated amine and the HCrO4- show good affinity towards EGO in the form of cation-p and electrostatic interactions with adherence to second order kinetics. The -ΔG, -ΔH and -ΔS showed that adsorption is spontaneous, exothermic along with decreased randomness at the amine-EGO–Cr(VI) (solid-solution) interface. Moreover, Cr(VI) and Cr (III) can be removed by amine modified EGO.

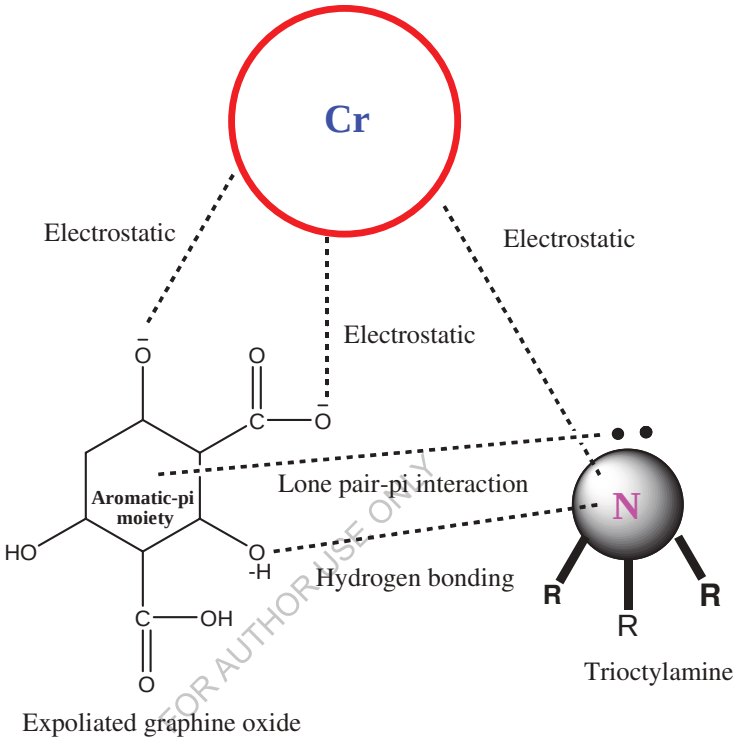

Figure 5: Chromium removal by expoliated graphene oxide

Karthik and Meenakshi (2014) found that cross linked-chitosan–grafted-polyaniline composite (CCGP) was better adsorbent than that of chitosan–grafted-polyaniline(CGP) composite due to intraparticle diffusion pattern. The spontaneous and endothermic adsorption process (pseudo-second-order kinetic) was well described by Freundlich isotherm model for both the composites. The maximum adsorption capacity of CGP and CCGP composite for Cr(VI) ions was 165.6 mg/g and 179.2 mg/g at 303 K. Kumar et al. (2008) observed electrostatic attraction of

acid chromate ion with protonated PANI-jute (short chain polyaniline synthesized on jute fiber) as an adsorbent to remove Cr(VI) (62.9 mg/g within 40–120 min). By ignition of Cr bounded PANI-jute, 94% Cr(VI) were able to recover as Cr(III) along with reduction in weight by 95%.

Lyu et al. (2017) observed external mass transfer along with hybrid sorption-reduction processby biochar supported nanoscale iron sulfide composite (CMC-FeS@biochar composite) for removal of Cr(VI) under acidic conditions. FeS particles adhered on biochar through oxygen-containing functional groups wascame out in enhanced surface area along with relatively higher Cr(VI) uptake (130.5 mg/g) than respective FeS (38.6 mg/g) and biochar (25.4 mg/g). Chen et al. (2011) used magnetic MCM-41 nanosorbents of large surface area (>550 m2 g−1) and high magnetization (≥8.0 emu g−1). Due to high cost of chemicals and production of toxic sludge, use of Cassia marginata seed gum functionalized with poly(methylmethacrylate) using microwave irradiation was preferred for efficient Cr (VI) adsorption (Singh et al. 2008). Kuang et al. (2012) used HPAM–chitosan gel beads for adsorption of Cr(VI)—82.9% and Cr(III)—67.6% from water according to pseudo-second-order rate kinetics. Both Langmuir equations and Freundlich equations were used for explaining the experimental data of adsorption isotherm, which demonstrated a better fit to the Lagmuir model i.e., a monolayer adsorption process onto the gel beads.

Geng et al. (2009) observed both physical adsorption of Cr(VI) onto the chitosan-Fe0 surface and subsequent reduction of Cr(VI) to Cr(III). After the reaction, relative to Cr(VI) and Fe(0), Cr(III) and Fe(III) are the predominant species on the surface of chitosan-Fe0 . Chitosan has also been found to inhibit the formation of Fe(III)–Cr(III) precipitation due to its high efficiency in chelating the Fe(III) ions.

Table 6. Adsorption Capacities of Different Adsorbents for Chromium(VI)

adsorbent	maximum ads. capacity(mg/g)	pH	maximum initial concn (mg/L)	ref
activated carbon (Filtrosorb 400)	125.5	6.0	260.0	Huang and Wu, 1977
sawdust	3.3	6.0	50.0	Srivastava et al. 1986
coconut shell activated carbon	20.0	2.5	-	Alaerts et al. 1989
activated carbon (Filtrosorb 400)	145.0	2.5	1000.0	Sharma and Forster, 1994b
sphagnum moss peat	119.0	1.5	1000.0	Sharma and Forster, 1994b
compost	101.0	1.5	1000.0	Sharma and Forster, 1994b
leaf mould	43.0	2	1000.0	Sharma and Forster, 1994b
sawdust	39.7	2	1000.0	Sharma and Forster, 1994a
sugar beat pulp	17.2	2.0	500.0	Sharma and Forster, 1994a
maize cob	13.8	1.5	300.0	Sharma and Forster, 1994a
sugar cane bagasse	13.4	2.0	500.0	Sharma and Forster, 1994a

coconut husk fibers	29.0	2.1	-	Tan et al. 1993
palm pressed-fibers	15.0	2.0	-	Tan et al. 1993
pinus sylvestris bark activated by 0.05 N NaCl	19.5	4.5	20.0	Alves et al. 1993
leather based activated carbon	241.0	3.0	1000.0	Manuel et al. 1995
Biogas residual slurry	5.87			Namasivayam and Yamuna, 1995
Wool Pine needles	8.66 5.36	2	69.3% adso 42.9%	Dakiky et al. 2002
Eucalyptus bark	45.00			Sarin and Pant, 2006

Liu et al. (2015) used nanoscale zero-valent iron on pumice (P-nZVI) for removal of heavy metals from wastewater from industrial effluents. At the optimum condition, NZVI with a mean

diameter of 20.2 nm was distributed uniformly and consistently on the surface of pumice. Freundlich isotherm suggested the heterogeneous surface of P-NZVI (106.9 mg/g) and removal of Cr (VI) was an endothermic and spontaneous and followed pseudo-first-order kinetic model.

Pumice (Chitosan matrix) is a porous material with large surface area, which can provide more reaction sites for heavy metals thus leading to the removal of heavy metals from wastewater [Candy and Sharma, 1993]. Pumice can be used as an efficient low-cost adsorbent for heavy metals [Yavuz et al. 2008]. Furthermore, pumice particles were effective as a support media infiltration and heterogeneous

catalytic reactions [Farizoglu et al 2003, Rachel et al. 2002]. Iron-coated pumice performed well both in maintaining the long-term hydraulic conductivity and eliminating contaminants [Moraci and Calabrò, 2010].

Altundogan, (2005) observed the hydrolysing product of ferric chloride impregnated-saponified sugar beet pulp (PSFH) most suitable adsorbent for removal of 83.1% Cr(VI) at the final pH of 4.4. Yavuz et al. 2008 carried out the adsorption of Cr3+ (100–500 mg/g) from water onto pumice (Pmc) and polyacrylonitrile/pumice (PAn/Pmc) composite within 6h at room temperature and pH values of 8.0. Adsorption Cr3+ in the solutions was in following order: PAn/Pmc(87% removal; capacity: 0.268 mmol/g) composite > Pmc(80%; 0.031). Effective removal of metal ions was demonstrated at. The mechanism for cations removal by the Pmc and (PAn/Pmc) composite includes complexation and sorption. Al-Othman et al. (2012) studied adsorption, kinetics, equilibrium and thermodynamic of Cr (VI) removal from aqueous medium by activated carbon prepared from peanut shell. Baroni et al. (2008) evaluated batch adsorption of chromium ions on natural and crosslinked chitosan membranes.

Jung et al. (2013) investigated that a positively charged surface under acidic conditions or low pH (pH 4) attracted the predominant Cr(VI) species (i.e.,$HCrO^-_4$) by both physisorption and chemisorption and hence, pseudo second-order fitted models. Adsorption was dependent on surface area, pore size, and surface functional groups while ion exchange and complexation were involved in the Cr(VI) adsorption process, although the most plausible Cr(VI) adsorption mechanism was electrostatic attraction. Protonated functional groups on the carbonaceous adsorbents and amine groups in chitosan were responsible for Cr(VI) electrostatic attraction. Furthermore, the adsorption behavior of chitosan for heavy metal removal is widely known to be attributable to its high hydrophilicity, with

hydroxyl and primary amino groups allowing a high activity and a flexible structure of the polymer chains having suitable configurations for the adsorption of metal ions.

Cr adsorption mechanism:

Cr(VI) mainly can be removed by two mechanisms

Mechanism I

The pH of the aqueous solution influences Cr speciation and the dissociation of active functional groups (–OH, –COOH, –NH2). Therefore, Cr adsorption is critically associated with solution pH that control the adsorption process or adsorption capacity of adsorbent as it affects the surface charge of the adsorbents, the degree of ionization, and the species of adsorbate i.e., Cr(VI) speciation. Cr(VI) exists as CrO4 2−, Cr2O7 2−, HCrO4−, HCr2O7− in aqueous solutions from pH 1 to 8, and $HCrO_4^-$ and $Cr2O7^{2-}$ are the predominant species in acidic media. Chromium uptake in the pH range 2.0–5.0 occurred correspond to bichromate anion and involve the ion exchange, ligand-exchange, ion-pair, electrostatic attaraction (Rajesh et al. 2011) whereas Cr(III) was retained at alkaline pH due to the interaction of the amine with $Cr(OH)_2^+$ and $Cr(OH)^{2+}$ species. The electrostatic attraction in complex reactions of Cr(VI) adsorption could be explained by used hard acid soft base (HSAB) principle where Cr (negatively charged bichromate anion) and nitrogen (positively charged nitrogen) are classified as hard acid and hard base, respectively (Choppin and Morgenstern, 2000). Less adsorption, beyond pH 5.5 or higher pH values, could be attributed to several factors: 1)deprotonation of the surface hydroxyl groups in the biopolymer composite (Hu et al. 2006; A.S.K. Kumar et al. 2012); 2) competition of the hydroxide anion OH− with the bichromate anion for the effective adsorption sites (the end-pH was lower than the

initial pH) (Wu et al. 2007; Rajesh et al. 2011;Zimmermann et al. 2010) 3) The pHpzc that determined the range of pH sensibility and allows the surface active and adsorption capacities to be predicted [Pintor et al., 2013]. At pH> pHzpc, the net surface charge becomes negative, resulting in repulsive forces between composite and Cr(VI) (Bohli et al. 2015; Doke and Yadav, 2014;Zubair et al 2008 Bayramoglu and Arica, 2008; Demiral et al. 2008).

At low pH, the functional groups in the surface of the bio material are protonated and restrict the approach of cationic species as the result of repulsive forces. As the pH increases, the degree of protonation decreases, and the functional groups become negatively charged (pH > pKa).

Table 7: Cr(VI) adsorption by Iron based composites

Adsorbent /composites	pH/ Det. method	Brief summary	Mechanism	References
nanoscale Fe^0 on pumice (P-nZVI)	-	106.9 mg/g; industrial wastewater; Adsorption: endothermic and spontaneous Freundlich isotherm and pseudo-first-order kinetic	-	Liu et al.2015
bio-functional magnetic beads (Rhizopus cohnii - Fe3O4)	1	6.73 mg/g; Cr (40 mg/l) ;Wastewater; 28 °C; regenerated (0.1 M NaOH) and reusable (n=5)	-	Li, et al. 2008
nano Fe^0 - waste rock wool (RW) ARW: acid treated RW	2	197.69 mg/g; Removal efficiency within 1 h: ARW/ZVI composites (1:2 w/w) 100%> ZVI (73%)> ARW (55%)>waste RW (~3%).	electrostatic attraction and the reduction of Cr (VI) to Cr(III)	Zhou et al. (2018)
magnetic hydrogels		76.87 mg/g; Cr(III) Langmuir and Freundlich adsorption isotherms	-	Ozay et al. 2009
iron(III) complex of a carboxylated polyacrylamidegrafted	2-3	144.20 mg/g at 20 °C to 172.74 mg/g at 60 °C; >99.0% removal of 25.0 mg/L	-	Unnithan and Anirudhan,

sawdust		;second-order kinetic model;Langmuir and Freundlich equations Reuse: 0.1 M NaOH		2001
iron (III) hydroxideloaded sugar beet pulp	4.4	5.1 mg/g; 83.1% removal of 10 mg /1of Cr(VI) in 120 min at 25 ºC; Water;	-	Altundogan, 2005
biocomposite (iron nanoparticles embedded in orange peel pith)	1	10 mg/Lof Cr(VI) adsorption: 71% with biocomposite (5.37 mg/g) > 34% biomass (1.90 mg/g)from industrial wastewater within 60 min.	reduction of Cr(VI) to Cr(III) by Fe or Fe(II) and adsorption of the Cr(III).	López-Téllez et al., 2011
bamboo charcoal-iron (Fe–BC) Microwave-assisted preparation	5	33.1 mg/g; 25 ºC; Langmuir model, pseudo-second-order; adsorption of Cr(VI) from water onto Fe–BC was spontaneous and exothermic. 0.12 mg/L of Cr(VI) reduced to to below 0.05 mg/L in 2 min regenerated by dilute NaOH	-	Wang et al. 2011
green nanocomposite (ZVI-PAC) Fe0-powdered activated carbon 60 nm; 107 m2/g	2	53.48 mg/g ; Cr(VI) removal; adsorption: endothermic, spontaneous, Langmuir model and Ho pseudo-second order model. adsorption mechanisms: intraparticle	-	Khosravi et al. (2018)

		diffusion and film diffusion		
biochar supported nanoscale iron sulfide composite CMC-FeS@BC (1;1;1) low-cost, ‘‘green”, and effective sorbent	5.5	Cr(VI) from aqueous solutions; enhanced adsorption capacity:130.5 mg/g > 38.6 mg/g for FeS and 25.4 mg/g for biochar; 57% reduction and 43% was sorption;Redlich-Peterson model.	-	Lyu et al. 2017
agarose-Fe nanoparticles hydrogel (green synthesis)	-	84.9% of Cr(VI); Chemical reduction 24 h; Fe(III)–Cr(III) complexes might be formed after reaction	-	Luo et al. 2016

Mechanism II

Nowadays, the "adsorption-coupled reduction" reaction (reduction of Cr(VI) to Cr(III) occurs after Cr(VI) is adsorbed) is widely accepted as the true mechanism of Cr(VI) adsorption by natural biomaterials under acidic conditions because of its high redox potential. Park et al. 2011, reported that Cr(VI) could be removed from solution by natural biomaterial through both direct and indirect reduction mechanisms:

i) Direct reduction mechanism: The reduction of Cr(VI) to Cr(III) occurs in the aqueous phase by contact with the electron-donor groups of the biomaterial that have lower reduction potential values than that of Cr(VI). Cr(III) ions remain in the aqueous solution or form complexes with the Cr-binding groups present in the biomaterial.

(ii) Indirect reduction mechanism consists in 3 steps: (a) binding of anionic Cr(VI) to the positively charged groups in the biomaterial surface such as amino and carboxyl groups, (b) reduction of Cr(VI) to Cr(III) by adjacent electron-donor groups and (c) release of Cr(III) into aqueous phase due to repulsion between positively charged Cr(III) and positively charged groups in the biomaterial surface, or complexation of Cr(III) with adjacent groups. Amino and carboxyl groups take part in step (a) of indirect reduction.

For adsorption of Cr(VI) ions by nanocomposites, mostly Langmuir and Freundlich isotherm have been investigated. The Langmuir model assumes homogeneous adsorption/active sites, whereas the Freundlich model takes into account heterogeneity in sites. Chitosan -Alginate nanocomposites (Gokila et al., 2017) and PGCP-NH3+Cl- (Unnithan et al. 2004) followed Freundlich model. Fe–crosslinked chitosan complex (Ch–Fe) (Zimmermann et al. 2010), Trialkylamine impregnated macroporous polymeric sorbent (Rajesh et al. 2011) followed Langmuir. Adsorption process by mesoporous cellulose– montmorillonite clay composite

(adsorption capacity of 22.2 mg/g) was spontaneous, in accordance with Langmuir isotherm model (A.S.K. Kumar et al. 2012). The model of Langmuir isotherm could be better used to fit the sorption process of bio-functional magnetic beads for removal of Cr(VI) (Li et al. 2008)., biocomposite of iron nanoparticles embedded in orange peel pith (López-Téllez et al., 2011), ceramic alumina-chitosan (Boddu et al. 2003).

Cr(VI) adsorbed onto the TOA–EGO adsorbent followed second order model as the t/Xt versus t plot (Fig. 10B) in the gave a nice fit to the experimental data in terms of the higher regression coefficient (Table 3). It was also observed that the Xe (calculated 24.72 mg/g) and the Xe (experimental 25.12 mg/g) values were in accordance with the second order kinetics. The adsorption of hexavalent chromium onto the TOA–EGO adsorbent could involve pore, surface or intraparticle diffusion [57]. The Weber–Morris [58] plot for this adsorbent–adsorbate system yields a straight line with a finite intercept. This feature could be attributed to the boundary layer mechanism for elucidating the kinetics of adsorption of Cr(VI) onto the TOA–EGO adsorbent. Adsorption of Cr(VI) on Ch-Fe follows pseudo-second order kinetics indicates chemisorption as the rate controlling step involving a sharing or exchange of electrons between the adsorbate and the adsorbent [30]. The suitability of the second order rate equation was reported in the literature for the removal of chromium for the adsorbents: active carbon from olive bagasse, magnetic beads, waste biomass and thermally activated weed. On the other hand, the results found in this work are different from those reported by Fagundes et al. 1998, for adsorption of As(V) by Ch-Fe.Pseudo-second-order kinetic model (Temp and conc dependent) was shown by PGCP-NH3+Cl- (Unnithan et al. 2004). Fe–crosslinked chitosan complex (Ch–Fe) (Zimmermann et al. 2010), Trialkylamine impregnated macroporous polymeric sorbent (Rajesh et al. 2011), mesoporous cellulose– montmorillonite clay composite

(A.S.K. Kumar et al. 2012) and Chitosan -Alginate nanocomposites (Gokila et al., 2017). While bio-functional magnetic beads for removal of Cr(VI), followed Lagergren (first order) (Li et al. 2008).

Zimmerman et al. (2010) found that adsorption of Cr(VI) with Ch-Fe is exothermic (ΔH◦: −499 kJ/mol), and spontaneous (ΔG°:−12.3 kJ/mol, −10.8 kJ/mol and −10.6 kJ/mol to 298 K, 308K and 328 K, respectively).Hence, the amount adsorbed at equilibrium must decrease with increasing temperature, because ΔG◦ decreases with increasing temperature of the solution. Similar results from ΔG◦ to ΔH◦ have been reported for Cr(VI) adsorption by iron (III) hydroxide-loaded sugar beet pulp Altungodan [2005]. The negative value _S◦ (−1.69 kJ/mol K) of Cr(VI) adsorption corresponds to a decrease in randomness at the solid/liquid interface during the adsorption of Cr(VI) on Ch-Fe. The results are in agreement with those reported by Zubair et al. [2008] for adsorption of Cr(VI) by waste biomass.

The spontaneity of the TOA–EGO–Cr interaction is reflected in the negative ΔG^0 (ΔG^0 = -RT lnK) values obtained at different temperatures.The free energy of adsorption essentially depends on the TOA–EGO as well as Cr(VI)-amine/EGO interactions. The negative ΔS^0 obtained from the Van't Hoff plot shows that there is more orderliness in the interaction between the tertiary amine and exfoliated graphene oxide. The overall adsorption process is exothermic. The negative entropy of adsorption that indicates the decreased randomness also depends on the $\Delta S_{TOA–EGO}$ and $\Delta S_{Cr–TOA–EGO}$interactions. This feature could be ascribed to the fact that entropy being a state function and an extensive property, the total ΔSads would depend on the sum of the above interactions.

Hence, $\Delta G_{adsorption} = \Delta H_{adsorption} — T (\Delta S_{Cr–TOA–EGO} + \Delta H_{Cr–TOA–EGO})$.

The lone pair-π, cation-π (R3NH+…..aromatic moiety) and the electrostatic ($HCrO^-_4$.....NH^+R_3) interactions are responsible for the compactness [59] and decrease in randomness at the solid-solution interface. The long chain protonated amine orients itself with the alkyl groups pointed away thereby facilitating the head group(NH+) to interact electrostatically with hexavalent chromium oxyanion

7. Utilization of green synthesized nanomaterials in remediation for environment

Nanomaterials generated via green route are cheap. Green synthesized nanoparticles acted same as other nanomaterials but showed enhanced efficiency due to introduction of phytoconstituents in crystal lattice. Currently, a lot of researchers worldwide are working on synthesis of nanoparticles using by employing sunlight, or plant-based surfactants or microorganisms and water or combination of those. For example, silver nanoparticles were biosynthesized extracellularly by bacteria *Bacillus cereus* with high activity against bacteria (Prakash et al., 2011). Shukla & Iravani (2017) reviewed green strategies for the preparation of metallic nanoparticles applied for water purification. The use of enzymes, vitamins, monosaccharides, polysaccharides and biodegradable polymers including microwave-assisted synthesis were discussed in detail. These biosynthesis methods are economical and eco-friendly, thus, can be used on large-scale. Application of these bioactive nanoparticles in the degradation of harmful PAHs will help in reconstructing the polluted environment. Green process not only control the morphology but are also efficient than chemically synthesized nanoparticles.Biosynthesized nanoparticles ZnO, copper oxide and ZnO/Graphene oxide showed good photocatalytic potential for anthracene and dyes [49-50]. Fardood and co-workers synthesiszed a number of nanomaterials (oxides of Zn, Cu and Ni; ferrites of Ni–Cu–Mg,

Ni-Cu-Zn and magnetic copper) via green routes employing gel, gum or plants and evaluated them as catalyst for organic synthesis as well as photocatalyst for remediation of organic pollutants. Superparamagnetic magnesium ferrite and $MgFe_2O_4$@γ–Al_2O_3 nanoparticles were prepared for degradation of reactive blue 21 and other organic dyes, respectively. Shanker and his research group fabricated nanomaterials of double metal cyanides, ferrates and metal oxides by use of sunlight, Sapindus mucrossi and A. marmelos forcatalytic oxidation of organic wastes (phenols, dyes, amines, PAHs). Lots of work have been done on estimation of photocatalytic activities of green (tea or starch) fabricated iron based nanoparticles. Green synthesized bimetallic Fe/Pd nanoparticles were better than Fe alone. Compared to constituents, doped Fe_2O_3@ZnHCF nanocubes prepared from *Azadirachta indica* were showedenhanced photocatalytic degradation of chrysene [Rachna et al. 2018]. Plant extract of*A. indica is (*locally found tree in India) would be prepared after crushing leaves with continued addition of deionized water. Ag-Cr-AC nanocomposites (pHpzc: 6.29) synthesisized via green route employing A. indica can be efficiently employed to remove the coloured effluent (64.92% to 82.47%) from aqueous media by ultrasonicated assisted adsorption process (Saad et al. 2017). Spontaneous adsorption obeyed Harkins-Jura model at temperature of 40 °C. Shahwan et al. ,observed that green tea-iron iron nanoparticles were a better catalyst than Fe nanoparticles produced by borohydride reduction.

Xing et al. (2018) developed a green nanocomposite of filter paper decorated with polyethylene glycol and polypyrrole to (FP/PEG/PPy) and found high adsorption capacity for Cr(VI). Moreover, it could be regenerated by electro-assisted or photo-assisted regeneration to reduce eluent use. Green syntheized magnetically separable g-Fe3O4/RGO nanocomposite (hydrothermal synthesis involving Averrhoa carambola leaf

extract) was showed potential reduction (97%) of Cr(VI) at room temperature (Padhi et al. 2017). The higher activity (including better antimicrobial activity) of g-Fe3O4/2RGO was attributed to the in situ loading of RGO, and the synergism developed between RGO and the super magnetic Fe3O4 nanoparticle. A. carambola played a major role in the modification of structural, optical, and electronic properties of the Fe3O4 nanoparticle.Li et al. (2017) carried out "Sol-Gel-like"condensation of dopamine (DA) and aminosilane coupling agents for fabrication of multifunctional magnetic hollow composites (Fe3O4@A/PDA). They concluded that process is green via post-grafting pathways that can avoid using organic solvents and high-temperature treatment. Magnetically separable Fe3O4@A/PDA exhibited the highest adsorption capacity (284.1 mg/g at 298 K and pH 2.0) for Cr(VI) removal (more than 70% even after five cycles). Adsorption was spontaneous and endothermic following pseudo-second-order and Langmuir model. Electrostatic attraction and reduction reaction could be used to explain the adsorption mechanism.

Cruz et al. (2017) carried out green synthesis of a magnetic hybrid adsorbent (CoFe2O4/NOM) using water rich in natural organic matter; for removal of chromium from industrial effluent. The hybrid obtained at ambient temperature (HbAmb) was calcined at 200, 400, and 800◦C for 2 h, and formation of thecobalt ferrite phase was confirmed by XRD, which indicated the presence of NOM in the structure of thematerial. Removal tests showed that HbAmb provided efficient removal of chromium at the natural pH ofthe effluent, while the other materials were effective at pH 6. Evaluation of the kinetics showed excellentperformance of the process, with 70–87% removal in 20 min, which provided a high degree of flexibility.The hybrid showed high removal during five reuse cycles, ranging from 96% in the first cycle to 82% in thefinal. The matrices containing the saturated adsorbent (HbAmb Sat) and recovered chromium

ions (CrD)showed high performance in the catalytic reduction of 4-nitrophenol, with conversion rates of 99.9% inshort periods of time, as well as excellent potential for reuse in three cycles. The results demonstrated thatthe production of a technological material and its use for remediation could be achieved in an ecologicallysustainable manner.

Dinari et al. (2018) carried out ultrasound-assisted synthesis of nanocomposites based on aromatic polyamide and surface modified ZnO nanoparticle with s-triazine heterocyclic ring for removal of toxic Cr(VI) from water. The surface of ZnO nanoparticle was modified by s-triazine core silane coupling agent (ZnOTSC) and PA/ZnO-TSC NCs with different amount of ZnO-TSC nanoparticles (0, 5, 10 and 15 wt%) were prepared by ultrasonic irradiation. The synthesized PA/ZnO-TSC NCs were characterized by FT-IR, XRD, FE-SEM, TEM and TGA methods. TEM images showed that ZnO nanoparticles were dispersed homogeneously in the polymer matrix. The adsorption experiments were carried out in batch mode to optimize various parameters like contact time, pH and concentration of metal ion that influence the adsorption rate. The maximum uptakes of Cr (VI) at pH 4.0 was 72%, 81%, 89% and 91% for pure PA, NC5%, NC10% and NC15%, respectively. The kinetic of adsorption was investigated and the pseudo second-order model is an appropriate model for interpretation of adsorption mechanism of Cr(VI) ions.

Liu et al., (2018) presents a novel sandwiched nanocomposite synthesized using graphene oxide (GO), manganese dioxide (MnO2) nanowires, iron oxide (Fe3O4) nanoparticles and polypyrrole (PPy) to remove hexavalent chromium ion Cr(VI) from water by an adsorption–reduction mechanism.In the sandwiched nanocomposites, GO provided enough surface area, functional groups, and hydrophilic surface for efficient absorption. Fe3O4 nanoparticles with excellent magnetic properties make it easy to separate

and recover from water. Under acidic conditions, MnO2 nanowires act as both template and oxidant to initiate the polymerization of pyrrole monomers on its freshly activated surface to obtain GO/MnO2/Fe3O4/PPy (designated as GMFP) nanocomposite. GMFP could effectively adsorb Cr(VI) through electrostatic attraction, and the adsorbed Cr(VI) ions were partly reduced to trivalent chromium Cr(III) (62%), resulting in the efficient adsorption and high removal of Cr(VI) from water. Hexavalent chromium adsorption by GMFP is strongly pH dependent and the adsorption kinetics followed the pseudo-second-order model. The Langmuir isothermal model described the adsorption isotherm data well and the maximum adsorption capacity was up to 374.53 mg g−1 at pH 2.0. These experimental results suggested that GMFP had great potential as an economic and efficient adsorbent of hexavalent chromium from wastewater, which has huge application potential.

Conclusions

Hazardous heavy metal pollution of wastewater is one of the most important environmental problems throughout the world. To meet the increased more and more stringent environmental regulations, a wide range of treatment technologies such as chemical precipitation, coagulation-flocculation, flotation, ion-exchange and membrane filtration, have been developed for heavy metal removal from wastewater. It is evident from the literature that ion-exchange, adsorption and membrane filtration are the most frequently studied for the treatment of heavy metal wastewater. Ion-exchange processes have been widely used to remove metals from wastewater. Adsorption by low-cost adsorbents and biosorbents is recognized as an effective andeconomic method for low concentration heavy metal wastewater treatment as an alternative AC. Membrane filtration technology can remove heavy metal ions with high efficiency.

There is lack of few reports on removal of Cr by green nano-biocomposites. Most of the studies are confined to microorganisms mediated degradation. Such methodologies need more time for complete metabolism from several days to month and are also very expensive, consequently, cannot be employed at industrial scale. The limited research facilitates the need for exploring new pathways, especially the use of nanomaterials as they have a unique property of high surface-to-volume ratio, which makes them excellent adsorbents. Moreover, green synthesized nanoparticles have been showing potential role in making environment green. Nanoadsorbents like TiO_2 or ZnO as such or doped are playing an excellent role in complete mineralization of PAHs than microorganisms in a time as short as few minutes (Figure 15). Furthermore, these advanced nanomaterials are observed to be highly potential candidates as revealed by either absence of toxic by-products or transient metabolites which get quickly mineralized into non-toxic smaller by-products. Photooxidation mechanisms of PAHs could be operated by singlet oxygen mechanism or radical chain mechanism (Calvert et al. 2002;) (Figure 16).

Use of nanoparticles for the degradation of high molecular weight PAHs like Dibenzo (*a,h*) anthracene, Indeno (1,2,3-*cd*) pyrene, Benzo (*g,h,i*) perylene, Benzo (*k*) fluoranthene is still awaited. Due to high aromaticity, these compounds are very stable and do no undergo biodegradation. Hence, must be degraded using effective nanoadsorbents due to their long half-lives from days to years and high persistence in nature.

9. Future Scope

This chapter covered the encouragingperformances of a variety of green nanomaterials and nanocomposites as adsorbentand heterogeneous redox catalyst for the effective removal of toxic and bioaccumulating Cr. The Cr(VI), appear to be one of the major heavy metal pollutants globally in

this century. Cr(VI), derived from industrial wastewater, is highly toxic and present a serious threat to human health and environment.Comparisons of different techniques are very difficult because of inconsistencies in the data presentation. Cr(VI) removal was evaluated at different conditions, such as pH, initial chromium concentration, temperature, ratios. Various chromium-contaminated water such as ground water, drinking water, tannery wastewater, electroplating wastewater, and synthetic industrial wastewater were used.Adsorption/biosorption is found best in terms of economy and efficiency. Extensively used green and commercial adsorbents is associated with several drawbacks like high cost, long time requirements, difficulty in handling and selectivity along with difficult to separate. Activated carbons with less adsorption capacity are expensive and difficult to regenerate. Chitosan is a good adsorbent for Cr(VI) because of high its hydrophilicity, large number of primary amino groups and flexible structure of polymer chain. Being inexpensive, facile synthesis, non-toxic in nature, and of high efficiency, green nanocomposites based on biomass and biopolymer including chitosan, iron and PANI have proven to be effective adsorbents in removing completely in short period of few minutes to hours .They not only adsorb the toxic Cr (VI), but also transform them into into less hazardous forms Cr (III) in an eco-friendly manner with minimum requirement of energy, time and cost. Synthetic nanocomposites worked on base of reduction and adsorption.

References:

Abdulrasaq, O.O. and Basiru, O.G. (2010) Removal of copper(II), iron(III) and lead(II)ions from mono-component simulated waste effluent by adsorption oncoconut husk. Afr. J. Environ. Sci. Technol. 4 (6), 382–3

Acharyaa, J., Sahub, J.N., Sahoob, B.K., Mohantyc, C.R., Meikap, B.C. (2009) Removal of chromium(VI) from wastewater by activated carbon developed from Tamarind wood activated with zinc chloride, Chem Eng J 150, 25–39

Agarwal, S. and Singh, N.B. (2014) Zinc ferrite–PVA nanocomposite and removal of chromium from aqueous solution, *Emerging Mater Res* 3 (5) 222-229

Agoubordea, L., Navia, R. (2009) Heavy metals retention capacity of a non-conventional sorbent developed from a mixture of industrial and agricultural wastes, *J. Hazard. Mater.* 167, 536-544.

Ahmad, M.J., Thyodan S.K. (2013) Microwave assisted preparation of microporous activated carbons from Siris seeds pods for adsorption of metronidazole antibiotic, Chem. Eng. J. 214, 310-318.

Ajjabi, L.C. and Chouba, L. (2009) Biosorption of Cu2+ and Zn2+ from Aqueous Solutions by Dried Marine Green Macroalga Chaetomorpha linum, *J Environ Manage* 90(11):3485-3489.

Aksu, Z. and Balibek, E. (2007) Chromium(VI) biosorption by dried Rhizopus arrhizus: effect of salt (NaCl) concentration on equilibrium and kinetic parameters, *J. Hazard. Mater.*145, 210-220.

Al-Jlil, S.A. and Alsewailem, F.D. (2009) Saudi Arabian clays for lead removal in wastewater, *Appl Clay Sci* 42, 671–674.

Al-Othman, Z.A., Ali, R., and Naushad, M. (2012) Hexavalent chromium removal from aqueous medium by activated carbon prepared from peanut shell: adsorption kinetics, equilibrium and thermodynamic studies, Chem. Eng. J. 184, 238–247.

AlperIsoglu, Z.A.I. (2005) Removal of copper(II) ions from aqueous solution bybiosorption onto agricultural waste sugar beet pulp. *Process Biochem.* 40 (9), 3031–3044.

Altundogan, H.S (2005) Cr(VI) removal from aqueous solution by iron (III) hydroxideloaded sugar beet pulp, *Process Biochem.* 40, 1443–1452.

Aman, T., Kazi, A.A., Sabri, M.U. and Bano, Q. (2008) Potato peels as solid waste for the removal of heavy metal copper(II) from waste water/industrial effluent. Colloid Surf 63:116–121

Amini, M., Younesi, H., Bahramifar, N. (2009) Statistical modeling and optimization of the cadmium biosorption process in an aqueous solution using Aspergillus niger, *Colloid Surf.* 337, 67e73

Apiratikul, R. and Pavasant, P. (2008) Sorption of Cu2+, Cd2+, and Pb2+ using modified zeolite from coal fly ash, *Chem Eng J* 144, 245–258.

Apiratikul, R., and Pavasant, P. (2008b) Batch and column studies of biosorption of heavy metals by Caulerpa lentillifera, *Bioresour. Technol.* 99, 2766-2777.

Arulkumara, M., Thirumalaia, K., Sathish kumar, P., Palvannan, T. Rapid removal of chromium from aqueous solution using novel prawn shell activated carbon, Chem Eng J 185–186, 178-186

Aydın, Y.A. and Aksoy, N.D. (2009) Adsorption of chromium on chitosan: optimization, kinetics and thermodynamics, *Chem. Eng. J.* 151, 188–194.

Babu, B V., Gupta, S. (2008) Removal of Cr(VI) from wastewater using activated tamarind seeds as an adsorbent, J. Environ Eng. Sci. 7(5), 553-557.

Bahadir, T., Bakan, G., Altas, L. and Buyukgungor, H. (2007) The investigation of lead removal by biosorption: an application at storage battery industry wastewaters, *Enzym. Micro. Technol.* 41, 98-102.

Baig, U., Rao, R.A.K., Khan, A.A., Sanagi, M.M., Gondal, M.A. (2015) Removal of carcinogenic hexavalent chromium from aqueous solutions using newly synthesized and characterized polypyrrole–titanium(IV)phosphate nanocomposite, *Chem Eng J* 280, 494–504.

Barakat, M.A. (2011) New trends in removing heavy metals from industrial wastewater, *Arabian J. Chem.* 4, 361–377.

Barakat, M.A. (2011) New trends in removing heavy metals from industrial wastewater, Arab. J. Chem. 4 361–377.

Baral, R.D. Engelken, Chromium-based regulations and greening in metal finishing industries in the USA, Environ. Sci. Policy 5 (2002) 121–133.

Baran A1, Biçak E, Baysal SH, Onal S. (2007) Comparative studies on the adsorption of Cr(VI) ions on to various sorbents, *Bioresour Technol.* 98(3), 661-665.

Baroni, P., Vieira, R.S., Meneghetti, E., da Silva, M.G.C., Beppu, M.M. (2008) Evaluation of batch adsorption of chromium ions on natural and crosslinked chitosan membranes, J. Hazard.Mater. 152, 1155–1163

Barquist, K., Larsen, S.C. (2010) Microporous mesoporous mater 130, 197

Bayramoglu, G. and Arıca, M.Y. (2008) Removal of heavy mercury(II), cadmium(II) and zinc(II) metal ions by live and heat inactivated Lentinus edodes pellets, *Chem. Eng. J*. 143, 133-140.

Bayramoglu, G. and Arica, M.Y., (2008) Adsorption of Cr (VI) onto PEI immobilized acrylatebased magnetic beads: isotherms, kinetics and thermodynamics study, Chem. Eng. J. 139, 20–28.

Betancur, M., Bonelli, P.R., Vela´squez, J.A. and Cukierman, A.L. (2009) Potentiality of lignin from the kraft pulping process for removal of trace nickel from wastewater: effect of demineralization, *Bioresour Technol* 100, 1130–1137.

Bhattacharyya, K.G. and Gupta, S.S. (2008) Adsorption of a few heavy metals on natural and modified kaolinite and montmorillonite: a review.*Adv Colloid Interface Sci.* 140(2), 114-131.

Bikshapathi, M., Singh, S., Bhaduri, B., Mathur, G.N., Sharma, A., and Verma, N. (2012) Fe nanoparticles dispersed carbon micro and nanofibers: surfactant-mediated preparation and application to the removal of gaseous VOCs, *Colloids Surf., A* 399, 46–55.

Boddu, V.M., Abburi, K. Talbott, J.L. Smith, E.D. (2003) Removal of hexavalent chromium from wastewater using a new composite chitosan biosorbent, *Environ. Sci. Technol.* 37, 4449–4456.

Chen, C. and Wang, J.L. (2008) Removal of Pb2+, Ag+, Cs+ and Sr2+ from aqueous solution by brewery's waste biomass, *J. Hazard. Mater.* 151, 65-70.

Chen, J.H., Xing, H.T. Guo, H.X. Weng, W., Hu, S.R. Li, S.X. Huang, Y.H. Sun, X., and Su, Z.B. (2014) Investigation on the adsorption properties of Cr(VI) ions on a novel grapheme oxide (GO) based composite adsorbent, J. Mater. Chem. A 2, 12561–12570.

Chen, S.X. and Zeng, H.M. (2003) Improvement of the reduction capacity of activated carbon fiber, Carbon 41, 1265–1271.

Chen, X., Lam, K.F., and Yeung, K.L.(2011) Selective removal of chromium from different aqueous systems using magnetic MCM-41 nanosorbents, Chem Eng J 172, 728– 734.

Cheng, A., Lin, W.T. Huang, R. (2011) Application of rock wool waste in cement-based composites, Mater. Des. 32, 636–642.

Chromium, investigating news, Amanda Kay - March 26th, 2018; 4 Countries With the World's Highest Chromium Production,https://investingnews.com/daily/resource-investing/industrial-metals-investing/chromium-investing/top-chromium-producers/

Cojocaru, C., Diaconu, M., Cretescu, I., Savic, J., Vasic, V. (2009) Biosorption of copper (II) ions from aqua solutions using dried yeast biomass, *Colloid Surf.* 335, 181-188

Costa, M. (2003) Potential hazards of hexavalent chromate in our drinking water, *Toxicol. Appl. Pharm.* 188, 1–5.

Cunha, C., Panseri, S., Iannazzo, D., Piperno, A., Pistone, A., Fazio, M., Russo, A., Marcacci, M. and Galvagno, S. (2012) Hybrid composites made of multiwalled carbon nanotubes functionalized with Fe3O4 nanoparticles for tissue engineering applications, Nanotechnology 23, 465102.

De Flora, S. (2000) Threshold mechanisms and site specificity in chromium(VI) carcinogenesis, *Carcinogenesis* 21 533–541.

Demiral, H., Demiral, I., Tumsek, F., Karabacakoglu, B. (2008) Adsorption of chromium (VI) from aqueous solution by activated carbon derived from olive bagasse and applicability of different adsorption models, Chem. Eng. J. 144, 188–196.

Demirbas, Ö., Karadaˇg, A., Alkan, M., Doˇgan, M., 2008. Removal of copper ions fromaqueous solutions by hazelnut shell. J. Hazard. Mater. 153, 677–684.

Deng, S., and Bai, R. (2004) Removal of trivalent and hexavalent chromium with aminated polyacrylonitrile fibers: performance and mechanisms, Water Res. 38, 2424–2432.

Doke, S.M., and Yadav, G.D. (2014) Novelties of combustion synthesized titania ultrafiltration membrane in efficient removal of methylene blue dye from aqueous effluent, Chemosphere, 117, 760-765

Dossing, L.N., Dideriksen, K. Stipp, S.L.S. Frei, R. (2011) Reduction of hexavalent chromium by ferrous iron: a process of chromium isotope fractionation and its relevance to natural environments.

Dreyer, D.R., Park, S., Bielawski, C.W., and Ruoff, R.S. (2010) The chemistry of grapheme oxide, *Chem. Soc. Rev.* 39, 228–240.

Duranoglu, D., Trochimczuk, A.W., Beker, U. (2012) Kinetics and thermodynamics of hexavalent chromium adsorption onto activated carbon derived from acrylonitrile–divinylbenzene copolymer, *Chem. Eng. J.* 187, 193–202.

El-Sikaily, A., Nemr, A.E., Khaled, A., Abdelwehab, O. (2007) Removal of toxic chromium from wastewater using green alga Ulva lactuca and its activated carbon, *J. Hazard. Mater.* 148, 216-228

EPA (1990) Environmental pollution control alternatives.E.P. Agency, Cincinnati, US.

Foo, K.Y., Hameed, B.H. (2012) Preparation of activated carbon by microwave heating of lang sat (Lansium Domesticum) empty fruit bench waste, Bioresour. Technol., 116, 522-525.

Fu, F. and Wang, Q. (2011) Removal of heavy metal ions from wastewaters: a review, *J. Environ. Manage.* 92, 407–418.

Fu, R.W., Lu, Y., Xie, W., Zeng, H.M. (1998) The adsorption and reduction of Pt (IV) on activated carbon fibre, Carbon 36, 19–23.

Fu, R.W., Zeng, H.M. and Lu, Y. (1995) The reduction of Pt(IV) with activated carbon fibers –an XPS study, Carbon 33, 657–661.

Fukai, R. (1967) Valency state of chromium in seawater, Nature volume 213, page 901 (04 March).

G. Zelmanov, R. Semiat, Iron (Fe^{3+}) oxide/hydroxide nanoparticles-based agglomerates suspension as adsorbent for chromium (Cr6+) removal from water and recovery, *Sep. Purif. Technol.* 80 (2011) 330–337.

Gabr, R.M., Hassan, S.H.A. and Shoreit, A.A.M. (2008) Biosorption of lead and nickel by living and non-living cells of Pseudomonas aeruginosa ASU 6a. *Int. Biodeterior. Biodegradation* 62, 195-203

Galera, M.M, Cho, E., Tuuguu, E., Park, S.J., Farnazo, D.M., Jee, C., Yoo, N.J. and Chung, W.J. (2007) Removal of NH3, H2S and toluene by biofilters packed with rock woolcompost media, *J. Ind. Eng. Chem.* 13, 895–902.

Garg, V.K., Gupta, R., and Gupta, R.K. (2004) Adsorption of chromium from aqueous solution on treated sawdust, *Bioresour. Technol.* 92 79–81.

Gillham, R.W., O'Hannesin, S.F. (1994) Enhanced degradation of halogenated aliphatics by zero-valent iron, *Ground Water* 32(6):958–967

Gokila, S., Gomathia, T., Sudha, P.N., Anil, S. (2017) Removal of the heavy metal ion chromiuim(VI) using Chitosan and Alginate nanocomposites, Int J Biolog Macromolecules 104, 1459–1468.

Goldstein, G. (1993) Evidence that lead acts as a calcium substitute in second messenger metabolism, *Neurotoxicol* 14:97-102

Gollavelli, G., Chang, C.C., Ling, Y.C. (2013) Facile synthesis of smart magnetic grapheme for safe drinking water: heavy metal removal and disinfection control, ACS Sustain. *Chem. Eng.* 5, 462–472.

Greenwood, N.N., Earnshaw, A. (1997) Chemistry of the Elements (2nd ed.). Butterworth-Heinemann.ISBN 0-08-037941-9. Figure 8.19 Ellingham diagram for the free energy of formation of metallic oxides, p. 308.

Gu, H., Rapole, S.B. Sharma, J. Huang, Y. Cao, D., Colorado, H.A. Luo, Z., Haldolaarachchige, N., Young, D.P., Walters, B. Wei, S. Guo, Z. (2012) Magnetic polyaniline nanocomposites toward toxic hexavalent chromium removal, RSC Adv. 2 11007–11018.

Gu, X.Y. and Evans, L.J. (2008) Surface complexation modelling of Cd(II), Cu(II), Ni(II), Pb(II) and Zn(II) adsorption onto kaolinite, *Geochim Cosmochim Acta* 72, 267–276

Gupta, S. and Babu, B.V. (2009) Utilization of waste product (tamarind seeds) for the removal of Cr(VI) from aqueous solutions: equilibrium, kinetics, and regeneration studies, *J Environ Manag* 90, 3013–3022.

Gupta, V. K., Pathania, D., Sharma, S., Singh, P. (2013) Preparation of bio-based porous carbon by microwave assisted phosphoric acid activation and its use for adsorption of Cr(VI), *J. Colloid Interface Sci.* 401, 125–132.

Gupta, V.K., Agarwal, S., Saleh, T.A. (2011) Chromium removal by combining the magnetic properties of iron oxide with adsorption properties of carbon nanotubes, *Water Res*. 45, 2207–2212.

Habib, A., Islam, N., Islam, A., Alam, A.M.S., 2007. Removal of copper from aqueoussolution using orange peel sawdust and bagasse.*Pak. J. Anal. Environ. Chem.* 8(1,2), 21–25.

Hamad, H. A. Abd El-latif, M. M..Kashyout, A. B Sadik, W. A. and Feteh, M. Y. (2015) Influence of calcination temperature on the physical properties of nano-titania prepared by sol-gel/hydrothermal method, *Russ. J. Phys. Chem.* 89, 1896.

Hamad, H., Abd El-Latif, H., Kashyout, A., Sadikd, W., and Fetehad, M. (2015) Synthesis and characterization of core/shell/shell magnetic ($CoFe_2O_4$/SiO2/TiO2) nanocomposite and TiO2 nanoparticle for photocatalytic activity under UV and visible irradiation,*New J. Chem.,* 39, 3116-3128

Han, Schlautman, M.A., and Batchelor, B. (2013) Removal of hexavalent chromium from groundwater by granular activated carbon, Water Environ. Res. 72 29–39.

Hench, L. L., and West, J. K. (1990) The sol-gel process Chem. ReV. 90, 33-72.

Ho, T.-L. (1975) The Hard Soft Acids Bases (HSAB) principle and organic chemistry, Chem. Rev. 75 (art. no. 1).

Ho, Y. (2003) Removal of copper ions from aqueous solution by tree fern, *Water Res.* 37, 2323–2330.

Hoch, L.B., Mack, E.J., Hydutsky, B.W., Hershman, J.M., Skluzacek, J.M., Mallouk, T.E. (2008) Carbothermal synthesis of carbon-supported nanoscale zero-valent iron particles for the remediation of hexavalent chromium, *Environ. Sci. Technol.* 42, 2600–2605.

Hsieh, T.-H., Ho, K.-S., Bi, X., Han, Y.-K., Chen, Z.-L., Hsu, C.-H., and Chang, Y.-C. (2009) Synthesis and electromagnetic properties of polyaniline-coated silica/maghemite nanoparticles, Eur. Polym. J. 45, 613–620.

Hu, F.X., Xie, J.L., Bao, S.J., Yu, L., Li, C.M., (2015) Shape-controlled ceria-reduced graphene oxide nanocomposites toward high-sensitive in-situ detection of nitric oxide. Biosens.Bioelectron. 70, 310–317.

Hu, J., Chen, C. Zhu, X. Wang, X. (2009) Removal of chromium from aqueous solution by using oxidized multiwalled carbon nanotubes, *J. Hazard.Mater.* 162, 1542–1550.

Huang, X., Yin, Z., Wu, S., Qi, X., He, Q., Zhang, Q., Yan, Q., Boey, F., and Zhang, H. (2011) Graphene-based materials: synthesis, characterization, properties, and applications, Small 7, 1876–1902.

Huang, Y., Lee, X., Macazoc, F.C., Grattieric, M., Caic, R., and Mintee, S.D. (2018) Fast and efficient removal of chromium (VI) anionic species by a reusable chitosan-modified multi-walled carbon nanotube composite, *Chem Eng J* 339, 259–267.

Jabeen, H., Chandra, V., Jung, S., Lee, J.W., Kim, K.S., Kim, S.B. (2011) Enhanced Cr(VI) removal using iron nanoparticle decorated graphene, Nanoscale 3, 3583–3585.

Jiang, M.Q., Jin, X.Y., Lu, X.Q., and Chen, Z.L. (2010) Adsorption of Pb(II), Cd(II), Ni(II) and Cu(II) onto natural kaolinite clay, Desalination 252, 33-39.

Jirickova, M., Cerny, R. (2006) Effect of hydrophilic admixtures on moisture and heat transport and storage parameters of mineral wool, *Constr. Build. Mater.* 20, 425–434.

Juang, M.W. Ahn, K.H. Lee, Y., Kim, K.P., Rhee, J.S., Park, J.T., Paeng, K.J. (2001) Adsorption characteristics of phenol and chlorophenols on granular activated carbons (GAC), Microchem. J. 70, 123–131.

Jung, J. H., Han, J., Her, N., Lee, S.-J., Oh, J., Ryud, J., Yoon, Y. (2013) Hexavalent chromium removal by various adsorbents: powdered activated carbon, chitosan, and single/multi-walled carbon nanotubes, Sep. Purif. Technol. 106, 63–71.

Kaczala, F., Marques, M., Hogland, W. (2009) Lead and vanadium removal from a real industrial wastewater by gravitational settling/sedimentation and sorption onto Pinus sylvestris sawdust, *Bioresour Technol* 100, 235–243.

Kalidhasan, S., Kumar A.S.K., Rajesh V, Rajesh N. (2012) Ultrasound-assisted preparation and characterization of crystalline cellulose-ionic liquid blend polymeric material: a prelude to the study of its application toward the effective adsorption of chromium, *J Colloid Interface Sci.* 367(1), 398-408.

Kashinath, L., Namratha, K. Byrappa, K., (2019) Microwave mediated synthesis and characterization of CeO_2-GO hybrid composite for removal of chromium ions and its antibacterial efficiency, *J Environ Sci.,* 76, 65-79.

Khare, P, Yadav, A., Ramkumar, J. and Verma, N., (2016) Microchannel-embedded metal–carbon–polymer nanocomposite as a novel support for chitosan for efficient removal of hexavalent chromium from water under dynamic conditions, Chem Eng J 293, 44–54.

Khare, P., Ramkumar, J., Verma, N. (2015) Control of bacterial growth in water using novel laser-ablated metal–carbon–polymer nanocomposite-based microchannels, Chem. Eng. J. 276, 65–74.

Khezami, L. and Capart, R. (2005) Removal of chromium(VI) from aqueous solution by activated carbons: Kinetic and equilibrium studies, *J. Hazard Mater* 123 (1–3), 223-231.

Khosravi, R., Moussavi, G., Ghaneian, M.T., Ehrampoush, M.H., Barikbin, B., Ebrahimi, A.A., Gholamreza Sharifzadeh Chromium adsorption from aqueous solution using novel green nanocomposite: Adsorbent characterization, isotherm, kinetic and thermodynamic investigation, Journal of Molecular Liquids, 256, 2018, 163-174

Kim, M. K., Sundaram, K.S., Iyengar, G.A., Lee, K.-P. (2015) A novel chitosan functional gel included with multiwall carbon nanotube and substituted polyaniline as adsorbent for efficient removal of chromium ion,Chem Eng J 267, 51–64.

Kimbrough, D.E., Cohen, Y., Winer, A. M., Creelmen, L. and Mabuni, C. (1999) A critical assessment of chromium in the environment, *Crit. Rev. Environ. Sci. Technol*. 29 (1).

Kohler, S.J., Cubillas, P., Rodriguez-Blanco, J.D., Bauer, C. and Prieto, M. (2007) Removal of cadmium from wastewaters by aragonite shells and the influence of other divalent cations, *Environ Sci Technol* 41, 112–118.

Kuang, W., Tan, Y., Fu, L. (2012) Adsorption kinetics and adsorption isotherm studies of chromium from aqueous solutions by HPAM–chitosan gel beads, Desal. Water Treat. 45, 222–228.

Kumar, A.S.K. and Rajesh, N. (2013) Exploring the interesting interaction between graphene oxide, Aliquat-336 (a room temperature ionic liquid) and chromium(VI) for wastewater treatment, RSC Adv. 2697–2709

Kumar, A.S.K., Kakan, S.S., Rajesh, N., novel amine impregnated graphene oxide adsorbent for the removal of hexavalent chromium, Chem. Eng. J. 230 (2013) 328–337.

Kumar, A.S.K., Kalidhasan, S. Rajesh, V. Rajesh, N. (2012) Application of cellulose–clay composite biosorbent toward the effective adsorption and removal of chromium from industrial wastewater, Ind. Eng. Chem. Res. 51, 58–69.

Kumar, R., Ansari, M.O., and Barakat, M.A. (2013) DBSA doped polyaniline/multi-walled carbon nanotubes composite for high efficiency removal of Cr(VI) from aqueous solution, *Chem. Eng. J.* 228, 748–755.

Kumar, U., Bandyopadhyay, M. (2006) Sorption of Cd(II) aqueous solution using pretreated rice husk, *Bioresour. Technol.* 97, 104–109.

Kurniawan, T.A., Chana, G.Y.S., Babelb, W.L.S. (2006) Comparisons of low-costadsorbents for treating waste waters laden with heavy metals, Sci. Total Environ. 366 (2-3), 409–426.

Kyzas, G. Z. and Kostoglou, M. (2014) Green adsorbents for wastewaters: a critical review,Materials 7, 333-364

Lazaridis, N.K., Bakoyannakis, D.N., Deliyanni, E.A. (2005) Chromium (VI) sorptive removal from aqueous solutions by nanocrystalline akaganeite, Chemosphere 58 65–73.

Li Y., Zhu, S., Liu, Q., Chen, Z., Gu J., Zhu, C., Lu, T., Zhang, D., and Ma, J. (2013) N-doped porous carbon with magnetic particles formed in situ for enhanced Cr(VI) removal, *Water Res.* 47, 4188–4197.

Li, D., Muller, M.B., Gilje, S., Kaner, R.B., and Wallace, G.G. (2008) Processable aqueous dispersions of graphene nanosheets, *Nat. Nanotechnol.* 3, 101–105.

Li, G.Y., Jiang, Y.R., Huang, K.L., Ding, P. and Yao, L.L. (2008) Kinetics of adsorption of accharomyces cerevisiae mandelated dehydrogenase on magnetic Fe3O4-chitosan nanoparticle, *Colloids Surf. A* 320, 11–18.

Li, H., Li, Z., Liu, T., Xiao, X., Peng, Z., Deng, L., (2008) A novel technology for biosorption and recovery hexavalent chromium in wastewater by bio-functional magnetic beads, Bioresour. Technol. 99, 6271–6279.

Li, Q., Su, H., Tan, T., (2008) Synthesis of ion-imprinted chitosan-TiO2 adsorbent and its multi-functional performances, Biochem Eng J 38:212-218.

Li, S., Lu, X., Xue, Y., Lei, J., Zheng, T., and Wang, C. (2012) Fabrication of polypyrrole/grapheme oxide composite nanosheets and their applications for Cr(VI) removal in aqueous solution, Plos one 7, 43328.

Li, X., Li, Y., Zhang, S., Ye, Z., (2012) Preparation and characterization of new foam adsorbents of poly(vinylalcohol)/chitosan composites and their removal for dye and heavy metal from aqueous solution, *Chem. Eng. J.* 183, 88–97.

Li, X.L., Peng, Q., Yi, J. X., Wang, X., and Li, Y. D. (2006) Near monodisperse TiO_2 nanoparticles and nanorods, *Chem. Eur. J.* 12, 2383-2391.

Lin, C.K., Chen, J.N., Lin, C.C. (1997) An NMR, XRD and EDS study of solidification/ stabilization of chromium with Portland cement and C3S, *J. Hazard. Mater.* 56, 21–34.

Liu, M., Wen, T., Wu, X., Chen, C., Hu, J., Li, J., Wang, X. (2013) Synthesis of porous Fe3O4 hollow microspheres/graphene oxide composite for Cr(VI) removal, *Dalton Trans.*, http://dx.doi.org/10.1039/C3DT50955A.

Liu, T., Yang, X., Wang, Z.L., Yan, X. (2013) Enhanced chitosan beads-supported FeO nanoparticles for removal of heavy metals from electroplating wastewater in permeable reactive barriers, Water Res. 47 6691–6700.

Liu, W.Y., Zhang, J., Zhang, C.L., Wang, Y.F., Li, Y. (2010) Adsorptive removal of Cr (VI) by Fe-modified activated carbon prepared from Trapa natans husk, *Chem. Eng. J.* 162 677–684.

Liu, Y.X., Yuan, D.X., Yan, J.M., Li, Q.L. and Ouyang, T. (2011) Electrochemical removal of chromium from aqueous solutions using electrodes of stainless steel nets coated with single wall carbon nanotubes, J. Hazard. Mater. 186, 473–480.

Liu, Z.R., Zhou, L.M., Wei, P., Zeng, K., Wen, C.X. and Lan, H.H. (2008) Competitive adsorption of heavy metal ions on peat, *J China Univ Min Technol* 18, 255–260.

López-Téllez, G., Barrera-Díaz, C.E., Balderas-Hernández, P., Roa-Morales, G. and Bilyeu, B. (2011) Removal of hexavalent chromium in aquatic solutions by iron nanoparticles embedded in orange peel pith, *Chem Eng J,* 173, 480-485.

Lu, Z. L., Lindner, E. and Mayer, H. A. (2002) Applications of sol−gel-processed interphase catalysts, Chem. ReV. 102, 3543-3578.

Lu,, A.H., Zhong, S.J., Chen, J., Shi, J.X., Tang, J.L., Lu, X.Y. (2006) Removal of Cr(VI) and Cr(III) from aqueous solutions and industrial wastewaters by natural clinopyrrhotite, *Environ Sci Technol* 40:3064–3069.

Luo, C., Tian, Z., Yang, B., Zhang, L., and Yan, S. (2013) Manganese dioxide/iron oxide/acid oxidized multi-walled carbon nanotube magnetic nanocomposite for enhanced hexavalent chromium removal, Chem Eng J 234, 256–265.

Luo, F., Chen, Z., Megharaj, M., Naidu, R.(2016) Simultaneous removal of trichloroethylene and hexavalent chromium by green synthesized agarose-Fe nanoparticles hydrogel, Chem Eng J 294, 290-297.

Lv, X.S., Xu, J., Jiang, G.M., Tang, J., Xu, X.H. (2012) Highly active nanoscale zero-valent iron (nZVI)-Fe3O4 nanocomposites for the removal of chromium(VI) from aqueous solutions, *J. Colloid Interface Sci.* 369 460–469.

Lv, X.S., Xu, J., Jiang, G.M., Xu, X.H. (2011) Removal of chromium(VI) from wastewater by nanoscale zero-valent iron particles supported on multiwalled carbon nanotubes, Chemosphere 85, 1204–1209.

Lyu, H., Tang, J., and Huang, Y. et al., (2017) Removal of hexavalent chromium from aqueous solutions by a novel biochar supported nanoscale iron sulfide composite, Chem Eng J 322, 516–524.

Ma, H.L., Zhang, Y., Hu, Q.H., Yan, D., Yu, Z.Z., Zhai, M. (2012) Chemical reduction and removal of Cr(VI) from acidic aqueous solution by ethylenediamine-reduced graphene oxide, *J. Mater. Chem.* 22, 5914–5916.

Ma, X., Anderson, P., and Chang, P.R. (2015) Modification of porous starch for the adsorption of heavy metal ions from aqueous solution, Food Chem, 181, 133-139.

Marques, P.A.S.S., Rosa, M.F. and Pinheiro, H.M. pH effects on the removal of Cu2+, Cd2+ and Pb^{2+} from aqueous solution by waste brewery waste, Bioprocess Eng. 23 (2000) 135–141.

Marquez-Reyes, J.M., Lopez-Chuken, U.J., Valdez-Gonzalez, A. and LunaOlvera, H.A. (2013) Removal of chromium and lead by a sulfatereducing consortium using peat moss as carbon source, *Bioresour Technol* 144, 128–134.

Martin, M., Salazar, P., Villalonga, R., Campuzano, S., Pingarron, J., Gonzalez-Mora, J. (2014) Preparation of core–shell Fe3O4@poly(dopamine) magnetic nanoparticles for biosensor construction, J. Mater. Chem. B 2, 739–746.

Mata, Y.N., Blázquez M.L., Ballester, A., González, F. and Muñoz, J.A. (2009) Sugar-beet pulp pectin gels as biosorbent for heavy metals: Preparation and determination of biosorption and desorption characteristics,*Chem Eng J* 150, 289-301

Mirzayi, B. Nematollahzadeh, A. F. (2014) Firouznia, S. Heydari, Nitrite removal from aqueous solution using surface modified maghemite nanoparticles, Nano, 9 (1450013-1-1450013-10)

Mohan, D. Pittman Jr. C.U. (2006) Activated carbons and low cost adsorbents for remediation of tri-and hexavalent chromium from water, *J. Hazard.Mater.* 137, 762–811.

Mohan, D., Singh, K.P. (2002) Single- and multi-component adsorption of cadmium and zinc using activated carbon derived from bagasse—an agricultural waste, *Water Res* 36, 2304–2318.

Namduri, H. and Nasrazadani, S. (2008) Quantitative analysis of iron oxides using Fourier transform infrared spectrophotometry, Corros. Sci. 50, 2493–2497.

Nematollahzadeh, A., Seraj, S., Mirzayi, B. (2015) Catecholamine coated maghemite nanoparticles for the environmental remediation: Hexavalent chromium ions removal, Chem Eng J 277, 21–29

Ngah, W.S. W., Hanafiah, M.A.K.M. (2008) Removal of heavy metal ions from wastewater by chemically modified plant wastes as adsorbents: A review, *Bioresource Technol.* 99, 3935-3948

Nordberg, G.F., Flower, B., Nordberg, M. and Friberg, L. (2007) Handbook on the Toxicology of Metals, third ed., Academic Press,.

Nriagu, J.O. and Pacyna, J.M. (1988) Quantitative assessment of world-wide contamination of air, water and soils by trace metals, *Nature* 333(6169), 134–139.

O'Hannesin, S.F., and Gillham, R.W. (1998) Long-term performance of an in situ 'iron wall' for remediation of VOCs, *Ground Water* 36, 164–170

Odoemelam, S.A., Iroh, C.U. and Igwe, J.C. (2011) Copper(II), cadmium(II) and lead(II)adsorption kinetics from aqueous metal solutions using chemically modifiedand unmodified cocoa pod husk (Theobroma cacao) waste biomass, *Res. J. Appl.Sci.* 6 (1), 44–52.

Oliveira, F.D., Paula, J., Freitas, O.M. and Figueiredo, S.A. (2009) Copper and lead removal by peanut hulls: equilibrium and kinetic studies, Desalination 248, 931–940.

Orth WS, Gillham RW (1996) Dechlorination of trichloroethene in aqueous solution using Fe(0) Environ Sci Technol 30:66–71

Owlad, M., Aroua, M.K., Daud, W.A.W., Baroutian, S. (2008) Removal of hexavalent chromium-contaminated water and wastewater: a review, *Water Air Soil Pollut.* 200 59–77.

Ozay, O., Ekici, S., Baran, Y., Aktas, N., Sahiner, N. (2009) Removal of toxic metal ions with magnetic hydrogels, Water Res. 43, 4403–4411.

Oze, C., Bird, D. K. and Fendorf, S. (2007) Genesis of hexavalent chromium from natural sources in soil and groundwater, Proceedings of the National Academy of Sciences of the United States of America 104 (16), 6544-6549.

Pan, J.H., Liu, R.X. and Tang, H.X. (2007) Surface reaction of Bacillus cereus biomass and its biosorption for lead and copper ions, J. Environ. Sci. 19, 403-408.

Pandey, S. and Mishra, S. B. (2011) Organic–inorganic hybrid of chitosan/organoclay bionanocomposites for hexavalent chromium uptake, J. Colloid Interface Sci. 361(2), 509-520.

Parga, J.R., Cocke, D.L. Valverde, V., Gomes, J.A.G., Kesmez, M., Moreno, H., Weir, M., and Mencer, D. (2005) Characterization of electrocoagulation for removal of chromium and arsenic, Chem. Eng. Technol. 28 (5), 605–612.

Park, D., Lim, S.L., Yun, Y.S., Park, J.M. (2008) Development of a new Cr(VI) biosorbent from agricultural biowaste, Bioresour. Technol. 99, 8810–8818.

Patterson, J. W. (1985) Industrial wastewater treatment technology, Second edition.Butterworth.

Pavasant, P., Apiratikul, R., Sungkhum, V., Suthiparinyanont, P., Wattanachira, S., Marhaba, T.F. (2006) Biosorption of Cu2+, Cd2+, Pb2+, and Zn2+ using dried marine green macroalga Caulerpa lentillifera, *Bioresour. Technol.* 97, 2321-2329.

Pellera, F., Giannis, A., Anastasiadou, K., Kalderis, D., Pentari, D., Gidarakos, E. (2010) Adsorption of Cu(II) ions from aqueous solutions using biochar prepared fromagricultural byproducts, *Hazard. Waste Manage.*(Third InternationalSymposium on Energy from Biomass and Waste).

Pierre, A.C., and Pajonk, G. M. (2002) Chemistry of Aerogels and Their Applications Chem. ReV. 102, 4243-4266.

Pillay, K., Cukrowska, E.M., Coville, N.J. (2009) Multi-walled carbon nanotubes as adsorbents for the removal of parts per billion levels of hexavalent chromium from aqueous solution, *J. Hazard. Mater.* 166, 1067–1075

Pintor, A., Ferreira, C., Ferreira, C. et al., (2012) Use of cork powder and granules for the adsorption of pollutants: A review, Water Res. 46(10), 3152-66.

Qu, X., Alvarez, P.J.J. and Li, Q. (2013) Applications of nanotechnology in water and wastewater treatment, *Water Res.* 47 (12), 3931–3946.

Quintana, M. Vazquez, E. Prato, M. (2013) Organic functionalization of graphene in dispersions, Acc. Chem. Res. 46, 138–148.

Quintelas, C., Rocha, Z., Silva, B., Fonseca, B., Figueiredo, H. and Tavares, T. (2009) Biosorptive performance of an Escherichia coli biofilm supported on zeolite NaY for the removal of Cr(VI), Cd(II), Fe(III) and Ni(II), *Chem. Eng. J.* 152, 110-115.

Rachna, Rani, M., Shanker, U. (2019a) Degradation of tricyclic polyaromatic hydrocarbons in water, soil and river sediment with a novel TiO2 based heterogeneous nanocomposite. J Environ. Manage., 248, 109340–109351.

Rachna, Rani M., Shanker, U. (2019b) Sunlight mediated improved photocatalytic degradation of carcinogenic benz[a]anthracene and benzo[a]pyrene by zinc oxide encapsulated hexacyanoferrate nanocomposite. J. Photochem. Photobiol. A Chem., 381, 111861–11175.

Rachna, Rani, M., Shanker, U. (2018) Enhanced photocatalytic degradation of chrysene by Fe2O3@ ZnHCF nanocubes. Chem. Eng. J., 348, 754–764.

Rachna, Rani, M., Shanker, U. (2019c) Sunlight active ZnO@FeHCF nanocomposite for the degradation of bisphenol A and nonylphenol. J. Environ. Chem. Eng., 7, 103153–103170.

Rajesh, N., Kumar, A. S. K., Kalidhasan, S. and Rajesh, V. (2011) Trialkylamine Impregnated macroporous polymeric sorbent for the effective removal of chromium from industrial wastewater, *J. Chem. Eng. Data* 56, 2295–2304.

Raji, C., and Anirudhan, T.S. (1998) Batch Cr(VI) removal by polyacrylamide-grafted sawdust: kinetics and thermodynamics, Water Res. 32, 3772–3780.

Rani, M., Shanker, U. (2017) Removal of carcinogenic aromatic amines by metal hexacyanoferrate nanocubes synthesized via green process. J. Env. Chem. Eng., 5, 5298–5311.

Rani, M., Shanker, U., Chaurasia, A. (2017a) Catalytic potential of laccase immobilized on transition metal oxides nanomaterials: Degradation of alizarin red S dye. J. Environ. Chem. Eng., 5(3), 2730–2739.

Rani, M., Rachna, Shanker, U. (2018) Metal hexacyanoferrates nanoparticles mediated degradation of carcinogenic aromatic amines. Environ. Nanotechnol. Monit. Manag., 10, 36–50.

Rani, M., Shanker, U. (2018a) Insight in to the degradation of bisphenol A by doped ZnO@ ZnHCF nanocubes: High photocatalytic performance. J. Colloid. Interfac. Sci., 530, 16–28.

Rani, M., Shanker, U. (2018b) Sun-light driven rapid photocatalytic degradation of methylene blue by poly (methyl methacrylate)/metal oxide nanocomposites. Colloids Surf., 559, 136–147.

Rani, M., Shanker, U. (2018c) Effective adsorption and enhanced degradation of various pesticides from aqueous solution by Prussian blue nanorods. J. Env. Chem. Eng., 6, 1512–1521.

Rani, M., Shanker, U. (2018d) Removal of chlorpyriphos, thaimethoxam and tebuconazole from water using green synthesized metal hexacyanoferrates nanoparticles. Environ. Sci. Pollut. Res., 25, 10878–10893.

Rani, M., Shanker, U. (2018e), Photocatalytic degradation of toxic phenols from water using bimetallic metal oxide nanostructures. Colloids Surf. A., 553, 546–561.

Rani, M., Shanker, U. (2018f), Promoting sun light-induced photocatalytic degradation of toxic phenols by efficient and stable double metal cyanide nanocubes. Environ. Sci. Pollut. Res., 25, 23764–23779.

Rani, M., Shanker, U. (2018g), Remediation of polycyclic aromatic hydrocarbons using nanomaterials. In The Handbook Green Adsorbents for Pollutant Removal. London: Springer Nature, pp. 343–387.

Rani, M., Shanker, U. (2018h), Advanced treatment technologies. In Handbook of Environmental Materials Management, ed. C. M. Hussain. Cham: Springer International Publishing AG, 2018h. https://doi.org/10.1007/978-3-319-58538-3_33-1.

Rani, M., Shanker, U. (2018i), Degradation of traditional and new emerging pesticides in water by nanomaterials: Recent trends and future recommendations. Int. J. Environ. Sci. Technol., 15, 1347–1380.

Rani, M., Rachna, Shanker, U. (2019) Mineralization of carcinogenic anthracene and phenanthrene by sunlight active bimetallic oxides nanocomposites. J. Colloid Interface Sci., 555, 676–688.

Rani, M., Shanker, U. (2019), Green solvents in chemical reactions. In book "Industrial Applications of Green Solvents" Millersville, PA: Materials Research Forum LLC.

Ramos, R.L., Martinez, A.J., Coronado, R.M.G. (1994) Adsorption of chromium (VI) from aqueous solutions on activated carbon, *Water Sci. Technol.* 30, 191–197.

Rao, C.N.R., Sood, A.K., Subrahmanyam, K.S., and Govindaraj, A. (2009) Graphene: the new two-dimensional nanomaterial, *Angew. Chem. Int. Ed.* 48, 7752–7777.

Rao, M.M., Ramesh, A., Rao, G.P.C., Seshaiah, K. (2006) Removal of copper and cadmiumfrom the aqueous solutions by activated carbon derived from ceiba pentandra hulls, J. Hazard. Mater. B 129, 123–129.

Reddy, D.H., Lee, S.M. (2013) Application of magnetic chitosan composites for the removal of toxic metal and dyes from aqueous solutions, *Adv. Colloid Interface Sci.*201–202, 68–93.

Renge, V. C., Khedkar, S. V. and pande, S.V. (2012), Removal of heavy metals from wastewater using low cost adsorbents: a review, *Sci. Revs. Chem. Commun*, 2(4), 580-584

Riahi, S.M. Mehdi, B.S. Ali, O. Javad, C.M. (2010) Removal of chromium from aqueous solution using polyaniline–poly ethylene glycol composite, *J. Hazard. Mater.*184, 248–254.

Roger, M. R. (2006) Removal of metal ions from contaminated water using agricultural residues. ECOWOOD 2006 - 2nd International Conference on Environmentally-Compatible Forest Products Fernando Pessoa University, Oporto, Portugal, 20-22 September 2006

Rubio, J., Souza, M.L., Smith, R.W. (2002) Overview of flotation as a wastewater treatment technique. *Miner. Eng.* 15, 139-155.

Ryu, J., Ku, S.H., Lee, H., Park, C.B. (2010) Mussel-inspired polydopamine coating as a universal route to hydroxyapatite crystallization, Adv. Funct.Mater. 20, 2132–2139.

Saeed, A., Iqbal, M. and Akhtar, W. (2005) Removal and recovery of lead (II) from single and multimetal (Cd, Cu, Ni, Zn) solutions by crop milling waste (black gram husk), *J Hazard Mater* 11, 65–73.

Saha, R. Nandi, R. and Saha, B. (2011) Sources and toxicity of hexavalent chromium, *J. Coord. Chem.* 64, 1782–1806.

Samani, M.R., Borghei, S.M. Olad, A. Chaichi, M.J. (2010) Removal of chromium from aqueous solution using polyaniline–poly ethylene glycol composite, J. Hazard. Mater. 184, 248–254.

Santhosh, C., Velmurugan, V., Jacob, G. and Jeong, S.K. et al. (2016) Role of nanomaterials in water treatment applications: A review, *Chem Eng J* 306, 1116–1137.

Sarin, V. and Pant, K.K. Removal of chromium from industrial waste by using eucalyptus bark, Bioresour. Technol. 97 (2006) 15–20.

Schiewer, S. and Patil, S.B. (2008) Modeling the effect of pH on biosorption of heavy metals by citrus peels, *J Hazard Mater* 157, 8–17.

Schwarz, J. A., Contescu, C., Contescu, A. (1995) Methods for preparation of catalytic materials, *Chem. ReV.* 95, 477-510.

Senthurchelvan, R., Wang, Y. Basak, S. Rajeshwar, K. (1996) Reduction of hexavalent chromium in aqueous solutions by polypyrrole. II. Thermodynamic, kinetic, and mechanistic aspects, *J. Electrochem. Soc.* 143, 44–51.

Seraj, S. Mirzayi, B. Nematollahzadeh, A. (2014) Superparamagnetic maghemite/ polyrhodanine core/shell nanoparticles: synthesis and characterization, *Adv.Powder Technol.* 25 1520–1526

Shanker, U., Jassal, V., Rani, M. (2016a) Catalytic removal of organic colorants from water using some transition metal oxide nanoparticles synthesized under sunlight. RSC Adv., 6, 94989–94999.

Shanker, U., Jassal, V., Rani, M., Kaith, B. S. (2016b), Towards green synthesis of nanoparticles: From bio-assisted sources to benign solvents. A review. Int. J. Env. Anal. Chem., 96, 801–835.

Shanker, U., Jassal, V., Rani, M. (2017a) Degradation of toxic PAHs in water and soil using potassium zinc hexacyanoferrate nanocubes. J. Environ. Manag., 204, 337–348.

Shanker, U., Jassal, V., Rani, M. (2017b) Green synthesis of iron hexacyanoferrate nanoparticles: Potential candidate for the degradation of toxic PAHs. J. Environ. Chem. Eng., 5, 4108–4120.

Shanker, U., Rani, M., Jassal, V. (2017c) Degradation of hazardous organic dyes in water by nanomaterials. Environ. Chem. Lett., 15(4), 623–642. Shen, W. Chen, S.Y. Shi, S.K. Li, X. Zhang, X.. Hu, W.L Wang, H.P. (2009) Adsorption of Cu(II) and Pb(II) onto diethylenetriamine-bacterial cellulose, Carbohydr. Polym. 75, 110–114.

Sheng, G.D., Wang, S.W., Hua, J., Lu, Y., Li, J.X., Dong, Y.H. and Wang XK (2009) Adsorption of Pb (II) on diatomite as affected via aqueous solution chemistry and temperature. *Colloid Surf* 339, 159–166.

Shyaa, A.A., Hasan O.A., Abbas, A.M. (2015) Synthesis and characterization of polyaniline/ zeolite nanocomposite for the removal of chromium (VI) from aqueous solution, *J. Saudi Chem Society* 19, 101–107.

Singh, V., Sharma, A.K., Kumari, P. and Tiwari, S. (2008) Efficient chromium (VI) adsorption by *Cassia marginata Seed* Gum functionalized with

poly(methylmethacrylate) using microwave irradiation, *Ind. Eng. Chem. Res.* 47, 5267–5276.

Sonawane, G.H., Patil, S.P. and Sonawan, S.H. (2018) Chapter 1 - Nanocomposites and Its Applications, Applications of Nanomaterials, Advances and Key Technologies, Micro and Nano Technologies, pp. 1-22

Souiri, M., Gammoudi, I., Ouada, H.B., Mora, L., Jouenne, T., Jaffrezic-Renault, N., Dejous, C., Othmane, A. and Duncan, A.C. (2009) Escherichia coli-functionalized magnetic nanobeads as an ultrasensitive biosensor for heavy metals, *Proced. Chem.* 1, 1027-1030.

Srivastava, N.K. and Majumder, C.B. (2008) Novel biofiltration methods for the treatment of heavy metals from industrial wastewater, *J. Hazard.Mater.* 151, 1–8.

Sud, D., Mahajan, G. and Kaur, M. P. (2008) Agricultural waste material as potential adsorbent for sequestering heavy metal ions from aqueous solutions – A review, *Bioresource Technol* 99, 6017-6027

Sureshkumar, V., Kiruba Daniel, S. C. G., Ruckmani, K., and Sivakumar, M. (2016) Fabrication of chitosan–magnetite nanocomposite strip for chromium removal, Appl Nanosci 6, 277–285

Thinh, N.N., Hanh, P.T.B., Ha, L.T.T., Anh, L.N., Hoang, T.V., Hoang, V.D, Dang, L.H., Khoi, N.V., Lam, T.D. (2013) Magnetic chitosan nanoparticles for removal of Cr(VI) from aqueous solution, Mater. Sci. Eng., C 33, 1214–1218.

Tocchi, C., Federici, E., Fidati, L., Manzi, R., Vincigurerra, V. and Petruccioli, M. (2012) Aerobic treatment of dairy wastewater in an industrial three-reactor plantEffect of aeration regime on performances and on protozoan and bacterialcommunities.*Water Res.* 46, 3334–3344.

Tonni, S.B. and Kurniawan, A. (2003) Low-cost adsorbents for heavy metals uptake from contaminated water: a review, *J Hazard Mater.* 97(1-3):219-43.

Tsekova, K., Todorova, D., Dencheva, V. and Ganeva, S. (2010) Biosorption of copper(II) and cadmium(II) from aqueous solutions by free and immobilized biomass of Aspergillus niger, *Bioresour. Technol.* 101, 1727-1731.

Tuzen, M. and Soylak, M. (2007) Multiwalled carbon nanotubes for speciation of chromium in environmental samples, J. Hazard.Mater. 147, 219–225.

Tuzen, M., Saygi, K.O., Usta, C., Soylak, M. (2008) Pseudomonas aeruginosa immobilized multiwalled carbon nanotubes as biosorbent for heavy metal ions, *Bioresour. Technol.* 99, 1563-1570.

U.S. Environmental Agency, Drinking Water Contaminants <http://www.epa.gov/safewater/contaminants/index.html>, May 17, 2015. World Health Organization International Standards for Drinking Water, WHO, Geneva, 2008, pp.177

Uchida, M. Shinohara, Q. Ito, S. Kawasaki, N. Nakamura, T. Tanada, S., (2000) Reduction of iron(III) ion by activated carbon fiber, *J. Colloid Interface Sci.* 224, 347–350.

Unnithan, M.R. and Anirudhan, T.S. (2001) The kinetics and thermodynamics of sorption of chromium(VI) onto the iron(III) complex of a carboxylated polyacrylamidegrafted sawdust, *Ind. Eng. Chem. Res.* 40 2693–2701.

Unnithan, M.R., Vinod, V. P. and Anirudhan T. S. (2004) Synthesis, characterization, and application as a chromium(VI) adsorbent of amine-modified polyacrylamide-grafted coconut coir pith, *Ind. Eng. Chem. Res.* 43, 2247-2255.

Wafwoyo, W., Seo, C.W., Marshall, W.E. (1999) Utilization of peanut shells asadsorbent for selected metals, *J. Chem. Technol. Biotechnol.* 74, 1117–1121.

Wan Ngah WS, Teong LC, Hanafiah MAKM (2011) Adsorption of dyes and heavy metal ions by chitosan composites: a review, *Carbohydr Polym*, 83:1446-1456.

Wang, H., Sun, Y. B., Chen, Q. W., Yu, Y. F. and Cheng, K. (2010) Synthesis of carbon-encapsulated superparamagnetic colloidal nanoparticles with magnetic-responsive photonic crystal property, *Dalton Trans.* 39, 9565–69.

Wang, J., and Wang, X. et al., (2018) Polyvinylpyrrolidone and polyacrylamide intercalated molybdenum disulfide as adsorbents for enhanced removal of chromium(VI) from aqueous solutions, *Chem Eng J,* 334, 569-578.

Wang, J., Pan, K., Giannelis, E.P., Cao, B., (2013) Polyacrylonitrile/polyaniline core/shell nanofiber mat for removal of hexavalent chromium from aqueous solution: mechanism and applications, RSC Adv. 3, 8978–8987.

Wang, W., Wang, X., Wang X., Yang, L., Wu, Z., Xia, S., Zhao, J. (2013) Cr(VI) removal from aqueous solution with bamboo charcoal chemically modified by iron and cobalt with the assistance of microwave, J. Environ. Sci. 25, 1726-1735.

Wang, X., Zhuang, J., Peng, Q., Li, Y. D. (2005) A general strategy for nanocrystal synthesis, Nature 437, 121.

Wang, X.J., Wang, Y., Wang, X., Liu, M., Xia, S.Q., Yin, D.Q., Zhang, Y.L., and Zhao, J.F. (2011) Microwave-assisted preparation of bamboo charcoal-based iron-containing adsorbents for Cr(VI) removal, *Chem. Eng. J.* 174, 326–332.

Wang, X.S., Chen, L.F., Li, F.Y., Chen, K.L., Wan, W.Y., Tang, Y.J. (2010) Removal of Cr(VI) with wheat-residue derived black carbon: reaction mechanism and adsorption performance, J. Hazard. Mater. 175, 816–822.

Wang, Y., Wang, S., Niu, H. Ma, Y. Zeng, T. Cai, Y. Meng, Z. (2013) Preparation of polydopamine coated Fe3O4 nanoparticles and their application for enrichment of polycyclic aromatic hydrocarbons from environmental water samples, *J. Chromatogr. A* 1283, 20–26.

Warren, L.M., Julian, C.S., Harriott, P. (2005) Unit Operations of Chemical Engineering, 7th ed. McGraw Hill Book Company.

Wei, H., Deng, S., Huang, Q., Nie, Y., Wang, B., Huang, J., Yu, G. (2013) Regenerable granular carbon nanotubes/alumina hybrid adsorbents for diclofenac sodium and carbamazepine removal from aqueous solution, Water Res. 47, 4139–4147.

Wen, Y., Tang, Z., Chen, Y., Gu, Y. (2011) Adsorption of Cr(VI) from aqueous solutions using chitosan-coated fly ash composite as biosorbent, *Chem Eng J* 175, 110-116.

Wight, A. P. and Davis, M. E., (2002) Design and preparation of organic– inorganic hybrid catalysts, *Chem. ReV.* 102, 3589-3614.

Wu, Y., Jiang, Y., Han, D., Wang, F., Zhu, J. (2007) Speciation of chromium in water using crosslinked chitosan-bound FeC nanoparticles as solid-phase extractant, and determination by flame atomic absorption spectrometry, Microchim. Acta 159, 333–339.

Xi, Z.-Y., Xu, Y.-Y. Zhu, L.-P.Wang, Y. and Zhu, B.-K. (2009) A facile method of surface modification for hydrophobic polymer membranes based on the adhesive behavior ofpoly(DOPA) and poly(dopamine), *J. Membr. Sci.* 327, 244– 253.

Xiao, Y., Liang, H. Chen, W. Wang, Z. (2013), Synthesis and adsorption behavior of chitosan-coated MnFe2O4 nanoparticles for trace heavy metal ions removal, Appl. Surf. Sci. http://dx.doi.org/10.1016/j.apsusc.2013.08.083.

Xing, J., Shen, Y., Yang, B., Feng, D., Wang, W., and Bai, B. (2018) A green method based on electro-assisted and photo-assisted regeneration for removal of chromium(VI) from aqueous solution, *Water Sci Technol* 2017 (3), 896-902.

Xu, J., Ge, J. P., Li, Y. D. (2006) Solvothermal Synthesis of Monodisperse PbSe Nanocrystals, *J. Phys. Chem. B* 110, 2497-2501.

Xu, Y., and Zhao, D. (2007) Reductive immobilization of chromate in water and soil using stabilized iron nanoparticles, Water Res. 41 2101–2108.

Xuan, S. H., Hao, L. Y., Jiang, W. Q., Gong, X. L., Hu, Y. and Chen, Z. Y. (2007) A facile method to fabricate carbon-encapsulated Fe3O4 core/shell composites Nanotechnology 18, 035602

Yadav, S. K. (2010) Heavy metals toxicity in plants: An overview on the role of glutathione and phytochelatins in heavy metal stress tolerance of plants, *South African Journal of Botany* 76, 167-179.

Yang Z., Ren, L. and Jin, L.et al. (2018) In-situ functionalization of poly(m-phenylenediamine) nanoparticles on bacterial cellulose for chromium removal, Chem Eng J 344, 441-452,

Yuan, X., Wang, Y., Wang, J., Zhou, C., Tang, Q., Rao, X. (2013) Calcined graphene/Mg-Al layered double hydroxides for enhanced Cr(VI) removal, *Chem. Eng. J* d221, 204–213.

Yuan, Y., Zhang, G., Li, Y., Zhang, G., Zhang, F., Fan, X. (2013) Poly(amidoamine) modified graphene oxide as an efficient adsorbent for heavy metal ions, *Polym. Chem.* 4, 2164–2167.

Zhang, D., Wei, S.Y., Kaila, C., Su, X., Wu, J., Karki, A.B., Young, D.P. and Guo, Z.H. (2010) Carbon-stabilized iron nanoparticles for environmental remediation, *Nanoscale* 2 917–919.

Zhang, J., Zhang, G., Wang, M., Zheng, K., Cai, D., Wu, Z. (2013) Reduction of aqueous Cr(VI) using nanoscale zero-valent iron dispersed by high energy electron beam irradiation, Nanoscale 5, 9917–9923.

Zhang, N., Lin, L.S. and Gang, D.C. (2008) Adsorptive selenite removal from water using iron-coated GAC adsorbents, *Water Res.* 42 3809–3816.

Zhang, S., Zhang, Y., Bi, G., Liu, J., Wang, Z., Xu, Q., Xu, H., Li, X. (2014) Mussel-inspired polydopamine biopolymer decorated with magnetic nanoparticles for multiple pollutants removal, J. Hazard. Mater. 270, 27–34.

Zhang, S., Zeng, M., Xu, W., Li, J., Li, J., Xu, J., and Wang, X. (2013) Polyaniline nanorods dotted on graphene oxide nanosheets as a novel super adsorbent for Cr(VI), *Dalton Trans*. 42, 7854–7858.

Zhang, S.J., Li, X.Y., and Chen, J.P. (2010) Preparation and evaluation of a magnetite doped activated carbon fiber for enhanced arsenic removal, Carbon 48, 60–67.

Zhang, X.X., Tang, S.S., Chen, M.L., Wang, J.H. (2012) Iron phosphate as a novel sorbent for selective adsorption of chromium(III) and chromium speciation with detection by ETAAS, *J. Anal. At.Spectrom.* 27, 466–472.

Zhao, G. Wen, T. Chen, C. Wang, X. (2012) Synthesis of graphene-based nanomaterials and their application in energy-related and environmental-related areas, RSC Adv. 2, 9286–9303.

Zhao, Y. Zhao, D. Chen, C. Wang, X. (2013) Enhanced photo-reduction and removal of Cr(VI) on reduced graphene oxide decorated with TiO2 nanoparticles, J. Colloid Interface Sci. 405, 211–217.

Zheng, J., Liu, Z. Q., Zhao, X. S., Liu, M., Liu X. and Chu, W. (2012) One-step solvothermal synthesis of Fe_3O_4@C core–shell nanoparticles with tunable sizes Nanotechnology 23, 165601-165608.

Zhou, L., Li, R., Zhang, G., Wang, D., Cai, D. and Wu, Z. (2018) Zero-valent iron nanoparticles supported by functionalized waste rock wool for efficient removal of hexavalent chromium, Chem Eng J 339, 85–96.

Zhu, J., Wei, S., Gu, H., Rapole, S.B., Wang, Q., Luo, Z., Haldolaarachchige, N., Young, D.P., Guo, Z., (2012) One-pot synthesis of magnetic graphene

nanocomposites decorated with core@double-shell nanoparticles for fast chromium removal, Environ Sci Technol. 46(2), 977-85.

Zhuang, L., Li, Q., Chen, J., Ma, B. and Chen, S. (2014) Carbothermal preparation of porous carbon-encapsulated iron composite for the removal of trace hexavalent chromium, Chem Eng J 253, 24–33

Zimmermann, A.C., Mecabo, A. Fagundes, T. Rodrigues, C.A. (2010) Adsorption of Cr(VI) using Fe–crosslinked chitosan complex (Ch–Fe), J. Hazard. Mater. 179, 192–196.

Zubair, A., Bhatti, N.N. Hanif, M.A. and Shafqat, F. (2008) Kinetic and equilibrium modeling for Cr(III) and Cr(VI) removal from aqueous solutions by Citrus reticulate waste biomass, *Water Air Soil Pollut.* 19, 305–318

Authors' Biography

Ajay Kumar Mishra (*MSc, MPhil, PhD, CSci, FRSC*) is currently working as 'Full Professor' for University of South Africa and also working as 'Adjunct Professor' at Jiangsu University, China. His research interests include nanomaterials & water research. Prof. Mishra has edited several books and also serves as member advisory board of a number of international scientific societies, conferences and workshops. He also served as Associate Editor as well as member of the editorial board of many peer-reviewed international journals. He has delivered a number of including Plenary/Keynote/Invited Lectures. For his outstanding research profile, he was awarded a number of international awards. Prof. Mishra also served as Associate Editor as well as member of the editorial board of many peer-reviewed international journals. He is serving as member advisory board of a number of international scientific societies, conferences and workshops.

Deepak Pathania is Professor Cum Head Cum Dean, Central University of Jammu, Jammu and Kashmir, India. He is presently also serving as founder President of Him Science Congress Association, Himachal Pradesh, India, scientific society. He is members of different professional scientific societies. He had guided a number of Ph.D, M.Phil and M.Sc research projects for their respective degrees. He had authorized several books in different areas of interest from believed publishers. He has edited books from international publisher. He is editorial members and reviewer of different national and international journals. He had number of publications in reputed Journals and publications in conferences to his credit. He is reviewers of different international journals. He is life members of different scientific societies. His area of research includes polymer based composites, nanocomposite ion exchangers, graft copolymerization; fiber reinforced composite, environmental chemistry, metal sensors, photocatalysis degradation of organic and inorganic pollutants.

CHAPTER

Photocatalytical degradation of pesticides

9

Deepak Pathania[a], Manita Thakur[b], Arush Sharma[c]

Department of Environmental Sciences, Central University of Jammu, Samba, India[a] Department of Chemistry, IEC University Baddi, Solan, India[b] School of Sciences, Baddi University of Emerging Sciences and Technology (BUEST), Solan, India[c]

1 Introduction

A variety of toxic organic and inorganic pollutants are generally released into the aquatic system, which pollute the aquatic system. These pollutants are of most toxicological concern because of their bioaccumulation and nonbiodegradability. The main sources of these pollutants into water system are mining, metallurgical, chemical manufacturing, tannery, battery manufacturing industries, fossil fuel, chemical industries, etc. The presence of organic pollutants in water is carcinogenic and nonbiodegradable and persists in the environment for long time and caused harmful effects in mammalian and aquatic life. A large number of herbicides are applied on the agricultural fields, which, apart from killing their respective weed, due to their chemical stability, resistance to biodegradation, and sufficient water solubility, either can penetrate deep into the groundwater aquifers or can be washed away to the surface water bodies (Hettige, Mani, & Wheeler, 2000).

These compounds, due to their toxicity, stability to natural decomposition, and persistence in the environment, have been of much concern to the societies and regulation authorities around the world (El-Geundi, 1997). 2,4-Dichlorophenoxy acetic is commonly known as 2,4-D. It is one of the most commonly used herbicides for controlling broadleaf weeds and other vegetation. 2,4-D is used to control broadleaf weeds in a variety of places such as home lawns, cereal and grain crops, commercial areas, commercial turf, rights-of-way, and forests. Because of the toxicity, conventional treatment methods are not suitable for wastewaters containing 2,4-D, as they can destroy the microbial population of the treatment plants. Therefore the development of an effective degradation process for this herbicide is very important (Khan, Zia, & Qasim, 2010; Li & Zhang, 1999; Malhat, Haggag, Loutfy, Osman, & Ahmed, 2015; Thuy, Van Geluwe, Nguyen, & Vander Bruggen, 2012).

The presence of pesticide contaminants in various water sources such as surface water and groundwater has increased manyfold in recent years due to their significant use in agricultural field for plant and crop protection. The contamination of water bodies may be due to direct applications of insecticides, rainwater runoff from agricultural fields, and disposal of outdated stocks and discharge of waste water from industries (Colabuono, Taniguchi, & Montone, 2010; Hu et al., 2011). To meet the global food demand, yearly, tonnes of pesticides have been used without apprehending their consequences (Karami-Mohajeri & Abdollahi, 2011). Currently, India involved in biggest producer of pesticides

Nano-Materials as Photocatalysts for Degradation of Environmental Pollutants. https://doi.org/10.1016/B978-0-12-818598-8.00009-2

in Asia, after China. India ranks as fourth largest pesticide-producing nation in the world after the United States, Japan, and China. Pesticides in Jammu with the highest consumption rates include monocrotophos, endosulfan, phorate, chlorpyriphos, methyl parathion, quinalphos, mancozeb, paraquat, butachlor, isoproturon, and phosphamidon. In India, due to intense agricultural activities, some organophosphates and organochlorine pesticides were detected abundantly in groundwater (Freire, Koifman, & Koifman, 2015).

Organophosphorus pesticides represent the most applied group of insecticides for the last two decades. OPs are composed of 10 most widely used pesticides all over the world. They have been used as an alternative to organochlorine compounds for pest control. However, they are considered as extremely toxic compounds. Organophosphorus pesticides like monocrotophos and chlorpyrifos are commonly used in India and noticed in various environmental segments, such as soil, water, and air due to their extensive use (Calle, Frumkin, Henley, Savitz, & Thun, 2002). Chlorpyrifos is another widely used organophosphorus pesticide in agriculture. This compound was first developed in 1965 and applied in over 100 countries across the world. Chlorpyrifos has become the largest organophosphate insecticide in world in both volume and value. It is used to control the populations of insects, soil grubs, rootworms, subterranean termites, foliage, and soil-born insects (Robinson et al., 2015). Chlorpyrifos is not readily soluble in water and easily comes out of solution. However, temperatures above 63 °C allow chlorpyrifos to dissolve at a faster rate into solution. Exposure to chlorpyrifos and its metabolites has resulted in a variety of nerve disorders in humans. Its acute poisoning causes headache, nausea, muscle twitching, and convulsions and in some extreme cases even death (Gasnier et al., 2009; Jaga & Dharmani, 2003; McKinlay, Plant, Bell, & Voulvoulis, 2008). Despite the major role of pesticides in increasing productivity, there is a concern about the progressive pesticide contamination of groundwater.

2 Entry of pesticides into animals

Insecticides are used to kill insects by getting inside their bodies where they then act as poison. There are three different ways of entry of pesticides into animals.

2.1 Dermal entry

The insecticides enter into the body of animals through the skin. In the case of insects, the skin is called the cuticle. Insecticides of this type are called as contact poisons. Dermal enter into the body of insect takes place when aerosol spray droplets hit the insect and insects walk over and in doing so come into contact with powder or granule forms of insecticide. In most work situations, absorption through the skin is the most common route of pesticide exposure. People can be exposed to a splash or mist when mixing, loading, or applying the pesticide. Pesticides can also be absorbed through eyes. In addition, pesticides can cause injuries to the eye itself.

2.2 Oral entry

When the insecticide enters the body through the mouth, then it is called oral entry. It occurs when the insect eats the insecticides. Insecticides of this type are called ingested poisons. The insecticides are ingested by the insect as poisonous bait and when it cleans itself after the poison comes into contact

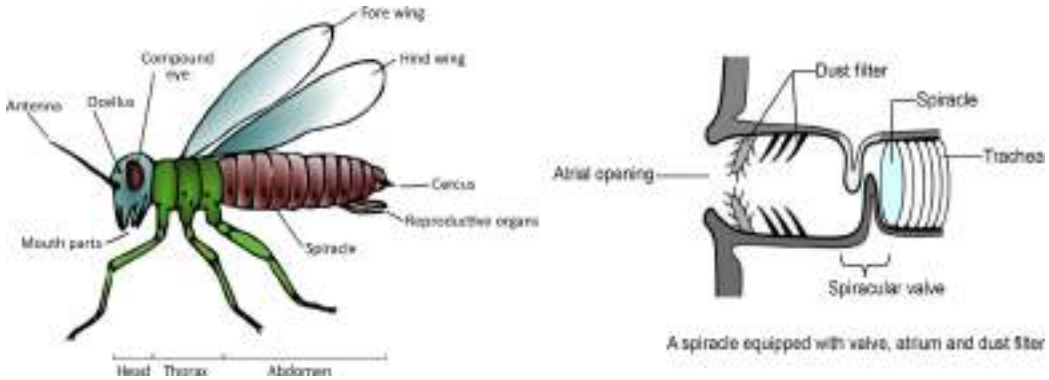

FIG. 1

Respiratory entry of pesticides.

with its body. There are numerous reports of people accidentally drinking a pesticide that has been put into an unlabeled bottle or beverage cup/container (including soft drink cans or bottles). Workers who handle pesticides may also inadvertently ingest when eating or smoking if they have not washed their hands first.

2.3 Respiratory entry

The insecticides are breathed in by the insect then it is called respiratory entry. These insecticides are called inhaled poisons. Insects do not breathe through the mouth as observed in most of animals. They breathe through spiracles. The pesticides with a high inhalation hazard will be labeled with directions to use a respirator. Fig. 1 shows the respiratory entry of pesticides.

3 Types of insecticides

3.1 Classification based on types of pests that they kill

The main groups of pesticides are categorized into the following six groups:

1. Insecticides—Killing insects
2. Herbicides—Killing plants
3. Rodenticides—Killing rodents, like mice and rats
4. Bactericides—Killing bacteria
5. Fungicides—Killing fungi
6. Larvicides—Killing larvae

3.2 Classification based on biodegradability

Pesticides can also be classified into two types based on biodegradability:

3.2.1 Biodegradable

The biodegradable pesticides are those that can be broken down by microbes and other living beings into harmless compounds.

3.2.2 Persistent

The persistent pesticides are those that may take months or years to break down.

3.3 Chemically related pesticides

3.3.1 Organophosphate

Most organophosphates are insecticides; they affect the nervous system by disrupting the enzyme that regulates a neurotransmitter. Organophosphates, which were promoted as a more ecological alternative to organochlorines, include a great variety of pesticides, the most common of which is glyphosate. This class also includes other known pesticides, such as malathion, parathion, and dimethoate; some are known for their endocrine-disrupting potential. This class of pesticides has been associated with effects on the function of cholinesterase enzymes (Jaga & Dharmani, 2003; McKinlay et al., 2008); decrease in insulin secretion; disruption of normal cellular metabolism of proteins, carbohydrates, and fats; also genotoxic effects (Li et al., 2015); and effects on mitochondrial function, causing cellular oxidative stress and problems to the nervous and endocrine systems. Population-based studies have revealed possible relations between the exposure to organophosphorus pesticides and serious health effects including cardiovascular diseases, negative effects on the male reproductive system and on the nervous system, dementia, and also a possible increased risk for non-Hodgkin's lymphoma. Furthermore, prenatal exposure to organophosphates has been correlated with decreased gestational duration and neurological problems occurring in children (Jamal, Haque, Singh, & Rastogi, 2015).

3.3.2 Carbamate

Similar to the organophosphorus pesticides, the carbamate pesticides also affect the nervous system by disrupting an enzyme that regulates the neurotransmitter. However, the enzyme effects are usually reversible. Carbamate pesticides, such as aldicarb, carbofuran, and ziram, are another class of chemical pesticides that have been associated with endocrine-disrupting activity, possible reproductive disorders (Goad, Goad, Atieh, & Gupta, 2004), and effects on cellular metabolic mechanisms and mitochondrial function. Moreover, in vitro studies have revealed the ability of carbamate pesticides to cause cytotoxic and genotoxic effects in hamster ovarian cells and to induce apoptosis and necrosis in human immune cells and natural killer cells and also apoptosis in T lymphocytes (Li, Kobayashi, & Kawada, 2011; Soloneski, Kujawski, Scuto, & Larramendy, 2015).

Furthermore, it has been confirmed that carbaryl, which belongs to the category of carbamate pesticides, can act as a ligand for the hepatic aryl hydrocarbon receptor, a transcription factor involved in the mechanism of dioxin toxicity. There is also evidence for the ability of carbamate pesticides to cause neurobehavioral effects, increased risk for dementia, and non-Hodgkin's lymphoma (Denison, Phelan, Winter, & Ziccardi, 1998; Lifshitz, Shahak, Bolotin, & Sofer, 1997).

3.3.3 Organochlorine insecticides

They were commonly used earlier, but now, many countries have removed organochlorine insecticides from their market due to their health and environmental effects and their persistence (e.g., DDT, chlordane, and toxaphene). Exposure to organochlorines occurs through ingestion of contaminated food or water, inhalation of vapor, and absorption through the skin. Dietary exposure results in bioaccumulation of these chemicals in the human body. The accumulation of organochlorine compounds is a result of their chemical structure and their physical properties such as polarity and solubility. These fat-soluble compounds persist in both the body and the environment. Consequently, researchers and regulatory agencies have banned several organochlorines (Gomathi, Devi, & Kumar, 2009). The main symptoms of organochlorine intoxication are dizziness, headache, anorexia, nausea, vomiting, malaise, dermatitis, diarrhea, apprehension, excitement, irritability, gait disorders, excessive sweating, altered reflexes, muscle weakness, tremors, spasms, mental confusion, anxiety, seizures, coma, and death. The carcinogenicity of this class of compounds is assigned to polychlorocyclodiene compounds that form epoxides during their biotransformation. Because organochlorines have long half-life, these levels in the serum constitute a marker of exposure to these pesticides (Hossain, Fakhruddin, Chowdhury, & Alam, 2013).

3.3.4 Pyrethroid

These are a synthetic version of pyrethrin, a naturally occurring pesticide, found in chrysanthemums (flower). They were developed in such a way as to maximize their stability in the environment. They comprise active agents (pyrethrins I–VI), but pyrethrins I and II are the most active. These compounds decompose rapidly in the presence of light, but synthetic production of pyrethroids around 1950 overcame some disadvantages of natural pyrethrins (Hossain et al., 2013). After absorption, rapid pyrethroid distribution occurs in the organism. Therein, these compounds undergo biotransformation via two mechanisms: hydrolysis of the ester linkage by carboxylesterases and oxidation of the alcohol moiety by cytochromes P450. Pyrethroids exert the same mechanism of action in insects and mammals.

3.3.5 Sulfonylurea herbicides

The sulfonylureas herbicides have been commercialized for weed control such as pyrithiobac-sodium, cyclosulfamuron, bispyribac-sodium, terbacil, sulfometuron-methyl, sulfosulfuron, rimsulfuron, pyrazosulfuron-ethyl, imazosulfuron, nicosulfuron, oxasulfuron, flazasulfuron, primisulfuron-methyl, halosulfuron-methyl, flupyrsulfuron-methyl-sodium, ethoxysulfuron, chlorimuron-ethyl, bensulfuron-methyl, azimsulfuron, and amidosulfuron.

3.3.6 Biopesticide

The biopesticides are certain types of pesticides derived from such natural materials as animals, plants, bacteria, and certain minerals.

4 Usage of pesticides in India

The pesticide use has been started during the times of ancient Romans. The people burn the sulfur for destroying pests and employed the salt, ashes, and bitter for controlling weeds. A Roman naturalist insisted the use of arsenic as an insecticide (History of pesticide use 1998). Mixture of honey and

arsenic has been employed for monitoring ants in 1600. During the 1800s, the US farmers used certain chemicals such as nicotine sulfate, calcium arsenate, and sulfur as pesticides (Wasse, Salmon, & Delaplane, 2000). In 1867, an impure form of copper, arsenic, has been utilized to check the potato beetle in the United States. The major burst through pesticide growth has been found in the era around and after the Second World War. The numerous operative and economical pesticides have been manufactured. This period is marked by the discovery of aldrin, dichlorodiphenyltrichloroethane (DDT) in 1939, dieldrin, β-benzene hexachloride (BHC), 2,4-dichlorophenoxyacetic acid (2,4-D), chlordane, and endrin. In 1962 an American scientist Rachel Carson emphasized in her book, *Silent Spring*, that DDT spray has found to cause the sudden death of nontarget creatures using direct or indirect noxiousness. (Delaplane, vander Steen, & Guzman-Novoa, 2013; Jabbar & Mallick, 1994).

The production of pesticides started in India in 1952 with the establishment of a plant for the production at Calcutta. Today, India is the second leading manufacturer of pesticides in Asia after China and ranks 12th globally (Mathur, 1999). There has been a steady increase in the production of pesticides in India, from 5000 metric tons in 1958 to 102,240 metric tons in 1998. The demand for pesticides in terms of value was estimated to be around Rs. 22 billion (USD 0.5 billion), which is about 2% of the total world market during 1996–97. The pattern of pesticide usage in India is different from has been shown Fig. 2. It was recorded that in India 76% of the pesticide used is insecticide, as against 44% globally (Mathur, 1999). The use of herbicides and fungicides usage is less compared with pesticides. The major use of pesticides in India has been recorded for cotton crops (45%), followed by paddy and wheat.

5 Harmful effects of pesticides

The harmful effects accompanying the pesticide usage have suppressed their positive effects. Pesticides have life-threatening effects on nontarget species including animal, plant biodiversity, and aquatic as well as terrestrial ecosystems. As per the data available, approximately 80%–90% of applied pesticides should volatilize after few days of applications (Majewski & Capel, 1996). The volatilized pesticides rapidly vaporize and consequently pose danger to nontarget creature. Abandoned uses of pesticides have threatened the existence of erratic species such as bald eagle, peregrine falcon,

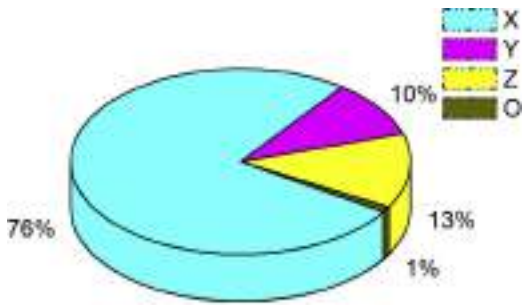

FIG. 2

Pattern of pesticides in India.

and osprey (Helfrich, Li, Sharp, & Sales, 2009). Furthermore, air, water, and soil have been polluted with these chemicals to the noxious level.

Depending upon the solubility of pesticides, they enter the ecosystem by two different methods. Water-soluble pesticides dissolved in water and arrive in the watercourse, rivers, and lake, therefore posing damage to the untargeted species. Secondly, fat-soluble pesticides enter into the animals using bioamplification process.

5.1 Effect on human

Pesticides have amended the standard of human well-being by monitoring vector-borne ailments, but long-term and random use has resulted in serious health issues. Human beings chiefly newborns and children are extremely prone to poisonous effects of pesticides due to nonspecific nature and inadequate usage of pesticides. The pesticide use has become augmented over past few decades. The exposure to these chemicals has also significantly increased. According to World Health Organization, approximate 3,000,000 cases of pesticide poisoning and 220,000 deaths have been reported in developing countries (Haakstad & Bø, 2011). Nearly about 2.2 million people in the developing countries are at threat to exposure of pesticides (Hicks et al., 2013).

Pesticides reach the human body by ingestion, inhalation, or the upper layer of the skin. Though, human bodies have mechanism for the removal of toxins. However, in some cases, it retains them through absorption in the circulatory system. Studies have revealed the close association of pesticides and the development of cancers in both children and adults. The close exposure with pesticide impart greater risk to various malignancies such as leukemia, Burkitt's lymphoma, neuroblastoma, Wilm's tumor, non-Hodgkin's lymphoma, soft tissue sarcoma, ovarian cancer, lung cancer, stomach cancer, colon cancer, bladder cancer, and rectal cancer (Bonner & Laskey, 1974). Many childhood cancers are found to be associated with pesticide exposure. Compared with other cancer types, more convincing evidence was presented in a population-based case-control study of acute myelocytic leukemia (AML). A comparison of 491 cases between an age group of 0–9 years was done for polymorphisms in CYP1A1, CYP2D6, GSTT1, and GSTM1 genes responsible to encode enzymes responsible to metabolize carcinogenic substances (Infante-Rivard, Labuda, Krajinovic, & Sinnett, 1999). Fig. 3 shows effect of pesticides on various cellular activities.

5.2 Effect on biodiversity

Pesticide-polluted water poses a hazard to aquatic life. It can affect aquatic plants. It declines the dissolved oxygen in the water system and causes physiological and behavioral change in the fish populations. Lawn care pesticides have been reported in the surface water and water bodies such as ponds, streams, and lakes. Pesticides applied to land drift to aquatic ecosystem are noxious to fish and nontarget organism. These pesticides not only are poisonous themselves but also interact with stressors and include harmful algal blooms. However, excessive use of pesticides causes decrease in the populations of different fish species (Scholz, 2012). Roughly 80% of the dissolved oxygen has been supplied by aquatic plant. It is essential for the survival of aquatic life. The aquatic fauna have been killed by herbicides causing low O_2 level, hence finally leading to asphyxia and decreased fish productivity (Helfrich et al., 2009). Mostly, level of pesticides is too much higher in the surface water than groundwater. It was probably due to surface runoff from the farmland and contaminations using spray drift.

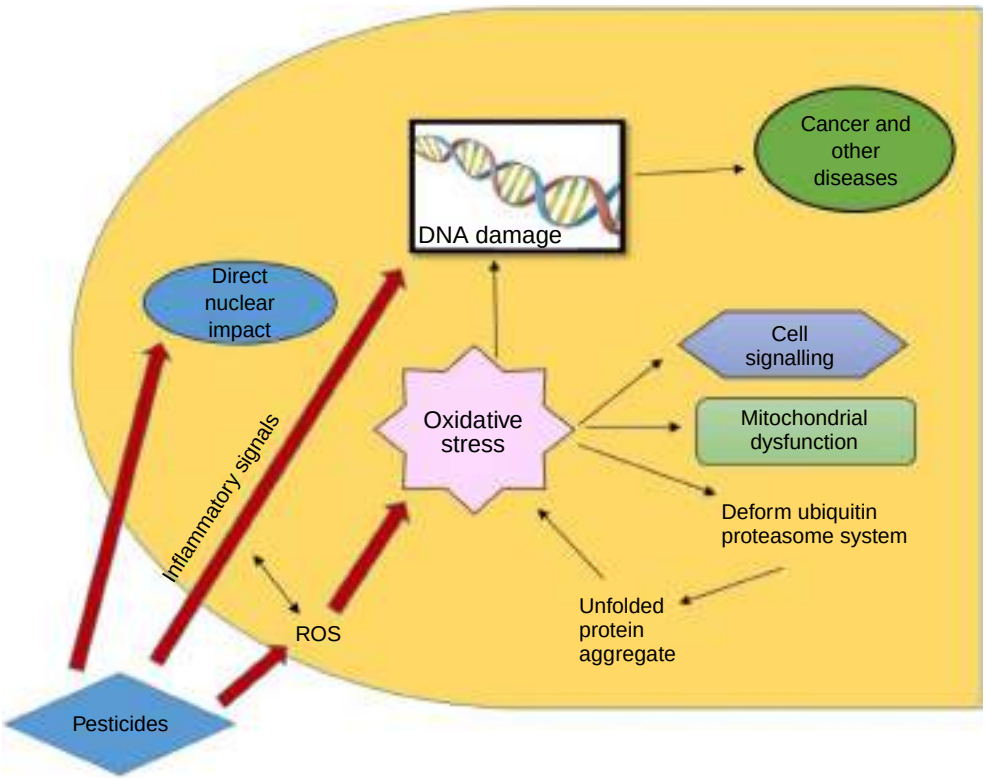

FIG. 3

Effect of pesticides on various cellular activities.

However, pesticides enter the underground by the seepage of polluted surface water, improper dumping, and accidental spill and leakage.

Pesticide exposure is also responsible for the lethal effect on the terrestrial plant apart from killing of nontarget plant. The volatilization of phenoxy herbicides caused harm to nearby trees and shrub. Herbicide such as glyphosate enhanced the susceptibility of plant to various noxious diseases (Brammall & Higgins, 1988), hence decreasing the quality of seed. However, low doses of herbicide, sulfonylureas, sulfonamides, imidazolinones, etc. have posed noxious effect onto the productivity of nontarget crop, natural plant, and wildlife (Fletcher, Pfleeger, & Ratsch, 1993).

5.3 Soil contamination

A large number of transformation products (TPs) from a widespread range of pesticides have been reported (Hutson & Roberts, 1999). Persistency and movement of these pesticides and their TPs have been measured using some parameters such as water solubility, soil-sorption constant, and half-life in soil (DT50). They can be moved from soil by runoff and leaching, thereby constituting a problem for the supply of drinking water to the population. The most researched pesticide TPs in soil are undoubtedly those from herbicides. Several metabolic pathways have been suggested, involving transformation

through hydrolysis, methylation, and ring cleavage that produce several toxic phenolic compounds. The pesticides and their TPs are retained by soils to different degrees, depending on the interactions between soil and pesticide properties. The most influential soil characteristic is the organic matter content. The larger the organic matter content, the greater the adsorption of pesticides and TPs. The capacity of the soil to hold positively charged ions in an exchangeable form is important with paraquat and other pesticides that are positively charged. Strong mineral acid is required for extracting these chemicals, without any analytical improvement or study reported in recent years. Soil pH is also of some importance. Adsorption increases with decreasing soil pH for ionizable pesticides (e.g., 2,4-D,2,4,5-T, picloram, and atrazine) (Andreu & Pico, 2004).

6 Different methods for the degradation of pesticides

Several attempts have been made for the treatment of pesticides and its residues from surroundings. The degradation of pesticides is the breakdown of toxic chemicals into nontoxic compounds. The process of breakdown can take a wide range of time, that is, from hours, to days, to years. It depends on the chemical properties of the pesticide and environmental conditions. Degradation of pesticide occurs by chemical and biological processes (Berg, Hagmeyer, & Gimbel, 1997; Gupta, Gupta, Rastogi, Agarwal, & Nayak, 2011). The pesticides that quickly breakdown do not persist in the environment and have short time control on crop. Due to adverse effects of using pesticides, researchers are encouraged to explore and design proficient techniques for the removal of different harmful pesticides. Several physical, chemical, and biological methods such as adsorption, catalytic degradation, membrane filtration, biological treatment, and advanced oxidation processes (AOP) have been investigated as shown in Fig. 4.

FIG. 4

Different methods for the degradation of pesticides.

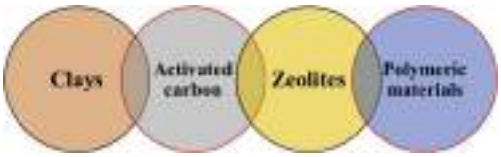

FIG. 5

Different physical methods for removal of pesticides.

6.1 Physical processes for remediation of pesticides

Various methods have been explored for the remediation of pesticides on large scale as shown in Fig. 5.

6.1.1 Clays

Natural clay particles are hydrophilic, negatively charged, and used for the retention of cationic pesticides because of their high surface area, low cost, and high availability. Natural clays have been modified to improve the retention of pesticides. Therefore, in recent years, much attention has been paid to the expansion of modified clays with enhanced sorption capacities for both polar and nonpolar pollutants (Haderlein, Weissmahr, & Schwarzenbach, 1996; Li, Sheng, Teppen, Johnston, & Boyd, 2003). Various parameters that effect the adsorption include initial pesticide concentrations, adsorbent mass, pH, contact time, ionic strength, and temperature. The efficiency of organoclays for the adsorption of different pesticides from water including prometron, butachlor, metsulfuron, and bensulfuron has been reported. But there is difficulty in the separation of clay minerals from water after treatment process and limits their use as adsorbent. Introduction of clay minerals as a coagulant aid made it easy for the separation of clay minerals after treatment because of improved sedimentation (Sanchez-Martin, Rodriguez-Cruz, Andrades, & Sanchez-Camazano, 2006). There are numerous benefits of using small amounts of clay minerals as a coagulant aid.

The pesticides get removed through flocculation process, and pesticides get adsorbed over the clay mineral, which improves the removal efficiency. In the presence of chemical coagulants, the low negatively charged organic clay may act as a sorbent for pesticides or nucleus for flocculation. Also, surfactant-modified nanomontmorillonites have been used to enhance the sorption capacity of the adsorbent as compared with commercial normal bentonites, which helps to remove the pesticides even at low concentration (Gerstl, Nasser, & Mingelgrin, 1998; Manisankar, Selvanathan, & Vedhi, 2006).

6.1.2 Activated carbon

Charcoal is porous, soft, black substance made by heating substances containing carbon such as material from hardwood trees and coconut shells. Activated charcoal has been used for many years to exclude organic contaminants from wastewaters and in water purification. Powdered activated charcoal is made up of very small carbon particles and has a high affinity for organic chemicals such as pesticides. Activated charcoal is used to adsorb and deactivate organic chemicals such as pesticides in soil. When pesticide has been adsorbed onto activated charcoal, it is biologically inactive and cannot cause injury to the turfgrass (Ayranci & Hoda, 2005; Hameed, Salman, & Ahmad, 2009). Due to its dark color, it has ability to absorb heat; therefore activated charcoal is also used to artificially warm the soil to minimize the effects of light frosts or to allow earlier seeding of an area.

Activated charcoal is an excellent adsorbent with large surface area and has high adsorption of pharmaceuticals and pesticides from water. The adsorption process of activated carbon depends on different

aspects like structure, surface chemistry, and nature of adsorbate and the properties of the adsorption solution (Salman, Njoku, & Hameed, 2011). Activated charcoal materials are of different types including granular active carbon, powder active carbon, black electrodes, fiber, and carbon. Powder active carbon is employed as an efficient approach to eliminate pesticide from drinking water treatment due to its cost-effectiveness and flexibility (Humbert, Gallard, Suty, & Croué, 2008; Zhang et al., 2017).

6.1.3 Zeolites and polymeric materials

Zeolites are widely used in pollution control, agriculture, and industry to remove pesticides and heavy metals. In recent years, zeolite has attracted much attention because of its excellent physicochemical properties, availability, and low cost. Zeolites are crystalline aluminosilicate materials and have extremely high adsorption capacity with interconnected micropores. They have superior catalytic properties and thermally stable and good resistance to most compounds (Kanan, Kanan, & Patterson, 2006).

Zeolites used as an adsorbent to treat water contaminated with pesticides are imidacloprid, bentazon, isoproturon, etc. The adsorption rate mainly depends on the mobility and polarity of pesticides. The high adsorption rate for carbamate pesticides has been detected by cetyltrimethyl ammonium bromide–modified zeolite (Kyriakopoulos & Doulia, 2006). The immobile pesticides like imidacloprid, isoproturon, and metalaxyl-m have been associated with zeolite, whereas more mobile pesticides like bentazon and clopyralid are partitioned in water. Isoproturon and metalaxyl-m are nonionic pesticides and show higher affinity for the zeolites on the basis of their polarity. Therefore the rate of trapping by zeolites mainly depends on the mobility and polarity of pesticide. Polymeric materials such as cyclodextrins, dendrimers, and hypercross-linked polymers have been employed for the elimination of pesticides. The most important advantages of polymeric materials in contrast to carbonaceous material are that they require lower energy and lower cost for the regeneration of adsorbents (Badawy, Ghaly, & Gad-Allah, 2006; Roy, Singh, Bajpai, & Bajpai, 2014).

6.2 Chemical treatment for removal of pesticides

Chemical treatment involves various processes including advanced oxidation process, adsorption, and biological treatment as shown in Fig. 6.

FIG. 6

Chemical processes for removal of pesticides.

6.2.1 Advanced oxidation process (AOP's)

Advanced oxidation processes are the oxidation techniques in which hydroxyl radicals have been produced by different methods. These are used for the removal of pollutants that have high chemical stability and low biodegradability. The hydroxyl radicals are efficient enough to initiates a series of reactions and convert pollutants completely to carbon dioxide and water (Cheng et al., 2016; Ikehata & El-Din, 2006). These are environmental friendly because they do not transfer pollutants from one phase to another. AOP's mechanisms involved various processes such as the following:

Fenton process

Fenton reaction is one of the efficient tools used for the oxidation of organic pollutant. In this, oxidation of organic substrates by Fe (II) and hydrogen peroxide occurs. The reaction involves in situ generation of a strong oxidizing agent, hydroxyl radical from hydrogen peroxide. The chemical equation of Fenton reaction is

$$Fe^{2+} + H_2O_2 \rightarrow Fe^{3+} + OH^* + OH^- \quad (1)$$

Fe^{3+} forms further react with hydrogen peroxide, and catalyst is regenerated again.

$$Fe^{3+} + H_2O_2 \rightarrow Fe^{2+} + HO_2^* + H^+ \quad (2)$$

These OH* radicals will react with organics (RH) by the abstraction of proton and producing organic radicals (R*), and these are highly reactive and can be further oxidized (Malato et al., 2002). Two major drawbacks of this process are requirement of acidic pH and formation of iron sludge. H_2O_2 dosage, pH, and iron dosage are the main factors affecting the efficiency of the process. Fenton process has been extensively used for the removal of total organic carbon, dyes, pigments, phenolic compounds, etc. It is very difficult to oxidize highly colored effluents from textile industries at low concentration. Therefore Fenton oxidation was effectively used for the removal of such compounds (Hamby, 1996). This process was also explored for the degradation of specific compounds like cresols, phenols, EDTA, cyanides, and organics. Another main application is wastewater treatment from oil recovery industry wastewater, landfill leachate, and natural gas plant wastewater.

UV and UV/H2O2 process

In this method the compounds will absorb the radiation passing to excited state promoting reactions. Degradation may be by either direct photolysis or indirect photolysis. Effectiveness of UV treatment for the removal of pharmaceuticals was observed only for ketoprofen, diclofenac, and antipyrine. The applicability and productivity of UV process depend on the stability of the compound, pH, and the nature of light source (Galindo, Jacques, & Kalt, 2000; Yuan et al., 2011). When H_2O_2 is used in the presence of UV, there is the formation of hydroxyl radicals by the photolysis of H_2O_2.

In this the oxidation of compounds can occur by either direct photolysis or reaction with hydroxyl radicals. Different parameters including pH, intensity of UV light, and H_2O_2 dosage affect the performance of system. It has been observed that acidic condition favors UV/H_2O_2 process because the acidic pH favors the hydroxyl radical formation. The rate of photolysis of H_2O_2 is pH dependent and increases when more alkaline conditions are used. But at higher pH, H_2O_2 autodecomposes forming water and oxygen. Excessive dose of H_2O_2 will reduce the degradation of pollutant; therefore, sufficient dose of

H_2O_2 is necessary to absorb UV to accelerate the generation of hydroxyl radicals (Gupta, Ali, & Saini, 2006).

6.3 Adsorption

Adsorption process by solid adsorbents is one of the most effective methods for dealing with the organic impurities from wastewater (Al-Qodah, Shawaqfeh, & Lafi, 2007). It is an excellent technique for the remediation of pesticides as compared with other traditional methods because of its simple design, high efficiency, low maintenance cost, highly economic benefits, and insensitivity for toxic substances. In recent years, the low-cost adsorbents with intensified pollutant removal capacities have been explored. Agricultural wastes, natural materials, and industrial wastes produced low-cost adsorbents like activated carbon that are used in wastewater treatment. Natural adsorbents have more advantages including technical feasibility, local availability, inexpensive, treatability, and their disposal (Kyriakopoulos, Doulia, & Anagnostopoulos, 2005; Lafi & Al-Qodah, 2006). There are some natural adsorbents that have excellent pesticide removal capacity as shown in Fig. 7. The role of various adsorbents for the removal of pesticide has been summarized in Table 1.

6.4 Biological treatment

Biological remediation involves complete transfer of organic compounds into less toxic end products like CO_2 and H_2O. This method is environmentally friendly and highly economic as compared with other tools for eliminating pollutants (Shawaqfeh, 2010).

There are three types of bioremediation with micro scale organism:

- Remediation through improved natural attenuation
- Bioaugmentation
- Biostimulation

The microorganisms capable of degrading organic pollutants can be isolated from surroundings including contaminated site or marine sediment. In recent decades, fungi have been used for biodegradation and bioremediation of pesticides. It has been observed that fungal isolates have found to be effective bioresource to degrade different pesticides such as lindane, methamidophos, atrazine, cypermethrin, endosulfan, chlorpyrifos, dieldrin, methyl parathion, and heptachlor. (Gerhardson, 2002). The main disadvantage is the speed of fungal degradation of pesticides, which depends on temperature, pH,

FIG. 7

Natural adsorbents used for the removal of pesticides.

Table 1 List of adsorbents used for the remediation of pesticides from aqueous system.

Adsorbent	Pesticides	Q_{max} (mg/g)	Reference
Activated carbon	Bromopropylate	18.9×10^{-2}	Ioannidou, Zabaniotou, Stavropoulos, Islam, and Albanis (2010)
Activated carbon	Bromopropylate	11.6×10^{-2}	Ioannidou et al. (2010)
Activated carbon	Bromopropylate	12.3×10^{-2}	Ioannidou et al. (2010)
Commercial activated carbon	4,4 DDT	163	Boussahel, Irinislimane, Harik, and Moussaoui (2009)
Cork wastes	4,4 DDT	2.03–19.08	Boussahel et al. (2009)
Wood saw dust	4,4 DDT	4.25–69.44	Boussahel et al. (2009)
Bagasse fly ash	9DDD	7.69×10^{-3}	Zolgharnein, Shahmoradi, and Ghasemi (2011)
Bagasse fly ash	DDE	6.67×10^{-3}	Zolgharnein et al. (2011)
Bagasse fly ash	Lindane	2.51×10^{-3}	Zolgharnein et al. (2011)
Bagasse fly as	Endrin	43.71	Zolgharnein et al. (2011)
Bagasse fly as	Aldrin	19.54×10^{-3}	Zolgharnein et al. (2011)
Tea leaves	Quinalphos	196.07×10^{-3}	Islam, Sakkas, and Albanis (2009)
Cork	α-Cypermethrin	303×10^{-3}	Ahmad et al. (2010)
Activated carbon	2(3H)-one	4.32	Arvand et al. (2009)
Commercial activated carbon	2,4D	8.13–10.48	Chingombe, Saha, and Wakeman (2006)
Vegetable activated carbon	Prometon	23.51	Moreno, López, Galvín, Cordón, and Mellado (2010)
Coconut activated carbon	Prometon	26.02	Moreno et al. (2010)
Vegetable activated carbon	Propazine	25.62	Moreno et al. (2010)
Coconut activated carbon	Propazine	27.15	Moreno et al. (2010)
Lignocellulosic material	Terbumeton	11.2	Boudesocque, Guillon, Aplincourt, Martel, and Noël (2008)
Lignocellulosic material	Isoproturon	61.8	Boudesocque et al. (2008)
Ayous saw dust	Praquat	9.47	Nanseu-Njiki, Dedzo, and Ngameni (2010)

nutrient availability, oxygen level, and soil moisture content. Different enzymes such as peroxidase, hydrolase, lactase, esterase, dehydrogenase, manganese peroxidase, lignin peroxidase mediate the biodegradation of a wide range of pesticides. Different biochemistry processes such as hydroxylation, dechlorination, demethylation, dioxygenation, dehydrochlorination, esterification, and oxidation have been employed on the fungal strains during the biodegradation of pesticides (Reddy & Kim, 2015). Biological processes for the elimination of pesticides may be affected by various environmental factors such as nutrients, pH, temperature, inoculum density, pesticide concentration, and chemical and physical characteristics of substrate (Chishti, Hussain, Arshad, Khalid, & Arshad, 2013).

6.5 Photocatalysis

Photocatalysis is one of the effective and competent advanced oxidation processes (AOPs) used to detoxify the contaminants emitted from the various industrial processes with negligible waste. Photocatalysis typically ensues with the illumination of solar light and photon generated catalytically species. The process of photodegradation involves the following steps: Initially, solar irradiation of certain wavelength is incident onto semiconductor. If the energy of incident radiation is equal to band energy or band gap of the photocatalyst, then electrons are excited from the valence band (VB) to the conduction band (CB) of photocatalyst and holes (h^+) left in the valence shell.

The electrons (e^-) and holes (h^+) endure the successive oxidation and reduction reactions with active compounds adsorbed onto the semiconductor surface to produce the degraded products. The photocatalytic processes involve the highly reactive hydroxyl radicals (OH*). These radicals are capable of degrading the organic pollutants into innocuous product from aqueous system. It has high capacity to mineralize nearly all organic pollutants into harmless substance such as CO_2 and H_2O under ambient conditions. The schematic representation of photocatalytic process under visible region is shown in Fig. 8.

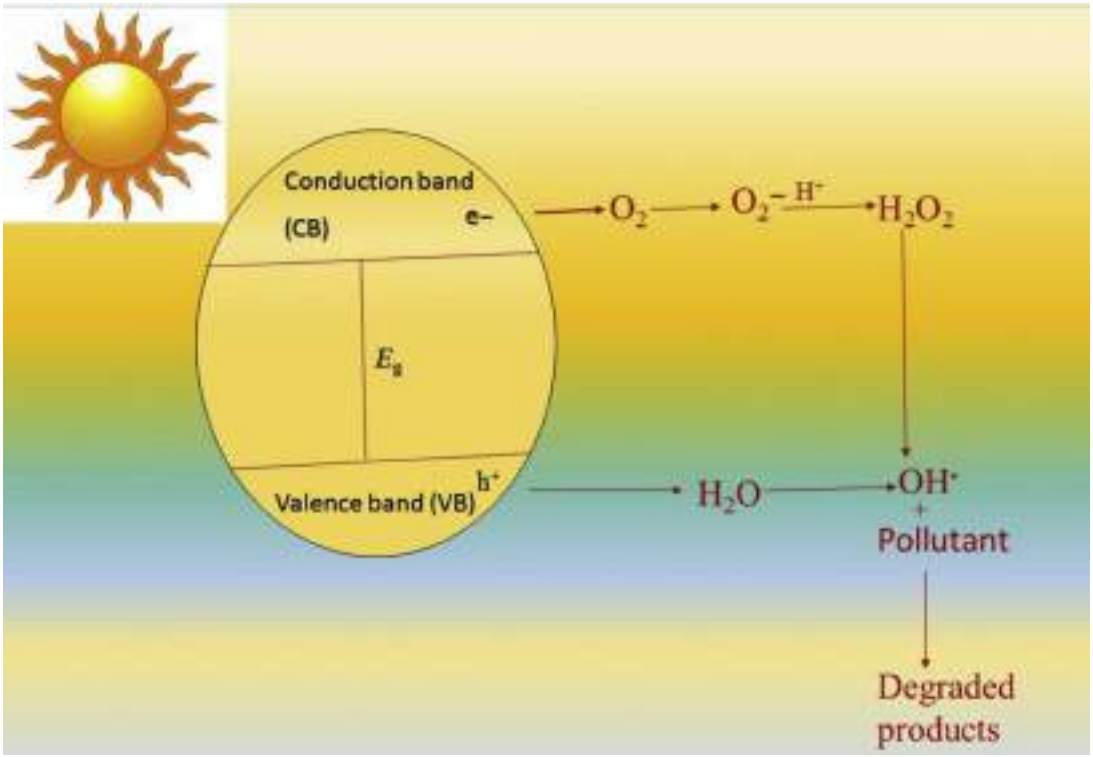

FIG. 8

Photocatalytic mechanism.

Since the revolutionary work in the 1970s, semiconductor-based nanocomposites have revealed the higher degradation rate for various pollutants (Liu, Chen, Hu, Wu, & Wang, 2011). Semiconductor-based composites were used as excellent photocatalytsts due to their potential applications for environmental decontamination. Photocatalysis using heterogeneous semiconductor appeared as most agreeable mean of degradation due to economical, nontoxic, higher–surface area, broad absorption spectra with greater absorption and capability for multi–electron transfer, etc.

Higher adsorption increased the catalytic degradation of organic and inorganic pollutants. Therefore nanoparticles are incorporated into some organic moieties and provide the enhanced surface area for the photodegradation of pollutants. Some of the advantages of carbon supported nanoparticles are as follows:

- They are innocuous in nature.
- Carbon suppresses the electron–hole pair recombination by acting as an electron acceptor.
- Organic moieties keep the metal nanoparticles in dispersed phase, hence preventing the agglomeration of nanoparticles.

7 Conclusions

Aquatic pollution is the biggest and most alarming problem that requires effective solutions. However, various initiatives have been taken to tackle this problem. Further, research dedicated to this problem is still needed. Recently, bionanocomposites have been widely explored for the removal of various pesticides from water system. Photodegradation is an abiotic method for the removal of pesticide. In this method, molecular excitation occurred by the absorption of solar energy. This results in the generation of various highly reactive species such as oxide and peroxide radicals. This specifically or nonspecifically oxidize the functional group present in a pesticide. However, extensive research has been conducted for the degradation of pesticide. However, additional research is required to evaluate the environmental impact of these ubiquitous pesticides.

References

Ahmad, T., Rafatullah, M., Ghazali, A., Sulaiman, O., Hashim, R., & Ahmad, A. (2010). Removal of pesticides from water and wastewater by different adsorbents: A review. *Journal of Environmental Science and Health. Part C*, *28*(4), 231–271.

Al-Qodah, Z., Shawaqfeh, A. T., & Lafi, W. K. (2007). Adsorption of pesticides from aqueous solutions using oil shale ash. *Desalination*, *208*, 294–305.

Andreu, V., & Pico, Y. (2004). Determination of pesticides and their degradation products in soil: Critical review and comparison of methods. *Trends in Analytical Chemistry*, *23*, 772–789.

Arvand, M., Latify, L., Tajmehri, H., Yagubov, A. I., Nuriyev, A. N., & Pourhabib, A. (2009). Comparative study for the removal of oxadiazon from aqueous solutions by adsorption on chitosan and activated carbon. *Analytical Letters*, *42*(6), 856–869.

Ayranci, E., & Hoda, N. (2005). Adsorption kinetics and isotherms of pesticides onto activated carbon-cloth. *Chemosphere*, *60*, 1600–1607.

Badawy, M. I., Ghaly, M. Y., & Gad-Allah, T. A. (2006). Advanced oxidation processes for the removal of organophosphorus pesticides from wastewater. *Desalination*, *194*, 166–175.

Berg, P., Hagmeyer, G., & Gimbel, R. (1997). Removal of pesticides and other micropollutants by nanofiltration. *Desalination*, *30*, 205–208.

Bonner, W. M., & Laskey, R. A. (1974). A film detection method for tritium-labelled proteins and nucleic acids in polyacrylamide gels. *European Journal of Biochemistry*, *46*, 83–88.

Boudesocque, S., Guillon, E., Aplincourt, M., Martel, F., & Noël, S. (2008). Use of a low-cost biosorbent to remove pesticides from wastewater. *Journal of Environmental Quality*, *37*(2), 631–638.

Boussahel, R., Irinislimane, H., Harik, D., & Moussaoui, K. M. (2009). Adsorption, kinetics, and equilibrium studies on removal of 4, 4-DDT from aqueous solutions using low-cost adsorbents. *Chemical Engineering Communications*, *196*(12), 1547–1558.

Brammall, R. A., & Higgins, V. J. (1988). The effect of glyphosate on resistance of tomato to Fusarium crown and root rot disease and on the formation of host structural defensive barriers. *Canadian Journal of Botany*, *66*, 1547–1555.

Calle, E. E., Frumkin, H., Henley, S. J., Savitz, D. A., & Thun, M. J. (2002). Organochlorines and breast cancer risk. *CA: A Cancer Journal for Clinicians*, *52*, 301–309.

Cheng, M., Zeng, G., Huang, D., Lai, C., Xu, P., Zhang, C., et al. (2016). Hydroxyl radicals based advanced oxidation processes (AOPs) for remediation of soils contaminated with organic compounds: A review. *Chemical Engineering Journal*, *284*, 582–598.

Chingombe, P., Saha, B., & Wakeman, R. J. (2006). Effect of surface modification of an engineered activated carbon on the sorption of 2, 4-dichlorophenoxy acetic acid and benazolin from water. *Journal of Colloid and Interface Science*, *297*(2), 434–442.

Chishti, Z., Hussain, S., Arshad, K. R., Khalid, A., & Arshad, M. (2013). Microbial degradation of chlorpyrifos in liquid media and soil. *Journal of Environmental Management*, *114*, 372–380.

Colabuono, F. I., Taniguchi, S., & Montone, R. C. (2010). Polychlorinated biphenyls and organochlorine pesticides in plastics ingested by seabirds. *Marine Pollution Bulletin*, *60*, 630–634.

Delaplane, K. S., vander Steen, J., & Guzman-Novoa, E. (2013). Standard methods for estimating strength parameters of Apis mellifera colonies. *Journal of Apicultural Research*, *52*, 1–2.

Denison, M. S., Phelan, D., Winter, G. M., & Ziccardi, M. H. (1998). Carbaryl, a carbamate insecticide, is a ligand for the hepatic ah (dioxin) receptor. *Toxicology and Applied Pharmacology*, *152*, 406–14.10.

El-Geundi, M. S. (1997). Adsorbents for industrial pollution control. *Adsorption Science and Technology*, *15*, 777–787.

Fletcher, J. S., Pfleeger, T. G., & Ratsch, H. C. (1993). Potential environmental risks associated with the new sulfonylurea herbicides. *Environmental Science & Technology*, *27*, 2250–2252.

Freire, C., Koifman, R. J., & Koifman, S. (2015). Hematological and hepatic alterations in brazilian population heavily exposed to organochlorine pesticides. *Journal of Toxicology and Environmental Health. Part A*, *78*, 534–548.

Galindo, C., Jacques, P., & Kalt, A. (2000). Photodegradation of the aminoazobenzene acid orange 52 by three advanced oxidation processes: UV/H_2O_2, UV/TiO_2 and VIS/TiO_2: Comparative mechanistic and kinetic investigations. *Journal of Photochemistry and Photobiology A: Chemistry*, *130*, 35–47.

Gasnier, C., Dumont, C., Benachour, N., Clair, E., Chagnon, M. C., & Séralini, G. E. (2009). Glyphosate-based herbicides are toxic and endocrine disruptors in human cell lines. *Toxicology*, *262*, 184–191.

Gerhardson, B. (2002). Biological substitutes for pesticides. *Trends in Biotechnology*, *20*, 338–343.

Gerstl, Z., Nasser, A., & Mingelgrin, U. (1998). Controlled release of pesticides into soils from clay – polymer formulations. *Journal of Agricultural and Food Chemistry*, *46*, 3797–3802.

Goad, E. R., Goad, J. T., Atieh, B. H., & Gupta, R. C. (2004). Carbofuran-induced endocrine disruption in adult male rats. *Toxicology Mechanisms and Methods*, *14*, 233–239.

Gomathi, L., Devi, B., & Kumar, G. (2009). Photocatalytic activity of V^{5+}, Mo^{6+} and Th^{4+} doped polycrystalline TiO_2 for the degradation of chlorpyrifos under UV/solar light. *Journal of Molecular Catalysis A: Chemical*, *308*, 174–181.

Gupta, V. K., Ali, I., & Saini, V. K. (2006). Adsorption of 2, 4-D and carbofuran pesticides using fertilizer and steel industry wastes. *Journal of Colloid and Interface Science*, *299*(2), 556–563.

Gupta, V. K., Gupta, B., Rastogi, A., Agarwal, S., & Nayak, A. (2011). Pesticides removal from waste water by activated carbon prepared from waste rubber tire. *Water Research*, *45*, 4047–4055.

Haakstad, L. A., & Bø, K. (2011). Exercise in pregnant women and birth weight: A randomized controlled trial. *BMC Pregnancy and Childbirth*, *11*, 66.

Haderlein, S. B., Weissmahr, K. W., & Schwarzenbach, R. P. (1996). Specific adsorption of nitroaromatic explosives and pesticides to clay minerals. *Environmental Science & Technology*, *30*, 612–622.

Hamby, D. M. (1996). Site remediation techniques supporting environmental restoration activities—A review. *The Science of the Total Environment*, *191*, 203–224.

Hameed, B. H., Salman, J. M., & Ahmad, A. L. (2009). Adsorption isotherm and kinetic modeling of 2, 4-D pesticide on activated carbon derived from date stones. *Journal of Hazardous Materials*, *163*, 121–126.

Helfrich, C. D., Li, Y. F., Sharp, N. D., & Sales, A. E. (2009). Organizational readiness to change assessment (ORCA): Development of an instrument based on the promoting action on research in health services (PARIHS) framework. *Implementation Science*, *4*, 38.

Hettige, H., Mani, M., & Wheeler, D. (2000). Industrial pollution in economic development: The environmental Kuznets curve revisited. *Journal of Development Economics*, *62*, 445–476.

Hicks, J. K., Swen, J. J., Thorn, C. F., Sangkuhl, K., Kharasch, E. D., Ellingrod, V. L., et al. (2013). Clinical Pharmacogenetics implementation consortium guideline for CYP2D6 and CYP2C19 genotypes and dosing of tricyclic antidepressants. *Journal of Clinical Pharmacy and Therapeutics*, *93*, 402–408.

Hossain, M. S., Fakhruddin, A. N., Chowdhury, M. A., & Alam, M. K. (2013). Degradation of chlorpyrifos, an organophosphorus insecticide in aqueous solution with gamma irradiation and natural sunlight. *Journal of Environmental Chemical Engineering*, *1*, 270–274.

Hu, Y., Qi, S., Zhang, J., Tan, L., Zhang, J., Wang, Y., et al. (2011). Assessment of organochlorine pesticides contamination in underground rivers in Chongqing, Southwest China. *Journal of Geochemical Exploration*, *111*, 47–55.

Humbert, H., Gallard, H., Suty, H., & Croué, J. P. (2008). Natural organic matter (NOM) and pesticides removal using a combination of ion exchange resin and powdered activated carbon (PAC). *Water Research*, *42*, 1635–1643.

Hutson, D. H., & Roberts, T. R. (1999). *Metabolic pathways of agrochemicals:-insecticides and fungicides.* RSC Publishing.

Ikehata, K., & El-Din, M. G. (2006). Aqueous pesticide degradation by hydrogen peroxide/ultraviolet irradiation and Fenton-type advanced oxidation processes: A review. *Applied Journal of Environmental Engineering Science*, *5*, 81–135.

Infante-Rivard, C., Labuda, D., Krajinovic, M., & Sinnett, D. (1999). Risk of childhood leukemia associated with exposure to pesticides and with gene polymorphisms. *Epidemiology*, 481–487.

Ioannidou, O. A., Zabaniotou, A. A., Stavropoulos, G. G., Islam, M. A., & Albanis, T. A. (2010). Preparation of activated carbons from agricultural residues for pesticide adsorption. *Chemosphere*, *80*(11), 1328–1336.

Islam, M. A., Sakkas, V., & Albanis, T. A. (2009). Application of statistical design of experiment with desirability function for the removal of organophosphorus pesticide from aqueous solution by low-cost material. *Journal of Hazardous Materials*, *170*(1), 230–238.

Jabbar, A., & Mallick, S. (1994). *Pesticides and environment situation in Pakistan.* Islamabad: Sustainable Development Policy Institute.

Jaga, K., & Dharmani, C. (2003). Sources of exposure to and public health implications of organophosphate pesticides. *Revista Panamericana de Salud Pública*, *14*, 171–185.

Jamal, F., Haque, Q. S., Singh, S., & Rastogi, S. (2015). The influence of organophosphate and carbamate on sperm chromatin and reproductive hormones among pesticide sprayers. *Toxicology and Industrial Health*, 1–10.

Kanan, S. M., Kanan, M. C., & Patterson, H. H. (2006). Silver nanoclusters doped in X and mordenite zeolites as heterogeneous catalysts for the decomposition of carbamate pesticides in solution. *Research on Chemical Intermediates*, *32*, 871–885.

Karami-Mohajeri, S., & Abdollahi, M. (2011). Toxic influence of organophosphate, carbamate, and organochlorine pesticides on cellular metabolism of lipids, proteins, and carbohydrates: A systematic review. *Human & Experimental Toxicology*, *30*, 1119–1140.

Khan, M. J., Zia, M. S., & Qasim, M. (2010). Use of pesticides and their role in environmental pollution. *World Academy of Science, Engineering and Technology*, *72*, 122–128.

Kyriakopoulos, G., & Doulia, D. (2006). Adsorption of pesticides on carbonaceous and polymeric materials from aqueous solutions: A review. *Separation and Purification Reviews*, *35*, 97–191.

Kyriakopoulos, G., Doulia, D., & Anagnostopoulos, E. (2005). Adsorption of pesticides on porous polymeric adsorbents. *Chemical Engineering Science*, *60*, 1177–1186.

Lafi, W. K., & Al-Qodah, Z. (2006). Combined advanced oxidation and biological treatment processes for the removal of pesticides from aqueous solutions. *Journal of Hazardous Materials*, *137*, 489–497.

Li, D., Huang, Q., Lu, M., Zhang, L., Yang, Z., Zong, M., et al. (2015). The organophosphate insecticide chlorpyrifos confers its genotoxic effects by inducing DNA damage and cell apoptosis. *Chemosphere*, *135*, 387–393.

Li, H., Sheng, G., Teppen, B. J., Johnston, C. T., & Boyd, S. A. (2003). Sorption and desorption of pesticides by clay minerals and humic acid-clay complexes. *Soil Science Society of America Journal*, *67*, 122–131.

Li, Q., Kobayashi, M., & Kawada, T. (2011). Ziram induces apoptosis and necrosis in human immune cells. *Archives of Toxicology*, *85*, 55–61.

Li, Y., & Zhang, J. (1999). Agricultural diffuse pollution from fertilisers and pesticides in China. *Water Science and Technology*, *39*, 25–32.

Lifshitz, M., Shahak, E., Bolotin, A., & Sofer, S. (1997). Carbamate poisoning in early childhood and in adults. *Journal of Toxicology. Clinical Toxicology*, *35*, 25–27.

Liu, M., Chen, C., Hu, J., Wu, X., & Wang, X. (2011). Synthesis of magnetite/graphene oxide composite and application for cobalt (II) removal. *Journal of Physical Chemistry C*, *115*(51), 25234–25240.

Majewski, M. S., & Capel, P. D. (1996). *Pesticides in the atmosphere: Distribution, trends, and governing factors*. CRC Press.

Malato, S., Blanco, J., Cáceres, J., Fernández-Alba, A. R., Agüera, A., & Rodrıguez, A. (2002). Photocatalytic treatment of water-soluble pesticides by photo-Fenton and TiO_2 using solar energy. *Catalysis Today*, *76*, 209–220.

Malhat, F. M., Haggag, M. N., Loutfy, N. M., Osman, M. A., & Ahmed, M. T. (2015). Residues of organochlorine and synthetic pyrethroid pesticides in honey, an indicator of ambient environment, a pilot study. *Chemosphere*, *120*, 457–461.

Manisankar, P., Selvanathan, G., & Vedhi, C. (2006). Determination of pesticides using heteropolyacid montmorillonite clay-modified electrode with surfactant. *Talanta*, *68*, 686–692.

Mathur, V. K. (1999). Human capital-based strategy for regional economic development. *Economic Development Quarterly*, *13*, 203–216.

McKinlay, R., Plant, J. A., Bell, J. N. B., & Voulvoulis, N. (2008). Endocrine disrupting pesticides: Implications for risk assessment. *Environment International*, *34*, 168–183.

Moreno, R. F., López, C. J., Galvín, M. R., Cordón, M. M., & Mellado, R. J. (2010). On the removal of s-triazine herbicides from waters using commercial low-cost granular carbons. *Journal of the Serbian Chemical Society*, *75*(3), 405–412.

Nanseu-Njiki, C. P., Dedzo, G. K., & Ngameni, E. (2010). Study of the removal of paraquat from aqueous solution by biosorption onto Ayous (Triplochiton schleroxylon) sawdust. *Journal of Hazardous Materials*, *179*(1), 63–71.

Reddy, P. V., & Kim, K. H. (2015). A review of photochemical approaches for the treatment of a wide range of pesticides. *Journal of Hazardous Materials*, *285*, 325–335.

Robinson, T., Ali, U., Mahmood, A., Chaudhry, M. J., Li, J., Zhang, G., et al. (2015). Concentrations and patterns of organochlorines (OCs) in various fish species from the Indus River, Pakistan: A human health risk assessment. *The Science of the Total Environment*, *541*, 1232–1242.

Roy, A., Singh, S. K., Bajpai, J., & Bajpai, A. K. (2014). Controlled pesticide release from biodegradable polymers. *Central European Journal of Chemistry*, *12*, 453–469.

Salman, J. M., Njoku, V. O., & Hameed, B. H. (2011). Adsorption of pesticides from aqueous solution onto banana stalk activated carbon. *Chemical Engineering Journal*, *174*, 41–48.

Sanchez-Martin, M. J., Rodriguez-Cruz, M. S., Andrades, M. S., & Sanchez-Camazano, M. (2006). Efficiency of different clay minerals modified with a cationic surfactant in the adsorption of pesticides: Influence of clay type and pesticide hydrophobicity. *Applied Clay Science*, *31*, 216–228.

Scholz, E. (2012). *Karl Fischer titration: Determination of water*. Springer Science & Business Media.

Shawaqfeh, A. T. (2010). Removal of pesticides from water using anaerobic-aerobic biological treatment. *Chinese Journal of Chemical Engineering*, *18*, 672–680.

Soloneski, S., Kujawski, M., Scuto, A., & Larramendy, M. L. (2015). Carbamates: A study on genotoxic, cytotoxic, and apoptotic effects induced in Chinese hamster ovary (CHO-K1) cells. *Toxicology In Vitro*, *29*, 834–844.

Thuy, P. T., Van Geluwe, S., Nguyen, V. A., & Vander Bruggen, B. (2012). Current pesticide practices and environmental issues in Vietnam: Management challenges for sustainable use of pesticides for tropical crops in (south-east) Asia to avoid environmental pollution. *Journal of Material Cycles and Waste Management*, *14*, 379–387.

Wasse, J. C., Salmon, P. S., & Delaplane, R. G. (2000). Structure of molten holmium and erbium trichlorides and tribromides. *Physica B: Condensed Matter*, *276*, 433–434.

Yuan, F., Hu, C., Hu, X., Wei, D., Chen, Y., & Qu, J. (2011). Photodegradation and toxicity changes of antibiotics in UV and UV/H_2O_2 process. *Journal of Hazardous Materials*, *185*, 1256–1263.

Zhang, S., Yang, Q., Yang, X., Wang, W., Li, Z., Zhang, L., et al. (2017). A zeolitic imidazolate framework based nanoporous carbon as a novel fiber coating for solid-phase microextraction of pyrethroid pesticides. *Talanta*, *166*, 46–53.

Zolgharnein, J., Shahmoradi, A., & Ghasemi, J. (2011). Pesticides removal using conventional and low-cost adsorbents: A review. *Clean—Soil, Air, Water*, *39*(12), 1105–1119.